

AD-A045 603

SYSTEMS CONTROL INC PALO ALTO CALIF

F/G 15/7

PROCEEDINGS OF THE SYMPOSIUM ON CONTROL THEORY AND NAVY APPLICA--ETC(U)

N00014-72-C-0327

AUG 77 M D CILETTI, J S TYLER

NL

UNCLASSIFIED

1 OF 8
ADA045603



AD A 045603

12

PROCEEDINGS OF THE SYMPOSIUM ON

**CONTROL THEORY
AND
NAVY APPLICATIONS**

Held at the
**U.S. NAVAL POSTGRADUATE SCHOOL
MONTEREY, CALIFORNIA**

July 15-17, 1975

Michael D. Ciletti
James B. Tyler

SPONSORED BY THE

OFFICE OF NAVAL RESEARCH
ARLINGTON, VIRGINIA

DDC
OCT 17 1975

11 AUG 77

298p.

100014-72-C-13276



DISTRIBUTION STATEMENT A
Approved for public release.
Distribution Unlimited

AD No. _____
DDC FILE COPY

ORGANIZED BY

SYSTEMS CONTROL, INC. (Vt)
1801 Page Mill Road
Palo Alto, California 94304

389335

4/B

UNCLASSIFIED

SECURITY CLASSIFICATION OF THIS PAGE (When Data Entered)

REPORT DOCUMENTATION PAGE		READ INSTRUCTIONS BEFORE COMPLETING FORM
1. REPORT NUMBER	2. GOVT ACCESSION NO.	3. RECIPIENT'S CATALOG NUMBER
4. TITLE (and Subtitle) CONTROL THEORY AND NAVAL APPLICATIONS; PROCEEDINGS OF THE SYMPOSIUM HELD AT U.S. NAVAL POST-GRADUATE SCHOOL, MONTEREY, CA, JULY 1975		5. TYPE OF REPORT & PERIOD COVERED CONFERENCE PROCEEDINGS
7. AUTHOR(s) M.D. CILETTI, J.S. TYLER		6. PERFORMING ORG. REPORT NUMBER
9. PERFORMING ORGANIZATION NAME AND ADDRESS SYSTEMS CONTROL, INC. (Vt) 1801 Page Mill Road Palo Alto, CA 94304		8. CONTRACT OR GRANT NUMBER(s) N00014-72-C-0327
11. CONTROLLING OFFICE NAME AND ADDRESS OFFICE OF NAVAL RESEARCH 800 North Quincy Road Arlington, VA 22217		10. PROGRAM ELEMENT, PROJECT, TASK AREA & WORK UNIT NUMBERS 5124
14. MONITORING AGENCY NAME & ADDRESS (if different from Controlling Office) SAME		12. REPORT DATE AUGUST 1977
		13. NUMBER OF PAGES 697
		15. SECURITY CLASS. (of this report) UNCLASSIFIED
		15a. DECLASSIFICATION/DOWNGRADING SCHEDULE
16. DISTRIBUTION STATEMENT (of this Report) UNLIMITED		
17. DISTRIBUTION STATEMENT (of the abstract entered in Block 20, if different from Report)		
18. SUPPLEMENTARY NOTES		
19. KEY WORDS (Continue on reverse side if necessary and identify by block number) Control Theory & Applications Navy Control Applications Control Estimation Identification		
ABSTRACT (Continue on reverse side if necessary and identify by block number) This report contains the proceedings of a conference on the application of control theory to Navy problem areas. Papers are included on Navy and other Government program areas where control theory has been applied; and on the state-of-the-art of various aspects of control theory, including control, estimation, and identification. Summaries of panel discussions are included which address where control theory has been applied and where additional research efforts should be directed.		

DISTRIBUTION STATEMENT A

Approved for public release;
Distribution Unlimited

DD FORM 1 JAN 73 1473

EDITION OF 1 NOV 65 IS OBSOLETE

UNCLASSIFIED

SECURITY CLASSIFICATION OF THIS PAGE (When Data Entered)

11

FOREWORD

The Conference on Control Theory and Naval Applications was sponsored by the Office of Naval Research and organized by Systems Control, Inc. (Vt) with the goal of assessing the current status of control theory; including where it has been applied and where it could be applied to Navy systems. Invited and contributed papers were given by government personnel on where control theory is being applied to current Navy, Army, Air Force, and Maritime problems, and by industry and academic experts on the state-of-the-art of control theory from a current and future applications point of view.

The proceedings include papers which were submitted by the authors and transcriptions of oral presentations by authors and the panel discussions.

The Technical Monitor for this project at the Office of Naval Research is Dr. Stuart L. Brodsky.

ACCESSION FOR	White Section	<input type="checkbox"/>
NTIS	Ref Section	<input type="checkbox"/>
DDC		
UNANNOUNCED		
JUST RECEIVED		
BY		
DATE		
RECEIVED		
SP-001		
A		

CONTENTS

	PAGE
SUMMARY by M.D. Ciletti and J.S. Tyler	1
INTRODUCTORY REMARKS by Rear Admiral Isham Linder, USN	9
 SESSION I: SURFACE AND SUBSURFACE VEHICLES	
INTRODUCTORY REMARKS ON SURFACE AND SUBSURFACE VEHICLES by W.E. Cummins	13
AN OVERVIEW OF SHIP DYNAMICS AND THE CONTROL OF SHIP MOTIONS by G.R. Hagen	15
HARDWARE IMPLEMENTATION OF SUBMARINE CONTROL SYSTEMS by W.E. Smith	23
VERTICAL AND HORIZONTAL PLANE CONTROL FOR AIR-CUSHION- SUPPORTED VEHICLES by D.D. Moran	31
STABILITY AND CONTROL OF SWATH SHIPS BY STABILIZING FINS by C.M. Lee	65
STATE-OF-THE-ART FOR PREDICTING THE HYDRODYNAMIC CHARACTERISTICS OF SUBMARINES by J.P. Feldman	87
"TRIDENT SHIP CONTROL" SYSTEMS DEVELOPMENT PROGRAM by R.A. Stankey	129
 SESSION II: AIRCRAFT AND OTHER NAVAL SYSTEMS	
NAVY FLIGHT TESTING AND SYSTEMS IDENTIFICATION by R. Burton	143
THE APPLICATION OF ESTIMATION THEORY TO THE TRANSFER ALIGNMENT OF INERTIAL SYSTEMS by W.F. Ball	165
CONTROL AND ESTIMATION THEORY: AN INTEGRAL PART OF THE ELECTRICALLY SUSPENDED GYRO NAVIGATOR (ESGN) by W.R. Diamond	177
APPLICATION OF CONTROL THEORY IN NAVY COMMAND, CONTROL AND COMMUNICATION SYSTEMS by R.C. Kolb	195
 SESSION III: OTHER GOVERNMENT CONTROL PROGRAMS	
STATUS OF MARITIME SHIP AUTOMATION by T.J. Williams	205
AIR FORCE FLIGHT CONTROL PROGRAMS by P.E. Blatt	229

	PAGE
SESSION III: OTHER GOVERNMENT PROGRAMS	
ARMY FLIGHT CONTROL PROGRAMS by D.L. Key	261
NASA'S ACTIVE CONTROL AIRCRAFT PROGRAM by L.W. Taylor, Jr.	281
SESSION IV: IDENTIFICATION	
SYSTEM IDENTIFICATION - AN OVERVIEW by W.E. Hall, Jr. ..	301
SYSTEM IDENTIFICATION TECHNIQUES FOR SHIP MANEUVERING TRIALS by M.A. Abkowitz	337
IDENTIFICATION OF MULTIVARIABLE GAS TURBINE DYNAMICS FROM STOCHASTIC INPUT-OUTPUT DATA by G.J. Michael and F.A. Farrar	393
CALIBRATION OF HIGH PRECISION NAVIGATORS WITH MAXIMUM LIKELIHOOD ESTIMATION by C.E. Mueller and G. Stein	415
SESSION V: ESTIMATION	
ESTIMATION OVERVIEW by R.A. Nash	443
CONTROL OF STABLE PROPORTIONAL NAVIGATION LAWS FOR MANEUVERING TASKS by R.B. Leipnik, G.A. Hewer and T. Newton	469
EXTENDING THE RANGE OF TACTICAL MISSILES AGAINST JAMMING TARGETS by D.J. Yost and J.E. Kain	471
SESSION VI: CONTROL	
CONTROL OVERVIEW by E.E. Yore	513
THE APPLICATION OF STOCHASTIC CONTROL THEORY TO NAVY FIRE CONTROL SYSTEMS by C.F. Price	559
THE CARRIER AIRCRAFT APPROACH PATH CONTROL SYSTEM AS AN OPTIMAL CONTROL SYSTEM by L.G. Hofmann	577
F14A AIR COMBAT MANEUVERING CONTROL SYSTEM by W. Bihrlé	603
APPLICATION OF THE AUTOMATIC RUDDER INTERCONNECT (ARI) FUNCTION IN THE F-14 AIRCRAFT by J.H. Lindahl	619
LQG APPROACH TO SUBMARINE CONTROLLER DESIGN FOR NEAR SURFACE DEPTH KEEPING by J. Ware	637

	PAGE
SESSION VII: SUMMARY OF PANEL DISCUSSIONS	
IDENTIFICATION PANEL SUMMARY by W.E. Hall, Jr.	653
ESTIMATION PANEL SUMMARY by R.A. Nash, Jr.	663
CONTROL PANEL SUMMARY by E.E. Yore	669
SESSION VIII: INFORMAL CONTRIBUTIONS	
REMARKS ON LQG SUBMARINE CONTROL by D.L. Kleinman	677
LIST OF ATTENDEES	689

SUMMARY

Michael D. Ciletti*

James S. Tyler**

INTRODUCTION

The Office of Naval Research Symposium on Control Theory and Naval Applications met with the objectives of: (1) reporting on Navy problem areas where control theory, identification and estimation have been successfully applied and where a need for application of this technology exists, and (2) to define areas where control theory research is needed for future Navy applications. This summary is intended to review the major Navy applications of identification, estimation and control technologies that were reported at the symposium, and to indicate additional potential applications and areas where further research appear to be needed.

Modern control theory has evolved into a powerful tool for designing improved control systems and for improving the actual design process. With the aid of high-speed digital computers and sophisticated software, certain areas of this technology have matured to the point of being routinely used in the design process. Time domain and frequency domain technologies, on the so-called modern and classical approaches, have made significant impacts on Navy systems. For this discussion, these applications of control, estimation, and identification can be grouped into the categories of ships, aircraft, missiles, and other systems.

CONTROL APPLICATIONS

For surface ships, there are four general areas where control problems arise: course-keeping, roll control, engine control, and replenishment operations. Automatic course keeping and adaptive autopilots are areas where applications of control technology are being made. Coupled with an onboard digital computer, these systems provide a capability for automatic great circle navigation and optimum route selection. Roll control by means of activated anti-roll fins are in wide

* Assistant Professor of Electrical Engineering, University of Colorado, Colorado Springs, CO 80919

** President, Systems Control, Inc. (Vt), 1801 Page Mill Road, Palo Alto, CA 94304

spread application today. The use of such devices is warranted for more reasons than crew comfort, since a number of weapon fire control subsystems require a stabilized environment. The degree of roll stabilization provided by active fins reduces the demand for subsystem stabilization. Research is presently underway to examine use of the ship's rudder as an anti-roll device. This scheme depends on rudder oscillations being made at a frequency and amplitude sufficient to effect anti-roll torques without adversely affecting heading.

Replenishment of stores at sea involves controlling two ships in quarters close enough that the hydraulic suction generated between them is appreciable. It was indicated that this area is being investigated for application of control technology to provide assistance to the helmsman's sensory and decision making capabilities.

Air-cushion-supported vehicles or surface-effect ships have speed characteristics which make them particularly attractive to the Navy. These vehicles couple high speed capability with excellent sea keeping characteristics. Two major problems inherent to these vehicles are the control of motion in the vertical plane and the lack of stability in the horizontal plane. Various cushion configurations, lift systems, and dynamic seals for the cushion have been studied in an attempt to solve the problem of controlling vertical motion, and both active and passive aerodynamic stabilizers have been combined with active thrust vector control to provide horizontal plane stability.

Small water-plane area twin hull ships (SWATH) are another example of an application of control technology to improve the ship's dynamic response characteristics. SWATH ships are characterized by low restoring capability for heave and pitch motion caused by waves. An active control system using stabilizing fins was seen to provide greatly improved response characteristics.

Submarines are a major area where the technology of control theory provides new approaches for meeting the goals of depth keeping, course keeping, depth changing, and course changing. Solutions to these problems have been advanced in the form of new control effectors and automatic digital control systems. In the case of the Trident submarine, control theory was applied to solve the problem of depth-keeping near the surface. Relatively large suction forces tend to cause this large vessel to broach, and the problem is compounded by the reduced effectiveness of the control effectors at low speeds. The approach to solving this problem consisted of developing an automatic control system which uses the forward and stern planes to

control pitch and depth. Statistical variations in the sea state environment led to development of a sea state filter to reduce the response to high frequency wave motion. The system is to be implemented in a time-shared digital computer.

Several new control effectors are being studied for submarines. Partial open flaps are being considered for use in near-surface depth keeping modes, and differential sail planes and sail planes are being examined for roll control. A transfer of technology from the aircraft industry is also being seen in the form of lift augmentation devices, such as blown flaps and flow circulation control.

From the standpoint of crew safety and mission performance, the reliability of any automatic control system must be unquestionable. Manual control may be adequate to ensure crew safety, but the mission requirements of submarines such as the Trident can be better met by automatic control.

Control of the F-14 aircraft at high angles-of-attack and the control of the A-7E aircraft on its approach path to a carrier were presented as applications of classical and modern control theory. In the case of the F-14, a control system was designed to enable the pilot to utilize the aircraft's inherent stability at high angles-of-attack using ordinary pilot control functions. The system includes the capability of automatically coupling the rudder to the lateral stick and minimizing the differential tail deflections, thereby providing subsonic roll maneuverability.

Optimal control theory was used to model the carrier approach problem and to develop a control system comparable to the classically designed approach path control system for the A-7E aircraft. This application demonstrated the applicability of the theory to complex Navy problems, and the techniques used are transferrable to other aircraft. The optimal system was found to have superior performance in changing the approach path angle and reducing the throttle activity. A need was indicated for additional research to determine designs which incorporate carrier wake burble characteristics.

Air Force flight control activities that were reported included a digital multimode flight control system for the A-7D aircraft, active controls for store flutter prevention, a program for a digital avionics system, fault tolerant digital flight control systems, control configured propulsion systems, and the impact of weapon delivery requirements on fire control systems.

A discussion of Army flight control programs considered handling qualities for helicopters, flight tests to identify helicopter parameters, displays and vision aids for use in poor weather, night or non-terminal area operations, hydro-fluidic stability augmentation systems, and system technology demonstrations.

Three problem areas were discussed where control theory is being applied to the needs of the U.S. maritime community. In ship control, the application of control theory is being made to navigation problems, anti-collision and anti-grounding problems, automatic docking and to adaptive autopilots. Machinery control includes alarm systems, diesel and steam turbine control, and plant monitoring. Tanker and cargo loading problems were also described as areas where control theory has potential application.

IDENTIFICATION AND MODELING APPLICATIONS

Applications of identification and modeling theory were reported for submarines, aircraft, engines, cargo-type ships and other systems. Development of the theory has progressed to the point where more widespread application of existing identification algorithms can be made. Identification of submarine parameters is essential for establishing safe operating limits and crew procedures, and for establishing the submarine's ability to perform specific maneuvers effectively.

Use of advanced aircraft identification techniques such as maximum likelihood identification algorithms has made possible the use of more efficient flight tests at a reduced cost. The parameter data provided by these tests is more accurate than flight test data produced by conventional methods. It is expected that these improved test and evaluation procedures stemming from application of this theory will lead to improvements in Navy aircraft.

Identification theory is also being applied to the problem of identifying the parameters of turbo fan engines. A more accurate model for the engine is expected to support an overall effort to improve the thrust response of these engines.

Kalman filter identification methods have been applied with success to Mariner class cargo vessels. Both linear and nonlinear model coefficients have been identified through use of suitably chosen input maneuvers. Efforts are presently being made to identify model parameters for very large crude carriers (VLCC).

Although most of the reported successes for application of identification theory deal with aircraft and ship dynamics models, there are other applications to areas such as instrument calibration, and the calibration of high precision navigators.

ESTIMATION APPLICATIONS

One of the most significant applications of estimation theory has been to the problem of transfer alignment of a strap-down inertial navigation system for shipboard and airborne applications. A Navy program to apply optimal filtering theory to this problem led to successful development of reliable techniques which have been proven effective in field tests. In another program, modern estimation techniques led to improved gyro error models for use in electrically suspended gyro navigators. The effort produced optimized orientations for calibration of the gyro, and resulted in significantly reduced calibration times and shorter factors acceptance tests.

Navy command, control, and communication problems are a major area of current application of estimation theory. In the problem of surface ship navigation, a Kalman filter is being developed to perform navigation information processing within the onboard command control computer. The scheme uses a Kalman filter to estimate the ship's position, velocity, and ocean current set and drift. A second application of estimation theory is to the correlation of data from multiple sensors. Work in this area includes development of algorithms for data combination and for determining the partition of functions between the sensors and the command control system.

Another area for application of control and estimation is to the problem of pointing and tracking. State-of-the-art narrow beam optical and microwave communications systems require automatic acquisition pointing and tracking control systems. Part of the effort includes a transfer of technology and digital control hardware that was developed for weapon systems application, such as missile launchers and gun mounts.

Estimation theory is being applied to the problem of fault detection and isolation for CCV type aircraft. System state information is being used to detect failures and to differentiate between sensor failure and effector failure. Statistical methods are used with data from multiple sensors to detect unexpected data and to determine if it is due to a particular sensor's failure. Unexpected data from more than one sensor is used to detect an effector failure. On-line fault detection and identification techniques are expected to lead to significant reductions in preventive maintenance and highly reliable system designs at reduced cost.

Modern Navy missile systems rely heavily upon Kalman filtering and estimation theory for their fire control and guidance algorithms. One application that was described uses state estimators to provide guidance information for tactical missiles in a range-derived environment. Another author reported on significant improvements in missile guidance law design through use of modern state estimation and control techniques.

CONTROL RESEARCH

There is a need for additional control research directed towards the requirements of specific systems and towards the growth of the technology itself. A major trend towards digital control systems is evident. The main problem that exists is the problem of interfacing the physical hardware with the computer. Analog data converters characterize systems which use digital control systems. There is a question in this area about whether a direct digital design is necessary or whether an analog should be converted to a digital form. Although the present trend is toward digital control with a central computer, the increasing availability of reliable and cheap microprocessors creates a clear need for research to exploit this technology. The trade-offs between central digital control and distributed microprocessor control need to be identified, and a whole theory of design must be developed for systems using microprocessor control systems. The potential for application of these systems is enormous and ranges from control actuator management to sensor data compression.

Problems encountered in high performance systems such as CCV aircraft and the Trident submarine strongly suggest a need for research in the control of systems in regimes where some or all of the control effectors are saturated. This important problem has been overshadowed by the linear control problem, and has not received sufficient attention. Future systems will have to rely on this technology base.

High-speed turning performance for submarines is not sufficiently modeled or understood. There is a need to develop models for submarine turning performance at high speeds and to develop automatic control system capability to expand the operating envelope of present control systems.

Digital implementation of a complex control system in a time-shared environment requires allocation of processing speed to the various control loops, as well as to the other functions. There is an increasing need to develop a theoretical basis for the design allocations that are made in a multiloop environment.

IDENTIFICATION RESEARCH

Identification theory has evolved into a state of maturity that makes it readily applicable to several important Navy problems. There is a need to transfer recent technology developments in aircraft identification to other Navy systems, such as ships, submarines, and missiles. Work is needed to develop models for nonlinear regions of submarine operation. The input design problem for ships and submarines is an area where additional research is needed to develop maneuvers to replace the classical zig-zag and spiral maneuvers. Identification of ship models for use in ship simulators is an additional area where very little work has been done. The clear trend towards larger and more realistic simulations increases the need for research in this area.

Existing algorithms appear to be sufficient from the standpoint of being able to treat a variety of physical problems. However, there are many areas where the model structure problem is important. Nonlinear identification has not been developed to the maturity that characterizes linear identification theory.

Additional work is needed to improve existing models for sea wave spectra, and to model the wake burble behind an aircraft carrier. These models are needed to provide input data for development of ship and submarine control systems, and for carrier landing systems.

Virtually no research has been done to apply modern identification theory to the problem of modeling the helmsman in ship steering tasks. This research could lead to improved control and information systems, definition of operator limitations, and specification of operational procedures.

ESTIMATION THEORY RESEARCH

Like control and identification, a solid and mature foundation has been developed for estimation theory, and many successful applications have been made. There are indications that modeling is the fundamental problem which must be solved to permit application of estimation theory. The modeling problem is made difficult by a lack of the kind and quantity of data necessary for specification and identification of the model. Given this situation, there is a need for continued research in the development of designs which have a minimum sensitivity to the poor quality of the data.

Modular estimation with microprocessors located at the sensors will become increasingly important. There is a need to develop techniques to match microprocessor capabilities with special-purpose algorithms for modular estimation.

Other areas for potential application of estimation theory are in sonar and map-making. In sonar, there is the potential for using estimation theory to detect the characteristic spectral lines of target submarines. This could have a major impact on the training and manning requirements for submarine sonar operating. Estimation theory has been developed for one dimensional processes. Problems in map-making and data base integration give rise to two and three dimensional processes. There is a clear need for research to extend the theory to these problems.

INTRODUCTORY REMARKS

REAR ADMIRAL ISHAM LINDER, USN
Superintendent
Naval Postgraduate School

Welcome to the Postgraduate School. I have looked at the program for your symposium and I must say that you are going to cover some very interesting things. I believe the approach is one that will be most useful to the Navy in describing the control theory applications as we now have them in Naval systems and, hopefully, in projecting these to new ideas and new developments.

The school, of course, is very pleased to be able to provide the facilities, and to act as host for the Conference this week. I can't pass that by without saying a few words about what we have here, for those of you who may not be familiar with the activities of the School.

The Postgraduate School is on a 12-month cycle, so we do have classes in session at this time. We have four quarters a year and this is the summer quarter. The present enrollment of 1,000 or so students includes about 150 to 200 foreign officers, about 100 officers of services other than the Navy, and the rest of the officers are Naval officers. They are here for about two years at a time, and the programs they're in are in Engineering, Science, and Management -- for the most part at the Masters level. We have a few who are studying beyond that at the professional engineer level or at the Ph. D. level.

We have excellent facilities for a technical university, and we hope that you have the opportunity while you are here to look around at them. The Library is adjacent to this building. It may be new to some of you who have been here in the past. It is only about three or four years old, and it represents really the latest ideas in a technical library for a university. You might be interested in seeing some of the facilities there for study and for learning.

The Computer Center is in this building, and you may have an opportunity to look in it. It's on the main floor of this building. We have an IBM 360/67 for student use.

The facilities that are technically aligned with your interests are in the large building at the opposite end of the academic quadrangle. Academic departments located there provide computer studies, electronics programs, and related studies.

If you have the opportunity, we hope you will tour the campus and become better acquainted with what we have here, and what we provide.

As I mentioned, our primary purpose is the education of the thousand or so students who are here for about two years. In support of this effort, we have a research program which is about a three and one-half million dollar effort in which the faculty and students engage in individual projects. Perhaps individuals may work for some of you in this research.

If you have been here on other occasions for other meetings, you may have been to the Management Center. We have short programs that run generally for four weeks at a time in Management Principles and, in fact, there is a class in session now. Some of you may have attended a previous class.

Please take every chance you have to look around, and if you have questions we would be pleased to discuss them with you.

I hope that the conference you have today, tomorrow, and the next day is a very successful one; and I am confident that the Navy's needs for the future application of control theory, can be clearly identified so that we can get on with the work. As a Naval officer who has operated with your concepts and inventions in the past, I want to say that I have been pleased with the steady progress in a vital area of naval operations. I look forward to the new level of capability that can come from meetings such as this.

SESSION I

SURFACE AND SUBSURFACE VEHICLES

INTRODUCTORY REMARKS ON SURFACE AND SUBSURFACE VEHICLES

WILLIAM E. CUMMINS
David W. Taylor Naval Ship R&D Center

Men have been building ships and craft for a good many centuries. It has been said that you really have to be rather clever in order to design a very bad ship. If you use any care at all, it will float, and usually float upright. You put on a propeller (and it really takes a pretty good designer to design a bad propeller), you turn the propeller and the ship will move; and if you put the rudder at an angle, the ship will turn. If the engine stops, nothing very serious happens because the ship just sits there until you can fix things. This is the sort of reasoning that leads to a relatively small amount of research on ships and craft. But, like most generalizations, this one is completely invalid and you will hear more about that this morning.

I will just give you a few examples. Consider the super-tanker, which is a very real problem now. Many of them are directionally unstable. But that's not the important part of the problem. The important part of the problem with the super-tanker is that it has such a long time constant that you could be in trouble beyond recovery, many seconds or even minutes before you realize that you are in trouble.

Then consider some of the other craft--the air cushion vehicle, for instance. Ordinarily, we recognize that course and heading are not necessarily the same thing, but on air cushion vehicles, the difference can get ridiculous. You can go sideways, or backwards, without any difficulty at all.

In the hydrofoil craft (which is a very beautiful craft when properly designed, and takes a lot of the roughness out of the ocean surface), if you go into a turn, the struts may ventilate, which results in sudden reversal in the lateral force on the strut and can put you in a rather nasty trajectory.

If we go below the surface, there are similar problems. A submarine operates in a layer of water which is only a very small number of ship lengths thick. It has been described as like trying to fly a plane through the Holland Tunnel. It takes only a few seconds to go from broach to crush depth; and, with the speed of submarines increasing as they have over the last several decades, this is a very, very real concern. This morning you are going to hear about these and other problems from a variety of speakers, mostly from the David W. Taylor Naval Ship R&D Center.

AN OVERVIEW OF SHIP DYNAMICS AND THE CONTROL OF SHIP MOTIONS

GRANT R. HAGEN

Naval Ship Research and Development Center

This morning you will hear several speakers, all from the Ship Dynamics Division of the Naval Ship Research and Development Center (NSRDC), whose presentations will deal, in some detail, with recent and current activities at the Center relating to ship dynamics and motion control. Their purpose is to acquaint you with some relatively new and unusual types of marine vehicles of current interest to the Navy, and of the potential opportunities for control applications for these vehicles; to familiarize you, to some extent, with the technology at the Center for making investigations in dynamics and control; and to discuss recent work directed toward providing controllers for the Navy's newest submarines. The purpose of this paper, as its title suggests, is to discuss ship dynamics and control in a very general way, and, hopefully, to provide a background for the somewhat specific topics to be treated by the speakers to follow.

It should be made clear at the outset that the subject matter to be considered does not include machinery dynamics and the control of the machinery. Rather, it is concerned with the rigid body (except for movable appendages) dynamics of waterborne vehicles and the control of their motions through the application of forces which generally are of hydrodynamic, or aerodynamic, origin. Of course, it is recognized that such forces, for example the steering forces associated with a rudder, are not developed in the desired amount without the appropriate control of machinery.

The vehicles which are considered today under the general heading of "ships" are of such varied types that one might have

some difficulty in thinking of some of them as ships. However, all are waterborne, and, in this sense, belong to the family of craft that man has used since his earliest days to move about on the water. It is interesting to reflect on man's use of control devices for even the most primitive of such craft. Perhaps the most primitive one is a raft, constructed by lashing a few logs together and transported by the flow of a stream or river, i.e., by simply drifting with the current. At some point in history, it was discovered that a measure of control of the drifting raft could be achieved by use of drogues or by steering oars, so that the raft was not completely at the mercy of the currents. Rafts were used on the oceans too, and sails as well as currents were employed for motive power. We also know that man devised a relatively sophisticated control device for his rafts, although he did not understand why it worked. Captain Saunders, in Volume III of his monumental work, "Hydrodynamics in Ship Design" [1], makes reference to the use of rafts by the early inhabitants of South America, and quotes from J. Charnock's "History of Marine Architecture" (London, 1801, Vol. 1) which uses as source material the book "Relacion Historica del Viage a la America Meridional, Impresa de Orden de Rey en Madrid (Historical Account of Journey to Central America, Printed by the Order of the King in Madrid)," 1748:

"These rafts work, and ply to windward like keeled vessel, and keep their course before the wind almost as exactly, which is the effect of another contrivance besides the rudder: some large planks, three or four yards long, and half a yard broad, called quares, are set up vertically at the stern, and also forward between the main logs. By pushing some of these under the water, and taking others a little up, the float sails large, bears up, tacks, or lies to, according as the machine is worked; an invention which has hitherto escaped the acuteness of the most ingenious Europeans: and though the Indians have indeed contrived the instrument, yet they are utter strangers to the principles of mechanics, and the causes of its operation."

By one means or another, man has found methods of controlling the directions of the craft which he has built, whether they be birch bark canoes or the square-rigged sailing ships of days gone by. The control systems for all of these utilized man as the "black box," or computer, and for the most part, as the "machinery" as well. The use of man as the computer in the control system persists to this day, and it is perhaps not being too brash to suggest that he will continue to be indispensable in many instances involving the control of ships. Consider, for example, the problem that was recently presented to us: it was desired to bring one of our large aircraft carriers into a drydock in a foreign country, but it was necessary to approach the drydock through a very restricted access area, and the carrier had to maneuver in this area to change its heading by 180 degrees. The maneuver would have to be executed by backing and filling at dead slow speed, without aid of tugs. The question which was raised was whether the maneuver could be executed in the space available. While it may be assumed that the captain would have been highly pleased to have this task taken over by an automatic controller, the likelihood that such a thing might ever happen seems remote indeed. There are many circumstances in which it seems that man will have to continue to be the controller. On the other hand, some of the current problems of ship control are of such a nature that manual control is not possible; and others can be dealt with more economically and effectively by use of automatic, rather than manual, control.

The beginnings of the application of automation to the control of ship motions occurred in 1923 when automatic steering tests were conducted with an experimental installation on the U.S. battleship NEW MEXICO. The experiments were made possible by the advent of the gyroscopic compass in the early 1910's and the availability of electrohydraulic steering gear on the NEW MEXICO. Measurements made during the ship trials

showed that the automatic steering gear held the ship to within $\pm 1/6$ degree of the desired heading, with occasional excursions to $\pm 1/3$ degree. The analytic basis for controller was developed by Minorsky. His controller used the second derivative of yaw angle with respect to time, and this enabled the controller to anticipate the necessary rudder changes from 3 to 6 seconds ahead of a helmsman using manual control.

Although the NEW MEXICO trials must be considered highly successful, it has been observed by Nomoto [2] that the subject of directional control of ships was not established scientifically until 1946 when the equations of motion which embraced the dynamics of the ship were set forth, notably by Davidson and Schiff [3]. Within the U.S. Navy, the late 1940's also saw the beginnings of analytical and experimental investigations into the dynamics of submerged submarines, particularly with regard to their directional stability characteristics. This work coincided with the metamorphosis of the submarine from what was basically a surface ship to the true submersible which it is today. During the latter 1950's and in the 1960's, the scope of submarine dynamics investigations expanded from consideration of directional stability to the computer simulation of submarine motions in six degrees of freedom. In the 1970's the scope had been expanded further to embrace automatic controls. Within the Navy, investigations into the dynamics of surface ship maneuvering have not been pursued as actively as those related to seakeeping, but the development of the discipline of ship dynamics has progressed both for submerged submarines and for surface ships, including hydrofoils and such recent comers as semisubmerged craft and air-cushion supported vehicles. Mathematical models, or equations of motion, exist or are being developed for various vehicles, and, to the extent that they are valid, they provide a fundamental ingredient in the prediction of ship motions and in the development of automatic systems for motion control.

The motivation for automatic control can range from laziness on the part of an operator to the inability of human operators to perform the control tasks. Presumably the Navy is not motivated by the laziness argument, but it might well be motivated by the argument of fatigue, and the consequent need for additional men to give continuous attention to the control of ship motions. For long ocean crossings in calm seas the control function for surface ships is almost entirely one of coursekeeping--a rather obvious application of automatic control, and the one which was discussed earlier. When rough seas are encountered, little, if anything, can be done to alleviate pitching except change of speed and heading. However, rolling can be reduced substantially, and anti-roll fins are in fairly common use today for this purpose. The rudder-like fins which are located in the vicinity of the bilges are oscillated in response to a controller to produce rolling moments which oppose those induced by the sea. This is clearly a situation in which manual control is not feasible. Not only would manual control be less effective, it would also be very fatiguing for any substantial length of time. It is of interest to note that the use of the rudder as an anti-roll device is being investigated currently. For some ships the rudder is capable of producing substantial roll moments, and the concept requires that the rudder be oscillated at the natural frequency of roll without producing any appreciable changes in ships heading. This is envisioned as a device for certain ships not fitted with anti-roll fins, and would be used only for short periods when roll must be controlled to enable certain tasks to be performed--such as landing aircraft aboard ship. Presumably, manual control would be adequate for implementing this concept, but automatic control would appear to be highly desirable. An evaluation of the scheme is awaiting ship trials which should be performed within the next year. Anti-roll tanks and moving weight systems are also schemes which have been devised for

for roll control, and they have been investigated both as active and passive systems.

Probably the strongest motivation for the roll stabilization of naval ships in the modern era is related to the multitude of subsystems which are required for weapons fire control. In general, the motions of each of these various subsystems must be stabilized to enable them to function. If the degree of stabilization required for each of these subsystems can be reduced by stabilization of the entire ship as a unit, then it is to be expected that substantial gains in economy and effectiveness would be realized.

Replenishment of ships at sea is an operation which places heavy demands on control. Two ships are required to stream on parallel courses in close proximity to one another so that stores can be transferred from one ship to the other by means of interconnecting transfer lines. The hydrodynamic interaction forces and moments between the ships vary widely in magnitude and direction as the ships change their relative positions during the maneuver, and the helmsman cannot rely solely on his experience in open-water maneuvering. He is in somewhat the same situation as a novice attempting to back a tractor-trailer rig, and his difficulties are attested to by the occasional case wherein ships have found that the clearance between them became negative! This would appear to be a likely case for the use of automatic control, and some work is being done in this area.

Turning now to the consideration of submarines, they seem particularly amenable to the use of automatic control. The modern submarine operates submerged most of the time, and the human controllers must take action in response to information which comes to them by way of the ship's sensors rather than by their own observations of the environment and their relation to it. The sensor information can be inputted to an automatic controller rather than a human controller, and the

functions of depthkeeping, coursekeeping, depth changing and course changing can be provided by the automatic controller. Such controllers have been placed in submarines, but the option for manual control is always available, and there is a general impression that manual control is often used in preference to automatic control. There are various reasons for this, but probably the outstanding one relates to the matter of reliability. If reliability is questionable, and if manual control is both available and acceptable, manual control will be used, and understandably so. However, as speeds increase, the safety of the ship may require that automatic control be used, and the control systems must be 100 percent reliable. As you will hear from a later speaker, depthkeeping of a submarine operating near the surface and subject to the disturbances from the seaway is a control problem that is amenable to solution by automatic control, and in which better performance is obtained by automatic, rather than by manual, control.

Probably any craft that moves slowly enough can be manually controlled and the craft motions can be attenuated provided the necessary forces can be developed. As speeds increase, the need for automatic controls becomes more compelling, and this is certainly true of hydrofoils, one of a group of relatively new vehicles which are currently the subject of considerable research and which are lumped together under the heading "High-Performance Vehicles." Included in this group are semisubmerged ships and craft supported by air cushions. All of these craft have their own peculiar motion problems. Some of these relate to the seakeeping qualities of the craft, and others relate to the improvement of ride quality and to the alleviation of structural loading. Later speakers will discuss the dynamics of some of these vehicles, and will point out apparent opportunities for the application of controls which should enhance their performance and enable them to take their places alongside the traditional naval vessels of the past.

REFERENCES

1. Saunders, H.E., "Hydrodynamics in Ship Design," Volume III, published by SNAME 1965.
2. Nomoto, K., "Problems and Requirements of Directional Stability and Control of Surface Ships," Proceedings of International Symposium of Directional Stability and Control of Bodies Moving in Water, Published by the Institution of Mechanical Engineers, London 1972.
3. Davidson, K.S.M. and Schiff, L.I., "Turning and Course Keeping Qualities of Ships," Trans. SNAME 1946.

HARDWARE IMPLEMENTATION OF SUBMARINE CONTROL SYSTEMS *

WILLIAM E. SMITH
Naval Research and Development Center

This paper will deal with digital instrumentation of submarine control systems. The material treated will be very esoteric, but they are real world problems that we are wrestling with now.

In developing control systems in our group, we feel that we have a number of basic truths (Fig. 1). First, we have to have a reasonably good simulation of the craft, and since we are in ships and seaways, we have to have a simulation or a representation of the seaways disturbance; we have to have techniques or we employ techniques based on optimal control in the development of a control system at this point. In addition to optimal control, there's a lot of personal art in making a control system and a craft react in a specified way. Also, the designer has to look at available hardware in which to implement the control equations; he has to be sustained by what is possible, the state-of-the-art as well as the capacity of the system.

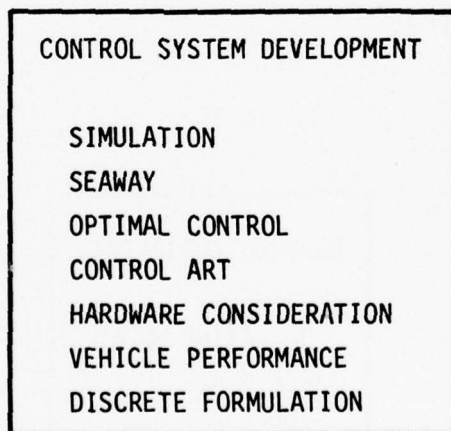


Figure 1

* This paper was typed from a taped version of the oral presentation.

Always in developing control systems for seagoing vehicles, we have the problem or concern of determining what performance is desirable--just what the craft must do and under what conditions. Also, as is pretty well standard now, the Naval craft are being built with digital control systems, therefore, the control equations or control algorithms must be in a discrete format.

The controls that are under development for seagoing craft have a number of similar requirements or components (Fig. 2). The first is the operating mode, such as course keeping, depth keeping, course changing, etc. The sea state is always involved; however, when you consider the craft speed, and heading, in respect to seaway and availability of the seaway, it's been our experience that every one of these controllers must necessarily be sea state adaptive. Similarly, speed adaptors (that's nothing new to many controllers), in the case of submarines, must adapt to depths.

Once a set of control algorithms is developed, it becomes necessary to test them out with the simulations and adjust them to behave very close to what is desirable. Then there is the problem of converting the algorithms into hardware. That's what this paper primarily addresses (Fig. 3).

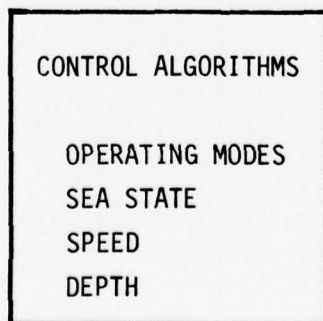


Figure 2

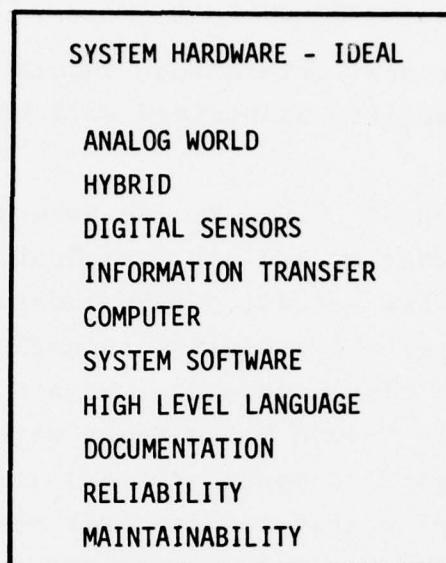


Figure 3

First, it is an analog world. The craft itself operates in an analog fashion; therefore, no matter what you tell it, your control is still a hybrid system. Sensors have to lick the analog world and convert the output to a digital computer. In control systems, it would be nice to have a digital information transfer system and computer with recent software and programming languages to put this together easily. Now, in all of this, a major concern is advanced maintainability or reliability. We would like to have very few filters; we'd like to have a redundant fail-safe system. With these reliability groups we seem to admire, we have not yet been able to locate completely reliable digital sensors and information transfer systems to a point in a real world craft.

The other items, computers, are noted as being systems available--the software one is doing very well. The Navy is tentatively trying to develop standard software with high level languages and documentation so the control systems that come along

later, or even in the next generation, should be much easier to implement. The reliability maintained will be a major item of concern.

What do we have now? (Fig. 4) We have analog sensors, and the control systems that we are now implementing use analog sensors, and, at this point, what we call a signal data converter, which converts analog to digital or digital to analog. Even with the best of computers, or best components, we are finding that consistent reliability is around 5,000 hours with a redundant system. Also, a number of digital computer systems are designed so that they have plug-in replaceable modules that make the repairability time rather short.

The systems that we recommend should be dual redundant (Fig. 5) in order to obtain reliability. The output from these sensors should be put through dual data converters to dual computers and then to dual output components. The systems we are using are, for the most part, dual redundant as most of the systems are, with

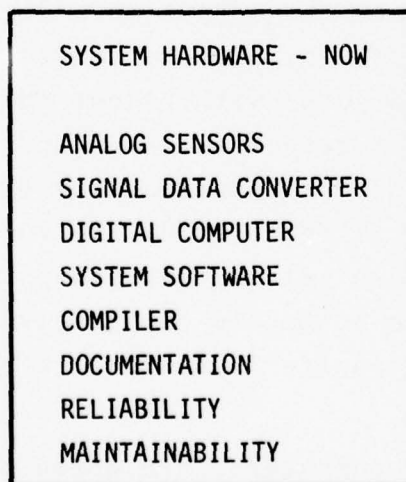


Figure 4

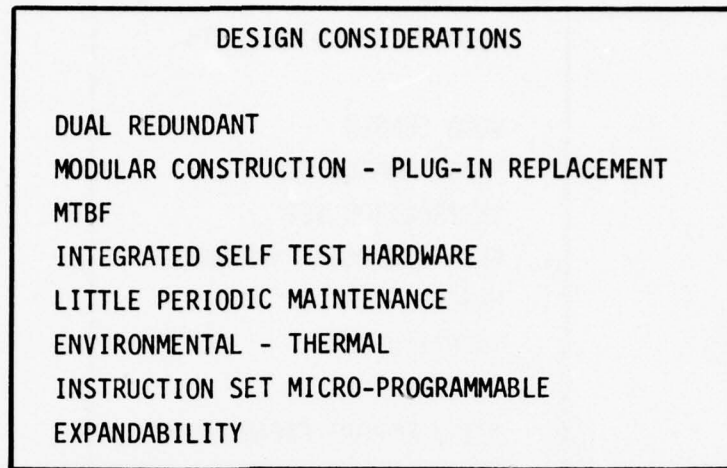


Figure 5

modular construction, and they have very good mean time between failure.

It is necessary to look at the system being built, in terms of self-test. They will fail regardless of MTBF numbers, and so the requirement that they have self test procedures is almost mandatory. Also, due to systems measures or growth, little periodic maintenance should be required, and the system should be able to cope with a wide range of environmental conditions, particularly thermal; and, in terms of implementing the control algorithms, it's very important that they have a micro-programmable instruction set. As all systems are inclined to grow as they begin working, if they work, it is necessary to be able to expand them.

There are a number of problems associated with components (Fig. 6).. For instance, when selecting the analog to digital converters, there's always a question of word length for the digital signal, which primarily goes as sample rates and conversion rates. Most of the signals require band lengthening of some form, and at

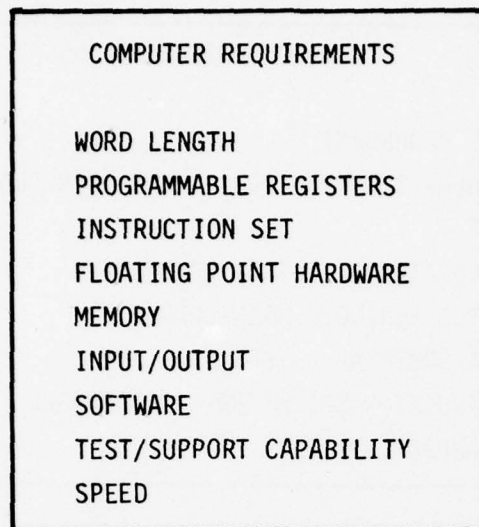


Figure 6

that point, the accuracy of your measurements also have made demands on the necessary size of the receiver.

The word length is a critical item, and the submarine systems being implemented will get by with a 16 bit word. We find that programmable registers are a problem--you can't find the program. You need a very good hardware programmable instruction test.

An item of input that we've run into over and over again is floating point hardware. All of these control problems require a great deal of scaling. They have a very large dynamic range for some of the signals. The scaling problem for floating point computers re-occurs time and time again. It always limits what can be done with a given digital control system. A proper floating point hardware set in the machine can avoid these problems. The memory must be 16K or larger. We have consistently selected core memories for reliability. It's also important that the memory itself has a good input/output structure. The computer itself is in a closed-loop and should be able to handle input data and output

data simultaneously. Also, software that is appropriately designed can be the bulk of the programming and program language which, while it requires more computer capabilities to do that, makes a system modification and updates considerably cheaper.

VERTICAL AND HORIZONTAL PLANE CONTROL FOR AIR CUSHION-SUPPORTED VEHICLES

by

DAVID D. MORAN
Naval Ship Research and Development Center

INTRODUCTION

The air cushion-supported vehicle (ACV) or surface-effect ship (SES) is a new and unique concept in several respects. The system components, which constitute the ACV/SES design, function together to produce a dynamic response to sea-wave excitation which requires study and investigation unique to the concept. The high speed and low directional stability characteristics of fully skirted ACV's make them prime candidates for thorough horizontal plane control.

Four unique characteristics of air cushion-supported craft precipitated their design and construction. The first is the very low hull resistance which these craft exhibit. Sidewall type SES's can be designed to optimize surface-piercing hull drag. Two sidewall type surface-effect ships are currently in operation by the U.S. Navy verifying the low hull drag obtainable through the slender hull design. The wave-making drag of the cushion pressure distribution is amenable to a degree of control and optimization. In general, the ACV/SES is capable of a greater design speed than a comparable displacement ship.

The second unique characteristic of some air cushion-supported craft is an amphibious capability. The benefits of amphibious high speed vehicles are obvious both for military and commercial uses. The British have indeed made a commercial success (Hoverloyd) from fully skirted ACV ferry operations

across the English Channel. Although the amphibious nature of the craft is not required in this specific case, it does facilitate the operation of loading and unloading the vehicles. The U.S. Navy is presently constructing two prototype air cushion vehicles which will serve as evaluation craft for ACV implementation in amphibious assault warfare. In this application, the amphibious capabilities will be exploited fully since the craft will operate over water, over land, in surf zones and upon the decks of support ships.

The third characteristic of ACV performance is concerned with directional stability. Fully skirted or amphibious vehicles have no intrinsic hydrodynamic stability in the horizontal plane. In the absence of aerodynamic stability or control, an air cushion vehicle will, in general, show no preferred orientation and may simply spin in yaw while moving forward. The small forces due to skirt drag are usually not sufficient to maintain horizontal stability in a moving hovercraft. The burden of stability and control in the horizontal plane must, therefore, be carried by active and passive aerodynamic stabilizers and by active control over thrust vectoring. The maneuvering system of an ACV is designed equally for directional maneuverability and horizontal plane stability control. The two prototype air cushion vehicles designed by the Navy's Amphibious Assault Landing Craft Program [1,2] have been designed according to this requirement and exhibit all of the control methods described above.

Sidewall type surface-effect ships derive their yaw and sway stability from the action of the surface piercing sidewalls and from the hydrodynamic response of rudders and control planes. Aerodynamic control is generally not required for surface-effect ships.

The fourth characteristic of air cushion ships which has been noted historically as a major reason to consider ACV

implementation, is the seakeeping response. The ACV from its inception was expected to be a very good seakeeper. The expectation was that the vehicle would ride over the waves on its air cushion shock absorber with a ride quality better than other vehicles. This expectation could not, of course, hold up either to dynamic analysis or to actual ACV testing. The surface-effect vehicle is a dynamic system and like all dynamic systems will exhibit response which is a function of the frequency and amplitude of the excitation. The excitation is, in this case, the wave field or overland terrain over which the vehicle travels. Air cushion-supported vehicles do have a great promise as good seakeepers, but the details of their behavior in a seaway must be known in order to make use of their benefits and minimize their disadvantages. The ACV offers some very attractive characteristics which would allow active or automatic control of the vehicle in a seaway. These features must also be examined in future designs to produce a vehicle which will perform well in a variety of marine applications.

The dynamic response of the ACV/SES may be examined in a number of ways. The total system or black-box approach is the fastest, easiest and most convenient. This technique does not, however, allow parametric analysis or performance improvement identification. Empirical analysis of the ACV/SES produces the most reliable dynamic performance criteria on a model scale but the technique suffers from great monetary expense and the unresolved questions of scaling of dynamic performance. An alternative to the total system approach is interactive systems component analysis. This method allows a great flexibility in design and evaluation of ACV/SES motions but suffers from the problem of cumulative errors produced by inaccurate mathematical models of physical systems. When the separate models are combined in a series constructure system, the individual component errors are multiplicative.

Each approach to the seakeeping problem has its own advantages and disadvantages. At present, none can be considered superior to any of the others. The problem is, therefore, still under active study and receives continued investigation by naval architects concerned with air cushion-supported craft.

ANALYTIC AND EXPERIMENTAL METHODS FOR PREDICTING MOTIONS AND TRAJECTORIES

There are five basic methods for analyzing the motion of an air cushion-supported vehicle in a seaway. These five techniques are:

- (1) oscillator model
- (2) physical system analysis
- (3) data base simulation
- (4) model experiments, seakeeping, and maneuvering
- (5) full scale trials

Each technique can be applied to both vertical and horizontal plane analyses. This presentation will include, however, only a discussion of maneuvering applications for the third and fifth techniques and a seakeeping application of the second on a model scale and the first on a prototype scale.

Oscillator Model

If the dynamic response of an ACV/SES is linear, the vehicle may be treated as a classical linear spring/mass/dashpot system. Unfortunately, the question of the linearity has not yet seen full resolution. Questions with regard to linearity are still frequently seen in the literature. However, more and more evidence is appearing to suggest that deviations from linearity in the dynamic response of air cushion-supported craft are not significant enough to discourage the use of linear analysis.

An example of such a demonstration was recently made for a high length-to-beam ratio surface-effect ship [3]. Linearity in the response of this craft is demonstrated through a comparison of frequency response functions based upon total energy in the craft motion and the first harmonic amplitude of the response for regular wave excitation. Comparisons are shown for pitch and heave motion in Figures 1 and 2, respectively. In general, the degree of linearity demonstrated is remarkably good.

Linearity in vehicle response is determined by the cushion geometry and other system characteristics. The example shown above cannot be taken as a general demonstration of linearity. It does serve, however, to demonstrate that certain craft may be modeled by linear systems.

The application of a simple linear system to the vertical plane dynamics of an air cushion vehicle is demonstrated best by examination of the results of a full-scale experiment on the pitch-heave response of a hovercraft. A spring/mass/dashpot oscillator model can be proposed to describe ACV motion. The excitation is the seaway and the response is the motion (taken as either the heave or pitch of the craft in separate consideration) of the vehicle. The response of this system to either translational or rotational excitation may be described by an overall system response amplitude operator (RAO), which is a frequency-dependent quantity equal to the square of the frequency response function or transfer function. For the present, the RAO is given as

$$RAO = \frac{f^2(\lambda)}{(1 - \omega^2/\omega_n^2)^2 + 4\zeta^2 \omega^2/\omega_n^2}$$

where a reduction factor $f(\lambda)$ as a function of wavelength λ has been introduced to empirically account for the effect of the free surface on the variable dynamic response of the cushion and the wave-induced leakage under the skirt. In this expression, ω is

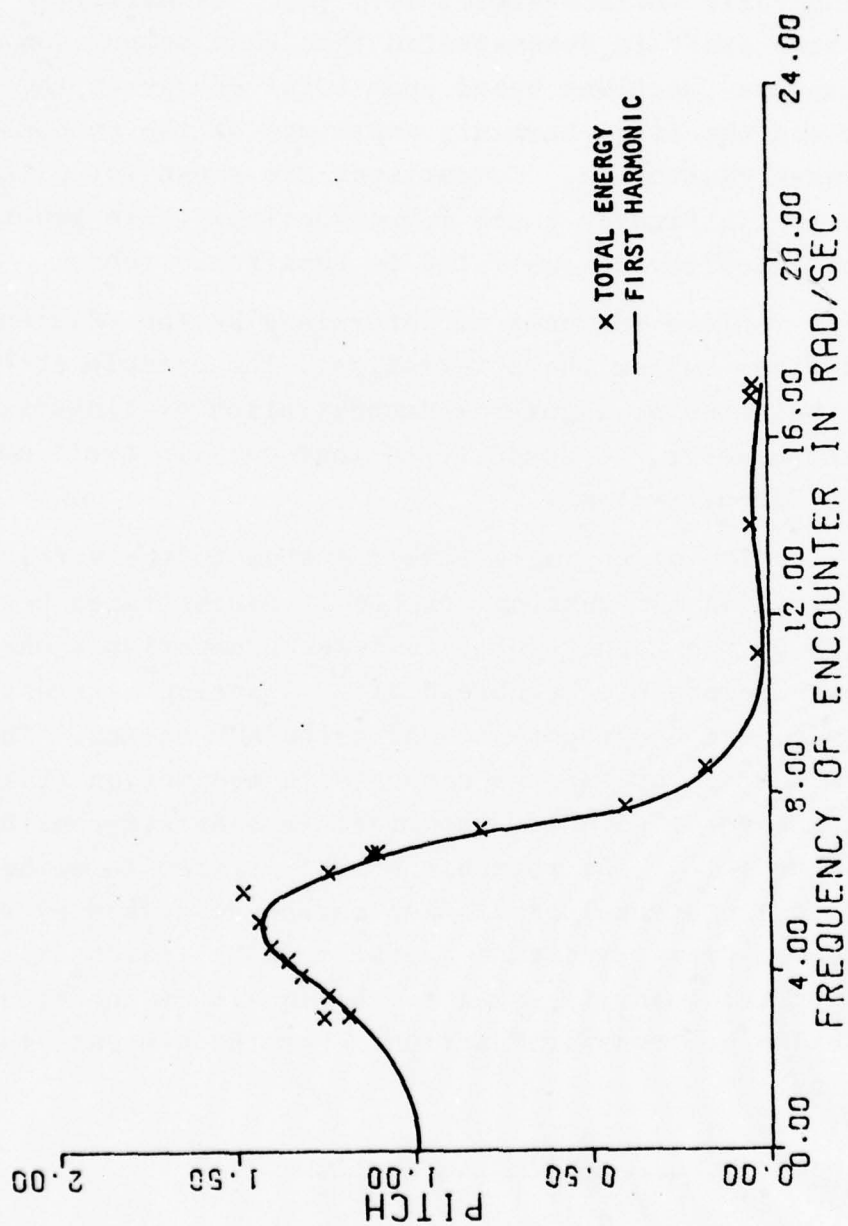


Figure 1 - Pitch Angle (Based on Total Energy) per Unit
 Wave Slope (Froude Number = 0.72)

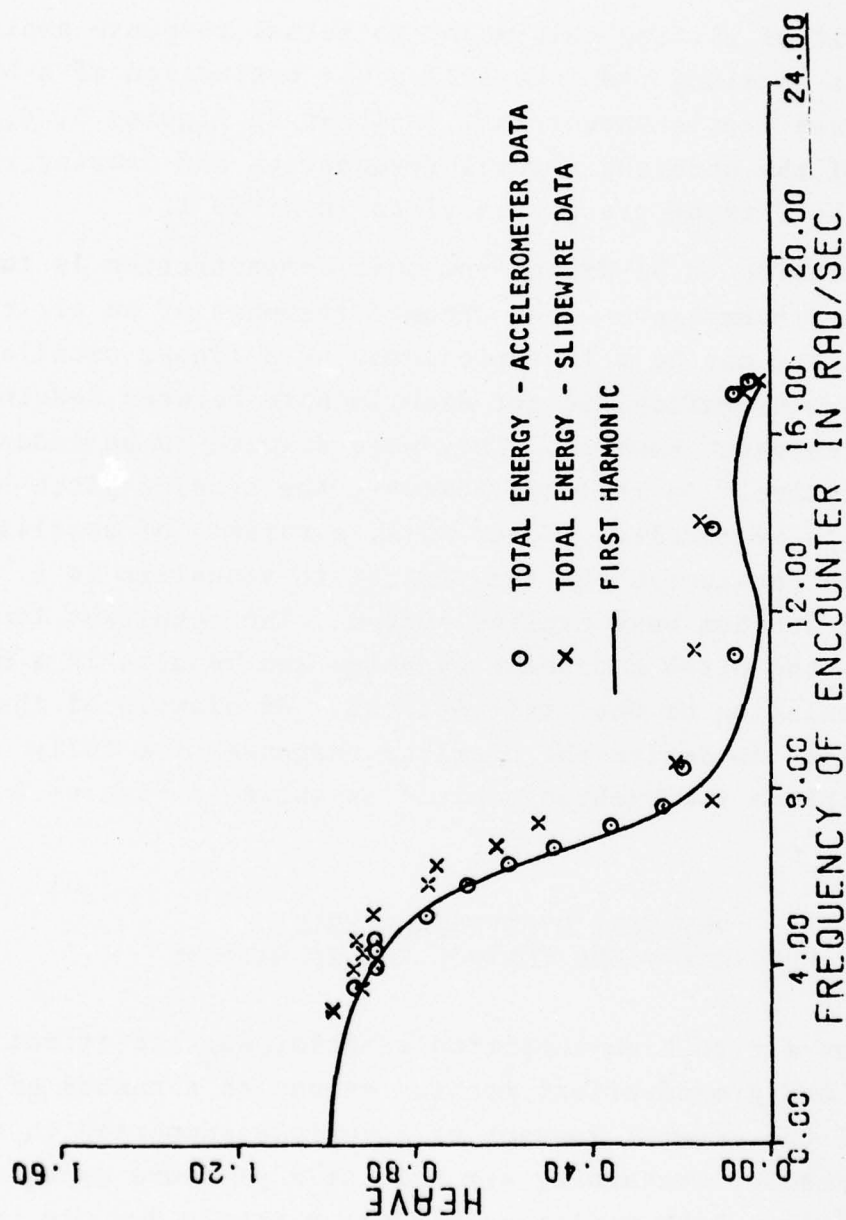


Figure 2 · Heave Motion (Based on Total Energy) per Unit
Wave Amplitude (Froude Number = 0.72)

the excitation frequency, ω_n is the natural frequency and ζ is the damping ratio.

The result of fitting this model to actual response amplitude operators obtained from the full-scale evaluation of a BH.7 Wellington Class British Hovercraft is shown in Figures 3, 4, and 5. A table of the observed natural frequencies and damping ratios employed in the fitting process is given in Table 1.

The conclusion to be drawn from this demonstration is that under certain circumstances, the dynamic response of an air cushion-supported vehicle may be well represented by a linear oscillator. The present demonstration did not discriminate between heaving or pitching response, however. They were assumed to be independent and noninteractive. In reality, however, the coupled pitch-heave response should be modeled. To do this, a variety of oscillator systems may be considered but the easiest to visualize is a two-degree-of-freedom base excited system. The resultant linear model couples the pitch and heave dynamics and results in a more realistic simulation of the craft motions. An example of the use of this analysis to derive the overland response of a fully skirted amphibious air cushion vehicle is shown in Figures 6 and 7.

PHYSICAL SYSTEMS ANALYSIS: VERTICAL-PLANE CONTROL CONSIDERATIONS

The terms air cushion-supported vehicle, surface-effect ship (or vehicle) and ground-effect machine encompass a number of variations of the general concept of a vehicle supported to some degree by a chamber containing air held at a pressure greater than atmospheric. Each variation defines a unique dynamic system and as such must be analyzed separately. In this presentation, however, the air-support concept may be discussed in general. The components which make up all types of ACV/SES's may be identified individually. The dynamic system defined by these

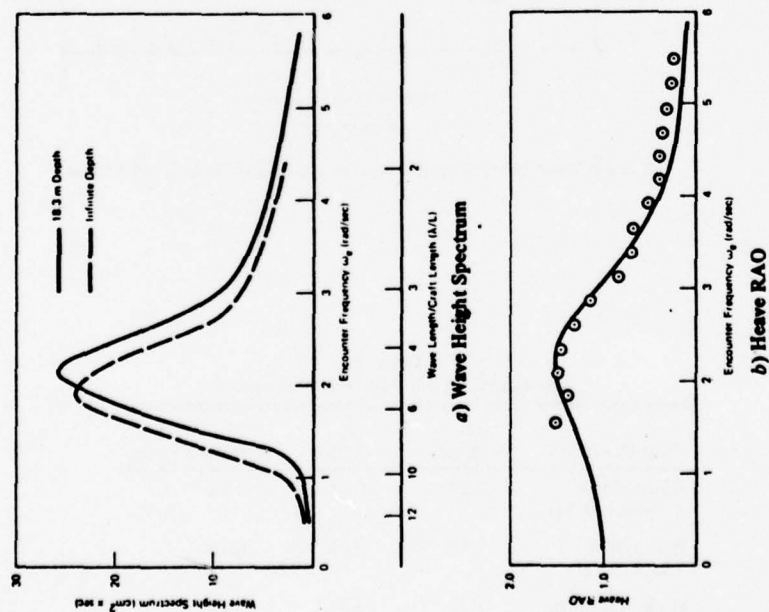


Figure 3 Wave Spectrum and RAO for Head Seas, Speed = 52 kt.

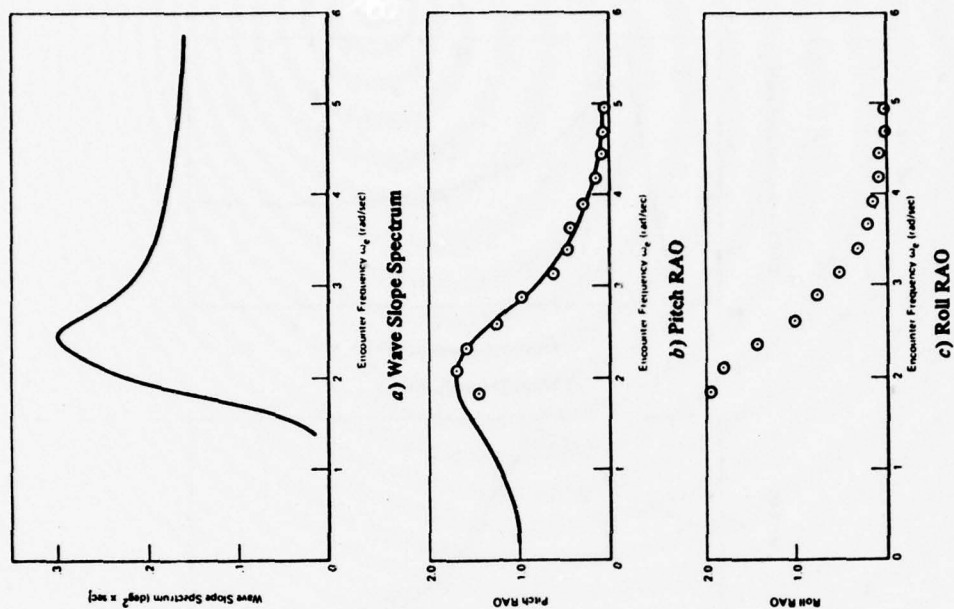
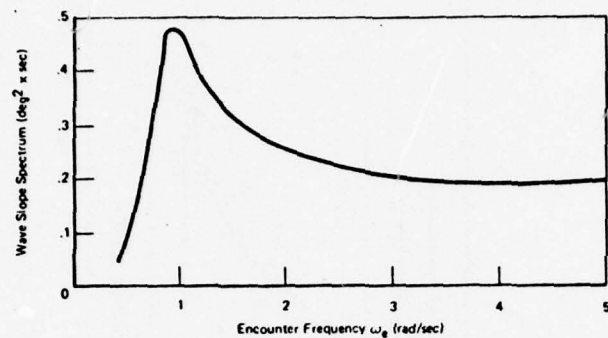
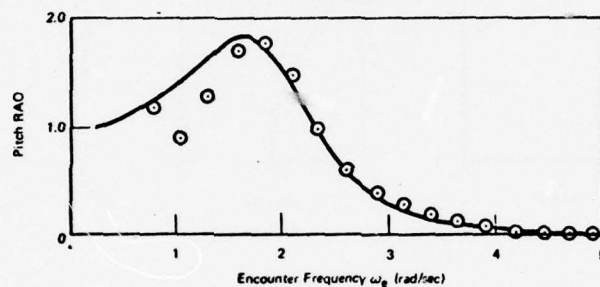


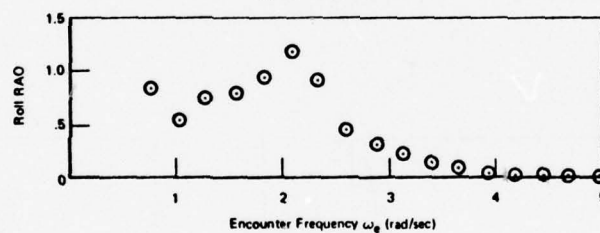
Figure 4 Wave Spectrum and RAOs for Head Seas, Speed = 52 kt.



a) Wave Slope Spectrum



b) Pitch RAO



c) Roll RAO

Figure 5 Wave Spectrum and RAOs for Following Seas, Speed = 55 kt.

Table 1
Damping Ratios and Natural Frequencies

Test Condition	ω_n (rad/sec)	ω_n (Hz)	ξ (Damping Ratio)
Heave, Head Seas (52 kt)	2.84	0.45	0.46
Pitch, Head Seas (52 kt)	2.50	0.40	0.42
Pitch, Following Seas (55 kt)	1.97	0.31	0.40

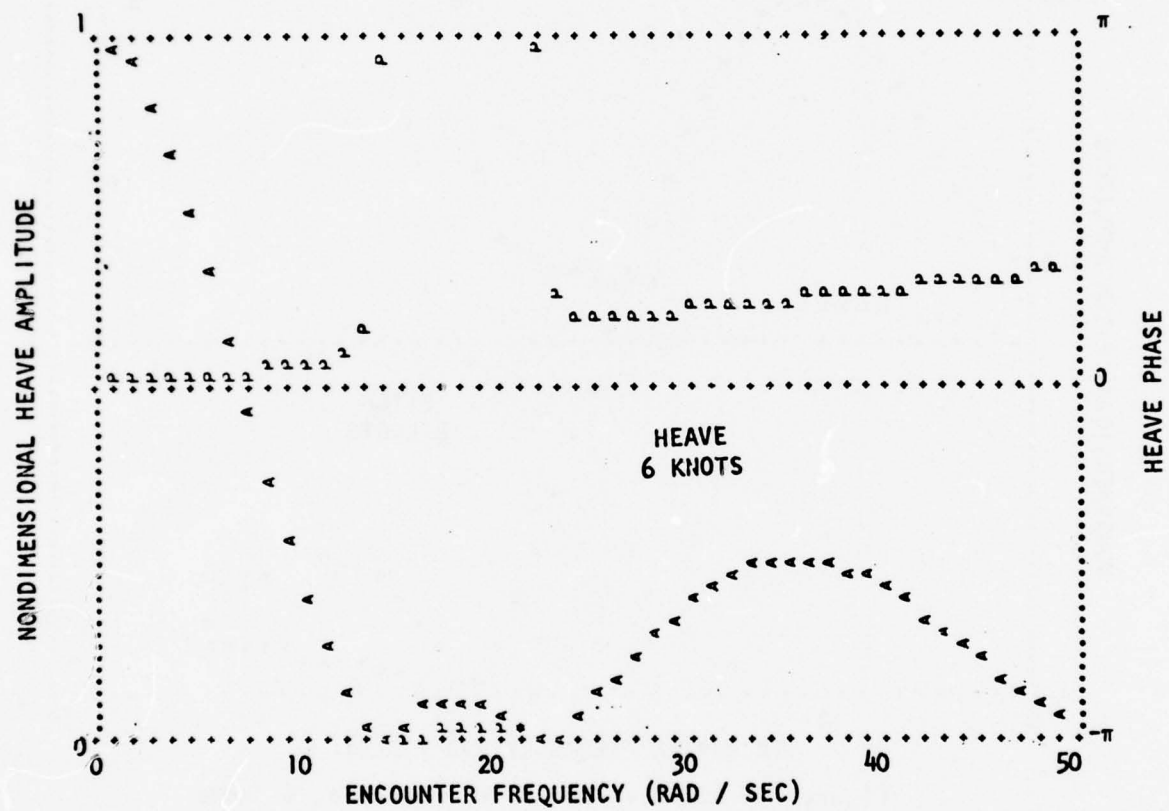


Figure 6 - ACV Overland Heave Response, 6 Knots.

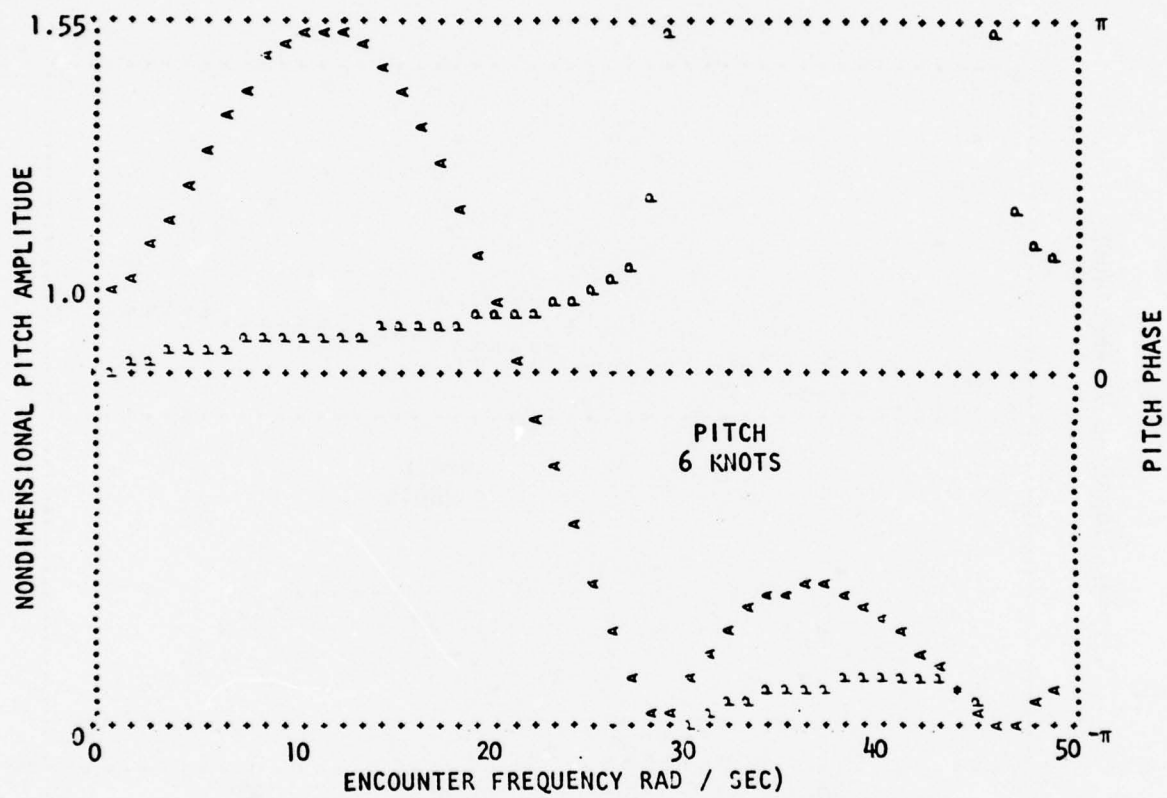


Figure 7 - ACV Overland Pitch Response, 6 Knots

components, therefore, may have to be visualized differently for each specific vehicle.

System Components

The SEV dynamic system can be divided into three distinct parts:

- (1) lift system
- (2) cushion system
- (3) seal system

plus two related processes

- (4) free surface behavior
- (5) rigid body motion

Lift System

The air cushion vehicle must be supplied with cushion fluid. (Without exception, the working fluid of prototype vehicles is air. Model vehicles may employ other gasses as cushion fluids.) The cushion fluid must be at a pressure sufficient to support the vehicle under dynamic conditions and at a discharge determined by the leakage characteristics of the seal system. The lift system consists of a lift fan, pump or compressor and air distribution duct work. The lift fan is the most important feature of the system. Properly designed, the lift fan must have a proven capability of functioning under conditions of varying load. This dynamic capability is one feature of the system which has been neglected until recently. As will be discussed in a later section, the dynamic performance of an ACV lift fan can differ dramatically from its static performance. An example [4] of this behavior is shown in Figure 8 which shows the pressure discharge relationships for both static and dynamic performance of an SES lift fan. The performance indicated was obtained from a dynamic fan testing device which is a dynamic system itself and, therefore, the indicated

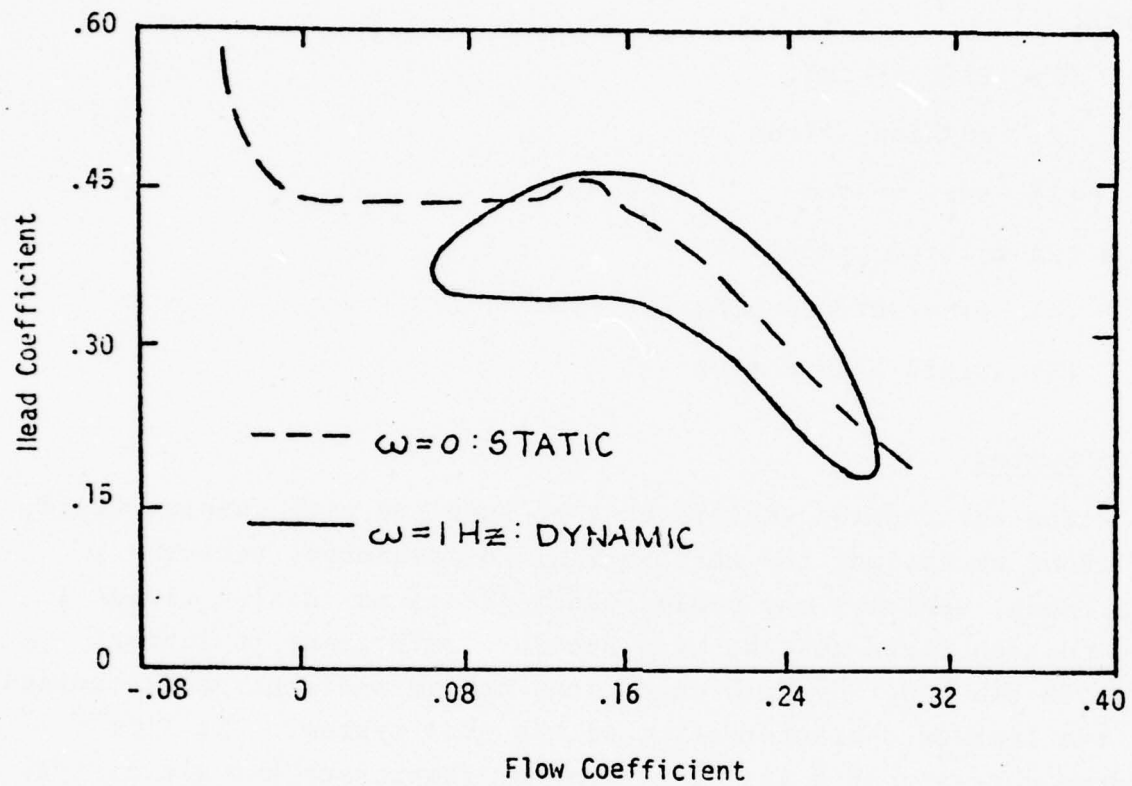


Fig. 8

Dynamic Characteristic of an
SES Lift Fan

behavior cannot be accepted as purely the result of the fan characteristics. The figure does show dynamic behavior which is indicative of that observed in SEV lift systems. The major point of this discussion is that the lift fan is a dynamic component and an element for vertical-plane control in the complete system.

The air distribution network connects the lift fan to the cushion and seals if they are of the inflatable type. The air distribution ducting may be of two types, either rigid pipes or flexible tubing. The rigid air transmission ducts are the more commonly encountered in ACV/SES lift systems. In addition to simple pipes, there usually exist diffusers and flow dividers. The flexible tubing indicated usually results from using part of the cushion seals as lift system flow ducting. When this is done, the ducting may change in size, shape and length depending upon the severity of the motions of the vehicle and the resultant seal deformation. For either type, rigid or flexible, the distribution is not a simple static system. Under conditions of dynamic excitation it will show some nonlinear behavior due to flow reversals, separation, constriction of the flexible tubing, pumping of flexible tubing, and diode behavior at bifurcations. The total response of these phenomena is hysteresis in the pressure discharge relation. The distribution system cannot, therefore, be treated as a simple linear device.

Cushion System

The cushion region or plenum of an SEV is a more complicated dynamic component than is immediately obvious. The plenum contains a volume of cushion fluid which is characterized by equilibrium values of pressure, density and volume.

Each of the properties is, however, a variable under dynamic conditions. The pressure in the plenum may vary over an extended range. It is not uncommon for the pressure to range between 25

and 200 percent of its equilibrium value for rather mild excitation. An example [5] of the time history of pressure measure in a high length-to-beam ratio surface-effect ship is shown in Figure 9. The experimental condition producing this pressure trace was regular-wave excitation at a model speed of 9 knots. The encounter frequency of 2.69 Hz corresponds to a wavelength to model length ratio of 0.58. The wave amplitude for this run was a mild 1.72 inches and yet the maximum pressure excursion is between positive .086 psi and negative .062 psi. (Negative pressures are guage pressures with respect to atmospheric pressure.) (Model length = 15 ft.)

A major variable for the SEV plenum is the volume contained by the vehicles, seals, and free surface. The volume of the cushion changes with the rigid body motion and the free surface forming the bottom boundary. Meaningful considerations of the total dynamic system must include the detailed volumetric behavior.

In summary, the cushion system should be modeled as a complete thermodynamic system with variable boundaries and unsteady non-uniform throughflow.

Seal System

The seals of a surface-effect vehicle may take any of the following forms: sidewalls, rigid planing seals, flexible planing seals, bags, bag and finger seals, pericell seals, curtain seals, air seals, or dynamic sealing by other fluids. Each of these seal types performs the double function of cushion sealing and providing dynamic stiffness and damping. The stiffness and damping of the seal are the more important characteristics in a discussion of vertical-plane dynamics. The dynamic characteristic of any type of seal are, however, closely associated with the sealing capability.

Sidewalls (rigid) provide the most effective form of cushion sealing. If the seal depth is sufficient and the sea state low, the rigid sidewall will seal perfectly. Rigid sidewalls have

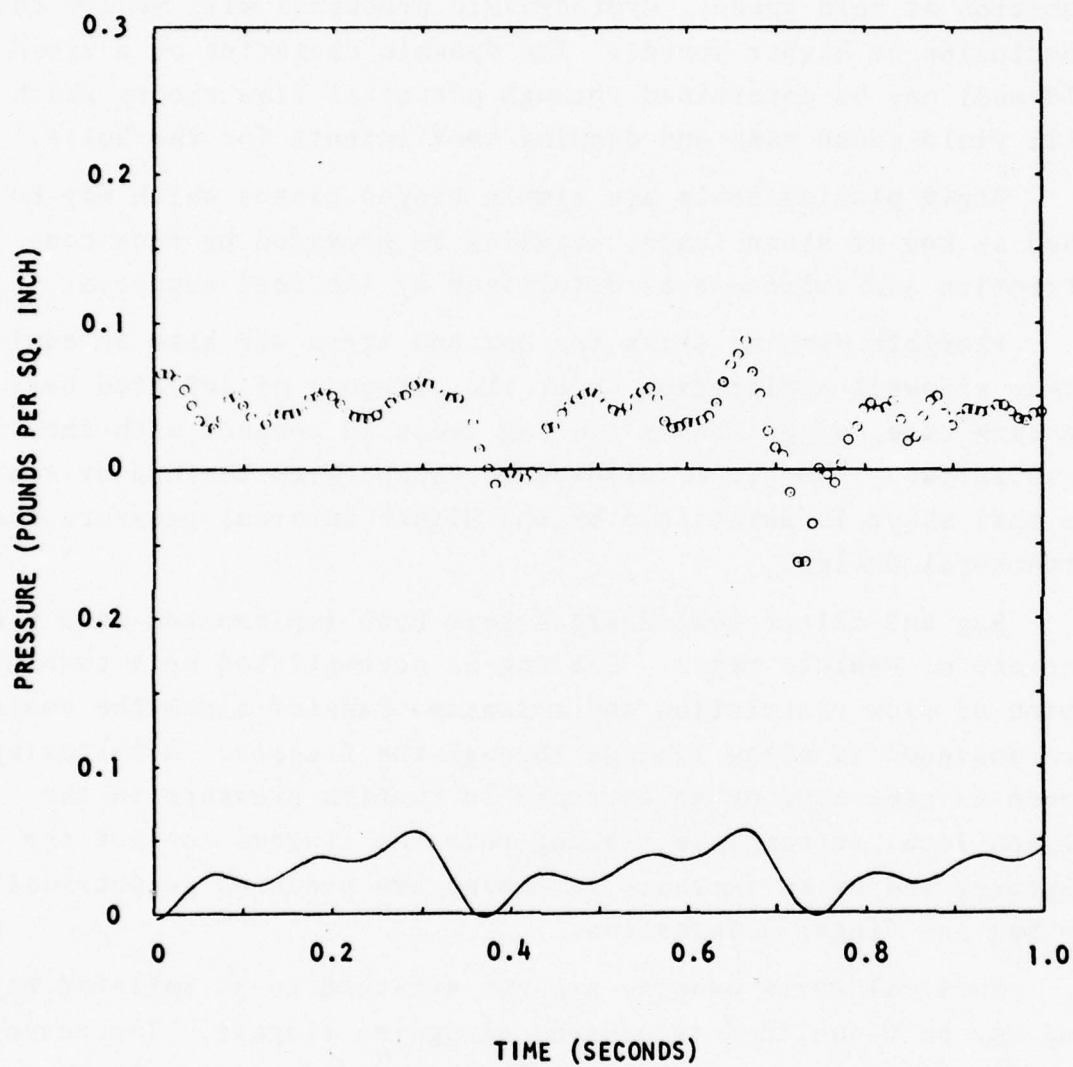


Figure 9 - Typical Time History of Cushion Pressure Measured in the Forward Part of the Cushion (Refer to Table 4 for Test Conditions) Upper Curve is Actual Time History, Lower Curve is Constructed from Harmonic Amplitudes and Phases

an easily calculated restoring or stiffness coefficient. With known hull shape, the stiffness is simply the draft displacement function at zero speed. Hydrodynamic processes will modify this conclusion at higher speeds. The dynamic character of a rigid sidewall may be determined through potential flow theory which will yield added mass and damping coefficients for the hulls.

Rigid planing seals are simple hinged plates which may be used as bow or stern seals. Sealing is provided by flow constriction and stiffness is determined by the seal supports.

Flexible planing seals for bow and stern use have an equivalent sidewall application under the category of inflated bags. In each case, a portion of the bag comes in contact with the free surface. No air is allowed to escape from the bag or seal so that shape is maintained by the higher internal pressure and structural design.

Bag and filter seal designs have been implemented on a wide variety of vehicle types. Sealing is accomplished by a combination of flow restriction and momentum transfer since the seals are designed to allow leakage through the fingers. A restoring force is generated by an increase in cushion pressure in the region local to complete sealing when the fingers contact the surface, and by an increase in moment arm produced geometrically by bag and finger deformation.

Pericell seals usually are not attached to an inflated bag and may be visualized as closed, elongated fingers. The restoring coefficient for a pericell seal is determined completely by geometry, i.e. by the slopes of edges of the cell. When the cell is compressed, a vertical force is generated by the increased area at a cell pressure higher than cushion pressure, and by the increased moment arm between the craft center of gravity and the center of pressure in the cell.

Curtain seals form a limiting case of pericell seals in which the cells are joined and open to the interior of the

cushion. Curtain seals exhibit extremely low stiffness and damping.

Air seals derive their sealing capability from momentum transfer. The seal is a jet of cushion air which must change direction through a large angle (approaching 180°) in order to exit from the cushion region. The dynamic characteristics of air seal systems are also determined by momentum considerations as the jet angle is changed by the craft motion. This type of seal was popular in early ground-effect machines (GEMs) but is now finding application only for tracked vehicles.

In summary, the seal system must be included as an integral component of the dynamic system representing an air cushion-supported vehicle. The cushion seals are not simple passive devices, but are control elements which may, under many conditions, significantly modify the response behavior of the vehicle.

Free Surface Behavior

The free surface is not an element of the dynamic system. It does, however, play such an important role in the seakeeping behavior of the vehicle that it deserves special attention. The free surface under an air cushion vehicle is deformed by the presence of the vehicle. Encountered waves are modified in amplitude by the body and, therefore, the free surface cannot be assumed to be rigid or undeforming. Modifications of the free surface result directly in perturbations to the cushion volume and hence to the dynamic function of the cushion.

Rigid Body Motion

The rigid body motion of an ACV/SES is the product of the seaway excitation acting through the dynamic system. The motion of the vehicle is, of course, a required input to the cushion dynamic system. The entire interactive system must, therefore,

be solved. Quasi-static solutions to the SES dynamics problem seldom have more than limited applicability.

System Component Interactions

The components of an ACV/SES dynamic system are not isolated. Each of the elements discussed in the preceding section has a strong excitation response relationship with the remainder of the system. The evaluation of the response of any individual element is, therefore, extremely difficult in a system of average complexity. The most critical flow characteristic which can be described as an interactive feature of the system is the relationship between the cushion region and the free surface. Since the cushion is bounded on its lower surface by water, the free surface profile under a moving air cushion vehicle determines the volumetric response of the cushion and strongly affects the cushion air leakage. The free surface is, of course, compliant so that it cannot be studied in the absence of the vehicle and the details of cushion and seal design.

Each component of the dynamic system provides available options for control of the vertical-plane dynamic response. Examples of control devices include the controlled fan dynamic response discussed earlier and mechanisms for controlled cushion discharge. The latter device may be either automatic or manual depending upon the nature of the application. An example of an automatic suchion discharge device is the heave attenuation system (HAS) [6] installed on one of the Navy's 100-ton surface-effect ships. The system is designed to bleed air from the cushion in response to high cushion pressures. The purpose of this technique is to lower the peak values of acceleration experienced by the SES in a seaway. The results of the use of the heave attenuation system during a full-scale trial under sea state 2 conditions resulted in a 47% reduction in the average 1/20 highest peak vertical acceleration at the craft center of gravity in head seas at a speed of 37 knots. The reduction in following

seas was nearly as impressive, being 39%. Further, no detrimental effects on the overall lift system were noted during the trials. In general, however, the response of the entire dynamic system must be considered in evaluating the effectiveness of any vertical-plane control device. It must be demonstrated that beneficial behavior in one respect does not produce detrimental behavior in another. Specifically, with regard to a control system which bleeds excess air from the cushion, adverse static (efficiency) and dynamic (control feedback) reactions may result from a system which is not tuned to the complete dynamic system.

Cushion Subdivision

Another vertical-plane control mechanism which may be employed in either an active or passive configuration is cushion subdivision [7]. The cushion region may be divided into a number of distinct cells by internal seals or by an arrangement of large pericell elements. This configuration modifies the pitching response of the vehicle by allowing a strong spatial pressure distribution to exist in the cushion with a pressure discontinuity across the internal seal. The restoring force in pitch is thereby increased over that produced in unsegmented cushions where the pressure is nearly uniformly distributed over the cushion area.

Experimental evidence demonstrating the vertical-plane control capabilities of cushion subdivision has been obtained recently for a fully skirted ACV operating at various speeds over a solid periodic terrain with a wavelength to cushion length ratio of 1.65. The model was operated with and without an internal pressurized bag or keel which divided the cushion into two nearly equal compartments. The results of this comparative experiment are shown in Figure 10 where pitch and heave transfer functions are indicated as functions of model scale encounter frequency for the two modes of operation. When the stability seal is removed from a segmented ACV the pitch natural frequency

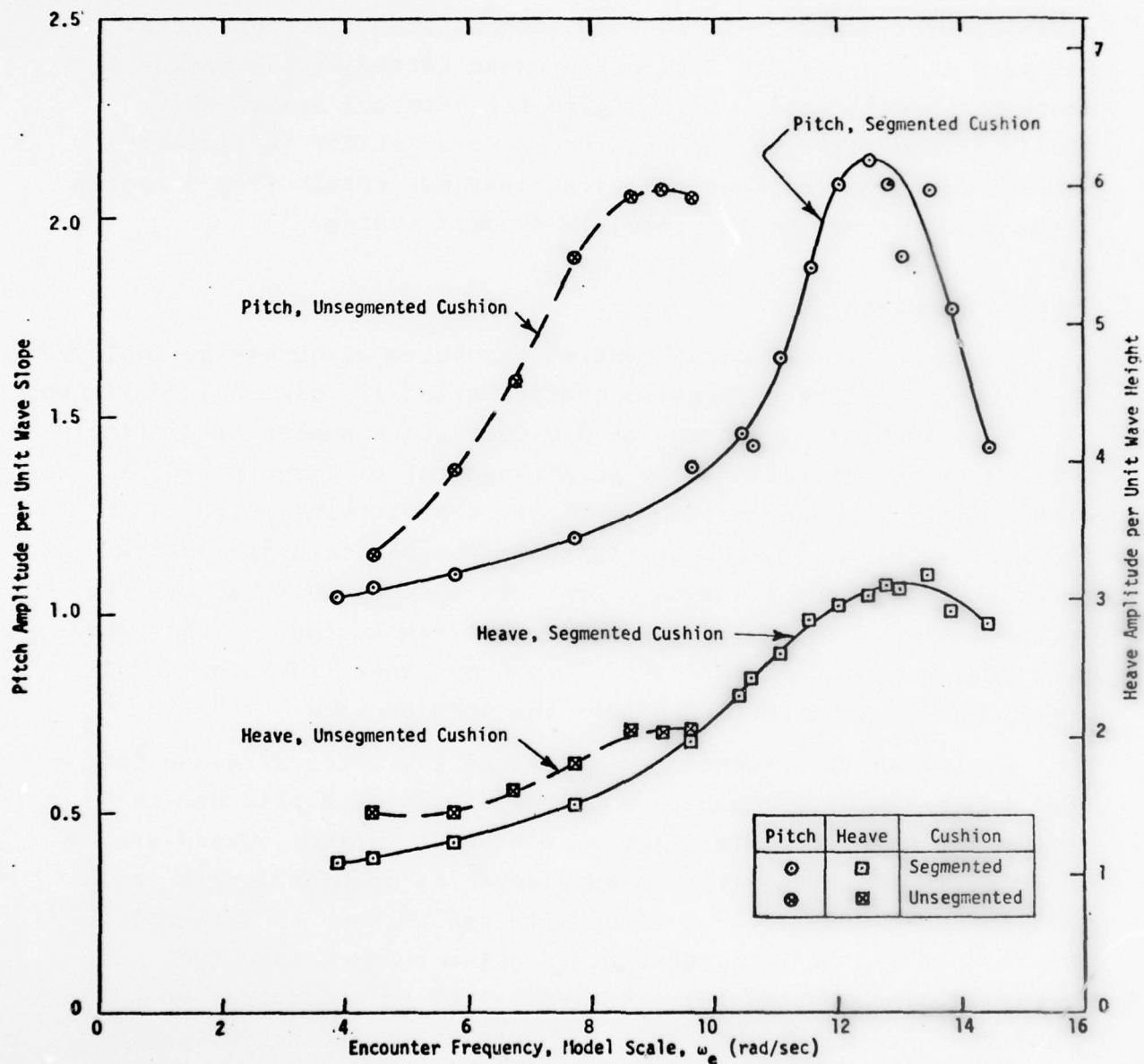


Figure 10 - Heave and Pitch Transfer Functions for ACV Overland Operation, $\lambda/L = 1.67$

is reduced and the pitch transfer function is shifted to a lower frequency range. The heave response is only slightly modified by the removal of the stability seal. This result is in keeping with the fact that the heave response is determined by the spatial integral of the pressure enclosed by the cushion, whereas the pitch response is proportional to the moment produced by the cushion pressure distribution. The unsegmented cushion experiments were frequency-limited due to the incidence of hard structure contact or slamming at the higher speeds. This motion is not evident in the transfer functions but arises from a shift in phase produced by the cushion segmentation. Phase angles for the pitching and heaving motion are shown in Figure 11 for both modes of vehicle operation. There it is evident that both the heave and pitch phase relationships are altered by cushion subdivision. It can be shown that the absolute bow motion is proportional to the cosine of the differences in heave and pitch phase angles. These differences are shown in Figure 12 and here the modification of craft motion produced by cushion subdivision is obvious. The accelerations of the bow and center of gravity (CG) of the model are presented in Figure 13. As expected, the CG acceleration is unchanged by cushion subdivision whereas the bow acceleration shows a response similar to the pitch response. Finally, the effect of bow impact for unsegmented cushion operation appears in the bow-bag pressure shown in Figure 14. There is a sharp increase in pressure for the unsegmented cushion experiment at the higher frequencies as the bow bag absorbs the shock of bow impact.

The benefits of active control over the spatial distribution of pressure in the cushion of an air cushion-supported vehicle are obvious. If the cushion may be segmented by the vehicle operator by inflating or deflating internal cushion seals, the pitch response of the vehicle may be tuned to the sea state in which it is operating by moving the peak pitching frequency in the frequency domain. Properly designed, therefore, the ACV/SES provides

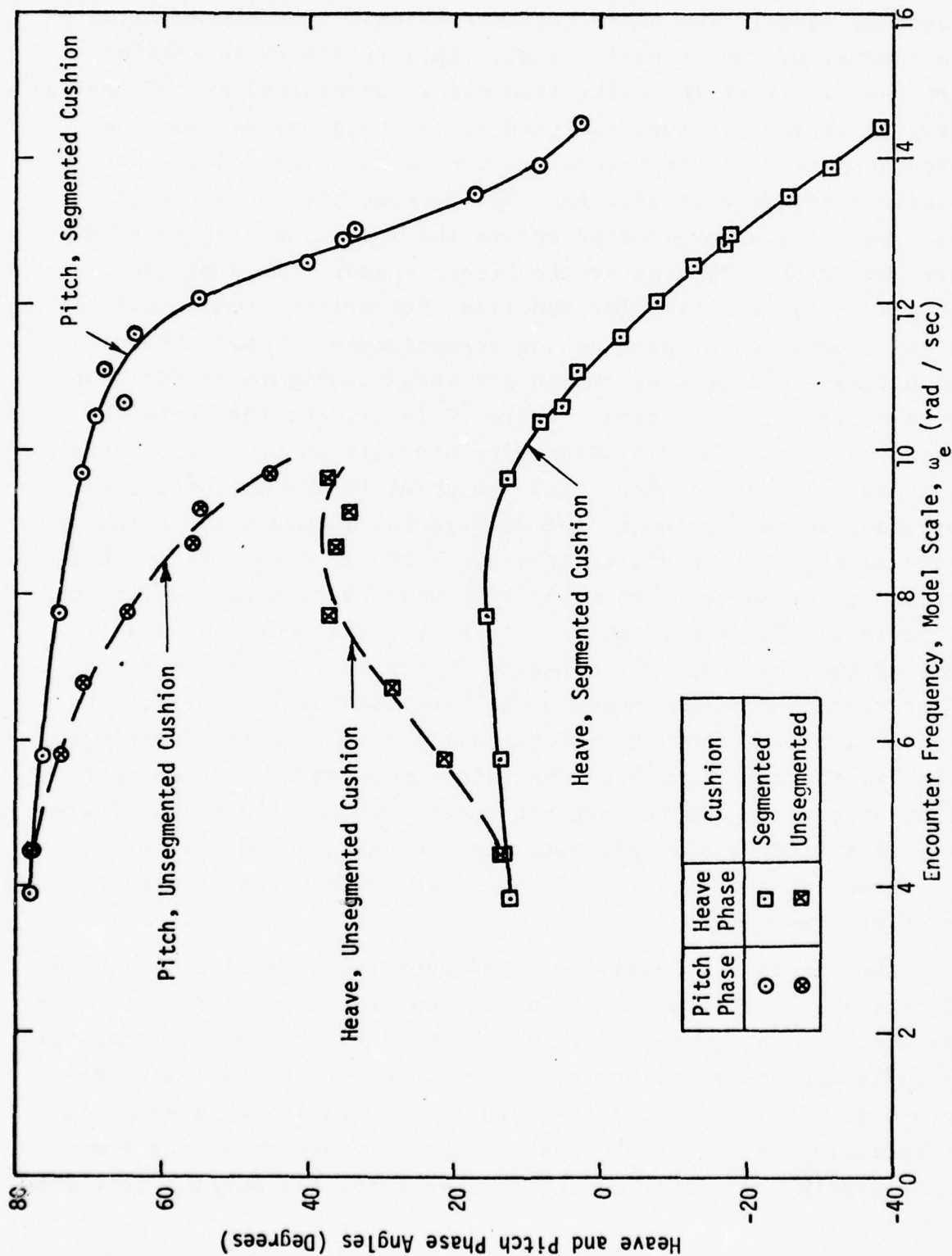


Figure 11 - Heave and Pitch Phase Angles for ACV Overland Operation, $\lambda / L = 1.67$

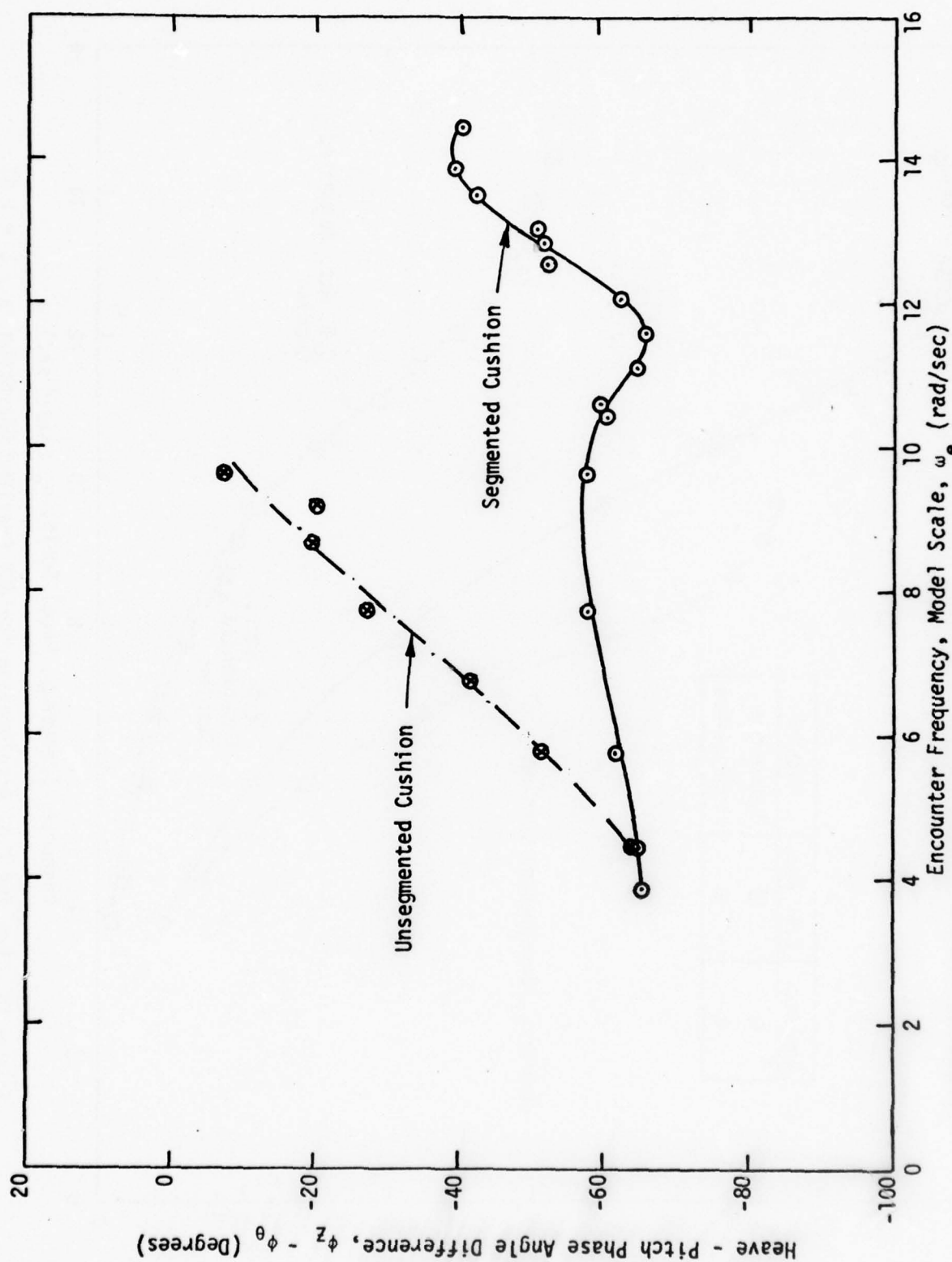


Figure 12 - Heave - Pitch Relative Phase Angle for ACV Overland Operation, $\lambda / L = 1.67$

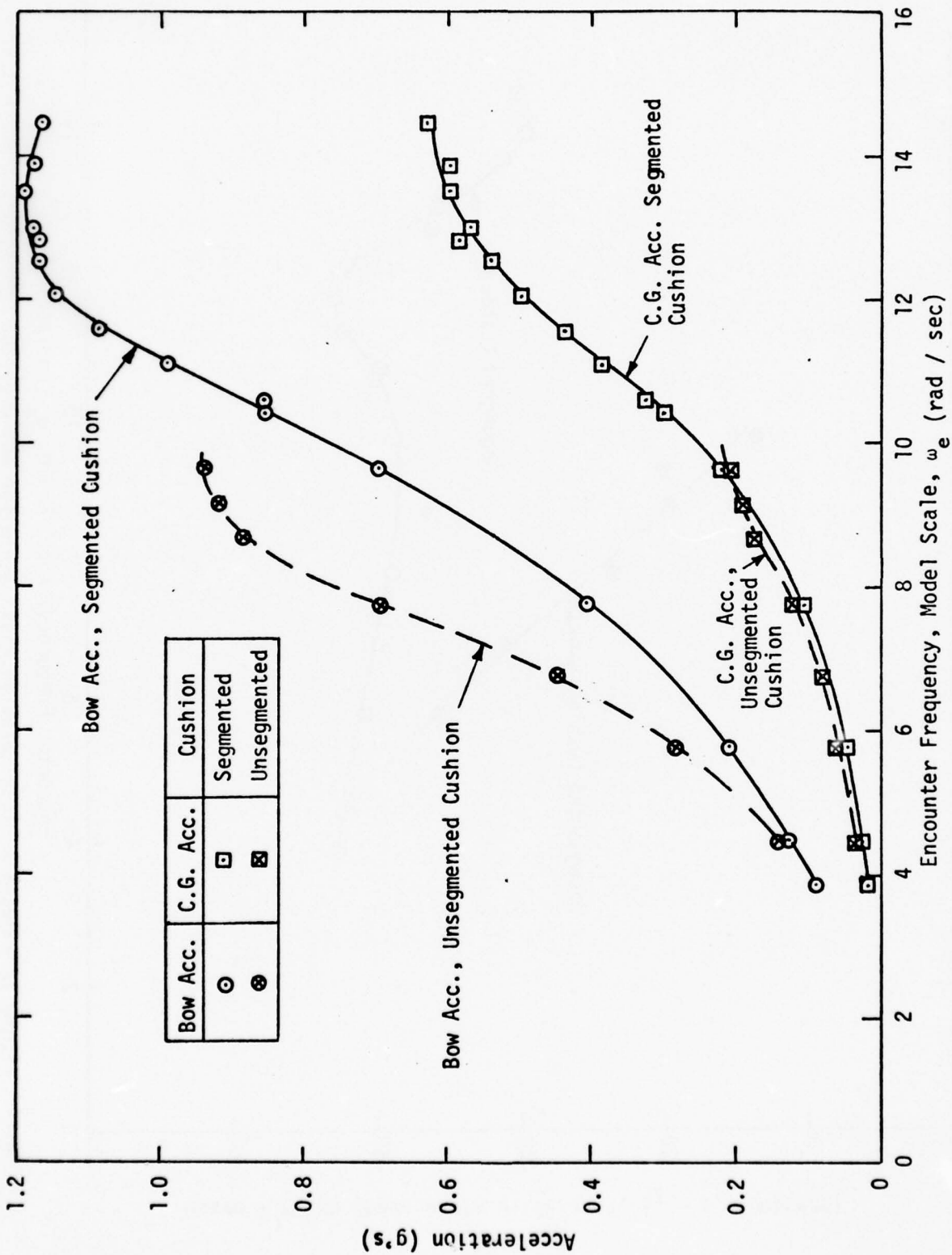


Figure 13 - Bow and C.G. Acceleration for ACV Overland Operation, $\lambda / L = 1.67$

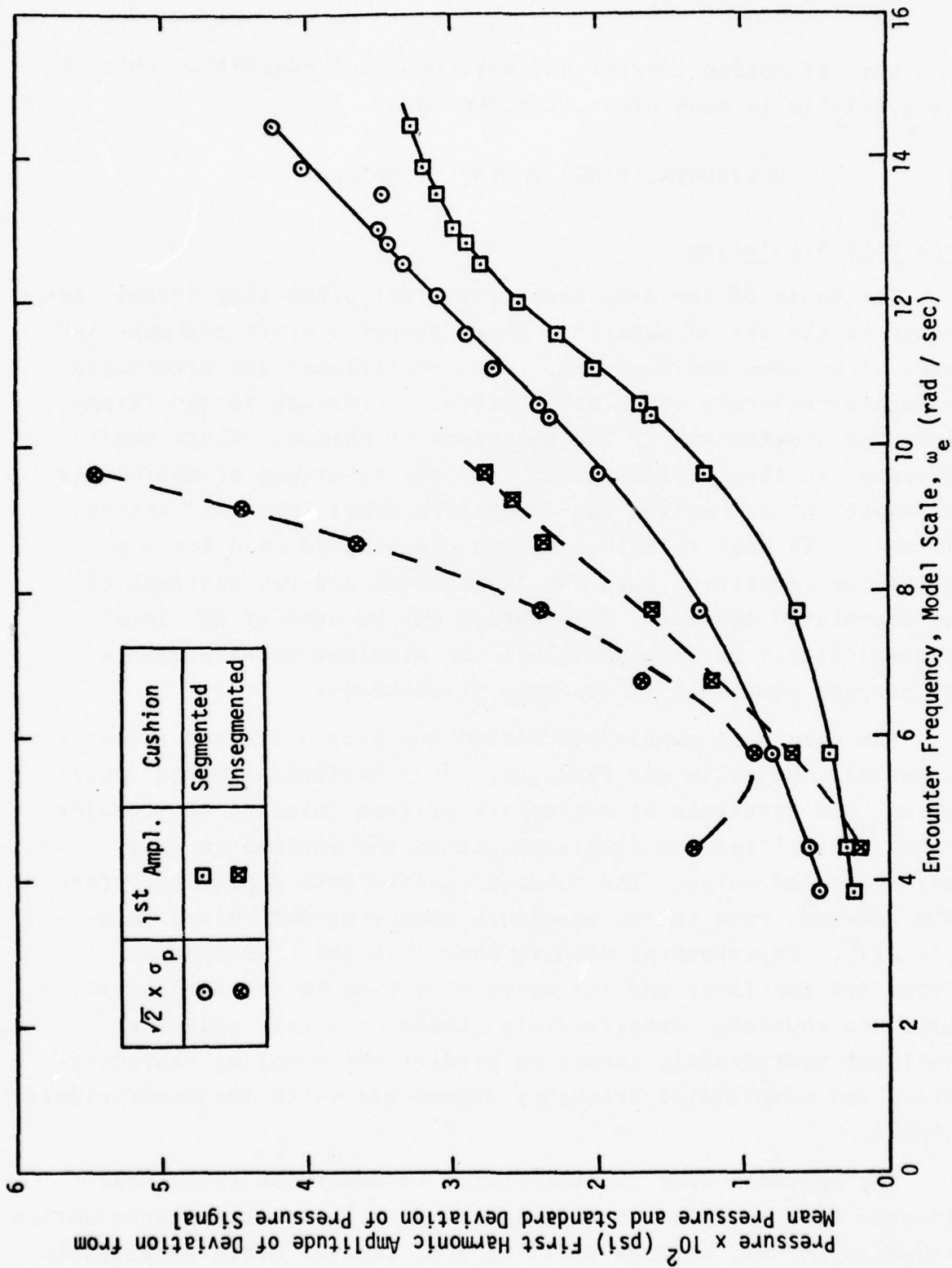


Figure 14 - Bow - Bag Pressure for ACV Overland Operation, $\lambda / L = 1.67$

a measure of motion control and environmental adaptation which is not available to many other ship concepts.

HORIZONTAL PLANE CONTROL CONSIDERATIONS

Data Base Simulation

The basis of the data base method for predicting dynamic response is the set of equations which describe craft response in terms of unknown coefficients. The coefficients are determined through experiments which are performed according to the assumptions and limitations of the equations of motion. These coefficients are then re-introduced into the equations of motion and the equations are solved for excitation other than that tested. The result is that vehicle response can be predicted for any excitation consistent with the assumptions and restrictions of the formulated problem. This method may be used at any level of complexity. One may postulate the simplest model possible and propose equations to describe its behavior.

The data base simulation method has been discussed recently by Wachnik, Messalle and Fein [8]. In a horizontal plane application, the equations of motion are written relating the accelerations, velocities and displacements of the vehicle in sway, yaw, roll, and surge. The unknown coefficients appearing before each inertial term in the equations should be determined theoretically. Experimental results show that the hydrodynamic forces are nonlinear and the modes of motion in the horizontal plane are coupled. Unfortunately, there presently exists no nonlinear hydrodynamic theory to predict the coupling characteristics and complicated frequency dependence which the coefficients exhibit.

The approach here is, therefore, to determine these coefficients from oscillation experiments on a horizontal planar motion mechanism (HPMM), through rotating arm, captive model experiments

and through measurements of the forces on a model towed at various headings. The HPMM experiments are the only method for determining the frequency-dependent coefficients. The full set of coefficients may be obtained through various modes of oscillation and data reduction.

The simultaneous equations of motion are finally solved for particular excitation and craft control functions. Excitation in the horizontal plane is primarily aerodynamic. The effects of wind velocity and relative heading are directly related to the operation of the maneuvering control devices.

In a horizontal plane motion simulation, vehicle control can be obtained in three ways. The first technique involves a table relating the effects of the various force effectors such as wind relative bearing, propulsor attitude, craft heading and the output of the main thruster, e.g. engine rpm. The table is used to compute the effect of any desired environmental and operational condition on the craft motion as a function of time. Characteristically, a linear interpolation is employed to use the table as a continuous function map.

The second method for controlling the simulated craft with time is through a model of a pilot's reactions. A particular course is set and the mathematical model is manipulated until a prescribed boundary condition on any mode of motion is exceeded. The mathematical pilot then introduces corrective commands to the model and the resultant maneuvers are computed until the next boundary condition is encountered.

The third means by which the mathematical model may be controlled is through the action of an automatic feedback control system which operates in a manner similar to the pilot above, but with machine-time-scale response. This technique is appropriate for simulating the effects of automatic course control or stationkeeping.

The mathematical model can be used to study maneuvering behavior but its main benefit is found in the ability to optimize the characteristics of the control devices and the responses to various control techniques. Propulsor angles, speed, and control device response rates are only a few of the quantities which may be treated as variables in control studies for ACV/SES design.

A final question concerns the validity of the output from the mathematical model of the craft under examination. Verification is one of the main objectives of the control simulation procedure, but verification of control responses must follow the accumulation of a reliable data base, preferably obtained through full-scale trials. One such verification was reported by Fein, Magnuson and Moran [9] for a data base simulation of the maneuvering response of a full-scale British Hovercraft. The equations of motion were solved by a fourth order Runge-Kutta-Merson method used to numerically integrate the differential equations in the horizontal plane. The result of performing this horizontal plane simulation is shown in Figures 15 and 16. In each figure, simulated maneuvers predicted from a model data base are compared with full-scale trajectories. The accuracy of these simulated maneuvers should serve as a testament to the value of the data base method of control simulation for air cushion-supported vehicles.

SUMMARY

The air cushion-supported vehicle poses several stability problems and control capabilities which are relatively new to the field of Naval architecture and unique to the concept itself. Vertical plane motion can be controlled through modifications of the dynamic performance of seals, cushion geometry, lift-system properties and a variety of techniques such as cushion segmentation. The possibilities of active motion control are

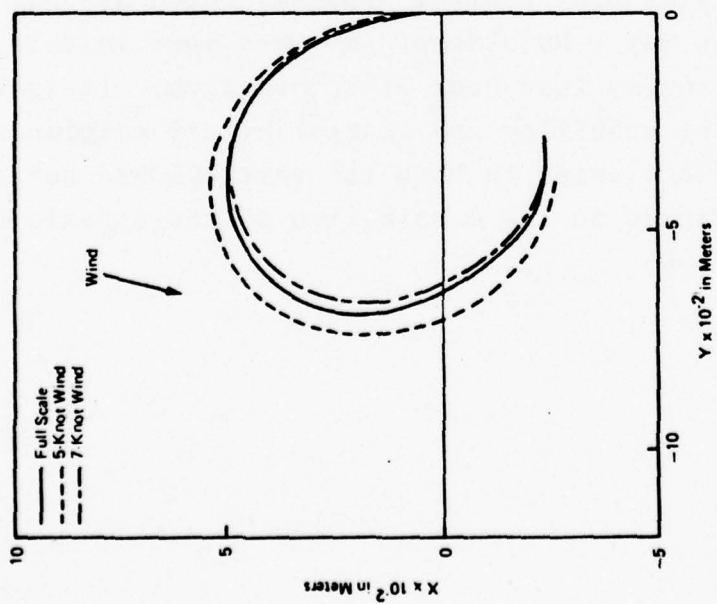


Figure 15 Comparison of Predicted and Full-Scale Trajectories for a Port Turn of the BH.7 with a 46-Knot Initial Speed.

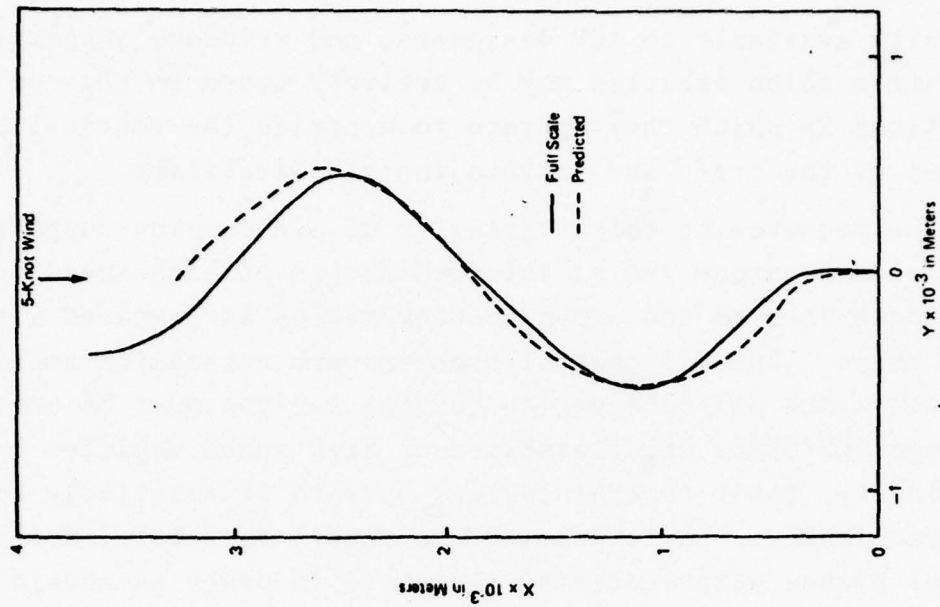


Figure 16 Comparison of Predicted and Full-Scale Trajectories for a Zig-Zag Manuever of the BH.7.

generally available to ACV designers, and evidence suggests that air cushion vehicles may be actively tuned to the sea conditions in which they operate to minimize the vertical plane motions of the craft and improve their habitability.

The maneuvering characteristics of air cushion-supported vehicles are unique due to the combination of high speed and low length-to-beam and depth-to-beam ratios as compared with other ships. Special control problems are raised for amphibious vehicles since all maneuvering control devices must be aerodynamic. Although ACV/SES's are classified as high-speed vehicles hydrodynamically, their control devices operate at relatively low speed aerodynamically. It is usually necessary, therefore, to augment control planes with vectoring thrusters in order to obtain sufficient maneuvering control of the craft.

The purpose of this presentation has been to introduce several ACV/SES control problem areas and discuss selected results covering only a few of these topics. The published literature in the ACV/SES field contains many control problems which are not specifically defined in that way. No attempt has been made in this presentation to thoroughly survey that body of information. It is sufficient to note that the stability and control of air cushion vehicles and surface-effect ships in both the vertical and horizontal planes is intrinsic to the examination of the dynamic behavior of these vehicles.

REFERENCES

1. Brown, M.W., "JEFF Craft - Navy Landing Craft for Tomorrow," AIAA/SNAME Advanced Marine Vehicles Conference, San Diego, February 1974.
2. Schuler, James L., "The Amphibious Assault Landing Craft Program," Naval Engineers Journal, April 1973.
3. Magnuson, A.H. and Wolff, K.K., "Seakeeping Characteristics of the XR-5, A High Length Beam Ratio Manned Surface Effect Testcraft: II. Results of Linearity Investigation, Effects of Changes from Reference Operating Condition and Trim and Draft in Regular Waves," NSRDC Ship Performance Department Report SPD 616-02, March 1975.
4. Durkin, J.M. and Langhi, W.E., "An Investigation of the Performance of a Centrifugal Lift Fan Operating Against Sinusoidally Varying Back Pressure," Proceedings of the International Symposium on Air Cushion Vehicle Technology, Canada, 1974.
5. Moran, D.D., "Cushion Pressure Properties of a High Length-to-Beam Ratio Surface-Effect Ship," NSRDC Ship Performance Department Report SPD 600-01, May 1975.
6. Bell Aerospace Company, "SES-1008 Program," Final Report No. 7308-94 8011, May 1974.
7. Bell Aerospace Company, "Preliminary Design Summary Report," AALC C150-50, Report No. 7385-950007, October 1970.
8. Wachnik, Z.G., Messalle, R.F., and Fein, J.A., "Control Simulation of Air Cushion Vehicles," Proceedings of the Fourth Ship Control Systems Symposium, The Netherlands, October 1975.
9. Fein, J.A., Magnuson, A.H., and Moran, D.D., "Dynamic Performance Characteristics of an Air Cushion Vehicle," Journal of Hydranautics, Vol. 9, No. 1, January 1975.

STABILITY AND CONTROL OF SWATH SHIPS BY STABILIZING FINS

C.M. LEE
Naval Ship Research and Development Center

ABSTRACT

The low restoring capability in heave and pitch modes of a small waterplane area, twin hull (SWATH) ship due to the small waterplane area causes a vertical-plane instability at and beyond a certain speed. Furthermore, SWATH ships can be excited to sharply tuned resonant motion in heave, pitch and roll by waves due to the inherent small wave-making damping.

To circumvent the aforesaid problems, the use of stabilizing fins on the submerged hulls is recommended. The stabilizing fins not only provide pitch stability but also contribute significantly to the damping of the heave, pitch and roll motions in a seaway. Model experiments have already exhibited significant improvements in overall motion characteristics with the use of stationary fins. Both analytical and experimental results reveal that a combination of fore and aft fins provides a definite improvement in the motion characteristics over aft fins alone.

Utilization of active fins for SWATH ships is expected to bring further improvements in controlling the motion in a seaway. A study is made to examine the feasibility of controlling the motion of a SWATH ship by active fins.

INTRODUCTION

Small waterplane area, twin hull (SWATH) ships with semisubmersible hull forms have larger natural period for the heave and

pitch modes than monohull ships of equivalent displacement due to the small waterplane area. The larger natural periods together with smaller wave excitation force due to submerged hulls provide SWATH ships with an advantage in seakeeping in moderate sea states. Furthermore, a large dry deck area which can be utilized as a helicopter pad, and deeply submerged sonar can make a SWATH ship an effective destroyer-escort ship. The smallness of the waterplane area, however, can result in a pitch instability when a SWATH ship cruises with speeds higher than a certain limit. The cause of the pitch-mode instability mainly stems from the so-called "Munk moment" on the submerged hull which is approximately proportional to the square of the speed and provides a destabilizing pitch moment.

This problem is eliminated by the use of stabilizing fins on the submerged hulls. The stabilizing fins not only provide pitch stability but also contribute significantly to the damping of the heave, pitch and roll motions in a seaway. Due to its characteristically small inherent damping, a SWATH ship normally has a sharply tuned response in heave, pitch and roll. The damping provided by stabilizing fins can, therefore, contribute significantly toward reducing the peak responses at the resonant frequencies and hence the overall motions in a seaway.

A theoretical investigation for stationary aft fins shows that the stability and damping are generally improved with increasing aft fin size only up to a point. Contrary to what one might expect, further increase in the fin size tends to result in a deterioration of the stability and can eventually, if carried far enough, cause the vehicle to become unstable. However, this deterioration can be significantly reversed by adding forward fins.

It is expected that more effective reduction of motion of SWATH ships in waves can be achieved by active fins. The

wave-exciting force on a SWATH ship is smaller by an order of magnitude compared to a monohull surface ship of equivalent displacement. It would be therefore feasible to counteract the wave-exciting force by active fins which do not need to be so large that they are impractical. The rate of fin deflection would be slow due to the fact that the resonant frequency of vertical motion of a SWATH ship is not only small but is also narrow banded. The foregoing facts all lead to the conclusion that the chances of successfully obtaining adequate control of vertical motion of SWATH ships in waves by active fins appear very good.

Since the vertical motion of a ship is caused by heave, pitch and roll, the size and location of the fins, and control strategy should be determined to offset the motion induced by these three modes of motion. From a control viewpoint, quatering stern seas (heading between following and beam) are expected to present the worst condition. This is because in a quatering sea, all the three modes of motion exist and, due to the difficulty of course keeping, the rudder is exercised more frequently which can further aggravate the roll motion.

It has been found from past investigations on the motion characteristics of SWATH models in waves that an adequate selection of the size and location of stationary fins can reduce the motion significantly. However, it can be expected that at certain critical conditions such as resonance in the heave, roll or pitch modes taking place individually or a large motion in heave, roll and pitch taking place simultaneously, an active control of fins would be desirable. Thus, it seems logical to determine the size and location of the fins based on the stationary-fins condition to ensure the necessary vertical-plane stability at high speeds and to reduce the motion at the resonant frequencies through the added damping by the fins. The second step is to check the feasibility of the active fins

to counteract the wave excitations. Most of the analysis in the first step has already been conducted by Lee and Martin [1] and a brief description of this analysis will be presented in this paper.

ANALYSIS FOR STATIONARY FINS

Assume that a SWATH ship translating with a forward speed U is momentarily disturbed so as to induce a coupled heave and pitch motion. Our objective is to study whether the ship at a given speed has sufficient stability to restore itself to its original equilibrium in a reasonable time. If the ship is found unstable, a stabilizing fin or fins will be introduced in the analysis.

The coupled heave and pitch equations of motion without excitation can be expressed in the form

$$(M + A_{33})\ddot{\xi}_3 + B_{33}\dot{\xi}_3 + C_{33}\xi_3 + A_{35}\ddot{\xi}_5 + B_{35}\dot{\xi}_5 + C_{35}\xi_5 = 0 \quad (1)$$

$$A_{53}\ddot{\xi}_3 + B_{53}\dot{\xi}_3 + C_{53}\xi_3 + (I_5 + A_{55})\ddot{\xi}_5 + B_{55}\dot{\xi}_5 + C_{55}\xi_5 = 0 \quad (2)$$

Equations (1) and (2) are formulated with respect to the body coordinate system at the equilibrium position of the ship, i.e., no motion except a steady forward translation. The origin of the coordinate system 0 is located on the calm water free surface and, together with the center of gravity, lies in the longitudinal plane of symmetry of the two hulls. The axes, Ox , Oy , and Oz are respectively directed toward bow, port, and vertically upward. $\xi_3(t)$ is the heave displacement, which is positive upward, and $\xi_5(t)$ is the pitch angular displacement about the y -axis, which is positive bow down. M is the mass of

of the ship; I_5 is the mass moment of inertia about the y-axis; A_{ij} , B_{ij} , and C_{ij} for $ij=3$ and 5 are, respectively, the added inertia, damping, and restoring coefficients.

In terms of the usual derivative notations, we can write

$$A_{33} = -\ddot{Z}_w, B_{33} = -\dot{Z}_w, C_{33} = -Z_h,$$

$$A_{35} = -\ddot{Z}_q, B_{35} = -\dot{Z}_q, C_{35} = -Z_\theta,$$

$$A_{53} = -\ddot{M}_w, B_{53} = -\dot{M}_w, C_{53} = -M_h,$$

$$A_{55} = -\ddot{M}_q, B_{55} = -\dot{M}_q \text{ and } C_{55} = -M_\theta$$

where h , w , and \dot{w} are, respectively, heave displacement, velocity and acceleration; θ , q , and \dot{q} are, respectively, pitch displacement (positive bow down), velocity and acceleration; Z the vertical force, positive upward; and M the pitch moment, positive for bow-down sense.

It will be assumed that the hydrodynamic coefficient A_{ij} and B_{ij} are made up of three contributing factors as

$$A_{ij} = A_{ij}^{(I)} + A_{ij}^{(R)} + A_{ij}^{(F)}$$

$$B_{ij} = B_{ij}^{(I)} + B_{ij}^{(R)} + B_{ij}^{(F)}$$

where the superscript (I) denotes the effect of irrotational flow with the free-surface boundary disturbed by the body without the fins; (R) denotes the real fluid effect on the bare hull, and (F) denotes the fin effects. $A_{ij}^{(I)}$ and $B_{ij}^{(I)}$ are obtained from the strip theory applied to twin hulls [2], $A_{ij}^{(R)}$ and $B_{ij}^{(R)}$ are obtained from the available experimental data of submerged bodies of revolution, and $A_{ij}^{(F)}$ and $B_{ij}^{(F)}$ are obtained from the lifting characteristics of fin-body combinations [3].

If we express the heave and pitch motion in terms of the stability index variable λ as

$$\begin{aligned}\xi_3(t) &= \alpha^{\lambda t} \\ \xi_5(t) &= \beta^{\lambda t}\end{aligned}\tag{3}$$

and substitute these into Eqs. (1) and (2), we can derive

$$a\lambda^4 + b\lambda^3 + c\lambda^2 + d\lambda + e \approx 0\tag{4}$$

where a , b , c , d and e are the functions of A_{ij} , B_{ij} and C_{ij} .

The Routh stability criteria are

$$\begin{aligned}a, b, d, e &> 0 \\ bcd - ad^2 - b^2e &> 0\end{aligned}\tag{5}$$

Obviously, we can obtain in general four complex roots of λ from Eq. (4). If the body is stable in its vertical-plane motion, we obtain two sets of conjugate-pair roots. One set, say λ_1 and λ_2 , is associated with the heave mode and the other set, say λ_3 and λ_4 , is associated with the pitch mode. For SWATH forms, the distinction of stability roots between the heave and pitch modes can be easily made by examining the stability roots for uncoupled individual modes.

If one of the four stability roots has a positive real root, then the ship is unstable in the vertical-plane modes. There is another quick method for finding whether a SWATH ship is stable or unstable in its vertical-plane modes for a given speed. That is done by checking the sign of the coefficient

e in Eq. (4) since this is the coefficient which becomes negative for an unstable SWATH ship.

The coefficient e is defined by

$$e = C_{33}C_{55} - C_{35}C_{53}$$

For $e > 0$, we find that

$$C_{55} = \frac{C_{35}C_{53}}{C_{33}} > 0$$

Since

$$C_{55} > \frac{C_{35}C_{53}}{C_{33}} > 0 \quad (6)$$

C_{55} for an unappended hull is given by

$$C_{55} = \Delta \overline{GM}_L - U^2 B_{53}^{(R)} \quad (7)$$

where Δ is the total weight of the ship, \overline{GM}_L the longitudinal metacentric height and U the forward speed. Since $B_{53}^{(R)}$ is usually positive, the second term of the right-hand side of Eq. (7) which is often called the Munk moment provides a destabilizing pitch moment due to its negative sign. Substitution of Eq. (7) into (6) yields

$$U < \left[\frac{\Delta \overline{GM}_L}{B_{53}^{(R)}} + \frac{C_{35}C_{53}}{C_{33}B_{53}^{(R)}} \right]^{1/2}$$

$$\approx \left[\frac{\Delta \overline{GM}_L}{B_{53}^{(R)}} \right]^{1/2}$$

since the term $\frac{C_{35}C_{53}}{C_{33}B_{53}^{(R)}}$ is usually negligibly small for a SWATH ship. Thus, the speed of inception for the vertical-plane instability U_o can be obtained by

$$U_o = \frac{\Delta \overline{GM}_q}{B_{53}^{(R)}}^{1/2} \quad (9)$$

If the inception speed U_o is less than the required operational speed limit of the ship, we should implement some stabilizing device of which horizontal stabilizing fins may be the most reasonable and practical choice.

If we assume that there are N number of horizontal fins attached to the SWATH hull, then the augmentation of pitch-mode stiffness contributed by the fins is obtained by

$$C_{55}^{(F)} = -U^2 \sum_{i=1}^N c_i s_i \ell_i C_{L\alpha_i} \quad (10)$$

where c_i is the mean chord of the i th fin, s_i the span, ℓ_i the x coordinate of the $\frac{1}{4}$ -chord point, and $C_{L\alpha_i}$ the lift-curve slope. If we add the fin-contributed stiffness to C_{55} , we find the inception speed of instability by

$$U_o = \left[\frac{\Delta \overline{GM}_q}{B_{53}^{(R)} + \frac{P}{2} \sum_{i=1}^N c_i s_i \ell_i C_{L\alpha_i}} \right]^{1/2} \quad (11)$$

The physical quantities in the right-hand side of Eq. (11) are positive except the moment arm l_i which takes a positive sign when the fins are located ahead of the longitudinal center of gravity of the ship and otherwise takes a negative sign. Thus, one can immediately observe that aft fins increase the inception speed. When the argument of the square root of Eq. (11) becomes negative, the ship is so stable that there exists no inception speed.

Once the vertical-plane stability of the ship is ensured by employing the stabilizing fins, we can find the response characteristics of the boat in waves in terms of the stability roots obtained from Eq. (4).

The natural periods for heave and pitch modes are obtained by

$$T_3 = 2\pi/I_m \lambda_1 \quad \text{for heave} \quad (12.1)$$

$$T_5 = 2\pi/I_m \lambda_3 \quad \text{for pitch} \quad (12.2)$$

where I_m means the imaginary part.

The damping ratios are obtained by

$$\xi_3 = - \frac{\lambda_1 + \lambda_2}{2\sqrt{\lambda_1 \lambda_2}} \quad \text{for heave} \quad (13.1)$$

$$\xi_5 = - \frac{\lambda_3 + \lambda_4}{2\sqrt{\lambda_3 \lambda_4}} \quad \text{for pitch} \quad (13.2)$$

If we replace the right-hand sides of Eqs. (1) and (2) by the wave-exciting terms $F_3^{(e)} e^{i\omega t}$ and $F_5^{(e)} e^{i\omega t}$, respectively, then we can show that the heave and pitch motion are, respectively, given by

$$\xi_3 = \frac{F'_3 e^{i\omega t}}{a(i\omega - \lambda_1)(i\omega - \lambda_2)(i\omega - \lambda_3)(i\omega - \lambda_4)} \quad (14.1)$$

$$\xi_5 = \frac{F'_5 e^{i\omega t}}{a(i\omega - \lambda_1)(i\omega - \lambda_2)(i\omega - \lambda_3)(i\omega - \lambda_4)} \quad (14.2)$$

where

$$a = (M + A_{33})(I_5 + A_{55}) - A_{53}A_{35} \quad (14.3)$$

$$F'_3 = F_3^{(e)} \left\{ -\omega^2(I_5 + A_{55}) + i\omega B_{55} + C_{55} \right\} - F_5^{(e)} (-\omega^2 A_{35} + i\omega B_{35} + C_{35}) \quad (14.4)$$

$$F'_5 = F_5^{(e)} \left\{ -\omega^2(M + A_{33}) + i\omega B_{33} + C_{33} \right\} - F_3^{(e)} (-\omega^2 A_{53} + i\omega B_{53} + C_{53}) \quad (14.5)$$

and λ_i , $i = 1, \dots, 4$ are the stability roots.

One motion criterion of great importance is the magnitude of the vertical motion (displacement, velocity and acceleration) at a certain point of the ship. The vertical motion can be obtained with respect to both calm water level and actual wave elevation beneath the point of the hull in question. The former is often called the absolute motion and the latter the relative motion. For a given sinusoidal head wave with frequency ω_0 and amplitude A , the absolute vertical displacement at $x = l_a$ is obtained by

$$z_a = \xi_3 - l_a \xi_5 \quad (15)$$

and the relative displacement is obtained by

$$z_r = \xi_3 - l_a \xi_5 - \eta \quad (16)$$

where the wave elevation η is given by

$$\eta = A e^{i \frac{\omega_0^2}{g} l_a + \omega t}$$

for the wave-encounter frequency given by

$$\omega = \omega_0 + \frac{\omega_0^2 U}{g}$$

The velocity and acceleration are obtained by multiplying the displacement by ω and ω^2 , respectively.

For SWATH ships the maximum z_a or z_r would occur when the peak heave motion occurs which takes place at the wave encounter frequency given by

$$\omega_H = \lambda_1 \lambda_2 \sqrt{1 - 2\xi_3^2} \quad \text{for } \xi_3 < \frac{1}{\sqrt{2}}$$

At $\omega = \omega_H$ we find that

$$\xi_3 = \frac{F'_3}{2aD_H} e^{i(\omega t + \delta)} \Big|_{\omega = \omega_H} \quad (17.1)$$

$$\xi_5 = \frac{F'_5}{2aD_H} e^{i(\omega t + \delta)} \Big|_{\omega = \omega_H} \quad (17.2)$$

where

$$D_H = 2 \lambda_{1R} \lambda_{1I} (i\omega_H - \lambda_3)(i\omega_H - \lambda_4) \quad (17.3)$$

for

$$\lambda_1 = \lambda_{1R} + i\lambda_{1I}$$

and $\delta = \text{argument of } \{(i\omega_H - \lambda_1)(i\omega_H - \lambda_2)(i\omega_H - \lambda_3)(i\omega_H - \lambda_4)\}.$

If we choose fins which provide good stability and small heave and pitch amplitudes, we are more likely to have smaller absolute and relative motions. That means that our objective of reducing the vertical motion of the ship would be to minimize the quantities $\frac{|F'_3|}{2aD_H}$ and $\frac{|F'_5|}{2aD_H}$. For stationary fins, the fins have little effect on a , F'_3 and F'_5 , but they can influence D_H significantly. Therefore, the selection of size and location of the fins should be directed toward increasing the value of D_H .

Numerical results for a SWATH ship designated as SWATH 4A will be given in the following as an illustration of the present analysis. The main geometric characteristics are given in Table 1 and a crude sketch of the profile and the midship section is shown in Figure 1. The inception speed for the vertical-plane instability obtained by Eq. (9) is 25 knots. Thus if the ship is required to cruise at a higher speed than 25 knots, the ship has to have stabilizing fins.

In Figure 2 the loci of the stability roots obtained from Eq. (4) are shown. In this figure only two roots, one for heave and the other for pitch, are shown since the other two roots are the conjugate pairs of roots shown, i.e. they have negative imaginary values. An aft fin of rectangular shape of 11.9-foot chord and 14.3-foot span inboard side of the main hulls at the 0.84L is designated as Fin-1.0. In Figure 2, the numbers beside the circle symbols denote the ratios of the plane area of the fins examined. The forward fins are located at the 0.15L of the inboard side of the main hulls. In the case for the fore and aft fins, the total plane area is taken twice the Fin-1.0 and the numbers beside the solid circles denote the plane area ratio of the aft fins to the Fin-1.0.

Table 1
Hull Characteristics of SWATH 4A

DESCRIPTION	UNIT	SWATH 4A
Displacement	Long tons	2379
Displacement Main Hull	Long tons	1852
Length Overall	Feet	239.7
Length of Strut	Feet	188.9
Maximum Strut Thickness	Feet	6.67
Maximum Hull Diameter	Feet	15.0
Beam Overall	Feet	70.0
Draft	Feet	25.0
Waterplane Area	Feet ²	1893
Waterplane Area Moment of Inertia	Feet ⁴	3.645×10^6
Center of Buoyancy from Nose of Hull	Feet	115.6
Center of Flotation from Nose of Hull	Feet	117.7
\overline{BG}	Feet	15.19
Longitudinal \overline{GM}	Feet	27.7
Radius of Gyration for Pitch	Feet	52.1

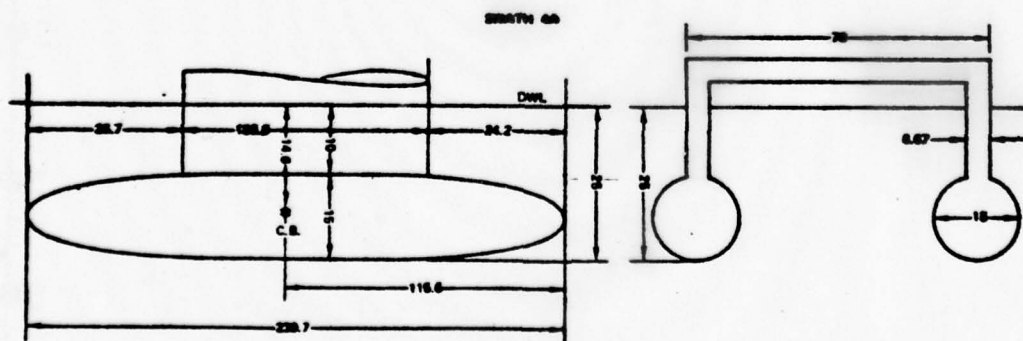


Figure 1 Profile and Midship Section of SWATH 4A

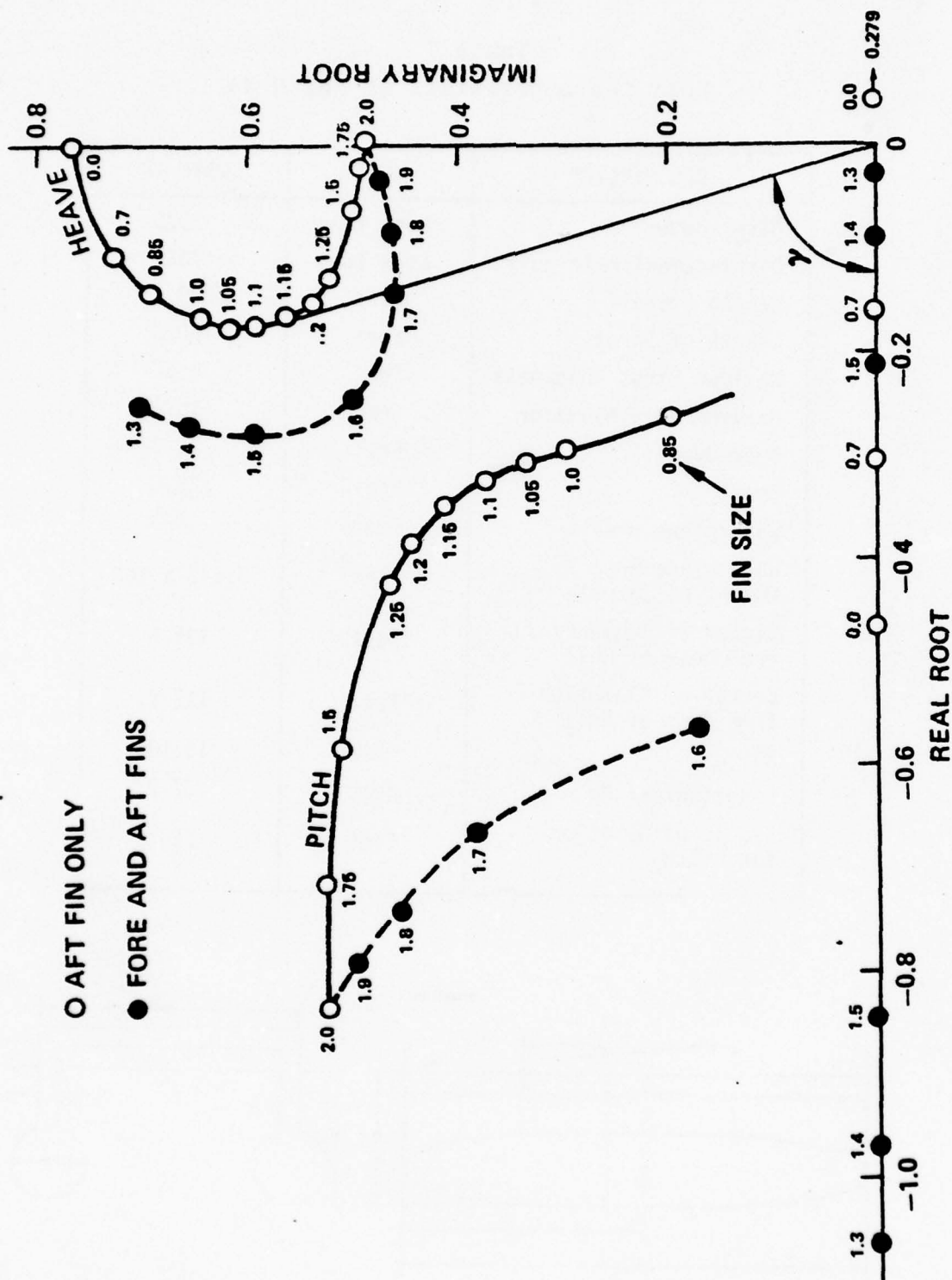


Figure 2 - Stability Roots for Various Fin Sizes for SWATH 4A at 35 Knots

The value of the imaginary root is the natural frequency of the mode indicated and the cosine of the angle of γ as shown in Figure 2 is the damping ratio, i.e., $\cos \gamma$ in Figure 2 is the heave-mode damping ratio of SWATH 4A with the aft fins of Fin-1.1. As the angle γ decreases, the damping ratio increases. As can be observed in Figure 2, SWATH 4A without fins, i.e., Fin-0.0, at 35 knots is unstable since it is a positive real root. Employment of aft fins provides the necessary stability (the larger the absolute value of the negative real root, the greater the stability and the pitch damping ratio). Note, however, that an increase in fin size beyond a certain size decreases the heave damping ratio. A decrease in the heave damping ratio naturally would result in an increase in the peak value of the heave motion and this would be undesirable. This is why the necessity of the fore and aft fins significantly increases the heave damping ratio. But, again, there appears to exist an optimum size combination of the fore and aft fins which provides adequate pitch stability as well as a maximum heave damping ratio. From Figure 2, one can judge that the Fin-1.6 is the best choice. The Fin-1.5, although it has the largest heave damping ratio, should be ruled out because of its smaller pitch stability.

As mentioned earlier, the absolute and relative motion criterion may be examined by checking the value of D_H given by Eq. (17.3). Table 2 shows the values of D_H for various fin combinations which provide sufficient pitch stability. From Table 2 the ranking of the desired fin selection can be made. Obviously, the first choice is the combination of the fore fins of Fin-0.4 and aft fins of Fin-1.6, the second choice is aft fins alone with the Fin-0.85 and the worst choice is the aft fins alone with the Fin-1.5. The correctness of the foregoing motion criterion is checked by computing the coupled heave and pitch motion in regular head waves following the theory described in Ref. 2. The results are shown in Figure 3, and the reliability of the criterion shown in Table 2 is confirmed.

Table 2
Motion Criterion of SWATH 4A at 35 Knots

FIN SIZE		D_H (EQ. 17.3)
AFT	FORE	
0.85	0	0.052
1.0	0	0.045
1.1	0	0.040
1.2	0	0.033
1.5	0	0.021
1.6	0.4	0.064
1.8	0.2	0.033

In the foregoing presentation, we have shown the results derived from the theoretical analysis. It is always safe to verify the theoretical analysis by experiments. Figure 4 presents the experimental results of the models of SWATH forms in waves. The results for the bare hull and the bare hull plus aft fins are obtained from the model of SWATH 4A. The size of the aft fin corresponds closely to the Fin-1.1. The results for the fore and aft fins combination are obtained for a slightly different model from SWATH 4A. The submerged hull shapes are essentially the same and the water plane areas are about the same but SWATH 4A model has a strut which is longer (189' versus 172'), narrower (6.7' versus 7.3'), and shallower (10' versus 11.7') than the other model.

ANALYSIS FOR ACTIVE FINS

As can be seen from Eq. (14) a minimization of the heave and pitch motion of a SWATH ship can be achieved by minimizing

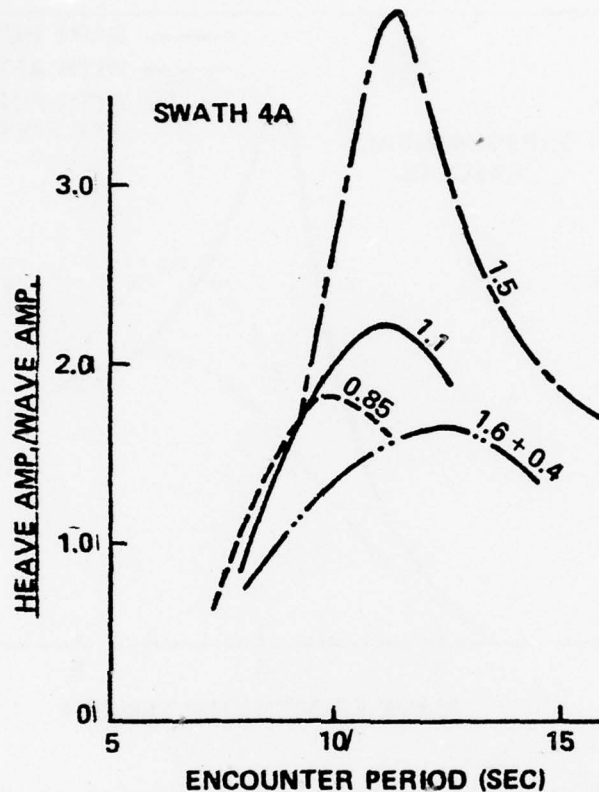


Figure 3 Heave Response of SWATH 4A in Regular Head Waves at 35 Knots

the right-hand sides of Eqs. (14.1) and (14.2). Specifically, if the fins are to be activated at the resonant conditions, say at the heave-mode resonance, then we can observe from Eqs. (17) that we should minimize $\frac{|F'_3|}{D_H}$ and $\frac{|F'_5|}{D_H}$.

For stationary fins, our effort was directed toward maximizing the denominator D_H . Once the fins are activated, we expect that the values of D_H can be changed. But if we assume that activation of the fin deflections are of periodic nature, we may regard the mean average value of D_H during one cycle of the fin deflections as unchanged. Then our task is to minimize

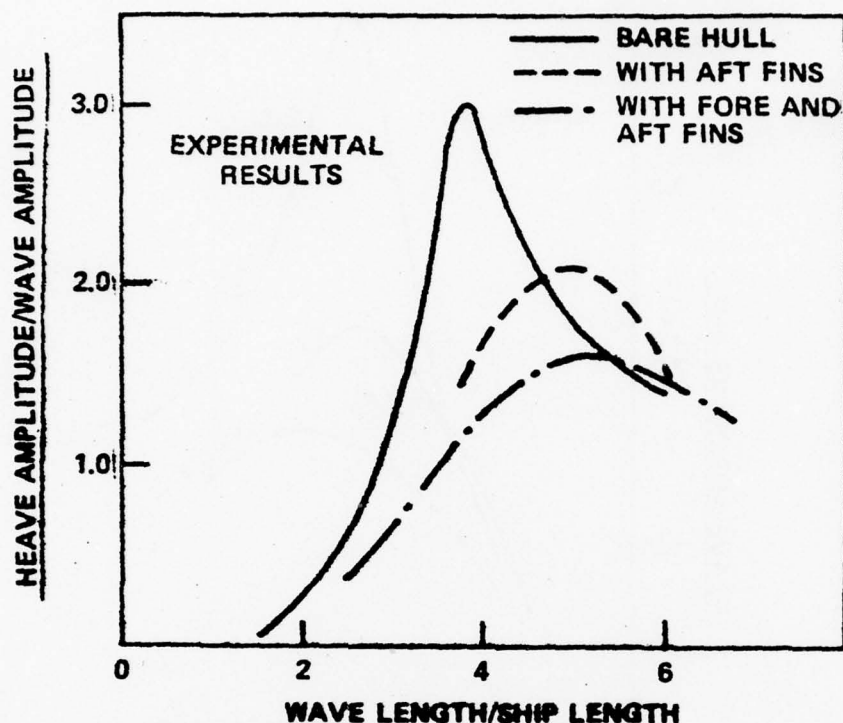


Figure 4 Effect of Fins on Heave Response of SWATH Ships in Regular Head Waves at 20 Knots

$|F'_3|$ and $|F'_5|$ by fin controls. From the definitions of F'_3 and F'_5 given by Eqs. (14.4) and (14.5) we see that the minimization of $|F'_3|$ and $|F'_5|$ by fin controls should be achieved by minimizing the wave-exciting force and moment, $|F_3|$ and $|F_5|$.

If we let the deflection angle of the j th fin to be $\delta_j(t)$ and the lift-curve slope to be $C_{L\delta_j}$, then the total exciting heave force and pitch moment can be expressed by

$$F_3 = F_3^{(e)}(t) + \frac{P}{2} \sum_{j=1}^N c_j s_j C_{L\delta_j} \delta_j(t) U^2 \quad (18.1)$$

$$F_5 = F_5^{(e)}(t) + \frac{P}{2} \sum_{j=1}^N c_j s_j \ell_j C_{L\delta_j} \delta_j(t) U^2 \quad (18.2)$$

An ideal goal should be to make $F_3 = F_5 = 0$. First, we would like to examine the magnitude of δ_j necessary to counteract the wave-exciting force and moment, $F_3^{(e)}$ and $F_5^{(e)}$. Figures 5 and 6 show respectively the amplitudes of the wave-exciting heave forces and pitch moments of a monohull surface ship and a SWATH ship having about the same displacement. Table 3 shows the principle characteristics of two ships. The wave-exciting heave force and pitch moment are almost independent of the speed of a ship. Thus, the results which are computed at zero speed can be regarded to be valid for any speed.

As can be seen in these figures, the SWATH ship has significantly smaller wave-exciting force and moment than the monohull ship. The heave force of the SWATH is less than 1/3 of the monohull and the pitch moment is less than 1/10 of the monohull. Roughly, if we take the total projected fin area to be 300 ft² and the lift-curve slope to be 3.0 per radian, then the necessary maximum fin deflection angle in degrees to cancel the maximum wave-exciting heave amplitude can be obtained by

$$\delta = 3918 \frac{A}{U^2} \text{ (degree)} \quad (19)$$

where A is the wave amplitude in feet. For example, take $A = 5'$ which corresponds roughly to the sea state 5 and $U = 20$ knots. The maximum required fin deflection angle is about 17 degrees. To cancel the wave-exciting pitch moment, the maximum required fin deflection should be even less than in the case of the heave force for a reasonable choice of the locations, and the division of fin areas between the fore and aft fins. From Eq. (19) one can immediately observe that as the ship speed decreases, the necessary fin deflection angle would increase. Of course, in real seas, it would be impossible to cancel completely the wave-exciting forces by any type of control means. The best one can expect from active fins would be to reduce the extent of the wave excitation.

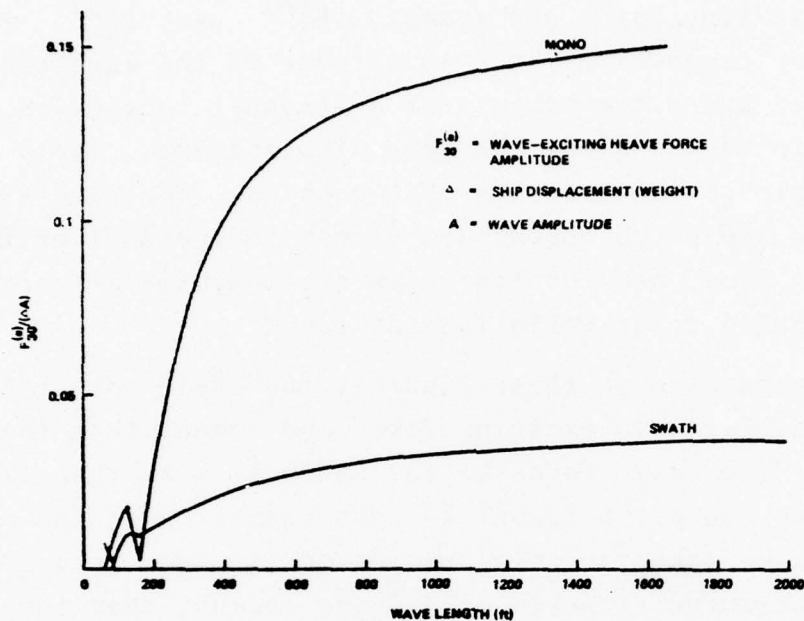


Figure 5 – Wave-Exciting Heave Force versus Wave Length in Head Waves

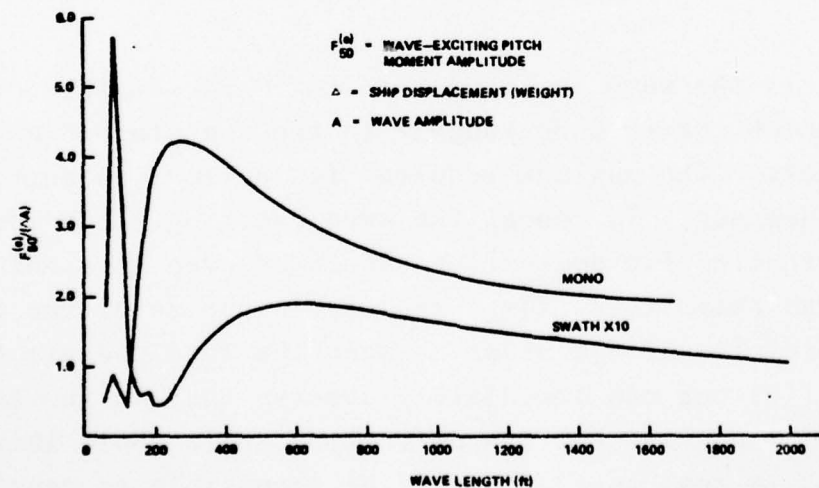


Figure 6 – Wave-Exciting Pitch Moment versus Wave Length in Head Waves

Table 3
Principle Characteristics of Monohull and SWATH

	MONOHULL	SWATH
Length (ft)	200	155
Beam (ft)	8.25	49.5
Draft (ft)	9.35	16.5
Displacement (ton)	741	785
Waterplane Area (ft ²)	4404	1166

We have not examined the feasibility of controlling the roll motion by active fins. But from a preliminary analysis, it was found that if the fin design is made to control the heave and pitch motions, a differential deflection of fins on the individual hulls should be capable of controlling the roll motion as well.

The next step in SWATH motion control is to develop optimum control logics for given sets of stabilizing fins. This subject is beyond the scope of the present paper. Concentrated efforts in this direction are going to be undertaken in the forthcoming year at the Naval Ship Research and Development Center.

To make any control design of the motions of marine vehicles successful, it is almost imperative to have reliable mathematical model for the equations of motion of the vehicle as well as the hydrodynamic and control coefficients in the equations. It is believed at the present that more investigations on the hydrodynamic fin-body interactions for an oscillating body below the free surface should be conducted.

CONCLUDING REMARKS

- (1) Stationary fins provide not only necessary vertical-plane Stability at high speeds but also damping to significantly reduce the peak motion at resonant conditions.
- (2) Determination of the size and location of stabilizing fins based on stationary find condition can be made satisfactorily.
- (3) Within the practical range of fin sizes, it appears that active fins on a SWATH ship can produce counteracting vertical forces and moments to the wave-exciting forces and moments to a much greater degree than on monohull ships because of the smaller magnitudes of the wave excitations.
- (4) Further investigations are necessary on body-fin hydrodynamic interactions when the body undergoes oscillatory motions under the free surface.

ACKNOWLEDGMENTS

This study was carried out under the support of the SWATH Ship Development Program at the Center. The author would like to extend his thanks to Mrs. M. D. Ochi for her encouragement for this study.

REFERENCES

1. Lee, C.M. and Martin, M., "Determination of Stabilizing Fins for Small Waterplane Area, Twin-Hull Ships," NSRDC Report 4495, 1974.
2. Pien, P.C. and Lee, C.M., "Motion and Resistance of a Low-Waterplane Catamaran," the 9th Symposium on Naval Hydrodynamics, Vol. 1, Office of Naval Research.
3. Pitts, W.C., Nielsen, J.N. and Kaattari, G.E., "Lift and Center of Pressure of Wing-Body-Tail Combinations at Subsonic, Transonic, and Supersonic Speeds," NACA Report 1307, 1959.

STATE-OF-THE-ART FOR PREDICTING THE HYDRODYNAMIC CHARACTERISTICS OF SUBMARINES

by

JEROME P. FELDMAN
Naval Ship Research and Development Center

ABSTRACT

This paper discusses some of the recent advances and the current status of various methods employed at NSRDC for evaluating the hydrodynamic force and moment coefficients of submarines and predicting their maneuvering and control characteristics. First, current captive-model test techniques are reviewed both for the straightline Planar Motion Mechanism type of experiments and for the more recent Rotating Arm tests. The need for improved experimental techniques and methods of analysis is discussed. Recent modifications to the equations of motion which have resulted in improved correlation with full-scale data are examined and additional problem areas are outlined. Investigations of several alternate control concepts for improved submarine control are discussed and some general conclusions are presented based on the relative effectiveness of these concepts. Concepts which require further development are outlined and the need for additional design data is indicated. Finally, an examination of some recent efforts to predict the roll motions of submarines submerged under a seaway is undertaken. Further areas for investigation are provided.

INTRODUCTION

It is highly desirable that the motions of the Navy's high speed submarines be predicted in advance of full-scale trials and operations to establish their safe operating limits and their ability to perform specific maneuvers effectively. To predict these motions and to establish a valid control strategy it is necessary that the hydrodynamic forces and moments acting on the submarine as a function of the velocities and accelerations in six degrees of freedom be determined either by experiment or analysis.

This paper gives a general description of the effort at the Center to predict, evaluate, and improve the stability, control, and maneuvering characteristics of submarines. Several specific topics are discussed to provide an over-view of some of the advanced techniques which are employed at the present time and the results of some current investigations. The objective is to provide at least an indication of where control theory and practice can be applied to the area of submarine dynamics.

First, current captive-model test techniques are reviewed both for the straightline Planar Motion Mechanism type of experiments and for the more recent Rotating Arm tests. The need for improved experimental techniques and methods of analysis is discussed. Recent modifications to the equations of motion which have resulted in improved correlation with full-scale data are examined and additional problem areas are outlined. Investigations of several alternate control concepts for improved submarine control are discussed and some general conclusions are presented based on

the relative effectiveness of these concepts. Concepts which require further development are outlined and the need for additional design data is indicated. Finally, an examination of some recent efforts to predict the roll motions of submarines submerged under a seaway is undertaken. Further areas for investigation are provided.

EXPERIMENTAL TECHNIQUES FOR DETERMINING THE HYDRODYNAMIC COEFFICIENTS OF SUBMARINES

The prediction of the depth keeping, depth changing, course keeping, and course changing maneuvers of the Navy's larger and faster submarines can be undertaken by either conducting free-running model experiments or by performing computer simulations employing an appropriate set of equations of motion in six-degrees-of-freedom with hydrodynamic force and moment coefficients determined from captive-model experiments or by analysis. The latter technique will be described briefly herein. The present standard equations of motion will be outlined first and then several proposed improvements will be presented.

First, the right-handed coordinate system which the equations of motion are referred, is shown in Figure 1. The positive directions of the axes, angles, linear and angular velocity components, forces and moments are shown by arrows. The six equations are as follows:

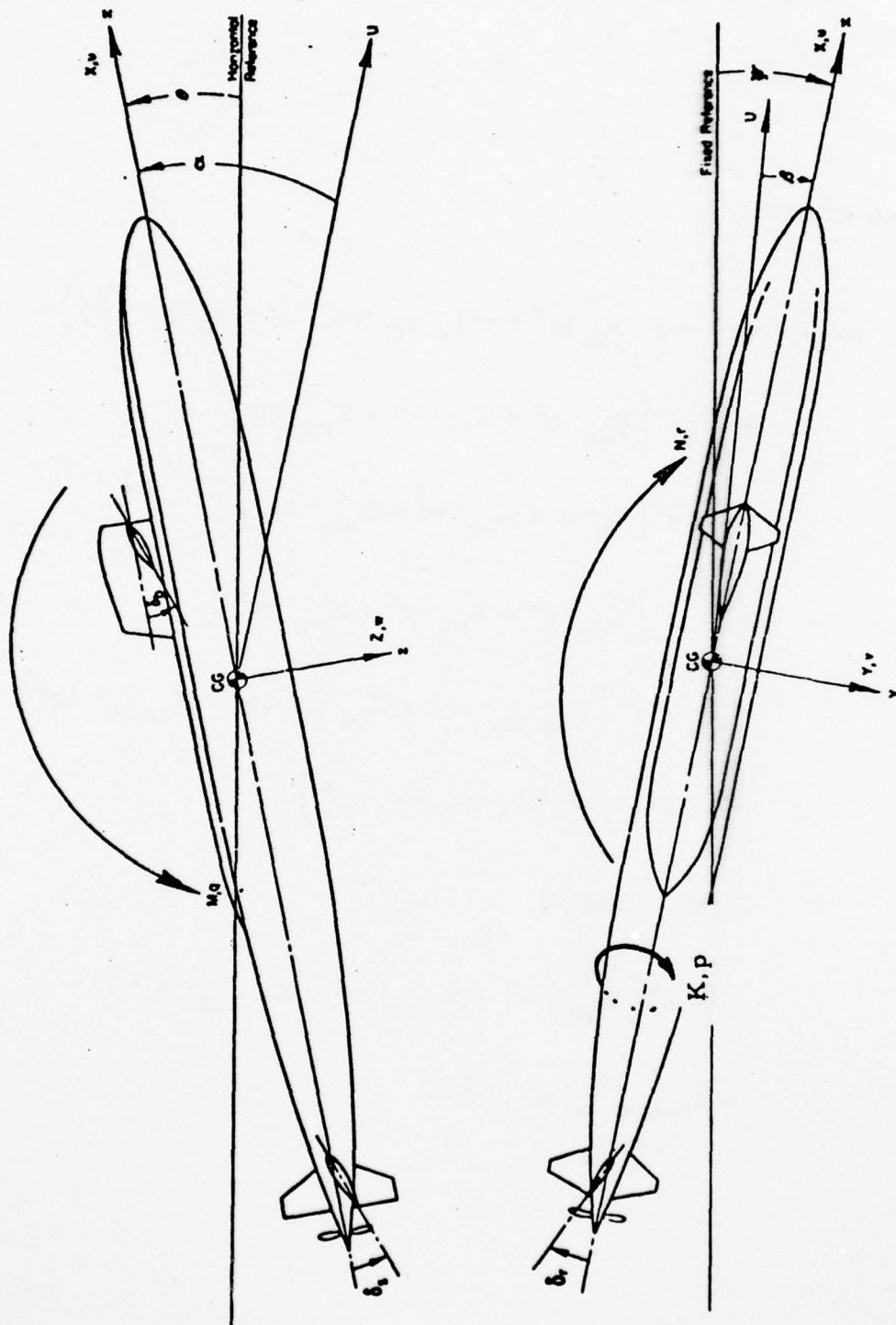


Figure 1 - Sketch Showing Positive Directions of Axes, Angles, Velocities, Forces, and Moments

AXIAL FORCE

$$\begin{aligned}
 m \left[\dot{u} - vr + wq - x_G (q^2 + r^2) + y_G (pq - \dot{r}) + z_G (pr + \dot{q}) \right] = \\
 + \frac{\rho}{2} \ell^4 \left[X_{qq}' q^2 + X_{rr}' r^2 + X_{rp}' rp \right] \\
 + \frac{\rho}{2} \ell^3 \left[X_{\dot{u}}' \dot{u} + X_{vr}' vr + X_{wq}' wq \right] \\
 + \frac{\rho}{2} \ell^2 \left[X_{uu}' u^2 + X_{vv}' v^2 + X_{ww}' w^2 \right] \\
 + \frac{\rho}{2} \ell^2 u^2 \left[X_{\delta r \delta r}' \delta r^2 + X_{\delta s \delta s}' \delta s^2 + X_{\delta b \delta b}' \delta b^2 \right] \\
 + \frac{1}{2} \rho \ell^2 \left[a_i u^2 + b_i uu_c + c_i u_c^2 \right] \\
 - (W - B) \sin \theta \\
 + \frac{\rho}{2} \ell^2 \left[X_{vv\eta}' v^2 + X_{ww\eta}' w^2 + X_{\delta r \delta r \eta}' \delta r^2 u^2 \right. \\
 \left. + X_{\delta s \delta s \eta}' \delta s^2 u^2 \right] (\eta-1)
 \end{aligned}$$

LATERAL FORCE

$$\begin{aligned}
 m \left[\dot{v} - wp + ur - y_G (r^2 + p^2) + z_G (qr - \dot{p}) + x_G (qp + \dot{r}) \right] = \\
 + \frac{\rho}{2} l^4 \left[Y_r' \dot{r} + Y_p' \dot{p} + Y_{p|p|}' p|p| + Y_{pq}' pq + Y_{qr}' qr \right] \\
 + \frac{\rho}{2} l^3 \left[Y_v' \dot{v} + Y_{vq}' vq + Y_{wp}' wp + Y_{wr}' wr \right] \\
 + \frac{\rho}{2} l^3 \left[Y_r' ur + Y_p' up + Y_{|r|\delta r}' u|r|\delta r + Y_{v|r|}' \frac{v}{|v|} |(v^2 + w^2)^{\frac{1}{2}} |r| \right] \\
 + \frac{\rho}{2} l^2 \left[Y_*' u^2 + Y_v' uv + Y_{v|v|}' v |(v^2 + w^2)^{\frac{1}{2}} | \right] \\
 + \frac{\rho}{2} l^2 \left[Y_{vw}' vw + Y_{\delta r}' u^2 \delta r \right] \\
 + (W - B) \cos \theta \sin \phi \\
 + \frac{\rho}{2} l^3 Y_{r\eta}' ur (\eta - 1) \\
 + \frac{\rho}{2} l^2 \left[Y_{v\eta}' uv + Y_{v|v|\eta}' v |(v^2 + w^2)^{\frac{1}{2}} | + Y_{\delta r\eta}' \delta_r u^2 \right] (\eta - 1)
 \end{aligned}$$

NORMAL FORCE

$$\begin{aligned}
 m \left[\dot{w} - uq + vp - z_G (p^2 + q^2) + x_G (rp - \dot{q}) + y_G (rq + \dot{p}) \right] = \\
 + \frac{\rho}{2} l^4 \left[Z_{\dot{q}}' \dot{q} + Z_{pp}' p^2 + Z_{rr}' r^2 + Z_{rp}' rp \right] \\
 + \frac{\rho}{2} l^3 \left[Z_{\dot{w}}' \dot{w} + Z_{vr}' vr + Z_{vp}' vp \right] \\
 + \frac{\rho}{2} l^3 \left[Z_q' uq + Z_{|q|\delta s}' u|q|\delta s + Z_{w|q|}' \frac{w}{|w|} \left(v^2 + w^2 \right)^{\frac{1}{2}} |q| \right] \\
 + \frac{\rho}{2} l^3 \left[Z_*' u^2 + Z_w' uw + Z_{w|w|}' w \left(v^2 + w^2 \right)^{\frac{1}{2}} \right] \\
 + \frac{\rho}{2} l^3 \left[Z_{|w|}' u|w| + Z_{ww}' |w| \left(v^2 + w^2 \right)^{\frac{1}{2}} \right] \\
 + \frac{\rho}{2} l^3 \left[Z_{vv}' v^2 + Z_{\delta s}' u^2 \delta s + Z_{\delta b}' u^2 \delta b \right] \\
 + (W - B) \cos \theta \cos \phi \\
 + \frac{\rho}{2} l^3 Z_{q\eta}' uq (\eta-1) \\
 + \frac{\rho}{2} l^3 \left[Z_{w\eta}' uw + Z_{w|w|\eta}' w \left(v^2 + w^2 \right)^{\frac{1}{2}} + Z_{\delta s\eta}' \delta s u^2 \right] (\eta-1)
 \end{aligned}$$

AD-A045 603

SYSTEMS CONTROL INC PALO ALTO CALIF
PROCEEDINGS OF THE SYMPOSIUM ON CONTROL THEORY AND NAVY APPLICA--ETC(U)
AUG 77 M D CILETTI, J S TYLER

F/G 15/7

N00014-72-C-0327

NL

UNCLASSIFIED

2 of 8
ADA045603



ROLLING MOMENT

$$\begin{aligned}
 & I_x \dot{p} + (I_z - I_y) q r - (\dot{r} + p q) I_{xz} + (r^2 - q^2) I_{yz} + (p r - \dot{q}) I_{xy} \\
 & + m \left[y_G (\dot{w} - u q + v p) - z_G (v - w p + u r) \right] = \\
 & + \frac{\rho}{2} \ell^5 \left[K_p' \dot{p} + K_r' \dot{r} + K_{qr}' q r + K_{pq}' p q + K_{p|p|}' p |p| \right] \\
 & + \frac{\rho}{2} \ell^4 \left[K_p' u p + K_r' u r + K_v' \dot{v} \right] \\
 & + \frac{\rho}{2} \ell^4 \left[K_{vq}' v q + K_{wp}' w p + K_{wr}' w r \right] \\
 & + \frac{\rho}{2} \ell^3 \left[K_\phi' u^2 + K_v' u v + K_{v|v|}' v |(v^2 + w^2)^{\frac{1}{2}}| \right] \\
 & + \frac{\rho}{2} \ell^3 \left[K_{vw}' v w + K_{\delta r}' u^2 \delta r \right] \\
 & + (y_G W - y_B B) \cos \theta \cos \phi - (z_G W - z_B B) \cos \theta \sin \phi \Big] \\
 & + \frac{\rho}{2} \ell^3 K_{*\eta}' u^2 (\eta - 1)
 \end{aligned}$$

PITCHING MOMENT

$$\begin{aligned}
 & I_v \dot{q} + (I_x - I_z) rp - (\dot{p} + qr) I_{xy} + (p^2 - r^2) I_{zx} + (qp - \dot{r}) I_{yz} \\
 & + m \left[z_G (\dot{u} - vr + wq) - x_G (\dot{w} - uq + vp) \right] = \\
 & + \frac{\rho}{2} l^5 \left[M_q' \dot{q} + M_{pp}' p^2 + M_{rr}' r^2 + M_{rp}' rp + M_{q|q|}' q|q| \right] \\
 & + \frac{\rho}{2} l^4 \left[M_w' \dot{w} + M_{vr}' vr + M_{vp}' vp \right] \\
 & + \frac{\rho}{2} l^4 \left[M_q' uq + M_{|q|\delta s}' u|q|\delta s + M_{|w|q|}' |(v^2 + w^2)^{\frac{1}{2}}| q \right] \\
 & + \frac{\rho}{2} l^3 \left[M_u' u^2 + M_w' uw + M_{w|w|}' w|(v^2 + w^2)^{\frac{1}{2}}| \right] \\
 & + \frac{\rho}{2} l^3 \left[M_{|w|}' u|w| + M_{ww}' |w|(v^2 + w^2)^{\frac{1}{2}}| \right] \\
 & + \frac{\rho}{2} l^3 \left[M_{vv}' v^2 + M_{\delta s}' u^2 \delta s + M_{\delta b}' u^2 \delta b \right] \\
 & - (x_G W - x_B B) \cos \theta \cos \phi - (z_G W - z_B B) \sin \theta \\
 & + \frac{\rho}{2} l^4 M_{q\eta}' uq (\eta-1) \\
 & + \frac{\rho}{2} l^3 \left[M_{w\eta}' uw + M_{w|w|\eta}' w|(v^2 + w^2)^{\frac{1}{2}}| + M_{\delta s\eta}' \delta s u^2 \right] (\eta-1)
 \end{aligned}$$

YAWING MOMENT

$$I_z \dot{r} + (I_y - I_x) pq - (\dot{q} + rp) I_{yz} + (q^2 - p^2) I_{xy} + (rq - \dot{p}) I_{zx}$$

$$+ m [x_G (\dot{v} - wp + ur) - y_G (\dot{u} - vr + wq)] =$$

$$+ \frac{\rho}{2} \ell^5 [N_r' \dot{r} + N_p' \dot{p} + N_{pq}' pq + N_{qr}' qr + N_{r|r}' |r|r]$$

$$+ \frac{\rho}{2} \ell^4 [N_v' \dot{v} + N_{wr}' wr + N_{wp}' wp + N_{vq}' vq]$$

$$+ \frac{\rho}{2} \ell^4 [N_p' up + N_r' ur + N_{|r|} \delta r' u |r| \delta r + N_{|v|} |v| (v^2 + w^2)^{\frac{1}{2}} |r|]$$

$$+ \frac{\rho}{2} \ell^3 [N_u' u^2 + N_v' uv + N_{v|v|} |v| (v^2 + w^2)^{\frac{1}{2}}]$$

$$+ \frac{\rho}{2} \ell^3 [N_{vw}' vw + N_{\delta r}' u^2 \delta r]$$

$$+ (x_G W - x_B B) \cos \theta \sin \phi + (y_G W - y_B B) \sin \theta$$

$$+ \frac{\rho}{2} \ell^4 N_{r\eta}' ur (\eta-1)$$

$$+ \frac{\rho}{2} \ell^3 [N_{v\eta}' uv + N_{v|v|\eta}' |v| (v^2 + w^2)^{\frac{1}{2}} | + N_{\delta r\eta}' \delta r u^2] (\eta-1)$$

As can be seen, the equations are nonlinear differential equations with coefficients which are due to the components of linear velocity of the submarine relative to the water (static coefficients), the components of angular velocity (rotary coefficients), and the components of linear or angular acceleration. The purpose of the captive-model experiments conducted at the Center is to determine the value of these coefficients. It would be desirable to acquire numerical values from hydrodynamics theory, but those coefficients which are primarily due to viscous flow, such as the static and rotary coefficients, cannot be obtained reliably from existing theory. However, theory has been employed in computing those contributions to the acceleration coefficients which are due primarily to potential flow.

The method used to perform the captive-model experiments at the Center is the Planar Motion Mechanism System (PMM) which was designed and built in 1956-7. It incorporates in a single device a means for experimentally determining all of the above types of hydrodynamic coefficients for a submerged submarine in six-degrees-of-freedom. Although the value of many of the coefficients indicated in the equations of motions can be obtained from the PMM, there are coupling terms and nonlinearities associated with large values of, for instance, nondimensional yawing angular velocity component which must be evaluated from experiments using the Center's Rotating Arm or possibly by estimates using other experimental results and/or theory.

The equations of motions are written in terms of the complete submarine configuration. The practice at NSRDC is to conduct all of the required tests with models that are fully equipped with all significant

appendages including bridge fairwater, deck, bowplanes or sailplanes, sternplanes, rudders, and propellers. These tests effectively cover the full range of motion variable, and of control surface angles and propeller rpm's. The resulting characterization of hydrodynamic forces and moments thus incorporates interaction effects involved in the various modes of rigid body motion including control surfaces and hull, propeller and hull, and propeller and stern control surfaces.

In addition to their being completely equipped and self-propelled the models used for tests involving specific submarine designs are usually about 20 feet in length. These large models used in conjunction with the large towing tank facilities permit the determination of hydrodynamic coefficients which are comparatively free of scale effects and other extraneous experimental problems. It is important that the Reynolds number be high enough to avoid the effect of premature stall on the hull and appendages of the model. This results in control coefficients at the larger control deflections which are lower than they should be for the corresponding full-scale submarine. With these large models, a sufficiently high Reynolds number can be obtained at a moderate speed, say about 5 to 6 knots for a 20-foot model, to avoid scale effects in most cases.

The hydrodynamic force and moment data obtained by the various experimental techniques are reduced to nondimensional form. These data can be plotted or tabulated as functions of each of the appropriate nondimensional kinematic variable. A least square fit is generally

applied to the static data in the form indicated by the equations of motion. Certain functional relationships are known to be linear from considerations of theory, such as those associated with the acceleration or added mass coefficients.

In addition to the hydrodynamic coefficients shown explicitly in the equations of motions for the deep submergence case, other hydrodynamic data is often required for use in submarine simulation. Typical data are the coefficients associated with proximity to the free surface, the ocean bottom, or other boundaries. These data are obtained by model experiment, by theory, or by a combination of both.

To determine how well the equations of motion, hydrodynamic force and moment coefficients, and experimental procedures combine to predict the maneuvering characteristics of the submarine, comparisons between full-scale trials data and computer simulations are required. These maneuvers are classified as either definitive, normal, or emergency maneuvers as follows:

1. Definitive maneuvers (open loop) to evaluate inherent handling qualities

- a. Meanders (vertical plane)
- b. Vertical overshoots
- c. Horizontal steady turns
- d. Horizontal overshoots
- e. Horizontal spirals
- f. Acceleration and deceleration in straightline motion

2. Normal maneuvers (operational or tactical)

- a. Near-surface depthkeeping and coursekeeping at various speeds, including hovering, using manual or automatic control
- b. Limit dives using manual, semi-automatic, or automatic control
- c. Transient horizontal turns using manual, semi-automatic, or automatic control
- d. Spiral descents
- e. Mission profiles of various types including target tracking, weapons delivery, and a variety of evasive maneuvers

3. Emergency Maneuvers

- a. Recovery from sternplane jam casualties using various combinations of recovery measures
- b. Recovery from flooding casualties using various combinations of recovery measures
- c. Buoyant ascents to develop safe procedures for exercising emergency ballast blow systems
- d. Maneuvers to determine load supportability as a function of speed

Since a large part of the effort described is devoted to prediction, namely providing solutions to problems before the fact, an active correlation program is required. Such a program has been undertaken recently. The overall objective of this program is to determine the accuracy with which the stability and control and maneuvering characteristics of submarines can be predicted by various alternative model and analytical techniques. The program has been devoted to establishing correlations between computer predictions based on techniques of the type described and measurements taken on full-scale trials of submarines.

On the basis of the correlations made to date, it appears that the equations and coefficients described previously, will for the most part, yield accurate predictions of trajectories associated with a variety of maneuvers in submerged ahead motion. In fact, the agreement in the majority of the cases investigated was well within the ability of the full-scale submarine to repeat the same maneuver. However, an area where improvement has been necessary is in the prediction of the depth changes, pitch angle, and roll angles of a submarine in a high-speed, tight turn. Three effects in the present equations of motion were investigated since it was anticipated that these effects contributed significantly to the forces and moments on the submarine in a turn. Each of these effects are discussed in the following paragraphs.

In the present lateral and normal force and pitching and yawing moments equations there are cross-flow drag type coefficients similar to $Z_{w|w|}'$, Z_{ww}' , and $Z_{w|q|}'$ in the normal force equation. These coefficients are multiplied, in part, by $w(w^2 + v^2)^{1/2}$ where v and w are the components of the linear velocity along the y and z axes through the center of gravity, respectively. In a turn the components of velocity vary along the hull due to the angular velocity. To account for this, a sectional cross-flow drag coefficient c_d is determined from the fitted value of $Z_{w|w|}'$. The force contribution of the three cross-flow drag type coefficients is then the integrated value of the sectional cross-flow coefficient multiplied by the local velocities over hull and the local projected area or

$$\int c_d w^2(x) D(x) dx$$

where $D(x)$ is the local diameter and

$$w_2(x) = (w - xq) [(w - xq)^2 + (v + xr)^2]^{1/2}$$

Similar integrations appear in the other three equations.

For a submarine going into a turn, lift is progressively developed on the bridge fairwater causing vorticity of varying strength to be shed and convected downstream along the hull and past the stern appendages. Since the vorticity caused both circulation around the hull and thus lift on hull and additional control force on the sternplanes and rudder, it would appear to be important to represent in the equations the time interval required for vorticity of some specific intensity to be convected from the bridge fairwater to some after location along the hull. First the equation

$$\int_0^{\tau} u(t) dt = x_f - x$$

is solved for τ which is the time for the vorticity to be convected from the longitudinal location of the sail x_f to the point x . Then, from the experimental values of Z_{vv}' and M_{vv}' the lift coefficient of the bridge fairwater in presence of the hull c_v can be determined. The instantaneous lift at a location on the hull after of the sail is then the product of the sail lift coefficient, the local lateral velocity component, and the local lateral velocity which was developed at the sail at the time the vortex was shed from the sail. The total force on the hull is the integration taken over the section of the hull after of the bridge fairwater as follows:

$$\int_{x_S}^{x_F} C_D (v + x r) v_F (E - \tau) dx$$

where x_S depends on the angle of drift and

$$v_F = v + x_F r - z_F p$$

Similar terms for the same effect are included in the lateral force, yawing moment, and rolling moment equations of motion.

The last effect investigated was the roll moment that is produced by a cruciform tail configuration when subjected to combined roll and yaw motions as occurs in a turning maneuver. During the initial portion of a turn the angle of drift on the sail increases to an angle generally less than ten degrees, while the effective angle on the sternplanes can be two or three times as great. In addition, a significant increase in local velocity due to yaw rate occurs. Thus, there are two additional effects which should be accounted for, namely, the roll induced on the stern appendages by the vorticity shed from the bridge fairwater and the masking effect of the hull in producing a differential lift on the sternplanes and rudders.

A comparison of full-scale trial trajectories and computer simulations conducted with all three effects incorporated in the equations of motion has indicated that significant improvements in the prediction process were made.

As mentioned previously, there are coupling terms and nonlinearities which occur in a tight turn which cannot be determined from straightline

model basin experiments. Rotating arm experiments would appear to be the answer. The original towing system used for the Center's Rotating Arm consisted of two vertical struts which were oriented so that their chords were parallel to their direction of motion. However, a varying angle of attack developed along the length of the struts due to cross-flow over the model. This angle of attack distribution produced lift on the struts which in turn induced forces and moments on the model thus giving unreliable results. To correct this situation a towing system was devised which consisted of two horizontal struts attached at right angles to the bottom of the original two vertical struts. Preliminary results of some recent experiments performed with the new struts indicate from comparisons with straightline data that the strut interference effects are no longer a serious problem.

IMPROVED CONTROL FOR ADVANCED SUBMARINES

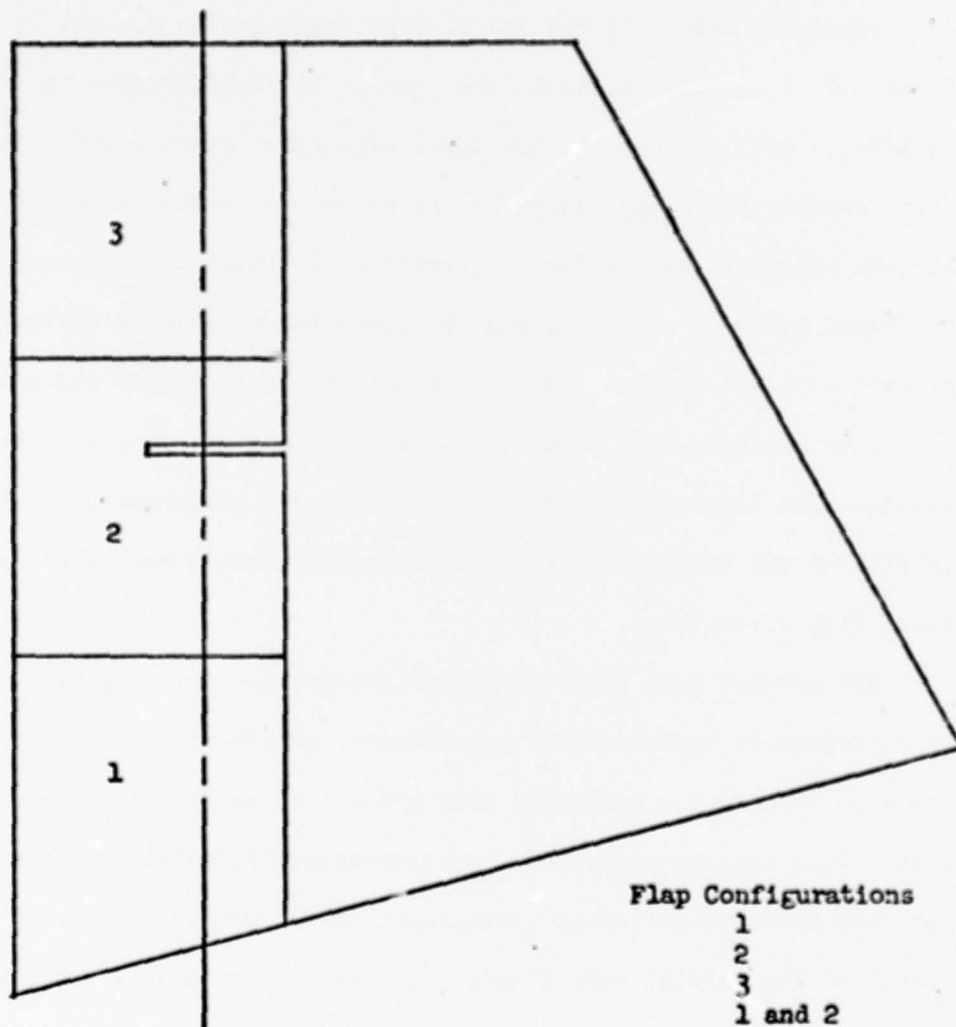
Several innovative methods of developing control force on high speed submarines have been investigated as part of an exploratory development project funded by the Naval Material Command. These methods are proposed as solutions to several control problems arising from the increased speed range of future submarines.

For example, conventional single-flap sternplanes provide adequate control at moderate speeds. But for low speed, near surface depthkeeping under a heavy seaway the sternplanes provide insufficient control. At high speeds a relatively small flap deflection can produce large pitch angles and depth excursions. Certainly with conventional sternplanes there is a problem of recovery from a sternplane jam at high speeds. The use of sternplanes with two partial span flaps has the potential for solving these problems. Both sets of flaps could be operated together for low-speed control. The use of one set of flaps would provide a satisfactory amount of control effectiveness at high speeds and, should a sternplane jam occur, the activation of the unused flaps would provide a recovery capability. As an additional advantage, one set of flaps could be used during turns for controlling excursions in roll angle while the other set in keeping depth. As another example, one of the important operational problems for modern attack type submarines is the occurrence of large roll angles during tactical turns at high speeds. A number of devices are potentially capable of reducing the roll angle. They include the use of the sailplanes or sternplanes

set differentially as ailerons, the dorsal flap, and retractable spoilers on the bridge fairwater. Finally, the problem of low speed control can potentially be solved by the use of lift augmentation devices as blown flaps and circulation control. The concept of replacing the conventional sailplanes with retractable bowplanes with circulation control to increase their control force capability at low speeds and reduce submarine drag at high speeds is particularly attractive. For high speed operation the bowplanes would be retracted and the sternplanes would be designed to provide adequate control force for depthkeeping and depth changing.

Five concepts will be discussed briefly herein. They are the partial span flap sternplanes, the differential sailplanes, the lift spoiler on the bridge fairwater, circulation control bowplanes, and blown flap sternplanes.

The partial span flap sternplane concept was investigated at NSRDC by a program of captive-model experiments, analyses, and simulations. The experiments were conducted with a model of an attack submarine fitted with various sternplane configurations, all with the same planform, but each having a different arrangement of the movable portions. A sketch of the partial span flap sternplane configurations which were tested are shown in Figure 2. Static stability and control, over-and-under propulsion, and sternplanes-as-ailerons experiments were conducted and the longitudinal and normal forces and pitching moments were measured. Based on the experiments, the hydrodynamic characteristics of a full-scale partial span flap sternplane design shown in Figure 3 were estimated.



Flap Configurations
1
2
3
1 and 2
2 and 3
1 and 2 and 3

Figure 2a - Partial Span Flap Sternplane Scheme A

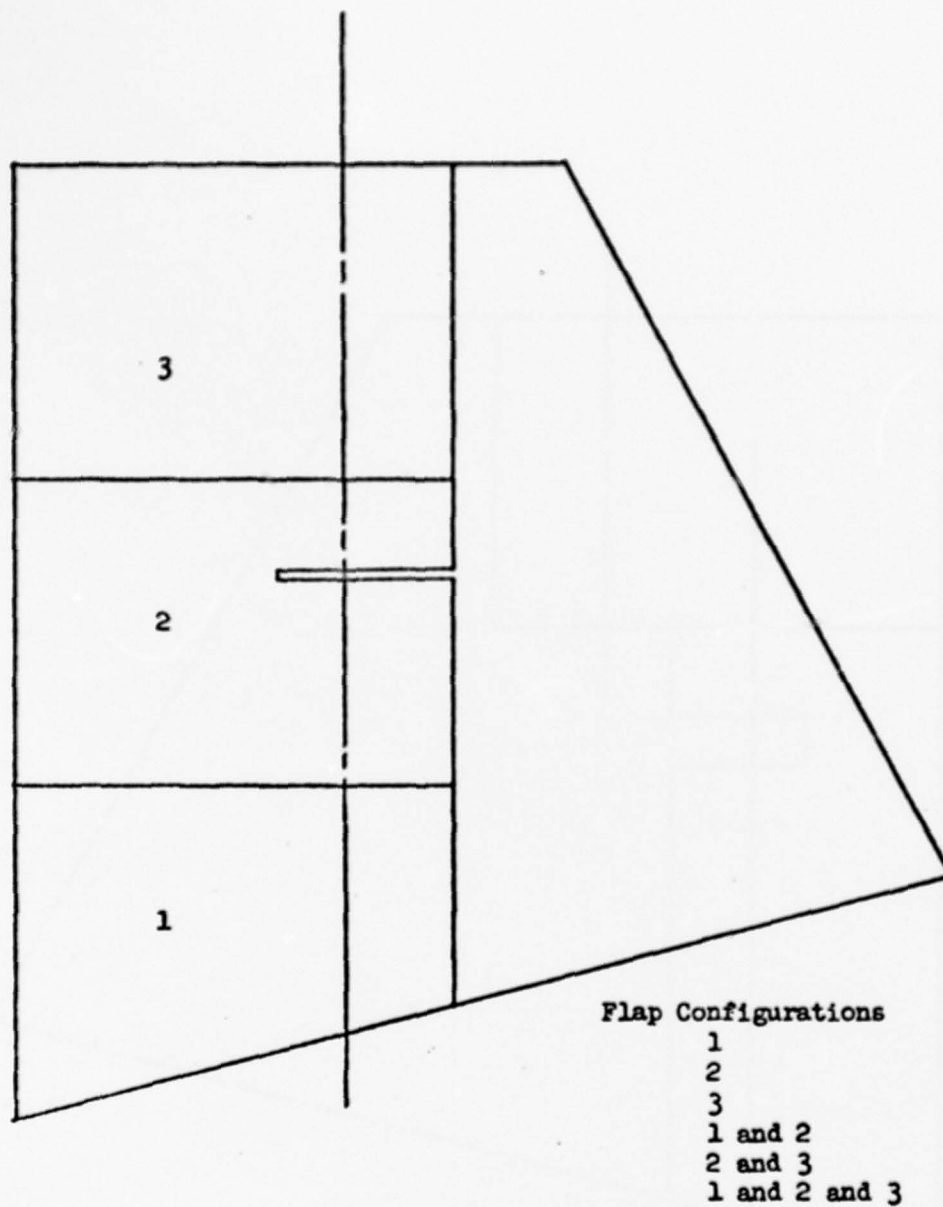


Figure 2b - Partial Span Flap Sternplane Scheme B

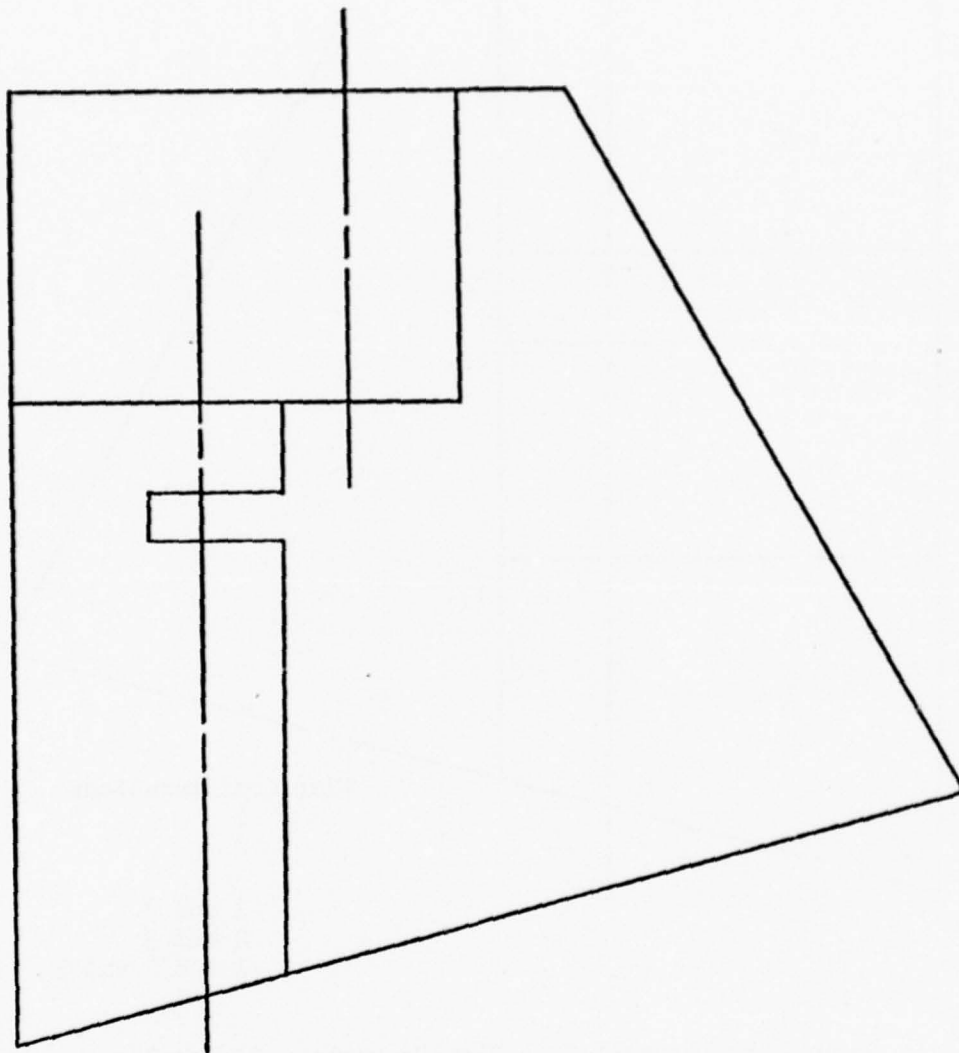


Figure 3 - Sketch of Full-Scale Partial Span Flap
Sternplane

Figure 4 shows qualitatively the improvement in the safe operating limits curves for a full-dive inner flap jam for a partial-span flap configuration having a 50 percent outer and inner flap. At the initiation of the maneuver the submarine is moving forward at constant speed and constant depth. Then one of the flaps moves to full-dive and jams. When the flap reaches full-dive (the time at which it is assumed that the recognition of the casualty occurs) the following orders are issued sequentially at two second intervals: full rise on the outer flap, back emergency, full rise on the sailplanes, and blow the forward main ballast tanks. Recovery is assumed when the submarine ceases to increase in depth. As can be seen in Figure 4, the effect of the sternplane jam can be reduced significantly, thus increasing the permissible operating envelope.

It should be mentioned that since reversing the propeller is a standard recovery procedure and since the effect of reversal is to decrease the effectiveness of the inboard flaps more than the outboard flaps, using the outboard flaps for recovery and the inboard flaps for high speed operations is the preferred mode.

In addition to using the outer flaps for recovery from a sternplane jam, they can be used as ailerons for roll motion reduction. Simulations conducted at the Center indicate that the roll angles experienced in a turn will be reduced if the outer flaps are used as ailerons. This control mode, however, would complicate the manual control of the submarine since two additional planes must be operated. The actuation of the aileron flaps in a turn must be carefully phased with the rudder, possibly by connected them to the rudder control stick.

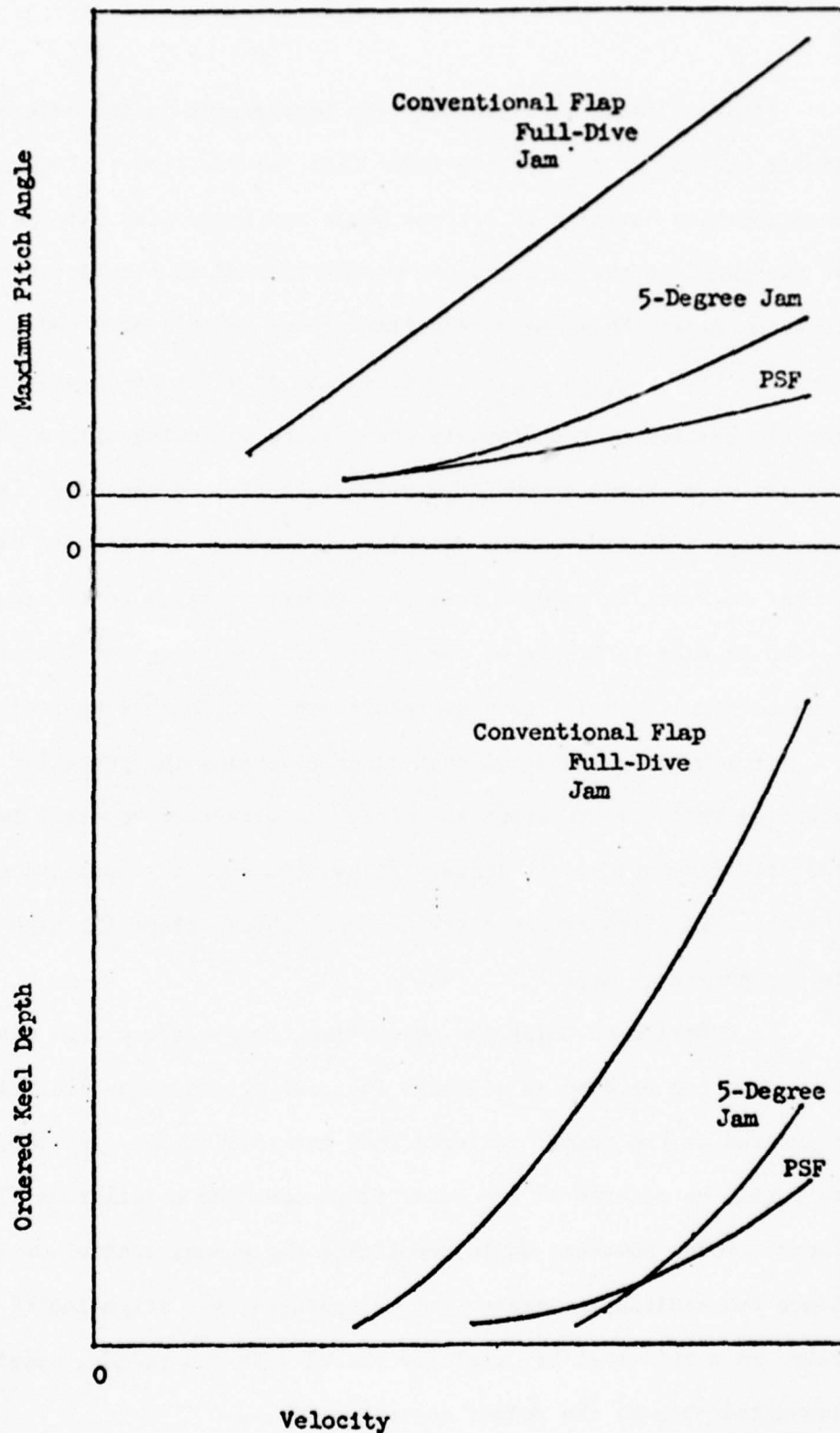


Figure 4 - Safe Operating Limits for a Sternplane Jam

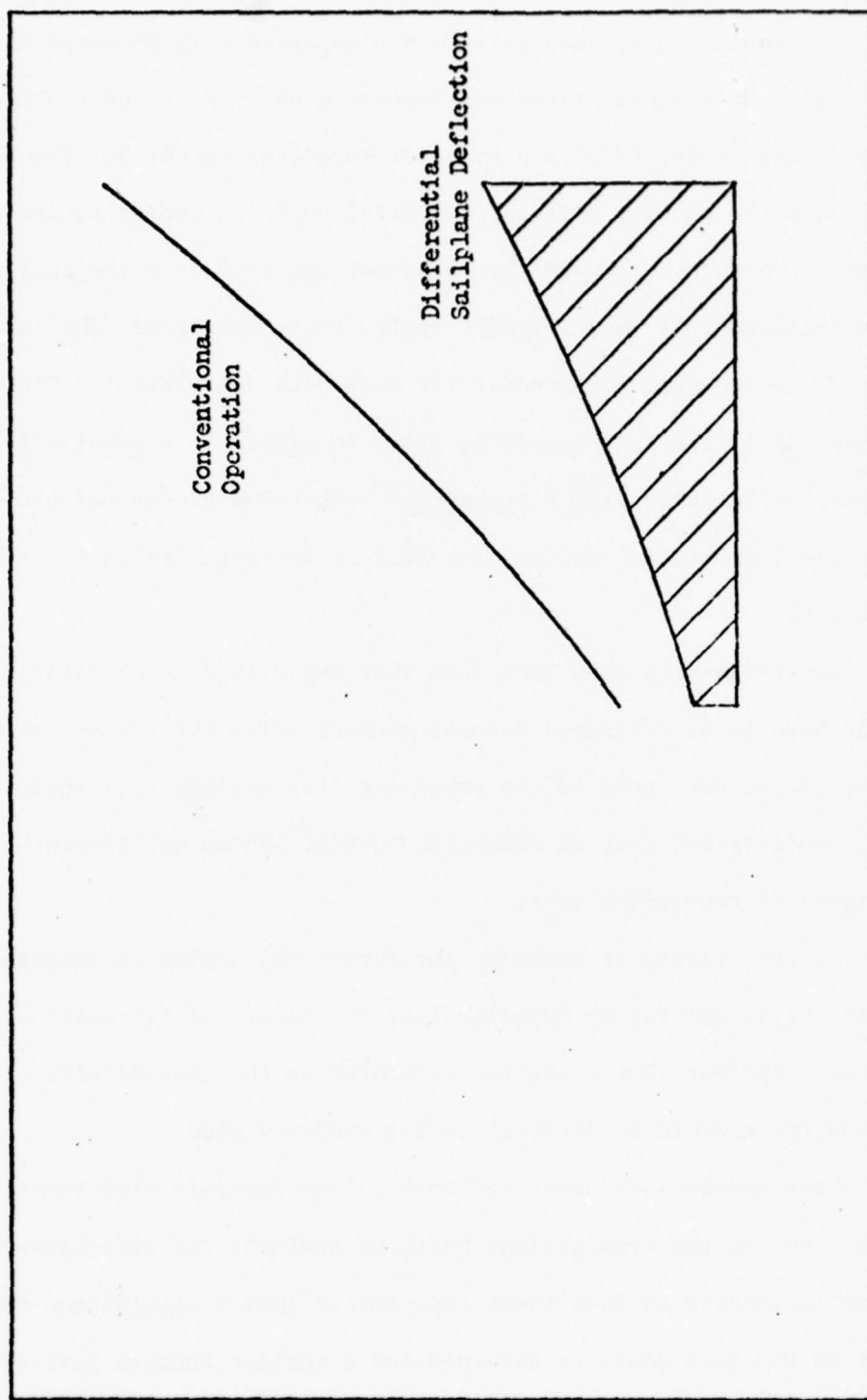
The reduction of snap roll in a high speed turn by using differential deflection of the sailplanes was demonstrated by radio-controlled model experiments conducted with a model of an attack submarine. The NSRDC radio-control package utilizes commercial FM-FM telemetry equipment to telemeter both the commands to the model and data from the model. The data included roll angle, rudder angle, and model speed. The experiments were conducted with full rudder for both with and without differential deflection of the sailplanes. As shown in Figure 5, a substantial reduction in snap roll occurs with differential deflection of the sailplanes. A conceptual mechanical design of a full-scale installation is shown in Figure 6.

Investigations have indicated that the differential sailplanes would have to be deflected several seconds after the rudders are thrown, depending on the speed of the submarine, for maximum roll angle reduction. It is anticipated that an automatic control system would have to be designed to accomplish this.

Another method of reducing the large roll angles on submarines in a turn is to develop an opposing lift on the bridge fairwater by the use of a spoiler. For a spoiler deflected on the leeward side of the sail, a side force would be directed to the windward side.

Experiments were conducted both in the subsonic wind tunnel at the Center and in the straightline basin to evaluate the effectiveness of spoilers. It was demonstrated from these experiments that a significant reduction in lift on the sail could be obtained for a spoiler located just aft of the sailplanes with a height to chord ratio of about 0.05 or more.

Snap Roll Angle



Approach Speed

Figure 5 - Submerged Snaproll Characteristics with the Sailplanes Differentially Deflected

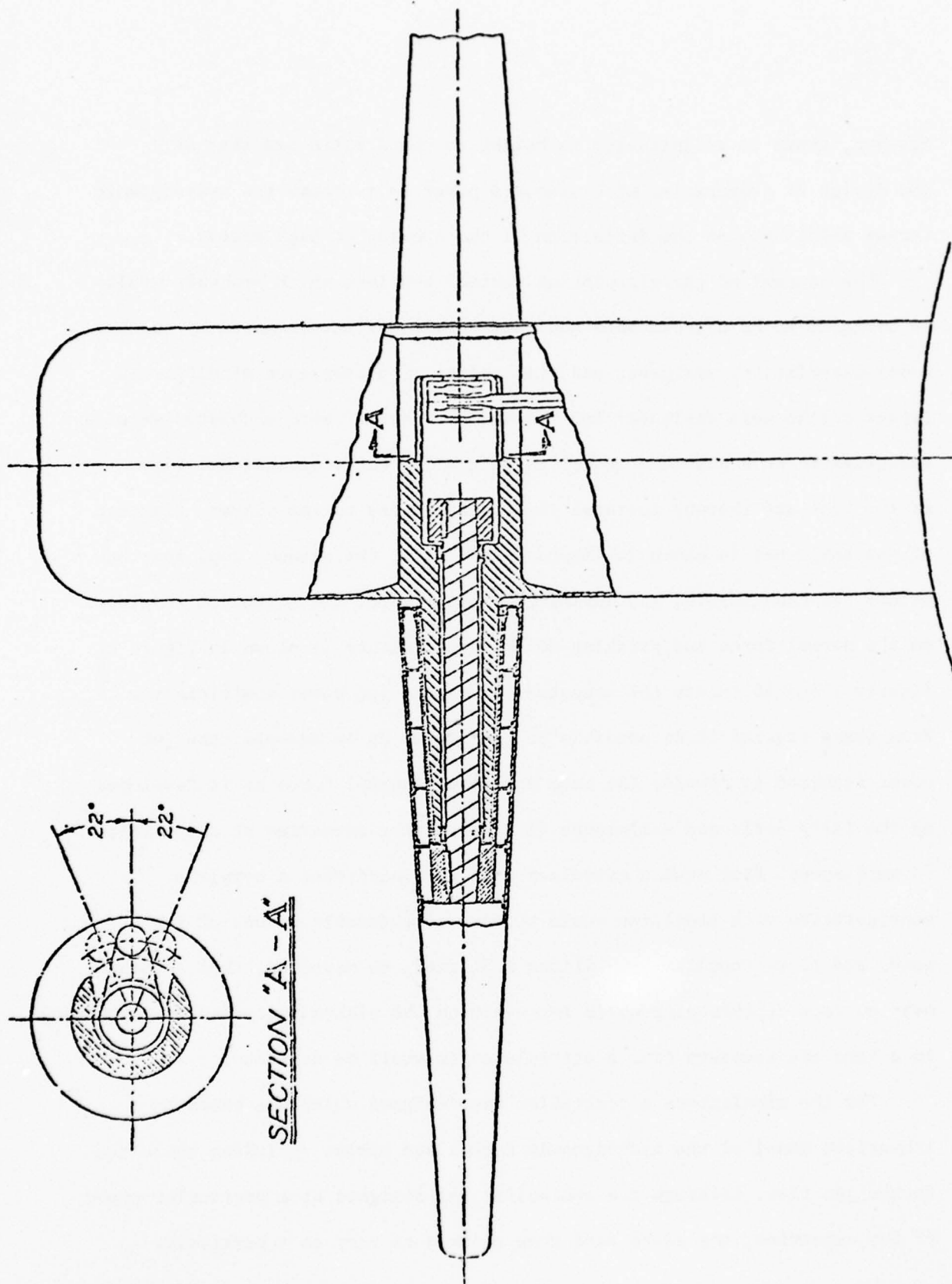


Figure 6 - Conceptual Mechanical Design for Differential Sailplanes

However, there is a limitation in height to chord ratio and that is the design of a mechanism with adequate power to overcome the hydrodynamic torque which opposes the deflection of the spoiler at high speeds.

The concept of the circulation control bowplane which probably would be designed to be nonrotatable and retractable was investigated by captive-model experiments, analyses, and simulations. Two bowplanes of different aspect ratios were designed. For the smaller aspect ratio endplates were investigated as a possible method to reduce the three dimensional flow at the tips and thereby increase the effectiveness of the planes. A sketch of the bowplanes is shown in Figure 7 indicating the plenum, gap, and the method for changing the gap during the model tests. The effect of endplates on the normal force and pitching moment coefficients is shown in Figure 8. Figures 9 and 10 relate the momentum, flow, and jet power coefficients. From these figures it is possible to calculate, as an example, the jet power required to develop the same amount of control force as is developed by the fully deflected sailplanes of a particular submarine at a specified forward speed. From such a calculation it was found that a bowplane configuration with endplates would require a reasonable amount of jet power and flow. Computer simulations indicated, as expected, that although near surface depthkeeping would improve with the planes retracted, depthkeeping in a turn and recovery from a sternplane jam would be degraded.

For the simulations a controller was designed which was based on a linearized model of the hydrodynamic forces and moment including those due to the jet flow. Although the controller was designed at a particular speed of the submarine, the gains were then assumed to vary as a particular

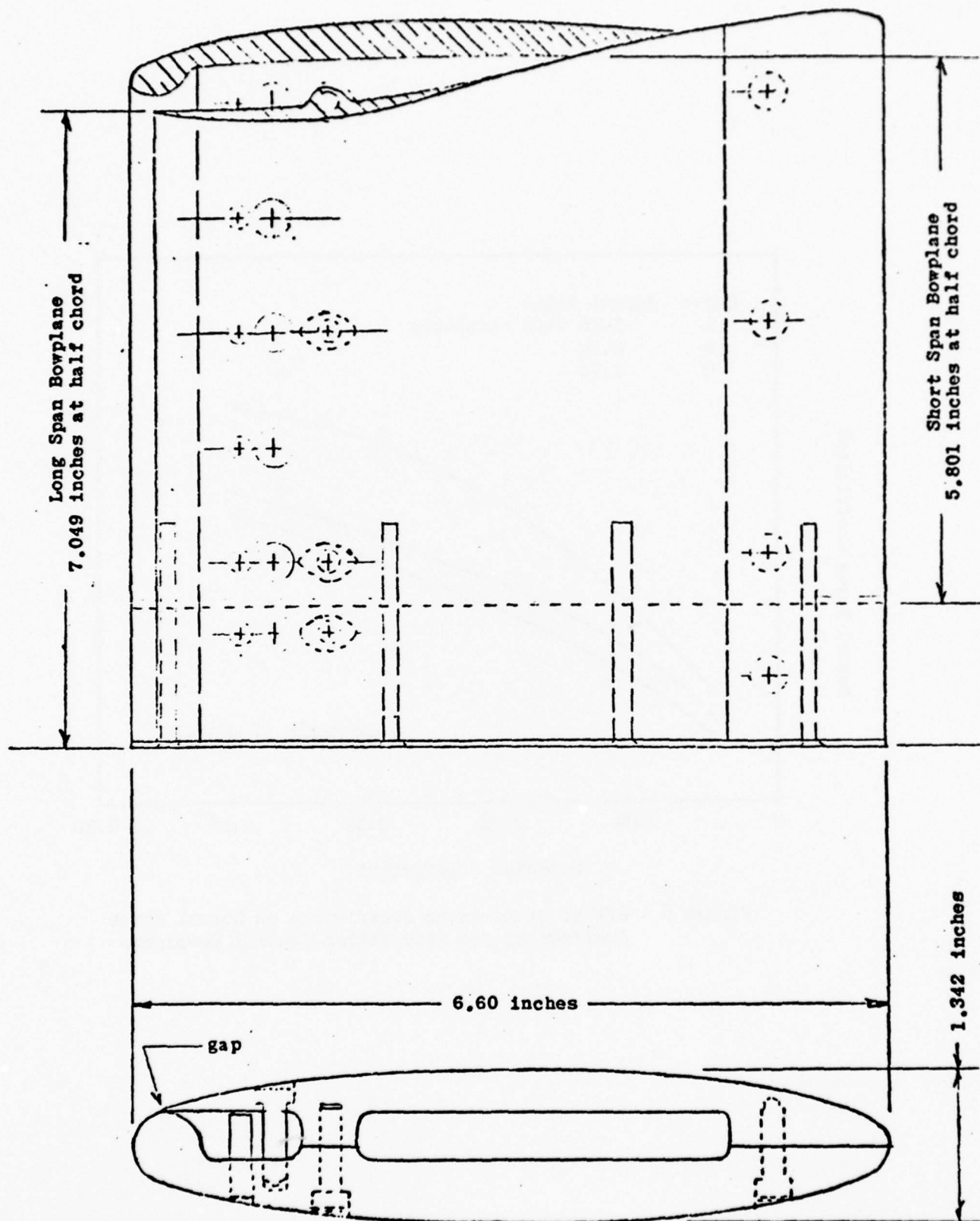


Figure 7 - Sketch of Circulation Control Bowplane Model

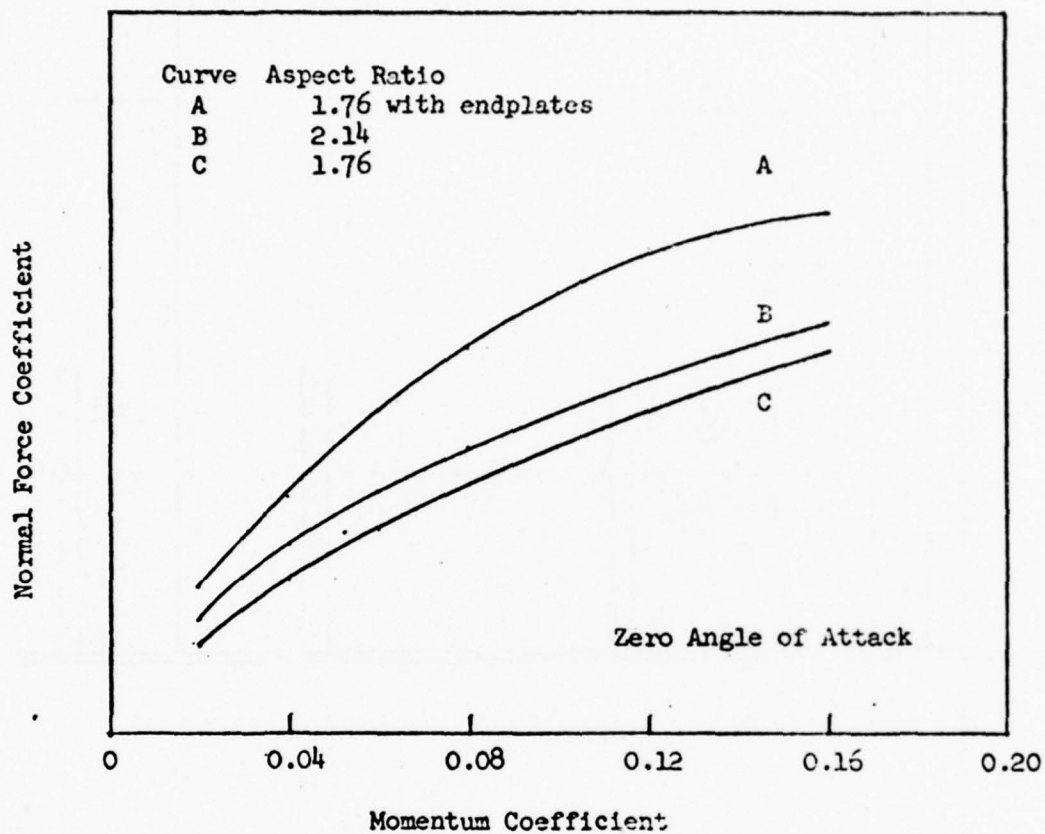


Figure 8 - Effect of Momentum Coefficient on Normal Force Coefficient for Circulation Control Bowplanes

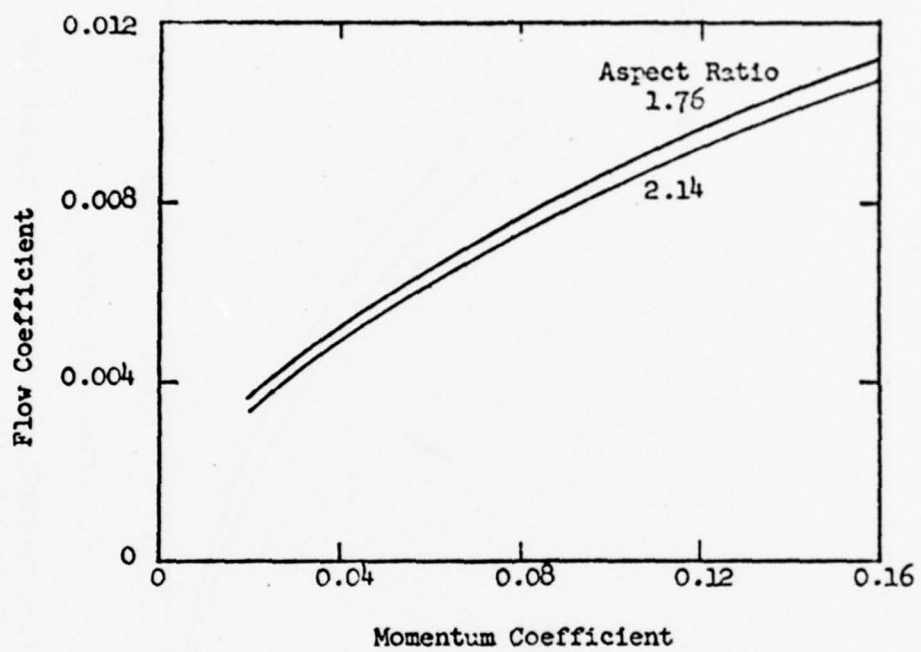


Figure 9 - Effect of Momentum Coefficient on Flow Coefficient for Circulation Control Bowplanes

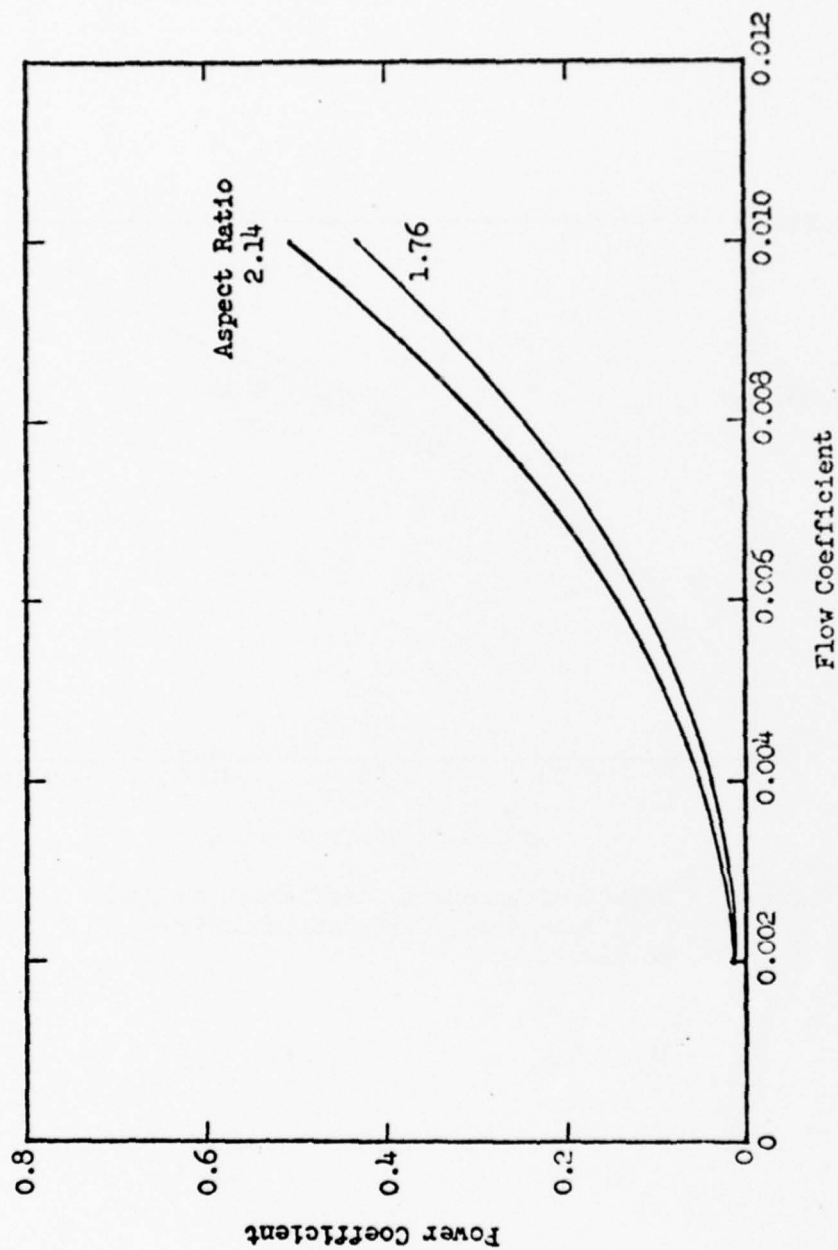


Figure 10 - Effect of Flow Coefficient on Power Coefficient for Circulation Control Bowplanes

function of speed. To compensate for the nonlinearities the linearized rates of force and moment with jet flow were determined at moderately high jet flows and various deadzones were introduced.

The investigation of the blown flap sternplanes was performed in a similar fashion to the circulation control bowplanes. The two configurations which were evaluated experimentally had flap chord to chord ratios of 0.1 and 0.2 instead of the conventional ratio of about 0.45. A sketch of one of the models is shown in Figure 11. Fluid is blown over the flap tangentially from a slot located at the aft end of the fixed section of the sternplane. At the larger flap angles moderate blowing acts to reattach the flow and thus significantly improve the lift of the sternplanes. At particularly low blowing rates or where the ratio of jet velocity to free-stream velocity is less than 2 there is no lift augmentation. For very high blowing rates the increase of force with momentum coefficient increases at a less steep rate indicating that there is supercirculation instead of flow reattachment. These region can be seen in Figure 12. At the higher submarine speeds the ratio of jet velocity to free-stream velocity is generally less than 2 for what are assumed to be presently attainable blowing rates. Hence, as has been shown from computer simulations, blown flaps are not particularly effective at high speeds with presently attainable blowing rates. However, the smaller than conventional flap chord to chord ratio means that recovery from a sternplane jam should be better.

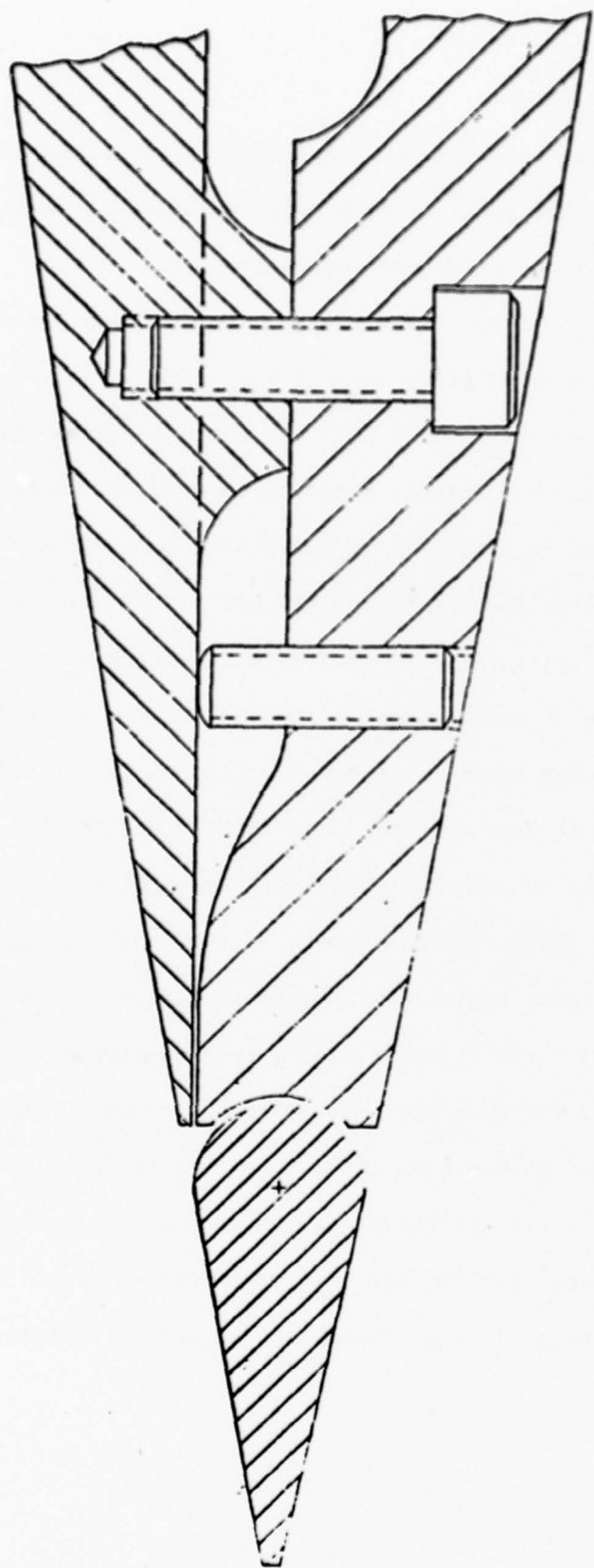


Figure 11 - Sketch of Blown Flap Sternplane Model

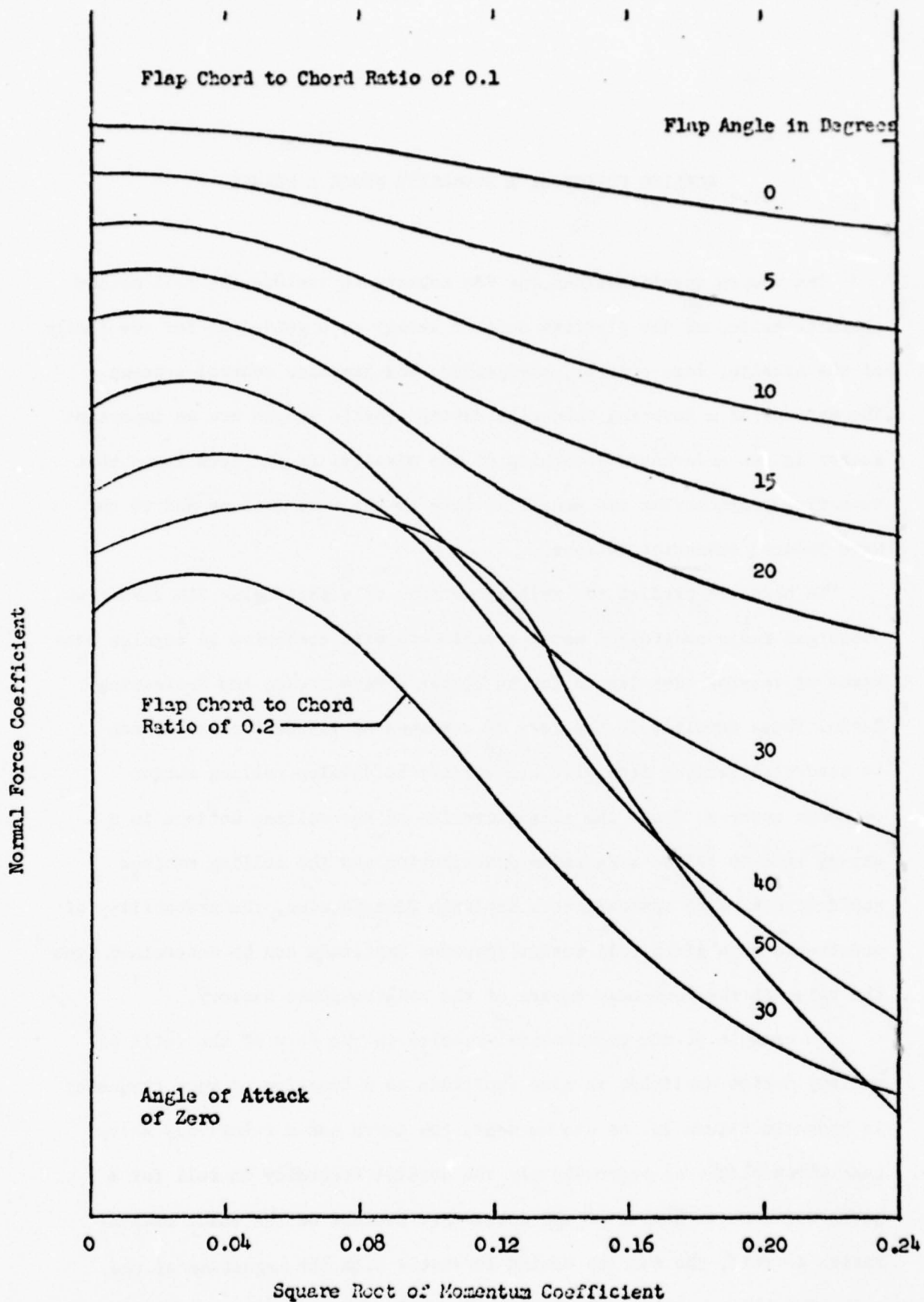


Figure 12 - Effect of Momentum Coefficient on Normal Force Coefficient for Blown Flap Sternplanes

ROLLING MOTION OF A SUBMARINE UNDER A SEAWAY

The weapon specifications for FBM submarines include the roll motion characteristics of the platform under a seaway as a guideline for the design of the missile, fire control, navigation, and launcher control systems. The motions of a hovering submarine during missile launch are an important factor in the underwater launching of the missile. It has been found that submarine trajectories are sensitive both to the wave motions and to the wave-induced submarine motions.

In order to predict the rolling motions of a particular FBM submarine, submerged radio-controlled model experiments were conducted in regular beam waves of varying wave length in the Center's Maneuvering and Seakeeping Basin. These results, in the form of response amplitude operators, can be used with various irregular sea spectra to develop rolling motion response spectra. Since the time histories of the rolling motions in a seaway tend to follow a Gaussian distribution and the rolling motions amplitudes tend to approximate a Rayleigh distribution, the probability of occurrence of a given roll motion response amplitude can be determined from the value of the root-mean-square of the roll response history.

An example of the experimental results in the form of the ratio of rolling motion amplitude to wave amplitude as a function of wave frequency is shown in Figure 13. As can be seen, the curve has a relatively sharp peak which occurs at approximately the natural frequency in roll for a given metacentric height of the submarine. Because of the small damping ratios in roll, the damping varies inversely with the magnitude of the peak. The linear theory, which compares well with the underway experiments,

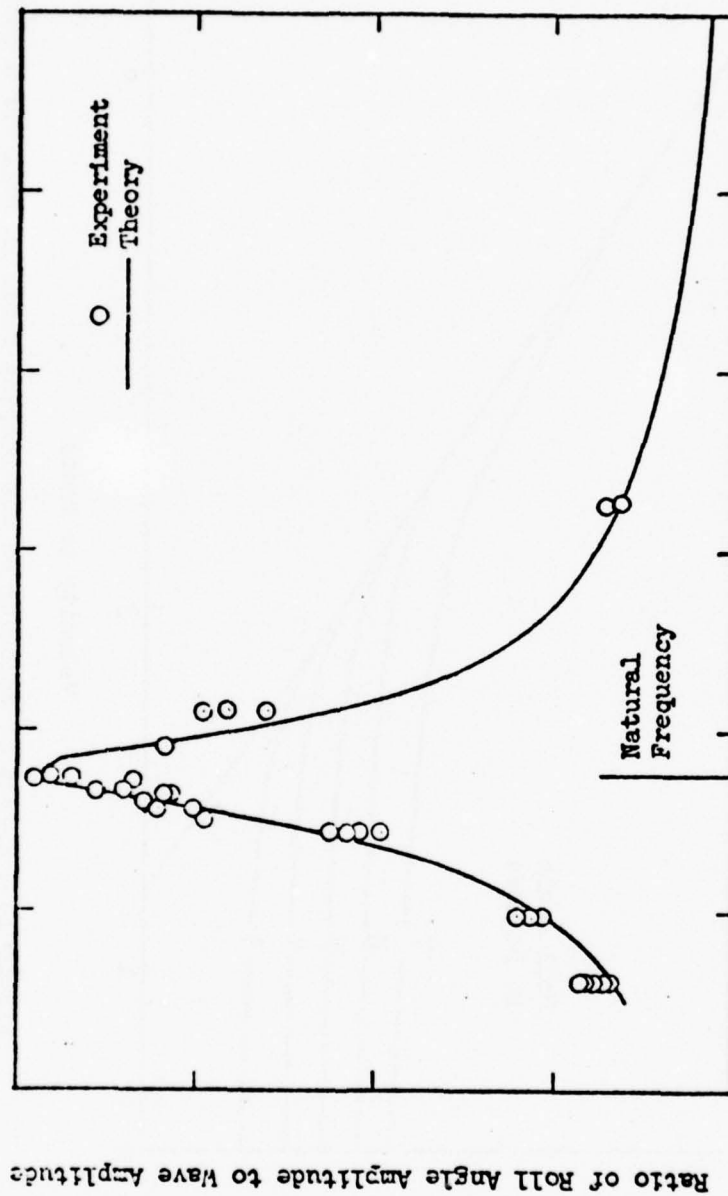


Figure 13 - Effect of Frequency on Roll Angle Amplitude for a Submarine Under a Train of Regular Waves with Beam Heading

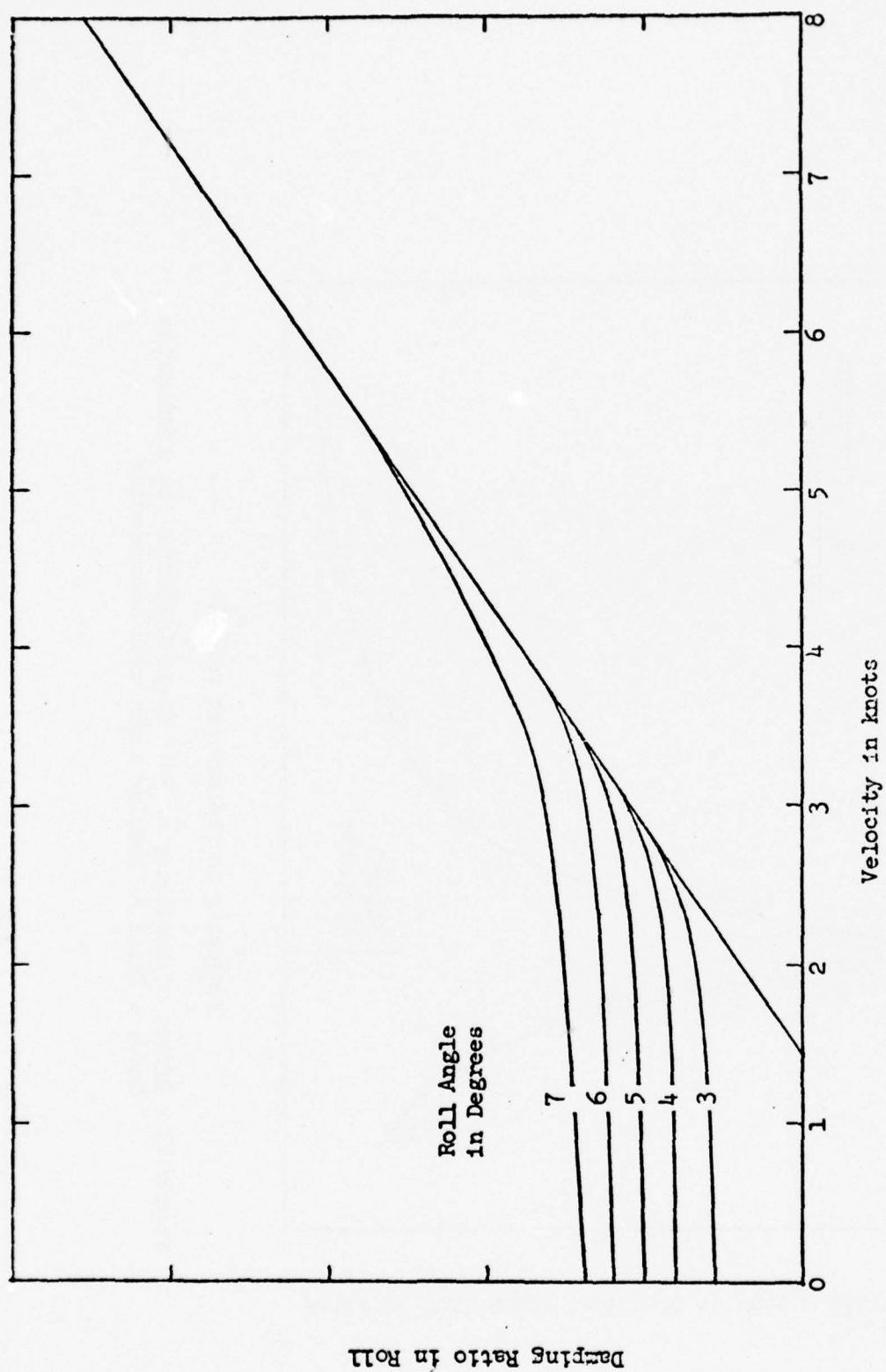


Figure 14 - Effect of Velocity on the Damping Ratio in Roll for a Submerged Submarine

is a one degree of freedom, second order differential equation for roll. The standstill experiments compare well with a nonlinear differential equation with nonlinear quadratic damping. In both cases the damping in roll was determined by performing free oscillation experiments in calm water. These results are shown in Figure 14.

Further investigation is required to determine accurately the scale effects for roll damping predictions at low speeds where the damping is nonlinear. In addition, systematic experimental data is needed not only for the effect of rolling angular velocity on rolling moment, but also the effect on lateral force and yawing moment. The proper representation of these coupling contributions in the equations of motion should significantly improve the predictions of submarine rolling in a seaway and thus facilitate the design of the inertial guidance system and the fire control system for FBM submarines.

"TRIDENT SHIP CONTROL" SYSTEMS DEVELOPMENT PROGRAM *

RICHARD A. STANKEY
Naval Ship Engineering Center

The TRIDENT submarine has a displacement of 18,736 tons, is 559 feet in length, and has a diameter of 42 feet. TRIDENT is the largest submarine under construction, approximately 2.5 times the displacement of an existing SSBN640 Class submarine.

The TRIDENT Ship Control Development Program began in March 1971 and is still in progress. Electric Boat Division of the General Dynamics Corporation was awarded the contract to design the Ship Control System for TRIDENT. The system would use the Command and Control (CCS) data processing resources for the automatic ship control operating modes.

The development of the automatic digital control capability for TRIDENT required a larger design and management effort than originally anticipated. This is due primarily because the system is operating in a multiprogrammed environment and also because of the software and system documentation requirements.

It is the purpose of this paper to discuss the design and management effort that is required not only during the stage of control equation development, but also into the implementation and testing stages of system design.

This talk will cover four subjects:

- Early Design Considerations
- System Development
- Tech Management
- Lessons Learned

* This paper was typed from a taped version of the oral presentation.

DESIGN OBJECTIVE

The mission requirement for the TRIDENT submarine is to provide a platform for missile launching. The Ship Control System operational requirement as specified in the TRIDENT Submarine Performance Requirements Baseline (SUPERB) requires TRIDENT to have the capability to maneuver and hover at desired depths near surface and deeply submerged in calm and rough seas, in support of this mission. The Shipbuilding Specification defines the performance requirements, general configuration, and operating modes that the Ship Control System will be designed to.

For a given hull form and bounded control force, the Ship Control System design begins with performance prediction studies in manual and automatic control modes. The control equations development begins with these imposed constraints. The design for TRIDENT has provided for manual, manual aided and automatic control modes for hovering/missile compensation. Steering and diving has manual (one or two men steering and diving), manual aided, automatic, and emergency control modes. The manual aided mode displays the control equation solution (such as stern plane angle command) to the operator for his aid in controlling ship depth.

The Ship Control Station provides a centralized man-machine interface for the following Ship Control functions:

- depth control
- course control
- hovering
- missile compensation
- variable ballast and trim
- snorkeling
- air systems control
- hydraulic systems control
- hull openings and alarms
- interior communications

For the first time, a combat submarine has been designed with a digital Ship Control System. The traditional and separate (hovering and course/depth keeping) analog control systems were not used because of their limited capability, and the major design consideration became one of dedicated vs. shared digital control. Sharing the data processing resources of the TRIDENT Command and Control System outweighed the dedicated system approach; therefore, Ship Control proceeded with the shared system design.

The increased resources of a digital system permitted a limited on-line performance monitoring/fault location (PM/FL) capability for the first time. With limited redundant elements, Ship Control could continue operations in the event of system element failures.

SYSTEM DEVELOPMENT

Analysis

The analysis effort consists of three major work areas:

- (1) control equations/simulation,
- (2) software, and
- (3) functional design.

Control Equations/Simulation

For TRIDENT, the Course and Depthkeeping control equations were developed using modern control theory. The Hovering control equations were developed classically. Because of the complexity of the ship dynamics and random forcing functions, extensive simulation is necessary even in the very early analysis stages. Control equations are programmed in Fortran to run in a conventional batch job environment. The simulation, also in Fortran, consists of the equations of motion, sensor and force producers, dynamics, sea forces, and control forces.

During this development, the preliminary control equations are modified to enhance system performance. Modifications such as, introducing control mode switching and additional filtering usually become evident and are evaluated during this exhaustive simulation period where most of the nonlinearities of the dynamics can be introduced for the first time.

Concurrent with this effort, an on-line hybrid simulation is used to introduce hardware elements and expedite the sensitivity analysis before the control equations approach their final form. The analysis is limited to investigating the sensitivity of controller gains as a function of ship dynamics and hardware variations.

Up until this time the control equations have been in continuous form. The equations are converted to the difference equation form using the Direct Transformation method. Further simulation is done to include data processing effects such as sample rate, random interrupts, throughput, truncations, skew, jitter, etc.

Software

Once the control equations are firm, a Computer Program Performance Specification is prepared that implements the results of the control system analysis. This specification addresses the functional requirements that are necessary to accurately carry out the control computations. This specification will also include the equations and logic to do data validation, data control, and function control operations necessary to carry out the control equation computation. In addition, software is necessary to carry out executive, maintenance, recording, and PM/FL functions.

Further analysis is required to prepare a Computer Program Design Specification from a performance specification. Here,

the program design is determined; such factors as modular structure, data formatting, table design, labeling, subroutine allocating, efficient computation forms, and high level program flow logic is specified.

Functional design is the process of ship control via ballast and planes/rudders that are moved in response to control commands from a computer that is activated by operator inputs from the ship control station (the cause and effect analysis of every state of the system, that is functional design). Subjects such as system initialization and operation procedures, data display, cause-effect analysis, control modes and scenario design, must be thoroughly analyzed before committing the system design to production. Considerable interaction and trade-offs are involved as for example in constraining the size of ballast tanks due to hardware design limitations. This has a severe effect on control that must be resolved in the early functional design stage. This process requires many design working group meetings among system engineers, analysis groups, hardware designers, and human engineering personnel before a functional design approach is accepted.

Ship Control Station (SCS)

Located in the Command and Control Center, the major ship control functions are centralized at this single location for coordinated system operation, and reduced manning. The TRIDENT Ship Control Station includes steering/diving control, ballast control, sensor data, alarms, and vital system status. Steering/diving control in the manual mode is done by helmsmen/planesmen seated inboard and outboard under the command of a Diving Officer who is behind and between them. Ballast control is done by a ballast control operator (hovering and missile compensation) under the command of the Compensation Officer.

Software

The Ship Control Application Program (SCAP) and the Ship Control Simulation/Stimulation Program (SIM/STIM) are the complete software. SCAP is tested in a simulated environment by SIM/STIM and is the operational program that will be aboard TRIDENT at the completion of the Navy Qualification Testing. SCAP provides the following Ship Control functions:

- (1) course and depthkeeping
- (2) hovering
- (3) missile compensation
- (4) variable ballast and trim
- (5) performance monitoring/fault location
- (6) maintenance and recording capability

SCAP is programmed in high level CMS-2 language where top down structured programming techniques have been used. SCAP consists of four modules:

- (1) Regional Control Module - the subsystem executive interfacing with the system executive.
- (2) Ship Control Module - performs control equation computations, data control, data validation, and function control.
- (3) Performance Monitoring/Fault Location - automatic recovery from position transmitter, position control unit, and SDC channel failures.
- (4) Maintenance and Recording Module - on-line recording of ship control functions, off-line testing of SDC, display alignment and test signal insertion capability.

SIM/STIM, the test software, is considerably larger than SCAP (35K vs. 20K 32 bit words). SIM/STIM is also modular and simulates the Signal Data Converter, Ship Control Station, Control Force Systems, Sea State Forces, and Ship Dynamics.

Hardware (Control Forces)

Hovering and Missile Compensation is done by moving water ballast to and from sea in accordance with control equation commands. This is accomplished by opening and closing valves in ballast tanks. This ballast system is a typical closed-loop servo system whose dynamics is much faster than the ship dynamics (hovering mode).

The Course and Depthkeeping systems apply control forces via rudder and stern planes. These are also closed-loop hydraulic servo control systems, receiving their plane angle command inputs from the Ship Control Software.

Testing

An extensive test program has been planned for TRIDENT Ship Control. To insure timely shipboard system operability, testing has been segmented into software, hardware, and hardware/software-- in a stand-alone environment and in an integrated system environment; all being done before the beginning of dockside and at-sea operational testing. The purpose is to eliminate as much shipboard testing as possible due to the difficulty of conducting tests aboard a submarine. Testing will be done in the following stages:

- (1) Software Testing. At the Software Development Facility. Here testing is done to verify the computer programs execute as per their performance and design specifications (both SCAP and SIM/STIM).
- (2) Integration Testing. Upon successful demonstration that the software executes as a stand-alone system, the Ship Control software will be turned over to the Integrator for extensive integration testing with the other subsystems at the Land Based Evaluation Facility (LBEF).
- (3) System Tests. Overall Ship Control System testing of hardware and software will be conducted both by the

integrator for integration testing and by the Ship Control subsystem for stand-alone testing.

- (4) Dockside and shipboard installation tests. This testing is essentially a limited set of tests to insure no defects during shipment. This also applies to software.
- (5) Operational Tests At Sea. Extensive Command and Control System testing will be done at sea, where Ship Control will be operational during the entire exercise. In addition, the Ship Control performance will be recorded and taken back for analysis and comparison with the land-based test results.

"The subject of technical management we all know, is to provide order and direction to the design process comprised of these individual events."

TECHNICAL MANAGEMENT

- (1) Integrated System - Data processing support for the TRIDENT Ship Control System is provided by the Command and Control System (CCS) Central Computer Complex (CCC). The CCS consists of the following subsystems:
 - (a) Sonar
 - (b) Defensive Weapons
 - (c) Command
 - (d) Monitoring
 - (e) Ship Control

For the first time, these systems will share the same data processing resources and operate in a multiprogramming environment. This integration of hardware and software resources, while conceptually straightforward, poses technical problems that severely stress management planning. Here, in addition to the normal subsystem level planning, planning for the new integration phase is necessary. An Integration Agency exists (Integrator) whose responsibility is to insure that all subsystems obtain enough resources to meet their respective system requirements.

Every stage of the design process that impacts the integrating hardware and software must go through a review cycle for overall concurrence and understanding by the Integrator as well as the other subsystems. This is

time-consuming and costly. Changes to a baseline design are well above normal because of the serious ripple effects. The management difficulty lies in stabilizing the development process in spite of the additional and differing requirements imposed by the Integrator.

- (2) The design requirements are a result of the Mission and Performance requirements established by the Navy. The Technical Manager has the responsibility to insure:
 - (a) The design satisfies these Mission/Performance requirements.
 - (b) The design is a practical and feasible concept (beyond the academic).
 - (c) The contractor brings maximum competence (technical and management) to the task.
 - (d) The design schedule satisfies the integration effort.
- (3) Design reviews at critical points in the design stage are an effective means of controlling task progress. The purpose of the design review is to officially approve the completion of an item of the design and invoke configuration control.
- (4) A subsystem Configuration Management Plan is necessary to clearly define the scope and procedures required for configuration control. For TRIDENT Ship Control, software documentation and code are the primary configuration control items. A Computer Program Library has been established that contains multiple master copies of software, a historical change log, master documents and test results, and a log containing the document and software distribution.
- (5) The technical management of a task generally becomes easier if the system documentation is complete. For TRIDENT Ship Control, the documentation is in four categories:
 - (a) management - configuration management plan, system management and development plans, status reports, maintenance plan, etc., to name a few.
 - (b) analysis - technical notes.
 - (c) software - Weapons Specification 8506
 - (d) T&E - plans and procedures

The documentation requirements of TRIDENT are more extensive than any previous ship acquisition project. There are many advantages to this:

- (a) early program planning - management plans force the design activity to forecast and distribute resources realistically.

- (b) provide maximum visibility and control for the technical management team to monitor and evaluate progress
- (c) clarifies the integration/subsystem relationship.

This degree of documentation is recommended for an integrated system development and in all probability will become more extensive in future developments.

Here I've discussed the more definable controls assisting the technical management effort. Documentation, configuration control, design reviews, schedules, etc., are the formal means for providing the maximum assurance that the project is under control. However, effective control often relies more on the project coordination, individual approach, direction, and decision making capability of the management team.

LESSONS LEARNED

Work Definition

Remember, it is the responsibility of the Technical Manager to deliver the system in accordance with the design requirements of the Shipbuilding Specification. I would insist he prepare the work statement. He must take the time to understand the scope of the work required in order to prepare a meaningful work statement. As a baseline for directing the design activity, this is absolutely necessary. If you have experienced first hand the problems arising from working to a vague and high level work statement, you will appreciate the importance of a detailed work statement.

Deliverables

Provide for as many meaningful deliverables as possible in support of program major milestones. Without supporting documents prepared in a timely manner, your chances of discovering a program milestone slip is completely in the hands of the performing activity.

Management Plan

This is the only formal document that will state the management control which the design agent will take to insure the job is complete on schedule, or to put it another way, it describes in detail the management necessary to accomplish all phases of the system design. A very sketchy and brief plan is a very early indication that the management team of the design activity does not clearly see its role in the program. It contains as a minimum:

- (1) organization structure and responsibilities
- (2) authority (who has)
- (3) relationship with the Navy Management Team
- (4) project controls (changes, slips, reporting, etc.)
- (5) working level responsibilities

Even with a Management Plan for the project, enough confusion and delay will always exist. You only hope to minimize it with a Management Plan.

Integrated Systems

While its purpose is to reduce system elements through common usage, its development requires additional people, tests, and documentation. The additional management effort required to keep informed of the integration process is more than tripled or quadrupled, and the overall progress is at the pace of the slowest member. Plan for it.

Impossible Situations (at the time)

As with most system developments, a number of occasions arise that are impossible to deal with but require resolution. To name three in this program:

- (1) A signal data converter was under procurement before the system was designed. Information such as number of channels, signal types, signal conditioning, system interfaces, etc., was required. The solution was to

design the I/O requirements before the system. The I/O became a design constraint.

- (2) Software design proceeded before system analysis due to the CCS schedule. The solution was to provide generalized algorithms to support the integration effort while analysis progressed.
- (3) Proceeding with code and analysis before hardware design is determined. Here is a case where one activity has scheduled to meet the ship construction schedule, and the other to meet Command and Control System schedule. Further complicating the problem is long lead material procurement and manufacturers not delivering as promised. This has already resulted in the redesign of missile compensation algorithms and we can't say it won't happen again. The software is being developed assuming certain hardware characteristics and will probably be modified to suit any hardware incompatibilities. So what is the lesson learned? I asked one consultant who said it was unacceptable and that the answer was simple, resign. He also said that he will not bid DOD contracts. But if you are not in that fortunate a situation, the lesson is to act; make a decision to go with the "less than best" way. If you wait you will create a new impossible situation.

MORE TEST DOCUMENTATION

Testing and associated documentation is usually the most neglected part of a program for a number of reasons:

- (1) Engineers like to design systems, not test them.
- (2) End of the project, funds allocated for testing have been spent due to unforeseen development problems.
- (3) The contractor doesn't want an excessive and detailed test program--tests can only uncover problems he has to fix.
- (4) Good test documents are just plain hard to prepare.

TRIDENT is the most extensive T&E program to date. It has been planned for early in design and documentation requirements are clearly stated.

SESSION 11

AIRCRAFT AND OTHER NAVAL SYSTEMS

NAVY FLIGHT TESTING AND SYSTEMS IDENTIFICATION*

ROGER BURTON
Naval Air Test Center

INTRODUCTION

This paper is intended to present an application of modern control theory to flight test problems at the Naval Air Test Center (NATC). Results obtained to-date indicate that the modern control theory application of systems identification will revolutionize conventional flight testing concepts presently available to the flight test industry. The original objectives of the program are shown in Table 1 and include primarily improved flight test efficiency (i.e., reduce the cost of a flight test) and data accuracy. In addition, an overall goal was to improve the Navy test and evaluation cycle, and convey system identification results to the aircraft industry and lead to improved Navy aircraft designs.

The scope of the Navy program at the Naval Air Test Center is shown in Figure 1. This particular program began at NATC in 1971, and during the last two years the participants in the

Table 1
Program Objectives

- IMPROVED FLIGHT TEST EFFICIENCY
- REDUCED COST
- IMPROVED DATA ACCURACY
- IMPROVED PRODUCT
 - NATC T&E
 - NAVY AIRCRAFT

* This paper was typed from a taped version of the oral presentation.

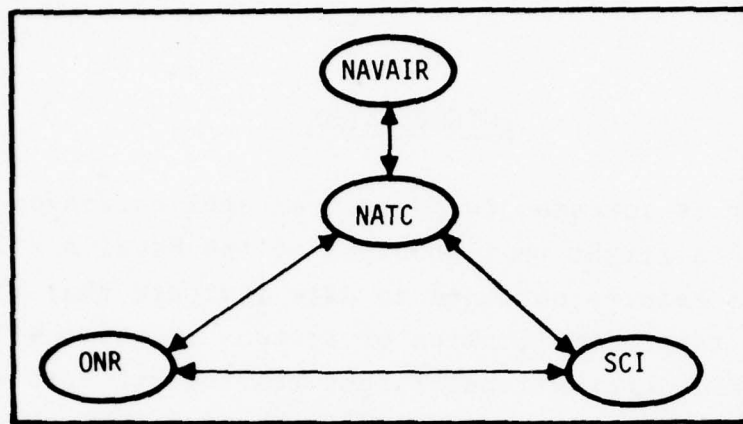


Figure 1 Scope of Navy Parameter Identification Program

program have included, in addition to NATC, the Naval Air Systems Command, the Office of Naval Research, and Systems Control, Inc. (SCI). This combination of organizations has evolved the current capability within the Navy.

LIST OF SYMBOLS

<u>Symbol</u>	<u>Definition</u>	<u>Units</u>
K	Gain	---
n_z	Normal acceleration	ft/sec ²
p	Roll rate	rad/sec
r	Yaw rate	rad/sec
α	Angle-of-attack	rad
β	Sideslip angle	rad
δ_a	Aileron deflection	rad
δ_R	Rudder deflection	rad
δ_{sp}	Spoiler deflection	rad
ζ	Damping ratio	---
τ	Time constant	sec
ϕ	Roll angle	rad
ψ	Phase angle	rad
ω	Natural frequency	rad/sec
<u>Nondimensional derivatives</u>		
C_{y_β}	Nondimensional partial derivative of sideforce with respect to sideslip angle	rad ⁻¹
C_{y_p}	Nondimensional partial derivative of sideforce with respect to roll rate	rad ⁻¹
C_{y_r}	Nondimensional partial derivative of sideforce with respect to yaw rate	rad ⁻¹
C_{n_β}	Nondimensional partial derivative of yawing moment with respect to sideslip angle	rad ⁻¹
C_{n_p}	Nondimensional partial derivative of yawing moment with respect to roll rate	rad ⁻¹
C_{n_r}	Nondimensional partial derivative of yawing moment with respect to yaw rate	rad ⁻¹

$C_{l\beta}$	Nondimensional partial derivative of rolling moment with respect to sideslip angle	rad^{-1}
C_{lp}	Nondimensional partial derivative of rolling moment with respect to roll rate	rad^{-1}
C_{lr}	Nondimensional partial derivative of rolling moment with respect to yaw rate	rad^{-1}
$C_{y\delta a}$	Nondimensional partial derivative of sideforce with respect to aileron position	rad^{-1}
$C_{y\delta R}$	Nondimensional partial derivative of sideforce with respect to rudder position	rad^{-1}
$C_{n\delta R}$	Nondimensional partial derivative of yawing moment with respect to rudder position	rad^{-1}
$C_{l\delta R}$	Nondimensional partial derivative of rolling moment with respect to rudder position	rad^{-1}
$C_{n\delta a}$	Nondimensional partial derivative of yawing moment with respect to aileron position	rad^{-1}
$C_{l\delta a}$	Nondimensional partial derivative of rolling moment with respect to aileron position	rad^{-1}
$C_{l\delta sp}$	Nondimensional partial derivative of rolling moment with respect to spoiler position	rad^{-1}
$C_{n\delta sp}$	Nondimensional partial derivative of yawing moment with respect to spoiler position	rad^{-1}
$C_{y\delta sp}$	Nondimensional partial derivative of sideforce with respect to spoiler position	rad^{-1}

PARAMETER IDENTIFICATION PROCEDURE

Figure 2 illustrates the nature of parameter identification. The basic idea is that in a given flight test, a control input from an automatic device or a pilot results in an aircraft response. (An important point to note is that the measured flight response is corrupted by instrumentation noise and gust noise.) Identification theory then provides a framework for mathematically modeling the aircraft dynamics, and identifying the coefficients of this model in order to obtain a match between the time response of this model and the actual aircraft response. Thus, a computed response based on a priori information is compared with the measured flight response to obtain a response

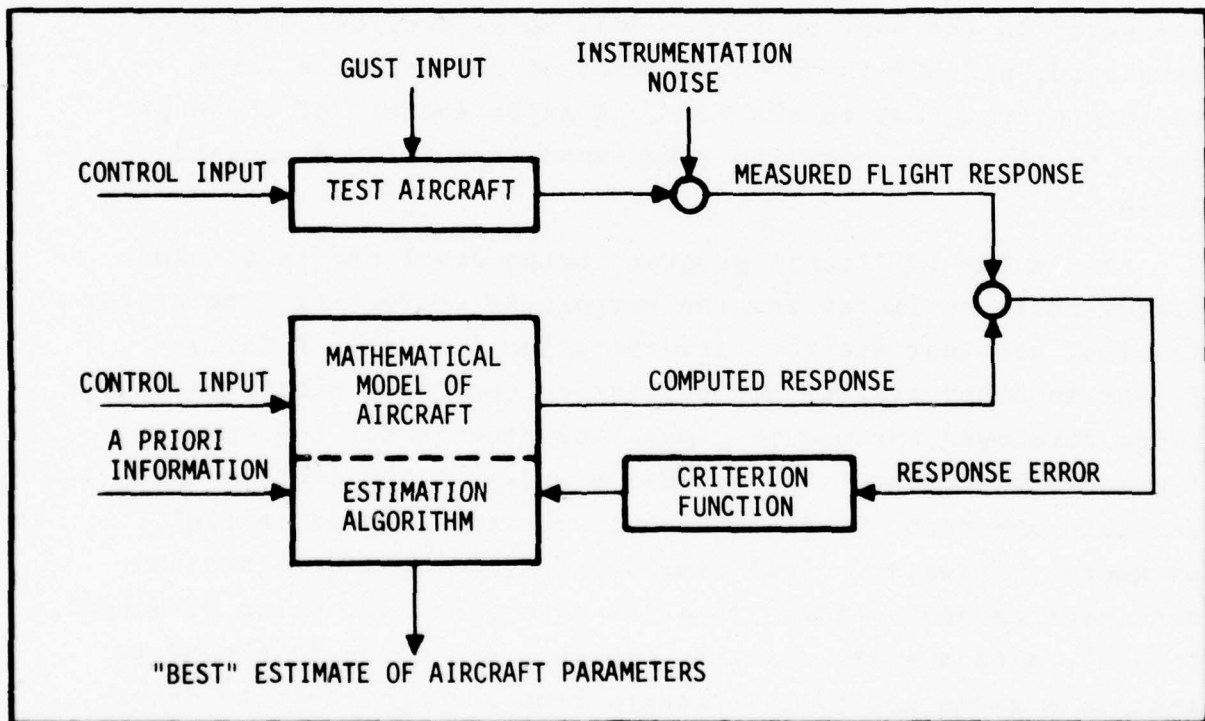


Figure 2 Parameter Estimation Procedure

error which is used in conjunction with a criteria function and an estimation algorithm to update the parameter estimates. An iterative scheme is used to successively reduce the error response to zero. The corresponding model parameter values then provide an estimate of the aircraft parameters. In terms of flight testing, the aerodynamic parameter values themselves are not as important as their use to satisfy flight test requirements.

STATUS OF NAVY PARAMETER IDENTIFICATION

It is appropriate at this point to briefly review the status of the Navy parameter identification capability. The initial capability consisted of an advanced state-of-the-art maximum likelihood identification computer program for linear analysis of flight test data [1]. This program was developed by SCI and delivered to the Navy in 1974. Additional programs have been developed, and SCI is in the process of delivering a large variety of programs to the Navy. A major feature of these programs is the linear maximum likelihood capability discussed above.

Among the additional programs being developed is a Kalman filter state estimator for the purpose of recreating time histories that are lost due to instrumentation failure. A Kalman filter smoother program for estimating gust time histories is being developed for use in simulation studies for the carrier landing environment. The technique known as the instrumental variable approach, is being used to obtain improved initial parameter estimates. Real time identification algorithms and nonlinear parameter identification algorithms are being examined. Finally, data quality analysis concepts are being developed to analyze a given set of instruments from a flight test to determine whether or not the interaction between the instruments is compatible.

FLIGHT TEST REQUIREMENTS FOR PARAMETER IDENTIFICATION

The objective of this program at the Naval Air Test Center is to develop the most complete capability in systems identification that is presently possible. Initially in the program, a set of requirements for developing parameter identification techniques was established, with the major requirement being determination of flying quality specification compliance [2]. This capability in itself is very important; however, in recent years, these specification requirements have increased in complexity and have posed a data analysis problem that cannot be handled by existing or conventional techniques. Thus, parameter identification was also being developed to address this data analysis problem. The final initial requirement was to reduce flight test time. The program has grown considerably from this initial concept of utilizing parameter identification in aircraft flight testing. Table 2 shows a list of many of the flight tests performed at the Naval Air Test Center, and in some way, parameter identification can be applied to each of these areas to satisfy Navy testing requirements.

Table 2
List of Vehicle Dynamics Flight Tests

FLIGHT TESTS
● MECHANICAL CHARACTERISTICS OF CONTROL SYSTEM
● TAKE-OFF
● LANDING APPROACH
● LONGITUDINAL FLYING QUALITIES
● LATERAL-DIRECTIONAL FLYING QUALITIES
● STALL CHARACTERISTICS
● PERFORMANCE
● ENGINE CHARACTERISTICS

This presentation will focus on applications to longitudinal and lateral directional flying qualities analysis. Tables 3 and 4 show the problems being addressed using parameter identification from flight tests. The longitudinal specifications of interest

Table 3
List of Longitudinal Specification Requirements

LONGITUDINAL SPECIFICATION REQUIREMENTS
<ul style="list-style-type: none"> • SHORT PERIOD FREQUENCY AND ACCELERATION SENSITIVITY ($\frac{n_z}{\alpha}$) • SHORT PERIOD DAMPING (ζ_{sp}) • PHUGOID FREQUENCY AND DAMPING (ω_{n_p}, ζ_p) • FLIGHT PATH STABILITY

Table 4
List of Lateral-Directional Specification Requirements

LATERAL-DIRECTIONAL SPECIFICATION REQUIREMENTS
<u>MIL-F-8785B</u>
<ul style="list-style-type: none"> • DUTCH ROLL DAMPING AND FREQUENCY (ζ_d, ω_{n_d}) • SPIRAL MODE TIME CONSTANT ($1/\tau_s$) • ROLL MODE TIME CONSTANT ($1/\tau_R$) • ROLL RATE SPECIFICATIONS
<u>DETAIL SPECIFICATIONS (S-3A, F-14A)</u>
<ul style="list-style-type: none"> • DUTCH ROLL COUPLING PARAMETER ($\omega_{n_\phi} / \omega_{n_d}$) • DUTCH ROLL EXCITATION PARAMETER (k_d / k_{ss})

are short period frequency and acceleration sensitivity and short period damping requirements. More importantly, new specifications have placed the maximum level of short period damping in an area where conventional analysis techniques do not provide sufficient accuracy. Requirements also exist for phugoid frequency, damping, and flight path stability.

A similar set of requirements exist in the lateral directional axis for dutch roll damping and frequency. Specific requirements on the spiral mode time constant, roll mode time constant, and roll rate specifications are written into the detailed specifications for the S-3 and F-14 [3,4]. Specifications are also given for the dutch roll coupling parameter and the dutch roll excitation parameter, which are requirements which limit the amount of dutch roll oscillation in the power approach configuration.

An important data analysis problem that is being approached with parameter identification techniques is that of determining the modal characteristics of heavily damped responses (Figure 3). Conventional hand measurement techniques are easily used in the lightly damped case to provide accurate frequency and damping estimates. However, for modern aircraft employing stability augmentation systems which result in heavily damped responses, these conventional data analysis techniques do not work as well. Thus, parameter identification is being used to solve this data analysis problem.

A similar problem exists for analysis of data in the lateral-directional axis. Table 5 presents the conventional roll rate to aileron transfer function. From this transfer function, it is apparent that the time domain response is separated into the spiral mode, roll mode, and the dutch roll oscillation. Under certain conditions using conventional analysis procedures, it is very hard to separate these parameters from flight test results. One objective of this program was to provide an advanced analysis capability to allow for separation of

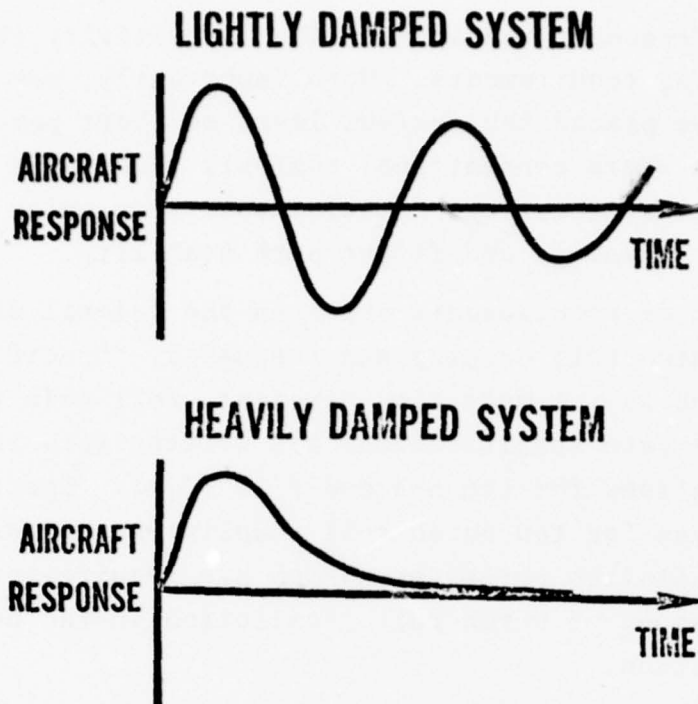


Figure 3 Comparison of Lightly and Heavily Damped Responses

these characteristics for determination of lateral-directional military specification compliance.

FLIGHT TEST RESULTS

Reductions in Flight Test Time Using Parameter Identification

Parameter identification analysis procedures can be used to reduce the flight time required to obtain data for determining flying qualities specification compliance [5]. An example of this application is presented in Table 6, which shows a comparison between the flight time and maneuvers required for conventional flight testing versus the parameter identification approach.

Table 5
Roll Rate to Aileron Transfer Function

THE $\frac{p}{\delta a}$ RESPONSE FUNCTION FOR A STEP INPUT CAN BE WRITTEN AS

$$\left. \frac{p(s)}{\delta a} \right|_{\text{STEP}} = \frac{K(s^2 + 2\zeta_\phi \omega_\phi s + \omega_\phi^2)}{\left(s + \frac{1}{\tau_S}\right)\left(s + \frac{1}{\tau_R}\right)(s^2 + 2\omega_d \omega_{n_d} s + \omega_{n_d}^2)}$$

TRANSFORMING TO THE TIME DOMAIN, THE ROLL RATE TIME HISTORY FOLLOWING A STEP AILERON INPUT IS GIVEN BY:

$$\left. \frac{p(t)}{\delta a} \right|_{\text{STEP}} = K_S e^{-\frac{t}{\tau_S}} + K_R e^{-\frac{t}{\tau_R}} + K_d e^{-\zeta_d \omega_{n_d} t} \cos \left[\omega_{n_d} \sqrt{1 - \zeta_d^2} t + \psi_p \right]$$

Table 6
Reductions in Flight Testing Using Parameter Identification

TEST	NUMBER OF MANEUVERS	
	CONVENTIONAL	PARAMETER IDENTIFICATION
<u>LONGITUDINAL</u>		
• SHORT PERIOD DAMPING (ζ)	1	} 2
• N_z/α	1	
• PHUGOID	1	
• STATIC STABILITY	1 (7 TEST PTS)	
<u>LATERAL-DIRECTIONAL</u>		
• DUTCH ROLL (ζ, w)	1	} 1
• SPIRAL MODE ($1/\tau_S$)	1	
• ROLL MODE ($1/\tau_R$)	1	
• DUTCH ROLL COUPLING AND EXCITATION	1	
• STATIC STABILITY	1 (7 TEST PTS)	
TOTAL MANEUVERS	9	3
ESTIMATED FLIGHT TIME	20 MIN	5 MIN

For longitudinal specification requirements, conventional methods require four maneuvers to obtain the flight test data, and only two are required using the parameter identification procedure. For the lateral directional tests, conventional methods require five specific maneuvers, while the parameter identification method requires only one. For the complete set of tests in Table 6, a reduction from nine maneuvers to three maneuvers is achieved using the parameter identification approach. This reduction in maneuvers required results in a reduction of flight test time from 20 minutes to five minutes or a savings of 75%. Excluding the phugoid maneuver, the parameter identification test can be performed in less than a minute which shows an even more dramatic savings in flight time.

In order to demonstrate this application of systems identification to aircraft flight testing, a specific test was conducted on the F-14 at the flight conditions shown in Table 7. Four specific trim points were used from 250 knots to 500 knots (a Mach range of 0.45 to 0.92). Using the parameter identification approach, eight maneuvers were needed to satisfy all the

Table 7

PARAMETER IDENTIFICATION
F-14A STABILITY FLIGHT TEST
(250-500 KEAS 30,000 FT)

TRIM AIRSPEED KEAS	NUMBER OF ⁽¹⁾ MANEUVERS	FLIGHT TIME
250	2	8 MIN. 1
350	2	
450	2	
500	2	
	<u>2</u> TOTAL 8	

NOTE: (1) CONVENTIONAL TESTING WOULD REQUIRE 32
MANEUVERS

specification requirements listed in Table 6, except for the phugoid. This flight test took eight minutes from start to finish and parameter identification results are shown in Figure 4.

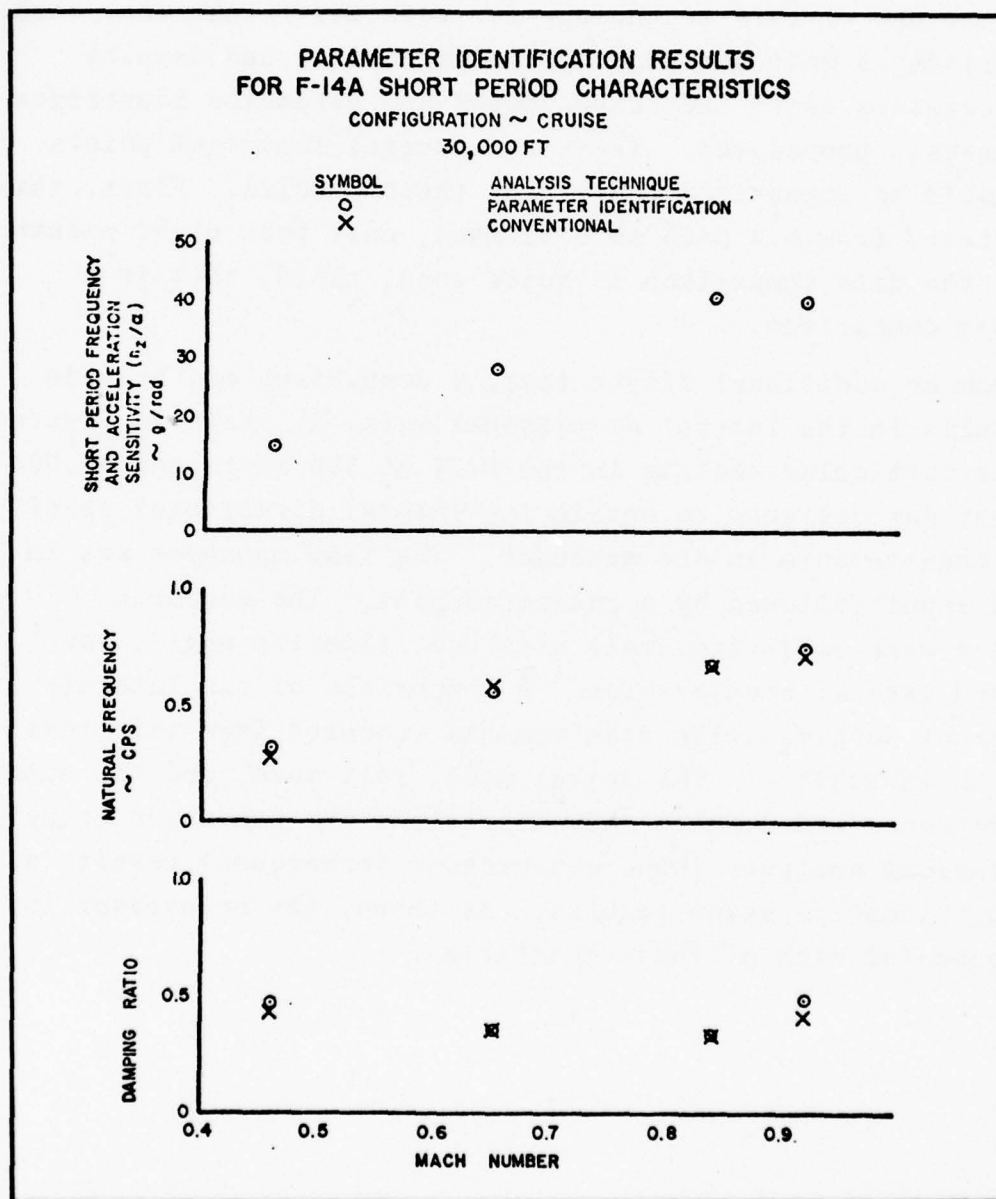


Figure 4 Parameter Identification Results for F-14A Short Period Characteristics

Where possible, a comparison was made between results from conventional flight test analysis and from the parameter identification method. From the test maneuvers used, it was not possible to compute the short period frequency and acceleration sensitivity parameter using conventional analysis methods; however, parameter identification results are presented which demonstrate the use of this technology for reducing flight test time. A comparison is made for short period frequency and damping characteristics using the conventional and parameter identification analysis procedures. There are several important points that should be emphasized concerning these results. First, this flight test, from 0.4 Mach to 0.92 Mach, only took eight minutes; second, the data comparison is quite good; third, this is a black box comparison.

From an additional flight test, a comparison can be made for results in the lateral directional axis, as shown in Figure 5. This particular test is in the F-14 at 396 knots and 30,000 ft. This test was designed to obtain the lateral directional specification requirements in one maneuver. The test maneuver was an aileron input followed by a rudder doublet. The measured responses were roll rate, roll attitude, sideslip angle, yaw rate, and lateral acceleration. A comparison of the lateral-directional specification requirements computed from this test are shown in Table 8. The spiral mode, roll mode, and the dutch roll frequency and damping characteristics are presented comparing classical analysis (hand measurement techniques) results with parameter identification results. As shown, the comparison is quite good for each of these quantities.

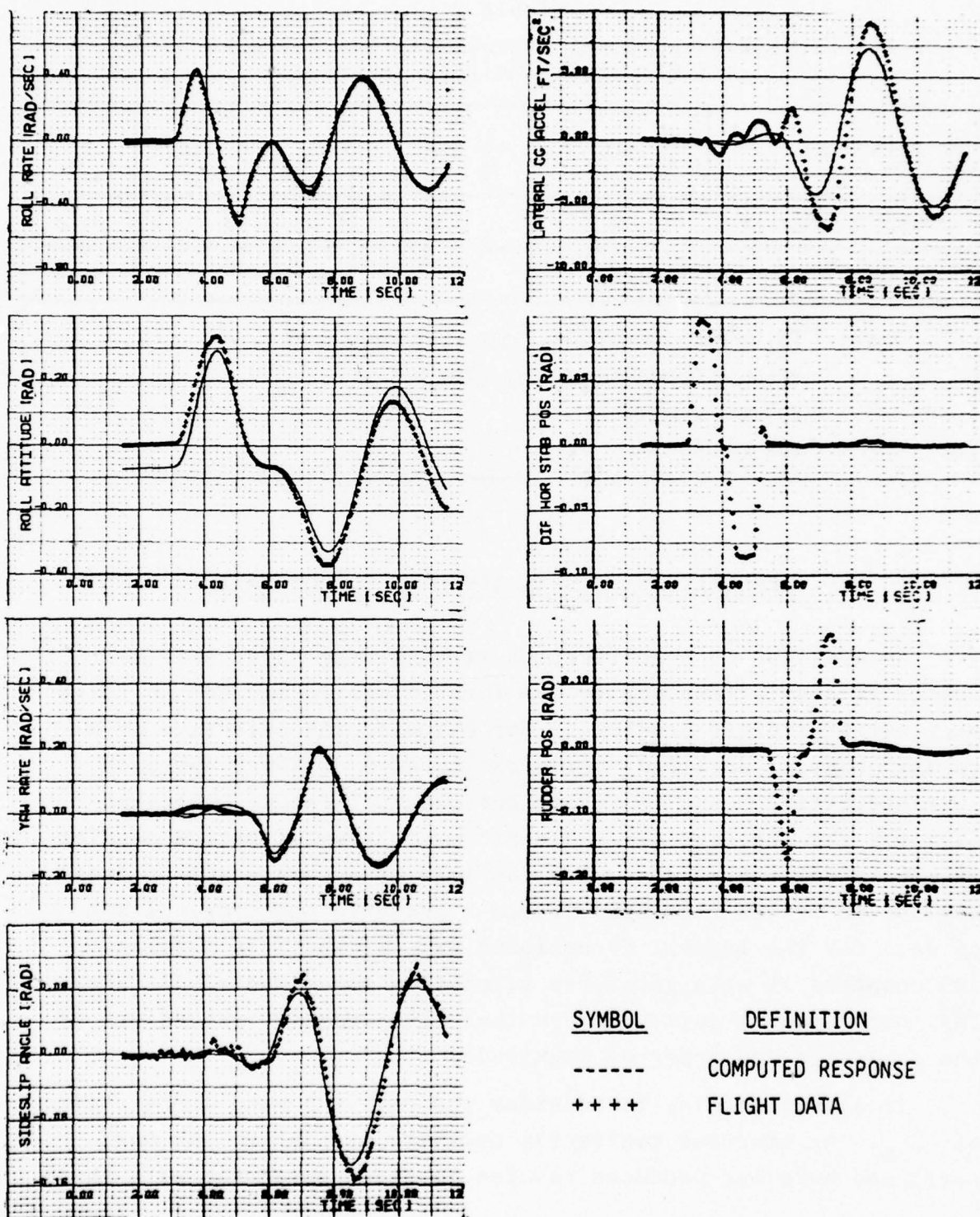


Figure 5 Time History Match for F-14A Aircraft Response to an Aileron-Rudder Doublet Input

Table 8
F-14A Lateral-Directional Characteristics Based on SCIDNT
and Classical Analysis Techniques

DATA SOURCE	$\frac{1}{\tau_S}$ (SEC ⁻¹)	$\frac{1}{\tau_R}$ (SEC ⁻¹)	ω_{n_d} (RAD/SEC)	ζ_d
CLASSICAL ANALYSIS	0	2.8	1.43	0.12
SCIDNT	0.0002	2.67	1.45	0.13
NOTES: (1) FLIGHT CONDITIONS - 368 KTAS, 30,000 FT (2) CONFIGURATION CRUISE, LOAD F (3) A - R INPUT (4) RUN 8				

APPLICATION TO S-3A AIRPLANE FLIGHT DATA

In addition to specification testing, the Naval Air Test Center is also attempting to use identification methods to solve particular aircraft problems. For example, the objective of a recent program, entitled "Verification of S-3A Power Approach Characteristics," was to verify the original set of published data for the airplane [7]. The parameter identification results will be used to provide a more complete or accurate set of data for use in system redesign. Table 9 presents the original set of data for the lateral directional axis of the S-3A airplane and compares it with parameter identification results. As shown, the comparison is quite good in that all parameter values are of the same sign and order of magnitude.

It is interesting to consider the original wind tunnel value of $C_{y\beta}$. An airframe contractor analysis similar to the one performed here has produced results in close agreement with the

Table 9
S-3A Power Approach Parameter Identification Results

S-3A POWER APPROACH PARAMETER IDENTIFICATION RESULTS		
DERIVATIVE	ORIGINAL PUBLISHED DATA (1/RAD)	NATC PARAMETER IDENTIFICATION RESULTS (1/RAD)
$C_{y\beta}$	-1.146	-1.238
C_{yp}	-0.08	----
C_{yr}	0.40	1.971
$C_{n\beta}$	0.1175	0.1194
C_{np}	-0.255	-0.2368
C_{nr}	-0.170	-0.1173
$C_{l\beta}$	-0.0888	-0.1412
C_{lp}	-0.435	-0.4607
C_{lr}	0.145	0.2937
$C_{y\delta R}$	0.0143	0.0192
$C_{n\delta R}$	-0.0974	-0.0872
$C_{l\delta R}$	0.269	0.326
$C_{n\delta a}$	0	----
$C_{l\delta a}$	0.0321	----

wind tunnel value in Table 9. However, a static test performed by the contractor has determined a value for $C_{y\beta}$ that more closely agrees with the estimate produced by the NATC parameter identification program than with the original wind tunnel data.

This comparison indicates that the original wind tunnel value is in error.

An important part of this analysis was to determine the aerodynamic characteristics to quantify the S-3A nonlinear response to spoiler inputs. Figure 6 presents the result obtained from this analysis. Different symbols represent different runs during the flight, and each run was at a stabilized test point with a specific level of lateral stick step input used to excite the airplane. A linear analysis capability in this case is being used very successfully to describe the nonlinear spoiler characteristics of the S-3A airplane. The results presented indicate a highly nonlinear rolling moment due to spoiler and a less severe nonlinear yawing moment spoiler characteristic.

In order to verify the complete aerodynamic model derived from this parameter identification analysis, a prediction test was conducted. Figure 7 presents results for this prediction test and compares both the original data base and the parameter identification time history matches. The input used for this test was a rudder doublet followed by an aileron doublet. Data is presented for roll rate, roll attitude, yaw rate, sideslip angle, and lateral acceleration responses of the airplane. As shown, a very good time history fit was obtained using the NATC estimates and in this light verifies the parameter identification result. This comparison also shows that the original data base did not successfully predict aircraft responses.

FUTURE APPLICATIONS

There are a number of areas for future Navy effort in the development of systems identification for application to aircraft flight testing. One is the problem of model structure determination. Developments in this area are a necessary

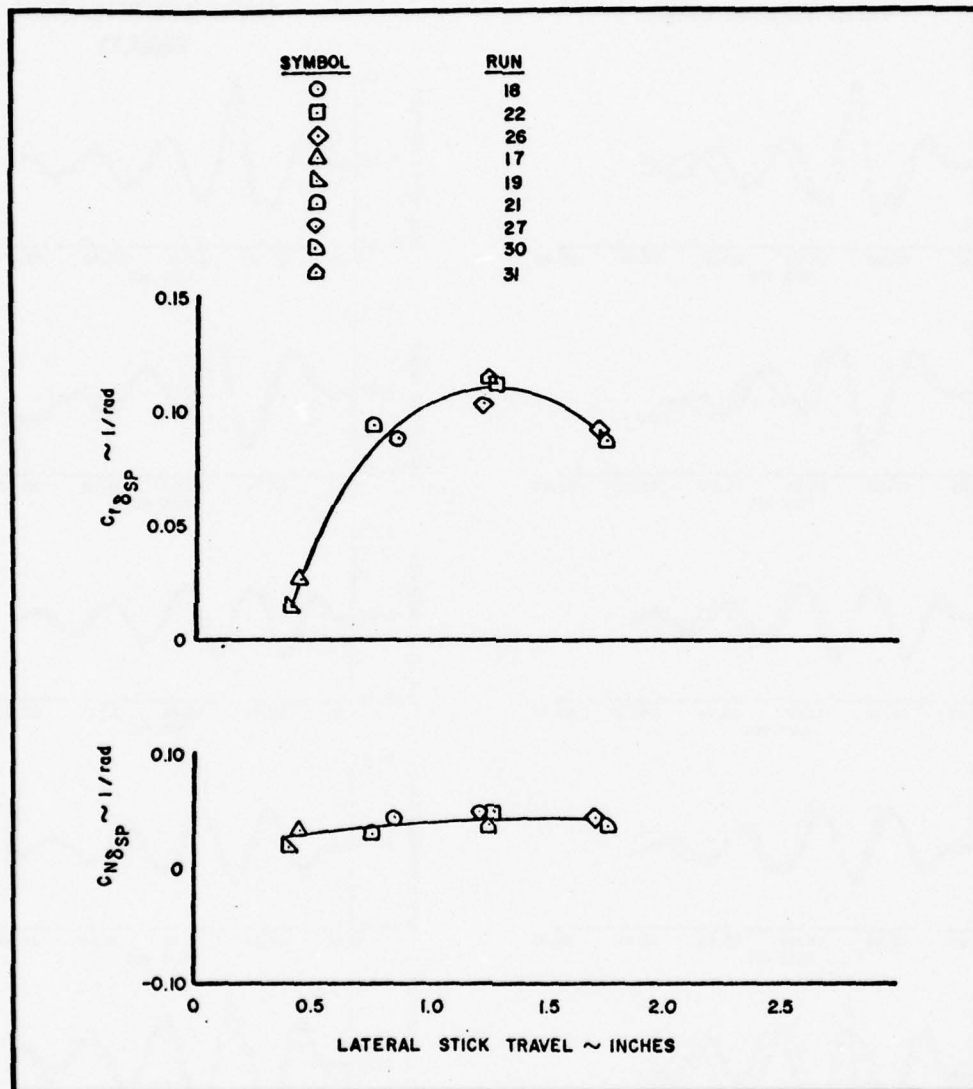


Figure 6 S-3A Power Approach Spoiler Characteristics Based On Parameter Identification Results

<u>SYMBOL</u>	<u>DEFINITION</u>
++++	MEASURED DATA
—	SIMULATED RESPONSE

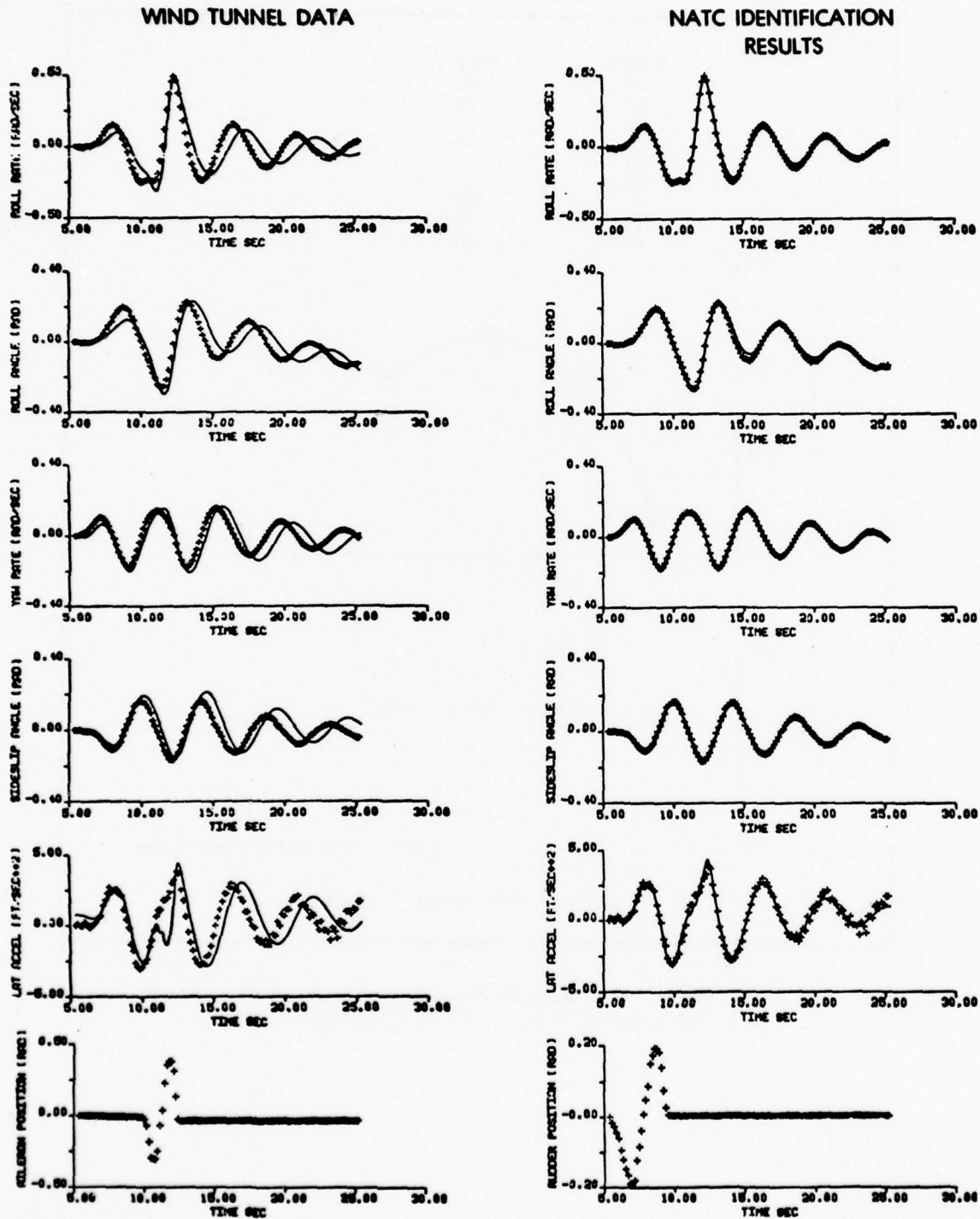


Figure 7 Prediction Test Comparing S-3A Power Approach Wind Tunnel Data and Parameter Identification Results

requirement for determining the nonlinear models to be used in the identification process. There is also a need for a technique for analyzing closed-loop dynamics. The data analysis problem here is to extract from a closed-loop environment the open-loop plane aerodynamics.

Future Navy flight test programs that will use system identification as a data analysis tool include the "EA-6B Catapult Launch Capabilities" and the "EC-130 Structural Evaluation." The EA-6B airplane program will use system identification to determine from flight tests the longitudinal aerodynamic characteristics of this airplane for use in a catapult launch simulation. This simulation will be used to define critical flight areas prior to any actual flight tests. The EC-130 program will use parameter identification to estimate frequency and damping characteristics of wing structural bending modes.

CONCLUDING REMARKS

This paper has presented an overview of the system identification program at the Naval Air Test Center. The use of this new technology to provide for more effective aircraft stability and control flight testing has been demonstrated. This is accomplished by either improving the efficiency of the flight test and/or providing for a more comprehensive data analysis.

REFERENCES

1. Stepner, D.E. and Mehra, R.K., NASA Contractor Report NASA CR-2200, Maximum Likelihood Identification and Optimal Input Design for Identifying Aircraft Stability and Control Derivatives, of Mar 1973.
2. Military Specification MIL-F-8785B (ASG), Flying Qualities of Piloted Airplanes, of 7 Aug. 1969.
3. Detail Specification for the Model S-3A Aircraft Weapon System SD-562-1, of 27 June 1969.
4. Detail Specification for Advanced Carrier Based Fighter Aircraft Weapon System, Model F-14A Airplane, SD-561-1, of 10 Jan. 1969.
5. Burton, R.A. Advancements in Parameter Identification and Aircraft Flight Testing, Paper 15, AGARD Conference Proceedings No. 172 on Methods for Aircraft State and Parameter Identification, of May 1975.
6. Humphrey, M.J., NATC Technical Report SA-C7R-75, First Interim Report - Flying Qualities Technical Evaluation of the F-14A Airplane, of 25 Nov. 1975.
7. Naval Air Systems Command Airtask/Work Unit Assignment, Airtask A510-5103/053-2/4241-000-265, Work Unit No. A53011A-25, Verification of S-3A Power Approach Characteristics, of 9 Jan. 1975.

THE APPLICATION OF ESTIMATION THEORY TO THE TRANSFER ALIGNMENT OF INERTIAL SYSTEMS

by

William F. Ball
Naval Weapons Center
China Lake, California

INTRODUCTION

The application of optimal estimation theory has been instrumental in the notable success of two inertial system programs at the Naval Weapons Center (NWC): the ATIGS (Advanced Tactical Inertial Guidance System) Program and the MRS (Missile Reference System) Program. ATIGS is a strapdown inertial system utilizing ring laser gyros being developed primarily for midcourse guidance of air-launched long-range tactical missiles. The MRS program is adapting the ATIGS technology to ship-launched missiles. Both of these programs require initial alignment of a strapdown inertial system. The technique chosen for this initialization is that of transfer alignment. Commencing in 1968, an optimal estimation theory approach to mechanizing the transfer alignment was pursued.

This paper will review the ATIGS and MRS programs and will discuss the estimation theory applications involved in each. Results of flight-test and sea-trial investigations will be given.

THE ATIGS PROGRAM

The goals of the ATIGS program are to (1) demonstrate the technical feasibility of Ring Laser Gyro (RLG) strapdown inertial systems, (2) establish a technology base for engineering development for an array of applications, and (3) establish a reasonable projected service cost base for production.

The key to the ATIGS development is the use of the RLG. Figure 1 shows the Honeywell GG-1300 RLG currently used by the ATIGS program. The salient features of this device are called out in the figure. NWC has selected the laser gyro because of its many advantages, which are delineated as follows. The RLG is truly a single-degree-of-freedom gyro in a strapdown environment. It has a highly stable input axis, has negligible g -sensitivity and, with development effort, can be made to have low thermal sensitivity. With the exception of the dithered block, which is

a noncritical moving part, the laser gyro has no moving parts. Limited only by the bandwidth of the readout electronics, the RLG has a very high rate capability with precise scale factor. The output is directly digital. It has a rapid warm-up time. Finally, because of simple construction, low parts count, and state-of-the-art optical technology, the RLG should be low-cost in production.

Figure 2 is a photograph of the first flight model of ATIGS. In the three-quarter view shown, two RLGs are visible. Below the RLG on the right is the Sundstrand Q-flex accelerometer triad box. The third RLG is on the bottom, the power supply on the right rear, and a Delco M-362, 8,000-word, 16-bit digital computer fits as a core in the center of the structure.

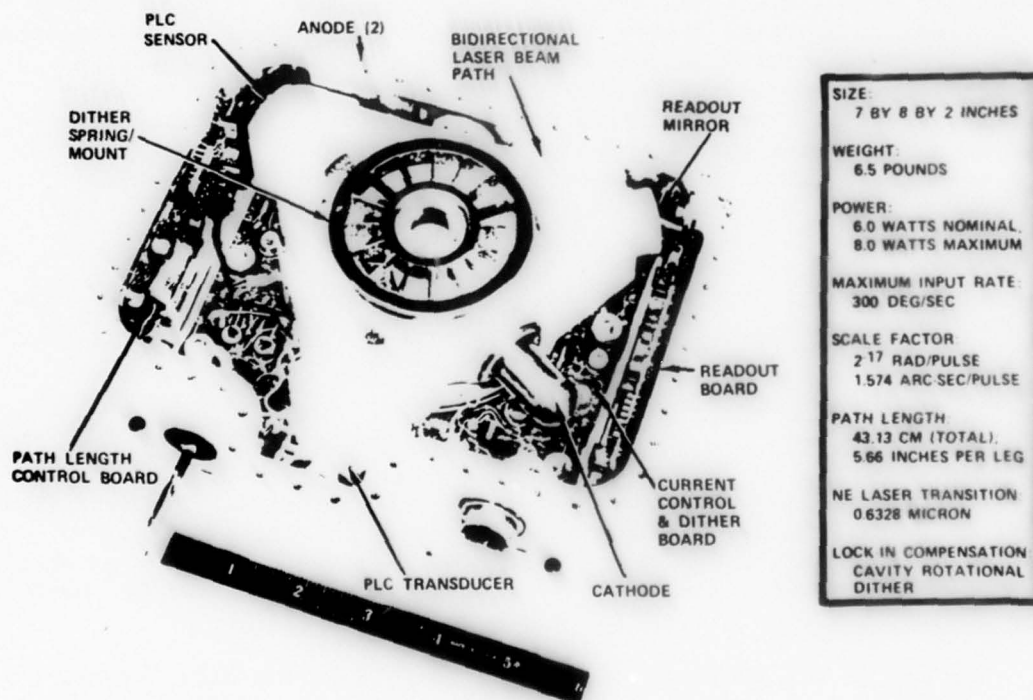


FIGURE 1. GG1300 Laser Gyro Characteristics.



FIGURE 2. ATIGS System.

ATIGS was first flight-tested in June and July 1974. The objective of this first flight series, in addition to being a shakedown series of tests for gaining experience with the RLG, was to evaluate the capability of the ATIGS system in an aircraft pod environment performing:

- (a) Navigation
- (b) Alignment transfer (optimal filter, velocity-matching mechanization, matching ATIGS velocity to the A-7E inertial navigator)
- (c) Utilization of position resets (simple position reset, no filtering).

All these objectives were demonstrated. The navigation performance is illustrated in Figure 3.

In Figure 3 each dot represents the radial error at a fix-point. Visual flyover fixes of surveyed landmarks were used as references for the tests. The error in the visual flyover fix is assumed to be equal to the altitude of the aircraft over the fix-point. The 4-nmi/hr line is drawn-in over the data points, with no attempt being made at fitting a curve. It was this data--more than adequate for missile midcourse

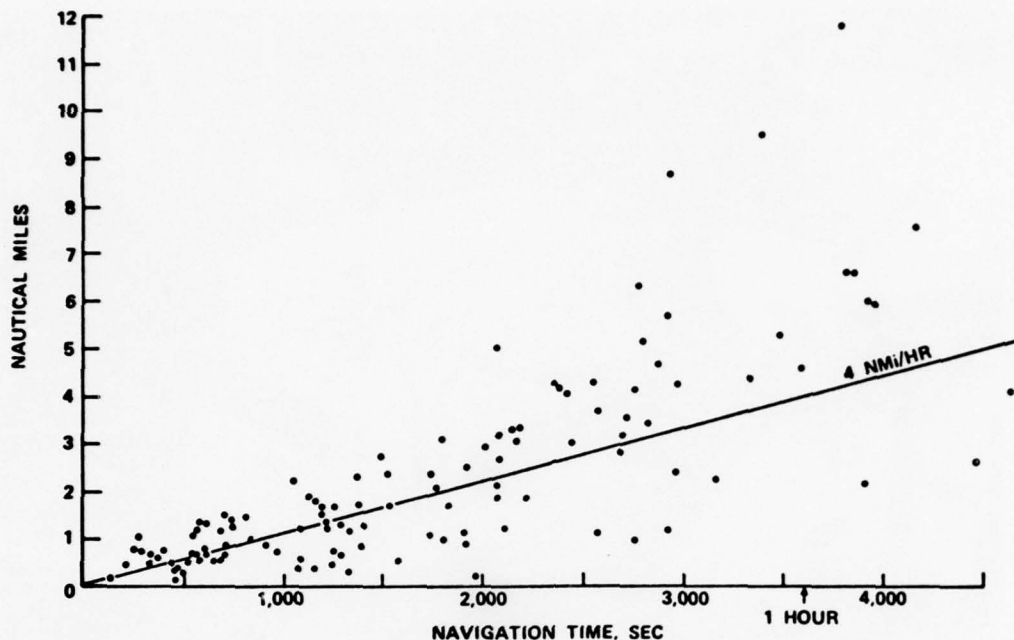


FIGURE 3. ATIGS June/July 1974 Flight Test, Composite Results, Radial Error.

guidance--that gave a first indication of the possibility that an aircraft navigation potential existed. The ATIGS system, as tested in the pod in these flights, had no thermal control except for the accelerometer box and the outside air blown over the system. No attempt was made at even coarse control of the pod inside temperature.

The June/July 1974 tests succeeded in creating interest at high levels. As a result of this interest, a second series of flight tests were defined, wherein an attempt would be made to improve the thermal control of the test pod. Therefore, for the flight tests of March 1975, a thermal control mechanism was installed in the pod, permitting coarse control to $\pm 10^{\circ}\text{F}$. Further, minor changes were made in the accelerometer electronics to improve the thermal characteristics of the A/D converters. These tests did not involve in-flight alignment transfer.

Figure 4 is a sample of ground-based navigation runs made during preflight preparations. In this configuration, it is estimated that the temperature in the pod was stable to $\pm 2^{\circ}\text{F}$. Inspection of Figure 4 shows that, for the 2-hour runs, all errors were below approximately 1 nmi/hr. It is felt that this is indicative of performance under conditions of good thermal control.

In the March tests, eight flights were made. Table 1 summarizes the results of the eight flights, with the flight number 2 data being rejected due to an inadvertent in-flight alignment transfer from the A-7E aircraft. The CEP for the seven accepted flights was 2.16 nmi/hr.

TABLE 1. ATIGS Phase II Flight Test Summary^a.

Flight	Position error rate, nmi/hr		No. of points	Navigation time, hr	Flight path	Comments
	CEP	90%				
1	2.95	4.92	13	3.0	3 CW ^b	Computer problem
2	2.40	4.11	13	2.9	3 CCW ^b	Inadvertent in-air align
3	2.08	3.80	16	4.4	4 CW	Missed 3 ckpts, weather
4	2.11	4.37	19	4.3	4 CW	...
5	2.82	5.59	13	2.9	3 CCW	...
6	1.90	5.67	13	2.9	3 CW	...
7	1.59	4.44	19	4.1	4 CCW	...
8	2.53	4.52	14	3.1	4 CCW	Abort early, low fuel
Total ^c	2.16	4.95	107	24.7

^a 4-24 March 1975 at NWC, China Lake.

^b CW = clockwise; CCW = counterclockwise.

^c Totals exclude flight 2.

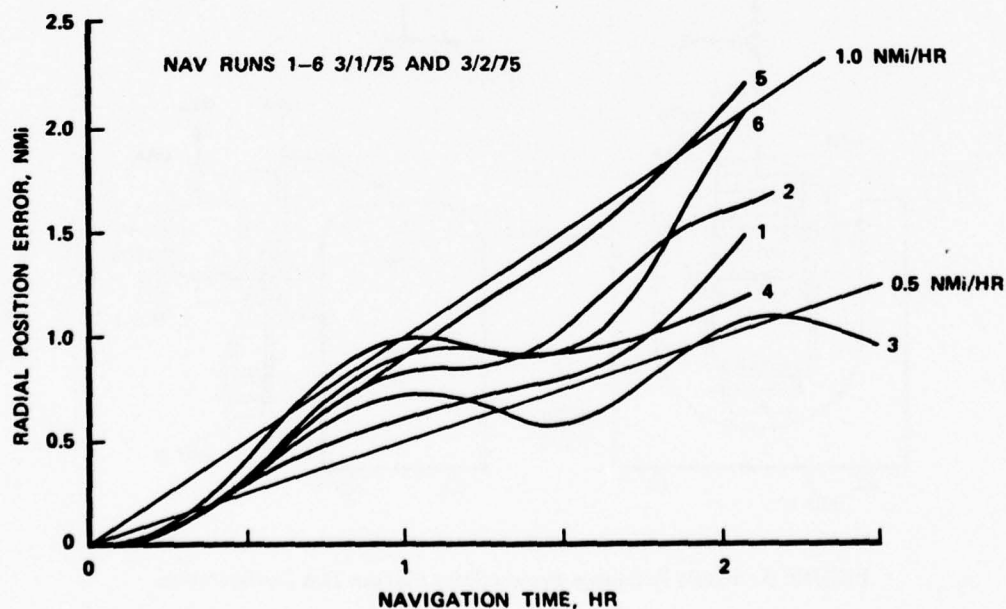


FIGURE 4. Ground Test-System In-Flight Configuration (In Pod).

THE MISSILE REFERENCE SYSTEM PROGRAM

The goals of the MRS Program are to (1) develop guidance system methods for strapdown inertial midcourse guidance of medium range tactical ship-launched missiles, and (2) develop and demonstrate guidance system alignment and initialization techniques. The program has concentrated on three areas of effort: pre-launch master-to-slave alignment, inertial midcourse guidance using ATIGS, and optimal in-flight target updating. Of particular interest to this paper is the master-to-slave alignment, which utilizes optimal filter techniques similar to the in-flight case of ATIGS. This program has progressed from early analytical investigations to laboratory demonstrations and finally to sea-trial. Figure 5 is a drawing of the ship-motion, ship-flexure simulator, used for laboratory investigations of alignment algorithm convergence under varying simulated sea-state, ship-flexure conditions. Figure 5 shows two motion tables, the smaller mounted on the larger. With the moment arm structure shown, various ship motion inputs could be imposed on the two strapdown inertial measuring units (IMUs). Figure 6 shows the location of the strapdown IMUs on the U.S.S. *Wainwright* (DLG-28), the ship used in the sea trial.

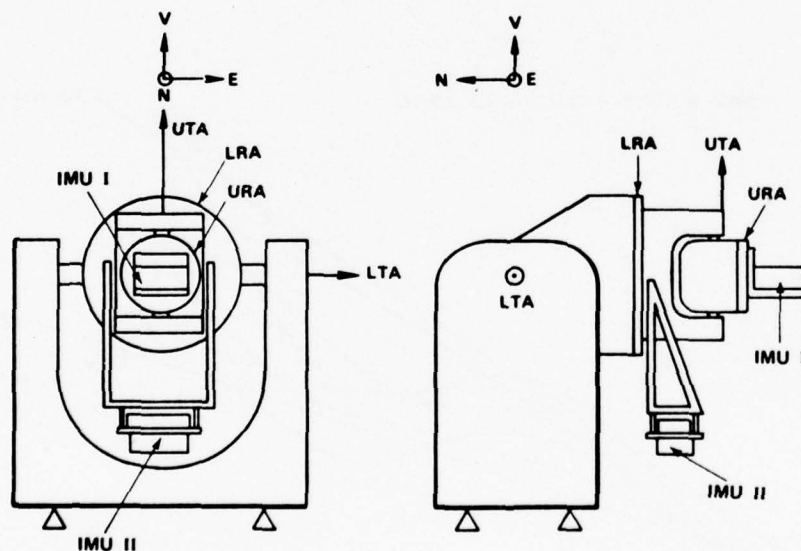


FIGURE 5. Missile Reference System Ships Flexure Test Configuration.

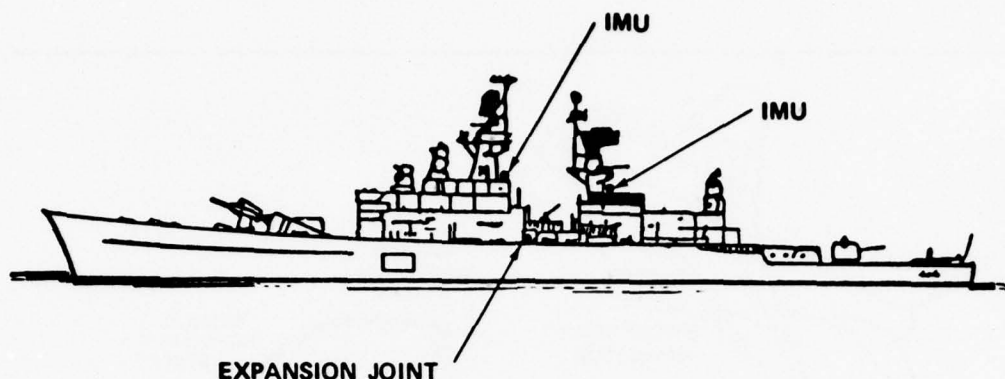


FIGURE 6. U.S.S. Wainwright (DLG-28).

THE OPTIMAL FILTER PROBLEM AND OUTLINE OF APPROACH EMPLOYED

The ATIGS and MRS optimal filters are quite similar. The aircraft case with ATIGS involves the transfer of attitude alignment data (North, East, Down) from an A-7E gimbaled inertial navigator to the strapdown ATIGS (missile) inertial navigator. In the MRS shipboard case, the transfer of altitude alignment data is from a strapdown master to a strapdown slave. In both cases, transfer alignment was chosen to eliminate the various sources of error present with mechanical alignments or shipboard synchro-resolver chains of previous alignment methods. None of the previously used alignment approaches were considered sufficiently accurate to meet the ATIGS or MRS requirements. Posing the problem in an inertial space setting was chosen to overcome these shortcomings. The two alignment situations are illustrated pictorially in Figure 7.

The optimal filter approach in both the ATIGS and MRS cases essentially was mechanized as shown in Figure 8. The outputs of the systems are observed and compared. The difference is inserted into the optimal filter and the proper direction cosine corrections are generated so that the two system outputs agree. When this occurs, the resulting direction cosine matrix represents the misalignment between the two reference systems.

Figure 9 shows the principal features of the two optimal filter mechanizations as used by NWC. Approach No. 1 was originally developed by The Analytic Science Corp. (TASC) under contract to NWC and was subsequently modified by NWC. In the TASC/NWC approach, the matrix C_M^S ,

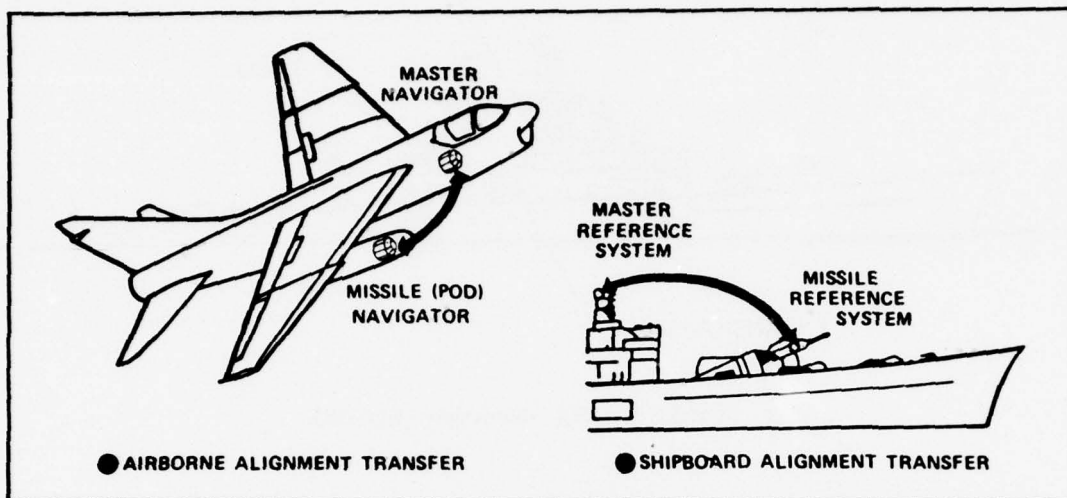


FIGURE 7. Alignment Transfer.

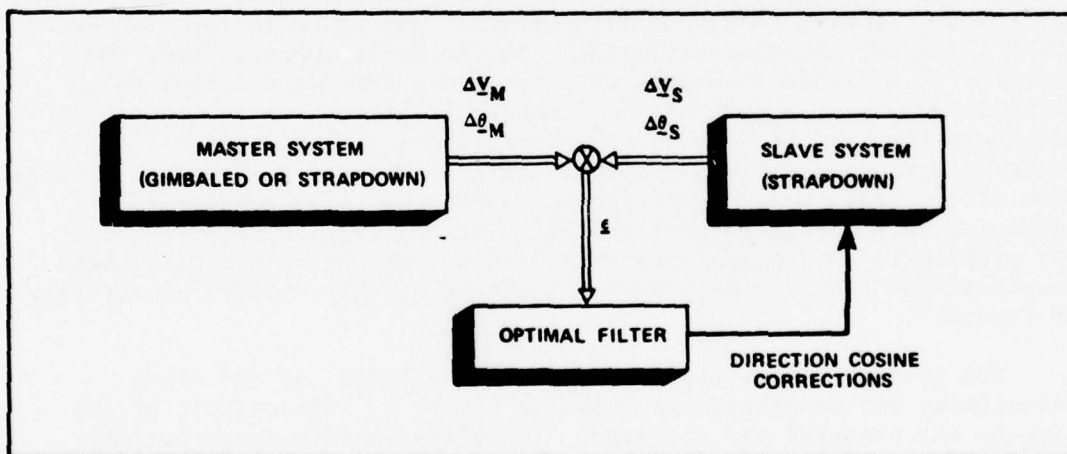


FIGURE 8. Master-to-Slave Alignment Approach.

relating the slave to the master system is the desired result. This is obtained by defining two inertial frames I and N, in such a manner that

$$C_I^M(0) = C_N^S(0) = \text{Identity matrix at } t \stackrel{M}{=} 0.$$

The desired matrix is then related by

$$C_M^S = C_M^I C_I^N C_N^S$$

Where, now, C_I^N is a constant matrix relating two arbitrary inertial spaces. C_M^I and C_N^S are propagated in the normal strapdown manner by solving the respective direction cosine differential equations. So, instead of estimating the time-varying parameters of C_M^S , the constant parameters of C_I^N are obtained. It is assumed that the angular rates and accelerations seen by master and slave are identical. This is not true, due to moment arm and flexure effects. However, simulation and demonstration has proven that violation of these assumptions within the limits of actual application is acceptable and does not represent excessively sensitive effects.

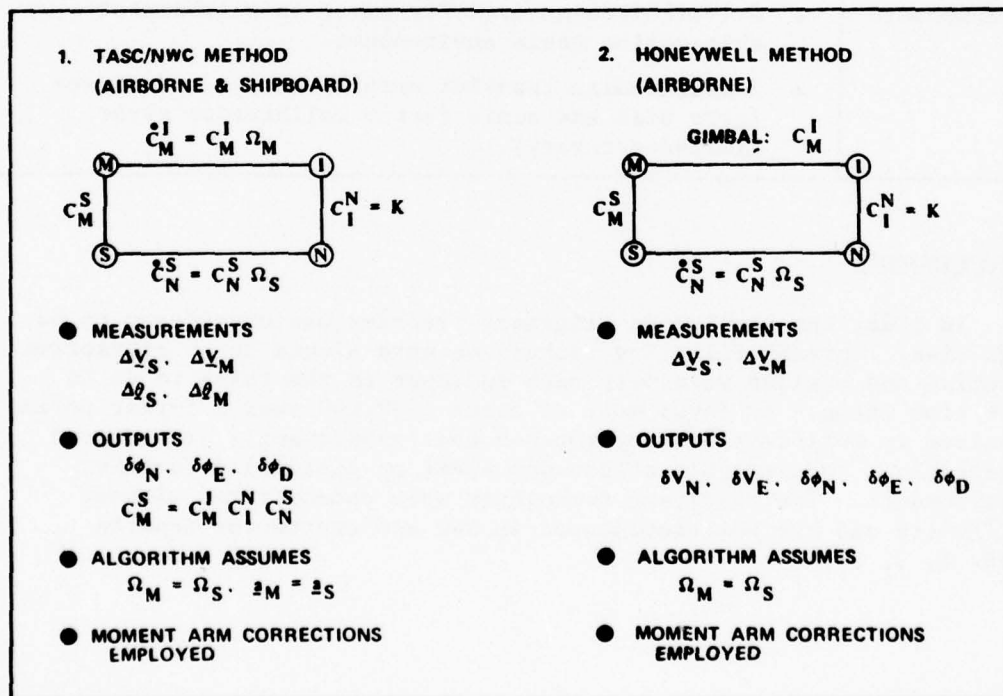


FIGURE 9. Alignment Transfer Mechanizations.

In Approach No. 2 by Honeywell under the ATIGS contract, the North and East velocities from the aircraft system are compared to the ATIGS North and East velocities. Moment arm corrections are employed to correct for the displacement of ATIGS from the aircraft navigator.

An optimal filter generates best estimates of the North and East velocity errors in ATIGS, and generates North, East, and Down alignment corrections for the quaternions and (ultimately) the direction cosine matrix C_M^S is obtained. In both cases, constant misalignment matrix corrections are obtained.

RESULTS ACHIEVED

The results of work in these areas are summarized in Table 2.

TABLE 2. Optimal Alignment Results.

Airborne	<ul style="list-style-type: none"> • 6-arc-minute transfer error demonstrated in flight. • 2-minute convergence time. • S-turn maneuver required.
Shipboard	<ul style="list-style-type: none"> • 0.1-milliradian transfer error in a laboratory ship-motion table environment. • 2-milliradian transfer error demonstrated at sea (gyro bias and scale factor calibration error limited accuracy).

CONCLUSIONS

In 1968, the problem of alignment transfer was considered to be high-risk. Optimal filtering techniques were viewed as an attractive solution and besides were very much in vogue as the thing to do in that time frame. An investment of about \$500,000 over a 5-year period resulted in well-developed approaches that subsequently were proven acceptable. Considerable effort was spent on minimizing computer requirements. The resultant techniques were demonstrated without difficulty and are well-documented in NWC and contractor reports (Ref. 1, 2, 3).

REFERENCES

1. Naval Weapons Center. *Strapdown IMU Alignment and Initialization*, by Larry D. Levsen. China Lake, Calif., NWC, June 1971. (NWC Technical Note 404-106, publication UNCLASSIFIED.)
2. Naval Weapons Center. *Strapdown IMU Alignment and Initialization*, by Larry D. Levsen. China Lake, Calif., NWC, December 1971. (NWC Technical Note 404-106, Supplement 1, publication UNCLASSIFIED.)
3. Honeywell, Incorporated. *Flight Program Requirements Document*, by Avery A. Morgan. St. Petersburg, Fla., HI, 23 May 1973. (ATIGS Contract N00123-73-C-0265, publication UNCLASSIFIED.)

CONTROL AND ESTIMATION THEORY: AN INTEGRAL PART OF
THE ELECTRICALLY SUSPENDED GYRO NAVIGATOR (ESGN) *

by

W.R. DIAMOND
Naval Ship Engineering Center

During the past decade, control and estimation theory has played a significant role in the development of the marine inertial navigation problem of accurate reset in the Ship's Inertial Navigation System (SINS). The role of estimation theory was expanded during the late 1960's and early 70's to include platform calibration (gyros and accelerometers) in the Ship Self-Contained Navigation System (SSCNS) and the Dual Miniature Ship Inertial Navigation System (Dual MINISINS). The purpose of today's discussion is to present an example illustrating how the application of estimation theory has become an integral part of the development of the Electrically Suspended Gyro Navigator (ESGN). The ESGN development program is sponsored by the Naval Sea Systems Command and is technically directed by the Naval Ship Engineering Center. The objective of this development program is to provide the SSN fleet with an accurate inertial navigation system employing ESG technology. We will see that during this development effort, the application of estimation theory was essential in achieving the Advanced Development program objectives. Figure 1 presents an overview of today's presentation.

First we will review the salient characteristics of the Electronically Suspended Gyro and its application to the marine navigation problem. The particular technology we will address is the Gimballed Airborne Navigation System (GEANS) which is manufactured by Honeywell, Inc. During the Navy's Advanced

* This paper was typed from a taped version of the oral presentation.

OVERVIEW

- ELECTRICALLY SUSPENDED GYRO /SYSTEM CONCEPTS
- WHY IS ESTIMATION THEORY REQUIRED?
- WHERE & HOW IS IT APPLIED?
- FUTURE APPLICATIONS TO ESGN TECHNOLOGY

Figure 1

Development program, a contract was awarded to Honeywell to modify the GEANS hardware and develop software for a marine application. While the application of control and estimation theory is exhibited in many areas of the Navy GEANS hardware and software, we will focus our attention to two particular areas, namely, the ESG drift prediction model (gyro calibration) and the attitude readout mechanization, to see why the application of estimation theory was required. Next, we will review where and how the theory was applied in the ADM configuration. Lastly, we will review several avenues where estimation theory can be applied to ESGN technology in the future.

The Electrically Suspended Gyro, shown in schematic form in Fig. 2, is a free rotor, two axis device, which consists of one moving part (a hollow beryllium rotor) which is supported by an electric field in a cavity composed of six electrodes maintained at hard vacuum. The rotor is spun-up, damped and maintained at operating speed by magnetic fields generated by the coils shown in the figure. Photodetection of the equatorial pattern is used to generate control signals to the coils to maintain rotor speed. The rotor is maintained at the cavity center via a three-axis capacitance bridge using an electrode to rotor capacitance measurement to provide feedback control voltages to the suspension electrodes. Angular displacement of the rotor spin axis is optically detected by the polar pick-off which generates control signals which can be used to servo the cavity to re-establish rotor spin axis and cavity axis alignment. This device is utilized in a space stabilized gimballed platform and consequently no gyro torquing for earth's rate, vehicle translational motion or self drift is applied as is done in Local Vertical systems. The high mechanical stability of the gyro, combined with its torque free operation are the two major characteristics which make this device suitable for high accuracy navigation. However, the self drift of the gyro (which is highly predictable) must be compensated for (in lieu of torquing) in the navigation algorithm by a mathematical

SCHEMATIC REPRESENTATION OF AN ESG

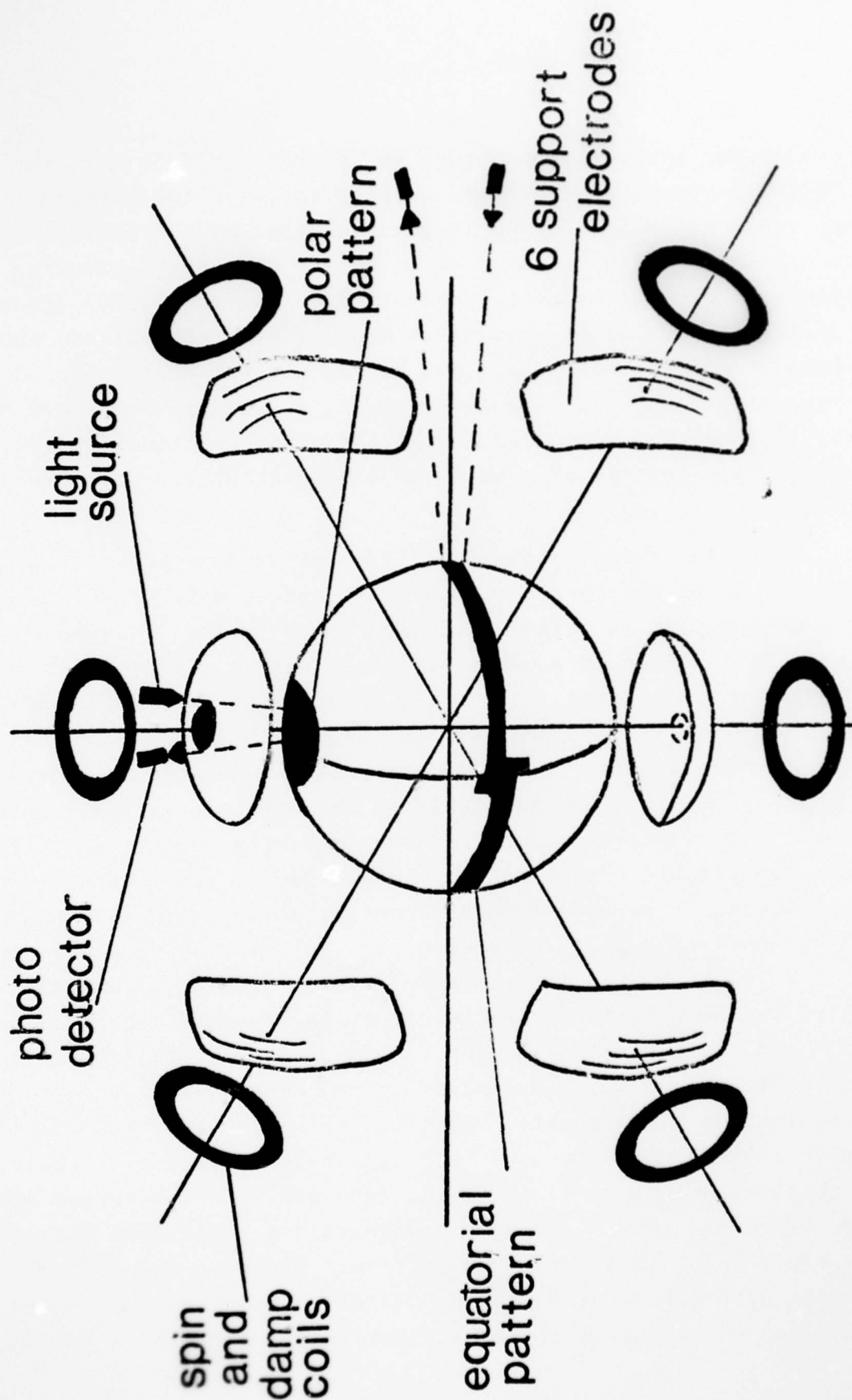


Figure 2

model which describes the motion of the spin axis as a function of the external forces acting upon it. ESG self drift is caused by the interaction of these external forces with the geometric imperfections of the device such as rotor mass unbalance, rotor non-sphericity, electrode structure mismatch, and rotor miscentering.

Since a space stable mechanization is instrumented vice a local vertical approach, the gimbal resolvers do not provide a direct ship's attitude readout. The gimbal resolver output signals must be converted to digital form and used in a coordinate transformation (deck to local vertical frame) from which ship's roll, pitch, and heading angles can be extracted. Resolvers are used vice higher accuracy inductosyns due to size constraints imposed on the design so that the ESGN binnacle will pass through a 25-inch circular hatch without disassembly. A general block diagram of the ESGN mechanization is shown in Figure 3.

Raw accelerometer information is compensated for instrument errors, resolved into the navigation frame and input into space stable Schuler loops which are closed in the computer by a gravity calculation which is subtracted from the measured inertial acceleration. The acceleration is integrated to obtain velocity and position. Ship's geographic position and velocity are then computed from the inertial quantities using geometric relationships between the local vertical and inertial frames. The box marked "Compute Platform to Inertial Transformation" in this figure represents the prediction of gyro self drift. We will explore this in greater detail momentarily. To round out the mechanization let us look at the attitude mechanization shown in Figure 4.

Raw gimbal resolver signals are digitized and used to compute the deck to platform transformation matrix. Since the platform to inertial matrix (gyro drift model) and the inertial to local vertical matrix (latitude, longitude and time) are known, the deck to local transformation matrix can be computed. From this matrix roll, pitch and heading can be extracted using the relationships

ESGN MECHANIZATION

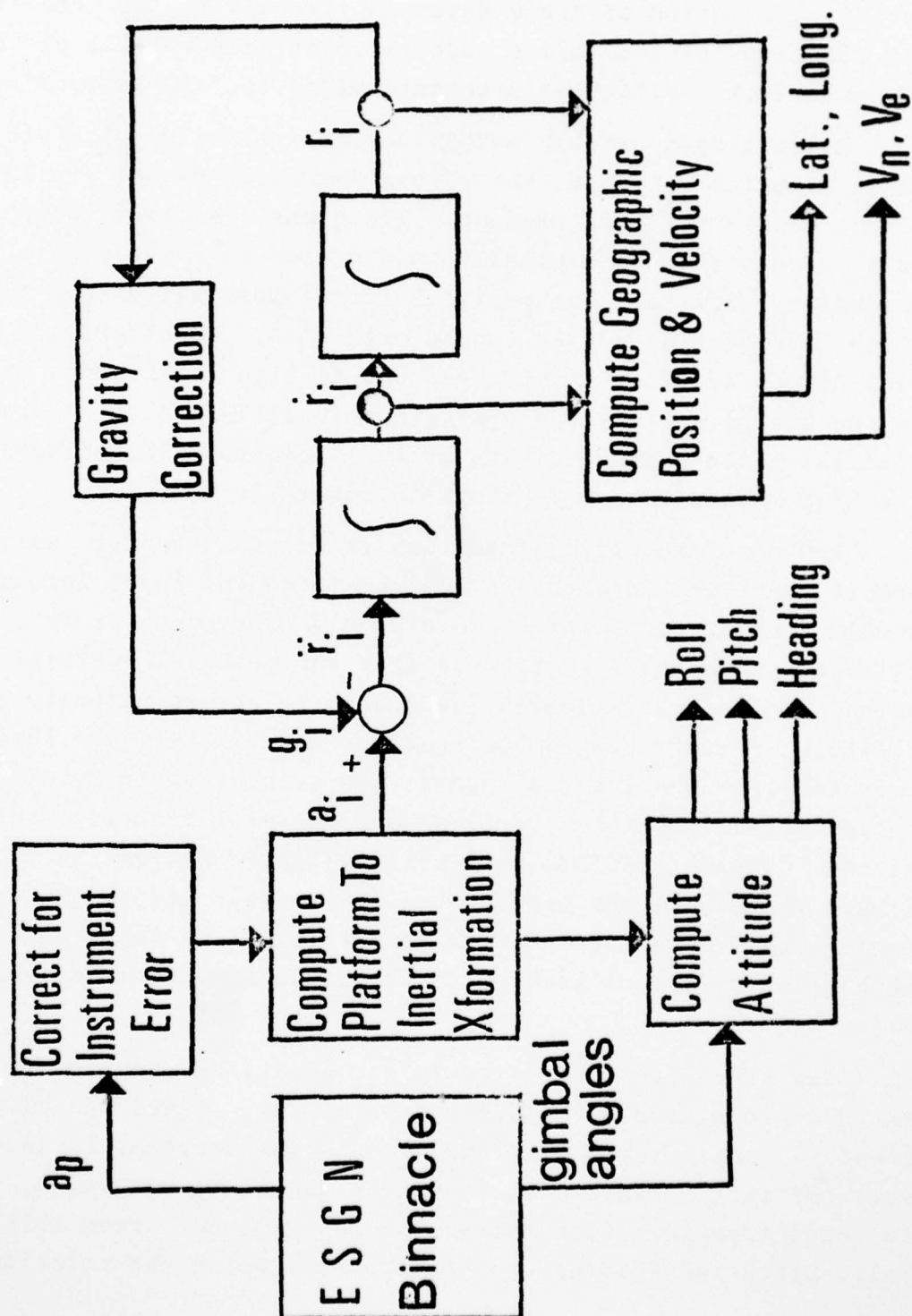
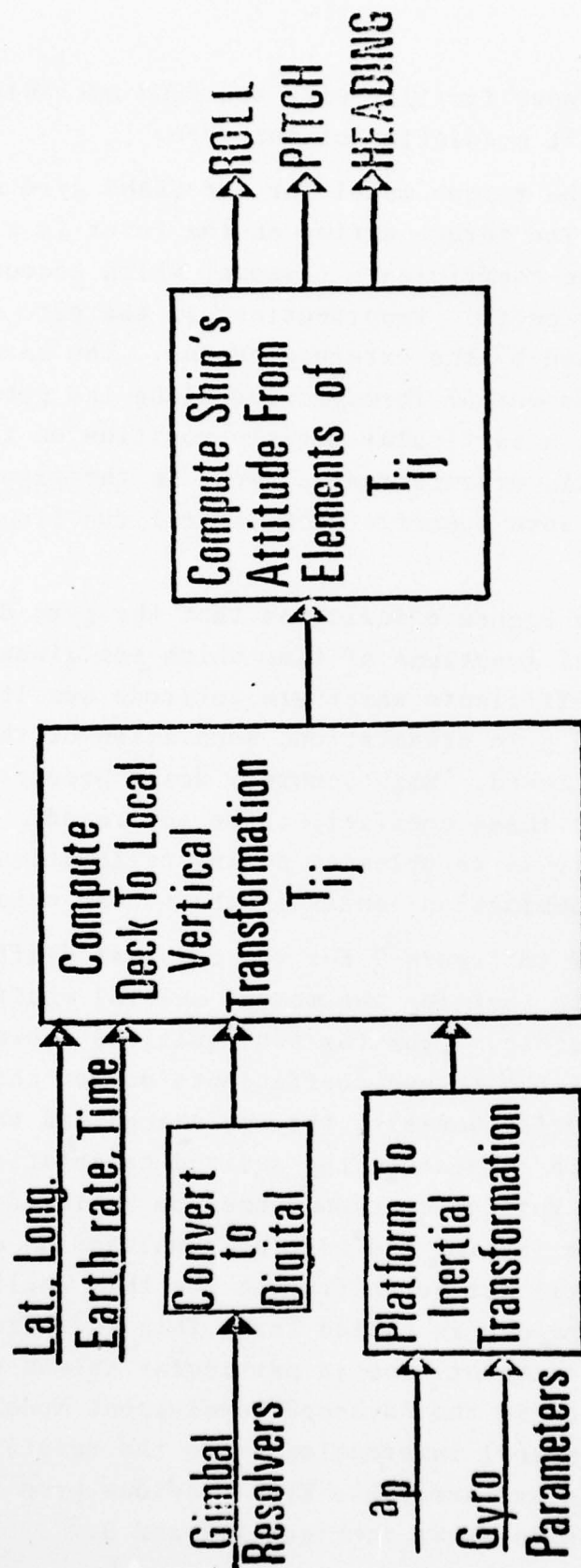


Figure 3

ATTITUDE COMPUTATIONS



$$\text{ROLL} = -\text{SINE}^{-1} (T_{13})$$

$$\text{PITCH} = \text{TAN}^{-1} (T_{12}/T_{11})$$

$$\text{HEADING} = \text{TAN}^{-1} (T_{23}/T_{33})$$

Figure 4

shown. Now that we are more familiar with the ESGN mechanization let us return to the drift prediction of the gyro.

Figure 5 presents the torque model for the GEANS gyro manufactured by Honeywell. The torque acting on the rotor is a linear combination of the torque coefficients (gammas) which account for the sensitivity of the geometric imperfections in the gyro to external force, multiplied by the external forces. The terms $g \cdot F_i$ represent the component of force acting along the gyro's ith axis. Let us select a particular vehicle position on the earth and a gyro spin axis orientation as shown in the figure and expand the torque model into specific mathematical functions of gyro drift.

The result shown in Figure 6 indicates that the gyro drift is described by mathematical functions of time which are linear combinations of the torque coefficients which are latitude sensitive. For a given latitude and gyro orientation, separation of the coefficients cannot be achieved. High accuracy drift prediction makes it imperative that these coefficients be separated. To achieve this end the gyro is re-oriented during calibration such that different linear combinations exist in the second orientation.

This is illustrated in Figure 7 for the constant drift term of the x gyro axis. Note that for the moment several coefficients have been assumed negligible. From the two equations shown, separation can be achieved if the torque coefficients do not change during reorientation. Unfortunately, they do change and their change is significant with respect to the desired calibration accuracy. Therefore, a full separation cannot be achieved, and the simple approach of curve fitting and solving simultaneous equations for gyro calibrations will not be sufficient for this application. A more sophisticated approach is called for. This is where the application of estimation theory and in particular Kalman filtering made a major contribution in the Advanced Development Model ESGN mechanization, since a priori information as to the relative magnitude of the coefficients was available from previous gyro test data. The filter mechanization is shown in Figures 8 and 9.

GEANS ESG TORQUE MODEL

$$T = (\gamma_{10} + \gamma_{11} (g \cdot F_x) + \gamma_{12} (g \cdot F_y) + \gamma_{13} (g \cdot F_z) + \gamma_{14} (g \cdot F_x)^2 + \gamma_{15} (g \cdot F_y)^2 + \gamma_{16} (g \cdot F_z)^2) F_x \\ + (\gamma_{20} + \gamma_{21} (g \cdot F_x) + \gamma_{22} (g \cdot F_y) + \gamma_{23} (g \cdot F_z) + \gamma_{24} (g \cdot F_x)^2 + \gamma_{25} (g \cdot F_y)^2 + \gamma_{26} (g \cdot F_z)^2) F_y$$

$$g \cdot F_x = -g \sin L \\ g \cdot F_y = -g \cos L \sin (\lambda + \Omega t) \\ g \cdot F_z = -g \cos L \cos (\lambda + \Omega t)$$

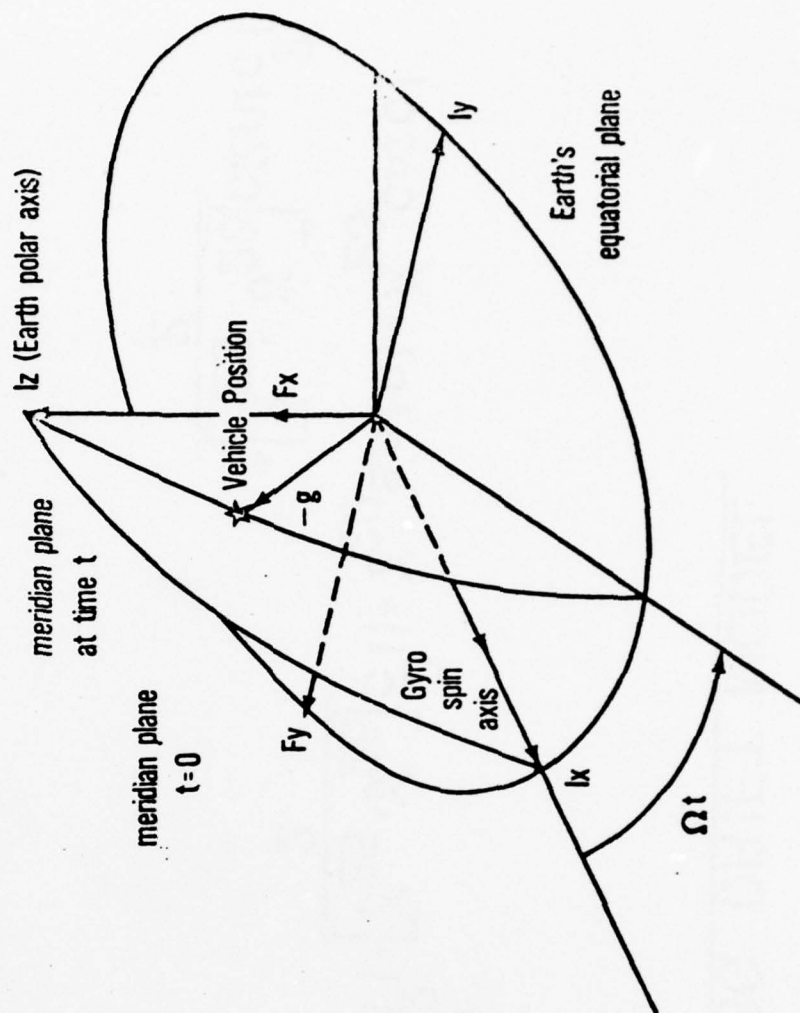


Figure 5

GEANS ESG DRIFT MODEL

$$W_x = -(\chi_{20} - \chi_{21} s_1 + \chi_{24} s_1^2 + \frac{[\chi_{25} + \chi_{26}] c_1^2}{2} + \chi_{22} s_1 c_1 + \chi_{23} c_1^2 + \frac{[\chi_{25} - \chi_{26}] c_2^2}{2})$$

$$W_y = (\chi_{10} - \chi_{11} s_1 + \chi_{14} s_1^2 + \frac{[\chi_{15} + \chi_{16}] c_1^2}{2} - \chi_{12} s_1 c_1 - \chi_{13} c_1^2 + \frac{[\chi_{16} - \chi_{15}] c_2^2}{2})$$

Figure 6

CLASSICAL SEPARATION APPROACH

$$W_x(1) = -\chi_{20} + \chi_{21}SL$$

$$W(2) = -\chi_{20} - \chi_{21}SL$$

$$\chi_{20} = -1/2(W_x(1) + W_x(2))$$

$$\chi_{21} = 1/2sl(W_x(1) - W_x(2))$$

Assumptions

1. $\chi_{24}, \chi_{25}, \chi_{26}$ negligible
2. Negligible change in χ_{20}, χ_{21} due to reorienting

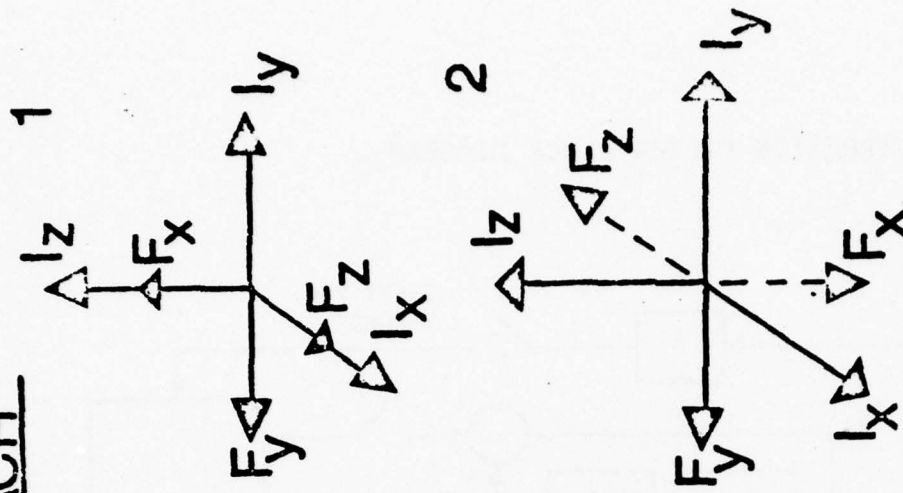


Figure 7

CALIBRATION FILTER BLOCK DIAGRAM

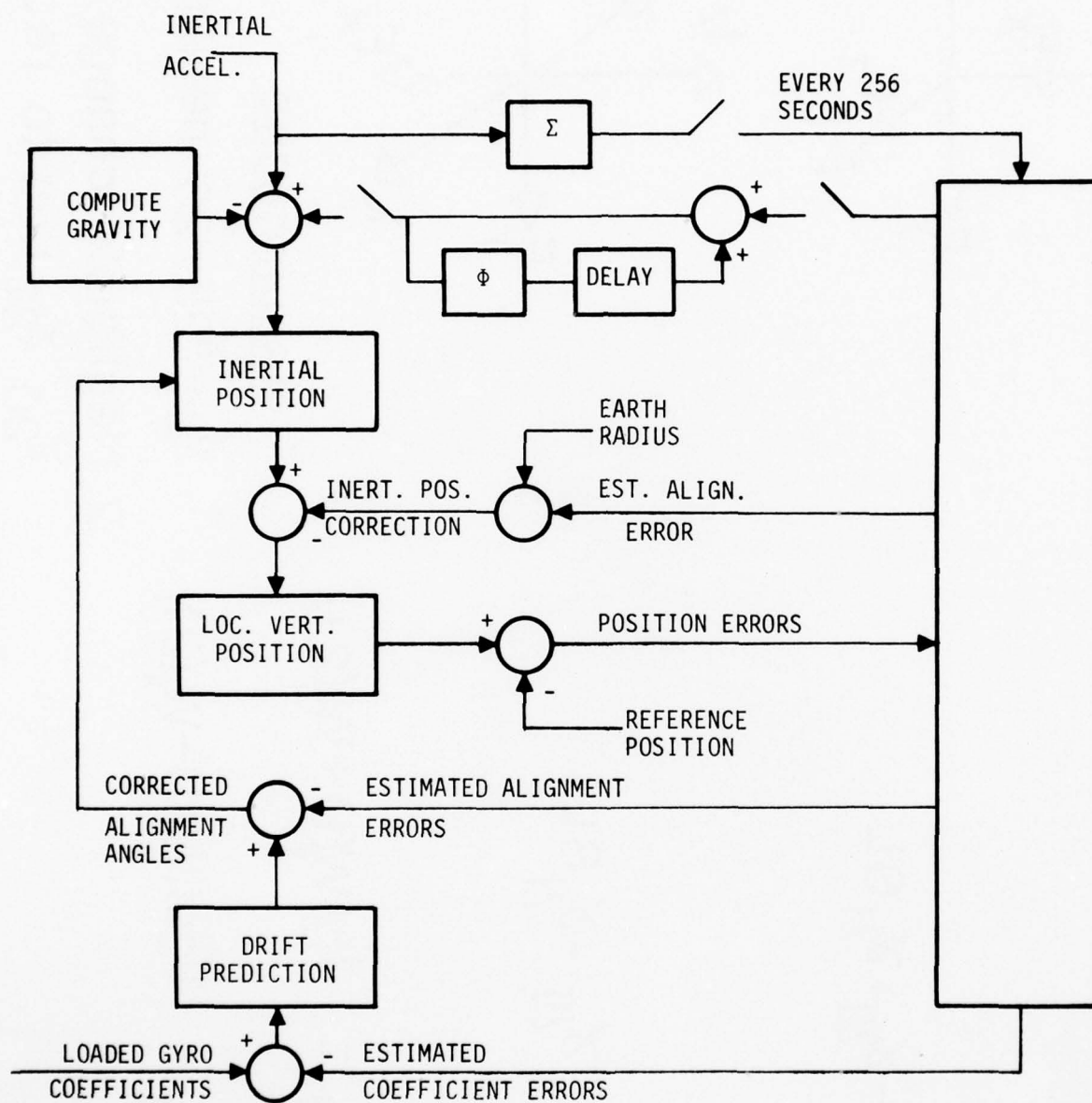


Figure 8

CALIBRATION/RESET FILTER STATES

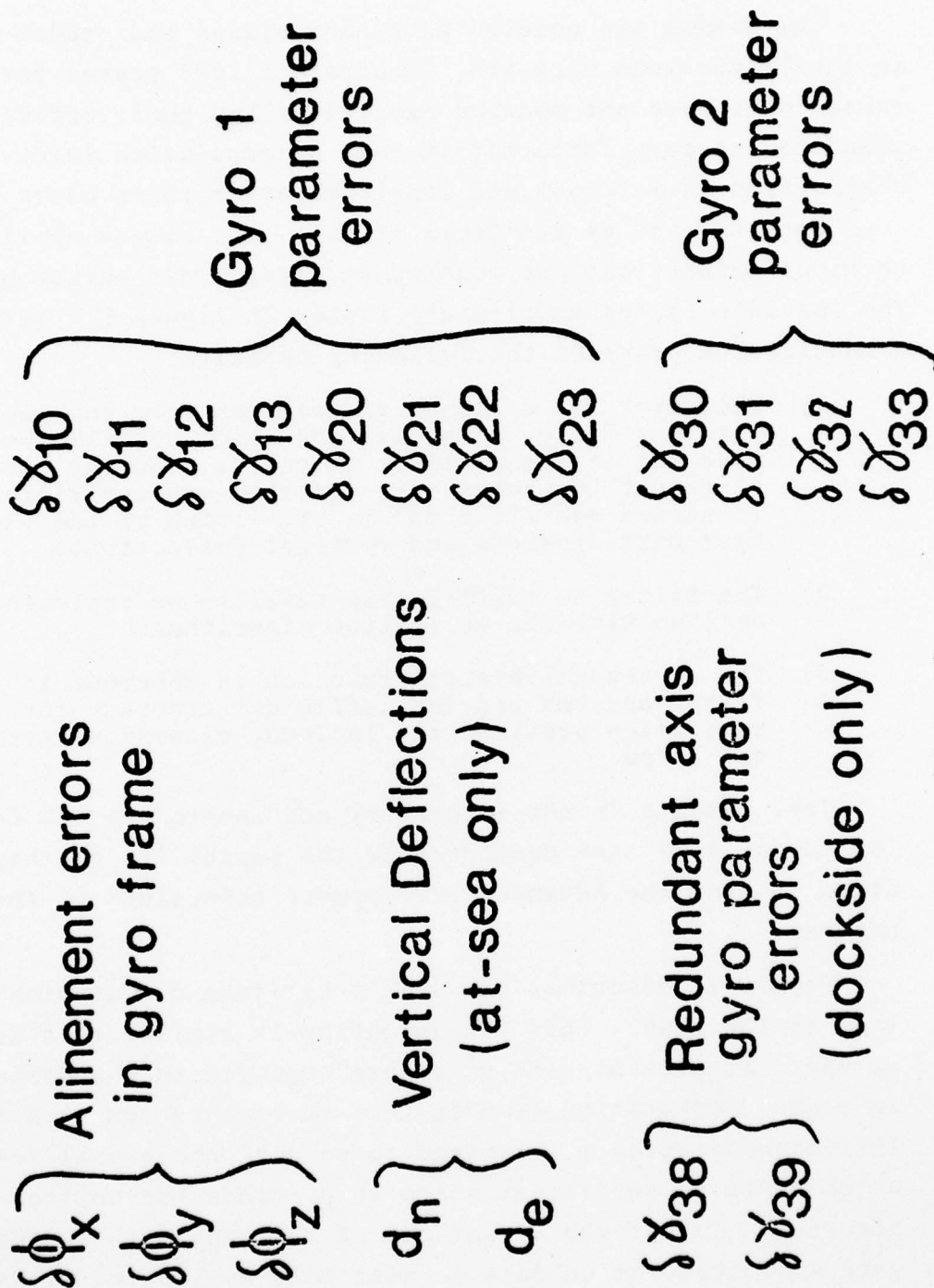


Figure 9

The gammas are modeled as random biases and random walks in the filter mechanization. Separate filter states for the random walks are not modeled explicitly but their effect is added to the covariance matrix each extrapolation interval. The observation is latitude and longitude error taken every six minutes dockside and as available at-sea. For at-sea application vertical deflections are modeled as first order markov processes. The specific states modeled are listed in Figure 9. This filter mechanization provides the following benefits:

- 1) The reset and calibration functions are combined into one filter mechanization which can also be used for at-sea platform alignment. During fine alignment the covariance for the gyro coefficients is zeroed and all error is attributed to the platform misalignments and vertical deflections.
- 2) The filter is sufficiently small to be implemented on-line with the navigation algorithm.
- 3) The at-sea calibration function is inherent in the filter and can provide sufficient accuracy for navigation provided the latitude excursions are not large.

Test results in the laboratory and aboard the USS Compass Island (AG 153) have demonstrated the capability of this mechanization to meet the Advanced Development objectives of the ESGN program.

Figure 10 describes the ship's attitude computation as mechanized in the ESGN. This mechanization is similar to a Kalman filter except that pre-computed gains are employed in the mechanization to reduce computation time as this routine is run at a 32 Hz rate. This mechanization is required to smooth the gimbal resolver data which contains sufficient noise to preclude the desired attitude accuracy. One of the advantages of this approach is that attitude rate and acceleration data is also made available. This data can be utilized by navigation users to avoid a data senescence problem in their application.

ATTITUDE FILTER BLOCK DIAGRAM

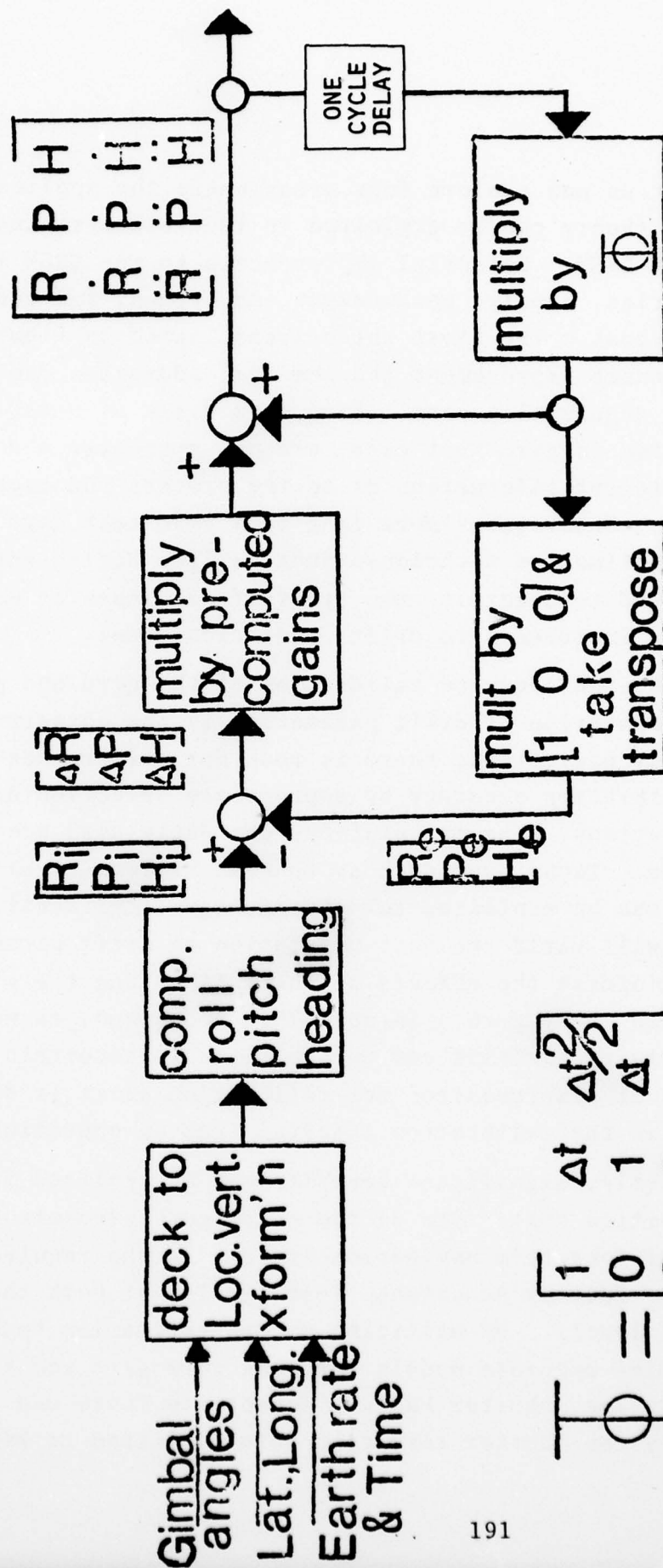


Figure 10

Let us now explore four areas where the application of estimation theory can be exploited in the future to improve the end product ESGN. Potential improvements to the ESGN fall into two categories, namely, performance improvement and reduced acquisition cost. The first three areas listed in Figure 11 address performance improvement and the last addresses one method to reduce acquisition cost. Long term drift effects, which are exhibited in gyro test data, are not currently modeled due to insufficient information as to the process and magnitude of the effect. However, as more long term gyro test data becomes available, estimation techniques such as Time Series Analysis can be exploited to determine the types of processes at work and provide an improved gyro drift prediction model.

Since an accurate calibration of the gyro and particularly a good separation of drift parameters is the cornerstone to high accuracy navigation, there is room for performance improvement in calibration accuracy by appropriate selection of calibration orientations. The orientations currently used are by no means optimum. Techniques such as General Maximum Likelihood Estimation can be exploited to determine gyro calibration orientations which will yield the best separation of drift parameters and which will minimize the effects of not calibrating the g-squared coefficients every gyro spin-up. This technique, as well as covariance sensitivity analysis can be exploited to ascertain the optimum amount of time required for calibration as it is desirable to minimize the calibration interval from an operational viewpoint.

Lastly, significant benefits can be realized from reduced acquisition cost. One of the major cost elements in the procurement of long term navigation systems is the requirement to have lengthy Factory Acceptance Tests (FATs) at both the gyro and system levels. By utilizing modern estimation techniques to determine accurate models for long term gyro and system error propagation, shorter Factory Acceptance Tests can be devised whereby the shorter term test data is fitted to known error models

FUTURE APPLICATIONS

◯IMPROVED GYRO ERROR MODELS

◯OPTIMIZE CALIBRATION ORIENTATIONS

◯OPTIMIZE CALIBRATION TIME

◯SHORTER FACTORY ACCEPTANCE TESTS

Figure 11

AD-A045 603

SYSTEMS CONTROL INC PALO ALTO CALIF

F/G 15/7

PROCEEDINGS OF THE SYMPOSIUM ON CONTROL THEORY AND NAVY APPLICA--ETC(U)

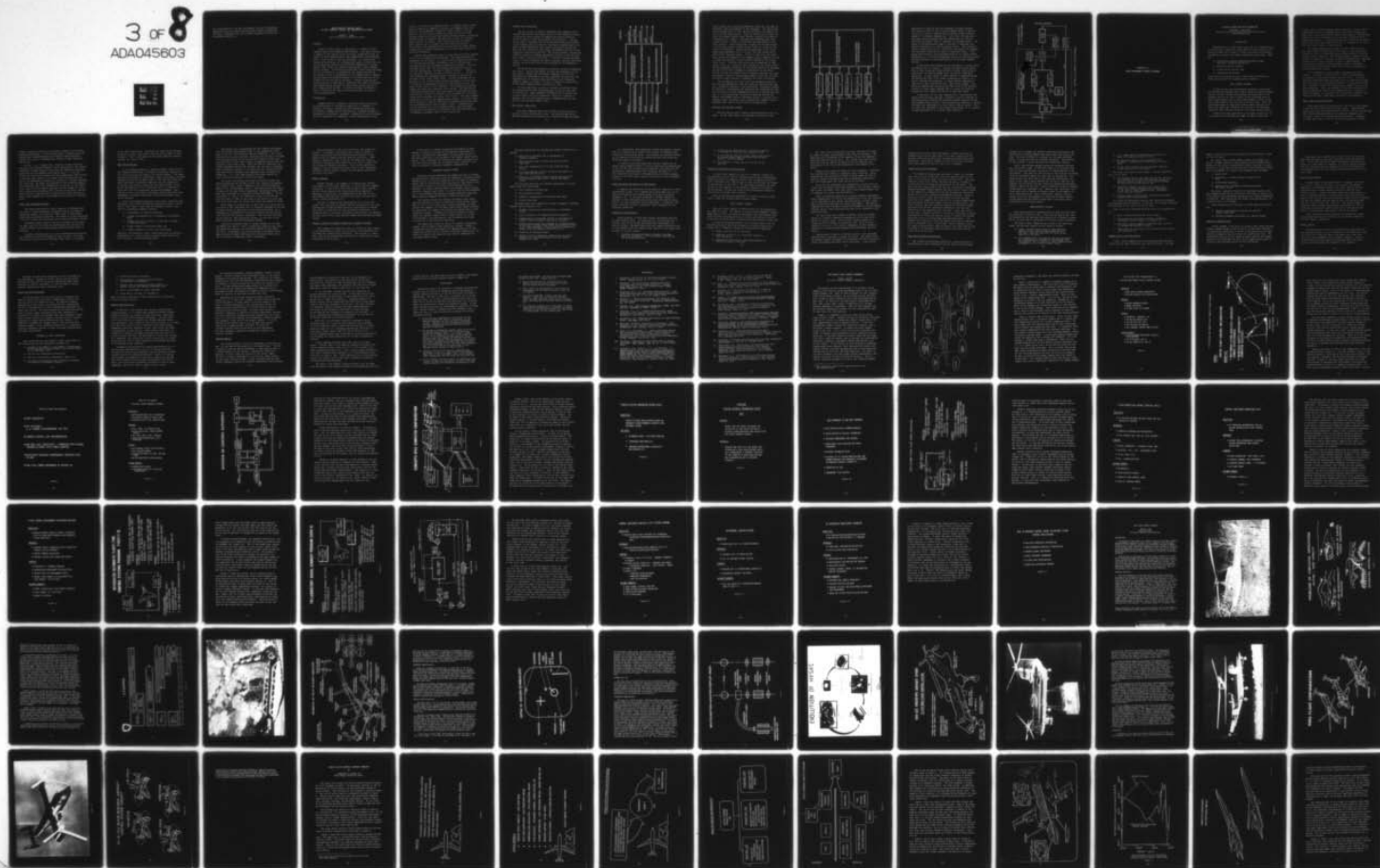
AUG 77 M D CILETTI, J S TYLER

N00014-72-C-0327

NL

UNCLASSIFIED

3 of 8
ADA045603



and extrapolated for the full performance interval to determine compliance with procurement specifications without compromising the Navy's confidence that the accepted equipment will meet the procurement objectives.

APPLICATION OF CONTROL THEORY IN NAVY COMMAND, CONTROL AND COMMUNICATION SYSTEMS

ROBERT C. KOLB
Naval Electronics Laboratory Center

ABSTRACT

Control systems theory is applicable to a number of Navy Command, Control and Communications problems. This paper provides a summary of the control system work being conducted at NELC in support of Navy Command Control and Communication system developments. Three areas of work are presented: (1) surface-ship navigation processing, (2) shipboard multisensor correlation, and (3) pointing and tracking for narrowbeam communication systems. Kalman filter theory has numerous applications in Navy Command Control Systems. The navigation processing system being developed for use on destroyers is presented as an example application. This Kalman filter is implemented in the command control computer. The multisensor correlation problem is described and some of the current work in the area is outlined. A typical pointing and tracking system is described to illustrate the control techniques and hardware being designed for future Navy optical and microwave communication systems. A universal digital controller is used to illustrate the impact of microelectronics on control system implementation.

INTRODUCTION

Command control is defined as the acquisition, processing and dissemination of information required by a commander in planning, directing, coordinating and controlling operations. In the Navy, command control functions are performed through an arrangement of personnel, equipment, communications and procedures which are employed by a commander in the accomplishment of his

mission. On major Navy combatant ships, a command control system, which is made up of computers, displays and communication links helps the ship commander perform his combat mission. The capabilities of this system include the processing of data from ownship sensor systems and from remote platform sensors, displaying processing data to command, and providing a means of assigning weapon systems to targets. The threats faced by the surface fleet require them to respond very accurately and rapidly. This requires the command control system to process large amounts of data and to respond automatically to threats that satisfy pre-specified conditions.

Control and estimation theory is applicable to several aspects of the at-sea command control problem. Three applications are summarized in this paper: (1) surface ship navigation processing, (2) shipboard multisensor correlation, and (3) pointing and tracking systems for narrowbeam communication systems. The first two applications deal with the acquisition and processing of tactical information. In today's complex threat environment, it is especially important to make use of all available data and to take advantage of overlapping sensor coverage to improve the estimate of the target state vector. Accurate knowledge of the position of all of the friendly forces operating in a task force is necessary if meaningful pooling of data held by each of the units of the force is to be achieved. The navigation processing example presented here addresses this problem. The multisensor correlation problem deals with the process of combining the data from multiple sensors to establish a non-redundant set of system tracks and to estimate the target state vector. The final example, pointing and tracking for communication systems, is used to illustrate the type of control techniques and hardware being developed for narrowbeam optical and microwave systems. Communications are an essential part of the command control, and narrowbeam systems have the potential of providing this required capability in jamming environments and in covert operations.

SURFACE SHIP NAVIGATION

The new classes of surface combatants have command control systems that process the outputs of all of the navigation sensors to obtain the best estimate of ownship position and velocity and the velocity of the ocean current (see Figure 1). The processed data is available for use by the other processing modules in the command control system, by the ship's navigator and by the other systems aboard ship that require navigation information. NELC has been involved in the design, development and test of the navigation system on the DD-963. The system includes a navigation satellite receiver, an Omega navigation receiver, a gun fire control system, a gyro and an EM log. A six-state linearized Kalman filter is used to estimate the ship's position, velocity and ocean current set and drift from the data provided by the navigation sensors.

The DD-963 and the navigation system are currently undergoing sea trials. Initial indications are that the navigation system will greatly enhance the operational capability of the ship. Throughout the development, the most difficult task has been the implementation of the processing algorithms in an integrated computer complex (4 AN/UYK-7's) that is required to perform all of the other command control processing as well.

The next generation system will include the NAVSTAR Global Positioning System (GPS) being developed by the Air Force for tri-service use. When completed, NAVSTAR GPS will provide very accurate global satellite navigation. NELC has a program to develop a low cost GPS receiver and to integrate this new capability into the Navy Surface Fleet.

MULTISENSOR CORRELATION

Most Navy combatant ships have several active and passive sensors in their surveillance suite. The type and quality of the data provided by the sensors are a function of many variables

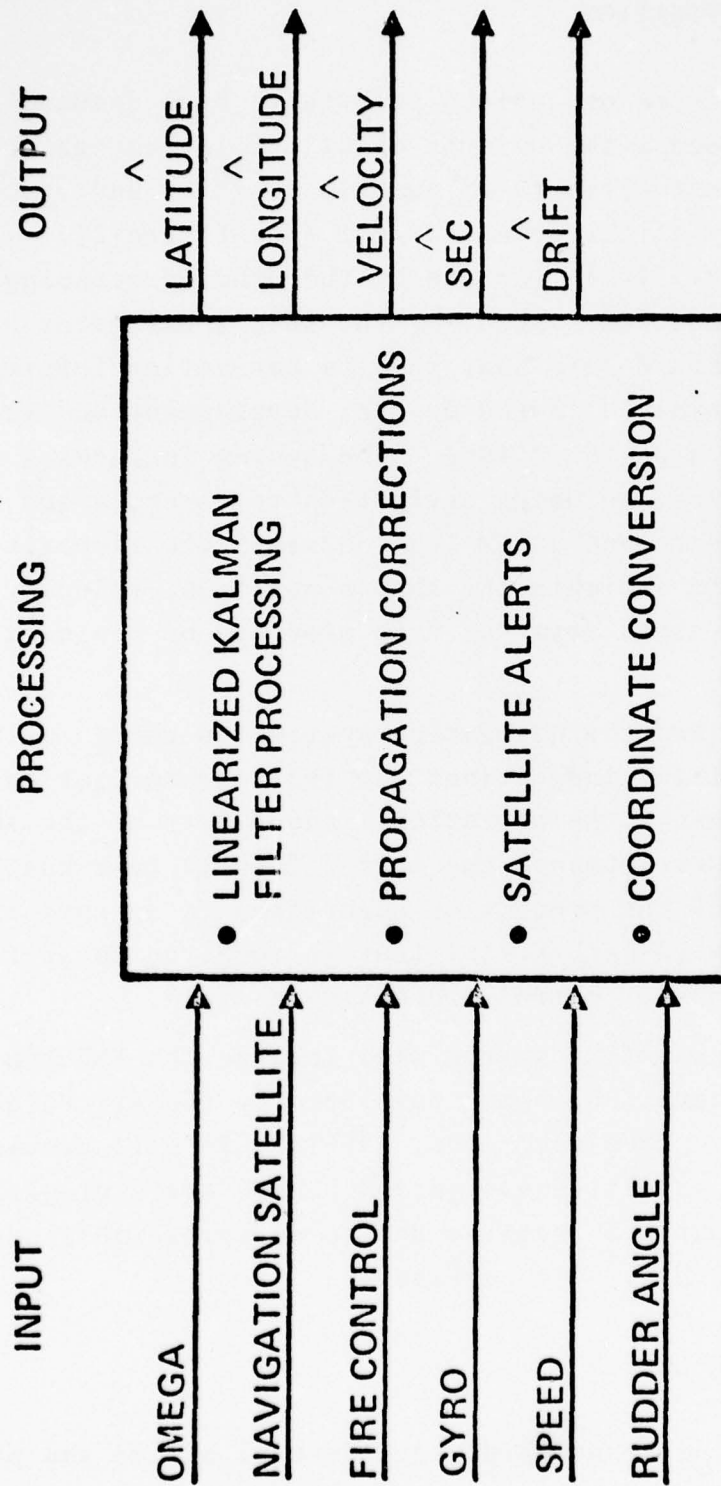


FIGURE 1. SURFACE SHIP NAVIGATION PROCESSING

which include the varying environmental conditions, the mode of operation, and the readiness of the equipment. The operational decision maker needs to have the best available information for use in his decision process. Since no single sensor always provides the highest quality data, the most accurate and complete information on a target is obtained from combining data from several sensors. Figure 2 illustrates the multisensor correlation process. After a detection is made, the new data report is associated with an existing target track or a tentative new track is established. Tracks may be maintained by the sensor processing equipment, and as a result, the same target may be held by more than one sensor. If this is the case, the redundant tracks are combined in the command control computer to form a single and hopefully a more accurate estimate of the target state vector. This new state vector may be augmented by additional states as a result of this combination, be revised based on the measurements provided by two similar sensors, be unchanged and one of the tracks dropped or combinations of the above. Current systems use various forms of gating techniques for report correlation, fixed or variable gain Kalman filters for tracking and mostly simple heuristic techniques for track correlation.

The introduction of sensor that have automatic detection and tracking capabilities into the Fleet has increased the need for a systematic approach to the multisensor correlation problem. In addition to determining the algorithms for combining the data, the structure of system implementation poses an interesting problem, i.e. determining the division of functions between the sensors and command control, designing sensors to operate in an automatic mode, designing sensor equipment and command control equipment that can be used in various configurations.

POINTING AND TRACKING SYSTEMS

NELC has had an active control system program for over ten years. In the early 1960's, the program was focused on the

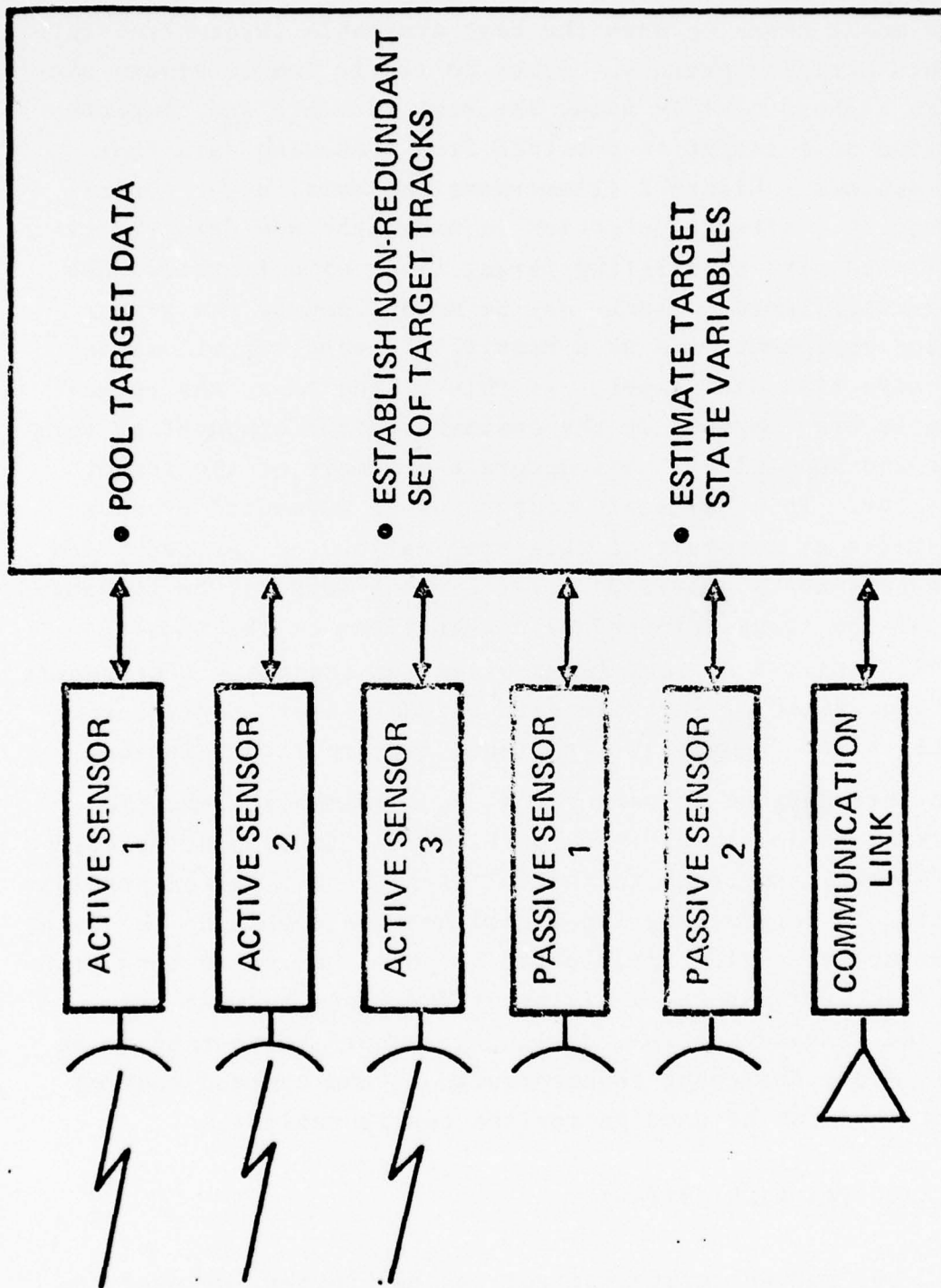


FIGURE 2. MULTISENSOR CORRELATION

application of digital control techniques in weapon systems. This led, in 1965, to the successful demonstration of digital control of a missile launcher using a general-purpose digital computer for dynamic compensation. Since then, the same basic dual-mode control approach has been demonstrated on several different gun mounts, missile launchers and antenna drives. The advent of microelectronics made it feasible to implement the control algorithms in a special-purpose device. The controller could be adapted for use in a particular application by changing the controller coefficients stored in read-only memory. Even though the controller was developed primarily for weapon system applications, it is readily adaptable for use in the pointing and tracking systems for narrowbeam optical and microwave communications.

A functional block diagram of the controller is shown inside the dotted lines in Figure 3. Because the power drives applicable to this design are characterized by torque (acceleration) saturation, the control scheme used is based on a dual-mode operation. A large signal or coarse control is employed during the period the plant is in torque saturation to bring it to a nearly synchronized condition. A linear control algorithm is then used in the relatively narrow, small signal region. The additive compensation section serves both as an aid in synchronization to large signal commands and as a means of achieving essentially zero steady-state error to ramp-type inputs.

A controller of this type coupled with a stabilization and acquisition processor provides a flexible, low-cost solution to the acquisition, pointing and tracking problems posed by narrowbeam communication systems. The microprocessor promises to provide even more cost advantages for this type of control system. Cost is especially important in this application because it is required on many platforms if it is to be truly effective.

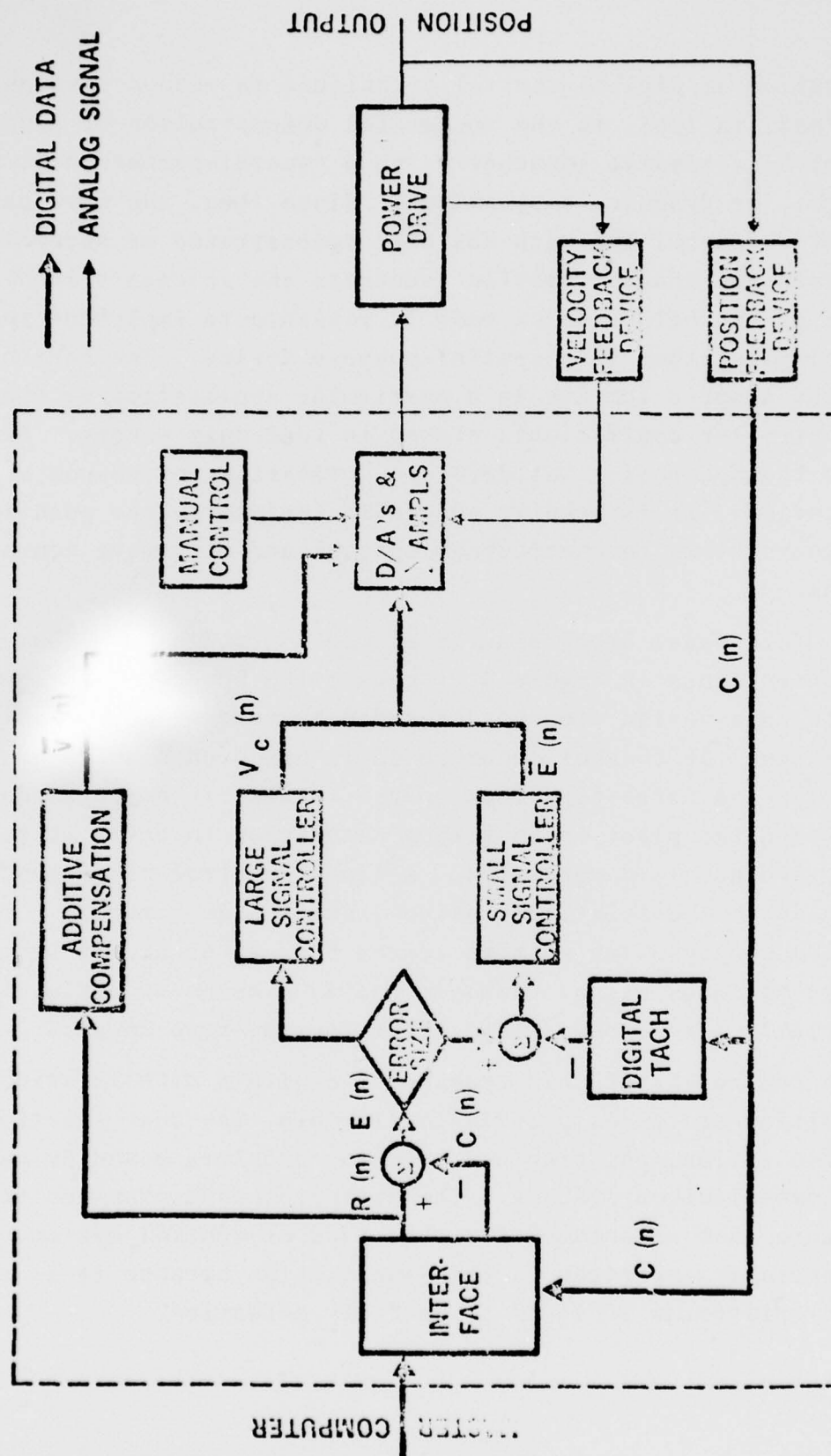


FIGURE 3. FUNCTIONAL BLOCK DIAGRAM OF DIGITAL CONTROLLER

SESSION III
OTHER GOVERNMENT CONTROL PROGRAMS

STATUS OF MARITIME SHIP AUTOMATION

THEODORE J. WILLIAMS
Purdue Laboratory for Applied Industrial Control
Purdue University

INTRODUCTION

Automation of the operational functions of a commercial ship or of the transit operation (non-combat) of a naval ship can be readily divided into a number of areas and indeed are generally considered as such by the company undertaking such tasks. These are:

- 1) Ship Control Systems (generally meaning bridge functions including navigation),
- 2) Machinery Control Systems,
- 3) Cargo Control Systems, and
- 4) Administrative Systems

These will be discussed in turn in this report followed by a brief discussion of the economic factors involved.

SHIP CONTROL SYSTEMS

As fast as new ship navigational equipment is developed, new navigational problems also seem to arise with equal rapidity. The most serious navigational problems existing today in the merchant service are those related to the increasing size of ships, particularly the so-called supertankers, and the extensive traffic density one can find in certain areas. Also, the increasing number of high speed surface effect vehicles will have to be given more attention as a result of the hazardous conditions that they may create for the slower moving vessels.

Recent tests have shown that it can take a distance of up to two miles for a 200,000-ton tanker to make a crash stop

without special control features being available. Devices may be constructed to allow a somewhat shorter controlled stopping distance, but so far these have not been widely applied. The physical dimensions of the supertankers can also cause a problem during docking operations. A reliable navigational system thus must keep these ships safely away from all hazards of grounding or of collision with other ships or fixed objects.

One common example used to show the high traffic density that the present day ships may have to face, is the Dover Strait. Frequently, 50 to 100 ships have been spotted within a five-mile radius of one's own ship. The constant growth in numbers of the world's shipping will soon pose an almost impossible anti-collision problem for the ship's officers to solve by hand methods. The only possible solution to this problem is then to implement efficient and safe automatic anti-collision and anti-grounding systems onboard the vessels.

It is becoming ever more urgent to optimize the ships' routing. In order to accomplish this, better instrumentation is necessary to give more accurate position fixes. In recent years new innovations have been made that are expected to accomplish these tasks in a satisfactory manner. At the present time, only a handful of ships carry significant examples of any of the above equipment. These are prototype ships with increased automation launched by a few of the leading nations in shipping. A rapid development is expected in the coming years, however, once these systems have proven their reliability and usefulness.

Ship's Anti-Collision Systems

Radar-based anti-collision devices have been in development by the Air Force and the Navy for many years. Companies have gained experience from these military systems, and are now offering well tested although perhaps still somewhat inadequate anti-collision systems for merchant marine application. Companies in Japan and Norway as well as the United States have tested

computer-integrated radar anti-collision systems for use onboard merchant marine ships. An increasing traffic situation and a projected future reduced manning will without a doubt eventually require this type of instrumentation onboard through regulatory body decree.

In Ref. 1 it is claimed that, "analysis of many collisions indicates that the main problem in radar navigation is the limited capability of human beings in utilizing the information available on the PPI with an adequate speed and accuracy." It is also stated that one of the problems with the conventional radar system is that the radar picture is a present-value presentation only, and as the measurements normally are relative to a moving reference, one's own ship, the human interpretation of the situation depends on considerable skill and concentration on the part of the ship's crew. Most of the presently available devices attempt to correct this situation by presenting both a history of own ship's and the other vessel's track and also a projection of future position as well as the computation of the probable closest point of approach (CPA).

Ship's Anti-Grounding Systems

The reports published by Lloyd's Registry of Shipping indicate that a larger percentage of shipping hazards are caused by groundings than by collisions with other ships or from damage caused during docking and mooring. The reason is given as piloting errors and insufficient detection and navigation equipment onboard.

Reasonable depth sounders have been available on the market for many years but they have the disadvantage that they are not forward looking, thus a sudden danger appearing ahead cannot be detected.

The anti-stranding sonar is a set of equipment for detecting the condition of sea bottom ahead of ship, by way of the transmitting and receiving of an ultrasonic beam, which is installed

at the ship's bow bottom. The detection range for the forward direction is about 2,000 meters, and for a water depth of about 60 meters. This is well short of the normal required stopping distance for large vessels.

Open Sea Navigation

As the shipping industry is meeting stronger competition in the transportation market, it becomes increasingly important to sail the ship across the oceans in an optimal manner. This means essentially to minimize a performance index consisting of the most important ship route variables such as time and fuel within the given constraints of weather conditions and ship capability. An optimal ship routing system like this cannot permit a navigation inaccuracy of 10 to 20 nautical miles, as sometimes is true today with the conventional navigation equipment. One problem is thus, to be able to determine accurate position fixes independent of weather conditions, such that an optimal route can be followed.

Today an overwhelming majority of all ships, both naval and commercial, solve their navigational problems by using a collection of "gray boxes" rather than an integrated system. This suite of instruments commonly includes:

- 1) A gyrocompass to determine heading,
- 2) A simple log (mechanical or electronic) to determine speed,
- 3) A LORAN-A or Decca receiver, a radar and a sextant to determine speed,
- 4) A depth sounder to determine depth, and
- 5) A human navigator to do all the calculations.

Typically, the results of such a navigational unit are position inaccuracies of 2 miles at best, and more often than not up to 10-20 miles, in the broad ocean areas.

The extreme case, representing the very highest performance that can reliably be achieved today, is the navigation system used in the U.S. Fleet Ballistic Missile Submarines. For a very high price this system provides continuous data on ship's attitude, position and velocity to the missile fire control system with a precision that is more than an order of magnitude better than that achieved in most other ships. While the devices themselves are indeed remarkably precise and reliable, the real key to achieving this navigational accuracy is to treat them as a system from the start and thus to integrate and complement their strengths and weaknesses. It is this same approach that holds promise for ships' navigation generally in the years ahead.

The recent innovations that hold the greatest promise for marine navigation are the Omega system [3], satellite navigation [4], Doppler sonar, digital computers, and inertial navigation. Omega is not an innovation, since it represents merely the latest-to-mature of the many kinds of hyperbolic navigation systems that have been developed in a continuous stream from LORAN-A. On the other hand, it truly is an innovation in that it can provide position fixes to ships on any ocean in the world, at a cost and with an accuracy that can satisfy most naval and commercial needs.

While Omega can provide day or night fixes to a precision of two miles or less, and while this is certainly adequate for all but the most unusual of operations in the broad ocean areas, it is inadequate for navigation in restricted waters, and for specialized tactical and strategic operations. Here one must fall back on more precise radio navigation systems, or else turn to the next innovation, satellite navigation systems.

Satellite navigation today is largely thought of in terms of TRANSIT [6], the U.S. Navy's pioneering system of polar orbiting satellites that has so successfully opened up this whole new field. Like Omega, this system provides a worldwide coverage, but with the major difference that position-fixing errors can be an order of magnitude smaller than Omega.

Other approaches to the use of satellites may change this picture. For example, the present Navy system is based on complex calculations derived from precise measurement of the Doppler shift in signals received from the satellites. Other technical approaches, such as the use of range data from synchronous or medium altitude satellites, may lead to simpler and less expensive shipboard receivers. Thus, quite significant changes in the use of satellites may result in this innovation becoming a central feature of most ship navigation systems by the end of the 1970's.

Weather Routing

Weather routing is an example of a routine that involves large amounts of data and, therefore, is well suited for computer processing. It has usually been carried out by shore stations and the results given to the ship master before departure. Updatings or corrections are communicated to the ship at sea. Considerable time has been saved for the vessel by using these special routing procedures [7].

The idea is based on the determination of a "least time track" from a forecast of weather and sea conditions for the area covering the sailing distance and from a description of allowed ship speed as a function of ocean and weather conditions. Although the object is usually to minimize sailing time, the methods can also lead to less cargo and hull damage and increased personnel comfort.

Channel, Coastal and Harbor Navigation; Automatic Docking

The problems of navigation today are related to heavy traffic in restricted waters, where ever-increasing ship dimensions can only make the situation more difficult. The interest is, therefore, centered on navigational aids that will contribute to safe navigation in these areas.

A discussion of "channel navigation and docking of super-tankers" is given in [8] and the navigational requirement of any ship, including the supertanker, are also given in Ref. 9. The deep ocean area is also germane to the subject under investigation. The requirements for coastal and channel navigation are such that their problems are of similar origin, and their solution is achieved by identical equipment configurations.

MACHINERY CONTROL SYSTEMS

Propulsion system automation and computerization is probably the most popular application area for automation in shipping today. Automation got its start on shipboard with the push for unmanned engine rooms by Det Norske Veritas starting in 1964, which action was quickly followed by the other Classification Societies. Likewise, the engine room has been a very popular early starting point for computer applications, as witness the T/T SEA SOVEREIGN and T/T SEA SERPENT experiments of Kockums Mekaniska Verkstads, Salen Shipping Companies and ASEA in 1969 and later [10].

The obvious similarities between stationary power plants and ship propulsion systems (in particular steam turbine ships) make it very easy to believe that similar advantages to those gained with computers in stationary power plants could be gained by application of computers for control and supervision of ship propulsion systems. Although the control problems on diesel ships are somewhat simpler than on turbine ships, it is also believed that a considerable gain can be obtained for these, particularly in insuring safer operation.

The propulsion systems on ships are normally considerably smaller than stationary power-generating systems. However, considering the high requirements for maneuverability of ship propulsion systems and the variable conditions onboard ship, the extent of control and supervision may well be comparable to stationary power plants.

The main motivations for introducing computer control are as follows:

- 1) Reduction in personnel due to automation of operator routines,
- 2) Safer operation due to faster and more reliable reactions,
- 3) Less fuel consumption due to more efficient operation,
- 4) Less down time due to early discovery and repair of worn and defective parts,
- 5) Reduction in invested capital through allowing more critical designs under better control and supervision.

The principal functions for computer application in a ship engine room are listed below:

- 1) Data logging and processing,
- 2) Safe operating system,
- 3) Automatic sequencing of startup and shut down,
- 4) Control functions.

The gains that can be expected by using a computer to perform various control functions are:

- 1) Economic savings and simplifications in instrumentation,
- 2) Great flexibility in changing control parameters,
- 3) Compensation for nonlinear effects in and undesired response from instruments and process actuators,
- 4) Modern control based upon computed or estimated values of physical variables which cannot be measured directly (e.g., flow, enthalpy). State variable estimation by Kalman filtering should be noted here [11].
- 5) Extension of operation range,
- 6) Adaptive control (automatic compensation of control parameters as physical parameters as the "plant" changes with time).

For conventional ship propulsion systems the greatest improvements are expected to be found in the control of turbine boiler systems on steam turbine ships. For instance, an improved control of the drum water level and its shrink and swell may extend the operating range of the boiler.

It should be mentioned again that the most common form of engine room automation today is to have sufficient instrumentation to satisfy the ship classification societies' specifications for periodically unmanned engine room, being EO, MO, UMS, etc. A more detailed description of the application of digital computer control of the ships power system will be given in the subsequent sections.

Alarm Functions and Control of Auxiliaries

A computerized monitoring system should be superior to a more conventional system. In a computerized system great care can be taken to eliminate false alarms during start-up of auxiliary equipment, etc. It has been attempted to include diagnostic programs in the alarm monitoring system such that when an alarm arises, the alarm condition can be pinpointed. In addition, the alarm system has variable (dynamical) limits depending on the operating conditions.

Propulsion System Control

Steady progress is being made towards unattended operation of steam turbine ships. An essential part in achieving this is careful study of the design and engineering requirements for control systems. The main reasons why most modern merchant ships are now being fitted with remote bridge control of the engine room is given in [12] as follows:

- 1) A quicker and more consistent response to bridge orders is obtainable. This facilitates maneuvering and berthing operations.

- 2) A more precise speed control is possible, and this is valuable on occasions when keeping station.
- 3) It is essential that the bridge officer have control of the main engine when operating with the main machinery spaces attended.
- 4) The engineer is freed from his position at the controls.

Condition Monitoring and Maintenance

A recent major emphasis in the use of computer systems for the machinery area is that of condition monitoring and maintenance prediction where the computer collects data on engine and auxiliaries performance over long periods of time and develops the trends in the readings of this data. The resulting information can then be used by the computer or the engineers themselves to predict when a machinery failure may occur or when maintenance should be carried out to prevent such a failure.

Such systems have been developed for diesel systems and much work is under way to apply them to steam systems.

CARGO CONTROL SYSTEMS

There are often a number of possibilities for distribution of the cargo in a ship. The choice of a particular arrangement should, among other factors, be based on achieving a load distribution that gives the best sea-going qualities possible and results in forces on the ship structure that are below certain permissible limits [13].

In order to determine measures for sea-going quality and the resulting action on the ship structure for a given cargo distribution, one is frequently faced with the problem of computing:

- 1) Depth, trim and list of the ship,
- 2) Stability of ship (e.g., metacenter height or other measures),
- 3) Magnitude of shear forces and bending moments at various sections of the ship.

The static forces acting upon the ship structure are caused by weight of cargo, steel weight of the ship, and buoyancy. The magnitude and distribution of the buoyancy forces are dependent upon depth and trim of the ship. For a given cargo distribution, depth and trim are implicitly given by the two equations for equilibrium of the forces and equilibrium of the moment of the forces.

Because of the implicit nature of these equations, a considerable computational effort is required to get a solution. These computations also necessarily involve a large number of data to describe weight distribution and the relationship between buoyancy and displacement (for each section of the ship).

As an aid for performing such computations, special devices called load calculators have been developed. For instance, approximate values for depth, trim, shear forces and bending moments can be computed for a given load distribution.

With the computing capacity of a digital computer available, these computations, as well as the computation of list and stability, can be performed in more detail and with greater accuracy, which may be especially important for large supertankers. The digital computer also offers greater flexibility through its stored program feature, while a load calculator will have to be tailored to each particular ship.

For bulk cargo this computer procedure could be extended further to include a complete determination of the best distribution of a given cargo. Since the best loading condition is characterized by a number of objectives with regard to trim, stability list, etc., the relative importance of each should be defined in a criterion whose maximum should determine the best choice.

Monitoring of stresses in the hull can be a very important addition here, especially in heavy sea states. The shear forces and bending moments determined in connection with the load calculations are nominal and under static conditions. To get better

account of the actual static and dynamic stresses occurring in different parts of the ship while at sea and in heavy wave conditions, these can be physically measured and continuously monitored [14]. The digital computer is well suited for recording such large amounts of data by statistical techniques.

Tanker Loading and Unloading

The problem of loading and unloading a tanker in a minimum time, and still be within the stress and bending limits of the hull, is very real in today's shipping industry [13]. The cargo handling systems will include the function which is normally carried out by the analog load calculators on the market. The data from the shipyard where the ship was constructed, concerning maximum allowable bending moments and shear forces, can be stored in the computer for comparison with the measured and calculated values for a certain loading and unloading operation. Based on the ship officer's input data with regard to cargo and ship properties, the computer can calculate all necessary bending moments and shear forces and suggest a specific loading plan. The ship's officers and crew could now perform an efficient loading operation based on the calculated information, but this will seem to carry the automation only half way. Since very little of the ship's computer capacity is utilized at the dock, it would seem natural to allow the computer system to control the loading operations such as starting pumps and operating valves. The computer will then be on-line, and making continuous calculations based on measured levels in each tank. Such a computer system for cargo handling will be able to minimize the time required for a loading or an unloading operation while still observing all stress restrictions [13].

Cargo Ship Loading and Unloading

The loading and unloading problem for a cargo ship may be characterized as quite different from the tanker cargo handling

problem [15], although the problems concerning measurements and calculation of bending moments and shear forces may be much the same. The major problem is to account for the many different pieces of cargo destined for different locations. The solution of this problem is called destination-preferential loading.

One of the problems making loading and unloading difficult on a cargo liner today, is that very often it is not known what kind of cargo and how much is going to be loaded onboard in the next harbor. Only when the ship arrives at the dock can one obtain reliable information about the cargo and its destination. The cargo officer must then feed in the new cargo information, and based on the cargo already onboard and the ship's capacity, the computer will calculate the most efficient loading and unloading program. Where the ship has a regular schedule, on-shore computers could handle this important task. However, the "nonlinear" situation would seem to demand an onboard system if the computer is to be used effectively. Such systems must, however, wait on further electronic developments to radically increase computer system capacities and further reduce their cost before such a system will be an economic payout.

ADMINISTRATIVE SYSTEMS

Fleet optimization is becoming more and more desirable from the ship owner's point of view. To be able to know at any time the location of the ship and what progress it is making is important in the home office scheduling of the ship's future operation.

The ship-to-shore communications system is not much used today, and the main reasons can be listed as follows:

- 1) Today's decentralized method of ship operation requires little contact between home offices and ships, when the ships are not close to the coast or in the dock.
- 2) The communications can often be poor and unreliable as a consequence of ionospheric fluctuations and disturbances, and is limited to radio communications, telegraph, or to a limited extent, telex.

- 3) It is cumbersome to obtain contact from ship to shore (for reading of traffic lists).
- 4) The passenger traffic is decreasing and the passenger's communications requirement is usually small.
- 5) Private calls between the crew and their families is not covered by the ship owner.

The future will require some changes. The most important are as listed here:

- 1) The changing form of ship operation and the resulting short periods at the dock will probably require an entirely different type of routine contact between the home office and the ship at sea.
- 2) Satellite transmission will in the future give stable and reliable communication of high quality at any time for radio communications, telegraph, telex, data and facsimile.
- 3) Systems with a selective call could ease the traffic sequence problem considerably.

The shipboard management functions that should be performed by the onboard digital computer, if present, are not much different from the ones we are used to seeing on shore.

Some of the most important functions that can be handled are [7]:

- 1) Work in connection with the ship's cargo,
- 2) Calculation of crew wages, overtime, income tax deductions, social security, insurance, etc.,
- 3) The ship's stores (supply of food and other articles of consumption onboard the ship),
- 4) Other functions that have to do with the crew's health and condition, etc.

Communications with Home Office

Today, little communication is performed between the home office and the ship, especially over large distances. The main

reason is that the quality and reliability of the present system are not very good.

The future form of fleet administration will probably require a stronger control of ship operation from the home office. Because of the capital concentrations which a ship and its cargo represents, it may even be necessary for a daily detailed control. Such a development will require interchanging data regarding:

- 1) Engine hull
- 2) Navigation, including optimal routing of the ship
- 3) Loading and unloading
- 4) Administrative information concerning payroll and ship's stores

The ship's computer system can be connected directly, such that communications can be carried out from shore to ship or vice versa without requiring human intervention if routine information is required. The transmission may either occur periodically, at a present time, or on command.

Video transmission by facsimile or other means may be used for:

- 1) Analyses and warning of general and specific weather conditions
- 2) Shipping documents and others in a special format

Satellite Communications

A major element in the drive to secure a more stable and more capable communications system as well as a much wider bandwidth or transmission capability is versed in the possibility of using satellite communications facilities for maritime use [16]. The availability and use of the satellite makes possible and indeed practical the fulfillment of each of the communication needs expressed in the previous section of this discussion.

Experiments have already been carried out by the U.S. Maritime Administration on the early satellite systems developed by NASA. In the near future the MARSAT experiments carried out by ships of a large number of companies in several countries should show the true value of this technique and the best methods for its implementation [18, 19] looking toward widespread use by the early 1980s.

Payroll Calculations

A major source of potential benefit in manpower relations is to be up to date on the ship's crew payroll calculations. Questions are frequently asked by the ship's officers and men concerning their account content, especially when the ship arrives in port. A desire has been expressed by many people to have a shipboard computer to perform these calculations based upon all the various rules and regulations, which are well defined, but many and complex and the cause of much time consuming work for one or more of the ship's officers. The digital computer should be able to update such payroll calculations as often as desirable and the crew could be paid for all overtime at each port on arrival rather than one port late as at present.

Such calculations could naturally be performed in a background mode and would not interrupt any of the more important on-line computer operations.

Ship's Stores

Record keeping on stores and supplies and suggestions for new purchases before a trip is started or at the next port based on stores facts about the ship's consumption are tasks that easily can be programmed into the digital computer. Likewise certain functions with regard to maintenance and spare parts onboard can be handled and scheduled by the computer.

Programs like the above mentioned can also be valuable to the home office. Through the direct contact with the ship's teletype the home office can acquire information about these functions as often as desirable, in order to make an overall economic comparison of ship's operating costs.

Safety and Fire Protection

The United States was the first nation to recognize the need for specialized training for shiphandling of super-size vessels, and is now leading the way. The American company, Standard Oil of New Jersey, was responsible for establishing the first training basin to teach shiphandling techniques for super-size vessels. The major hazards of the seven seas and the world's busiest tanker anchorages have been reproduced in microcosm on an eight acre man-made lake near Grenoble, France. There, master mariners go through a two-week course to prepare themselves to handle the 100,000-ton and over vessels. In addition to Standard Oil Company masters, one other American shipping company, Lykes Steamship Corporation, is planning to send its prospective masters of their new large containerships now under construction.

ECONOMICS OF SHIP AUTOMATION

Some of the factors that should be taken into account in the consideration of ship automation economics are:

- 1) Savings in the number of crew members (alternatively attracting crew by the alledgedly less onerous duties in an "automated" ship)
- 2) The cost of "automation installation"
- 3) The cost of ownership, maintenance, spares, etc.
- 4) The value to be obtained from continuous recording for machinery maintenance diagnosis

- 5) Projected period of ownership
- 6) Any alteration in insurance rates directly attributable to "automation"
- 7) Benefits due to optimizing passage length (i.e. weather routing) and reduced turnaround time
- 8) Effect on government or other subsidies
- 9) Trade unions attitudes to "automation"

Some of the most important of these concepts will be discussed in the following sections.

Reduced Operating Costs

In addition to the obvious cost savings resulting from reduced manning, it is claimed that automation affords further financial benefits in respect to lower fuel costs, lower maintenance costs and fewer machinery breakdowns. In these areas it is very difficult to quantify the savings which may result from automation. With respect to fuel costs, however, it is clear that the close control of fuel viscosity, fuel valve coolant temperature and early detection of poor valve action will make a contribution to fuel savings. These control facilities are essential on furnaces and engines burning heavy fuel and it is in this respect that they can contribute to a major cost savings. On a steamship, the savings can be even greater than on a motor ship since fuel rate is highly dependent on operating the plant at the optimum design conditions.

Automation can contribute to reduced maintenance bills by insuring that the machinery is run at its design conditions, by warning of deleterious conditions, and by producing accurate records essential to planned maintenance. Again, the savings attributable to automation are not easily quantified, and the only valid evidence would be long-term comparison of similar ships, with and without automation, operated by crews of equal competence, and on the same or similar service routes.

The fitting of automatic control equipment, however, itself imposes a further burden on the maintenance load, as the control equipment itself must be maintained. The situations are further complicated by the fact that machinery installations have advanced in complexity in parallel with the fitting of the automatic controls. On some medium-speed-engined ships the increased cost of maintaining the engines has completely blanketed out any maintenance saving contributed by automatic controls, particularly where the engines are operating on heavy fuel [20].

Regarding the claim that automation reduces machinery casualties, it is clear that a highly reliable alarm system and control equipment to reduce speed or stop the engine in the event of serious malfunction, will substantially reduce the damage resulting from failures in critical services such as lubricating and cooling systems. On motor ships the most essential safeguards in addition to normal temperature, pressure and level alarms are scavenge fire and crankcase oil mist detection, h.p. fuel line leakage, and turbocharger vibration monitoring equipment in the case of the largest engines. It is the feeling of the authors that it will be many years before statistical evidence becomes available to assess the savings resulting from the provision of such safeguards, but most shipowners regard this expenditure rightly as an insurance premium.

Reduced Manning

The situation after 10 years of automation is discussed in Ref. 20, and some of the points will be repeated here. The most attractive claim for marine automation is that applied even in a limited degree, it will permit a substantial reduction in manning. At first sight the statistics are fairly simple: the basic technical requirements to be met are remote control of the engine from the bridge; a highly reliable machine alarm system; automatic control of essential temperatures and pressures;

the maintenance of electrical supplies; and an adequate fire alarm system. The majority of new ships built in the last year have been fitted with some of these basic control elements, and engine room complements are generally half the size of those employed on ships of similar types built 10 years ago [20].

It is, therefore, evident that the first objective of marine automation has been realized. At the same time it must be admitted that the motivation of some shipowners to fit automation may be simply "force majeure." Shipping companies in general cannot recruit sufficient qualified staff to man engine rooms to the levels prevalent 10 year ago. The true situation is, therefore, almost certainly one that reduced manning is the result of the fortunate coincidence of staff shortage on one hand and the emergence of automation on the other. In short, automation has permitted the shipowner to cope with an inevitable reduction in available manpower.

Obviously, the shipowners would not continue to build automated ships if it were not both expedient and profitable. It is also mentioned that we have been advised that in certain European countries, it is becoming increasingly difficult to sell ships without Lloyd's UMS, Det Norske Veritas E0, or similar unmanned engine room certification, and even speculative new buildings are being fitted with all essential automation features.

Further manning reduction will take place in the near future. Similar ships to the Japanese computerized tanker will soon be operating with a crew size of 15 if the current tests show satisfactory results [21]. Also, various groups around the world have expressed their agreement to a future manning reduction down to eight or nine. Such reductions will not be possible without an extensive use of the digital computer in shipboard instrumentation and management.

The trend is now towards a general purpose crew, for both deck and engine, with combined navigation and engineering officers.

A future crew of nine may consist of one's captain, four general purpose officers and four general purpose crewmen [21].

CONCLUSIONS

Essentially every task involved in shipboard operation has already been carried out by automated means using analog or digital computer systems or is now in the process of being so implemented. The way is then clear, I believe, for us at any time we desire, to fit out a fully automated ship in which at least all of the at-sea and dock-side functions will be placed under the operation of a hands-off automation system. No one should seriously question our technological capability of doing this. We may, however, seriously question whether we can or should do this as a general practice at present for several important reasons:

- 1) First and most important, we still have serious questions about the overall reliability of the several components of the necessary automation system - sensors, the data transmission network, the data presentation devices and even of the computers themselves.
- 2) The payout of automation systems seems to be mainly in the subjective rather than in the directly measurable economic areas. At present systems costs, it is difficult to show a real payout for these systems from measurable quantities alone. We know that such systems can increase ship safety, that they can promote crew preferences for service on vessels equipped with them, that they can help decrease maintenance costs, and many other benefits. But, we do not know as yet how to put a real monetary value on many of these factors.
- 3) Hardware which can be used for automated ship functions is now in a rapid state of development. What type of this equipment, then, will we eventually standardize for our preferred installations?
- 4) Even assuming the final success of automation techniques, we have not worked out the best trade-offs between manpower and automation techniques in the

sea-going environment. We still must evaluate many things in this area. Among them are:

- a) Man's true position as a backup device for automation devices versus the use of redundancy or other related techniques.
- b) Man's value for maintenance at sea versus the carrying out of all such functions in port or in drydock.
- c) The social problems of small crews on long voyages - their pay, their duties and the hours of watch-standing, their use of off-duty time, the question of carrying families onboard, etc.
- d) The training required of the personnel of these ships must be established. Actually, of course, solution of the earlier problems will make plain the requirements in this latter area.

REFERENCES

1. Anonymous, "Definition of Collision Avoidance Requirements", Safety at Sea, No. 27, 14-19 (1971).
2. Anonymous, "The First Vessel Equipped with Anti-Stranding Sonar NICHIAN MARU Completed", Hitachi Zosen News Letter, No. 229, Hitachi Zosen, Tokyo, Japan, (August 3, 1970).
3. Dickerson, N.C., Jr., "Automatic Omega Receiver. Computer-Augmented Approach to Low Cost Marine Navigation", Navigation, 18, No. 2, 147-154 (Summer 1971).
4. Chernof, J., "Shipboard Equipment for Navigation and Position Fixing by Satellite", Electrical Communication, 44, 135 (1969).
5. Braddon, F.D., Ship Inertial Navigation, SNAME, New York, New York (November 2, 1962) 30 pp.
6. Stansell, T.A., Jr., "Satellite Navigation", Paper presented at the IFAC/IFIP Symposium on Ship Operation Automation, Oslo Norway, July 2-5, 1973.
7. Solsnaes, L. B., "Computer Applications on Board Merchant Ships", SFI Medd. M49 (1963).
8. Ohrström, Jan-Erik, "Navigation in Fairways", Paper presented at the IFAC/IFIP Symposium on Ship Operation Automation, Oslo, Norway, July 2-5, 1973.
9. Levy, J.F., and Adabie, D., "Data Acquisition System for the Docking of Large Ships", Paper presented at International Conference on Advances in Marine Navigational Aids, Institution of Electrical Engineers, London, England, July 25-27, 1972.
10. Anonymous, "Computerized Ships Make Debut in Sweden and Japan", Mar. Engng./ Log, 75, No. 4, 88-90 (April 1970).
11. Gustafson, R.D., Walters, R.C., and Williams, T.J., Digital Control of the Steam Propulsion System of a Naval Vessel, Final Report, Eight Quarterly Report, PEREC Report No. 44, The Purdue Energy Research and Education Center; PLAIC Report Number 7, The Purdue Laboratory for Applied Industrial Control, Purdue University, West Lafayette, Indiana (June 30, 1968).

12. Borsboom, A.C.H., et al., "Bridge Control of Marine Steam Turbine Plant, an Analytical Approach, "Trans., I. Mar. Engrg., 81, No. 2, 33-50 (1969).
13. Sten., L., "Computerized Cargo Handling on Large Tankers," Paper presented at the IFAC/IFIP Symposium on Ship Operation Automation, Oslo, Norway, July 2-5, 1973.
14. Golovato, P., "The Forces and Moments of a Heaving Surface Ship", Journal of Ship Research, 1, No. 1, 19-26, (April 1957).
15. Immer, J. R. Cargo Handling Systems for General Cargo, Unnumbered Report, Work Saving International, Washington, D.C., (1966) 76 pp.
16. Freisleben, H.C., "Advantages of Maritime Satellites for Ship Operation Automation", Paper presented at the IFAC/IFIP Symposium on Ship Operation Automation, Oslo, Norway, July 2-5, 1973.
17. Anonymous, Maritime Satellite VHF Communications Terminal, Prepared for U.S. Department of Commerce, Maritime Administration, Office of Research and Development, by Westinghouse Electric Corporation, Baltimore, Maryland, (1969).
18. Anonymous, Report to the International Conference on The Establishment of an International Maritime Satellite System, Inter-Governmental Marine Consultative Organization, London, England (September 1974).
19. Fiegelson, H.A., "Maritime Satellites are Here", Paper presented at the Eleventh Technical Meeting, American Institute for Aeronautics and Astronautics, Washington, D.C., February 24, 1975.
20. Anonymous, "A Systems Engineering Basis for Ship Automation", Naval Engrs. J., 74, No. 2, 293-308 (1962).
21. Bjurstrom, P-O., "Operational and Organizational Problems Regarding Centralized Control of a Highly Automated Ship", Paper presented at the IFAC/IFIP Symposium, Ship Operation Automation, Oslo, Norway, July 2-5, 1973.
22. Williams, T.J., "An Evaluation of the Present Status of Ship Automation", Paper presented at the IFAC/IFIP Symposium on Ship Operation Automation, Oslo, Norway, July 2-5, 1973.

AIR FORCE FLIGHT CONTROL PROGRAMS *

PAUL E. BLATT
Air Force Flight Dynamics Laboratory

The purpose of this presentation is to provide a brief summary of the control system development work at the Air Force Flight Dynamics Lab. Many of these programs are very strongly inter-disciplinary programs. We are trying to gain the benefits of some of these interfaces which have been neglected for many years. We believe we can gain greater performance benefits, and in many cases, quite a significant cost savings, through commonality of equipment. Many of these programs are also jointly sponsored by various Air Force Laboratories and, in some cases, the Army and Navy.

Figure 1 is intended to show just some of the recent flight control trends. Current aircraft are basically described like the A-7, which is a mechanical control system with a control augmentation system in parallel with it. It has very conventional rudder, aileron and stabilator controls, and is basically a stable airplane. A current Air Force fighter would be the F-16. It is a fully fly-by-wire controlled aircraft; it employs some preliminary control configured vehicle functions; it basically operates around a three per cent negative static stability margin; and it includes the differential stabilator, flaperon, programmed leading edge devices, and a basic rudder. In the future, we will be going to something significantly more advanced, fully employing the control configured vehicle principle and applying very strong propulsive interaction for both lift and drag modulation. We expect to see fully automatic fire and flight control combinations, and perhaps the areas of high acceleration cockpits. This is a typical study now underway; we term it the "advanced fighter

* This paper was typed from a taped version of the oral presentation.

FLIGHT CONTROL SYSTEMS DEVELOPMENT

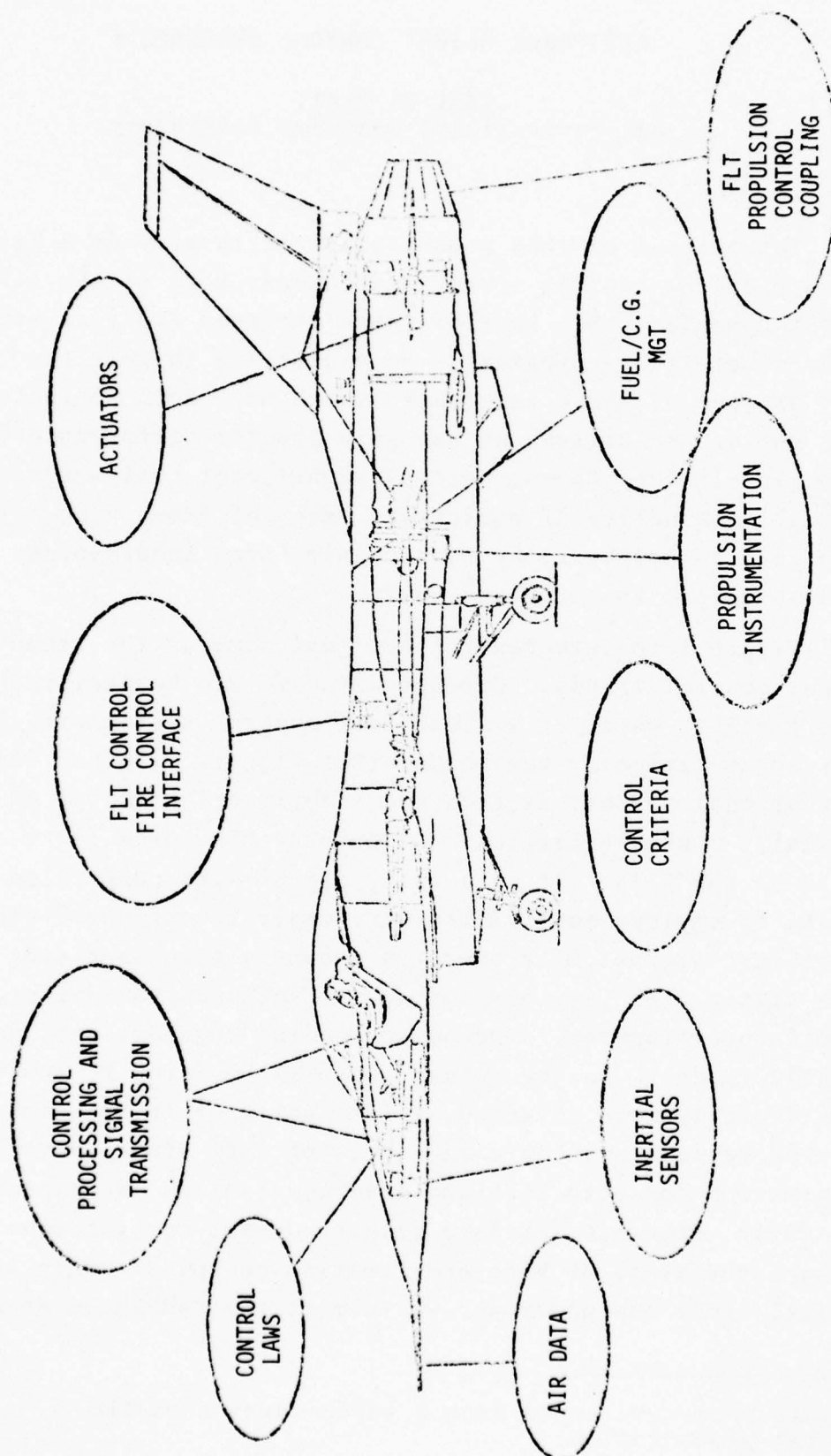


Figure 1

technology integrator," and there are several different versions of that out.

Figure 2 shows one of a number of programs leading up to such advanced technologies. The first one is our A-7D digital multimode control system under a contract with Honeywell, and it represents the Air Force's first flight test evaluation using digital computers in the stability and control aspect-- in this case, a control augmentation system. There are two things we are emphasizing here. First of all, the use of dual computers to provide a fail-op capability, through use of a considerable amount of on-line self-tests so we can detect which of the channels has failed and isolate it and continue to fly on the second channel. The second area we are emphasizing is that of the multimode control concepts in which we optimize the control as a function of the task being performed.

Figure 3 depicts some of the cases. First, we have implemented exactly what is currently onboard the A-7, analog control augmentation system, as a direct comparison means. We have termed that the standard mode used for most up-and-away cruise flights and landing and take-offs. It implements three axis control augmentation and some autopilot functions. We then added a second function for air-to-ground gunnery, termed a precision attitude mode. It gives much greater gunnery precision and emphasizes the attitude rate feedbacks. For dive bombing, a flight path mode is mechanized. These two are blended automatically so that when he exceeds something like 1, 2 or 3 pounds stick force, we go from the precision attitude into the flight path mode. Also, it looks like we may have slight differences between the precision attitude mode for air-to-ground gunnery and that for air-to-air gunnery. To date, we have had 16 flights onboard with just about 32 flight hours. The findings indicate that the digital flight control has given us additional flexibility for making changes

A-7D FLIGHT TEST EVALUATION OF A DIGITAL MULTIMODE FLIGHT CONTROL SYSTEM

OBJECTIVE:

- DUAL DIGITAL CONTROL AUGMENTATION
- MISSION-TAILORED FLIGHT CONTROL MODES

APPROACH:

- DEVELOP HARDWARE/SOFTWARE
- MANNED SIMULATION
- 50 HOUR FLIGHT TEST PROGRAM

CONTENT:

- CONTRACTOR - HONEYWELL, INC.
- A/A AND A/G CONTROL LAWS
- IN-LINE SELF-TEST, BITE
- DFCS AND DAIS ADP BASELINE
- DIG. HARDWARE, CONTROL LAWS, TECH RPT.

ACCOMPLISHMENTS:

- SYSTEM HARDWARE AND AIRCRAFT INSTALLATION COMPLETED
- FLT TEST BEGAN 7 FEB 75
- 18 HRS COMPLETED BY 1 MAY 75

Figure 2

SCOPE:

DIGITAL FLIGHT CONTROL IMPLEMENTATION

BENEFITS:

- MULTIMODE FLYING QUALITIES → INCREASED COMBAT EFFECTIVENESS
- INCREASED SAFETY / SURVIVABILITY (COMPUTER SELF TEST)

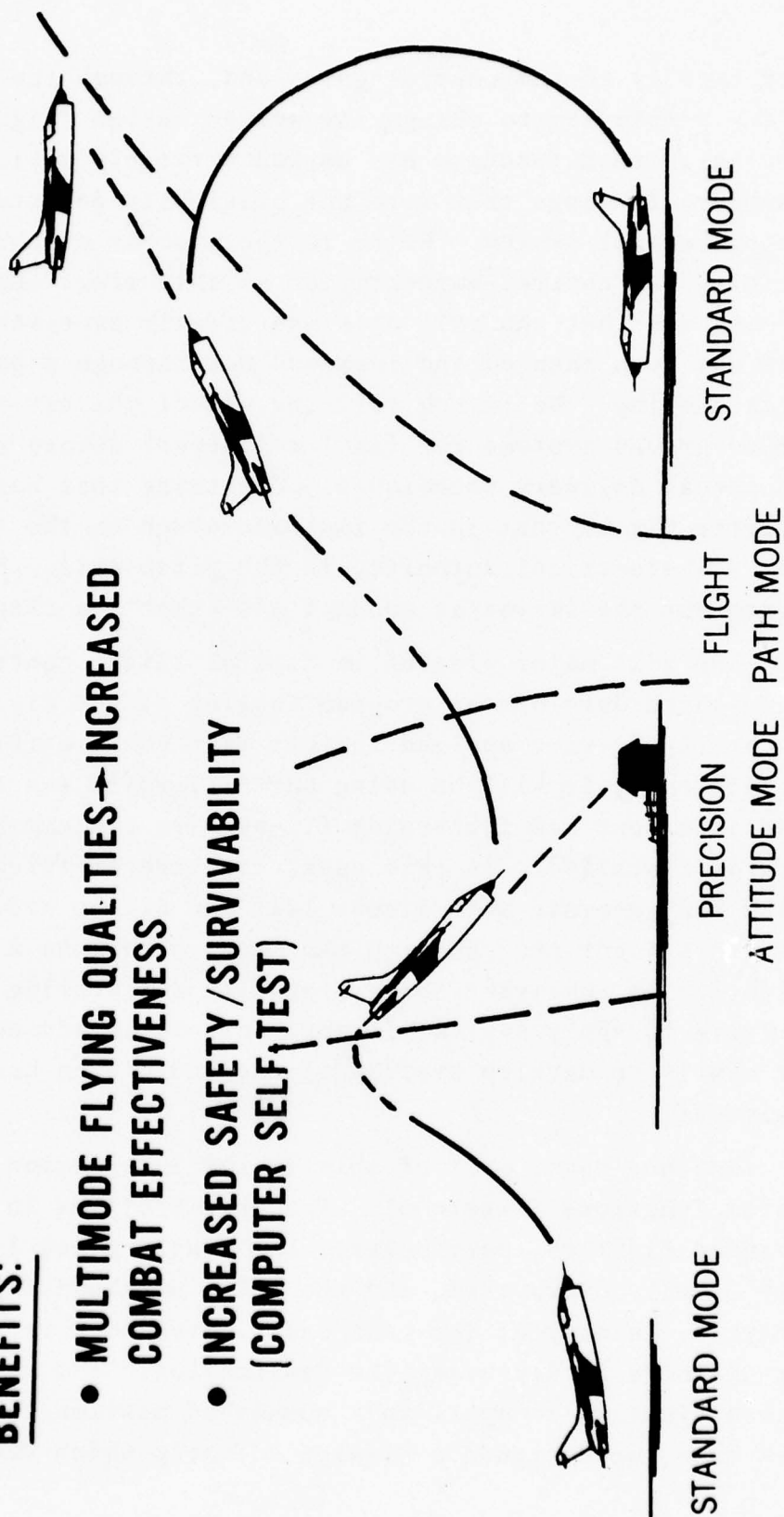


Figure 3

very rapidly to the control gains and, through the software, a very simple way to change the system design (Figure 4). A built-in test function has worked extremely well. We detected a number of things that were not previously detectable by the analog control system. We're in the process of correcting and refining the control augmentation at this time. Our initial finding was that the roll axis was greatly over-sensitive; that has been changed and improved now through a parabolic stick shaping. We're now refining all of the air-to-air and air-to-ground systems for final refinement before going into the actual delivery techniques. One thing that has limited us a little bit is that in the implementation on the A-7, we have just 25% electrical authority in the pitch axis. We begin to bottom out the servos at about 4 g's--that's a slight problem.

The next major program in digital flight control will be an advanced development program looking at the digital controls of the fly-by-wire applied to this test vehicle (Figure 5). In this case, it will be using our F-4, which was already used as a test bed for analog fly-by-wire systems and has canards installed. In this case, they are differential canards which can generate both direct lift and direct side force. This is a joint program with the Navy. There is a very common objective in achieving the reliability and proving out the criteria to apply digital flight controls in advanced fighters. Our aim is to develop specifications and proven hardware equipment.

Another major part of this is the integration of the crew system functions (Figure 6). The crew stations in many of our advanced fighters, particularly the single place fighters, are very heavily overworked, and the pilot workload for digital controls, in many of the past cases, have been very high. Our aim here is improving the "switchology" and using time-shared displays to apply to a number of mission tasks. In this case, we designed a mission scenario which was a typical

INITIAL FLIGHT TEST RESULTS

- DFCS FLEXIBILITY
- BIT EFFICIENCY
(i. e. LATERAL ACCELEROMETER, UHT POT)
- CORRECT CONTROL LAW IMPLEMENTATION
- MM ROLL AXIS SENSITIVITY - CORRECTED WITH UNIQUE
PARABOLIC-LINEAR STICK FORCE SHAPING
- AIR-TO-AIR TRACKING PERFORMANCE IMPROVED WITH
PA MM
- MM PITCH SERVO BOTTOMING AT APPROX 4G

Figure 4

ADP (FY 76 START)
DIGITAL FLIGHT CONTROL SYSTEMS

OBJECTIVES:

- APPLICATION SPECS, CRIT. & GUIDELINES
- MIL BENEFITS UNIQUE TO DIGITAL FBW
- ESTABLISH SAFETY, PERF. AND COST CHAR.

APPROACH:

- DES., INTEG., FLY REALISTIC DFCS
- ACTIVE, MULTI-VAR., COUPLED CONTROL CAPACITY
- OBJ. MEAS: COSTS, PERF., WORKLOAD
- DERIVE APPLICATIONS SPECS, CRIT., GUIDELINES

CONTENT:

- A/C UNSTABLE, DIRECT LIFT/SIDE FORCE
- FULL MISSION SCENARIO
- MISSION TASK MATCH: FLY QUAL. AND CREW SYSTEM
- ACTIVE WING/STORES FLUTTER SUPPRESS.

ACCOMPLISHMENTS:

- PLANNED JOINT AF/NAVY
- PRELIMINARY DESIGN, OP. PILOT EVAL. ACCOMPLISHED

Figure 5

DIVISION OF CONTROL AUTHORITY

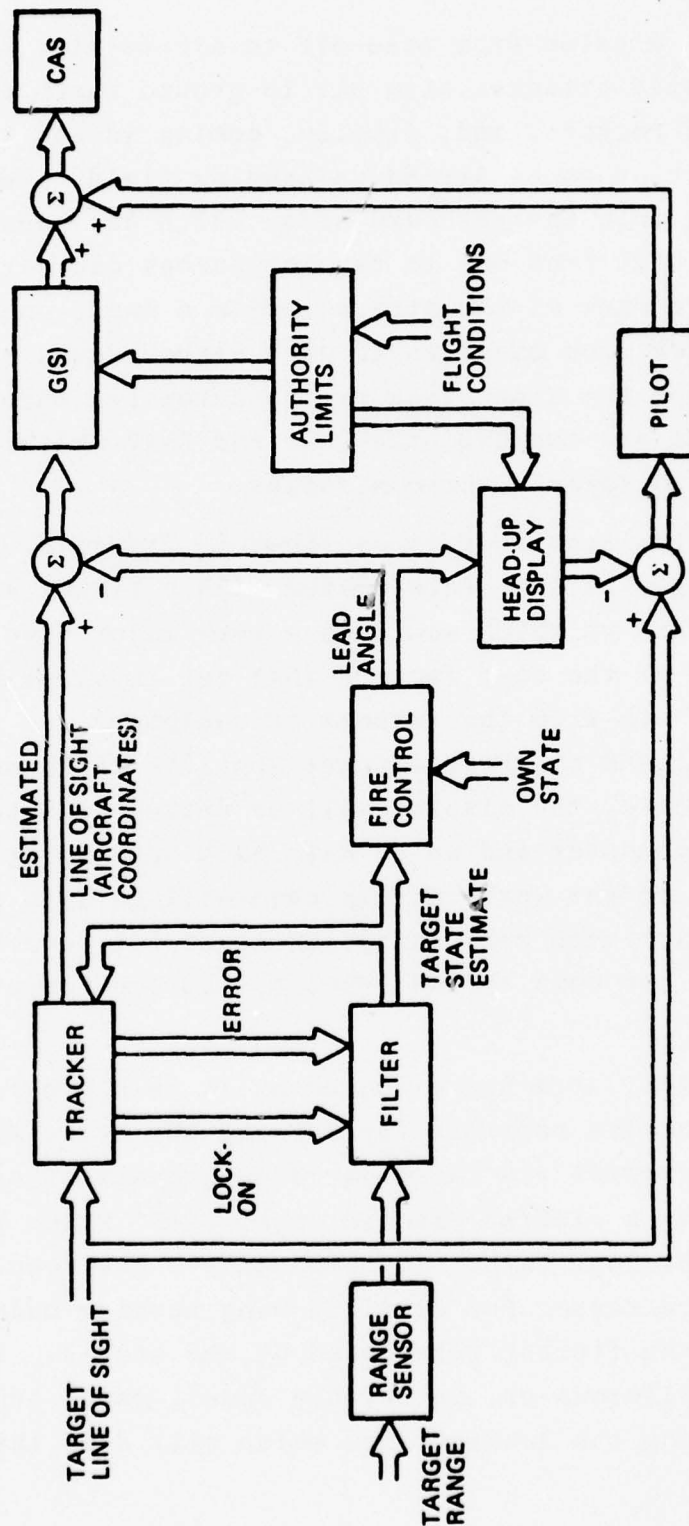


Figure 6

tactical mission from take-off to air-to-air, including gun and missile attacks; also air-to-ground which included bombs, guns and rockets, and, finally, coming in and landing on either a carrier or on an Air Force landing field. Much of the work is going into the keyboard area, which has been greatly simplified so that from one to two keypunches can satisfy the full need. In many of the attacks, it's a hands-on attack--you can switch from missiles to guns without even removing your hands from the side stick or the automatic throttle. The key functions are the HUD, the EADI and RNAV which has been militarized to satisfy those missions.

System architecture is shown in Figure 7. We expect to go to a two-fail operate system with a triplex set of architecture. This we think would be a very major payoff by eliminating many of the cost factors that get involved with the quad system, both from the amounts of equipment and the related hydraulic and electrical power supplies which must be provided. In this case, the display will be driven by a separate single digital computer and we do have back-up displays, as well. But much of the work in this case will go into proving that a triplex system can provide at least 98% coverage, so that once you get down to two systems, you can isolate and continue to fly.

Another area being looked at in this program is the concept of active controls for damping out store flutter. Many of our aircraft are carrying large amounts of external stores which have a flutter placard speed limit which restricts the flight envelope rather significantly. The concept is to carry an onboard sensor for critical wing bending modes that can pick up the flutter introduced by the stores. So then we can use the ailerons or, in certain cases, maybe separate little tabs along the leading edge which will damp this out,

CONCEPTS DFCS COMPUTER CONFIGURATION

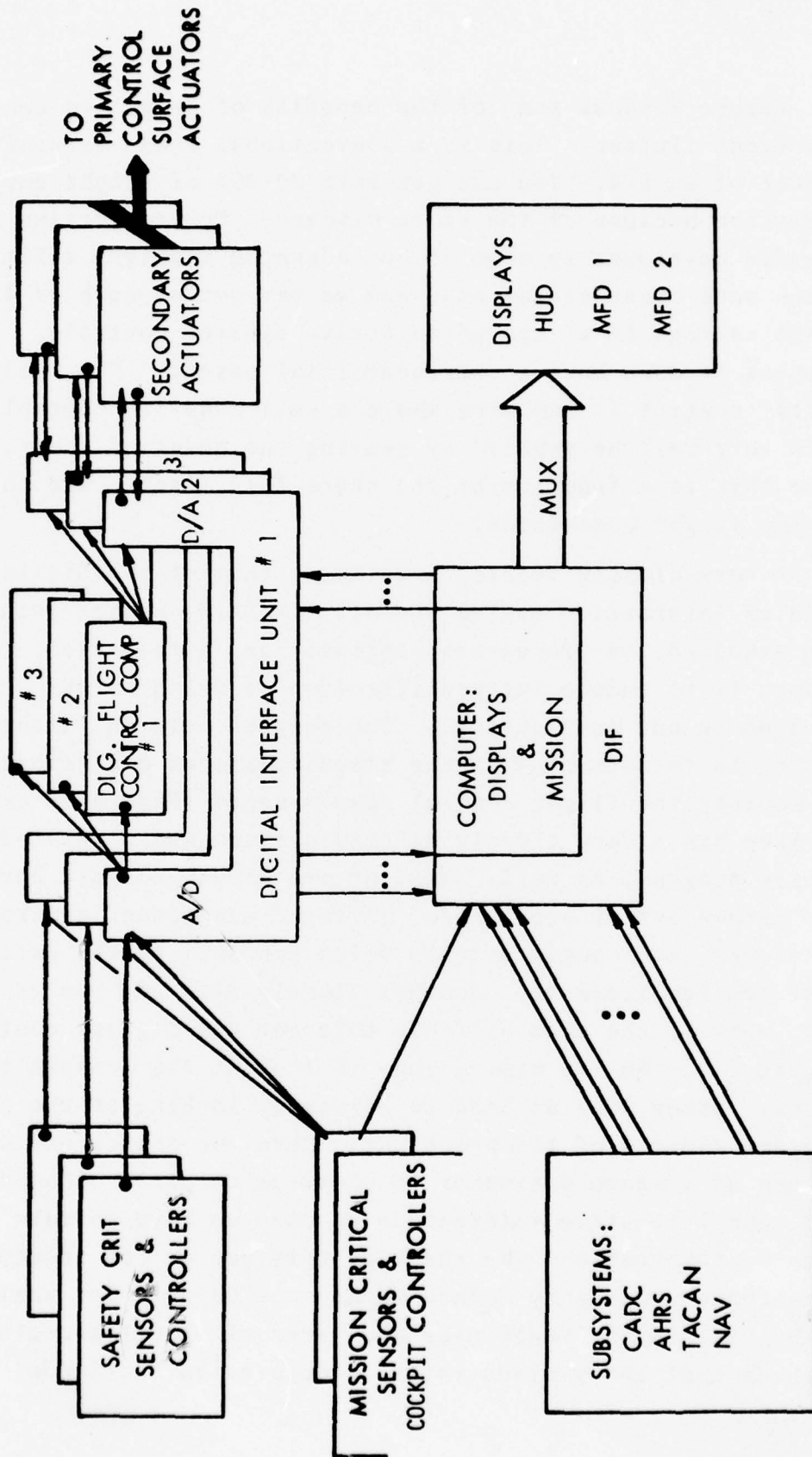


Figure 7

Figure 8 shows some of the benefits of an active control to prevent flutter. This is a conventional class aircraft typical of an F-4. You can get into 20-30% of flight envelope limitation because of the store placard. We are getting greatly expanded envelopes in some of our advanced fighters relative to the more conventional one, and we may get as much as 40% or 50% savings if we can go to active flutter controls. So, we think it does have a very beneficial payoff. The active flutter control is one area where a self-adaptive control could very well be applied by sensing the onset of the flutter, since this is a function of the store load itself, and the varying flight conditions.

A very closely related program is that of the digital avionics information system (DAIS). In DAIS, we are going into standardized processors, software and data busses. The purpose is to reduce the proliferation of avionics which is going on in our many systems. Our purpose here in flight control is to determine if the standard processors selected can satisfy the flight control requirements (Figures 9 and 10). The Navy has a very closely aligned program and a related display program, as well. What we are hoping to gain here is a common set of processors, software management control techniques, and common modules which can satisfy the various subsystem requirements. Another closely related, but exploratory, work is the area of fault tolerant and digital controls (Figure 11). We are aiming this to look at the sensors themselves. Other work at NASA is primarily looking at the fault tolerant aspects of the processor. Here, we anticipate seeing the use of a state estimator to continue to carry onboard good, complete state information in case we have certain breakdowns of information. We think in this way we can reduce the brute force redundancy method we are now using. Our analog fly-by-wire in the YF-16 uses quad sensors in all aspects. We think that the various rates, acceleration, attitude, and

FIGHTER FLUTTER PREVENTION SYSTEM (FFPS)

OBJECTIVE:

REMOVE FLUTTER SPEED RESTRICTIONS ON
ADVANCED FIGHTER/BOMBER AIRCRAFT WITH
EXTERNAL STORES

PAY-OFFS:

- EXPANDED SPEED - ALTITUDE ENVELOPE
- INCREASED SURVIVABILITY
- IMPROVED OPERATIONAL FLEXIBILITY
AND VERSATILITY

Figure 8

SOLUTION
DIGITAL AVIONICS INFORMATION SYSTEM
DAIS

PURPOSE:

PERMIT THE AIR FORCE TO ASSUME THE
INITIATIVE IN THE SPECIFICATION OF
AVIONICS CONFIGURATIONS FOR ACQUISITION
FOR FUTURE WEAPON SYSTEMS,

APPROACH:

DEVELOP AND TEST IN A HOT BENCH CON-
FIGURATION A DAIS ARCHITECTURE WHICH
WILL DEMONSTRATE A COHERENT SOLUTION
TO THE PROBLEM OF PROLIFERATION AND
NON-STANDARDIZATION OF AIRCRAFT
AVIONICS.

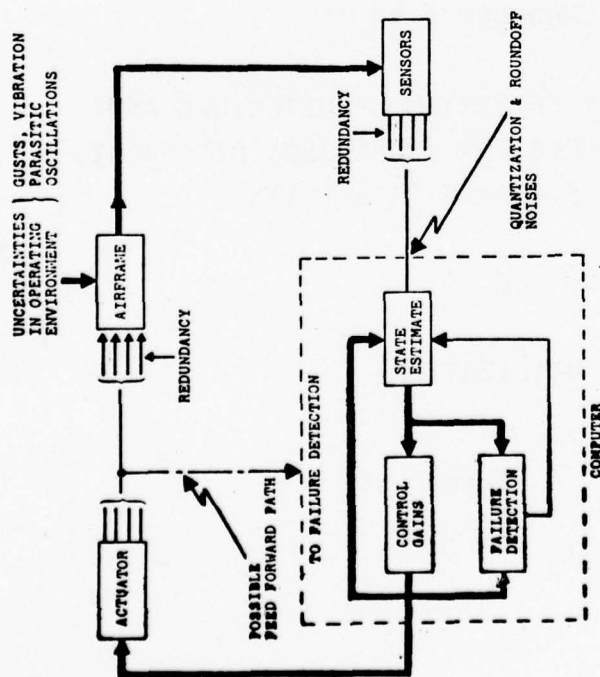
Figure 9

DAIS APPROACH TO LOW COST AVIONICS

- HIGH REPLICATION OF COMMON MODULES
- EXPLOITATION OF DIGITAL TECHNOLOGY
- SOFTWARE MANAGEMENT AND CONTROL
- COMPLIANCE WITH EVOLVING AIR FORCE STANDARDS
- MINIMUM TECHNOLOGY RISK
- FLEXIBILITY OF SYSTEM ARCHITECTURE AND COMMON MODULES FOR INCREASED, DIFFERENT, OR REDUCED AIRCRAFT CAPABILITY
- REDUCTION OF AGE
- REDUNDANCY UTILIZATION

Figure 10

FAULT-TOLERANT DIGITAL FLIGHT CONTROL SYSTEM STUDY



244

OBJECTIVE:

- REDUCE REDUNDANT FLIGHT CONTROL SENSOR REQUIREMENTS

APPROACH:

- FUNCTIONAL REDUNDANCY AND STATE ESTIMATION DEVELOPMENT
- FAULT DETECTION AND RECOVERY ANALYSIS
- CLOSED-LOOP SIMULATION

CONTENT:

- CONTRACTOR - HONEYWELL
- REDUCED HARDWARE REDUNDANCY
- INCREASED SURVIVABILITY THRU DEGRADED MODE OPERATION
- TECHNICAL REPORT

ACCOMPLISHMENTS:

- 1 JAN 76 START

Figure 11

position kinds of information available could be used more intelligently to reduce that total redundancy method, and as such reduce cost.

Another technology discipline program (Figure 12) we are looking at is a flight/propulsion control coupling (FPCC). We think that in the future many of our fighters will be using this 2-D nozzle as a way of gaining greatly increased maneuvering capability, both in generating additional lift and in use of drag modulations. So we need ways to fully understand and interpret and design the pilot's control of those very highly dynamically-coupled lift and propulsive forces. We have a contract with Lockheed with subs to Pratt and Whitney and Honeywell to study the methodology for these various designs. The baseline for this is a Lockheed IR&D study program which is an advanced vehicle relying on a 2D jet nozzle. The exhaust in the two F-100 engines are ducted out through the aft nozzle. It also has horizontal and vertical canards for both direct lift and direct side force, and relies heavily upon reduced static stability.

Another program we term control configured propulsion (CCP) is analogous to our control configured vehicle concept (Figure 13). Using CCP, we say in our initial design of the engine, "Let's include the control process for these vehicles, so we have a full understanding of what it does to engine design." In the past, we basically have looked at the airframe and engine cycle options together and really haven't looked at these other features around the airframe to the flight control option, or engine to control system option. With the jet flap flight control, these functions are very heavily involved. This is a contract we have with Pratt and Whitney, in turn with subs to Honeywell and Lockheed, to design those methodologies.

FLIGHT/PROPULSION CONTROL COUPLING (FPCC)

OBJECTIVE:

- TO DEVELOP METHODS AND DATA BASE FOR FPCC DESIGN IN FIGHTERS

APPROACH:

- FORMULATE GENERALIZED METHODOLOGY
- FPCC CONCEPT DEV. FOR JET FLAP AIRCRAFT

CONTENT:

- PRIME CONTRACTOR - LOCKHEED (+PWA, HWL)
- MISSION: A/A - A/G - SUPERSONIC DASH
- JF AC, PWA F-100
- FCS - RSS/DLC/DIGITAL

ACCOMPLISHMENT:

- METHODOLOGY
- POINT DESIGN AIRCRAFT
- STABILITY AND CONTROL LOOPS
- FOUR FLT CONTROL MODES

Figure 12

CONTROL CONFIGURED PROPULSION (CCP)

OBJECTIVE:

- TO FORMULATE METHODOLOGY FOR CCP DESIGN EMPHASIZING FLIGHT CONTROL REQS.

APPROACH

- EXTEND FPCC METHODOLOGY TO ENGINE DESIGN PARAMETERS AND CONTROL SELECTIONS

CONTENT:

- PRIME CONTRACTOR - PWA (+HWL, LAC)
- FIGHTER, BOMBER, STOL TRANSPORT
- COMPUTER GRAPHIC DEMO. - JF AIRCRAFT
- CCP WORK SHOPS

ACCOMPLISHMENT:

- STARTED 2 APRIL 75

Figure 13

Now getting into the other interaction of flight control with weapon delivery, the first area we were interested in was analytical techniques to predict the dynamic coupling between the pilot, his fire control sight displays, the control system, the weapon trajectory and release, and the geometry of the target attacks (Figure 14). In the past, we have designed almost all of our fire control systems somewhat independent of the aircraft itself and the control system, and there is a very strong interaction. The purpose of this program was to establish a computerized simulation method based upon a pilot model to analytically define the dynamic coupling between these various pilot displays, flight control aircraft dynamics, and the weapon themselves. There's been a contract with McDonnell-Douglas which is just about completed, and we'll be applying this on some of our future design techniques. We hope that in the future, it will be an early means of designing so that we have dynamic compatibility early in the design cycle, rather than waiting until we get into design testing to discover our problems.

Figure 15 shows a joint program with the Avionics Laboratory to look at the automatic features of fire control--automatic gun firing for final tracking purposes (FIREFLY). The Avionics Laboratory is looking at the automatic features of fire control. The program has investigated a number of advanced tracker systems, the EO, IR and radar techniques, in which we go through a filter technique, then combine into our automatic flight control system to deliver the bullet trajectory right on target. We have two contractors for this program; it's a parallel program, with General Dynamics using the F-16 as a baseline, and General Electric using the F-15 as a baseline. We'll be carrying this through quite a bit of simulation evaluation to determine just what the blends of manual and automatic control should be. One of the techniques being looked at basically relies upon a very good target state estimate derived

FLIGHT CONTROL REQUIREMENTS FOR WEAPON DELIVERY

OBJECTIVE:

- DEVELOP DYNAMIC ANALYTIC MODEL TO PREDICT A/A & A/G DELIVERY ACCURACY AND FORMULATE FLYING QUALITIES

APPROACH:

- TERMINAL AERIAL WEAPON DELIVERY SIMULATION (TAWDS) DIGITAL PROGRAM
- CONDUCT MANNED SIMULATION
- COMPARE DIGITAL AND SIMULATION RESULTS

CONTENT:

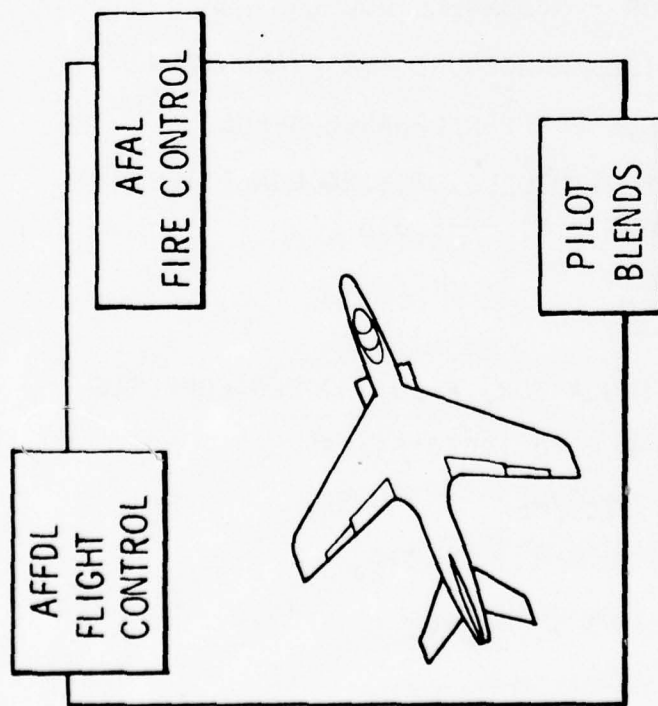
- CONTRACTOR - McDONNELL-DOUGLAS
- COMPUTERIZED PROCEDURE FOR EVALUATION
- DESIGN TOOL FOR PERFORMANCE SPECS
- TAWDS, PILOT MODELS, FLYING QUALITIES, TECH REPORT - MIL-F-8785B

ACCOMPLISHMENTS:

- TAWDS, SIMULATION, PILOT MODELS COMPLETE
- PILOT MODELS TO 19870154/64
- TAWDS TO JTCG/ME

Figure 14

INTEGRATED AUTOMATIC FLIGHT/FIRE CONTROL SYSTEMS PROGRAM (FIREFLY II)



OBJECTIVE:

- ESTABLISH TECHNOLOGY BASE OF INTEGRATED AUTOMATIC FLIGHT / FIRE CONTROL (IFFC)

APPROACH:

- PHASE I: CONTRACTOR DEFINE AND COMPARE AUTOMATIC VS MANUAL VS PILOT AIDED (BLENDED) SYSTEMS.
- PHASE II: GOV'T CONDUCT PILOTED SIMULATION TO VERIFY AND REFINE SYSTEMS

CONTENT:

- INCREASED WEAPON DELIVERY ACCURACY
- CONVENTIONAL UNGUIDED WEAPONS
- ATA AND ATG ATTACKS
- TECHNICAL REPORT
- BASELINE FOR FUTURE ADP

ACCOMPLISHMENTS:

- SYSTEMS DEFINED, PHASE I
- SIMULATION STARTED
- IMPROVEMENTS IN DELIVERY ACCURACY IDENTIFIED
- LARGE INCREASE IN SURVIVABILITY INDICATED.

Figure 15

from a range sensor and the target line-of-sight processed through the fire control and then input into the control augmentation, or in the case of the F-16, this will be the fly-by-wire system. So, the benefits here are to get good lock-on and be able to maintain it through this estimate of the target state.

A closely related program, but somewhat controversial, too, is a program we are looking at with the Avionics Laboratory and the Armament Lab (Figure 16). This is the movable gun concept in which we have small amounts of servo control (small excursion) in the gun, approximately plus or minus three degrees-of-freedom in elevation and transverse action. The purpose is that in the final tracking on a target, we believe we can totally eliminate the vehicle disturbances and small amount of pilot interaction. In this program, the Flight Dynamics Lab is responsible for the gun control laws and the interaction with the pilot; the Avionics Lab has responsibility for the revised fire control laws; and the Armament Lab for the M-61 gun and its gun servos.

Figure 17 shows one concept; we are actually going to investigate some 15 combinations, from a fully automatic gun which would be driven by a tracker-sensor, to a fully manual control where the pilot would directly control it. This is an intermediate kind of thing where the heart of the system is termed the "combat augmentation system," very similar in case to a model reference control. It also has some feedback to the pilot display function for information concerning the gun. Again, this is a rather small movement of the gun, but we feel we can gain, and should gain, some benefits by doing this, and should establish the benefits. There have been an awful lot of arguments about why these are good or bad, but very few facts have been established.

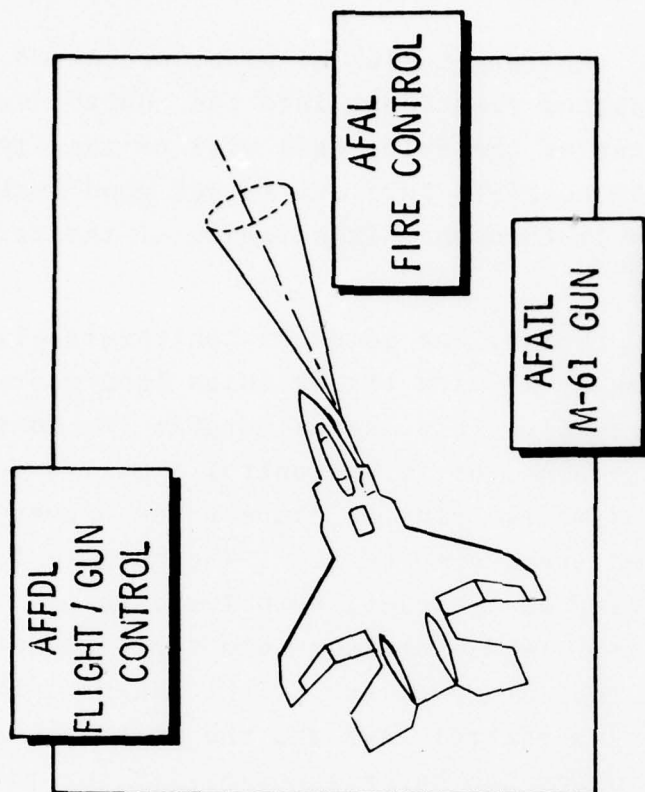
TRI-LABORATORY AERIAL GUNNERY PROGRAM (EXPO V)

OBJECTIVE:

- COMPARE FIXED VS MOVABLE GUN USING TRI-LAB TECHNOLOGIES

APPROACH:

- CONTRACTOR SIMULATION - F-15 / M61 GUN BASELINE
- CONFIGURATIONS - VARIETY OF FLIGHT / FIRE / GUN CONTROL SCHEMES
- CONFIGURATION DESIGNS - EXISTING OR SOA REALIZABLE HARDWARE
- REALISTIC SENSOR / AERO NOISE MODELS
- SIMULATION MODELS - DERIVED FROM HARDWARE DESIGNS



ACCOMPLISHMENTS:

- CONTRACT AWARD-MCAIR, MAY 75
- SIMULATION BASELINE - JUN 75
- GUN SYSTEM DESIGN - DEC 75
- CONFIGS EVALUATED - DEC 75
- SIGNIFICANT POTENTIAL IDENTIFIED

Figure 16

COMBAT AUGMENTATION SYSTEM MOVABLE GUN - COMBAT RETICLE DISPLAY

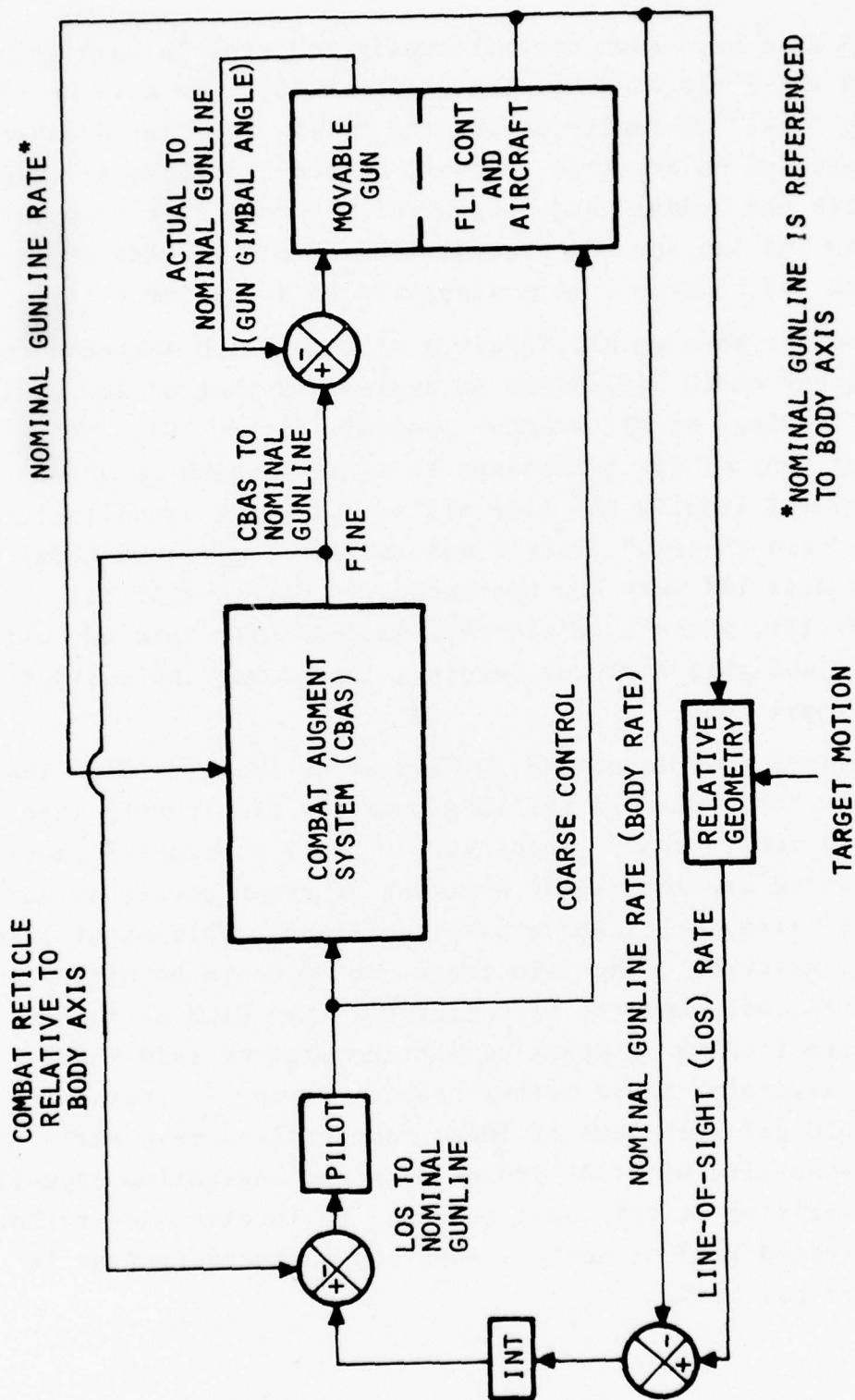


Figure 17

We also have some control configured vehicle work going on with the YF-16 at a baseline (Figure 18). We will be flight testing this. To really expand the YF-16, two canted canards are installed up front to generate direct sideforce in conjunction with the rudder, and it generates direct lift from the flaperon and the leading edge devices. We will also explore the areas of reduced static stability to a greater extent.

Another area we are involved with in which advanced control theory could definitely be applied is that of low visibility landing, or all weather landing (Figure 19). We're applying many of our techniques to a C-141 which is doing Category III landing and take-off's, but which are effectively termed "zero-to-zero" (that's not really a very good term). We have made 144 very low approaches in Category II and Category III, where they are very successfully into automatic control, and this includes landing, touchdown, and rollout to the final zone.

A final area is called 4D Navigation (Figure 20). The Air Force has a need to get large numbers of aircraft into some very remote spots, under very closely controlled conditions, so we are looking at arriving at given positions and altitude-latitude-longitude at given times. This might involve a mix of aircraft in hostile zones, so we could be mixing large transports, helicopters, FAC aircraft, that kind of thing. So, we are looking at means of getting what we term "pathfinder" aircraft--those rather heavily equipped aircraft--that could get into some of these remote sites very early and set up some kind of crude ground base and navigation capabilities. Arriving at this spot is going to involve some rather sophisticated kind of control laws and advanced systems in that terminal area.

CONTROL CONFIGURED VEHICLES (CCV) FIGHTER PROGRAM

OBJECTIVE:

- DEVELOP AND FLIGHT VALIDATE CCV TECHNIQUE
 - INCREASED PERFORMANCE/MISSION EFFECTIVENESS

APPROACH:

- ANALYZE/DESIGN/VALIDATE CONCEPTS ON YF-16
 - PROVIDE DESIGN DATA/CRITERIA

CONTENT:

- (CONTRACT F33615-73-C-3153 - GENERAL DYNAMICS/FT WORTH)
- RELAXED STATIC STABILITY - REDUCED TRIM DRAG
 - INCREASED TURN RATE - LOAD FACTOR - RANGE
- DIRECT SIDEFORCE
- DIRECT LIFT
 - FUSELAGE POINTING MODES
 - MANEUVER ENHANCEMENT
 - GUST ALLEVIATION

ACCOMPLISHMENTS:

- WIND TUNNEL TESTING (889 HR)
- ANALYSIS/DESIGN NEAR COMPLETION
- FABRICATION UNDERWAY
- YF-16 AVAILABLE

Figure 18

AUTO/MANUAL TAKEOFF/LANDING

OBJECTIVE:

- INVESTIGATE CAT III TAKEOFF/LANDING

APPROACH:

- AIRCRAFT CAT III MODIFICATION
- CAT III WEATHER FLIGHT TESTING

CONTENT:

- PROVIDE CAT III OPERATIONAL CAPABILITY
- CONTRACTOR SUPPORT (LSI/MSD)

ACCOMPLISHMENTS:

- 144 LOW VISIBILITY APPROACHES/LANDING
DOWN TO RVR = 0

Figure 19

4D INTEGRATED CON/DIS/NAV TECHNIQUE

OBJECTIVE:

- 4D CONTROL/DISPLAY/NAVIGATION SYSTEM
- DEFINITION FOR POSSIBLE 6.3 PROGRAM

APPROACH:

- FUNCTIONAL INTEGRATION DEFINITION
- PILOT-IN-THE-LOOP SIMULATION

CONTENT:

- CONFIGURATION VS. PERFORMANCE VS. COST
- REQUIREMENTS FOR NAVIGATION SENSORS
- GPS/JTIDS EFFECT
- CONTROL DYNAMIC IMPACT TO INTEGRATION DESIGN TECHNIQUES

ACCOMPLISHMENTS:

- MATHEMATICAL MODELS DEVELOPED
- MISSION PROFILES DEFINED
- SENSOR, FILTER, AND WIND MODELS DEVELOPED AND PROGRAMMED
- BASELINE SYSTEM SPECIFICATION DEFINED

Figure 20

Finally, in Figure 21 I have summarized what I saw as some of the roles of the advanced control theory in flight control and aircraft systems. The first one is a multiple subsystem integration; I've considered this interaction of various technologies. The propulsion/flight control, weapon delivery-- those kinds of things. It gives the means to dynamically understand state variable interactions, which are not intuitively apparent in certain cases. Closely aligned with this are multiparameter analysis and decoupling; being able to decouple the undesirable things and couple up the desirable terms in our control system, and have a full understanding of the important terms. Signal sensor refinement involves a blending of multiple navigation systems, the use of filters in radar sensors, and so on (e.g., lock-on, fire control). Fault tolerant redundancy is trying to use a state estimator to eliminate some of the high levels of redundancy we are now applying. In flight path optimization, a considerable amount of work has been done in optimizing time to climb, fuel management, and so on. Finally, the adaptive gain and phase changes are areas in which there has been a considerable amount of work in the past. It's lost its attractiveness, but I think there are many people who now realize that there are still a number of applications where it is beneficial.

ROLE OF ADVANCED CONTROL THEORY IN AIRCRAFT FLIGHT CONTROL APPLICATIONS

- MULTIPLE SUBSYSTEM INTEGRATION
- MULTIPARAMETER ANALYSIS & DECOUPLING
- SENSOR SIGNAL REFINEMENT
- FAULT-TOLERANT REDUNDANCY
- FLIGHT PATH OPTIMIZATION
- ADAPTIVE GAIN/PHASE CHANGER

Figure 21

ARMY FLIGHT CONTROL PROGRAMS

DAVID L. KEY
Ames Directorate
US Army Air Mobility R&D Laboratory

INTRODUCTION

The purpose of this paper is to show the scope of the Army's research and development programs in flight control, primarily those being performed by the Air Mobility Research and Development Laboratory (AMRDL). The particular topics covered are handling qualities, parameter identification, displays and vision aids, hydrofluidic SAS, and some of the major technology demonstrator programs. With such a broad survey, only brief descriptions will be given; details can always be obtained by a personal follow-up.

Army aviation is epitomized by the scene shown in Figure 1, a "Work Horse" UH-1H down amongst the trees. The increased threat from surface-to-air missiles and radar controlled guns means that any flying close to the battle area will have to utilize terrain masking to survive. This type of flying requires very good agility, maneuverability, navigation, and target acquisition, and involves tasks that are very difficult even during the daytime; however, the Army wants to perform these tasks in poor weather, and at night, making them even more difficult.

HANDLING QUALITIES

The first program to be discussed deals with handling qualities. A key theme for the program is the idea that manufacturers can now make helicopters and aircraft do almost anything: make them easy to fly, or even fly themselves. Such capabilities can be very expensive. We cannot really afford the very best systems. This is especially true for the Army which has 10,000 helicopters. We have to think simple. What do we really have to have? From the point of view of handling qualities, the question is: how do we find satisfactory stability and control characteristics which, when combined with adequate displays, give adequate performance and require a tolerable workload at a minimum cost? The cartoons on Figure 2 illustrate the generic flight phases for a low altitude mission: flying from A to B; making an approach to a hover or a landing; an unmasking maneuver to acquire and designate or attack a target. Agility and maneuverability are essential in these low-level flight phases. Precise control of the aircraft in various winds and turbulent conditions is critical. Also, at these low altitudes, navigation is very, very difficult. A helicopter going to a clearing in the

Paper presented at the Symposium on Control Theory and Navy Applications, US Naval Postgraduate School, Monterey, California, July 15-17, 1975.



Figure 1

PROBLEMS OF LOW-LEVEL OPERATIONS

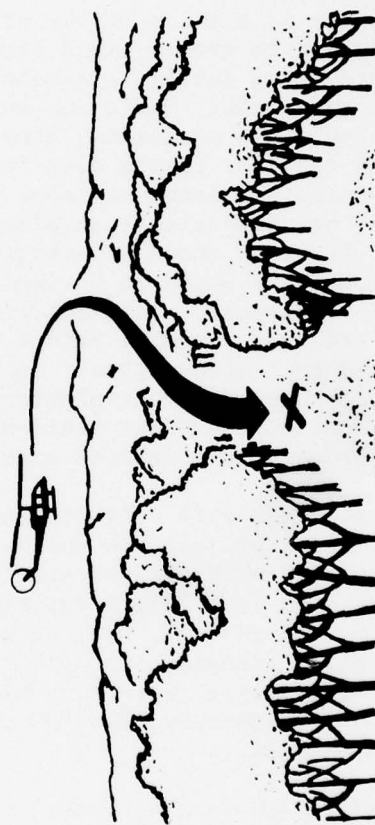
DAYTIME - GOOD VISIBILITY



AGILITY AND MANEUVERABILITY
NAVIGATION



PRECISION OF CONTROL
TARGET ACQUISITION



NAVIGATION, CONTROL, GUIDANCE

Figure 2

woods may be flying close to the treetops, so that if it misses the clearing by 100 meters the pilot may never see it. The Army wants to operate in poor weather and at night, and that creates additional problems such as the lack of visible details and possibly even the loss of the horizon which provides visual attitude cues.

In the handling qualities program depicted by Figure 3, an effort is being made to develop a handling qualities data base from which criteria can be developed and, hopefully, lead to a revision of the military specification for helicopter handling qualities, MIL-H-8501A. The program is a joint effort with NASA. This joint effort provides AMRDL access to ground-based simulators, both fixed-base and moving-base, and a new in-flight simulator which is being developed jointly by NASA and AMRDL. There are some limitations with existing ground-based simulators performing Army missions near the ground. Since the missions call for flying down in the trees, it is important to have trees on the simulated terrain. Until now, terrain models have been directed at conventional airplanes flying high, or landing in terminal areas. Figure 4 shows a photograph of some of the details required for a model terrain board to be used in nap-of-the-earth (NOE) simulations. On this test section, the natural features are well simulated and the trucks are good, but the bridge looks unrealistic. In the final design, we placed much more emphasis on realism of the man-made features and we expect this to be satisfactory. There is a need for not only more detail, but also a wider field-of-view, more like a real helicopter has. Plans for this year include examining wide field-of-view concepts.

Mission analysis efforts have been aimed at developing a good understanding of just how the Army uses the helicopters, what the problems are, and what the potential capabilities are. These results will be translated into a form for simulator experiment tasks. In helicopter stability and control, we have been compiling helicopter data packages which can be analyzed and used to generate helicopter models for the simulator. Having these data packages will contribute to an understanding of the parameters, desired changes in the parameters, and ranges for the changes.

Figure 5 shows a schematic of the pitch and roll axes of the UH-1H in-flight simulator being developed jointly with NASA. The system consists of a pair of digital computers interfacing with sensors, displays, a data acquisition system and the flight control system. The contractor, Sperry Flight Systems, is due to deliver the hardware and software by the end of July 1975. After installation and checkout in the ground simulator, it will be installed in the UH-1H for flight checkout. With a bit of luck, a useful tool may be available in six months to a year.

A program has been initiated to investigate the impact of rotor inertia on helicopter maneuverability and agility. Fifty-five pounds has been added to each rotor of an OH-58. Increasing the kinetic energy of the



6.2 CONTROL

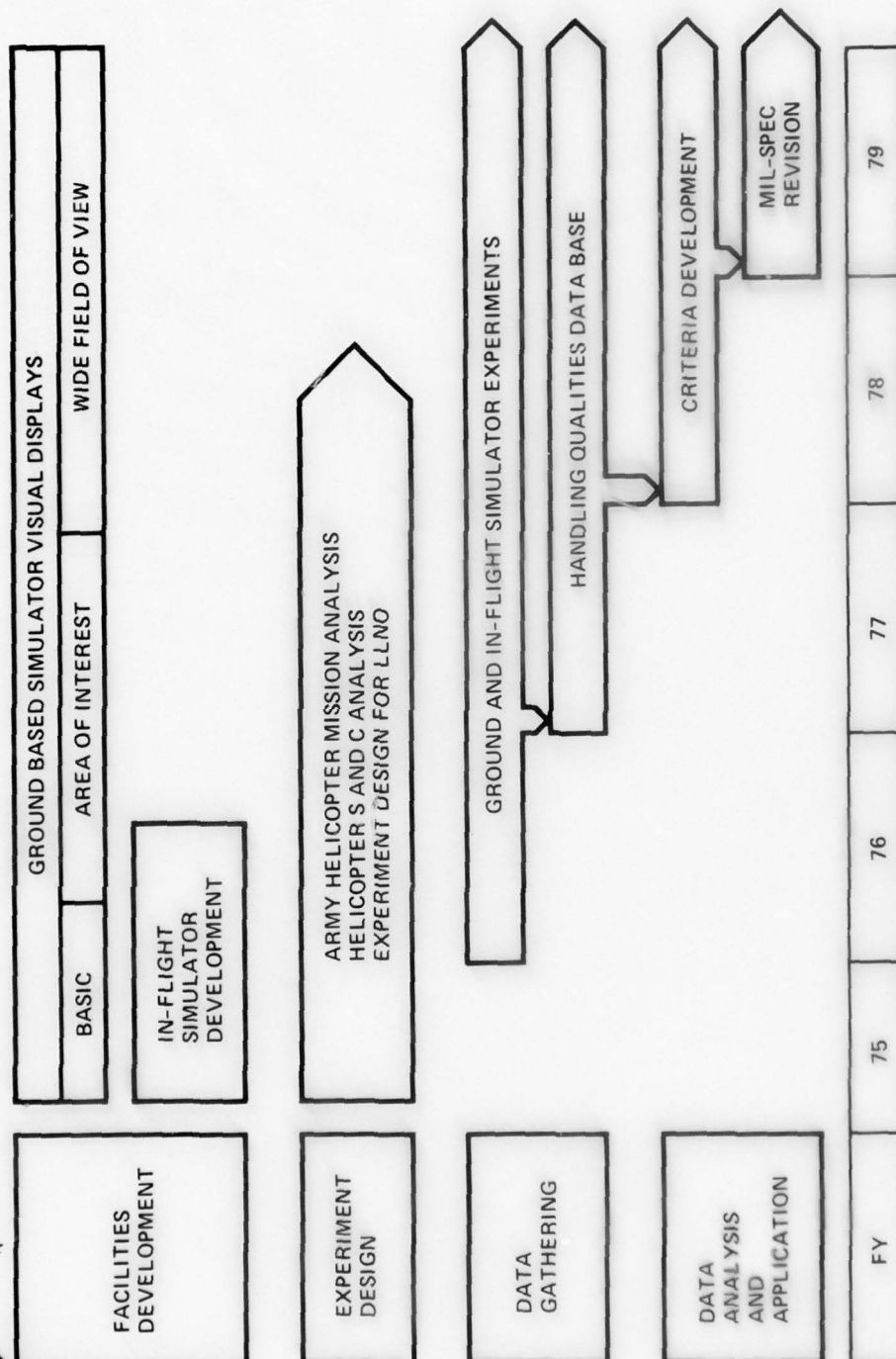


Figure 3



Figure 4

SCHEMATIC OF UH-1H IN-FLIGHT SIMULATOR

CONTROL SYSTEM:
PITCH AND ROLL AXES

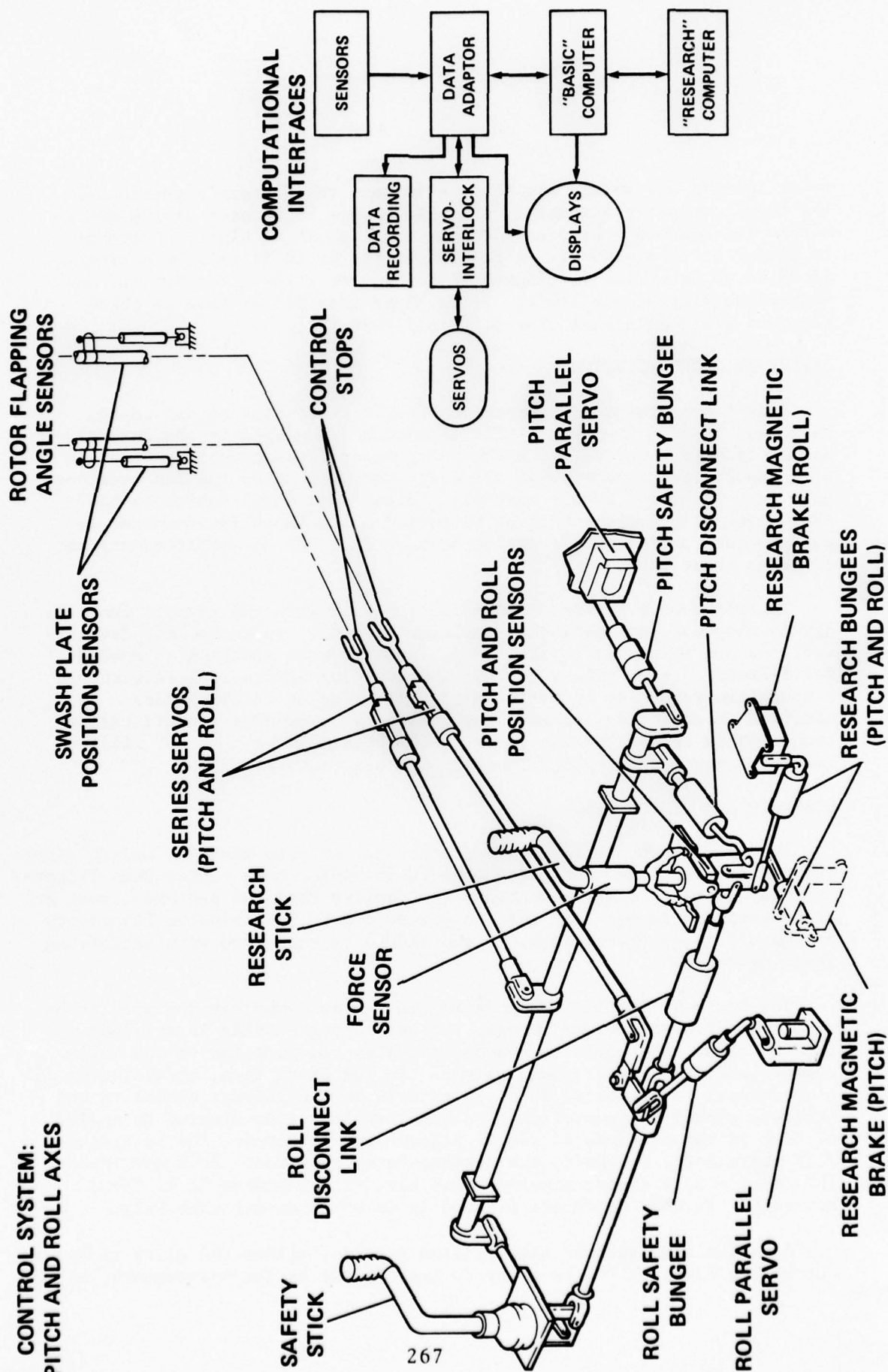


Figure 5

rotor in this way should shrink or eliminate the deadman's portion of the height velocity boundary. A single engine helicopter flying NOE is within the deadman's band most of the time, so it is highly desirable to shrink or eliminate it. A related effort is to install an engine in an OH-58 to determine how increased horsepower affects the agility and maneuverability of the craft. It is hoped that flight test on these programs will begin some time in fiscal year 1976.

PARAMETER IDENTIFICATION

Flight test parameter identification is being done on the CH-54, UH-1H and AH-1G helicopters. The technique being used is the extended Kalman filtering method, with a six-degree-of-freedom model. Compared with results for conventional aircraft, the helicopter results have been only fair to poor. Future work will investigate input design on the UH-1H, and flight tests will be performed on an AH-1G instrumented to measure the rotor flapping angles so that data can be extracted against a higher order model.

The plans on parameter identification fall into two areas: technology development and in-flight simulator support. In technology development, we are initially interested in learning what modeling is needed for different rotor types, such as the Bell two-bladed teetering rotor, a hingeless rotor, or an articulated rotor with up to six blades. In addition to answering the modeling questions, a routine identification technique is needed for the UH-1H in-flight simulator. An RFP will be issued to develop such techniques in the near future.

DISPLAYS AND VISION AIDS

The Army's need to fly at low altitudes, in poor weather, and at night has two implications: it puts emphasis on vision aids rather than flight-director types of instrumentation; and implies that the equipment must be self-contained rather than rely on ground aids. The Avionics Laboratory of the U.S. Army Electronics Command (ECOM) is concerned with satisfying these needs.

The Optic IV display shown in Figure 6 uses symbology designed to be superimposed over a video scene. The helicopter heading is straight up all the time. The position symbol indicates the position of the helicopter relative to the ground target. In the short term, acceleration is proportional to attitude, so a vector from the helicopter symbol to the attitude symbol is proportional to acceleration. The display is scaled so that if the attitude circle is placed over the cross, the helicopter will migrate to, and hold, the desired hover position. ECOM developed this device on a ground simulator and have flight tested it in CH-53 aircraft. Further tests are planned in an OH-6A during this Fall.

A vision aid, such as night vision goggles, allows the pilot to see out of the cockpit. If he tries to look inside at the instruments, he

OPTIC IV HOVER SYMBOLOGY

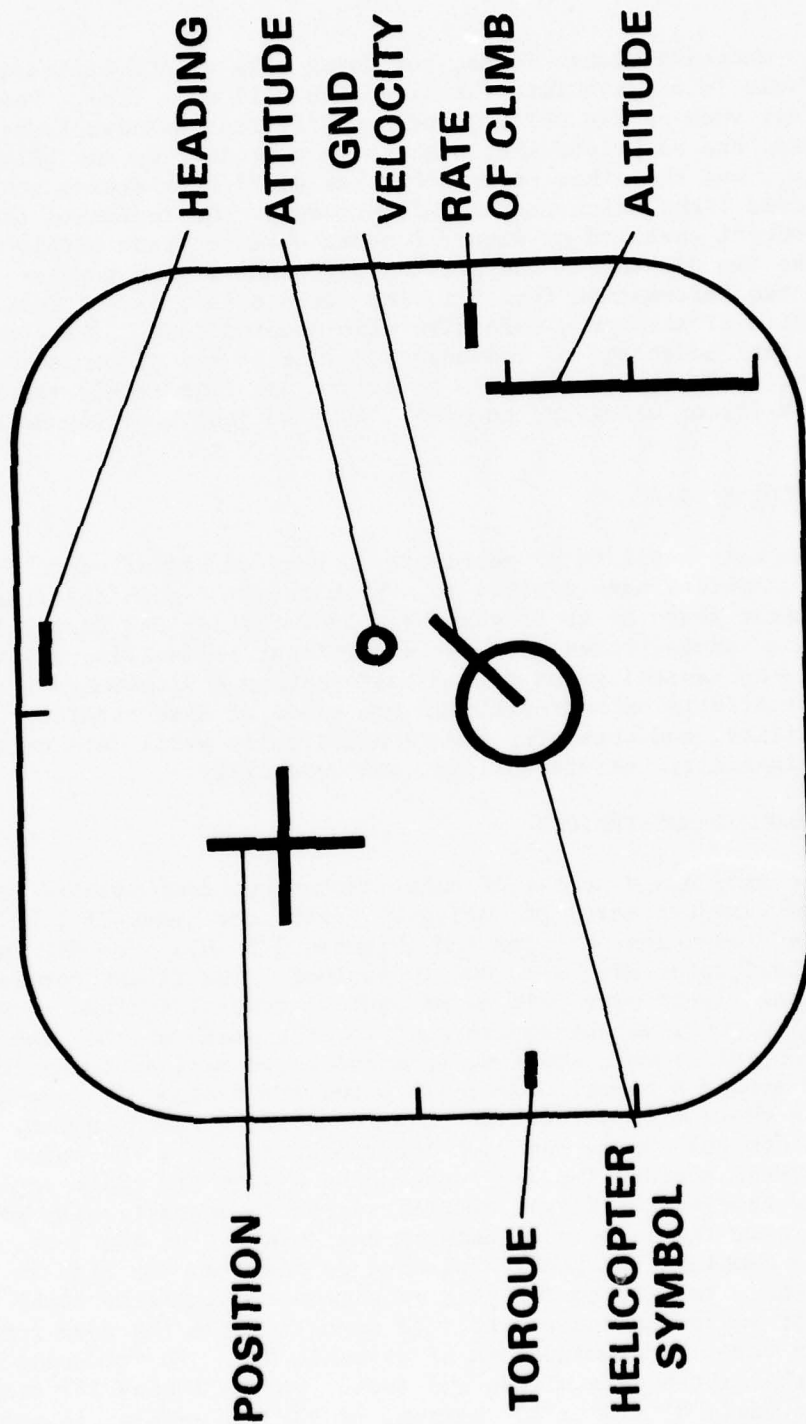


Figure 6

has to manually change focus, but doing this at NOE altitudes is likely to result in a crash into the side of a hill or a tree. Panel-mounted displays such as the OPTIC IV have a different disadvantage; the CRT displays are so bright that night vision is lost by the pilot flying the display, and the other crew member has difficulty seeing out, because of scattered light which causes reflections on the inside of the canopy. The concept sketched on Figure 7 would obviate these problems by combining the two displays. The pilot using night vision goggles would be presented information from a moving map display, flight instruments, or the Optic IV through a selective side-mounted lens. The concept has the additional advantage of redundancy, since if the pilot is flying using the Optic IV, and if there is a failure, he immediately transitions to contact flying using the goggles. ECOM is just starting to develop this idea.

HYDROFLUIDIC SAS

The next topic to be mentioned is that of hydrofluidic SAS. Hydrofluidic devices have evolved to a high level of sophistication during the last eight years or so (Figure 8). Hydrofluidic SAS uses a fluidic device to sense angular rates, and has significant reliability advantages over electro-mechanical gyros in the ever-shaking environment of a helicopter. Current efforts on hydrofluidics are aimed at demonstrating operational suitability, and obtaining some statistically valid data on reliability, maintainability, serviceability, and durability.

TECHNOLOGY DEMONSTRATORS

The Army has a number of major technology demonstrator programs which involve flight control technology. First, the heavy-lift helicopter/advanced technology program HLH (Figures 9 & 10). The HLH is a very large helicopter with a 22,000 lb payload. The flight controls are triply redundant fly-by-wire with no mechanical control system. Dual redundant hydraulic power actuators are used for the swash plate. The HLH has a load control crewman station, from which the helicopter can be controlled in and around a hover. Figure 10 shows the Boeing 347 test helicopter. It is a CH-47 with a fuselage plug and enlarged rotor pylon. The HLH flight control system has been incorporated, and a two-point load suspension system added. The load suspension system has cable angle sensing devices feeding the flight control system to automatically move the helicopter over the load, thus damping any swinging of the load. In addition to load damping, the HLH is required to position the load in hover within ± 4 inches. In testing for this requirement, simulator tests came within two feet while commanding the load manually from the load control station using a velocity command form of augmentation. In automatic position hold, the system came within one foot. On the Boeing 347 test vehicle, with an empty 8' x 8' x 20' milvan, on 30-foot cables, in gusty winds, the manual system achieved 12.3" circular error probability (CEP) (50% of the time the load is in a circle of that radius). With automatic position hold, the system achieved 7.5" CEP. The 347 has flown 315 hours

MULTIFUNCTION AVIATION DISPLAY (MAD)

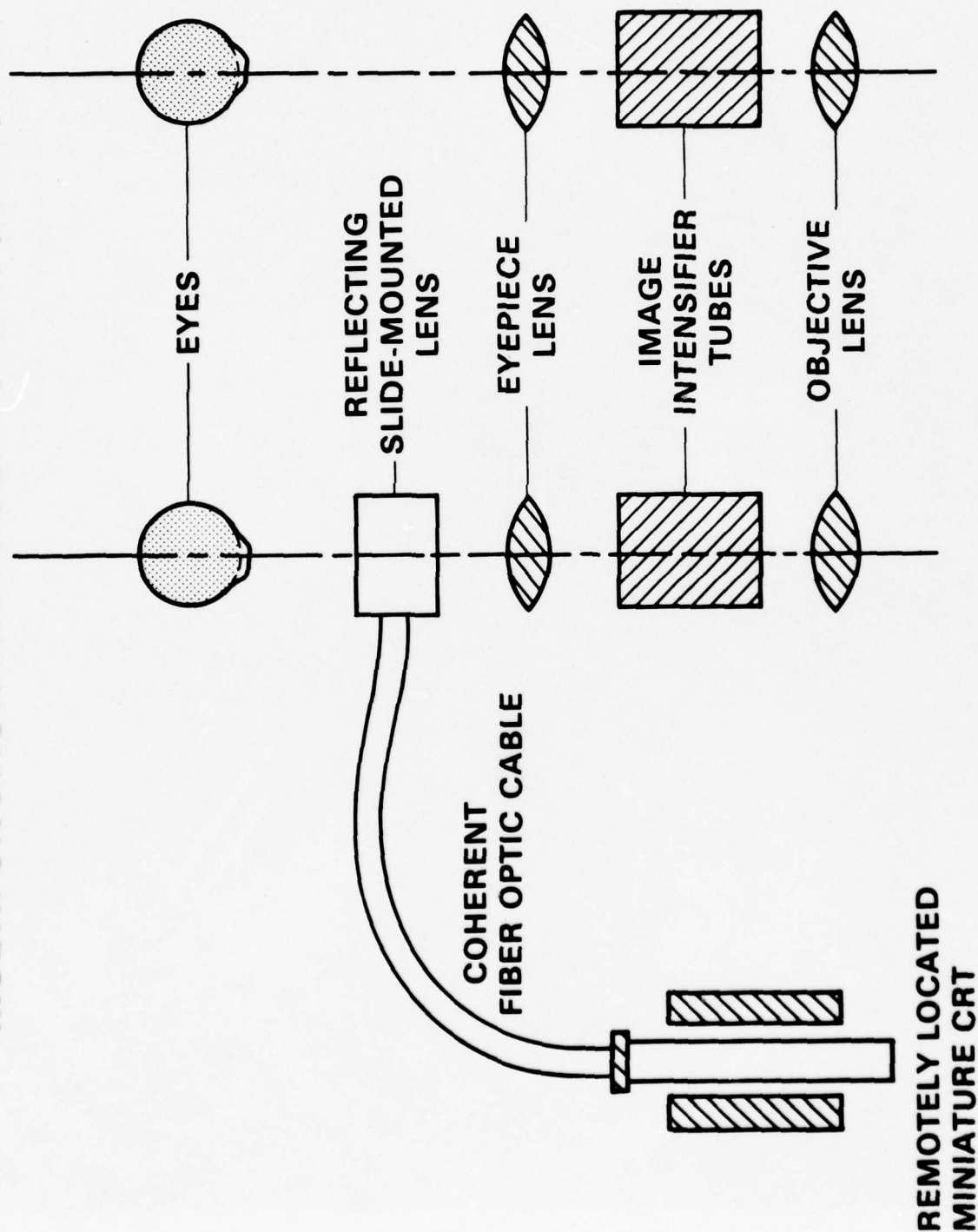


Figure 7

EVOLUTION OF HYSAS

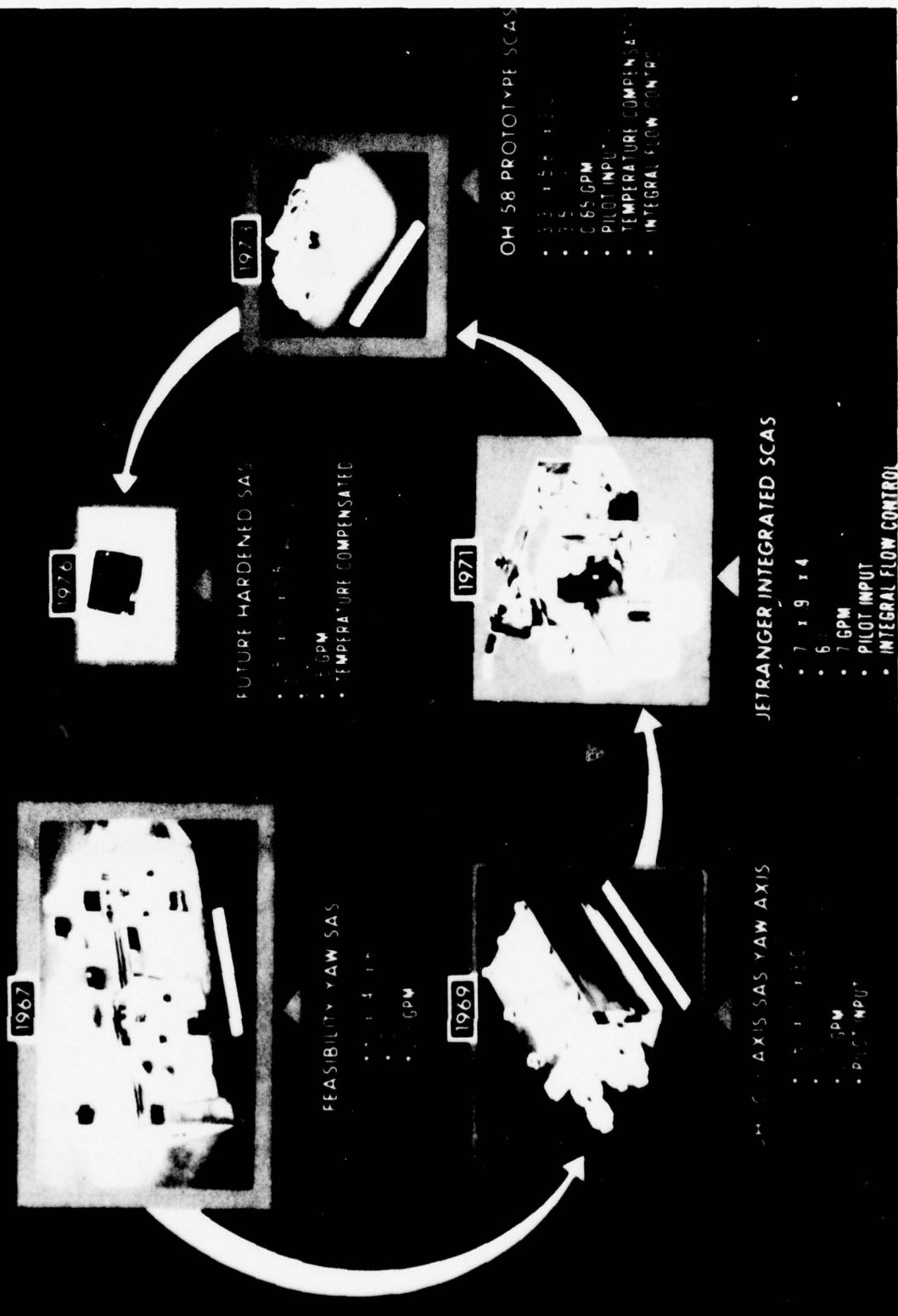


Figure 8

HLH/ATC PROTOTYPE AIRCRAFT EFFORT

FLY-BY-WIRE FLIGHT CONTROL SYSTEM

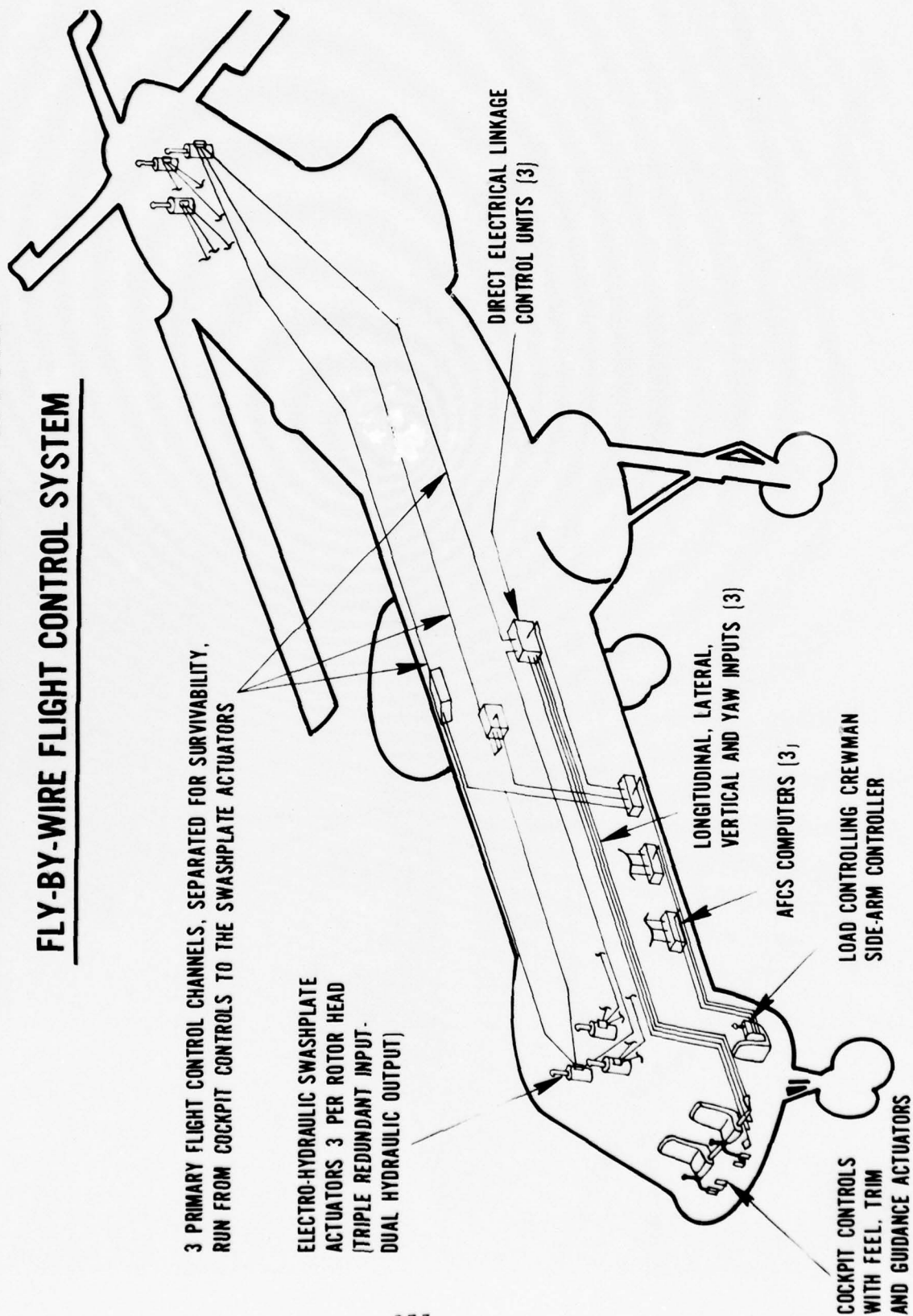


Figure 9

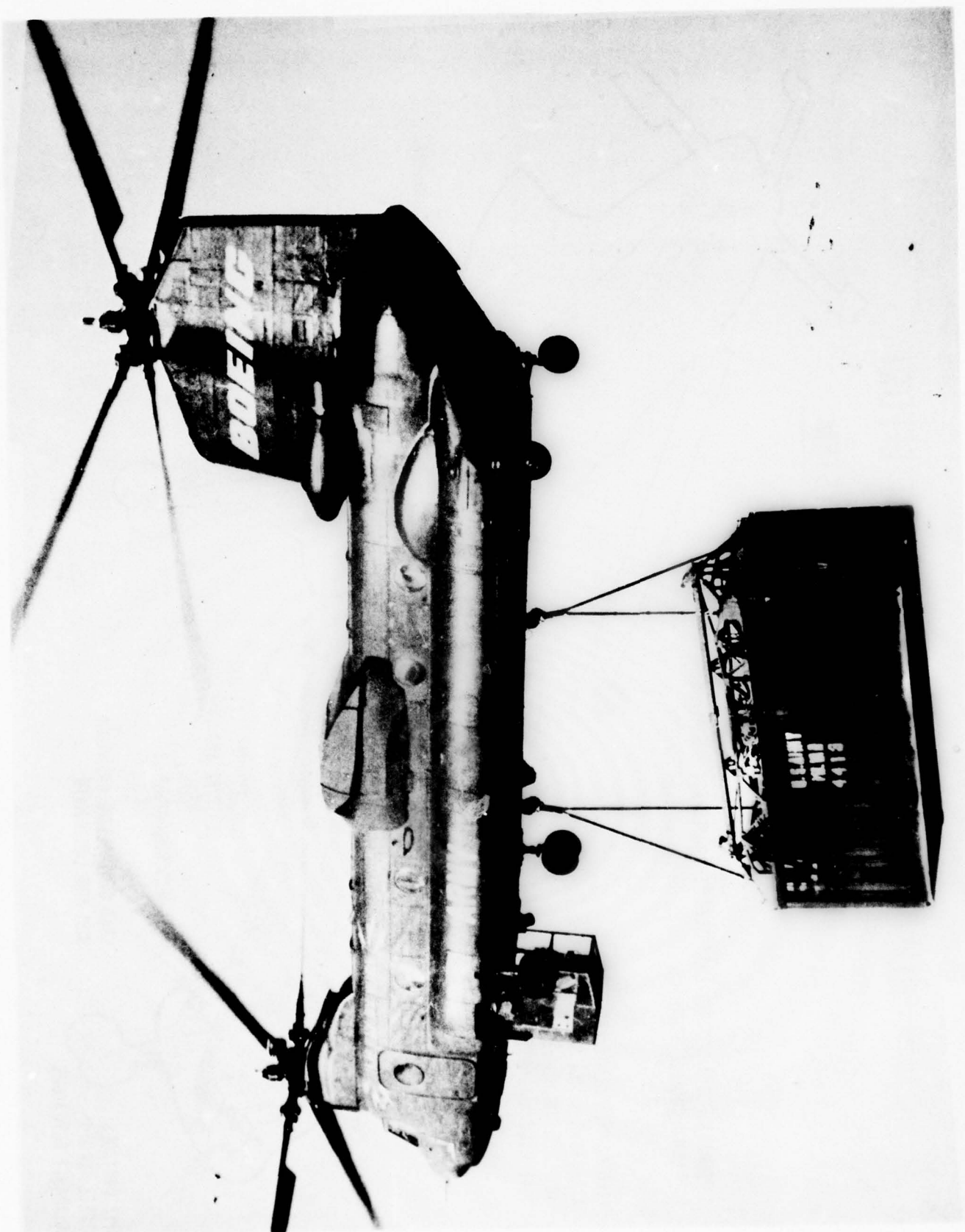


Figure 10

on fly-by-wire, 300 without any mechanical backup. The HLH program started in June 1971 as an advanced technology program to demonstrate the rotor systems, drive systems, cargo handling, and flight control system. A prototype was added a year later. First flight is due in March 1976, but the whole program is presently under review.

The next technology demonstration program to be mentioned is the Advancing Blade Concept (ABC) helicopter built by Sikorsky (Figure 11). This helicopter has counter-rotating, three-bladed, hingeless rotors. Counter-rotating blades allow the retreating blade to be unloaded to relieve retreating blade stall at high speeds. They also allow the tail rotor to be dispensed with. Two aircraft are being built in the ABC program. The first one crashed in August 1973 after about 3 hours of flight test because of a pitch-up problem in low speed (30 kt) flight. Over the past two years, a better understanding of counter-rotating rotor aerodynamics has been acquired. Based on this extended analysis, design improvements have been made and the second aircraft is due to fly this year.

The third demonstrator program is the Rotor Systems Research Aircraft (RSRA) being developed jointly with NASA (Figure 12). The RSRA is a test bed for rotors, and can fly as a helicopter, fixed-wing airplane, or as a compound craft. The compound mode is for testing rotors. With auxiliary engines variable incidence wing and conventional control surfaces, a range of forces and moments can be put on the rotor. This is also a two-aircraft program with Sikorsky as contractor. First flight is due in mid-1976, and delivery for research is scheduled for the Fall of 1977. Plans for the research rotors are an aeroacoustic rotor to investigate the effects of the tip planform and airfoil section. A composite structure 4-bladed hingeless rotor, and a variable geometry rotor will also be built.

The last program to be mentioned is the XV-15 tilt rotor which is also a joint Army/NASA program (Figure 13). The XV-15 has 25-foot diameter, 3-bladed, gimballed rotors. The engines are in the gimbal housing so the engine tilts up with the rotor. Figure 14 shows how the craft develops control moments in hover, and phases to conventional control surfaces in forward flight. Since the mid-50's when the XV-3 flew and encountered instabilities, a lot of work has been done to solve problems with the tilt rotor concept. This program will demonstrate that solutions have been found, and that a tilt rotor is a viable concept. Roll-out is due next April, and following tests in the NASA-Ames 40 x 80 ft wind tunnel, first flight is expected to be in October 1976. After a year of proof of concept flight tests, an advanced flight research program will be developed.

CONCLUSION

In conclusion, this paper has given an overview of Army flight control programs. Most of our money is spent with contractors to stimulate

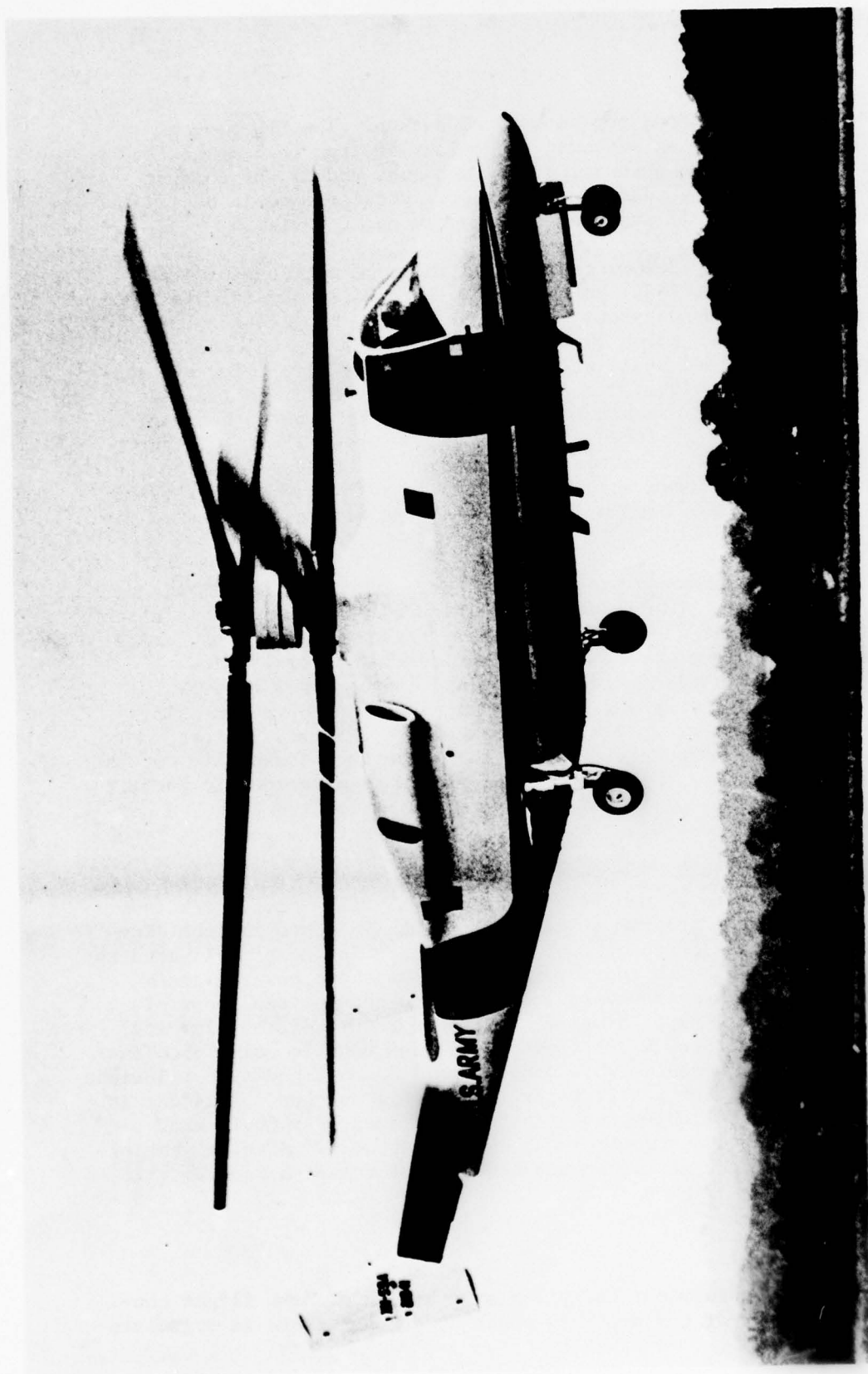


Figure 11

RSRA FLIGHT CONFIGURATIONS

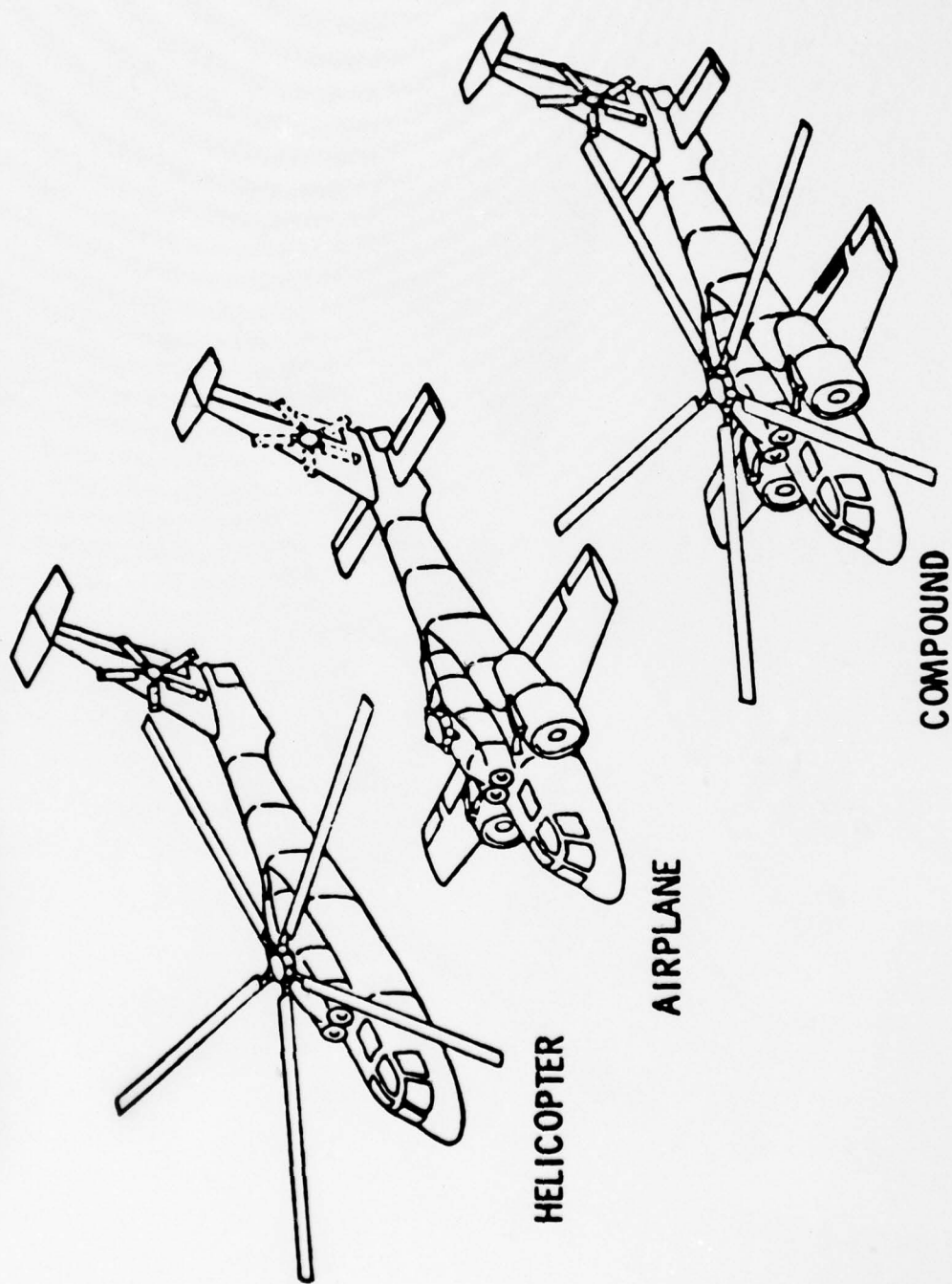


Figure 12

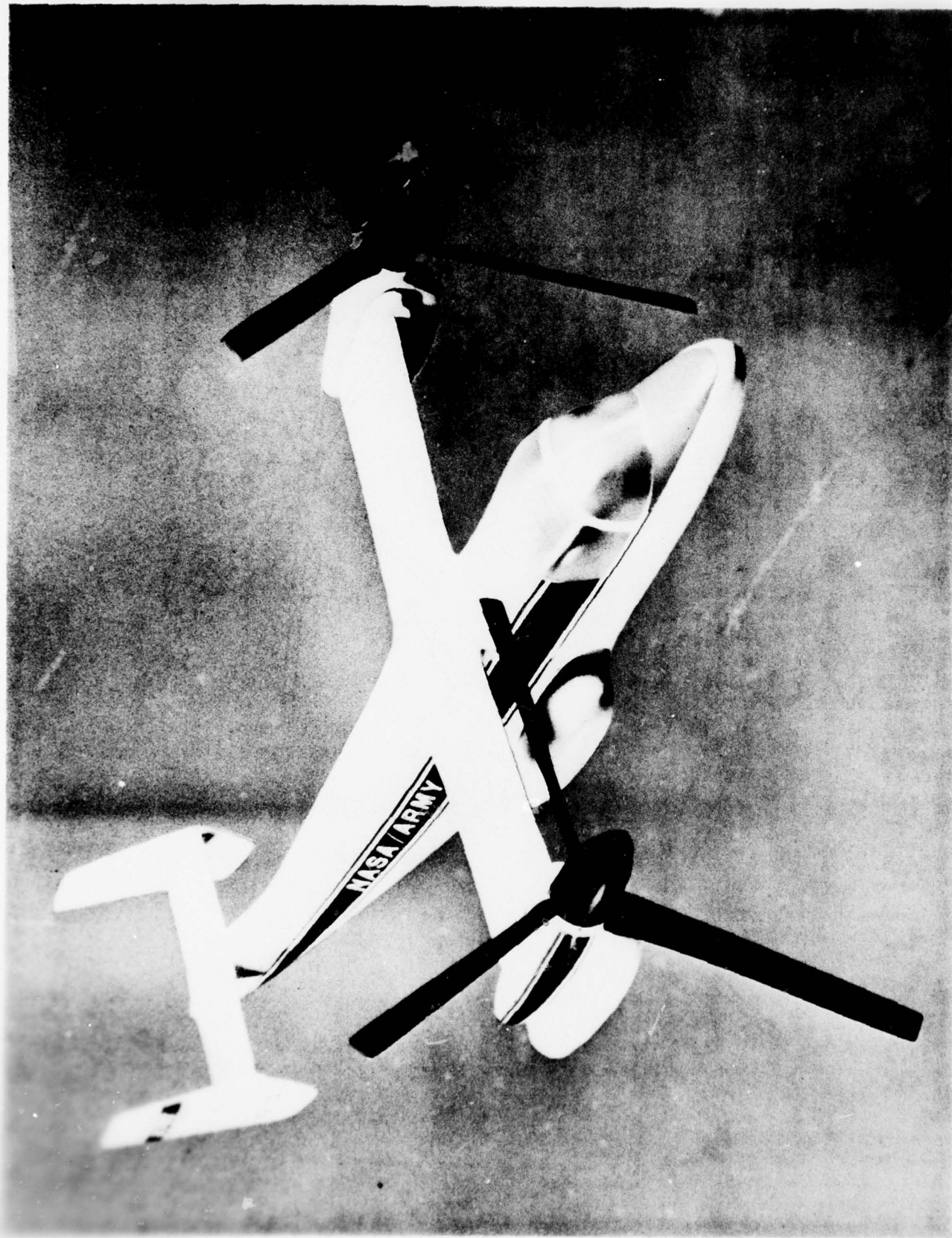
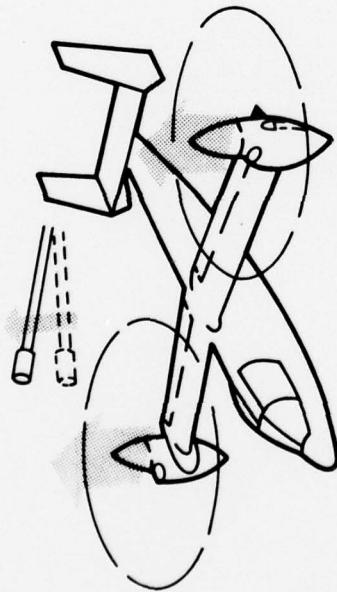


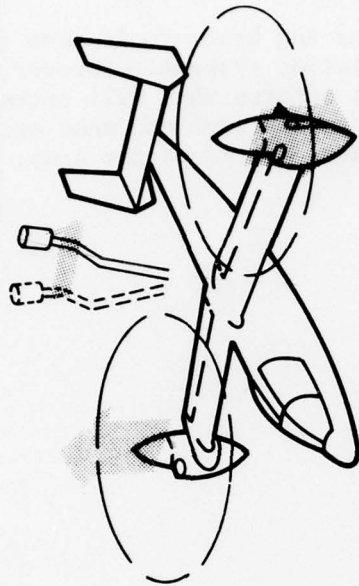
Figure 13

XV-15 TILT ROTOR RESEARCH AIRCRAFT CONTROL SYSTEM CONCEPT

COLLECTIVE



LAT. CYCLIC



LONG. CYCLIC



DIRECTIONAL



Figure 14

demonstration of advanced technology and hence to improve the contractor's abilities to build better aviation systems. However, we are also conducting research and development efforts that will extend our ability to set realistic requirements for Army systems and make astute assessments of the equipment and systems that are offered to the Army.

NASA'S ACTIVE CONTROL AIRCRAFT PROGRAM *

by

LAWRENCE W. TAYLOR, JR.
NASA Langley Research Center

This paper will discuss the Active Control Aircraft Program for civil transport aircraft. Of particular interest is the incorporation of active controls in the preliminary design of these aircraft. The objective of this program is given in Figure 1. The list of active controls considered is given in Figure 2: reduced static stability, gust load alleviation, maneuver load alleviation, ride qualities improvement, flutter suppression, envelope limiting, and decoupled control. We are trying to do everything possible with control systems to make the overall performance of the airplane better.

The program plan consists of the parts shown in Figure 3: (1) critical R&T, (2) validation flight and tunnel tests, (3) the active control analysis package, (4) the integrated conceptual designs, and (5) flight demonstrations. The first four parts are spread over about a three-year period, and terminate roughly in mid-1977, followed by some flight demonstrations of a special research vehicle, after that time period.

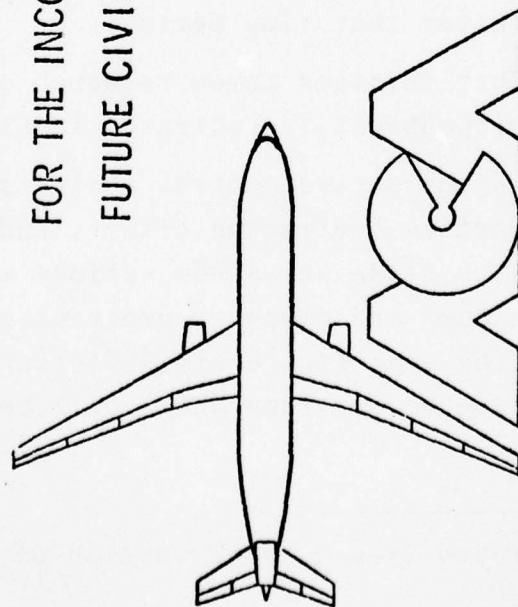
The total effort involves three research centers, with the areas of primary responsibility indicated in Figure 4.

Figure 5 shows the active control analysis package development. The upper part is contracted effort, and the bottom is in-house effort. The slide shows how various control synthesis and modeling techniques and computer programs are being integrated. Shown in the same figure are different module names or parts of a collection of programs which will be used in preliminary design.

* This paper was typed from a taped version of the oral presentation.

OBJECTIVE

"THE OVERALL OBJECTIVE OF THE ACTIVE CONTROL AIRCRAFT PROGRAM IS TO IDENTIFY, DEVELOP, AND VALIDATE TECHNOLOGY REQUIRED TO ESTABLISH DESIGN GUIDELINES FOR THE INCORPORATION OF ACTIVE CONTROLS IN FUTURE CIVIL AIRCRAFT."



ACTIVE CONTROL AIRCRAFT PROGRAM

Figure 1

ACTIVE CONTROLS:

- REDUCED STATIC STABILITY - LESS TRIM DRAG
- GUST LOAD ALLEVIATION - LESS STRUCTURAL WEIGHT
- MANEUVER LOAD ALLEVIATION - LESS STRUCTURAL WEIGHT
- RIDE QUALITIES - PASSENGER COMFORT, LONGER FATIGUE LIFE
- FLUTTER SUPPRESSION - LESS STRUCTURAL WEIGHT, LONGER FATIGUE LIFE
- ENVELOPE LIMITING - FLIGHT SAFETY
- DECOUPLED CONTROL - IMPROVED HANDLING QUALITIES



ACTIVE CONTROL AIRCRAFT PROGRAM

Figure 2

OVERALL ACTIVE CONTROL AIRCRAFT PROGRAM

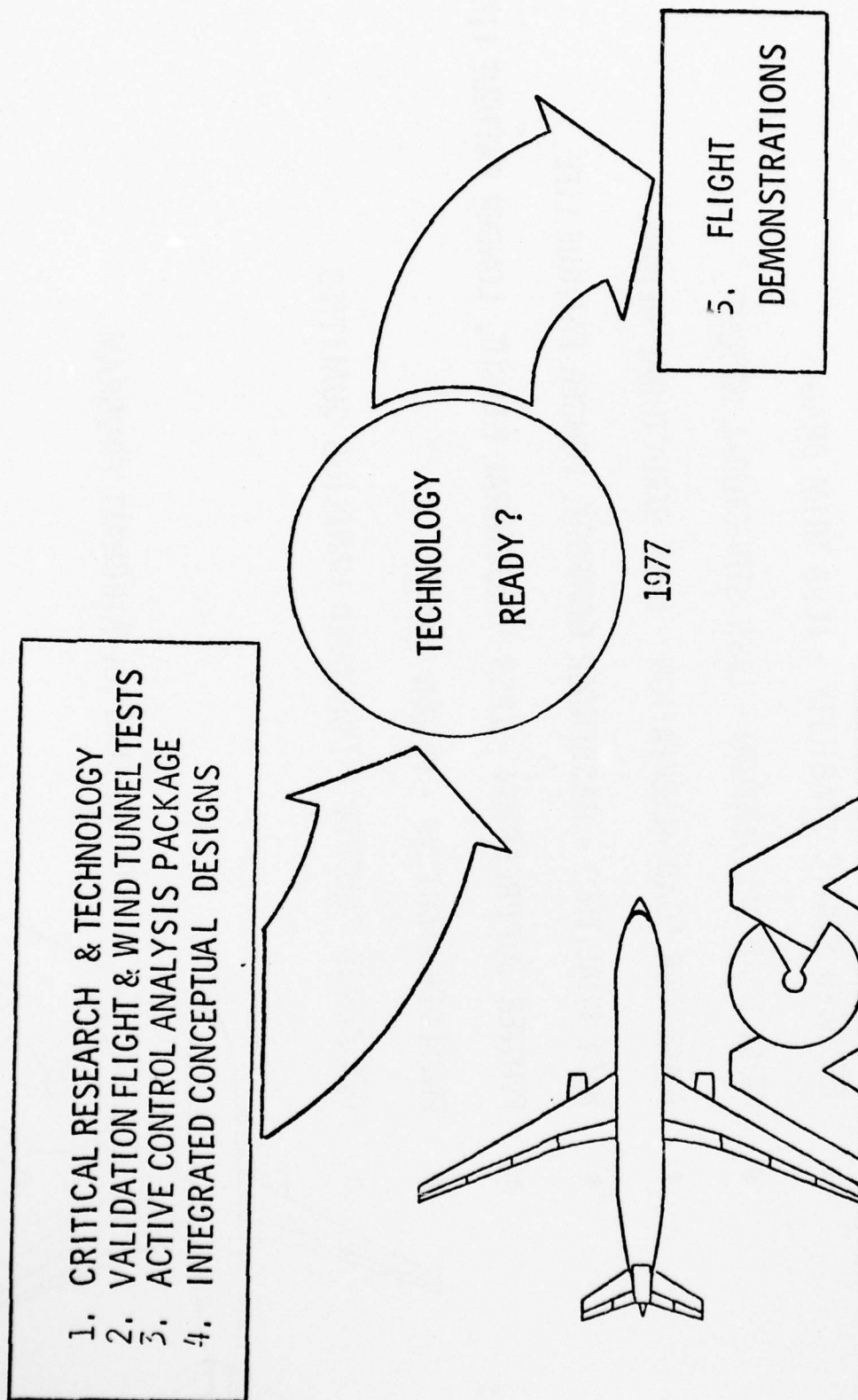


Figure 3

AREAS OF PRIMARY RESPONSIBILITY

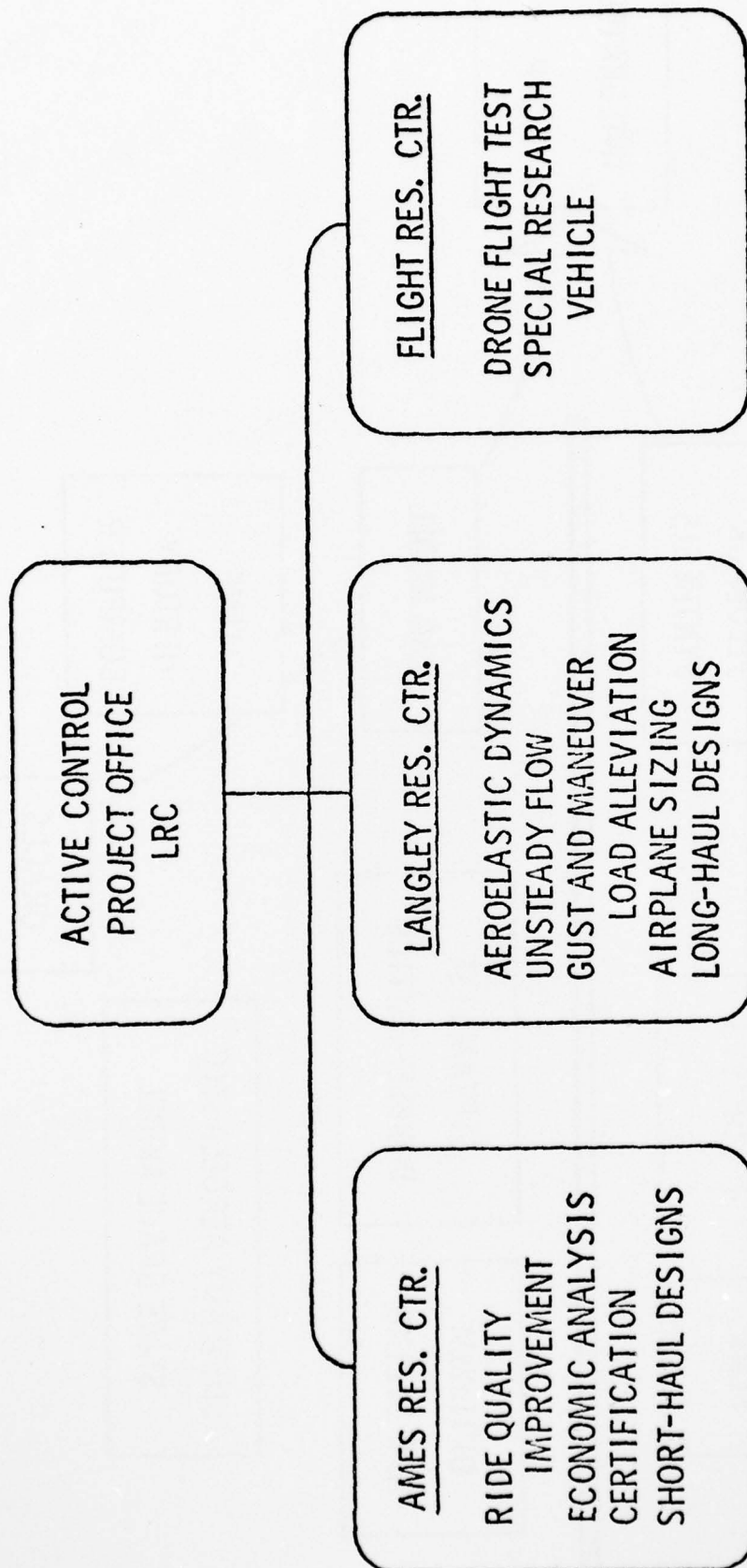


Figure 4

ACTIVE CONTROLS ANALYSIS PACKAGE

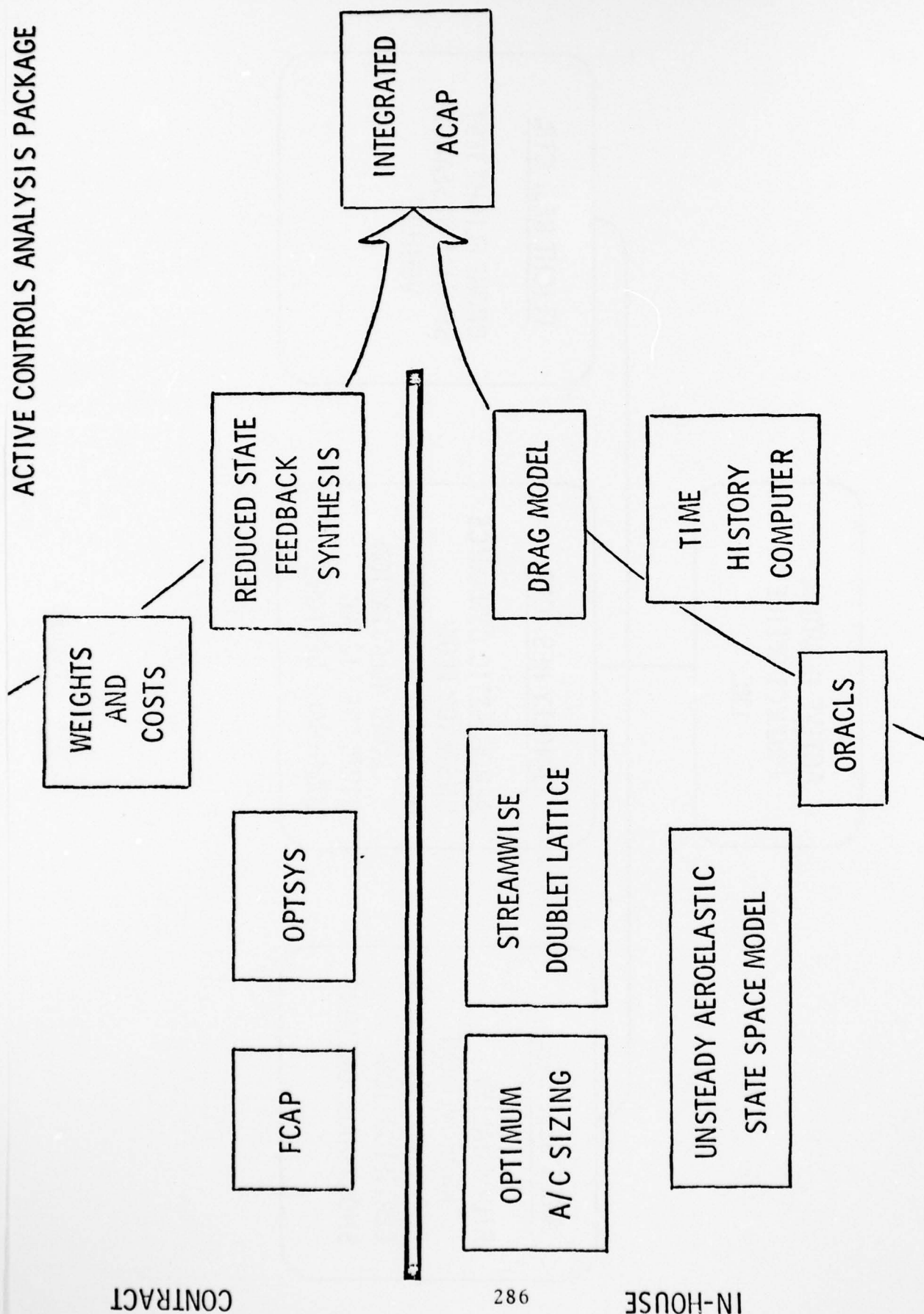


Figure 5

One of the validation flight tests involves the Air Force airplane shown in Figure 6. It is being used in a NASA program in cooperation with the Flight Dynamics Laboratory at Wright-Patterson AFB, and Calspan. The plane is the TIFS (total-in-flight- simulator), but it's being used as a regular airplane, instead of a simulated airplane. The TIFS airplane is unique because of its extensive direct lift flap system. In addition, the airplane will be modified to allow collective deflection of the ailerons as a means of getting additional direct lift. The purpose of this activity is to validate the performance of a gust load alleviation and maneuver load alleviation system in full-scale flight test.

Figure 7 shows the results of some work that Calspan did years ago on a gust load alleviation system. Hown is the power spectral density of the airplane's response to gusts versus frequency. You can see how the gust response is reduced in the moderate frequency range for the gust alleviated response, but made worse in the higher frequency range. It should be noted that this is a log plot before integrating visually the area under the curve. The net result was that the augmented gust response was made a little worse. The problem in this study was that models were not made of the structural dynamics or of the unsteady flow effects. We are trying to consider these effects this time, and use more advanced synthesis techniques. Time will tell how successful these new efforts at gust alleviation will be.

Drones, such as the Firebee 2 drone shown in Figure 8, will also be used in the validation flight tests. A different wing has been installed along with an active flutter suppression system to demonstrate the ability to provide flutter stability with such a flutter system. The drone will have a flutter boundary within the flight envelope, and then will be probed

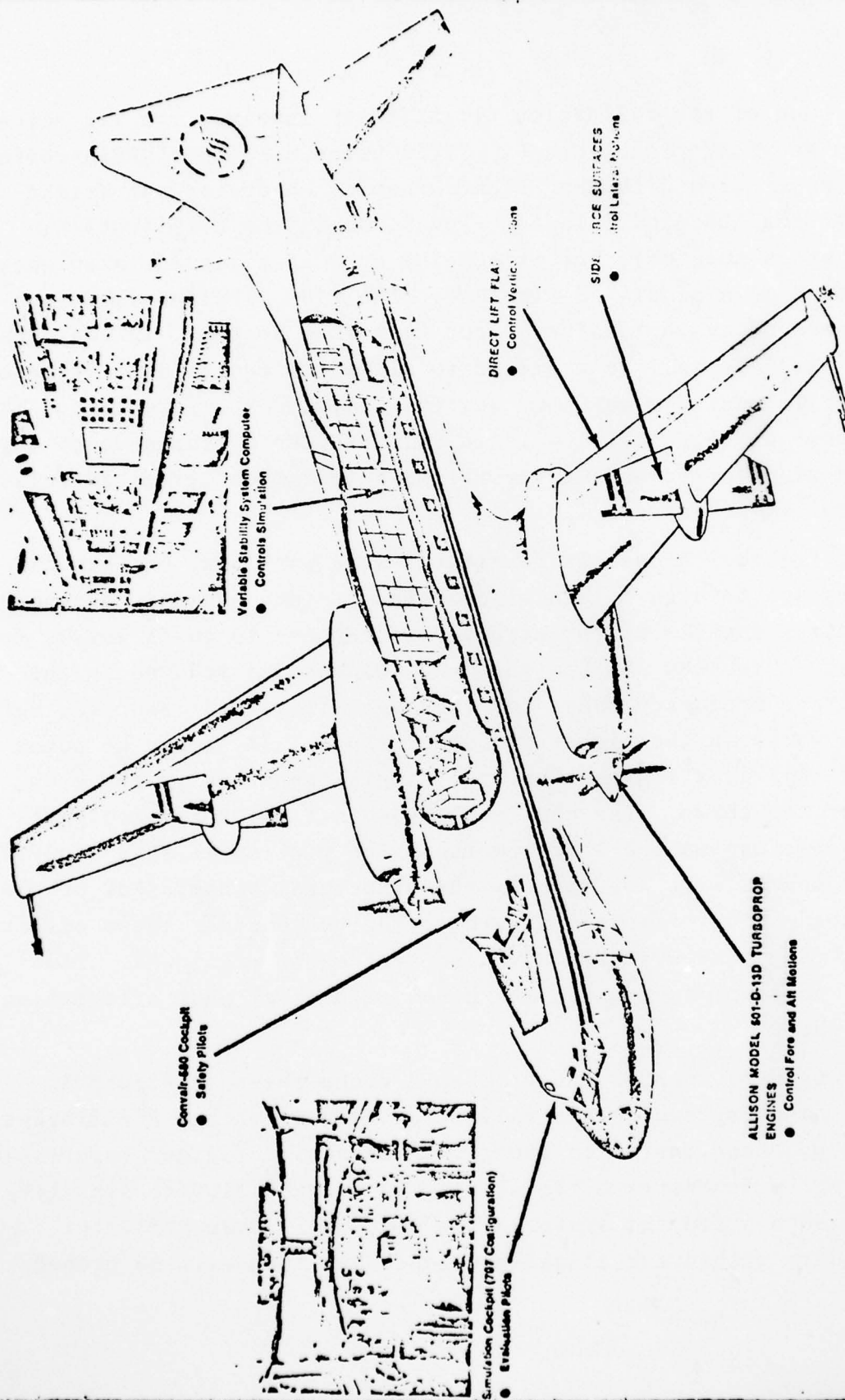
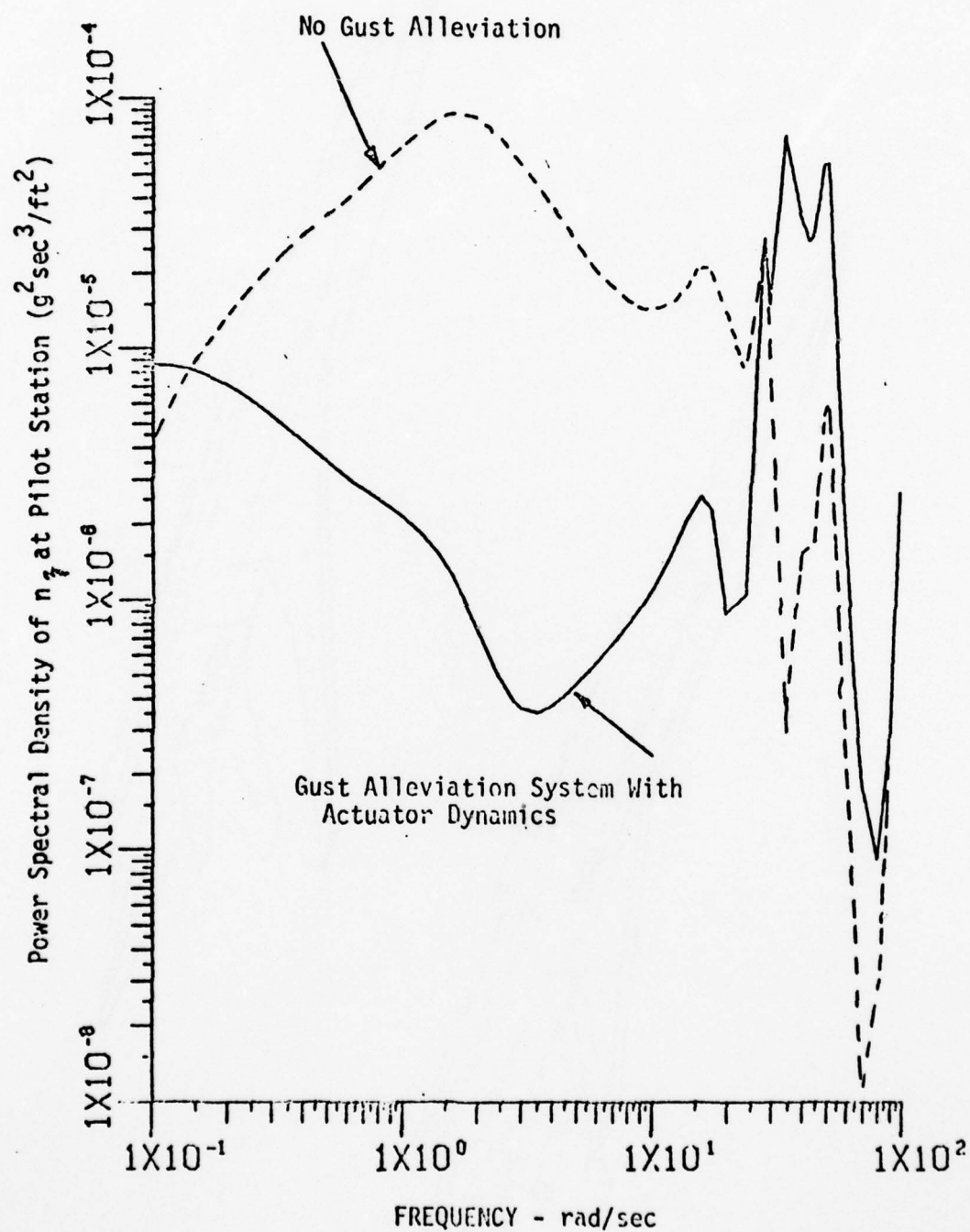


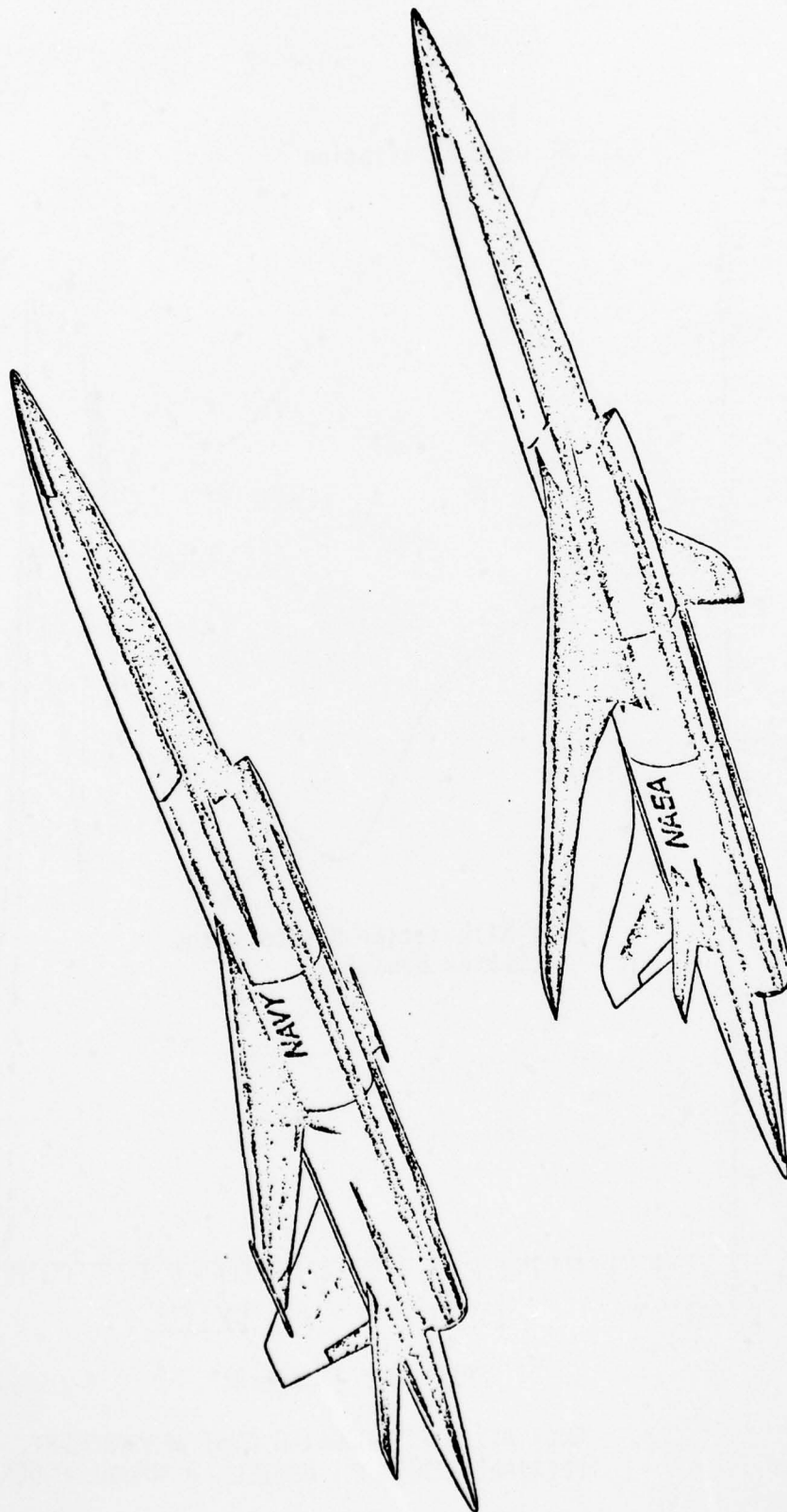
Figure 6



GUST ALLEVIATION USING GUST MEASUREMENT,
FLEXIBLE AIRPLANE, CRUISE, 8 NORMAL MODES

Figure 7

DRONES FOR AERODYNAMIC
AND STRUCTURAL TESTING



107.0530.30

Figure 8

with the system activated demonstrating that we can achieve a sizable margin in flutter speed with the active control system.

The final part of the program will have a fully integrated design using a special research vehicle as a test bed (Figure 9). It will be configured using active controls. It is likely to be a drone to keep costs down. The other part of the flight demonstrations will involve STOL applications and will probably use a modified Twin Otter airplane. The purpose of this activity will be to demonstrate a ride quality control system that will alleviate one of the most important limitations of airplanes with a light wind loading, the rough ride in stormy weather.

The remaining part of this paper will consider some ideas concerning applications of modern control theory to solve some of the problems associated with the application of active controls. One important consideration is to have the cost function that is used to synthesize the control laws be more closely tied to tangible benefits. One of these is the pilot rating. It has been possible to closely approximate contours of constant pilot rating with a quadratic performance index for the simple roll task of Figure 10. It is hoped that a similar approach can be as successful for other control modes. It is expected that other approaches can be used to make the cost functions used for synthesis closely tied to handling qualities considerations. Let us next consider the problem of synthesis for a flexible airplane.

Figure 11 shows a root locus plot with the real part having a different scale than that for the imaginary part. We have integrated the flutter analysis model and the rigid body A-matrix. The result is a single A-matrix that involves the so-called rigid body modes, the structural modes, and models of unsteady aerodynamics, sufficient in accuracy to give an

AD-A045 603

SYSTEMS CONTROL INC PALO ALTO CALIF
PROCEEDINGS OF THE SYMPOSIUM ON CONTROL THEORY AND NAVY APPLICA--ETC(U)
AUG 77 M D CILETTI, J S TYLER

F/G 15/7

N00014-72-C-0327

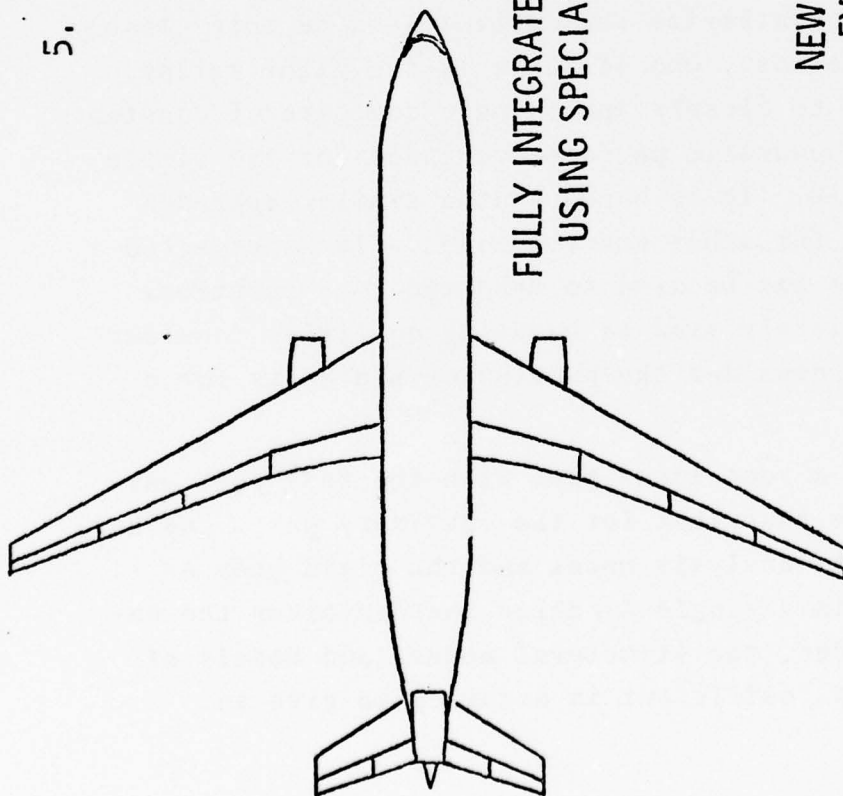
NL

UNCLASSIFIED

4 of 8
AD-A045603



5. FLIGHT DEMONSTRATIONS



FULLY INTEGRATED CTOL DESIGN
USING SPECIAL RESEARCH VEHICLE

NEW CONTROL SYSTEM APPLIED TO
EXISTING SHORT-HAUL AIRCRAFT

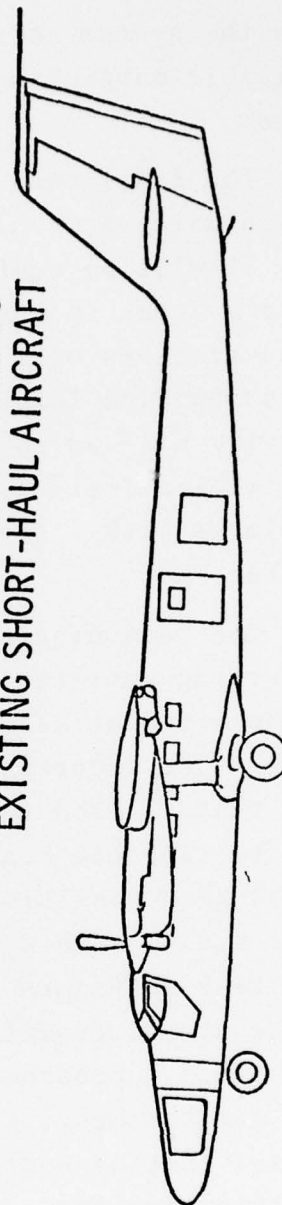


Figure 9

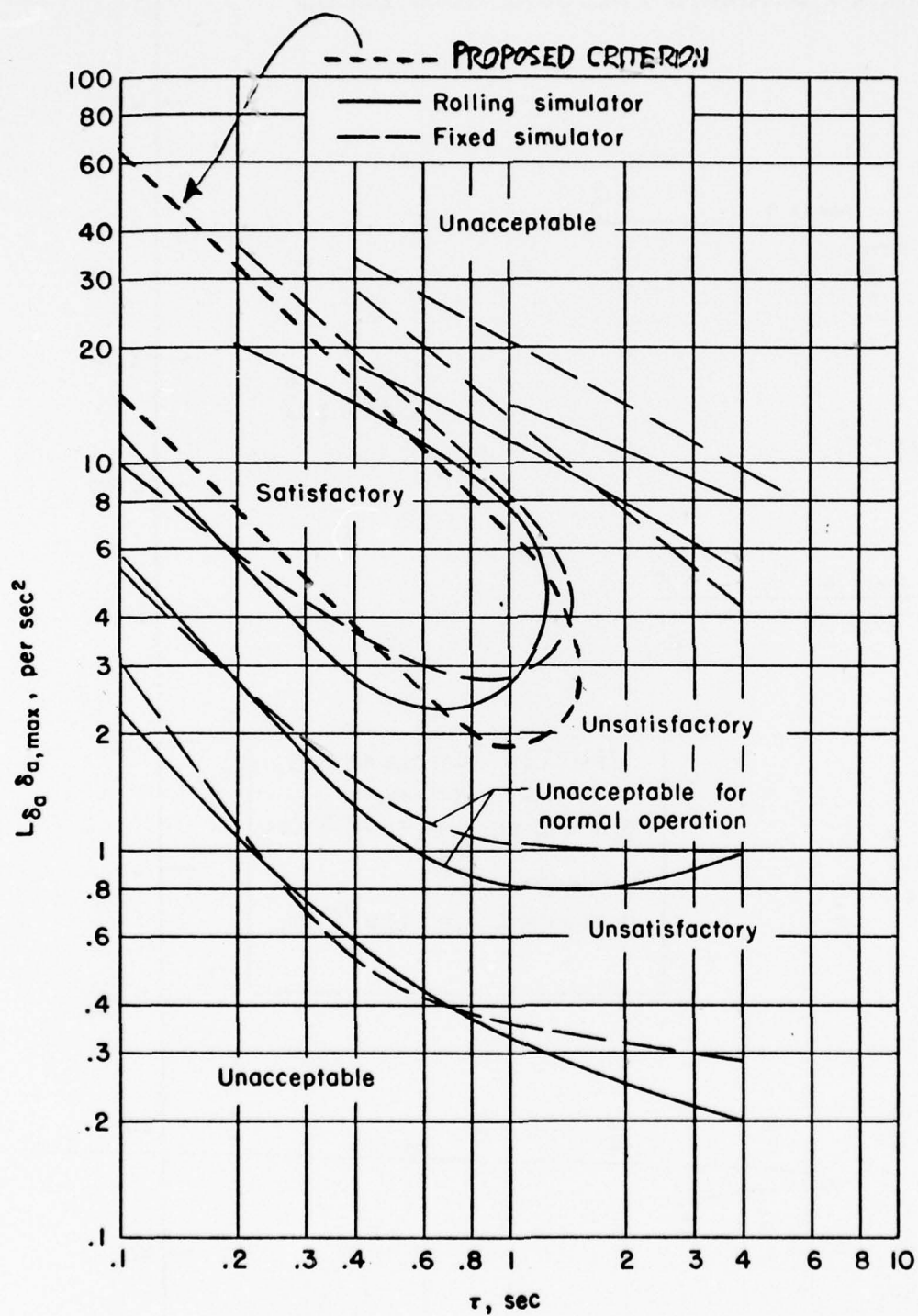


Figure 10 Comparison of pilot opinion boundaries obtained from the fixed and moving flight simulators.

MACH 0.9 DYNAMIC PRESSURE ROOT LOCUS

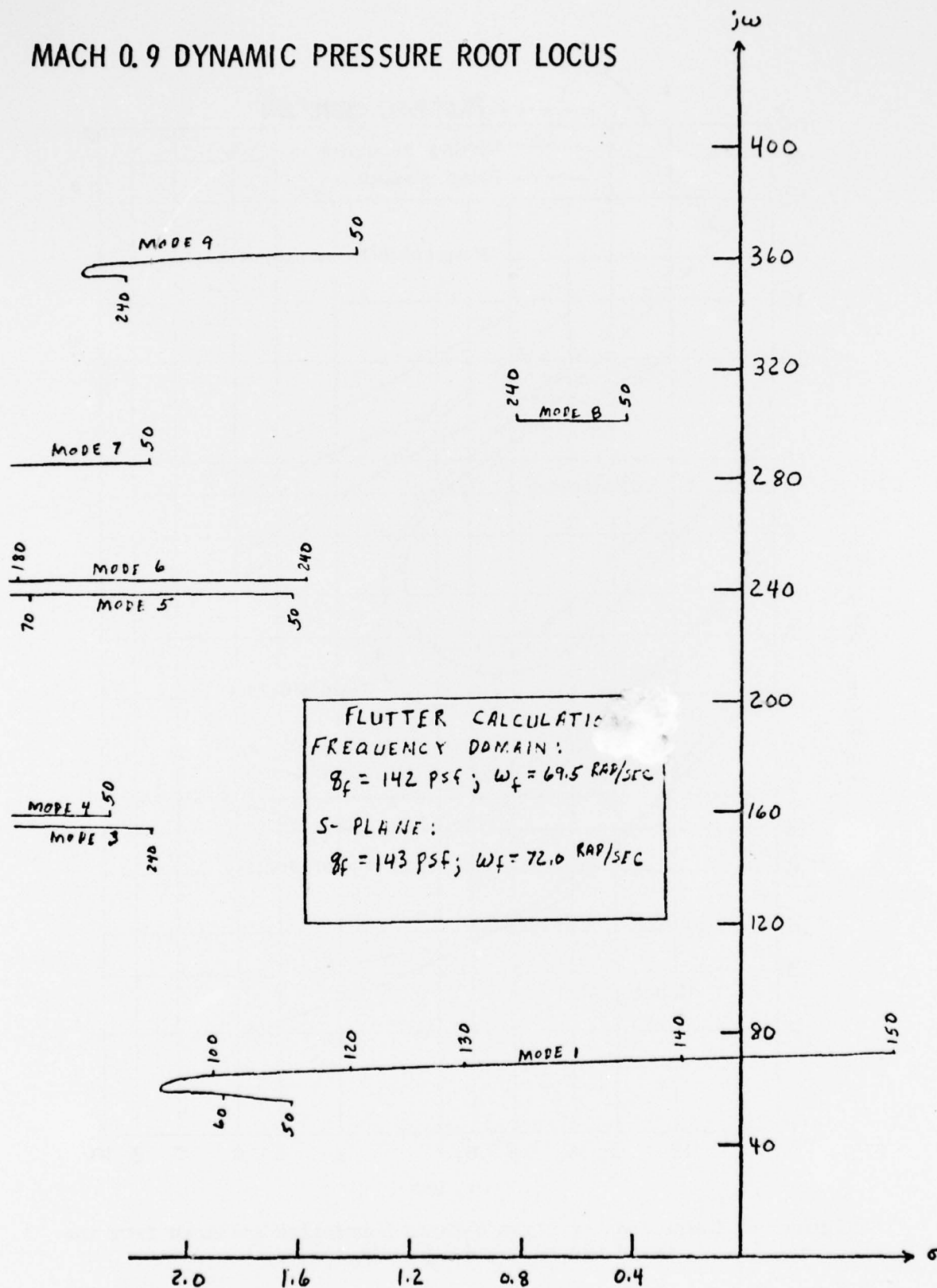


Figure 11

STATE VARIABLES FOR LONGITUDINAL, SYMMETRICAL MODES:

	<u>NUMBER OF STATES</u>
RIGID BODY MODES (α , q , θ , v)	4
AEROELASTIC MODES (9 SECOND ORDER MODES)	18
UNSTEADY FLOW (+2 EACH MODE, CONTROL)	26
ACTUATOR DYNAMICS	8
SENSOR DYNAMICS	10
FILTERS, COMPENSATORS	8
TOTAL	<u>74</u>

IF ALL MODES ARE COUPLED BECAUSE OF ENGINE MOMENTUM OR MALFUNCTIONING ACTUATOR, THE TOTAL STATES NUMBER IS ABOUT 150.

CONCLUSION:

NEED REDUCED STATE, INSENSITIVE CONTROL, SYNTHESIS TECHNIQUES, AND ALGORITHMS.

Figure 12

accurate flutter speed. We have made a comparison between this state variable approach and the classical approach. The two differed by one pound per square foot out of 143 for the dynamic pressure at the flutter condition. The flutter frequencies were $69\frac{1}{2}$ and 72 cycles per second.

One obvious observation that results from looking at such an A-matrix is the large unwieldy number of states. Figure 12 shows how the number of states can build up. It should be obvious that there are too many states to consider feeding back the entire state vector or to consider estimating those you can't sense directly. So, we've simply got to have better, more efficient ways of synthesizing with reduced state feedback.

Figure 13 is an attempt to illustrate an algorithm that addresses the synthesis problem in a general way. Represented are models of the disturbances, the intended response, and the plant. The disturbance model assumes that all of the noise can be injected at a single point, whether it be measurement noise, state noise, or noise due to uncertainties. If we can solve this problem using a quadratic cost function such as that shown in the figure, then we can synthesize both the feedforward and feedback control laws. The attraction of this approach is the ability to consider simultaneously a number of disturbances for a cost function which is directly related to pilot ratings. Considerable work remains, however, before this approach will be operational.

CONCLUDING REMARKS

NASA's Active Control Aircraft Program involves both theoretical and experimental activities concerned with the application of active controls to civil transport aircraft. Several aspects of the control synthesis problem are discussed and suggested and approaches.

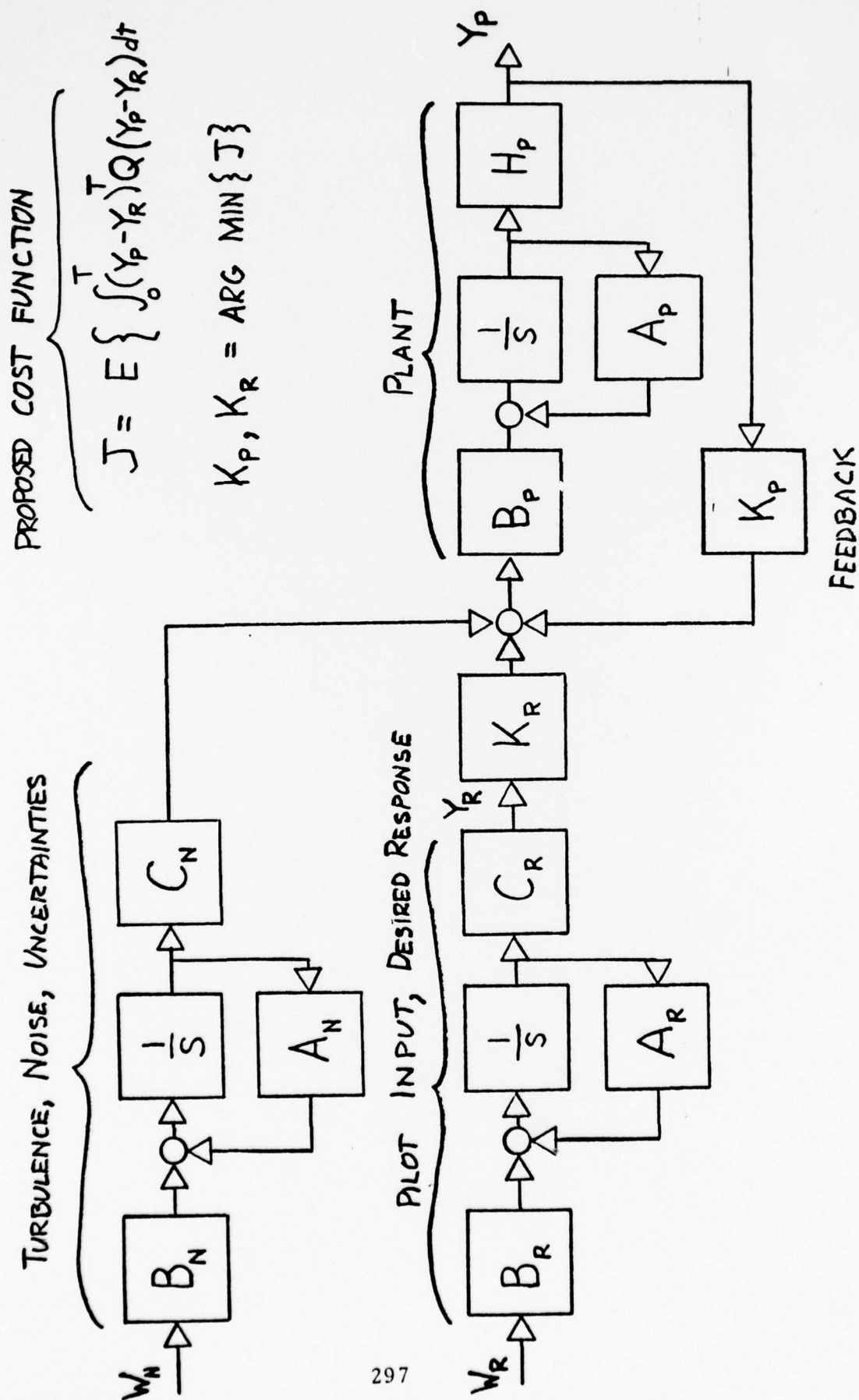


Figure 13

SESSION IV
IDENTIFICATION

SYSTEM IDENTIFICATION - AN OVERVIEW

by

W. EARL HALL, JR.
Systems Control, Inc. (Vt)

System identification, the technology of modeling vehicles and systems from their dynamic response, has emerged from its theoretical foundation to a practical Naval development, test, and evaluation tool. This paper reviews the status of this technology and its present and potential impact on the Navy.

INTRODUCTION

A vehicle (e.g. ship, submarine, aircraft) results from an extensive design process which is initiated by engineering knowledge of how basic physical laws can be controlled to perform a desired function. The more complex the machine, the more the engineer relies on mathematical models, from simple formulae to large systems of equations, to represent these laws and guide the design decisions throughout the design phase. This model also is used to develop quantitative specifications for evaluating performance of the vehicle and guide design modifications.

During the 1960's, there emerged another requirement on the accuracy of system models. These models were also used for the development of multivariable digital control and state estimation algorithms which were becoming an integral part of vehicle avionic systems. These new concepts, particularly that of state estimation (viz. Kalman filtering) for navigation systems, have played an increasingly important role in improving operational capabilities of Navy ships and aircraft. As these concepts were implemented, however, it became clear that accuracy of the design models was becoming a fundamental limitation to the potential improvements which could be practically realized.

The need for better models could be partially met with physical analysis and scale model tests. However, the uncer-

tainties involved in these approaches precludes sufficiently accurate models for many of the advanced vehicles of the 1970's and beyond. Examples are the difficulties in theoretically predicting flows in extreme aerodynamic or hydrodynamic regimes or in extrapolating from scale model results to full scale, because of nonsimilitude of viscous effects.

What was needed was a comprehensive technology for improving models based on tests of the actual system. Such a technology is that of system identification. This technology of system identification embodies more than estimation of model coefficients from data, but also the specification of tests by which that data is obtained. To explore this multi-faceted aspect of system identification, the following definition is discussed.

SYSTEM IDENTIFICATION - A DEFINITION

System identification is a highly mathematical technology and may be rigorously defined in statistical terminology. For application in engineering technology, however, the following definition has been found useful.

System identification determines, from a given input/output data record of vehicle test response, an estimate of the physical model which relates the observed data.

This definition implies that system identification involves the following:

- (1) A mathematical model: Though the governing equations for many vehicles are known, it is frequently found that other equations (e.g. effects) are present, and the data must be analyzed to isolate what the actual model is.
- (2) Parameters of the model: This is parameter identification, where the coefficients of the model are quantified from the data.
- (3) Random errors: Random errors in data arise from model errors, instrumentation or external forces such as from gusts. These errors must be identified and removed from the model effects.

Figure 1 shows an example of how the system identification procedure is used with submarine input and output data, corrupted

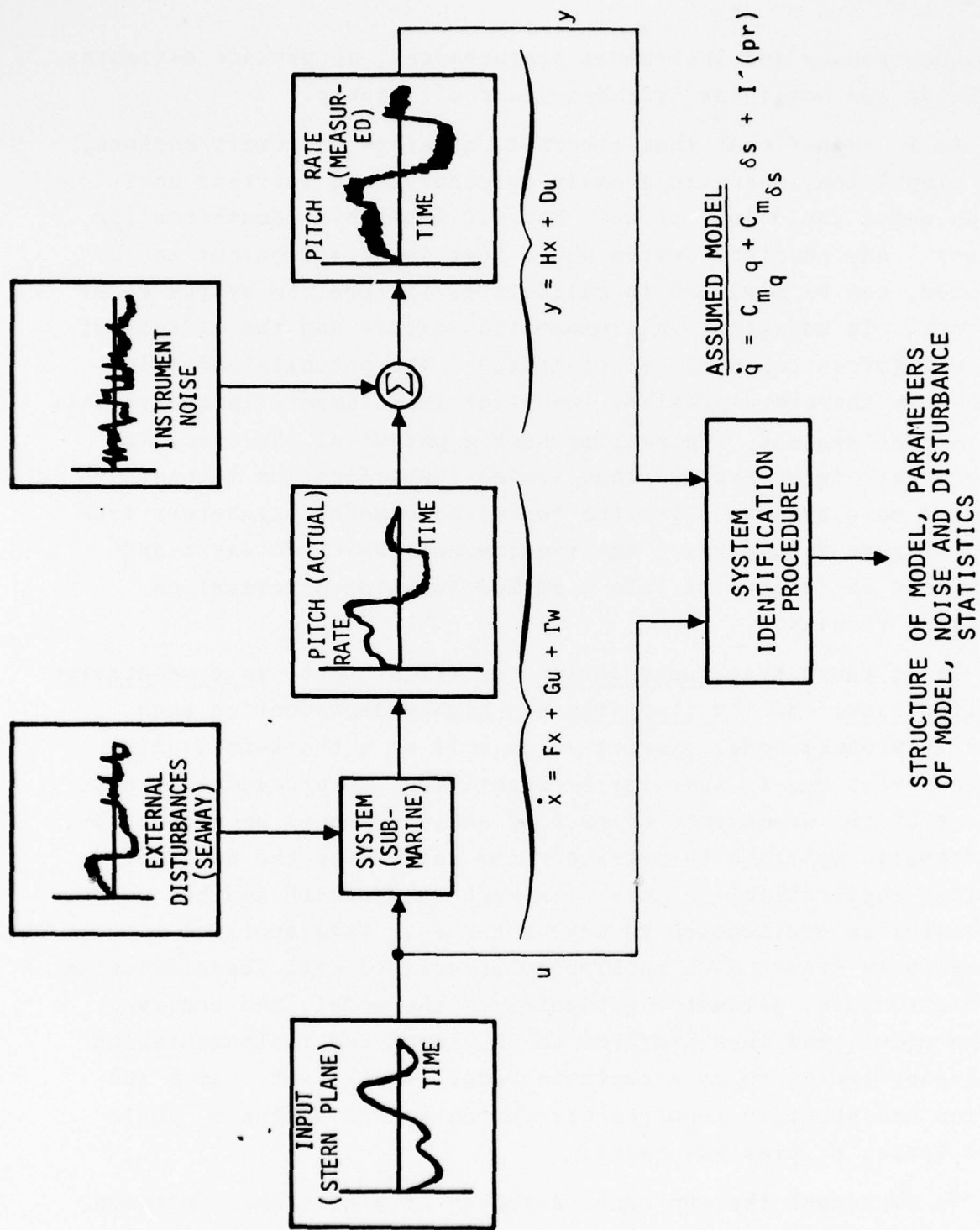


Figure 1

by random seaway and instrument disturbances, to produce estimates of linear and nonlinear hydrodynamic coefficients.

It is significant that aircraft, missiles, aircraft engines, ship propulsion, magnetic anomaly detectors, and inertial navigation units could just as well benefit from this identification process. Any physical system whose test input and output can be measured, can be analyzed to validate or improve the system model accuracy. In addition, instrumentation errors and the effects of external forces can also be calibrated. The potential of this technology therefore promises important improvements in the vehicle development process. To realize such a potential, however, it is necessary to understand that system identification technology requires more than an algorithm to estimate model parameters from data. Figure 2 summarizes the requirements which do exist and which must be integrated into a methodology for practical engineering results.

It is known that input design for flight test, instrumentation specification, and the algorithm are highly dependent on each other to produce model parameters as well as a characterization of the errors due to modeling or identification procedure errors. Because of the dependence of each of these elements on each other, a systematic approach is necessary for satisfying the needs of specific application. Figure 3 is such an approach and has proven successful in application to Navy vehicles. This approach successively treats each subproblem associated with identification model structure, parameter estimates of the model, and accuracy of the model, and then iterates on the input and instrumentation until convergence to an acceptable model is achieved. Each subproblem has specific requirements for data from analysis, scale model tests, or previous tests.

To implement the approach, a number of algorithms, software, and hardware considerations must be evoked. The status of these various considerations is now discussed.

THE INTEGRATED SYSTEM IDENTIFICATION PROCESS

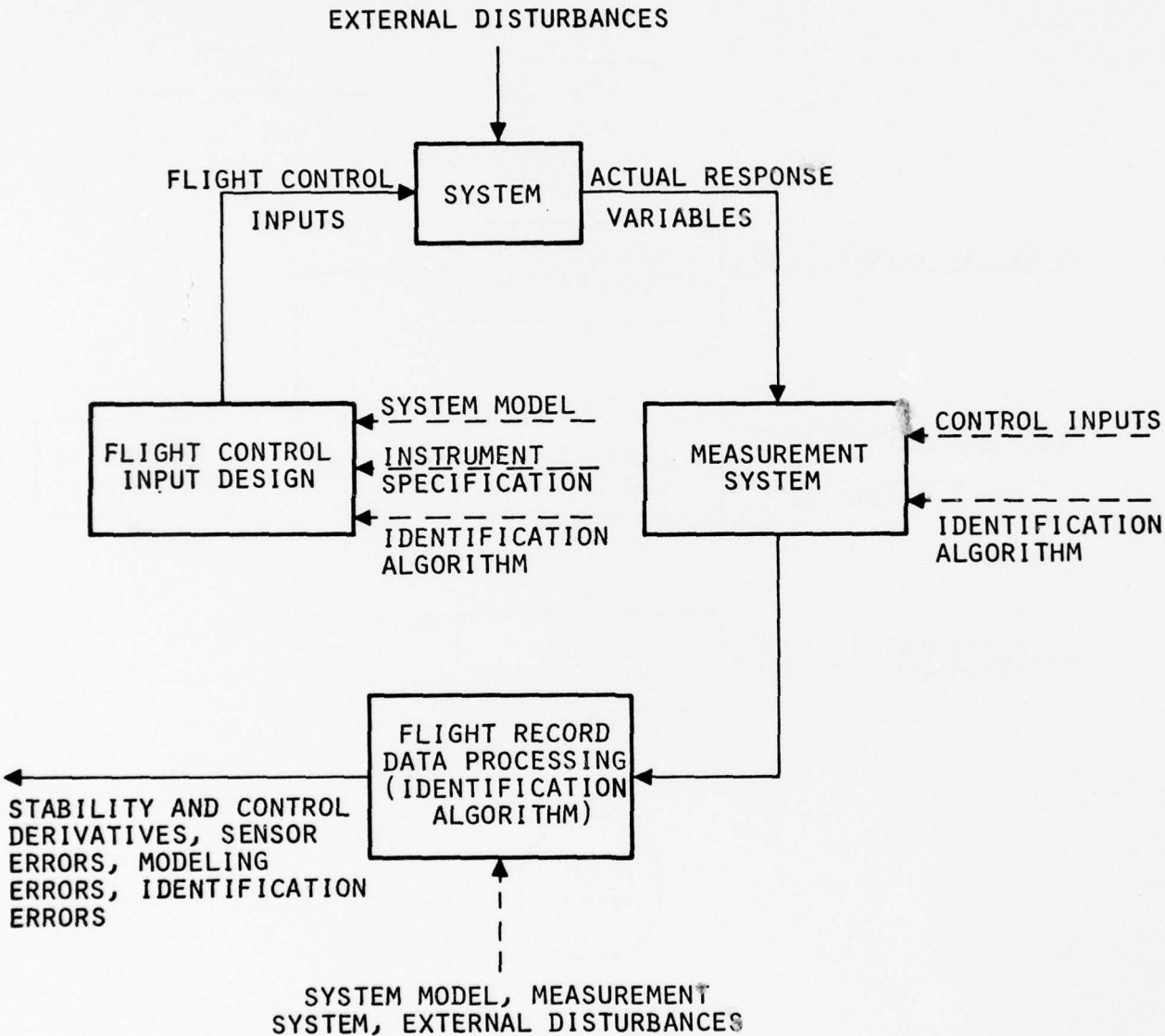


Figure 2

SUBPROBLEMS OF PARAMETER IDENTIFICATION

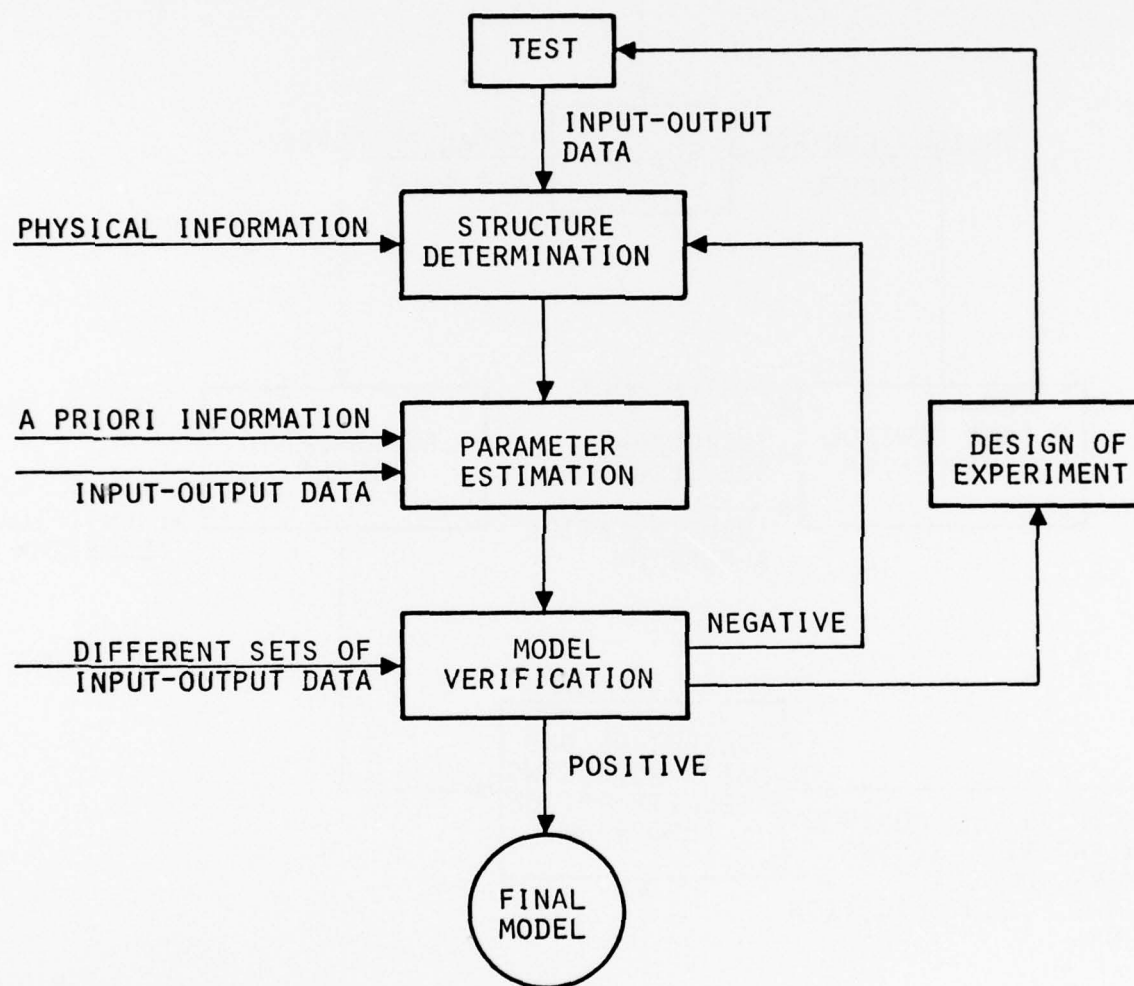


Figure 3

SYSTEM IDENTIFICATION - STATE-OF-THE-ART

The basic theoretical foundations of present applications of system identification were stated by Gauss, Fisher, Weiner, Komogorov, and Kalman. During the 1960's, system identification applications to Navy-type vehicles (notably aircraft) were limited to simple mathematical models from which basic stability and control parameters could be determined. More complete models were difficult to identify because of the effects of measurement noise, gust effects, lack of systematic input design capability, and the limited capability of computers to handle large-scale problems. A more subtle limitation to progressing the state-of-the-art was the lack of a clear requirement for better models after the vehicle had been built and flown.

What, then, has changed? Over the past six years, definite requirements for better vehicle models have emerged and significant improvements in system identification capability have been achieved. Specific requirements include:

- (1) Higher performance attainment for Navy vehicles and subsystems is dependent on better models upon which design decisions can be formulated, and estimation and control algorithms can be developed. Examples are shown in Figures 4 and 5.
- (2) Changes in design methods arising from higher performance requirements and cost considerations have placed more reliance on simulations and "fly-before-buy" specifications.
- (3) Changes in other technologies, such as lightweight composite materials and computer miniaturization, have lead to innovative concepts which place even more emphasis on integrating such advances with the effects on basic vehicle response characteristics.

To meet such requirements, the technology of system identification has undergone two important changes. First, the understanding of the theory and techniques for implementing the methods has improved.

WHY SYSTEM IDENTIFICATION IS NEEDED?

SYSTEM IDENTIFICATION CAN BE USED TO OBTAIN:

- STABILITY AND CONTROL PARAMETERS OF BASIC SYSTEM
- NONLINEAR REGIME MODEL STRUCTURE
- UNDERSTANDING OF SUBSYSTEM INTERACTION
- OBTAIN EXTRAPOLATIONS OF PHYSICAL (SCALE) MODEL ESTIMATES
- STATISTICS OF DISTURBANCES
- VALIDATE SIMULATORS
- DETERMINE CAUSE OF FAILURES
- CALIBRATION OF INSTRUMENTS

SYSTEMS IN WHICH IDENTIFICATION
IS INVOLVED TO VARIOUS DEGREES

● NAVY VEHICLES

- AIRCRAFT (FIXED AND ROTARY WING)
- SURFACE SHIPS
- SUBSURFACE VEHICLES
- MISSILES

● NAVY SYSTEMS

- NAVIGATION
- GUIDANCE
- CONTROL
- PROPULSION
- STRUCTURE

Figure 5

Secondly, the applications of the technology have become more widespread and some significant successes have been achieved (e.g. reduction of flight test time, upgrading of simulators).

For the purpose of this overview, the basic elements of system identification - algorithms for parameter and model structure identification, input design, and instrumentation - are now reviewed with respect to the state-of-the-art.

System Identification Algorithms

Even a cursory review of the literature reveals a confusing number of various identification algorithms. Some of the most frequently encountered are listed in Figure 6. Closer examination of those various methods, both from a theoretical and practical point of view, however, allows categorization into three principal methods which characterize modern system identification. These are:

- (1) Equation error methods (also known as least squares or regression)
- (2) Output error methods
- (3) Advanced methods

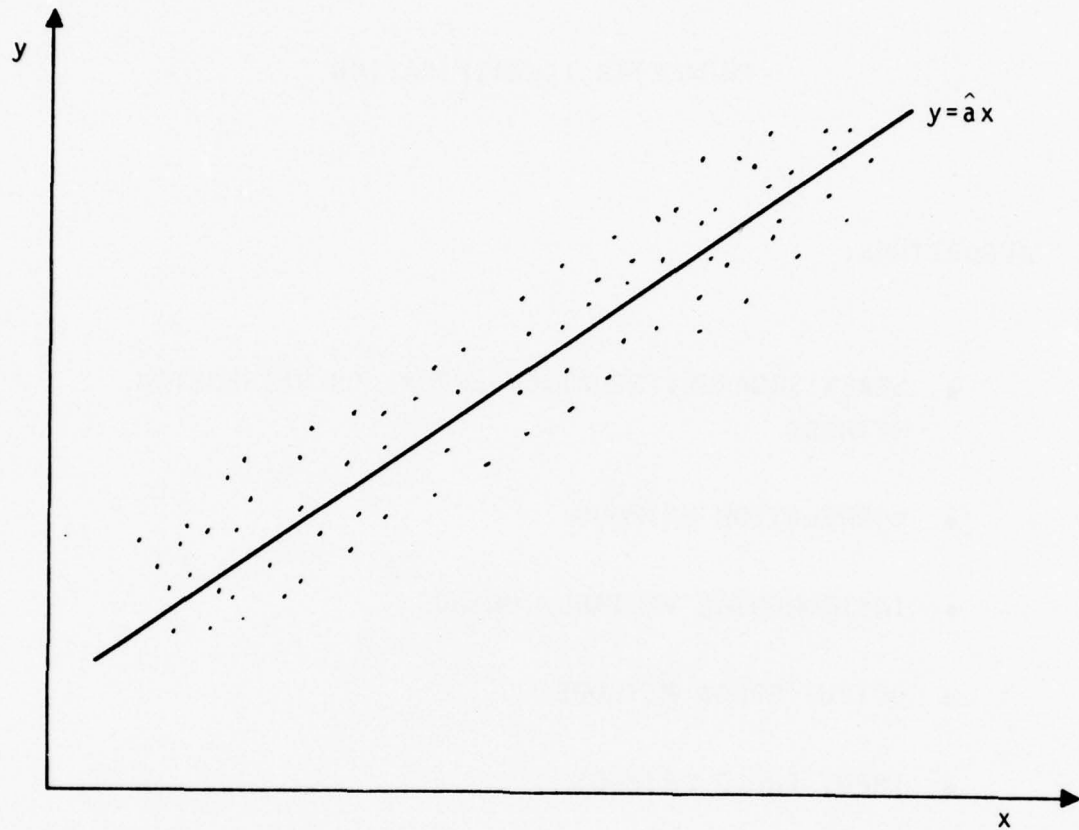
Equation error methods are the modern equivalent to Gauss' original least squares procedures which are used to model observations of planetary motion. Figure 7 summarizes this least squares principle. Output error methods (Figure 8) are derived, in principle, from analog computer matching techniques of identification. Because of higher flexibility and accuracy, both of these basic methods are being replaced by advanced methods - extended Kalman filter and maximum likelihood being the most widespread. The maximum likelihood method, in particular (Figure 9), is rapidly achieving widespread use. This is based on two factors. First, both equation error and output error methods can be shown to be special cases of the maximum likelihood method. Secondly, the

PARAMETER IDENTIFICATION

ALGORITHMS:

- LEAST SQUARES, EQUATION ERROR, OR REGRESSION METHODS
- CORRELATION METHODS
- INSTRUMENTAL VARIABLE METHOD
- OUTPUT ERROR METHODS
- INPUT ERROR METHODS
- GENERALIZED ERROR METHOD
- MAXIMUM LIKELIHOOD ESTIMATION
- KALMAN FILTER/SMOOTHING
- STOCHASTIC IDENTIFICATION

LEAST SQUARES



$$y = ax + \text{NOISE}$$

FIND $a = \hat{a}$ SUCH THAT

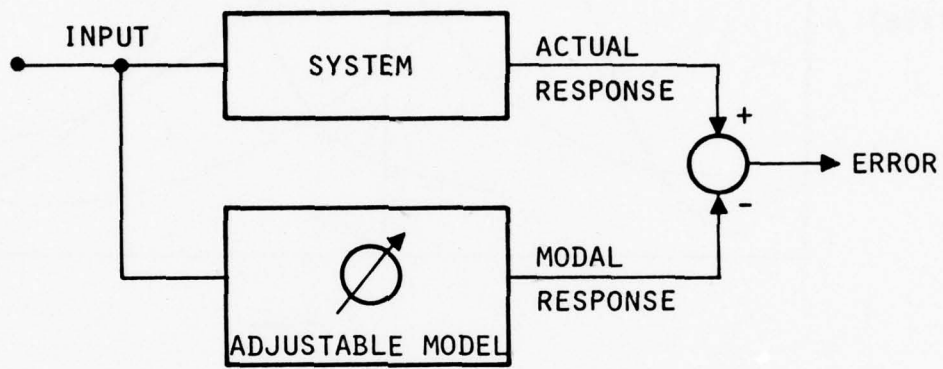
$$(y - \hat{a}x)^2$$

IS "SMALL".

Figure 7

OUTPUT ERROR

- o BASED ON ANALOG MATCHING, ALSO CALLED MODEL REFERENCE

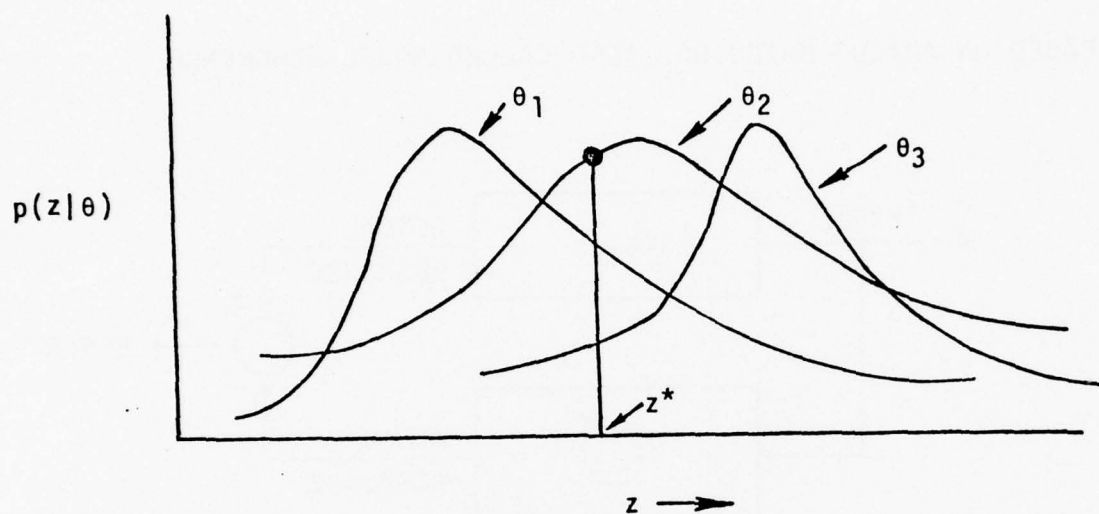


- o ADJUST PARAMETERS TO MINIMIZE ERROR

(NOTE: PARAMETERS IN ERROR IF HAVE PROCESS NOISE)

Figure 8

MAXIMUM LIKELIHOOD



SUPPOSE θ CAN TAKE ONE OF THREE VALUES: θ_1 , θ_2 AND θ_3 .

IF z^* IS THE OBSERVED VALUE OF z , THEN θ_2 IS THE
MAXIMUM LIKELIHOOD ESTIMATE OF θ .

Figure 9

maximum likelihood method has undergone extensive development under ONR research and is now being adopted by the Navy as well as NASA, Air Force, and Army agencies. A flow chart of one implementation of the maximum likelihood method is shown in Figure 10. Figure 11 lists some of the various computational techniques associated with each of these basic methods.

All three of these basic techniques can be used both for estimating model structure from input/output data or for parameter estimation for a specified model. Practical system identification requires both model and parameter estimation.

Model Structure Determination

Model structure determination procedures consist of testing input/output data successively against several assumed identification models and testing for "goodness of fit" in some sense. Equation error identification methods are frequently used for such structure estimation because they do not generally require start-up values of model parameters and thus provide estimates of both model and parameters. These parameter estimates are usually biased, however, because of the sensitivity of the equation error techniques to uncertainties on the state of the system. Maximum likelihood methods may also be used successively but there may be a significant penalty in computation time and possibility of divergence because of required start-up estimates in many implementations. Regardless of the particular algorithm, however, the ultimate success of a model structure procedure depends on the "goodness-of-fit" test. This is because of the so-called identifiability problem which arises because the basic algorithm cannot, on the basis of the data provided, distinguish between parameters or alternative model structures.

One approach which has been found useful for determining the model structure which relates input and output data is to plot some "goodness-of-fit" parameters as a function of the

FLOW CHART OF MAXIMUM LIKELIHOOD IDENTIFICATION PROGRAM

FLIGHT TEST DATA, WIND TUNNEL VALUES OF
AERODYNAMIC PARAMETERS

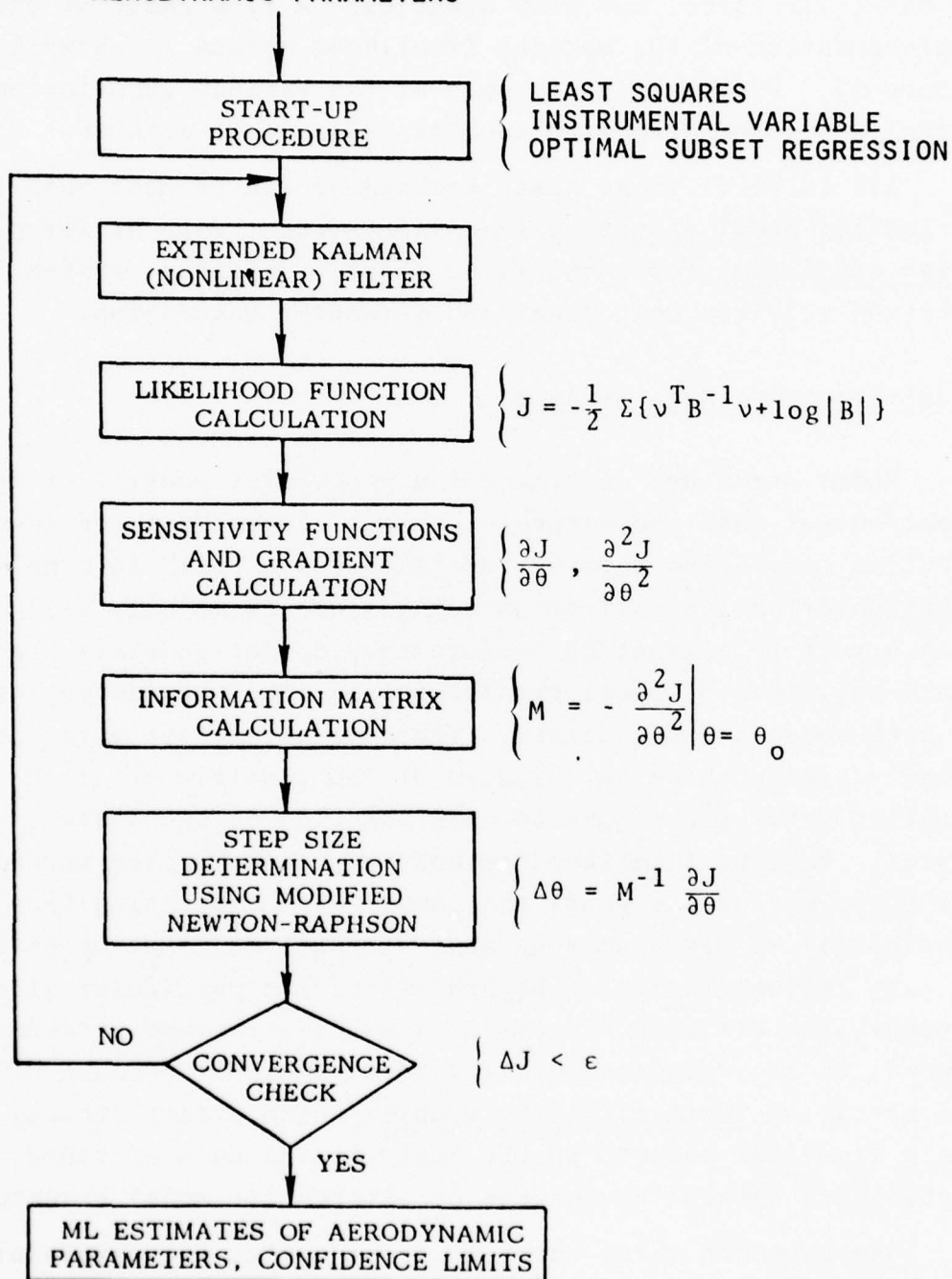


Figure 10

CATEGORIES OF PARAMETER IDENTIFICATION
AND COMPUTATION METHODS

I. EQUATION ERROR METHOD

- LEAST SQUARES
- WEIGHTED LEAST SQUARES
- METHOD FUNCTIONS
- TRANSFORM METHODS
- SPLINE FUNCTIONS

II. OUTPUT ERROR METHOD

- NEWTON-RAPHSON
- MODIFIED NEWTON-RAPHSON
- QUASI LINEARIZATION
- KALMAN FILTER
- GRADIENT TECHNIQUES
- CONJUGATE GRADIENT
- STEEPEST DESCENT

III. ADVANCED METHODS

(THOSE THAT ACCOUNT FOR BOTH
MEASUREMENT AND PROCESS NOISE)

- MAXIMUM LIKELIHOOD
- KALMAN FILTER/SMOOTHING

Figure 11

number of parameters in a model. Figure 12 shows such a plot with two such goodness-of-fit parameters - the multiple correlation coefficient, R^2 , and the model F-ratio. Details of these quantities may be found in any good statistics book. For our purposes, the R^2 parameter measures the decrease in fit error as parameters are added, while the F-ratio takes into account the fact that some additional parameters explain the data better than other parameters. The R^2 , therefore, increases with the number of parameters, while the F-ratio reaches a maximum when the "best" parameters are reached and indicates no further parameters should then be added.

Use of such methods to estimate model structure is an effective way to avoid divergence and incorrect results in subsequent parameter identification.

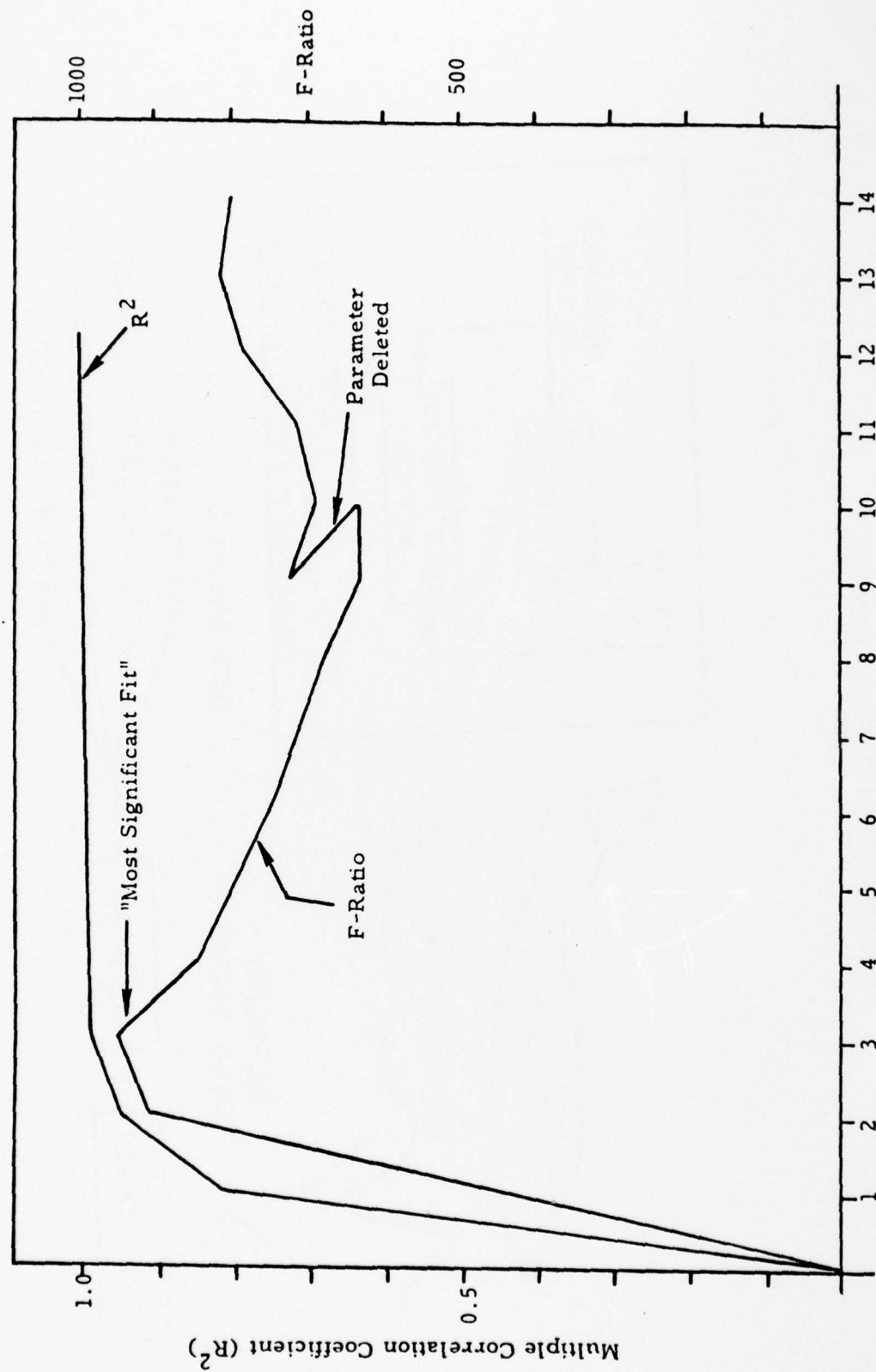
Parameter Identification

Parameter identification for a given model historically has been the focus of system identification. It has only been recently recognized that parameter identification is a subproblem of system identification, since results depend so heavily on the validity of the model for which the parameters are identified.

One particular application of parameter identification where extensive effort has been made is the determination of aircraft stability and control derivatives. For this application, at least for most handling-quality evaluation objectives, the linear aircraft model is reasonably well represented by well known sets of developed linear longitudinal and lateral differential equations of motion.

Figures 13 and 14 summarize one example of an extensive flight test program in aircraft derivative estimation performed by the Naval Air Development Center (see Roger Burton's paper, "Navy Flight Testing and Systems Identification," pp.143-164).

MULTIPLE CORRELATION COEFFICIENT (R^2) AND F-RATIO VARIATION AS PARAMETERS ARE ADDED
TO MODEL (LATERAL CASE)



Number of Parameters in Model

Figure 12

AIRFRAME DYNAMICS IDENTIFICATION

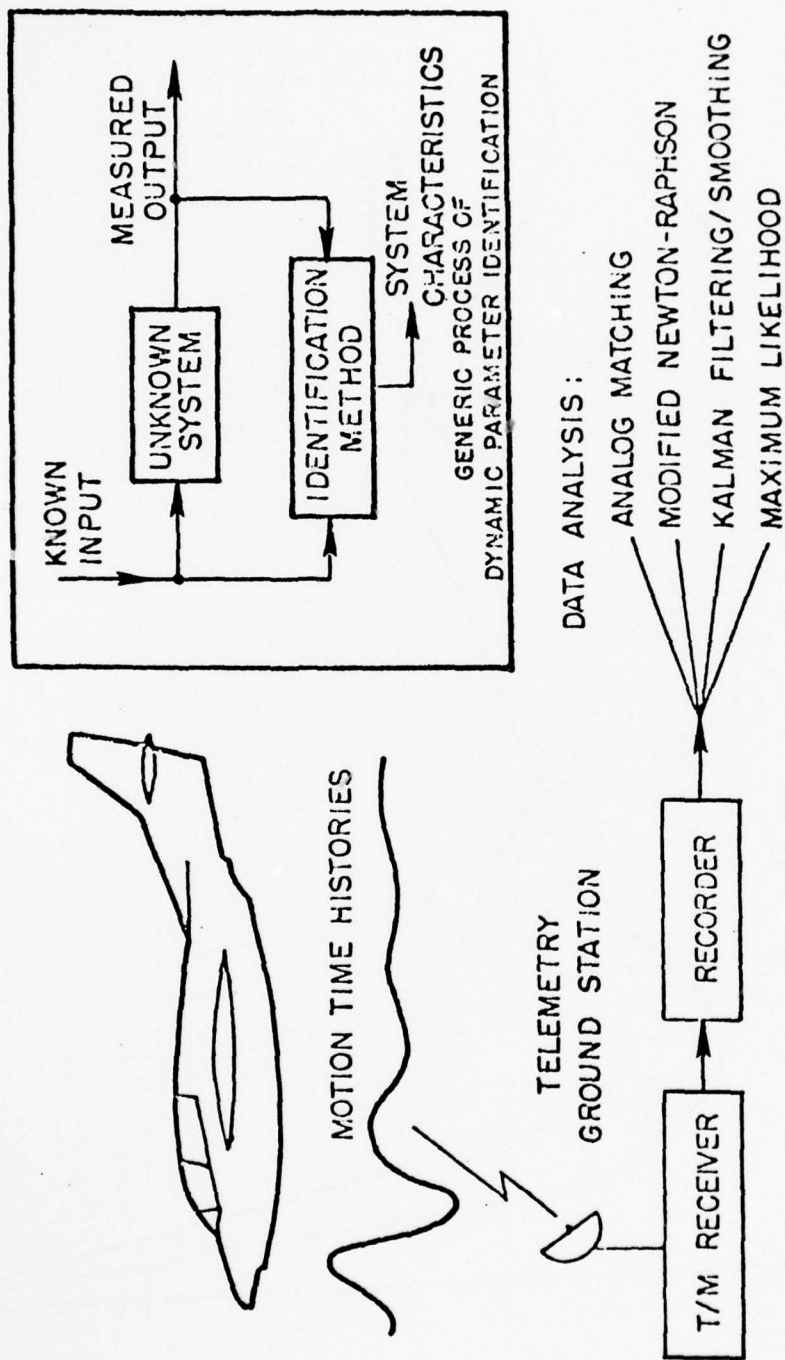


Figure 13

Figure 14 is a summary of results from maximum likelihood methods applied to flight data from a NADC T-2B aircraft. These outputs consist of a set of parameter values (the circles) and an estimated 20 confidence bounds of these estimates (brackets). These estimated confidence bounds are an important aspect of evaluating the reliability of the parameter estimates. In general, the wider the brackets, the less confidence one should assign to to estimate.

When low confidence of parameter estimates results from processing of data, there are several alternatives for improving that confidence. If the confidence has been degraded because of noise, a maximum likelihood algorithm can be used to extract more reliable estimates by using various computational options. If, however, the responses which are most affected by the desired parameters are not sufficiently excited by the system inputs, it is necessary to redesign these inputs for a subsequent test. Such input designs are optimized for improving parameter estimate confidences, and are hence denoted as optimal inputs.

Optimal Inputs

The input design process is shown in Figure 15. It is seen that the process requires some a priori knowledge of the aircraft characteristics and data collection parameters. In addition, it is necessary to specify the objectives of the identification procedure (e.g. what model response parameters are to be identified).

An optimal input for a C-8 aircraft is shown in Figure 16 (simulated data). Also shown is a stepwise approximation to that input. It has been verified that the approximated input produces very accurate results relative to the true optimal input. Such stepwise inputs are, in some cases, easier to implement.

Figure 17 shows the improvement in estimated standard deviations of parameter estimates for the input of Figure 16 versus

COMPARISON OF STABILITY AND CONTROL DERIVATIVES
AT LOW SPEED APPROACH CONFIGURATION (236 FT/SEC)

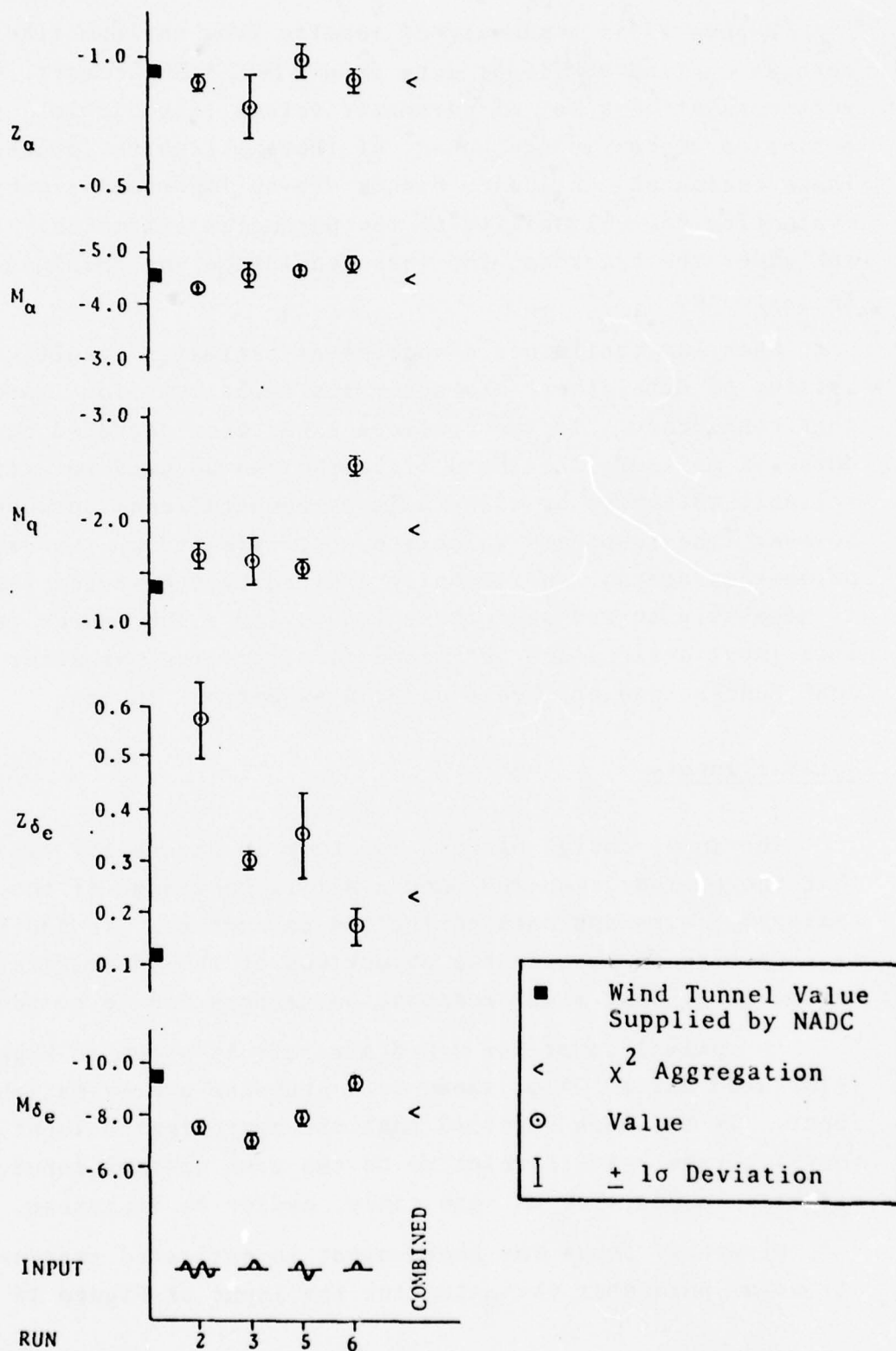
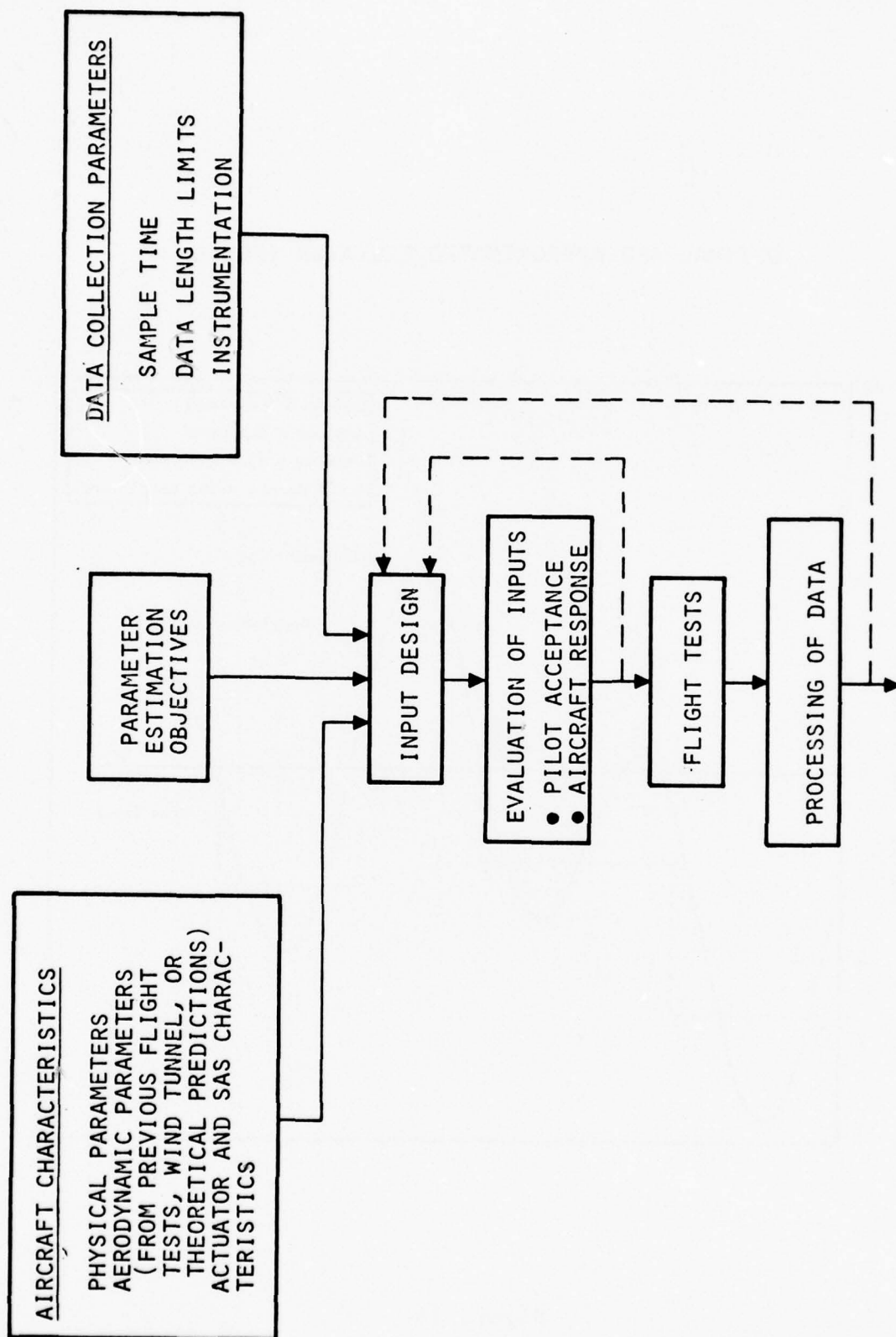


Figure 14
322

USE OF OPTIMAL INPUTS FOR FLIGHT TEST DESIGN



PARAMETER ESTIMATES (EVALUATE AGAINST OBJECTIVES)

Figure 15

OPTIMAL AND APPROXIMATED ELEVATOR INPUTS

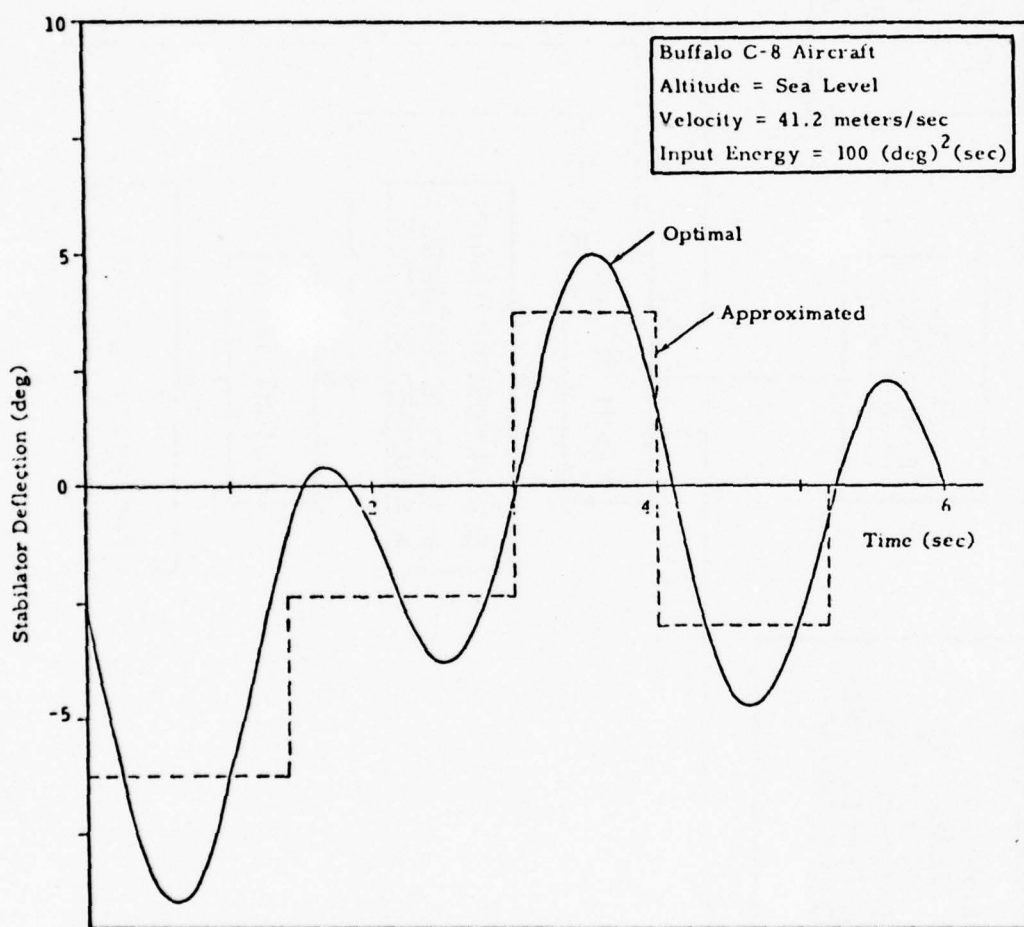


Figure 16

COMPARISON OF STANDARD DEVIATION IN PARAMETER
ESTIMATES FOR OPTIMAL INPUT AND DOUBLET
(SAME INPUT ENERGY)

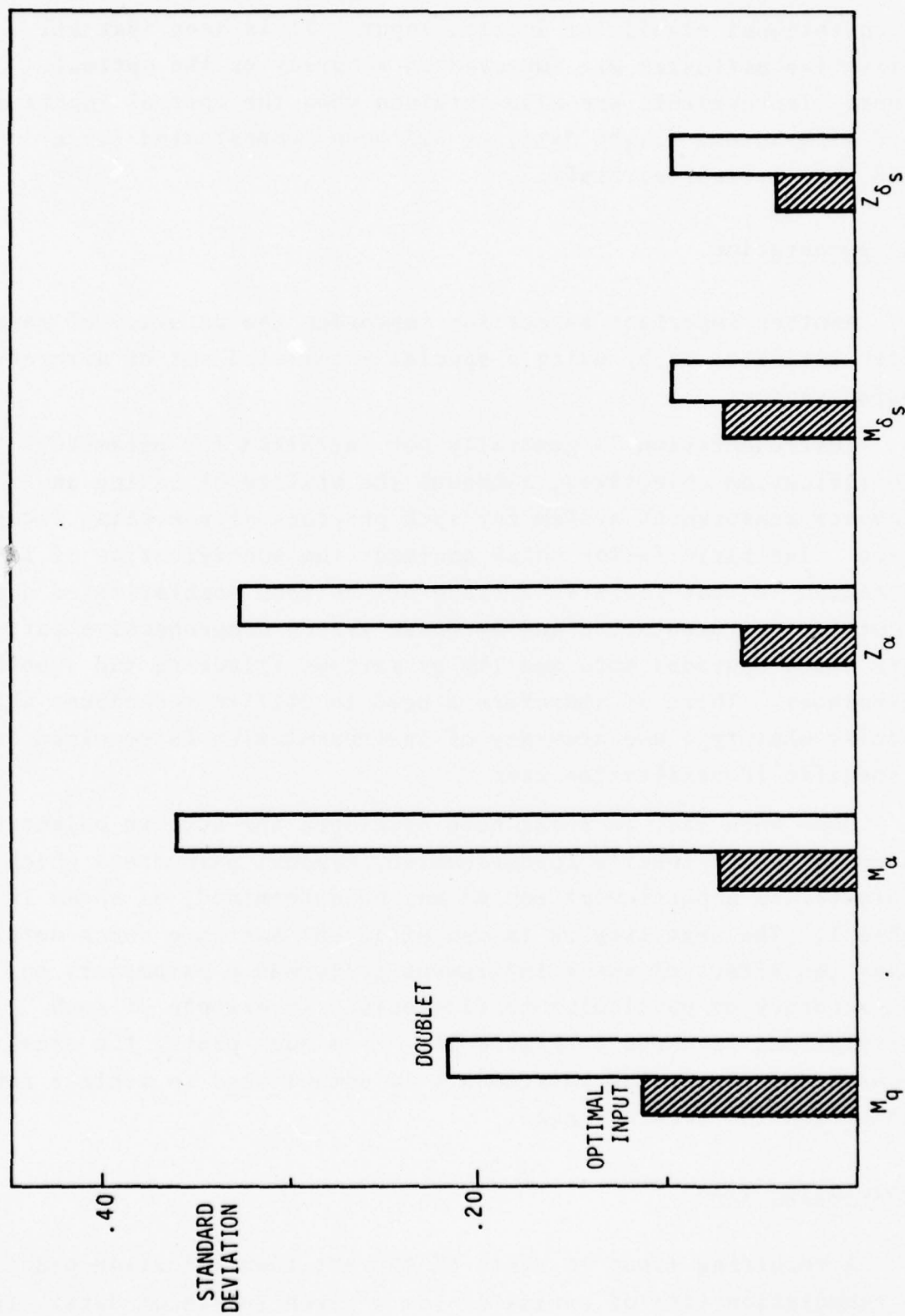


Figure 17

a conventional stabilator doublet input. It is seen that all derivative estimates are improved in accuracy by the optimal input. Improvements are also obtained when the optimal inputs are used with actual flight data, as has been demonstrated for a T-2B Navy trainer aircraft.

Instrumentation

Another important aspect for improving the accuracy of parameter estimates is by using a specially selected set of aircraft motion sensors.

Instrumentation is generally not installed for parameter identification objectives, although the utility of having an adequate measurement system for such purposes is now being recognized. The basic factor which confuses the specification of instrumentation is that there is a trade-off between sophisticated and accurate instrumentation and hardware versus comprehensive software which upgrades data quality by various filtering and smoothing techniques. There is therefore a need to utilize techniques which specify what type and accuracy of instrumentation is required for a specific identification task.

Some work has, in fact, been developed for such an objective. Based on manufacturer's specification, typical parameters which characterize a particular sensor may be determined, as shown in Table 1. The next step is to use efficient software which determines the effect of these instrument performance parameters on the accuracy of particular coefficients. An example of such calculations is shown in Figure 18. From such plots, the necessary accuracy of particular instruments is established to achieve some identification accuracy goal.

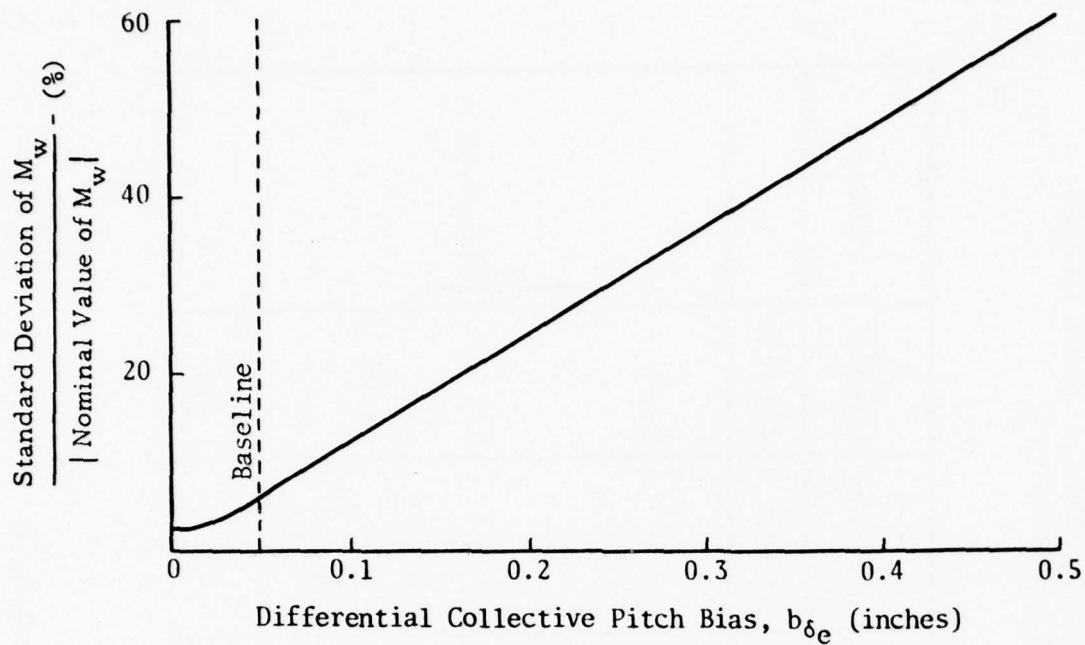
Computation Time

A recurring issue in state-of-the-art identification practice is computation time of estimates for a given length of data. It

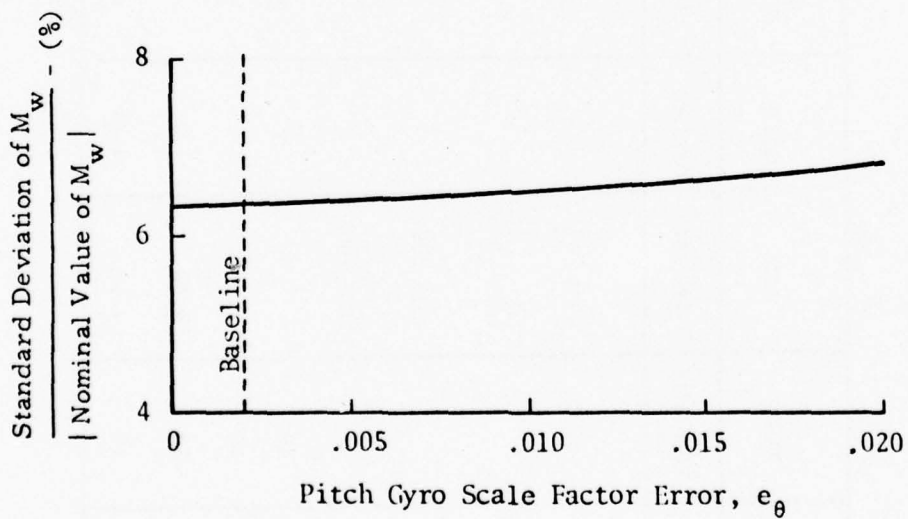
Table 1
 ACCURACY CHARACTERISTICS OF TYPICAL COMMERCIAL RATE GYROS
 (Values Given are Manufacturers' \pm Quotes Unless Noted)

TYPE	RANGE	BIAS	NOISE	NONLINEARITY OR SCALE FACTOR	RESOLUTION	MASS UNBALANCE	COMMENT
	deg/sec	deg/sec	deg/sec	% Full Scale	deg/sec	deg/sec g	
Timex SD-060	60	$\pm .03$ -.12	$\pm .18$	± 2	$\pm .01$	$\pm .05$	a.
Sperry DG 312		.0011-.036		.04-.23			Numbers are 10
Northrup GI-G6		.015-.094		.07-.32			
Kearfott Alpha 2		.001-.003		.02-.09			
Kearfott T2010	40			$\pm .5$ -1	$\pm .04$	$\pm .01$	b.
Syston Donner 8160	40	$\pm .4$		± 1.0	$\pm .4 \times 10^{-3}$		
Lear Siegler	80	$\pm .03$	$\pm .1$				
Sperry	40	$\pm .1$	$\pm .04$	± 2.5 -5	$\pm .04$	$\pm .05$	

- a. Scale factor proportional to voltage and power supply frequency
 b. Scale factor and bias vary with temperature



VARIATION OF M_w ERROR WITH BIAS $b_{\delta e}$



VARIATION OF M_w ERROR WITH SCALE
FACTOR ERROR e_{θ}

Figure 18

is now clear that, for any given algorithm, computation time may be reduced by decreasing the number of parameters to be identified, decreasing the length of maneuvers, or reduce the accuracy required for the parameters. These alternatives are usually available as options in a generalized flexible computer program.

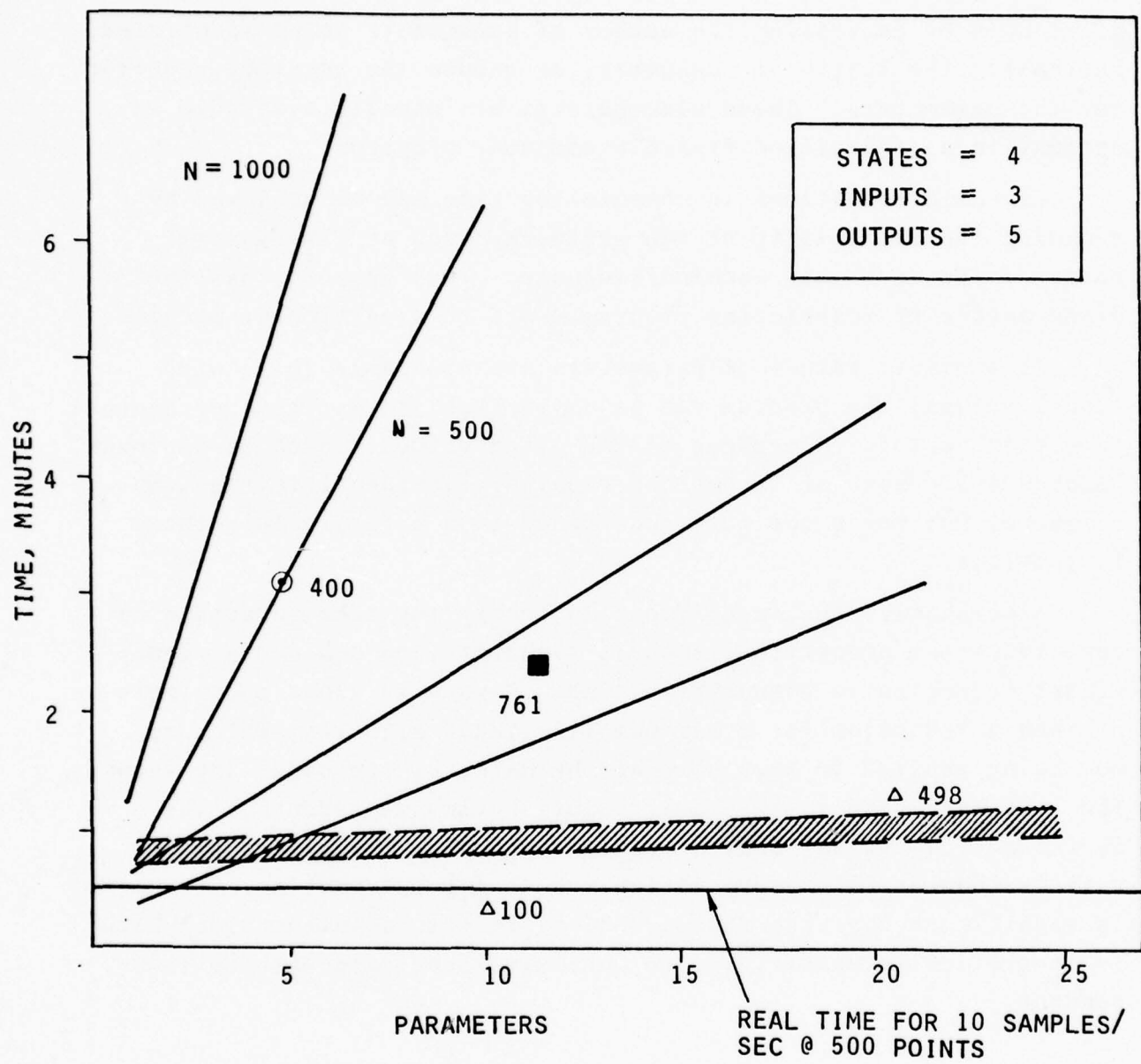
Dramatic reductions in computation time may be achieved by reducing the flexibility of the software, such as "hardwiring" parts of the code into machine language. This approach has the disadvantage of restricting program usage to a particular machine.

If a priori values of parameters are available (e.g. wind tunnel values) the program can be constrained to estimate parameters to within certain tolerances of the given values. Such an approach reduces the number of iterations required for identification convergence, but may place more confidence in a priori values than is justified.

Alternately, the identification theory may take advantage of certain system properties, such as linearity, to achieve a significant reduction in computation time. Figure 19 shows an example of such a reduction for a maximum likelihood algorithm which is now being applied to Navy aircraft by NATC. Three bands are shown. The left-hand band is the basic solution time dependence. The next band (clockwise) and the shaded band show the effect of various theoretical reformulations on this solution time. It is significant that the shaded band represents solution time which is theoretically exact (e.g. no approximations) and machine independent.

SUMMARY

In the time allotted, only a broad brush treatment of the comprehensive technology of system identification has been possible. It is concluded that system identification is rapidly having an impact on many Navy programs. As shown in Figure 20,



N = NO. OF DATA POINTS

Figure 19
330

PARAMETER IDENTIFICATION CAN PLAY AN INTEGRAL
PART IN NAVY SYSTEM TECHNOLOGY AND DESIGN

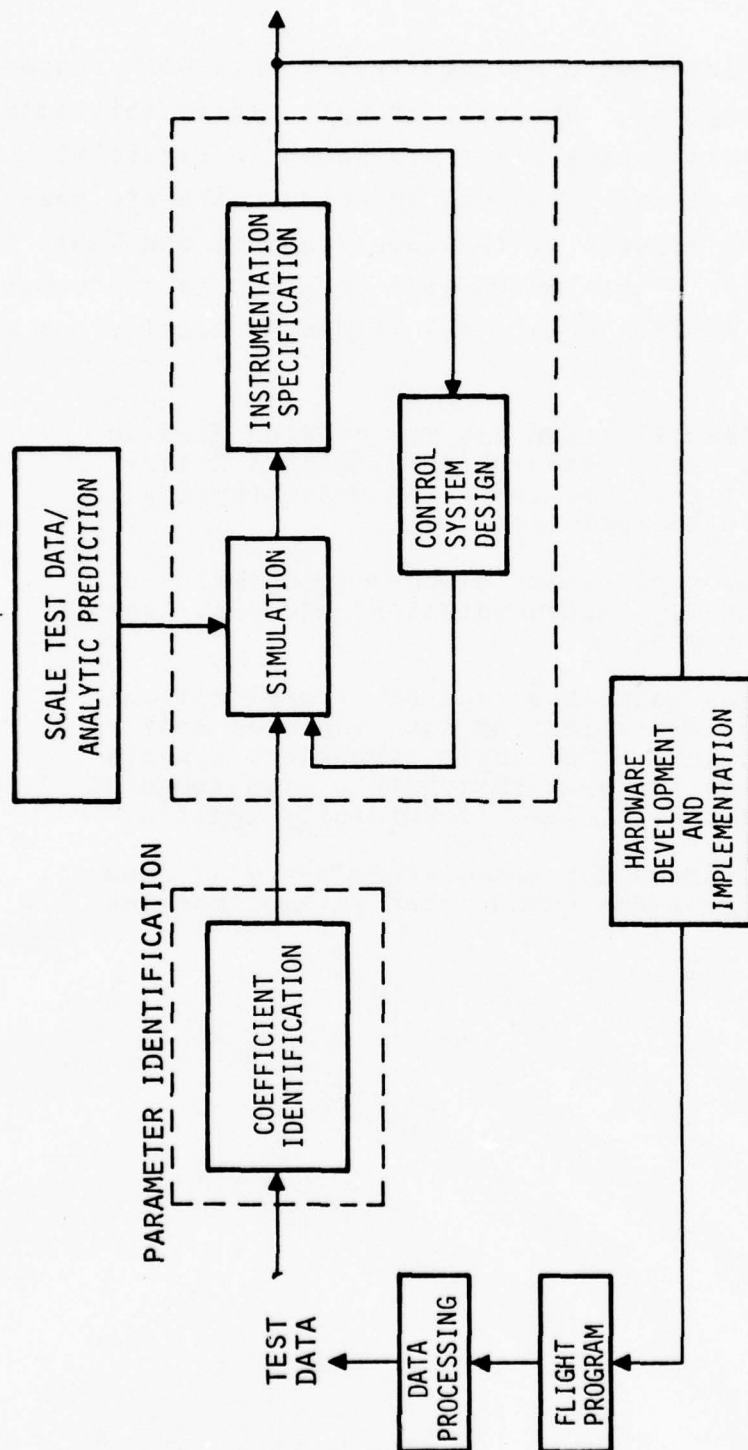


Figure 20

this input can be integrated systematically into both research and development programs. Specific examples where this integration has taken, or is taking place are shown in Figure 21.

Table 2 lists some of the principal agencies which are heavily involved in various aspects of this application, and Table 3

- lists the particular papers which will be given in the remainder of this session. At this point, the following conclusions are presented.

- System identification has now emerged from an extensive basic research program to a state-of-the-art tool for improving understanding of vehicle characteristics.
- Successful application demands integration of test planning, instrumentation, and post-test data processing.
- Past and on-going Navy and other applications of system identification have isolated most basic problems. The basic technology appears to be ready for application to a wide range of Navy systems/vehicles, if carefully applied.
- Future advances for this technology will come from the problems encountered in applications.

APPLICATIONS TO NAVY SYSTEMS

- PARAMETER IDENTIFICATION

- HYDRODYNAMIC COEFFICIENTS (FOR SUBMARINES, SES, SWATH)
- NAVIGATION SYSTEM COMPONENTS (PLATFORM MISALIGNMENT, GYRO BIAS)
- BALLISTIC AND REENTRY VEHICLE AERODYNAMIC COEFFICIENTS (ABLATION DISTURBANCES, HIGH MACH TRANSITION)
- DEFINITION OF GUST FIELD AROUND A CARRIER
- DEFINITION OF RANDOM SEAWAY FORCES AND MOMENTS
- STRUCTURAL STIFFNESS AND DAMPING COEFFICIENTS
- PRECISION TRACKING AND POINTING SYSTEM COEFFICIENTS
- NUCLEAR REACTOR PROPULSION SYSTEMS

- INPUT DESIGN

- TOW TANK TEST PLANNING
- FULL SCALE SHIP TESTING
- AIRCRAFT MANEUVER DESIGN

- INSTRUMENTATION ANALYSIS

- TRADEOFF OF INSTRUMENTS FOR DESIRED ACCURACY
- INSTRUMENT CALIBRATION
- POST-TEST DATA PROCESSING

Table 2

WHO'S DOING IT - BASIC AND APPLIED EFFORTS			
UNIVERSITIES		GOVERNMENT	INDUSTRY
ABKOWITZ	MIT	NATC	CALSPAN
ASTROM	LUND	NASA-FRC	HONEYWELL
BALAKRISHNAN	UCLA	NASA-LaRC	LOCKHEED
GERLACH	DELFT	NASA-AMES	NORTH AMERICAN
MEHRA	HARVARD		SCI
MENDEL	USC		UARL
NAHI	USC		
SARIDIS	PURDUE		
SCHWEPPE	MIT		

APPLICATIONS TO NAVY SYSTEMS

- **PARAMETER IDENTIFICATION**

- HYDRODYNAMIC COEFFICIENTS (FOR SUBMARINES, SES, SWATH)
- NAVIGATION SYSTEM COMPONENTS (PLATFORM MISALIGNMENT, GYRO BIAS)
- BALLISTIC AND REENTRY VEHICLE AERODYNAMIC COEFFICIENTS (ABLATION DISTURBANCES, HIGH MACH TRANSITION)
- DEFINITION OF GUST FIELD AROUND A CARRIER
- DEFINITION OF RANDOM SEAWAY FORCES AND MOMENTS
- STRUCTURAL STIFFNESS AND DAMPING COEFFICIENTS
- PRECISION TRACKING AND POINTING SYSTEM COEFFICIENTS
- NUCLEAR REACTOR PROPULSION SYSTEMS

- **INPUT DESIGN**

- TOW TANK TEST PLANNING
- FULL SCALE SHIP TESTING
- AIRCRAFT MANEUVER DESIGN

- **INSTRUMENTATION ANALYSIS**

- TRADEOFF OF INSTRUMENTS FOR DESIRED ACCURACY
- INSTRUMENT CALIBRATION
- POST-TEST DATA PROCESSING

Table 3
NEW APPLICATIONS

AUTHOR	APPLICATION	TECHNIQUE
ABKOWITZ	SURFACE SHIPS	KALMAN FILTER
MICHAEL	AIRCRAFT ENGINES	KALMAN FILTER
STEIN	NAVIGATION COMPONENTS	MAXIMUM LIKELIHOOD

SOME REFERENCES

BASIC PRINCIPLES

- Bryson, Jr., A.E. and Ho, Y.C., Applied Optimal Control, Xerox Blaisdell Co. (1969)
- Lee, R.C.K., Optimal Estimation, Identification, and Control, M.I.T. Press (1964)
- Nahi, N.E., Estimation Theory and Applications, John Wiley & Sons, Inc. (1969)
- Schweppe, F., Uncertain Dynamic Systems, Prentice-Hall (1973)

STATE-OF-THE-ART

- "Parameter Estimation Techniques and Applications to Flight Testing," NASA TND-7647, April 1974.
- AGARD Specialists Conference, NASA-LaRC, November 1974; AGARD Proceedings No. 172 (AGARD-CP-172).

APPLICATIONS TO NAVY SYSTEMS

- **PARAMETER IDENTIFICATION**

- HYDRODYNAMIC COEFFICIENTS (FOR SUBMARINES, SES, SWATH)
- NAVIGATION SYSTEM COMPONENTS (PLATFORM MISALIGNMENT, GYRO BIAS)
- BALLISTIC AND REENTRY VEHICLE AERODYNAMIC COEFFICIENTS (ABLATION DISTURBANCES, HIGH MACH TRANSITION)
- DEFINITION OF GUST FIELD AROUND A CARRIER
- DEFINITION OF RANDOM SEAWAY FORCES AND MOMENTS
- STRUCTURAL STIFFNESS AND DAMPING COEFFICIENTS
- PRECISION TRACKING AND POINTING SYSTEM COEFFICIENTS
- NUCLEAR REACTOR PROPULSION SYSTEMS

- **INPUT DESIGN**

- TOW TANK TEST PLANNING
- FULL SCALE SHIP TESTING
- AIRCRAFT MANEUVER DESIGN

- **INSTRUMENTATION ANALYSIS**

- TRADEOFF OF INSTRUMENTS FOR DESIRED ACCURACY
- INSTRUMENT CALIBRATION
- POST-TEST DATA PROCESSING

Figure 21

Table 2

WHO'S DOING IT - BASIC AND APPLIED EFFORTS			
UNIVERSITIES		GOVERNMENT	INDUSTRY
ABKOWITZ	MIT	NATC	CALSPAN
ASTROM	LUND	NASA-FRC	HONEYWELL
BALAKRISHNAN	UCLA	NASA-LaRC	LOCKHEED
GERLACH	DELFT	NASA-AMES	NORTH AMERICAN
MEHRA	HARVARD		SCI
MENDEL	USC		UARL
NAHI	USC		
SARIDIS	PURDUE		
SCHWEPPE	MIT		

Table 3
NEW APPLICATIONS

AUTHOR	APPLICATION	TECHNIQUE
ABKOWITZ	SURFACE SHIPS	KALMAN FILTER
MICHAEL	AIRCRAFT ENGINES	KALMAN FILTER
STEIN	NAVIGATION COMPONENTS	MAXIMUM LIKELIHOOD

SOME REFERENCES

BASIC PRINCIPLES

- Bryson, Jr., A.E. and Ho, Y.C., Applied Optimal Control, Xerox Blaisdell Co. (1969)
- Lee, R.C.K., Optimal Estimation, Identification, and Control, M.I.T. Press (1964)
- Nahi, N.E., Estimation Theory and Applications, John Wiley & Sons, Inc. (1969)
- Schweppe, F., Uncertain Dynamic Systems, Prentice-Hall (1973)

STATE-OF-THE-ART

- "Parameter Estimation Techniques and Applications to Flight Testing," NASA TND-7647, April 1974.
- AGARD Specialists Conference, NASA-LaRC, November 1974; AGARD Proceedings No. 172 (AGARD-CP-172).

SYSTEM IDENTIFICATION TECHNIQUES FOR SHIP MANEUVERING TRIALS

MARTIN A. ABKOWITZ

Introduction - The Need for Proper Mathematical Models to Simulate Vehicle Maneuvering

Ships and other ocean vehicles are designed, constructed, and operated to perform certain missions in the ocean environment. It is hoped that these missions are carried out at best in an optimum manner and at worst in an acceptable manner.

The ability to perform certain missions depends critically on the ability to control vehicle motions with confidence and without unreasonable demands on personnel and equipment. Hence, as far back as the vehicle design state, critical decisions are to be made as to the proper hull form, the proper number, type and design of control effectors, and the proper characteristics and any automatic control system that may be needed. Once the designer feels that he has done his best with the constraints of cost, constructional and operational realities, somewhere along the line someone has to decide whether there will be "unreasonable" demands on operators inexperienced in handling the ship in particular maneuvers demanded by the mission. The "unreasonable" demands may be reduced to "reasonable" by training operators with real time maneuvering simulators or "trainers."

To properly design for mission accomplishment one has to have the ability to predict from design characteristics the motion responses for all the maneuvers required. To do this, one needs to have a suitable simulation model. To develop a proper "trainer," one also needs a suitable simulation model.

Simulation models may be physical or mathematical - a scaled physical model run in a towing tank or a mathematical model run

on a computer. A free-running scaled ship model in the tank requires large maneuvering tanks, suffers extensively from "scale effect" (not satisfying Reynolds number), is very costly from time and funding considerations, and information is obtained on only a very limited number and type of maneuvers. Using a physical model in a tank for "pilot training" purposes suffers from two serious "scale effects" - one is the usual error in Reynolds' or viscous scaling and the other is "time" scaling, model time being scaled down by the square root of the model linear scale ratio. Hence, the model motions are not in real time while the pilot or operator is thinking and acting in real time.

Because of these many disadvantages of physical modeling in ship maneuvering, the mathematical model is the way to go. A general mathematical model form was introduced to ship motion studies in the late 1940s and was specifically developed for application to ship maneuvering in 1962 by the author (Ref. 1). This mathematical model form has been and is used rather extensively by the profession. This model uses motion variables referred to an axis system fixed in the vehicle with an origin not necessarily at the center of gravity, and an expression of the hydrodynamic forces by a Taylor series expansion in terms of the motion variables, with a certain order of nonlinearities maintained, advantage being taken of the existing symmetries in the vehicle shape and inertia distribution. Equations 1, 2, and 3 of Appendix I show this expanded form for the longitudinal force (X), the lateral force (Y), and the yaw moment (N), for the case when the motion is restricted to the horizontal plane without roll and the expansion includes up to third order terms. Equations 4, 5, and 6 of Appendix I show the solution for the longitudinal (\dot{u}), transverse (\dot{v}), and yaw (\dot{r}) accelerations for this case.

The hydrodynamic coefficients (or derivatives) of the linear and nonlinear terms depend on the geometry of the vehicle and the

conditions of the initial equilibrium condition such as straight line motion at a given speed. A few of these coefficients may be estimated by theoretical hydrodynamics, but most need to be determined through experimental methods, either testing of physical models in a laboratory (tank) or through experiments on the ship in full scale trials.

The linear coefficients and a few of the nonlinear coefficients are usually measured on a scaled model in a tank facility using either a rotating arm apparatus or a planar motions mechanism, wherein the apparatus impose constrained motion on the model. By this method, the linear coefficients and some, but not all, of the significant nonlinear coefficients are measured. However, the values of the coefficients as measured may suffer from scale effects arising from improper scaling of the viscous phenomena. The use of constrained testing does actually measure the partial derivative of a force or moment with respect to motion parameters. On the other hand, to specifically measure these coefficients at full scale on a constrained ship is out of the question. The obvious question arises - "Can these coefficients be 'evaluated' by experiments on the full size ship from planned unconstrained, and realizable, set of maneuvers of the ship at sea?" The purpose of this paper is to describe recent work done in the Department of Ocean Engineering at the Massachusetts Institute of Technology in an attempt to answer this question. It involves the development of a technique and associated computer program which analyzes the measurements obtained from full scale maneuvering trials so as to give the "best value" of the various coefficients which appear in the mathematical simulation model. The method is generally referred to as "system identification," i.e. the identification of what (math model) is inside the "black box" (system) from a proper analysis of the measured outputs of the system resulting from specific inputs into the system.

The author wishes to acknowledge the significant work and contributions of Michael N. Hayes, Hernani L. Brinati, and John G. Lundblad whose theses represent the major effort of this study to date and are listed as Refs. 2, 3, and 4 of this paper. Many of the figures presented are taken from these references. The author also wishes to acknowledge the support of the U.S. Navy and the Maritime Administration in certain portions of this research effort.

Identification Techniques

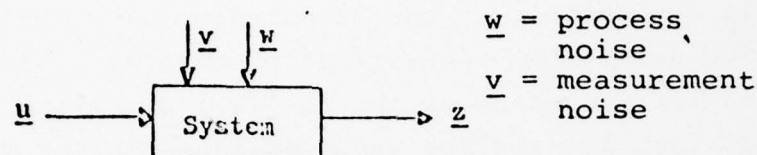
Two general types of identification techniques were investigated to determine their feasibility in evaluating the hydrodynamic coefficients from maneuvering tests on the full size ship. Computer programs were developed for applying the "model reference" technique and the "extended Kalman filtering" technique. Also, a program was developed to generate noisy measurement data to simulate data expected from actual ship trials in order to properly test the system identification methods in the absence of ship data.

The model reference technique as used here consists of the following. The mathematical model, using an original set of values for the coefficients, is used to generate a set of motion outputs (sway, yaw, yaw rate, etc. as functions of time) for a given set of inputs (rudder deflection as a function of time). As the maneuver proceeds in time, the actual measurements of these motions are compared to those estimated from the model, at specific increments in time, and the difference is squared and then integrated over the time of the maneuver. The integrated error-squares for each of the output parameters are combined (with allocated weighting factors if desired) to give the value of a "cost functional" which represents the total error-squared value for all the output measurements. The process is repeated for different selected values of the coefficients and

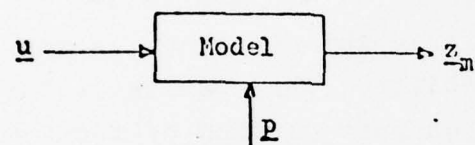
the "cost function" is evaluated for each of these cases - the coefficients being systematically varied over a given range of values. Those values of the coefficients which give a minimum cost function (representing the least squares fit) are the best estimate values of the coefficients. Figure 1 (taken from Ref. 2) shows a schematic of the computation steps used in the model reference parametric identification program. Since merely printing out the value of the coefficients which give the minimum cost function and the value at that minimum does not guarantee the identifiability of the coefficient. There can be minimum values at the end points of the range selected, there can be other values which give local minima which are not much greater in value than the minimum value, etc. One coefficient may be identifiable while another is not. To better determine the identifiability, the results of the model reference computation are "contour" plotted by the computer as shown in Figure 2 (taken from Ref. 3). The abscissa contains the range of values of one coefficient (p_1) and the ordinate represents the value of a second coefficient (p_2). It is clear from this figure that coefficients p_1 and p_2 appear to be identifiable and independent indicated by steep rising cost function slope about the minimum value indicated by 1 (with magnitude increases $1, 2 \rightarrow 9, A, B \rightarrow$). Figure 3 (taken from Ref. 2) indicates the variety of contour figures that may be obtained and how they can be interpreted with regard to the identification of the coefficients (parameters p_1 and p_2). Unfortunately, the contour presentation allows only two parameters (coefficients) to be handled at one time. Also, the model reference technique requires a great deal of computation time and costs to go through a systematic variation of many parameters.

The Kalman filter is a technique of data reduction which is used extensively to filter out noise to give a best estimate of a signal. The development of the filter equations and their adaptation for use in ocean vehicle dynamics identification

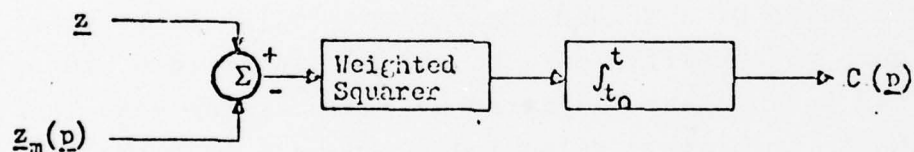
Step 1 Collect or generate noisy data \underline{z} and inputs \underline{u}



Step 2 Using the inputs \underline{u} run the model for a fixed set of parameters \underline{p}



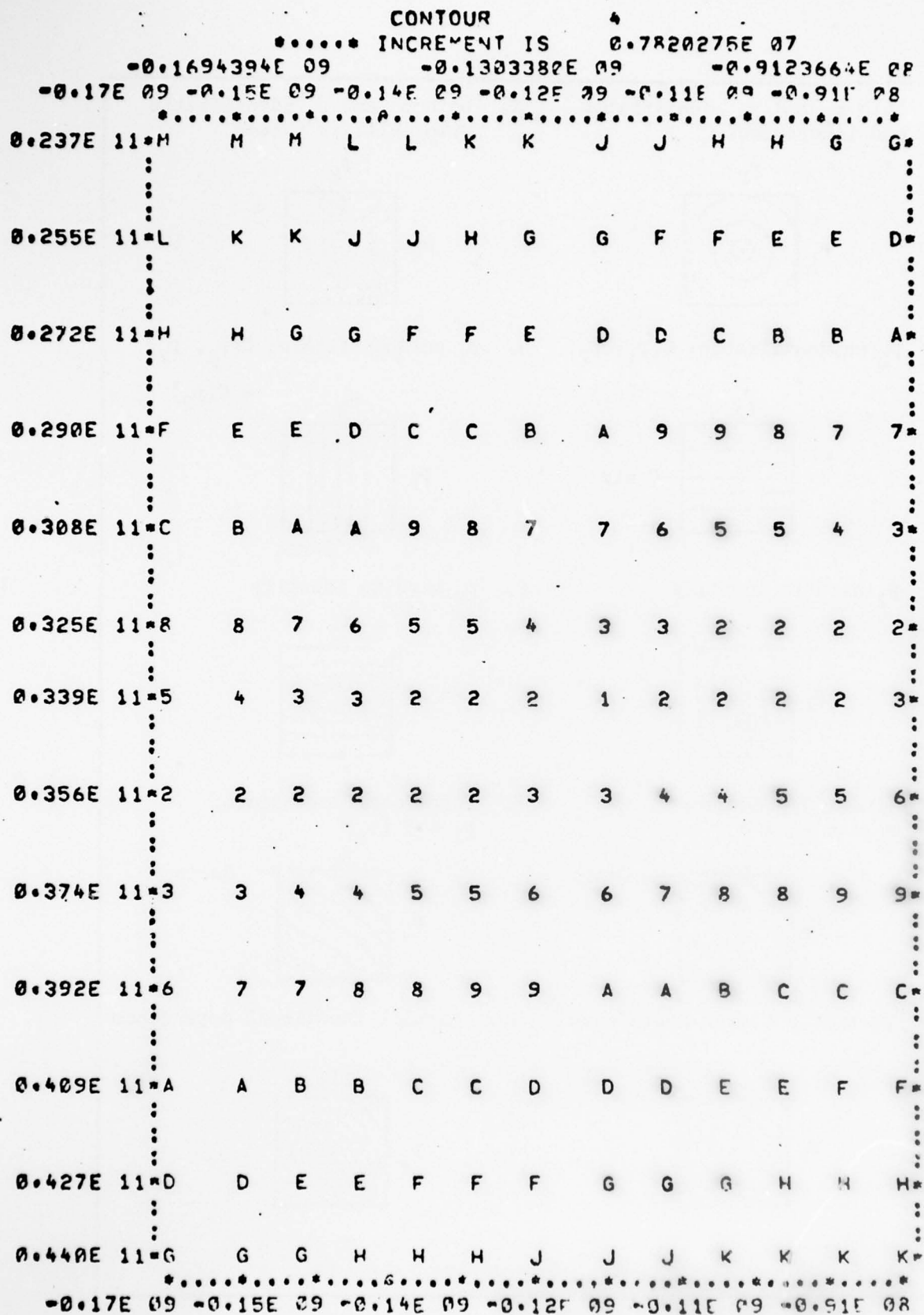
Step 3 Calculate the cost function $C(\underline{p})$



Step 4 Calculate a new value of \underline{p} by some decision and modification algorithm

Step 5 Branch to Step 2 and continue until complete or until $C(\underline{p})$ is minimum

Fig. 1 Model Reference Computation Steps



($I_z - N_r$) and N_δ contours 10% \underline{w} , (5., 0.5)% \underline{v} noises, linear model

Fig. 2 Typical Model Reference Contour Configuration

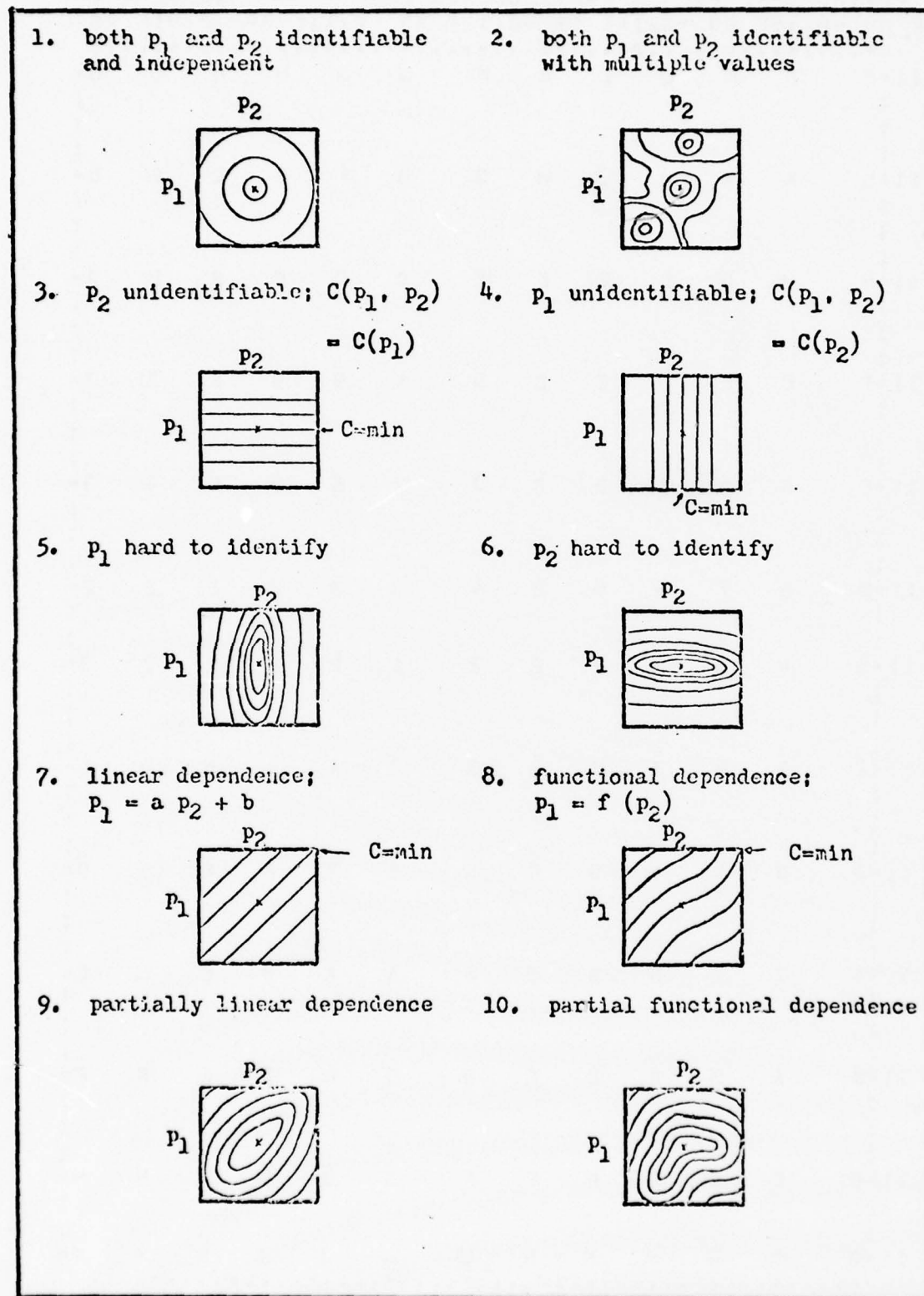


Fig. 3 Typical Model Reference Contour Configurations

procedures are described in Ref. 2. A summary of the computational procedures for the extended Kalman filtering (extended refers to an extension to nonlinear models) is given in Figure 4 (taken from Ref. 2). The state variables, such as displacements, velocities, and accelerations of the vehicle are represented in the vector \underline{x} which states vary with time during the maneuver. By obtaining the difference between the state estimated from the mathematical model with that as measured over intervals of time, one evaluates an error function. The Kalman filter error propagation matrix is used to update and improve the estimate of the state variables during the next time increment. The filter assumes that both the process noise vector \underline{w} and the measurement noise vector \underline{y} are Gaussian with zero mean, uncorrelated and with assumed covariance value of Q for the process noise and R for the measurement noise. The error propagation matrix involves the nature of the model function, the type and level of noise, and the measurement function matrix (H).

Since the Kalman filter identification technique essentially generates best estimates of the states, then treating the coefficients in the equations of motion as additional state variables, the technique provides best estimates of the values of the coefficients continually revising the estimates as the maneuver progresses. Hence, the matrix \underline{x} in Figure 4 includes the coefficient (parametric) matrix \underline{p} ; it also includes the input matrix \underline{u} , although \underline{u} , which in our case is represented by a rudder deflection, is a known function of time, i.e. a prescribed maneuver. The state variables are functions of time whereas the coefficients are assumed constant in time. The identification calculation procedure has to be started at a designated time $t = 0$, usually the start of the maneuver and initial estimates of the coefficients (\underline{p}_0) which are feasible but not necessarily accurate need to be included in the input (as well as estimated probable error). A block diagram depicting the extended Kalman

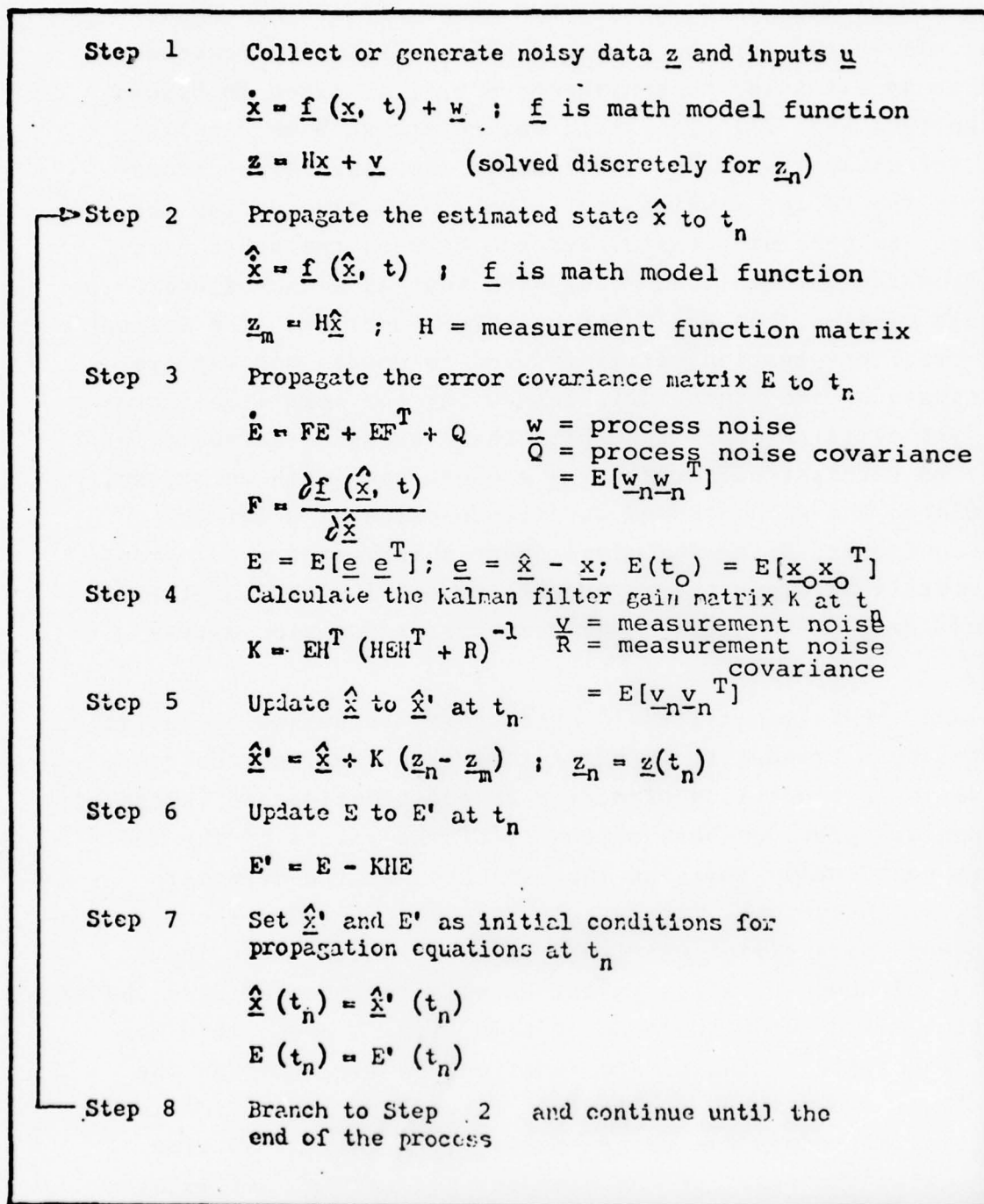


Fig. 4 Extended Kalman Filtering Computation Steps

filtering technique as well as that for the model reference technique are shown in Figure 5 (taken from Ref. 2).

A typical output of the Kalman filtering system identification program is shown in Figures 6 and 7. In Figure 6 one observes for the state variables of yaw velocity, sway acceleration, sway velocity, and yaw angle, the noisy measured data and the Kalman filtered estimate of the state as the maneuver progresses. In Figure 7 one observes the continuous estimating of the four major linear coefficients as the maneuver progresses, with the values settling down towards the end of the maneuver.

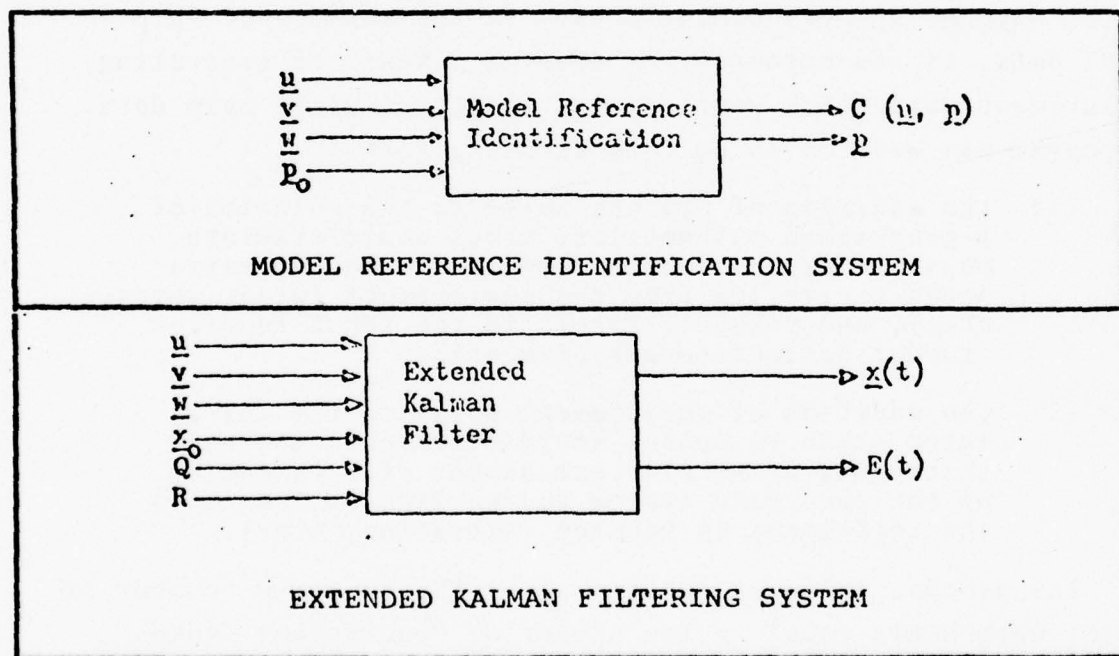


Fig. 5 Schematic of Identification Procedures

The program as it presently exists can handle output measurements of from one up to the 12 state variables of longitudinal and lateral position (x_0 and y_0), yaw angle (ψ), longitudinal and lateral velocity components (u and v), yaw rate (r) and the accelerations (\dot{u} , \dot{v} , and \dot{r}). The program can also handle the simultaneous identification of from one to 36 coefficients, although it is wise not to try to identify too many coefficients during any one maneuver as will be discussed later.

In order to evaluate the effectiveness of the system identification procedures and programs, the programs must be tested with noisy measurement data. In the absence of ship trial data, it was necessary to develop a means of generating measurement data which would realistically simulate ship data. A program was written to do this assuming that

- (1) the addition of process noise to the solution of a prescribed mathematical model would simulate possible errors in the form of the model, extraneous excitation from the environment (wind, waves, etc.), and possible errors in the input function (rudder deflection measurement);
- (2) the addition of measurement noise to the calculated state responses would represent internal instrument noise plus extraneous effects caused by the recording system and environment in which the instrument is located (vibration, etc.).

The process noise is designated by the vector \underline{w} (number of vector components equal to the number of "equivalent states" which appear in the math model) and the measurement noise is designated by the vector \underline{v} (number of vector components equal to the number of states being measured during the maneuver).

Both noises \underline{w} and \underline{v} are Gaussian white noise, uncorrelated and with zero mean. The magnitude of the noise is indicated by a percentage value, such as 5%. This number indicates that the root mean square value of the noise is equal to that percentage

of the maximum value of that state or measurement value during the maneuver. Hence, during certain parts of the maneuver, the noise-to-signal ratio could be many times the designated percentage.

The computer program as developed generates noisy output data simulating that which may be obtained from the actual vehicle by inputting the rudder action, the mathematical model, the specific type of motion measurements (measured states) of interest and the desired percentage value of process noise (w) and measurement noise (v). The computation process for generating noisy data is indicated in Step 1 of Figures 1 and 4.

Evaluation of the Model Reference and Extended Kalman Filter Identification Procedures and Programs

The "Mariner" was chosen as the ship type to be used in testing the identification programs because the values for the hydrodynamic coefficients, linear and nonlinear, as measured on scaled models (on either planar motion mechanisms and/or rotating arms at several establishments) are available from several publications. Using these coefficients and the associated mathematical form, noisy simulated trial data for various maneuvers were generated by the procedure previously described. This noisy data was then used as input data to the identification procedure and the final estimate of the coefficients were compared to the actual coefficients in order to determine the degree of identifiability.

In Ref. 3, the model reference procedure was investigated for various noise levels, initial estimates, length of maneuver and coefficients to be identified for the following conditions.

- (1) Using a linear model, various linear coefficients were selected to be identified from a mile maneuver which would not excite significant nonlinear forces (on the Mariner). The maneuver was a fixed deflection of 5° on the rudder resulting in small values

of drift velocity, v , and yaw velocity, r . Both model reference and the extended Kalman filter procedures were used in attempts to identify the linear coefficients from this maneuver. Some results from this study will be shown and discussed later.

- (2) Using a nonlinear model, various linear and nonlinear coefficients were selected to be identified from more violent types of maneuvers which would excite nonlinear forces. A fixed rudder deflection of 35° was the maneuver used in conjunction with the model reference technique, whereas a one cycle square wave rudder deflection of 35° was used in conjunction with the extended Kalman filter technique.

The results of the investigations covered in Ref. 3 indicated that the model reference technique has the following limitations.

- (1) Only two coefficients could be selected for identification during any one pass of the data.
- (2) Excessive computer time and costs were required with this method.
- (3) The method was much more sensitive to noise than the Kalman filter procedure.

It was then decided to concentrate on the more realistic nonlinear model and the extended Kalman filter procedure, since this procedure showed the most promise with noisy data, could handle many parameters during one pass, required reasonable computer time and costs, and gave a bonus of a "faired" curve of the noisy measurement data.

The investigations described in Ref. 4 concentrated on the extended Kalman filter technique applied to the case of the nonlinear mathematical model of the Mariner ship. Identification of the four major linear coefficients (Y_v , N_v , $(Y_r - \mu)$, and $(N_r - \mu x_G u)$) from the nonlinear model was attempted using a selected group of maneuvers, a variety of noise levels, a variation in length of maneuvers, and a variation in first estimates.

The maneuvers consisted of sinusoidal oscillation of the rudder at 10° and 35° amplitude, one cycle square wave rudder deflection of 10° , and fixed rudder deflection of 10° . In all these maneuvers and data passes attempts were made to identify the four major linear coefficients simultaneously during each pass of the data. The measured states used were those which could be realistically obtained during ship trials, i.e. yaw angle from a heading gyro, yaw velocity from a rate gyro, and transverse velocity v from integrating on a transverse accelerometer.

A few significant results from the investigations described in Refs. 3 and 4 will be discussed here and for more details the reader is referred to these publications.

Tables 1.1 and 1.2 (from Ref. 3) show some typical results of using the model reference procedure to identify the four major linear coefficients (from a linear model), based on minimum cost function and contour plotting as demonstrated in Figures 2 and 3. Since the model reference contour procedure handles only two coefficients at a time, it required two separate passes of the data to identify the four parameters. The maneuver is for a fixed rudder deflection of 5° and the measurements used were transverse velocity v and yaw rate r . It is seen from Tables 1.1 and 1.2 that for no process noise and no measurement noise all four coefficients are exactly identified. However, when 1% process noise, 5% noise on transverse velocity measurement (v) and 0.5% noise on the yaw rate measurement (r), Y_v and $(N_r - m_{x_G} u)$ are not identifiable even though $(Y_r - \mu)$ and N_v are identifiable. With 1% process noise and 50% on v - 5% on r measurement noise, none of the four coefficients are identifiable. However, with 10% process noise and 5% v - 0.5% r noise there is reasonable identification of all four coefficients. With 10% process noise and 50% v - 5% r noise, two of the four coefficients remain unidentifiable.

TABLE 1.1

Noise			$\underline{PA1} \equiv (Y_r - \mu)$	$\underline{PA2} \equiv N_v$			
% w	% v	$\frac{v}{r}$	$\underline{PA1}^* = -18.51 E 6$	$\underline{PA2}^* = -97.73 E 5$	$C(p^*)$	$C_{max}(p)$	Comment
0	0	0	-18.51 E 6	-97.73 E 5	-30.70	7.052	Many points
1	5	0.5	-18.51 E 6	-97.73 E 5	1.249	7.050	
1.	50.	5.			5.616	7.287	
10.	5.	0.5	-18.51 E 6	-97.73 E 5	1.123	7.063	
10.	50.	5.	-22.60 E 6	-104.80 E 5	5.827	7.207	

TABLE 1.2

Noise			$\underline{PA1} \equiv Y_v$	$\underline{PA2} \equiv (N_r - \mu \times G_u)$			
% w	% v	$\frac{v}{r}$	$\underline{PA1}^* = -81.51 E 3$	$\underline{PA2}^* = -32.51 E 8$	$C(p^*)$	$C_{max}(p)$	Comment
0	0	0	-81.51 E 3	-32.51 E 8	-19.41	7.783	Many points
1	5.	0.5			1.249	7.781	
1	50.	5.			5.615	7.908	Many points
10	5.	0.5	-75.15 E 3	-35.02 E 8	1.115	7.790	Many points
10	50.	5.			5.828	7.883	

Tables 1.3 and 1.4 (from Ref. 3) give the results using the extended Kalman filter technique (on a linear model) on the identification of the four major linear coefficients during a maneuver in which the rudder is fixed at a 5° deflection, with 10% process noise and 5% v - 0.5% r measurement noise. Table 1.3 indicates that doubling the length of time of recording the maneuver, the accuracy in identifying the coefficient Y_v is increased from within 10% of the true value to within 2% of the true value. The identification of $(Y_r - \mu)$ is improved from within 9% of the true value to within 2.5% of the true value, N_v is improved from within 19% to within 4% of the true value, and $(N_r - \mu_{Gu})$ is improved from within 14% to within 3.5% of the true value.

Table 1.4 gives an indication of the improvements of the degree of identification by repassing the data through the identification procedure by setting the value of the initial estimates for the second pass equal to the identified values of the first pass. The identification of Y_v is improved from within 2% to within 0.2% of the true value, $(Y_r - \mu)$ from within 2.5% to within 1% of the true value, N_r from within 3.5% to within 2.5% of the true value, with negligible improvement in the prediction of N_v which remains within 4% of the true value.

The results of the investigations associated with Ref. 4 are given in Figures 6 through 29 (6-19, 24-29 from Ref. 4). All the coefficient identifications were done on a nonlinear mathematical model of the Mariner using the extended Kalman filtering procedure with simultaneous identification of the four major linear coefficients. All the figures involve a process and measurement noise of 5% except Figures 20-27; Figures 20-23 have 1% noise and Figures 24-27 have 25% noise. Figures 6-13 and 24-29 refer to cases where the four state variables of v , \dot{v} (transverse velocity and acceleration) and ψ , r (yaw and yaw rate) are independently measured and Figures 14-24 refer to the cases where v , ψ , and r are independently measured, the

TABLE 1.3

Noise: $\% \underline{w} = 10;$ $\% \underline{v} = (5, 0.5)$				
	\underline{Y}_v	$(\underline{Y}_r - \mu)$	N_v	$(N_r - \mu \underline{x}_G)$
True Value	-81.515 E 3	-18.508 E 6	-97.735 E 5	-32.510 E 8
Initial Est.	-57.060 E 3 ± 24.454 E 3	-12.955 E 6 ± 55.525 E 3	-68.414 E 5 ± 29.321 E 5	-22.752 E 8 ± 97.581 E 7
F.Value T=188sec	-72.934 E 3 ± 12.696 E 3	-16.760 E 6 ± 31.644 E 5	-79.064 E 5 ± 15.481 E 5	-28.062 E 8 ± 37.366 E 7
F.Value T=376sec	-79.796 E 3 ± 10.585 E 3	-18.052 E 6 ± 28.213 E 5	-93.683 E 5 ± 12.959 E 5	-31.376 E 8 ± 32.591 E 7

TABLE 1.4

Noise: $\% \underline{w} = 10;$ $\% \underline{v} = (5, 0.5)$				
	\underline{Y}_v	$(\underline{Y}_r - \mu)$	N_v	$(N_r - \mu \underline{x}_G)$
True Value	-81,515E 3	-18.508E 6	-97.735E 5	-32.510E 5
Initial Estimate	-57.060E 3 ± 24.454E 3	-12.955E 6 ± 55.525E 5	-68.414E 5 ± 29.321E 5	-22.752E 8 ± 97.531E 7
First Pass	-79.796E 3 ± 10.585E 3	-18.052E 6 ± 28.213E 5	-93.683E 5 ± 12.959E 5	-31.376E 8 ± 32.591E 7
Second Pass	-81.642E 3 ± 64.705E 2	-18.677E 6 ± 18.061E 5	-93.987E 5 ± 84.216E 4	-31.651E 8 ± 20.228E 7

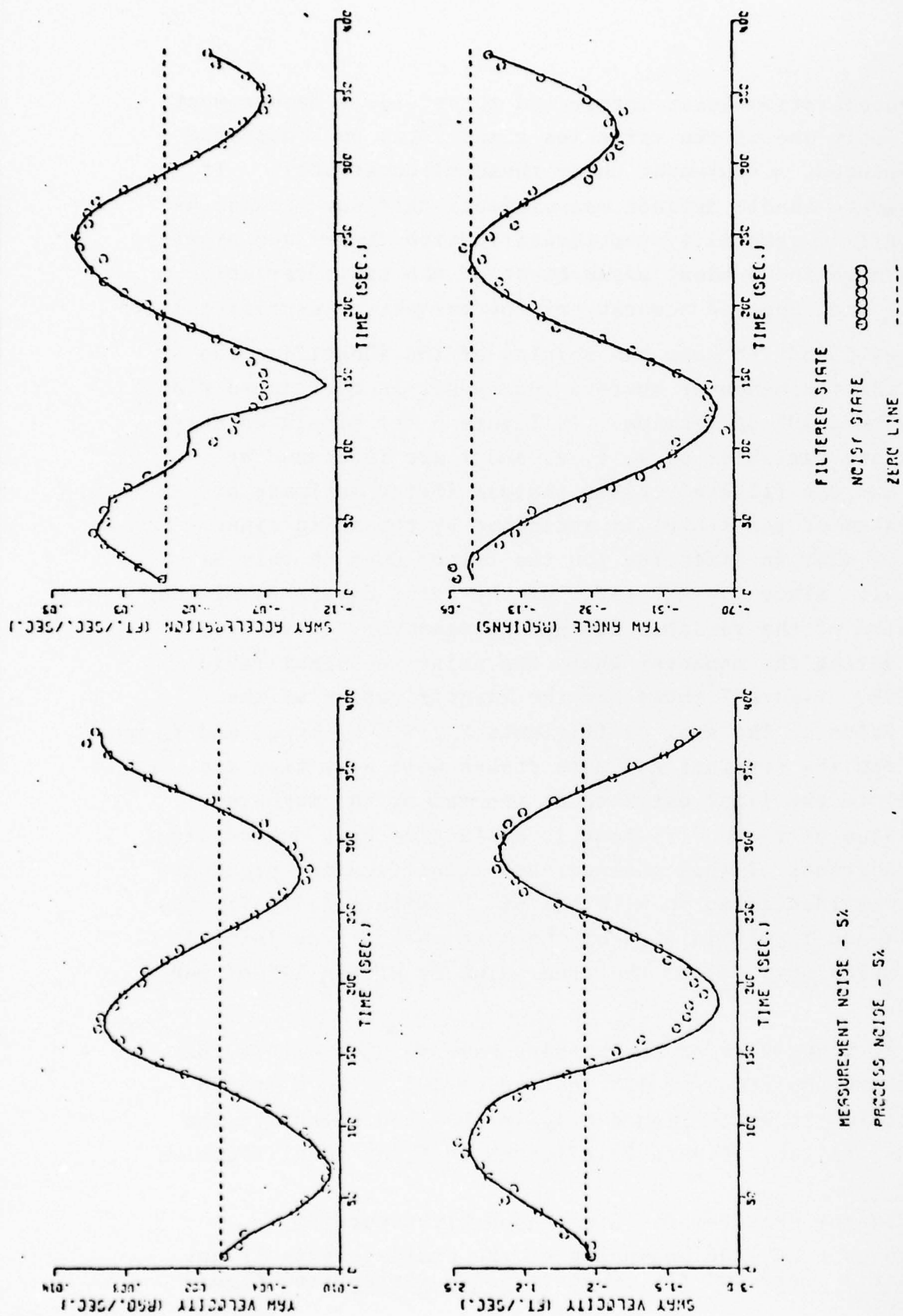
measured acceleration being integrated to provide a measurement of v (i.e. only one of the variables v and \dot{v} can be considered as an independent measurement under these circumstances). It is necessary to handle defined measurements this way because as it is known from general system identification theory and experience, the more independent measurement of the state variables, the more is the expected accuracy of the parameter identification.*

Figures 6 and 7** show the results of the identification procedure for the maneuver wherein the rudder is oscillated sinusoidally with a 10° deflection. In Figure 6 the simulated noisy measured state variables of v , \dot{v} , ψ , and r are indicated by circle 0, and the filtered states (Kalman filter estimate of the true value of the state) is indicated by the solid line. One observes what an effective job the filter does to this 5% noisy signal. Since the RMS value of the noise equals 5% of the maximum value of the variable during the maneuver, there are instances during the maneuver where the noise-to-signal ratio is over 100%. Figure 7 shows how the identification of the numerical value of the four coefficients N_v , Y_v , $N_r - mx_{Gu}$, and $Y_r - \mu$ proceeds from its original estimate (taken well away from the true value) to the final estimate at the end of the maneuver. The true value of the coefficient is designated by a dotted line. For the conditions of this maneuver and identification procedure ($N_r - mx_{Gu}$) was identified to within 1.6%, N_v within 1.4%, ($Y_r - \mu$) within 0.1% and Y_v within 5.8% of the true value, from initial estimates which were 67% of the true value or within 33% of the true value.

Figures 8 and 9 refer to the same maneuver but with a rudder deflection amplitude of 35° instead of 10° . The filtered state variables shown in Figure 8 again show how effective the filter does its job. Figure 9 indicates that the identification

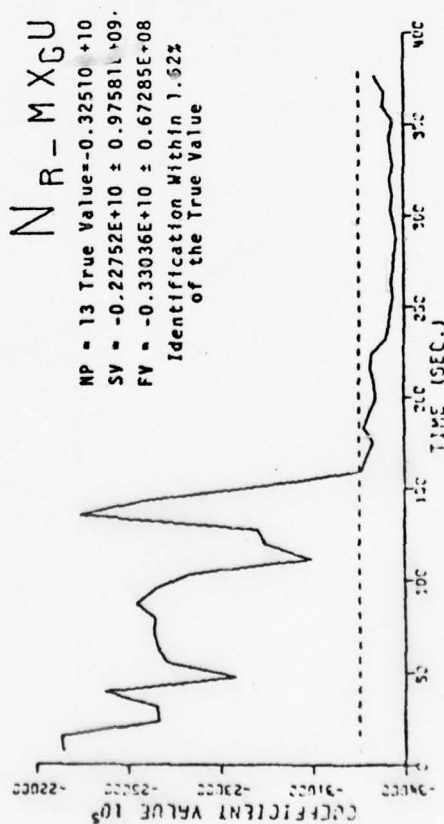
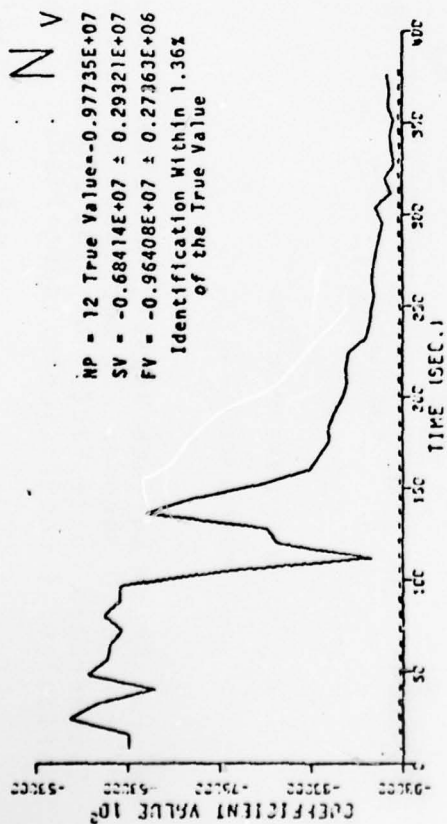
* Provided the measurements are reasonably accurate.

** In Figures 6-29, the beginning of the ordinate axis is not necessarily zero and the ordinate scale varies from figure to figure.



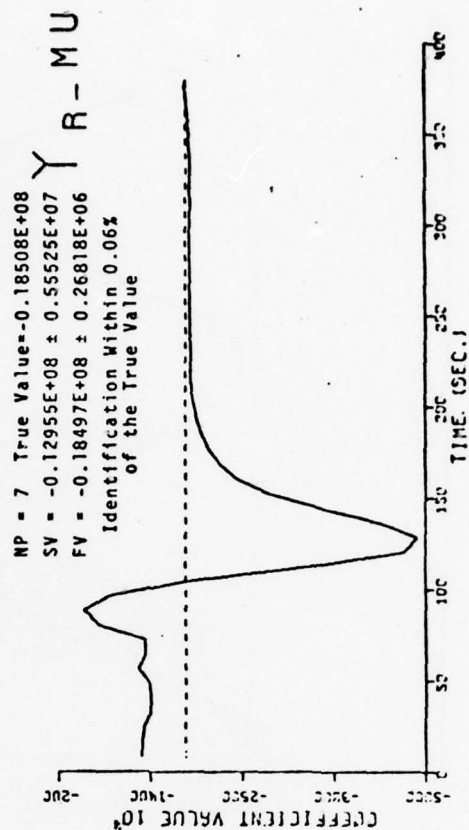
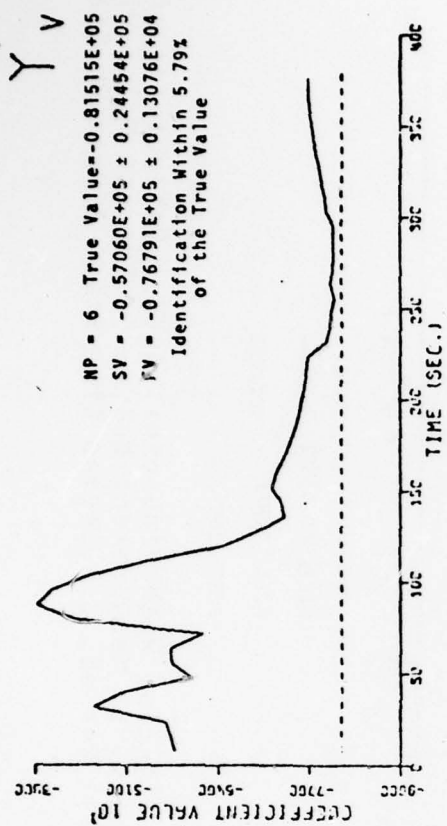
Mariner-Class Surface Vessel, Non-Linear Model, Zig-Zag, With Sinusoidal Rudder Deflections of Period 200.0 Seconds and Amplitude of 10.0 Degrees, 5% Measurement Noise, 5% Process Noise With Exaggerated Noise Factor of 1.0, 376 Second Trial Period, 2.0 Second Time Step, 4 Primary State Variables, 4 Coefficients Identified.

Fig. 6 FILTERED STATES



MEASUREMENT NOISE - 5%

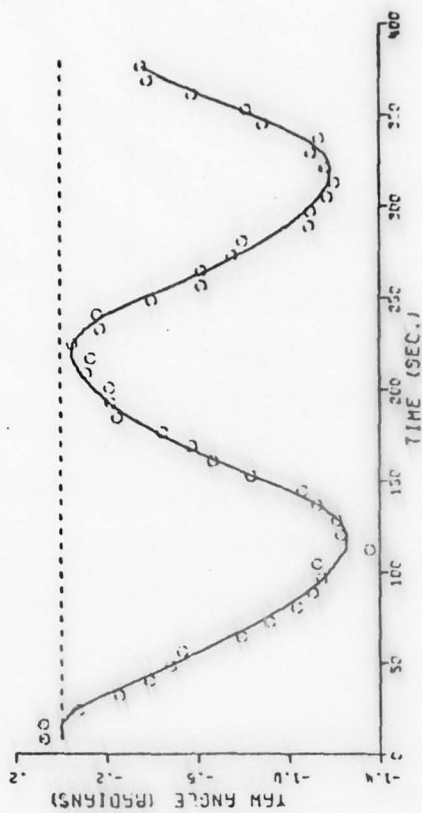
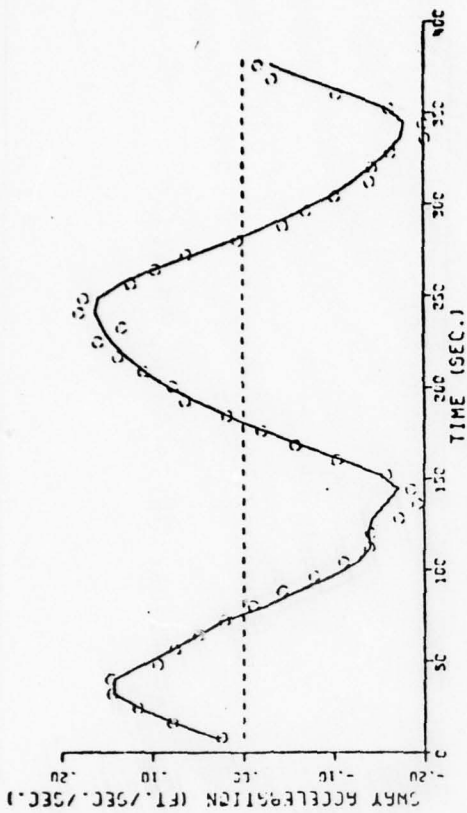
PROCESS NOISE - 5%



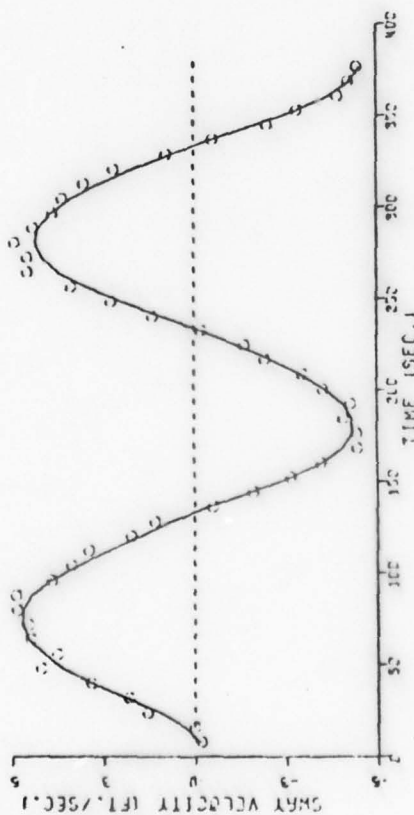
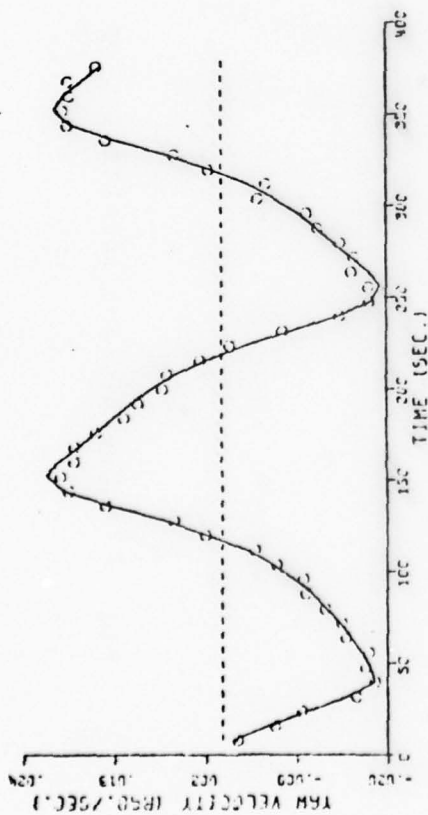
IDENTIFICATION —

TRUE VALUE - - -

Fig. 7 Coefficient Identification - 10 Degree Rudder Deflection, 5% Noise



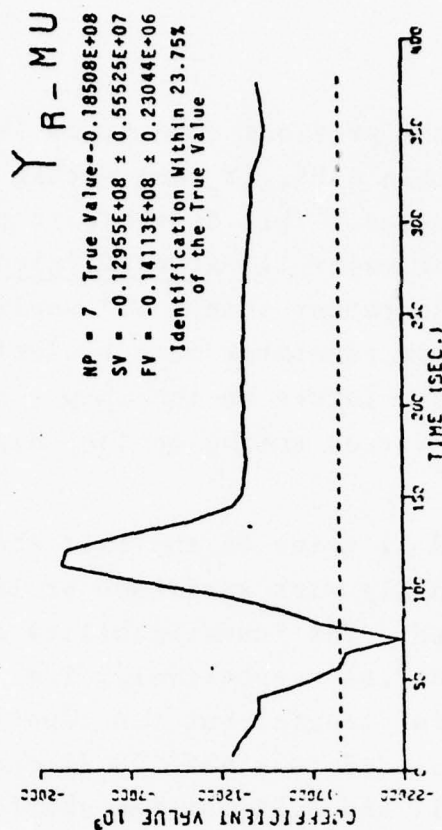
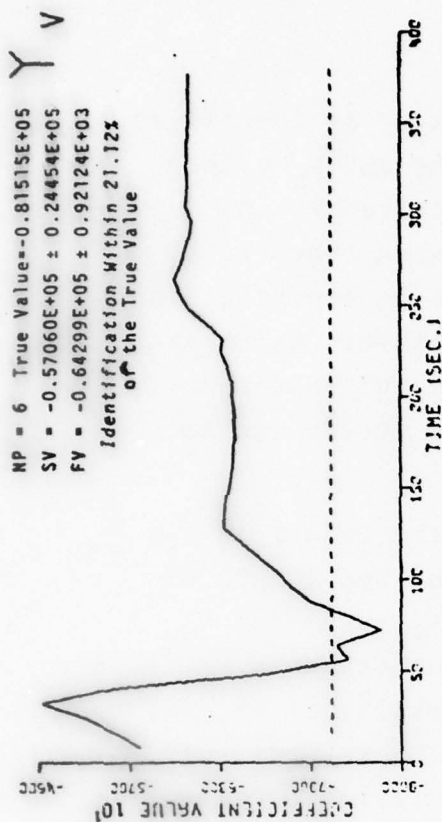
FILTERED STATE —
 NOISE STATE ○○○○○○
 ZERO LINE - - -



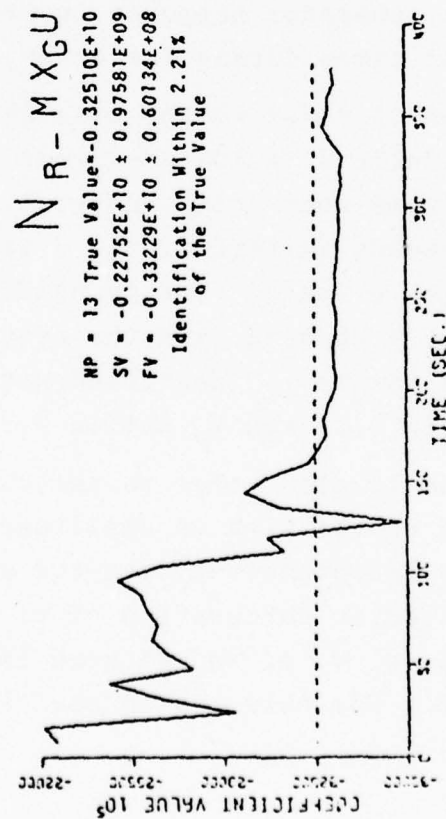
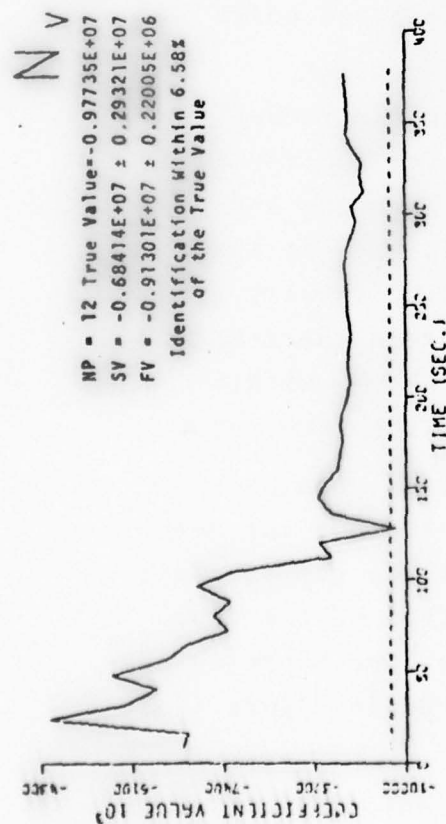
MEASUREMENT NOISE - 5%
 PROCESS NOISE - 5%

Mariner-Class Surface Vessel, Non-Linear Model, Zig-Zag, With Sinusoidal Rudder Deflections of Period 200.0 Seconds and Amplitude of 35.0 Degrees, 5% Measurement Noise, 5% Process Noise With Exaggerated Noise Factor of 1.0, 376 Second Trial Period, 2.0 Second Time Step, 4 Primary State Variables, 4 Coefficients Identified.

Fig. 8 FILTERED STATES



IDENTIFICATION —
 TRUE VALUE - - -



MEASUREMENT NOISE - 5%
 PROCESS NOISE - 5%

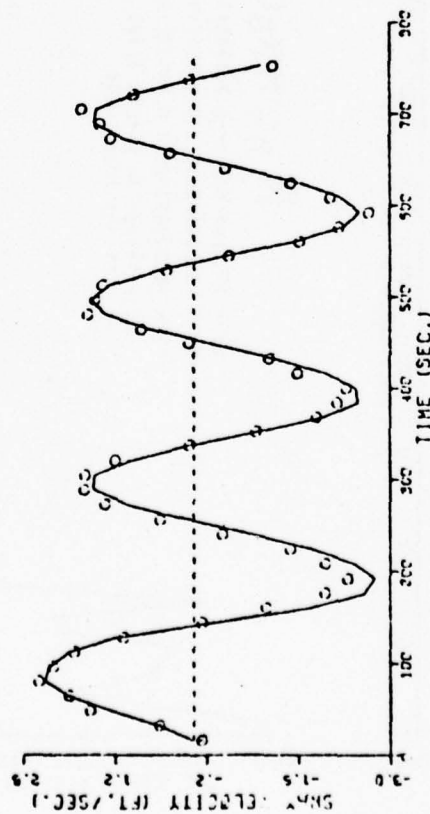
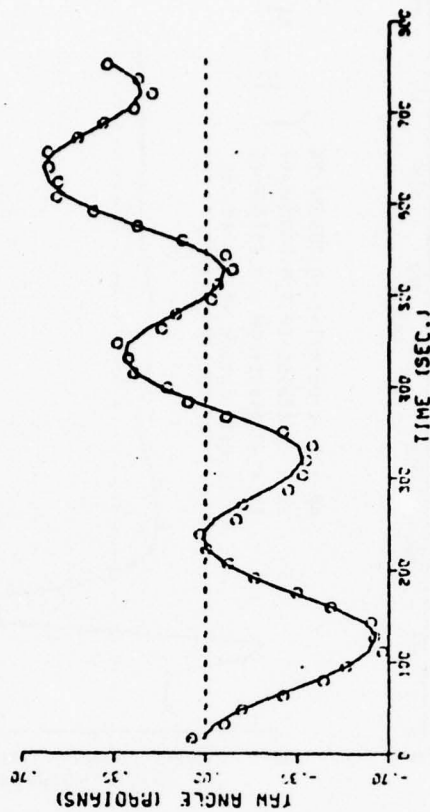
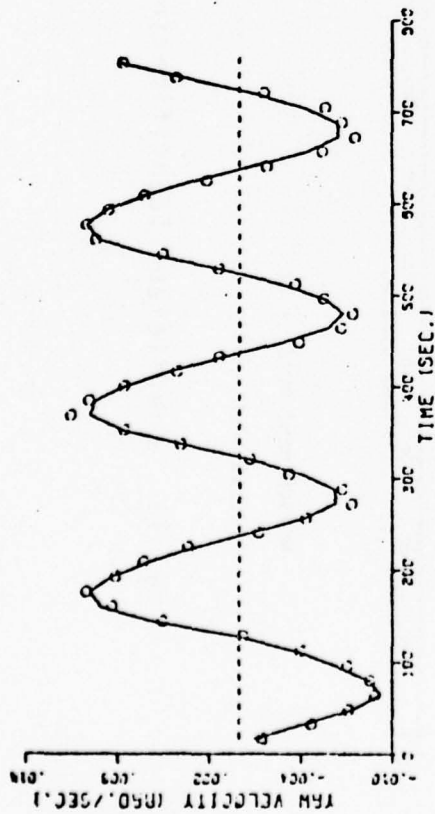
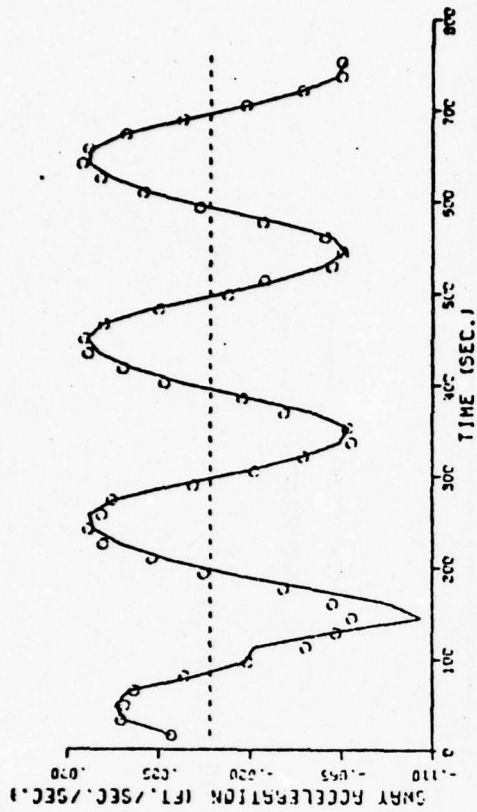
Fig. 9 Coefficient Identification - 35 Degree Rudder Deflection, 5% Noise

is not as good as the previous case since $(N_r - mx_G u)$ is identified within 2.2%, N_v within 6.6%, $(Y_r - \mu)$ within 23.8% and Y_v within 21.1% of the true value. This decrease in effectiveness in identifying the four major linear coefficients when there is a 35° rudder amplitude rather than a 10° amplitude is expected since the larger deflection generates more violent maneuvers which excite significant nonlinear forces on the ship. For a 10° rudder deflection the major forces acting on the ship are attributed to linear effects.

Figures 10 and 11 refer to the case where the rudder is oscillated sinusoidally with amplitude of 10° but the length of the trial is doubled. The identifiability of $(N_r - mx_G u)$ and N_v are within 1.5% and 2.6% respectively, i.e. about the same as for the shorter trial length, but the identifiability of $(Y_r - \mu)$ and Y_v has been degraded to within 10.2% and 16.5% respectively (as compared to 0.1% and 5.8% for the shorter duration trial). One rational explanation is that during the larger trial the random white noise generator happened to produce large noise outputs at critical times during the maneuver.

Figures 12 and 13 refer to the case wherein the rudder is oscillated sinusoidally at a 10° amplitude for the shorter trial duration, but the time step (time interval of recording and filtering) is 4 seconds instead of the 2 seconds used in the case described in Figures 6 and 7. The identifiability is very good and not significantly changed from the case wherein the 2-second step was used. $(N_r - mx_G u)$ is identified with 2.3%, N_v within 0.8%, $(Y_r - \mu)$ within 3.2% and Y_v within 2.2% of the true value.

Figures 14 and 15 also refer to the case of a sinusoidal oscillation of the rudder with an amplitude of 10° but the number of state variables independently measured are three (v , ψ , and r , with v resulting from an integration of \dot{v}) instead of the four measured variables (v , \dot{v} , ψ , and r) used in the case represented by Figures 6 and 7. For this reason one observes in Figure 14

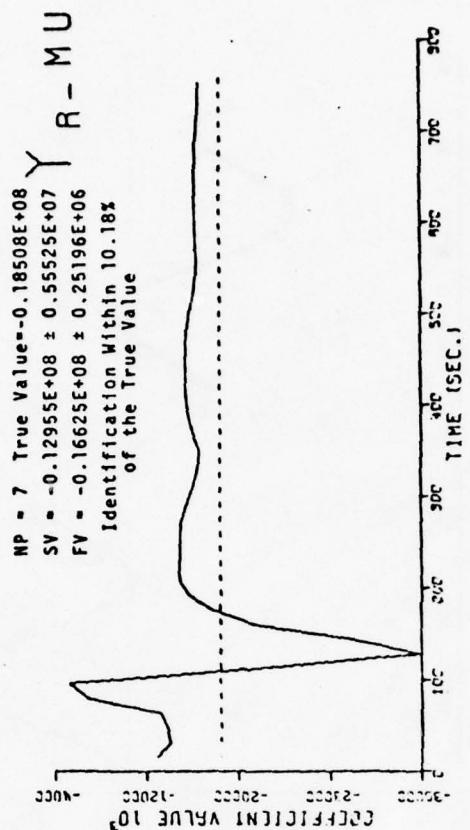
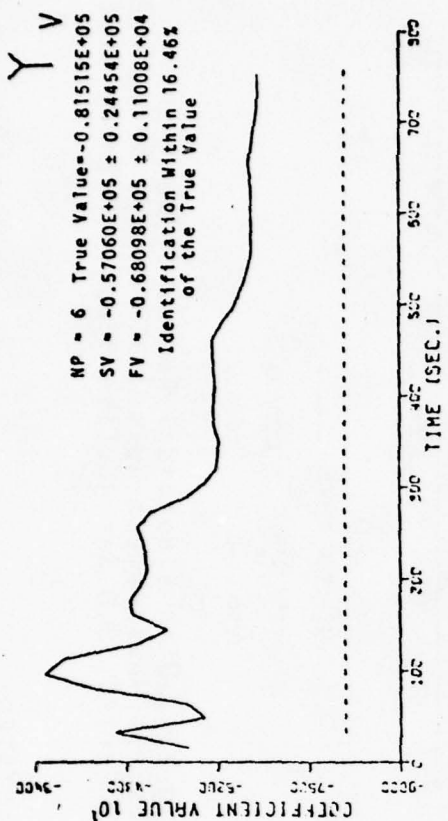
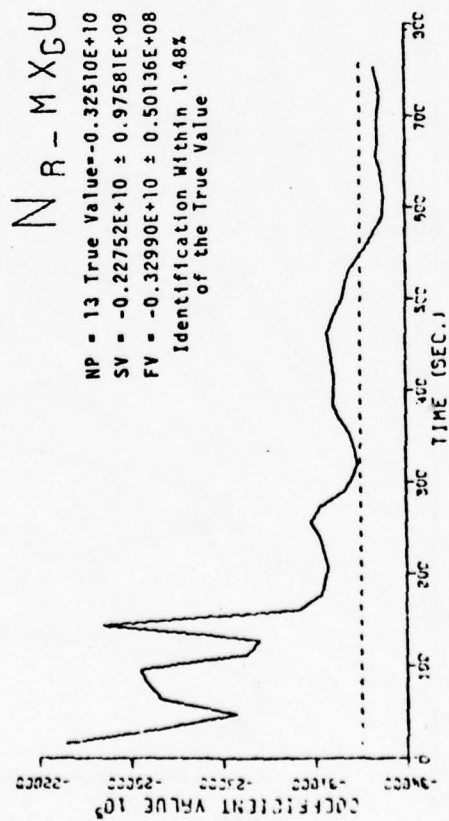
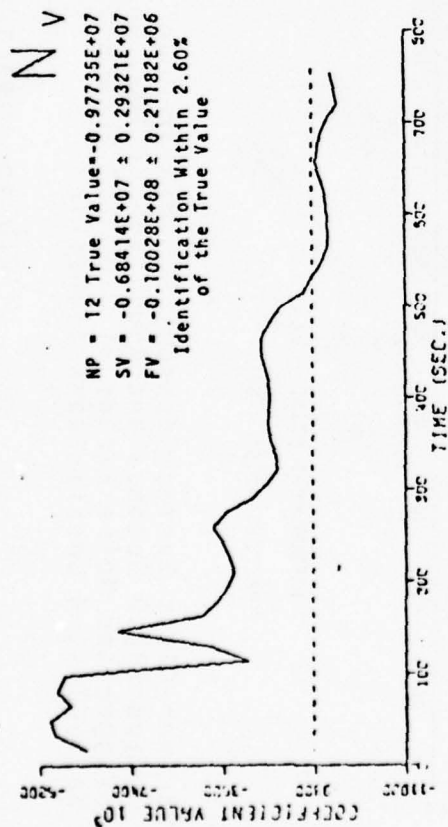


FILTERED STATE —
 NOISE STATE ○○○○○○
 ZERO LINE - - - -

MEASUREMENT NOISE - 5%
 PROCESS NOISE - 5%

Mariner-Class Surface Vessel, Non-Linear Model, Zig-Zag, With Sinusoidal Rudder Deflections of Period 200.0 Seconds and Amplitude of 10.0 Degrees, 5% Measurement Noise, 5% Process Noise With Exaggerated Noise Factor of 1.0, 752 Second Trial Period, 2.0 Second Time Step, 4 Primary State Variables, 4 Coefficients Identified.

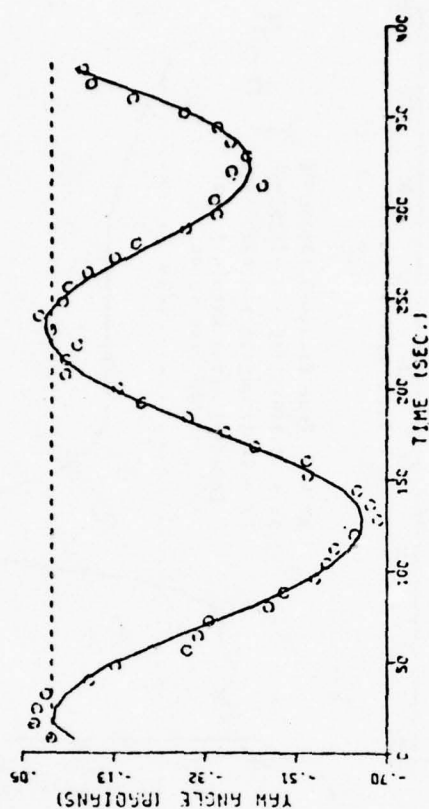
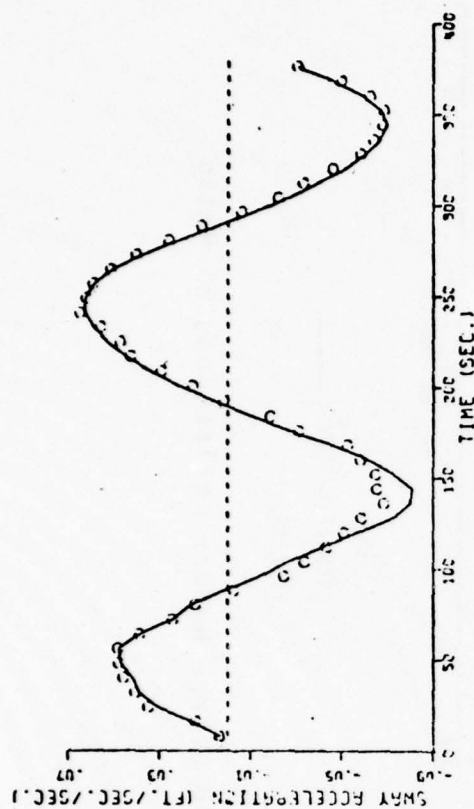
Fig. 10 FILTERED STATES



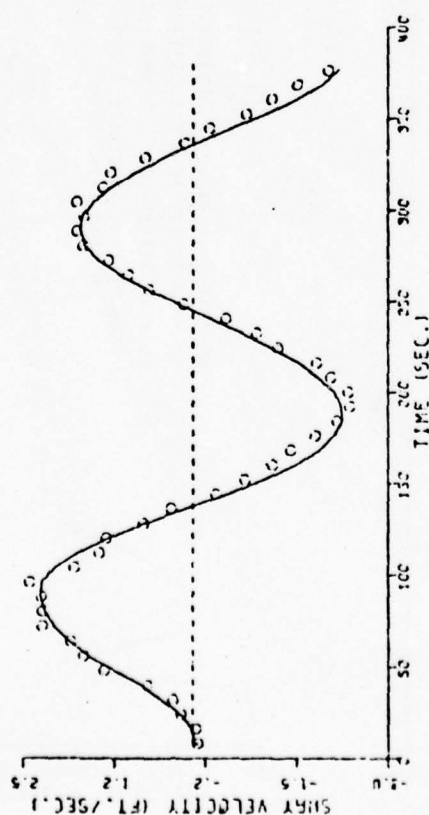
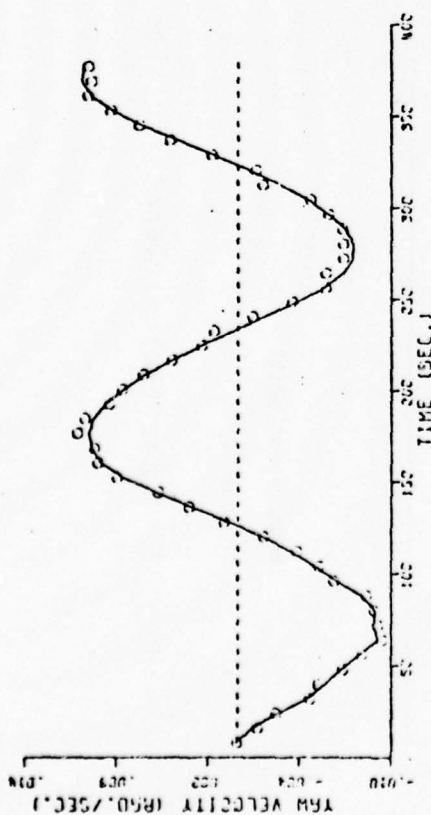
MEASUREMENT NOISE - 5%
 PROCESS NOISE - 5%

IDENTIFICATION —
 TRUE VALUE ----

Fig. 11 Coefficient Identification - 10 Degree Rudder Deflection, 5% Noise



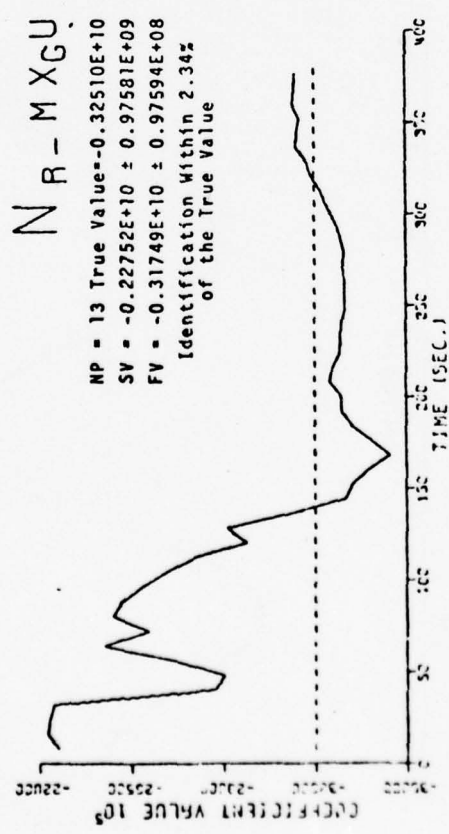
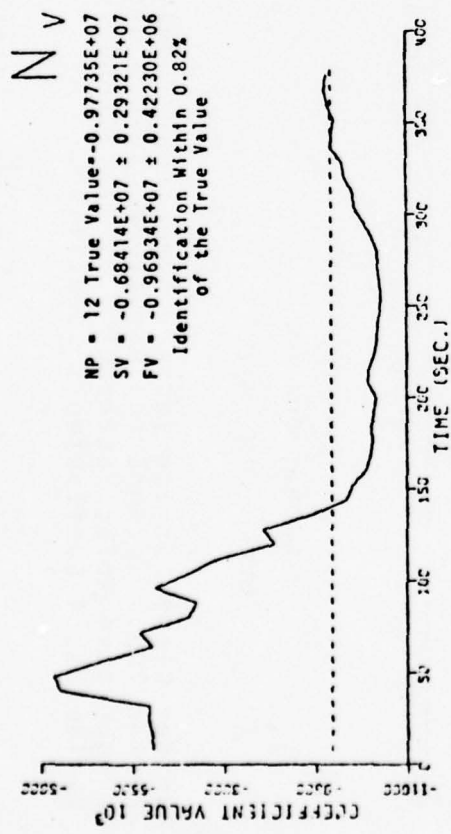
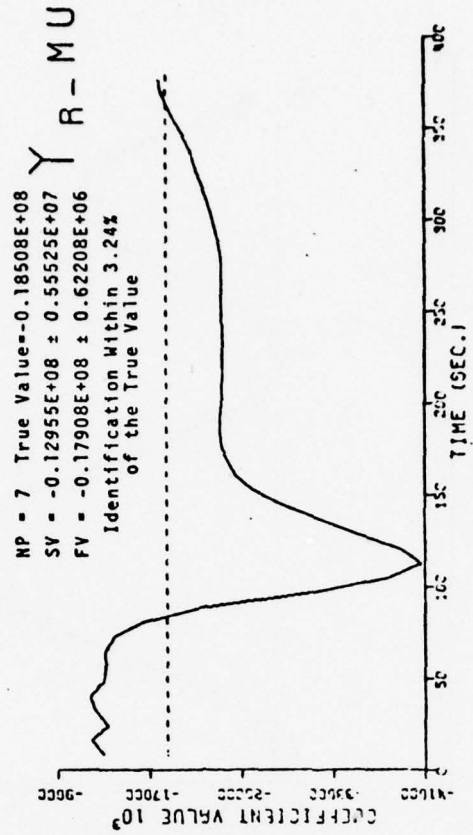
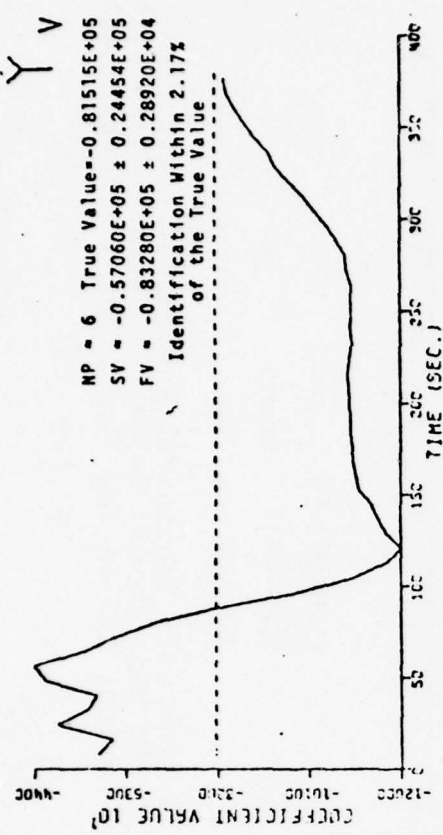
FILTERED STATE —
 NOISY STATE ○○○○○○
 ZERO LINE - - - -



MEASUREMENT NOISE - 5%
 PROCESS NOISE - 5%

Mariner-Class Surface Vessel, Non-Linear Model, Zig-Zag, With Sinusoidal Rudder Deflections of Period 200.0 Seconds and Amplitude of 10.0 Degrees, 5% Measurement Noise, 5% Process Noise With Exaggerated Noise Factor of 1.0, 376 Second Trial Period, 4.0 Second Time Step, 4 Primary State Variables, 4 Coefficients Identified.

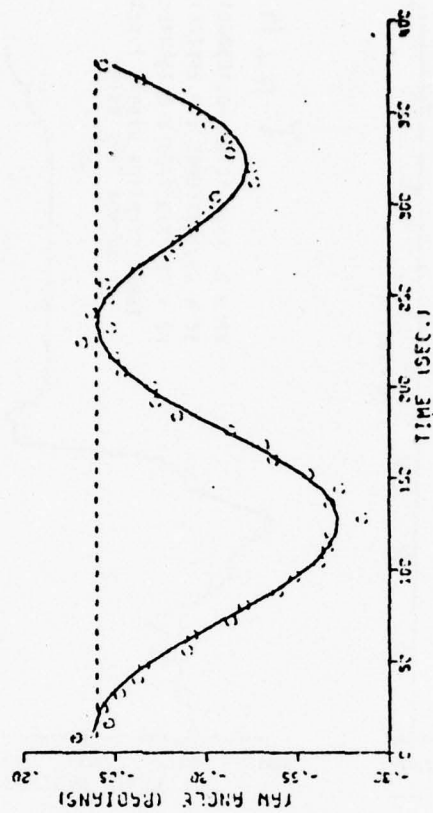
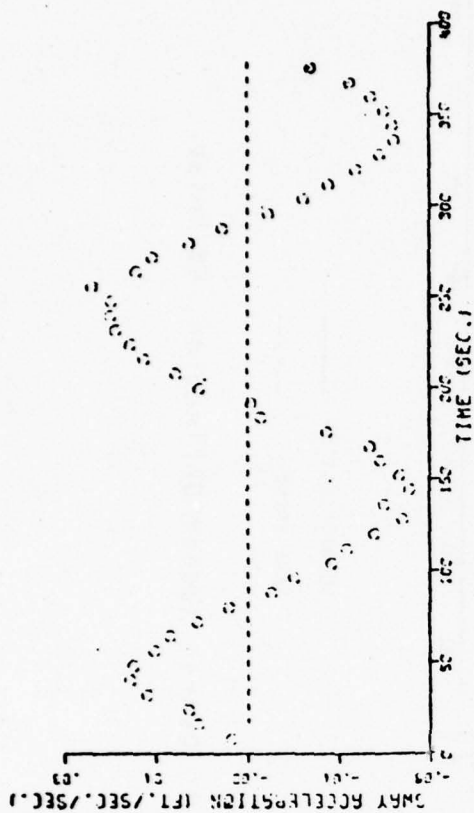
Fig. 12 FILTERED STATES



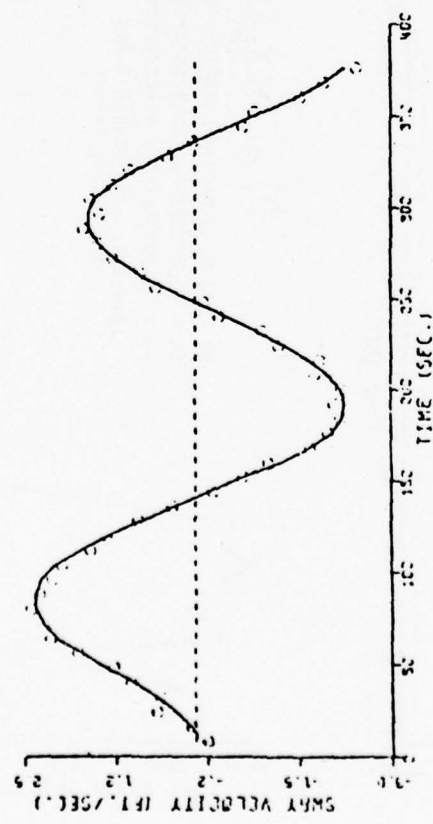
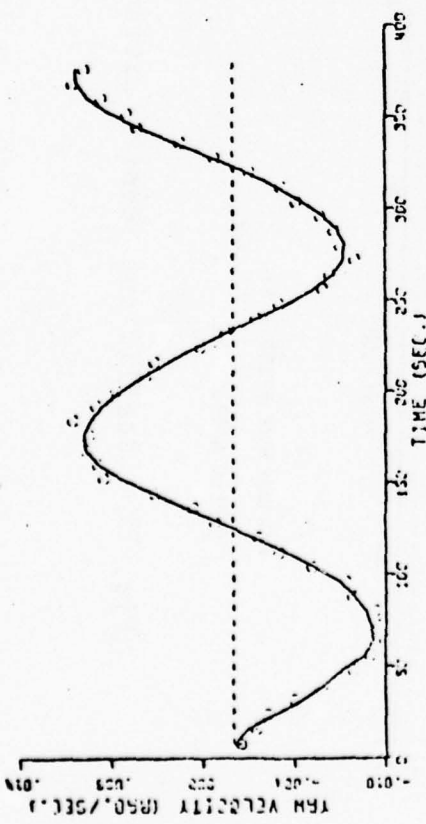
IDENTIFICATION —
 TRUE VALUE - - -

MEASUREMENT NOISE - 5%
 PROCESS NOISE - 5%

Fig. 13 Coefficient Identification - 10 Degree Rudder Deflection, 5% Noise



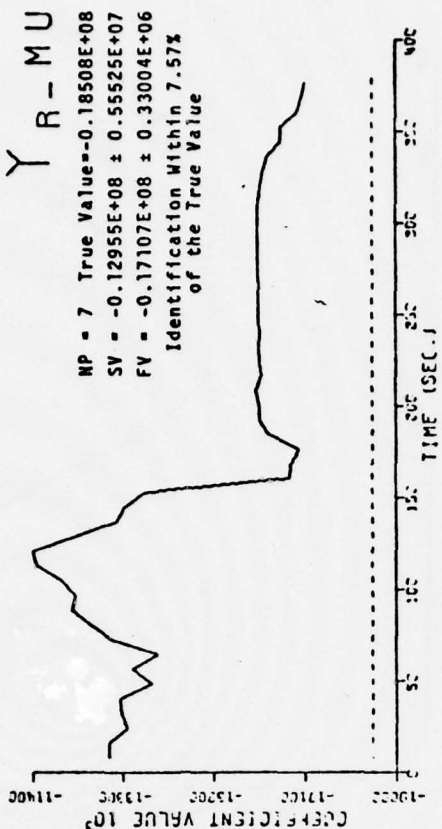
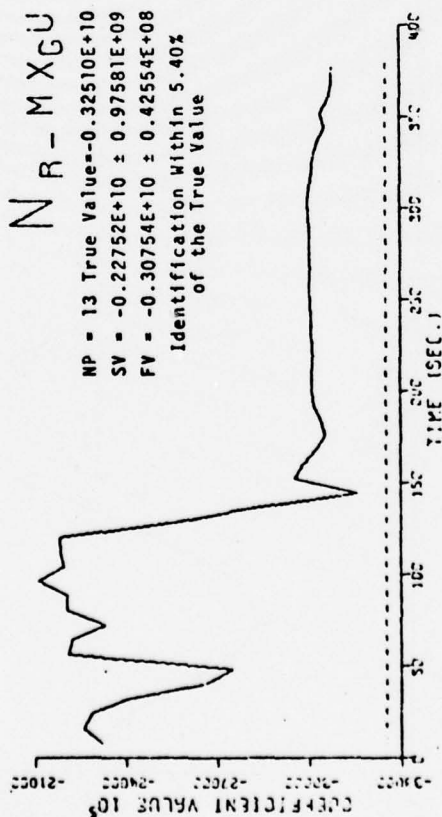
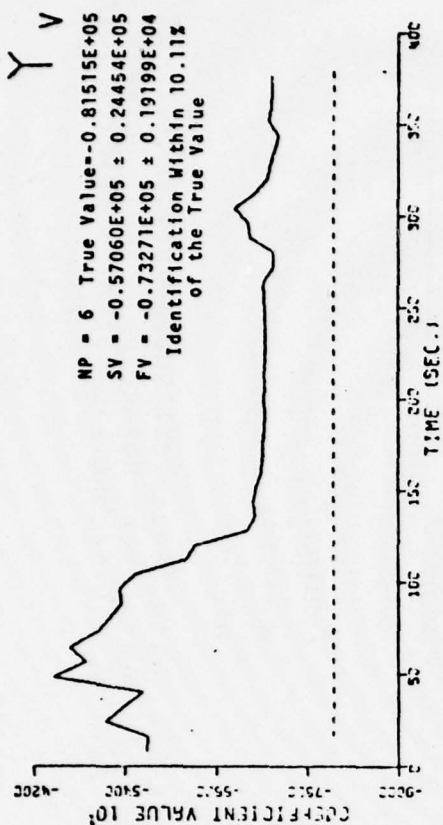
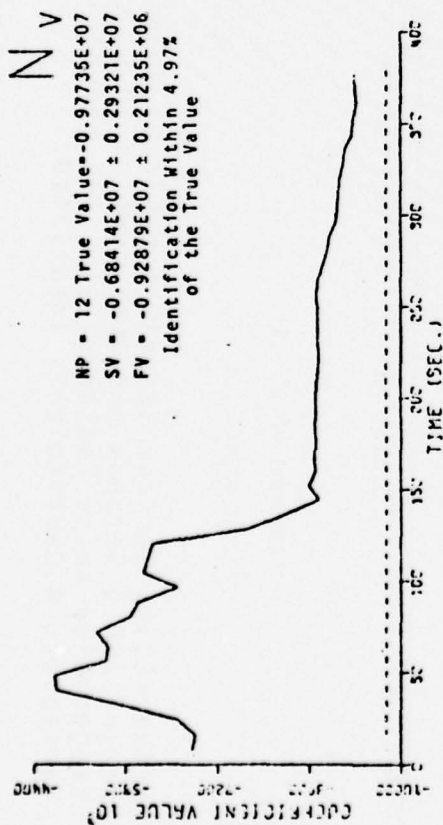
FILTERED STATE —
 NOISE STATE ○○○○○○
 ZERO LINE - - - -



MEASUREMENT NOISE - 5%
 PROCESS NOISE - 5%

Mariner-Class Surface Vessel, Non-Linear Model, Zig-Zag, With Sinusoidal Rudder Deflections of Period 200.0 Seconds and Amplitude of 10.0 Degrees, 5% Measurement Noise, 5% Process Noise With Exaggerated Noise Factor of 1.0, 376 Second Trial Period, 1.0 Second Time Step, 3 Primary State Variables, 4 Coefficients Identified.

Fig. 14 FILTERED STATES



MEASUREMENT NOISE - 5%
 PROCESS NOISE - 5%

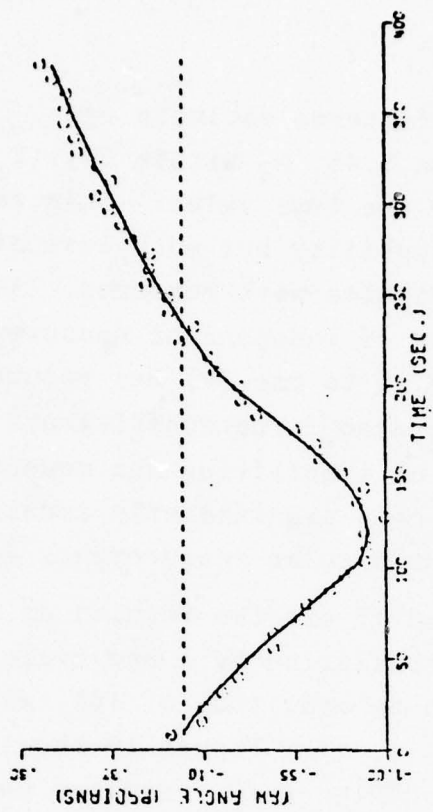
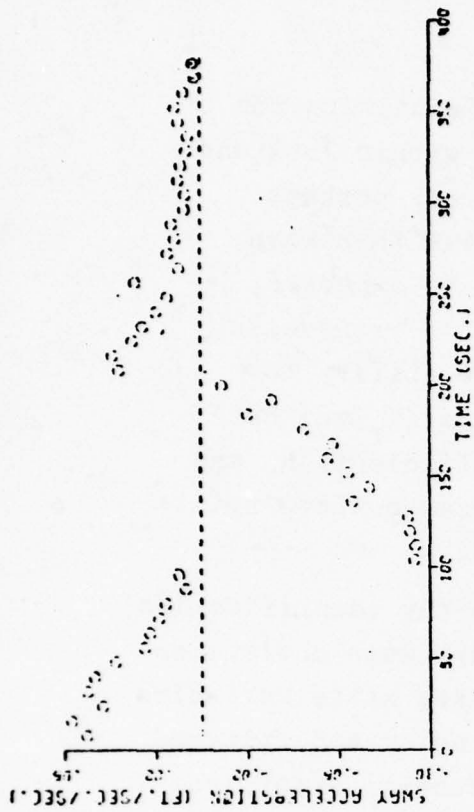
IDENTIFICATION —
 TRUE VALUE - - -

Fig. 15 Coefficient Identification - 10 Degree Rudder Deflection, 5% Noise

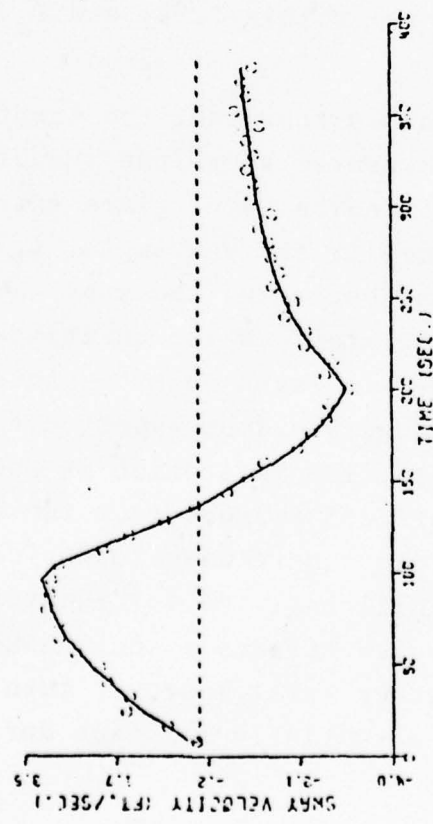
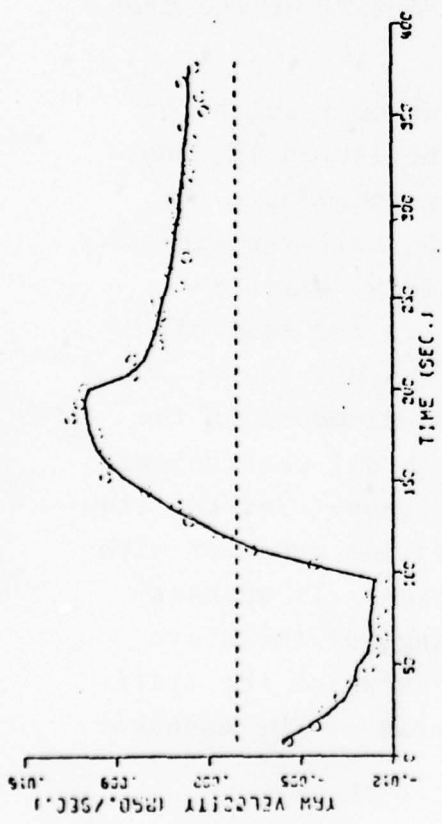
that there is not filtered estimate of \dot{v} . The identification of $(N_r - mx_G u)$ is within 5.4%, N_v within 5%, $(Y_r - \mu)$ within 7.6% and Y_v within 10.1% of the true value. This represents perhaps acceptable identifiability but much less effective than when all four state variables were measured. As may be expected, reducing the number of independent measurements of transverse motion from two (v, \dot{v}) to one (v) has reduced the ability to identify the transverse force coefficients Y_v and $(Y_r - \mu)$ but the effectiveness of identifying the moment coefficients N_v and $(N_r - mx_G u)$ has not been significantly reduced because there still are two independent angular measurements (ψ, r) .

Figures 16 and 17 are the results of parameter identification for the maneuver consisting of a one cycle square wave deflection of the rudder with an amplitude of 10° , with three state variables being measured (v, ψ, r) . Figure 16 shows the noisy and filtered state variables and Figure 17 indicates good identification from this maneuver with $(N_r - mx_G u)$ being identified within 6.4%, N_v within 12.2%, $(Y_r - \mu)$ within 7.7%, and Y_v within 8.2% of the true value.

Figures 18 and 19 represent the identification results for a steady turning maneuver where the rudder is deflected 10° and held there. The 5% noise level gives extremely noisy data for all signals, especially the yaw angle, ψ , which increases linearly during the maneuver and the sway velocity, v , which results from an integrated \dot{v} which quantity is zero for most of the maneuver. The simulated noisy measurements appear to be far in excess of what would be expected for measurements on the ship. In this case, identification is poor with all coefficients being estimated off 25% or more from the true value. Yet the sinusoidal and one cycle square wave rudder oscillation maneuver with 5% noise gave significantly better identification. It appears that a maneuver which effects a continuous change of the state variables is a better trial maneuver than one in which the state variables remain essentially constant during most of the maneuver,



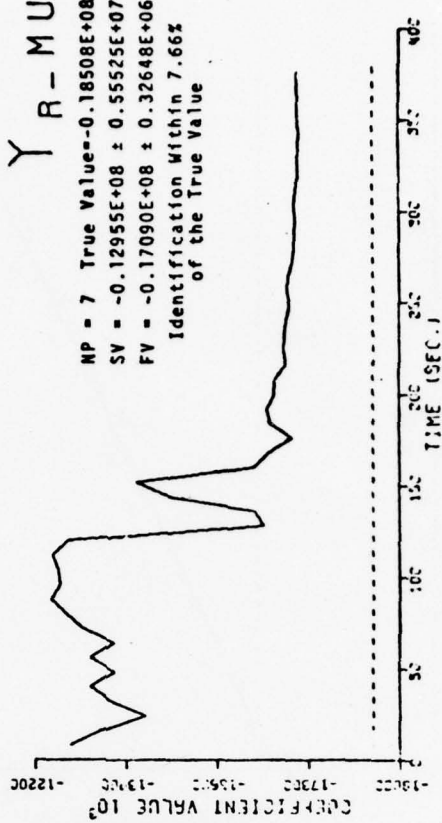
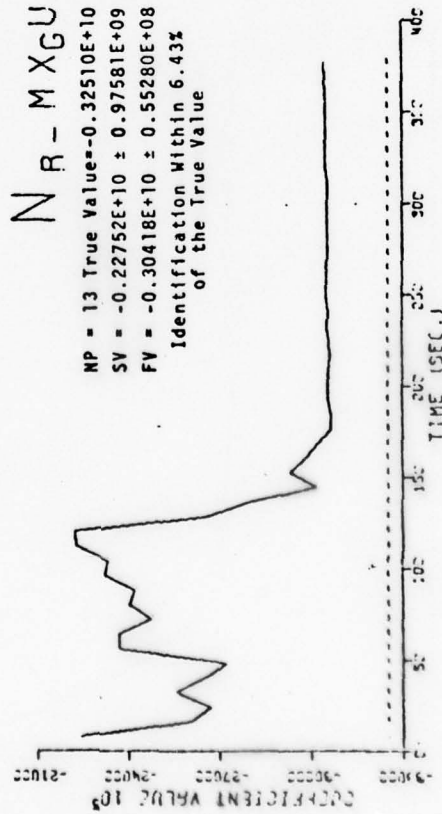
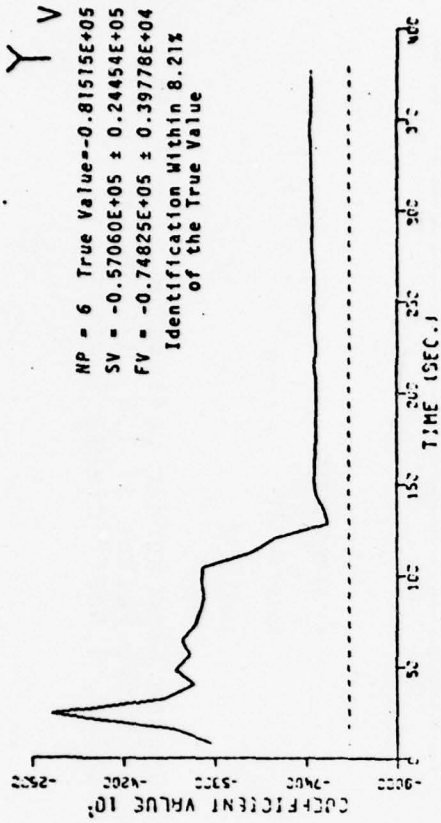
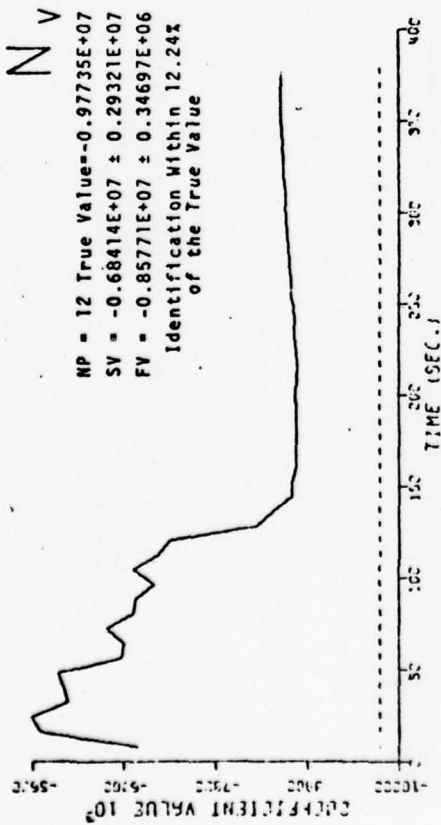
FILTERED STATE —
 NOISY STATE ○○○○○
 ZERO LINE - - -



MEASUREMENT NOISE - 5%
 PROCESS NOISE - 5%

Fig. 16 FILTERED STATES

Mariner-Class Surface Vessel, Non-Linear Model, Zig-Zag, With Step Rudder Deflections at Time $t=100$ and $t=200$ Seconds, 5% Measurement Noise, 5% Process Noise With Exaggerated Noise Factor of 1.0, 376 Second Trial Period, 1.0 Second Time Step, 3 Primary State Variables, 4 Coefficients Identified.



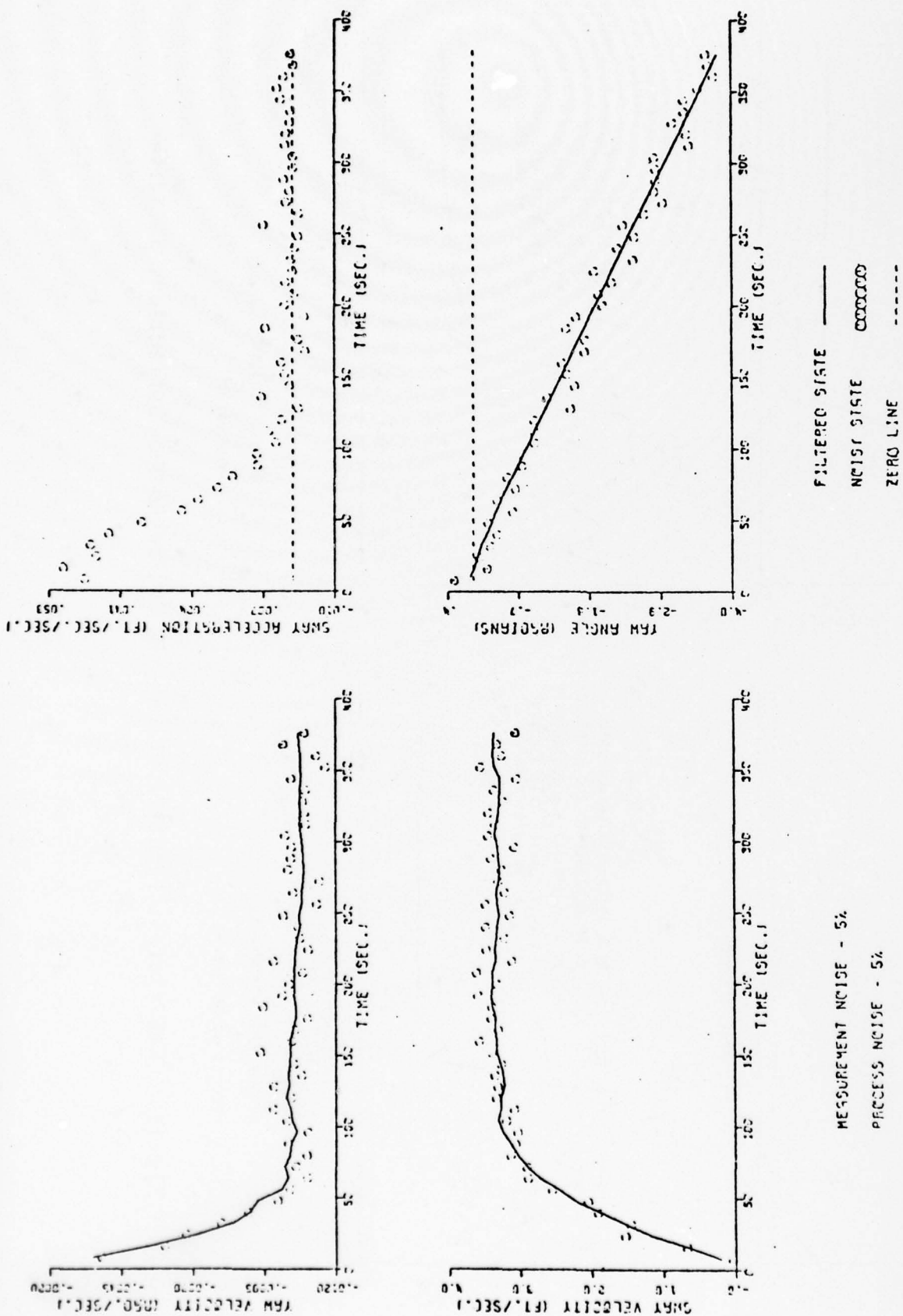
MEASUREMENT NOISE - 5%

PROCESS NOISE - 5%

IDENTIFICATION —

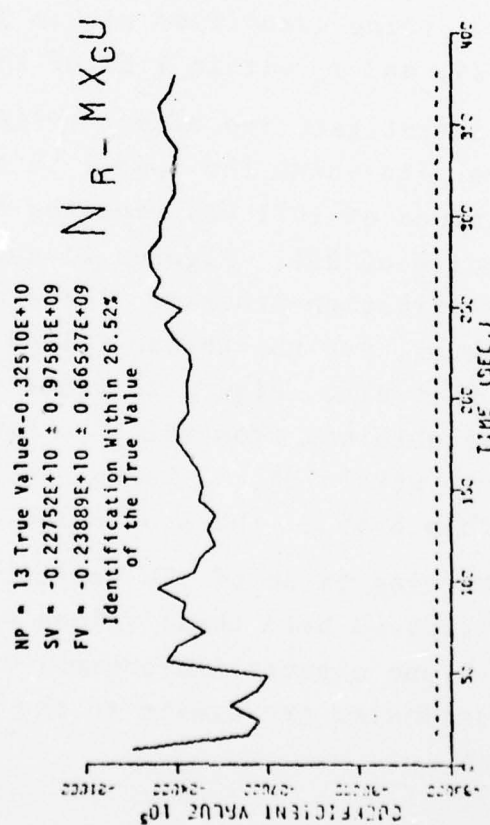
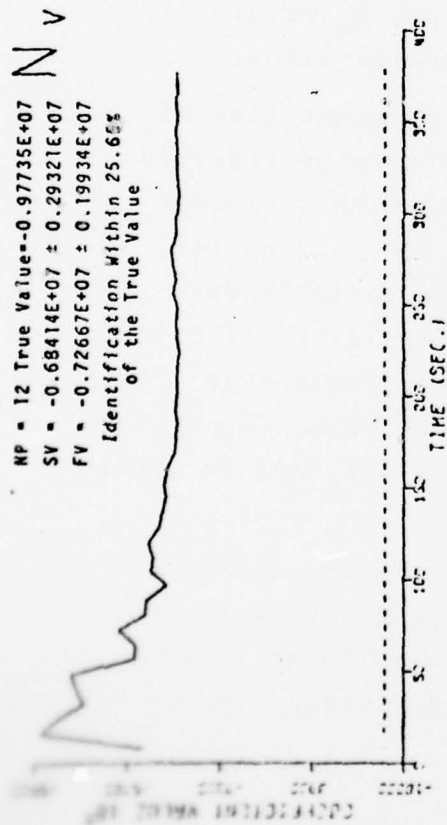
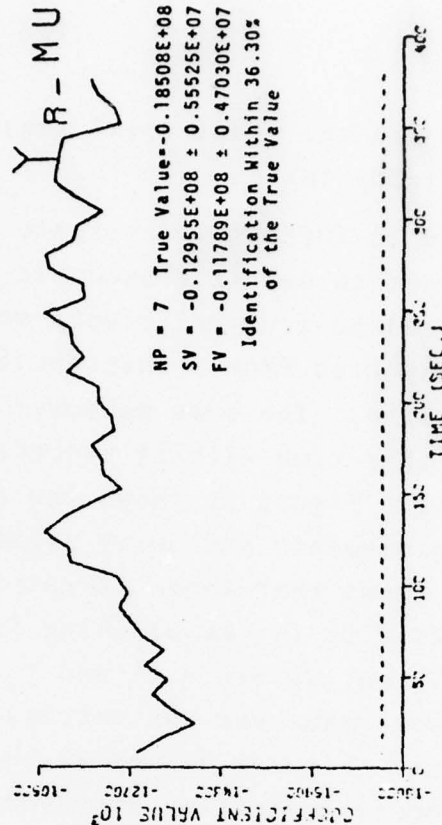
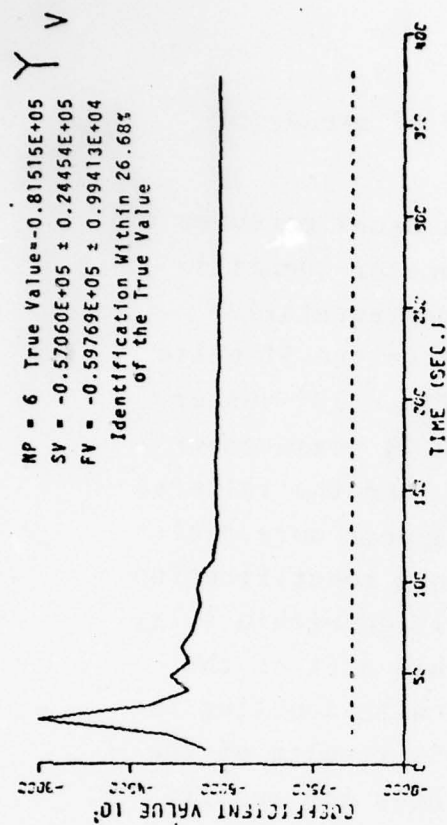
TRUE VALUE - - - -

Fig. 17 Coefficient Identification - 10 Degree Rudder Deflection, 5% Noise



Mariner-Class Surface Vessel, Non-Linear Model, 10 Degree Step Rudder Deflection at $t=0$, 5% Measurement Noise, 5% Process Noise With Exaggerated Noise Factor of 1.0, 376 Second Trial Period, 1.0 Second Time Step, 3 Primary State Variables, 4 Coefficients Identified.

Fig. 18 FILTERED STATES



IDENTIFICATION —
TRUE VALUE - - - -

MEASUREMENT NOISE - 5%
PROCESS NOISE - 5%

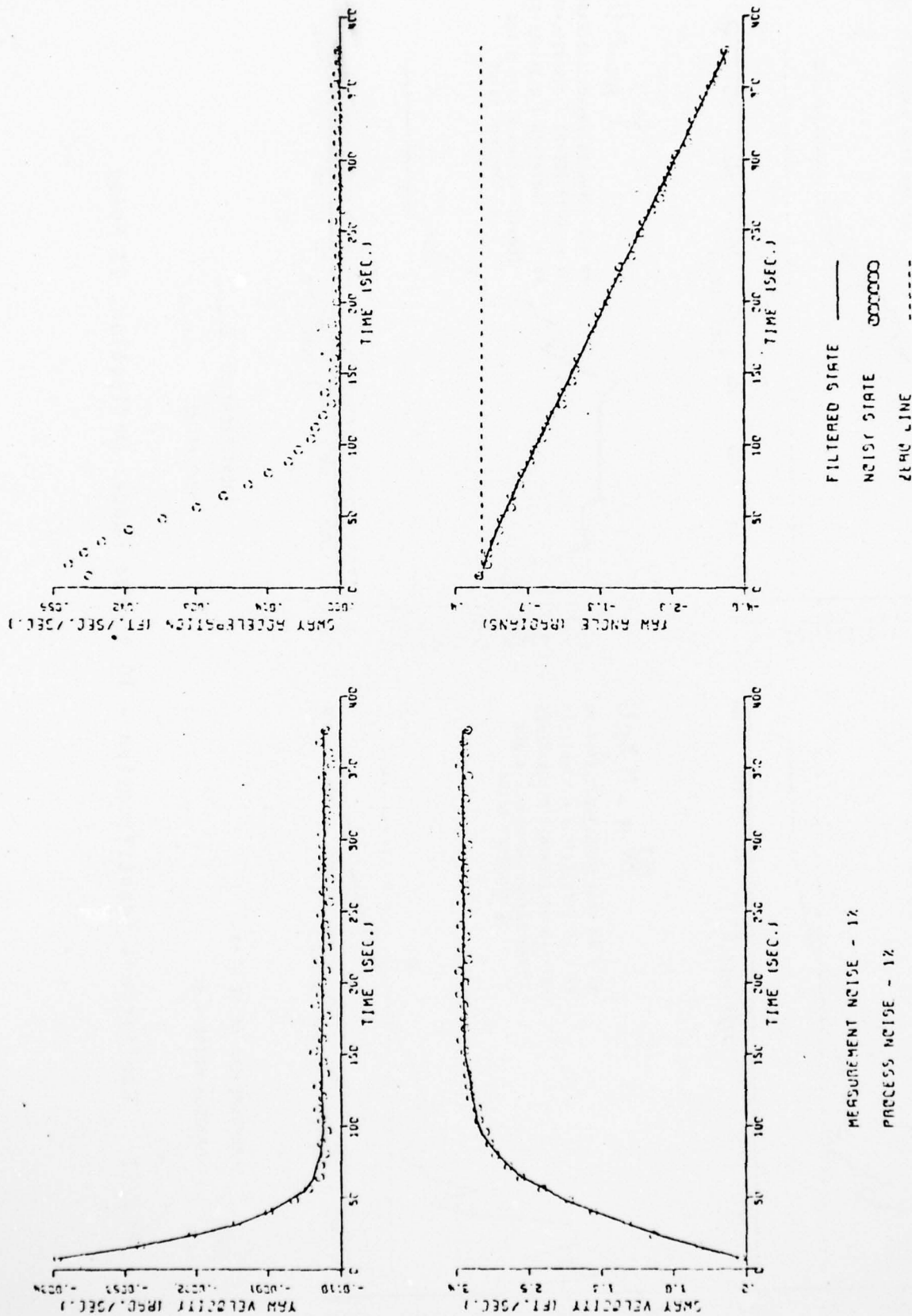
Fig.19 Coefficient Identification - 10 Degree Rudder Deflection, 5% Noise

such as v , \dot{v} , and r in the usual trial maneuver of steady or fixed rudder and steady turns.

It was decided to further investigate this usual maneuver of fixed rudder in order to see if reasonable parameter identification could be obtained from noisy data more representative of what would be expected from a ship trial, since the 5% noise appears very excessive. The same maneuver of fixed 10° rudder was analyzed, but this time with 1% process and 1% measurement noise instead of 5%. Figure 20 shows the noisy and the filtered state variable measurements and noisy signals appear more realistic. Figure 21 shows that there is rather good identification of the coefficients with $(N_r - mx_G u)$ being identified within 4.1%, N_v within 4.9%, $(Y_r - \mu)$ within 9.1% and Y_v within 6.6% of the true value. The same maneuver was carried out with doubling the length of trial run. Figures 22 and 23 show the results of the identification process indicating improvement over the results from the shorter run and very good identification of the coefficients, $(N_r - mx_G u)$ being identified within 3.8%, N_v within 5%, $(Y_r - \mu)$ within 2.2%, and Y_v within 1.3% of the true value.

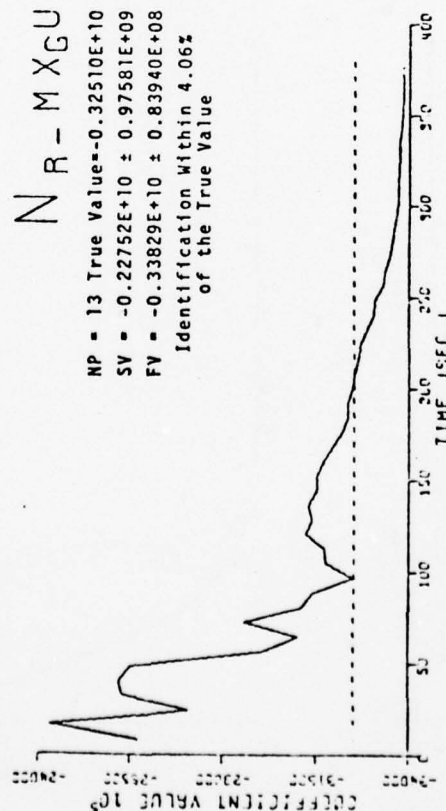
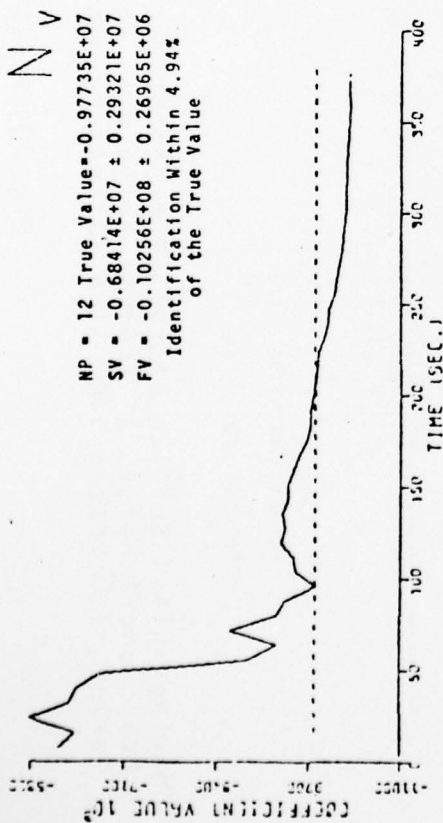
In order to investigate the effect of large quantities of noise, the maneuver (in which the rudder is oscillated sinusoidally with an amplitude of 10°) was repeated but with a process and measurement noise of 25%. Figures 24 and 25 show the results of the identification process. The state variable data is ridiculously noisy, yet the Kalman filter does a terrific job of making sense of it all. Figure 25 shows that reasonable identification was obtained from this "buckshot" data, $(N_r - mx_G u)$ being identified to within 9%, N_v to within 19%, $(Y_r - \mu)$ to within 2%, and Y_v to within 5.8% of the true value.

Since the starting value of the coefficients are estimates (in most cases discussed here these values were about two-thirds of the true value) one expects improvement in the identification if the original estimates are closer to the true value. Hence,



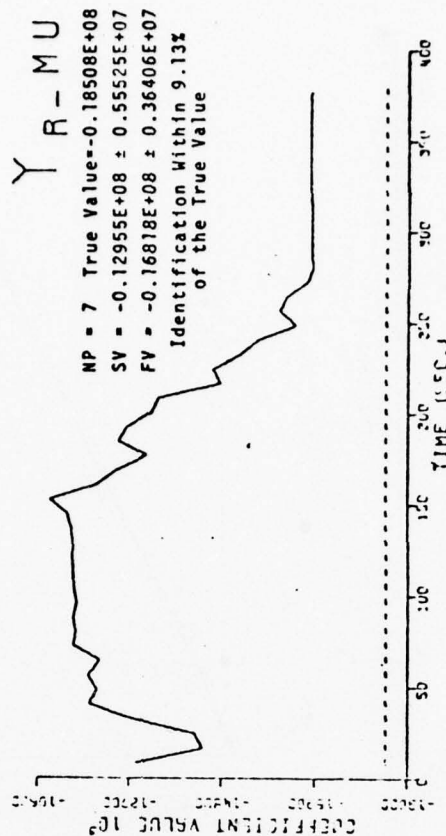
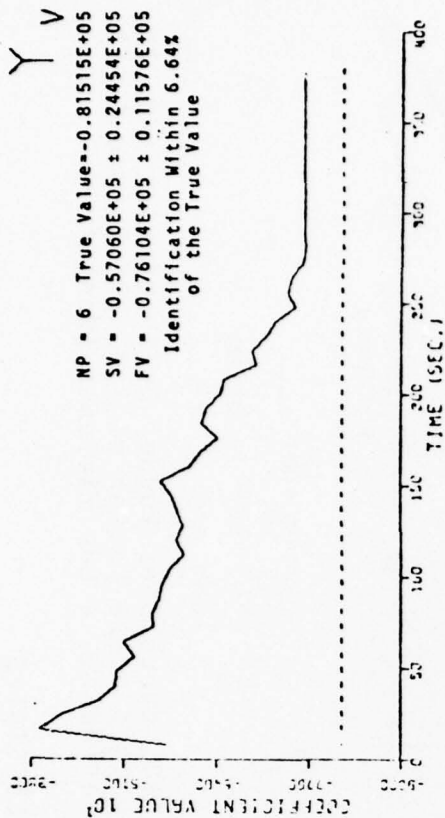
Mariner-Class Surface Vessel, Non-Linear Model, 10 Degree Step Rudder Deflection at $t=0$, 1% Measurement Noise, 1% Process Noise With Exaggerated Noise Factor of 1.0, 376 Second Trial Period, 1.0 Second Time Step, 3 Primary State Variables, 4 Coefficients Identified.

Fig. 20 FILTERED STATES



MEASUREMENT NOISE - 1%

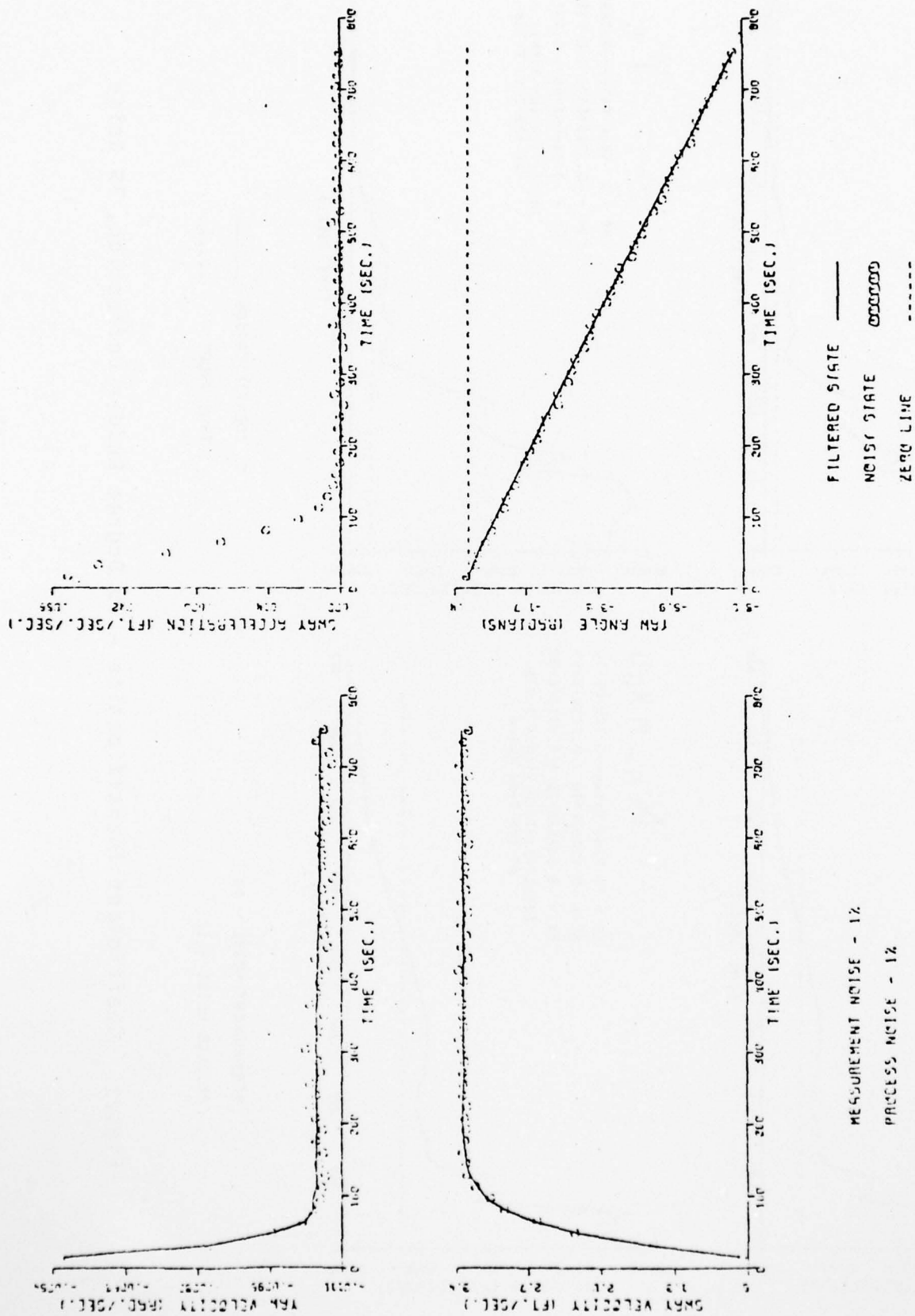
PROCESS NOISE - 1%



IDENTIFICATION —

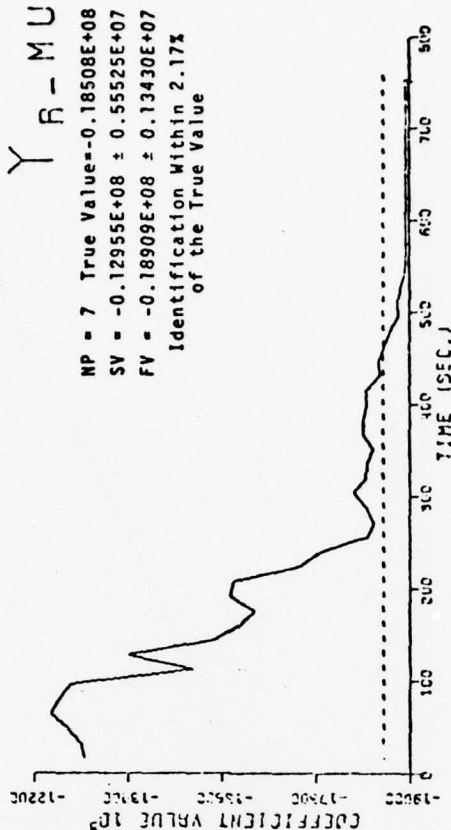
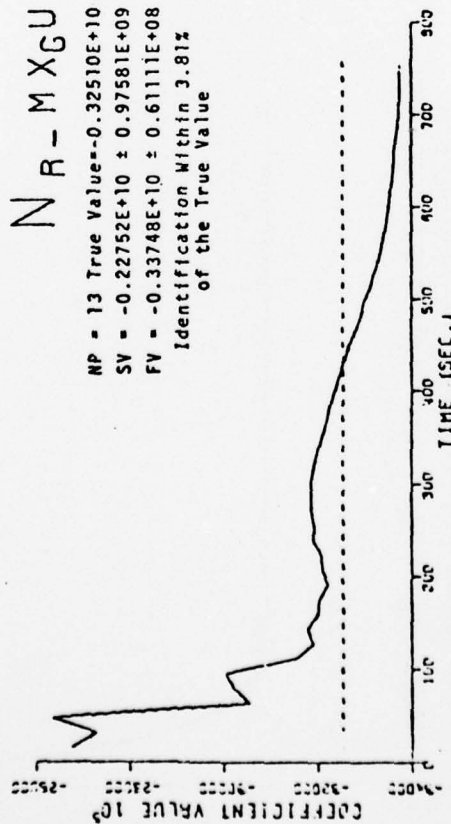
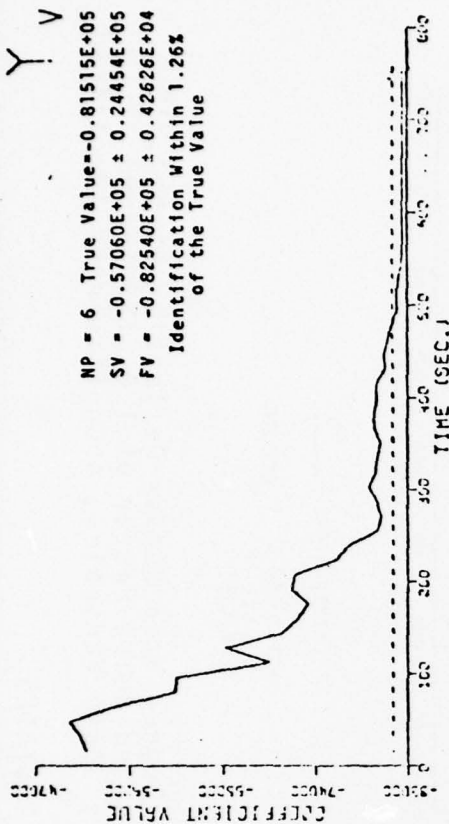
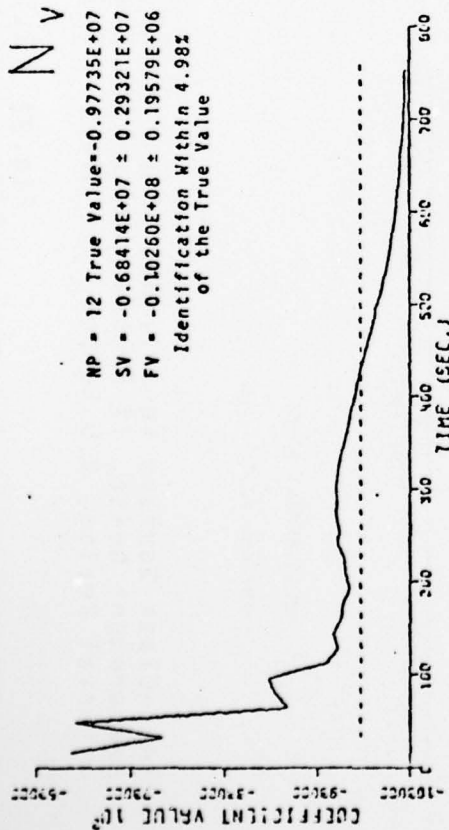
TRUE VALUE ----

Fig. 21 Coefficient Identification - 10 Degree Rudder Deflection, 1% Noise



Mariner-Class Surface Vessel, Non-Linear Model, 10 Degree Step Rudder Deflection at $t=0$, 1% Measurement Noise, 1% Process Noise With Exaggerated Noise Factor of 1.0, 752 Second Trial Period, 2.0 Second Time Step, 3 Primary State Variables, 4 Coefficients Identified

Fig.22 FILTERED STATES



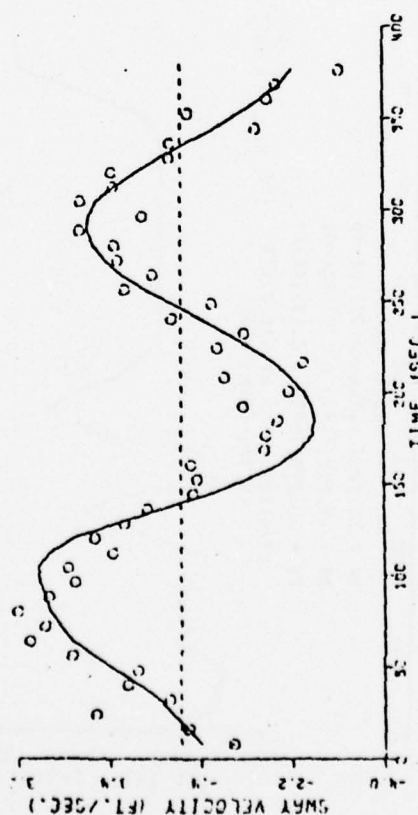
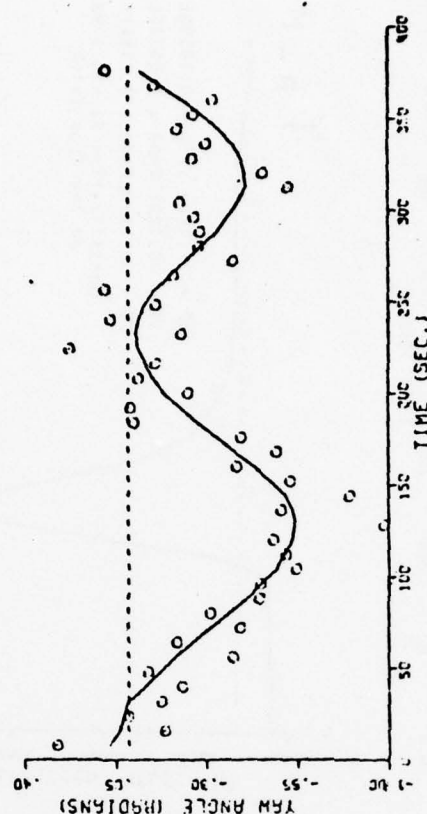
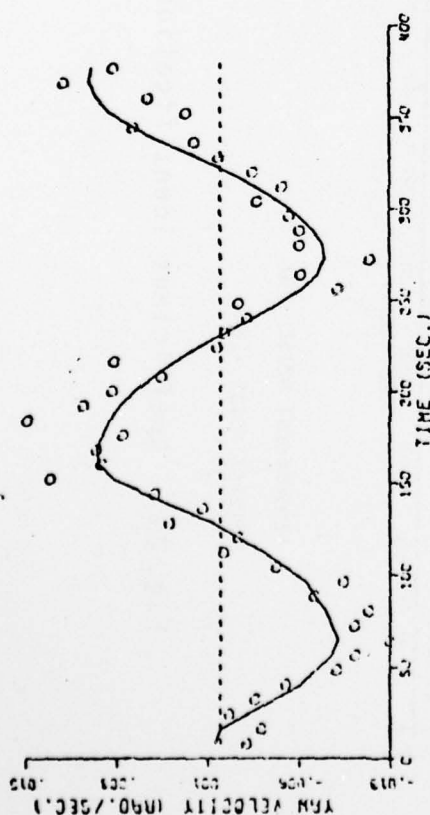
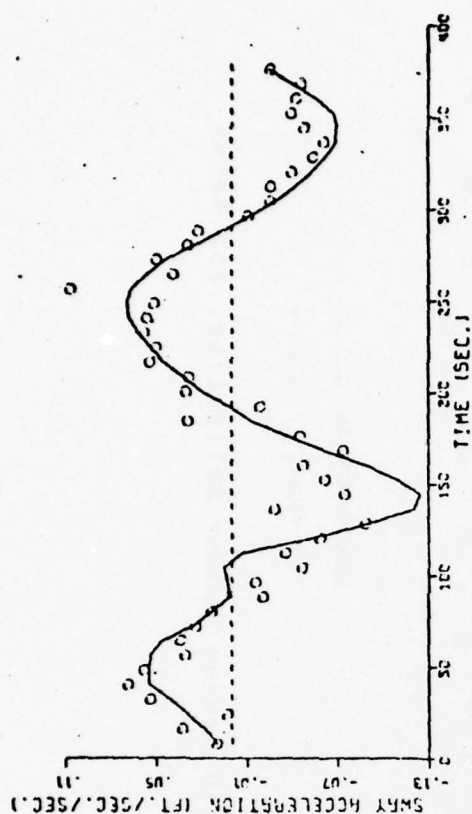
MEASUREMENT NOISE - 1%

PROCESS NOISE - 1%

IDENTIFICATION —

TRUE VALUE - - - -

Fig.23 Coefficient Identification - 10 Degree Rudder Deflection, 1% Noise

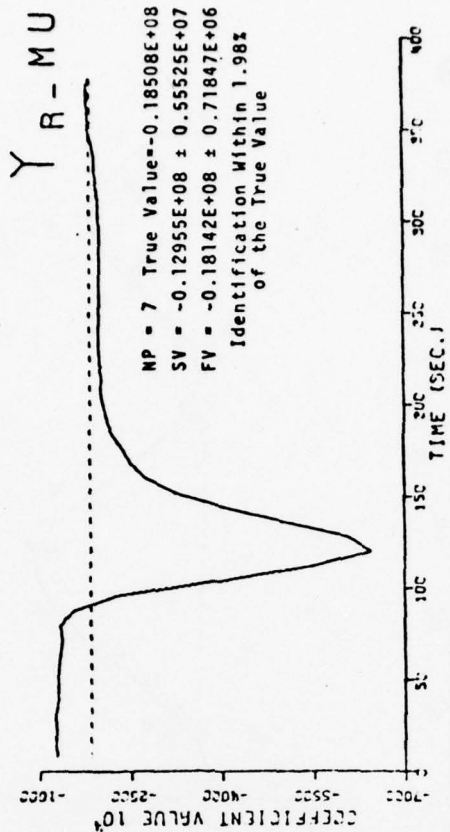
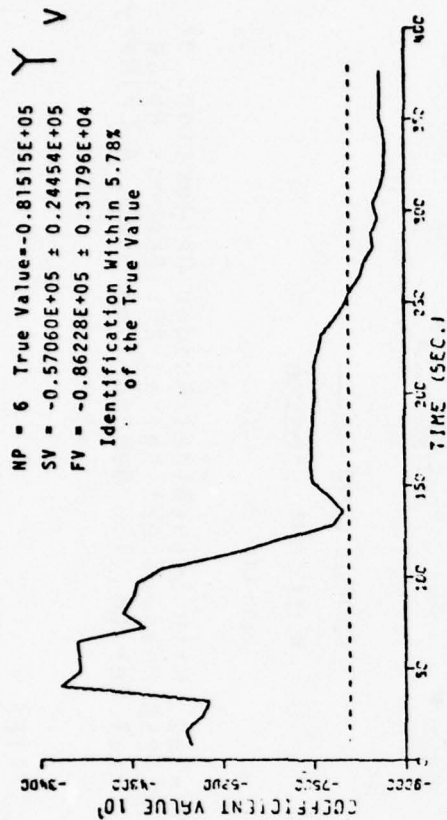
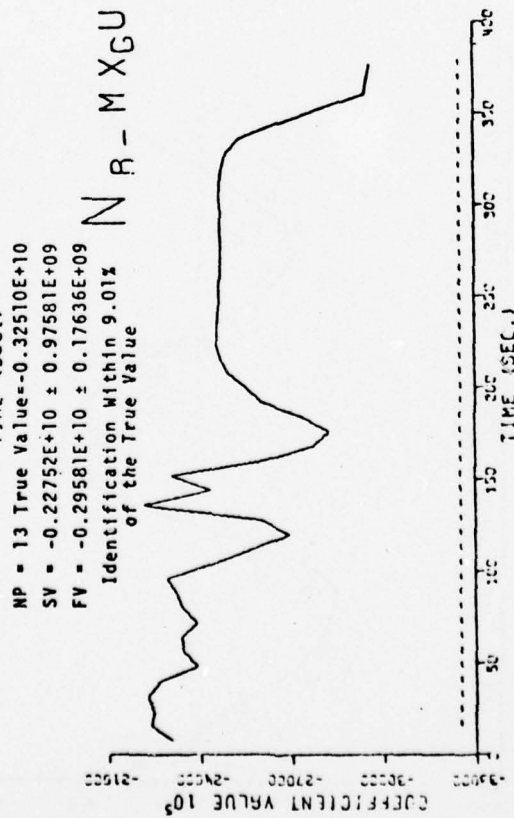
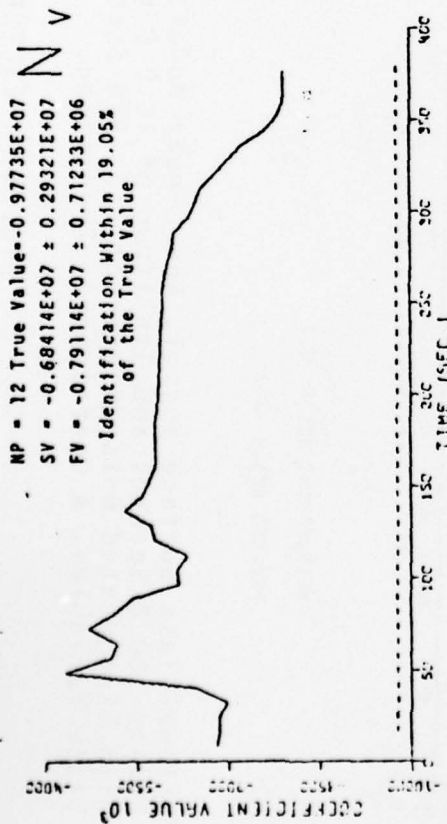


FILTERED STATE —
 NOISY STATE ○○○○○○
 ZERO LINE - - - -

MEASUREMENT NOISE -25%
 PROCESS NOISE -25%

Mariner-Class Surface Vessel, Non-Linear Model, Zig-Zag, With Sinusoidal Rudder Deflections of Period 200.0 Seconds and Amplitude of 10.0 Degrees, 25% Measurement Noise, 25% Process Noise With Exaggerated Noise Factor of 1.0, 376 Second Trial Period, 1.0 Second Time Step, 4 Primary State Variables, 4 Coefficients Identified.

Fig. 24 FILTERED STATES



IDENTIFICATION —
 TRUE VALUE - - -

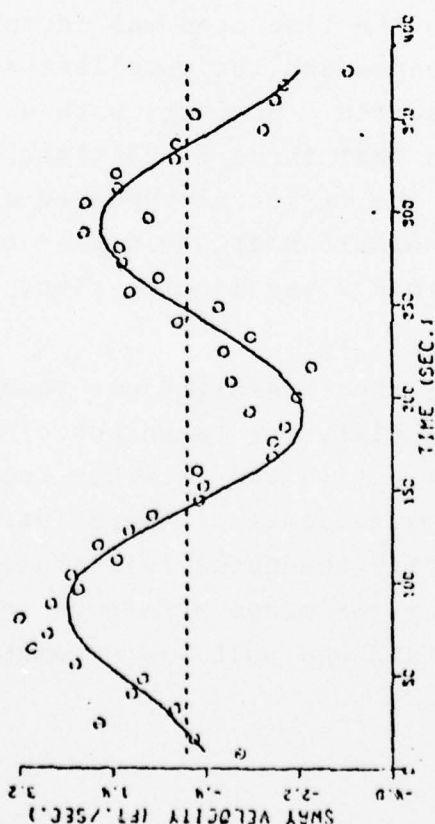
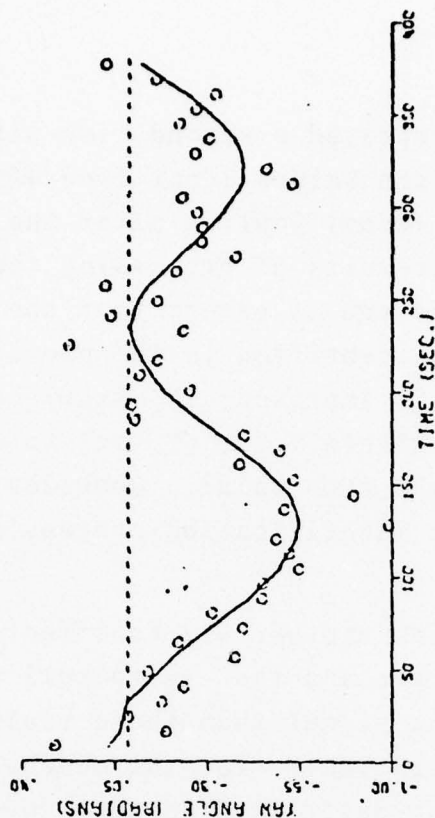
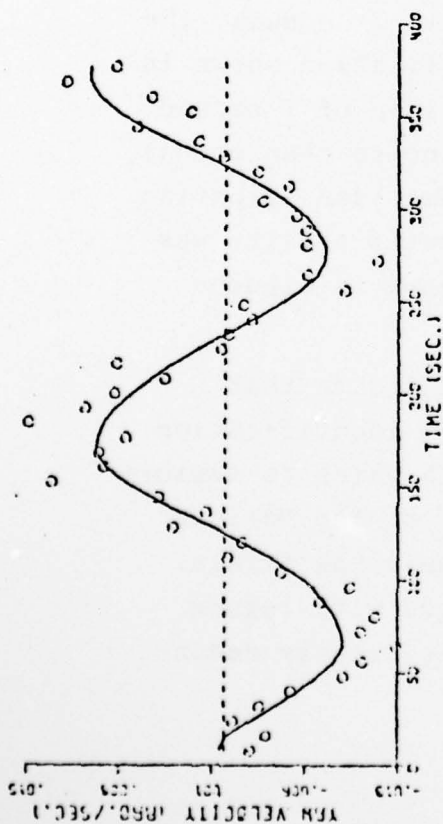
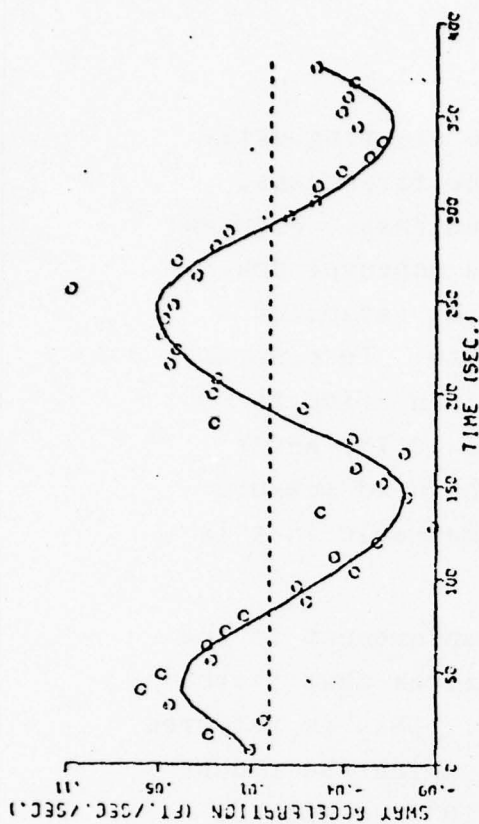
MEASUREMENT NOISE -25%
 PROCESS NOISE -25%

Fig. 25 Coefficient Identification - 10 Degree Rudder Deflection, 25% Noise

if the process is repeated a second time with the starting estimates set equal to the values identified after the first pass, one expects better identification after the second pass. Figures 26 and 27 show the results of processing the same maneuver described in Figures 24 and 25 except that the initial estimated values are those as identified in the previous case. In general, the identification is improved, $(N_r - mx_G u)$ being identified to within 6.4%, N_v to within 7.7%, $(Y_r - \mu)$ to within 10.7%, and Y_v to within 5.4% of the true value. Considering the wild measurement data used, the identification process is remarkable in this case.

There is perhaps another way to effect an improvement in the identification process and that is to tell the filter that there is more noise in the signal than there really is. This is referred to as "noise exaggeration." For the maneuver in which the rudder is oscillated sinusoidally with an amplitude of 10° and with 5% noise), no identification was obtained because the filter became unstable. Yet when the time step was increased to 2 seconds, the instability disappeared and the excellent identification shown in Figures 6 and 7 resulted. However, with a time step of 1 second and the filter told that there is 25 times more noise than actual, the instability in the filter disappeared and some identification was obtained, but nowhere near the degree of identifiability was obtained in going to a 2-second time step, as shown in Figures 28 and 29.

The results of the investigations to date indicate that the extended Kalman filtering technique of system identification is a potentially effective and flexible tool with which to measure the hydrodynamic coefficients of ships (at least of the Mariner type) through properly conducted full scale maneuvering trials. Its superiority over the model reference technique with regard to handling noisy data and multiple parameters is clearly demonstrated.

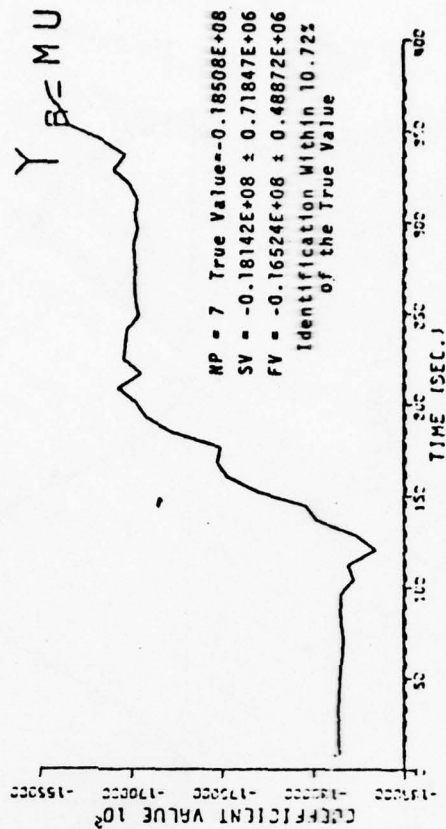
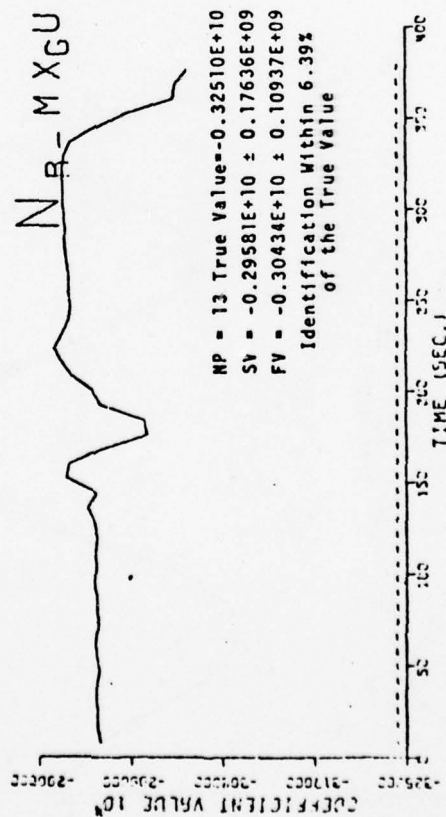
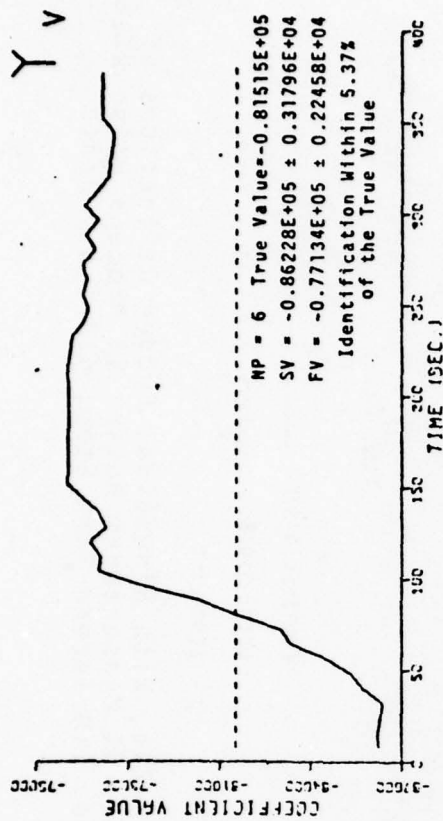
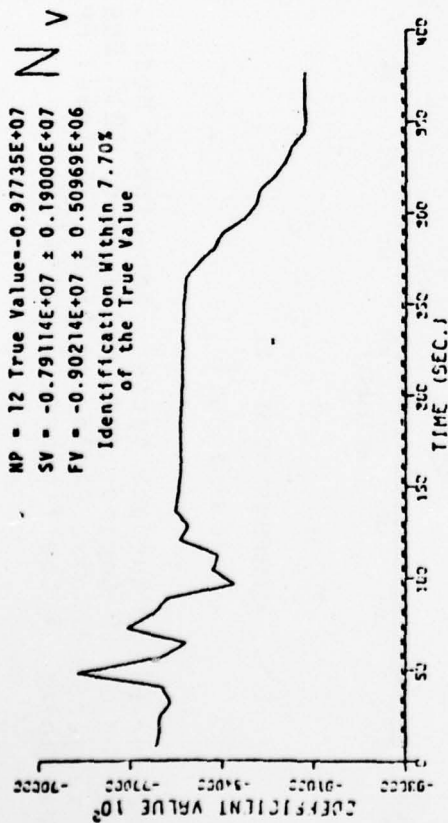


FILTERED STATE —
 NOISY STATE ○○○○○○
 ZERO LINE - - - -

MEASUREMENT NOISE -25%
 PROCESS NOISE -25%

Mariner-Class Surface Vessel, Non-Linear Model, Zig-Zag, With Sinusoidal Rudder Deflections of Period 200.0 Seconds and Amplitude of 10.0 Degrees, 25% Measurement Noise, 25% Process Noise With Exaggerated Noise Factor of 1.0, 376 Trial Period, 1.0 Second Time Step, 4 Primary State Variables 4 Coefficients Identified.

Fig. 26 FILTERED STATES



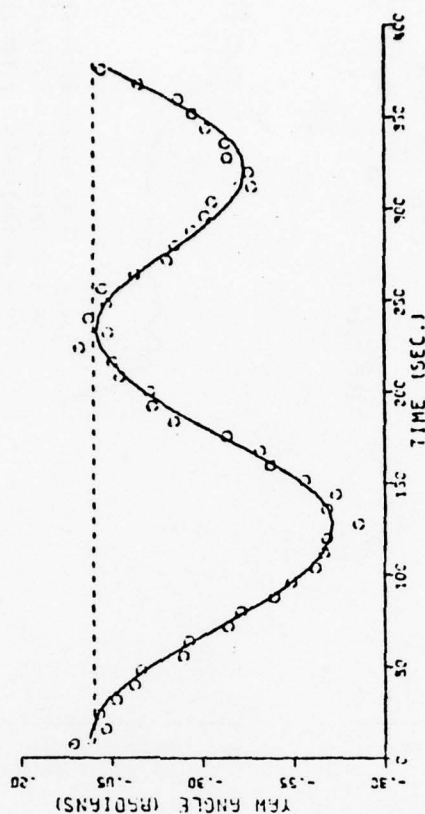
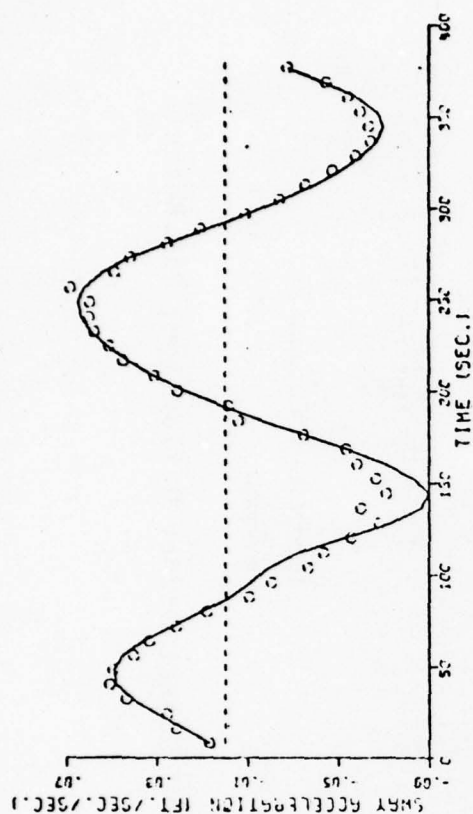
MEASUREMENT NOISE -25%

PROCESS NOISE -25%

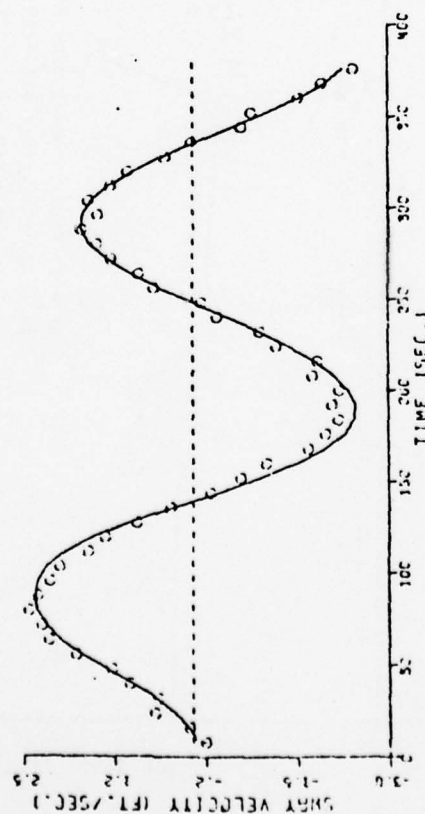
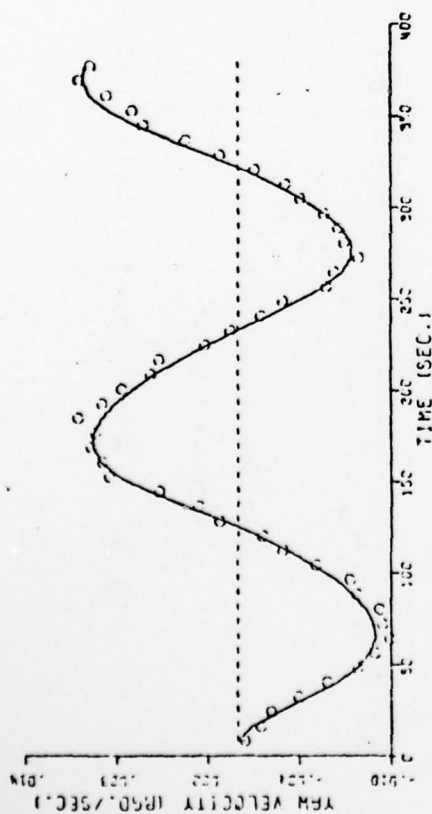
IDENTIFICATION —

TRUE VALUE ----

Fig. 27 Coefficient Identification - 10 Degree Rudder Deflection, 25% Noise



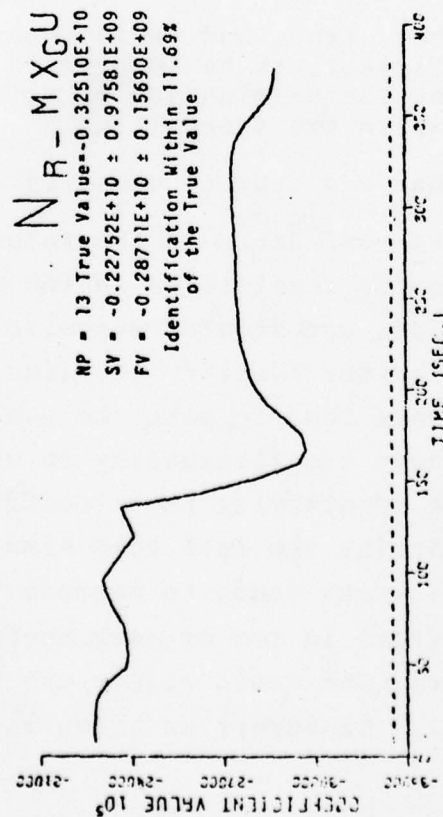
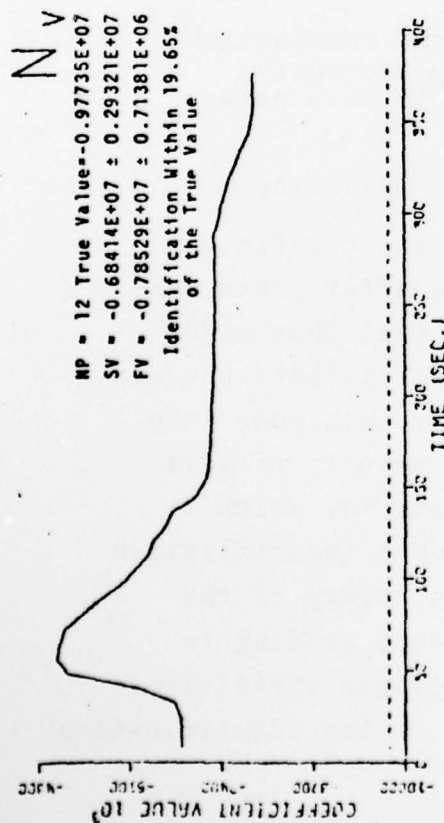
FILTERED STATE —
 NOISE STATE ○○○○○○
 ZERO LINE - - - -



MEASUREMENT NOISE - 5%
 PROCESS NOISE - 5%

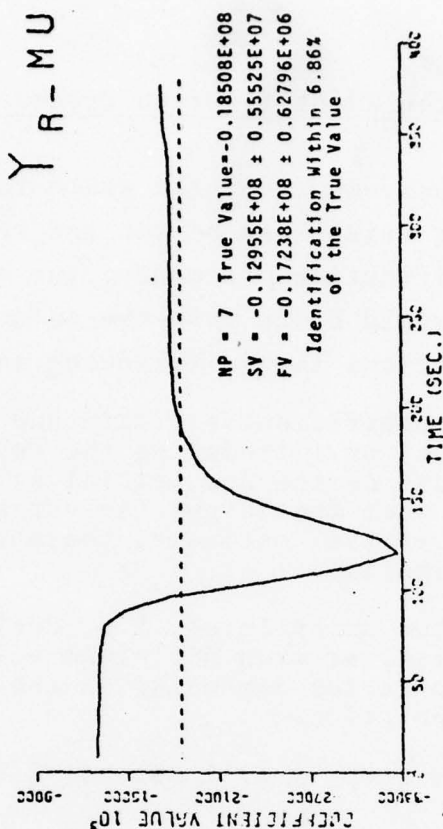
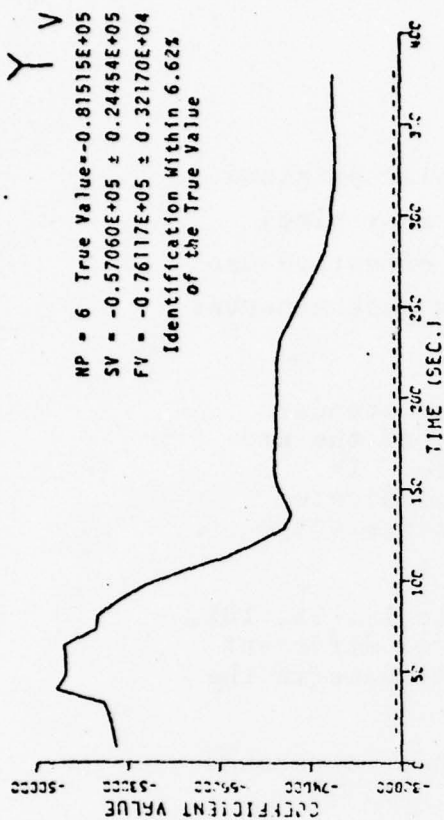
Mariner-Class Surface Vessel, Non-Linear Model, Zig-Zag, With Sinusoidal Rudder Deflections of Period 200.0 Seconds and Amplitude of 10.0 Degrees, 5% Measurement Noise, 5% Process Noise With Exaggerated Noise Factor of 25.0, 376 Trial Period, 1.0 Second Time Step, 4 Primary State Variables, 4 Coefficients Identified.

Fig. 28 FILTERED STATES



MEASUREMENT NOISE - 5%

PROCESS NOISE - 5%



IDENTIFICATION

TRUE VALUE

Fig. 29 Coefficient Identification - 10 Degree Rudder Deflection, 5% Noise

Effective Use of the Identification Process

Since the measurements of the state variables obtained during maneuvering trials can be run and rerun many times through the identification procedure, the most effective use of the technique would be to pass the data from each maneuver through with variations in the following items.

- (1) Initial coefficient estimate and their standard deviation, or introducing the results of the previous pass as the new initial estimate. It appears that the larger the variance indicated for the initial estimate, the more accurate the identification.
- (2) Designated noise level, i.e. designate 1%, 5%, 10%, etc. noise, or even different noise for different state variables depending on the confidence in the instrumentation.
- (3) The time step, i.e. 1 second, 2 seconds, 4 seconds, etc.
- (4) The length of record.
- (5) The number, type, and variations in the combination of coefficients to be identified simultaneously, including the elimination or setting to zero parameters which are insensitive.
- (6) The number and type of measured state variables.

One would have confidence in the value of the coefficient if there is reasonable consistence in the value after these many passes. In addition, one should recognize the fact that mild maneuvers tend to better identify the linear coefficients whereas the more violent ones tend to make the nonlinear ones come into play. Hence, we have the flexibility in using results of sets of maneuvers, each identifying those coefficients for which it is best suited. Noting the fact that simultaneous identification of too many coefficients tends to degrade the accuracy of the identification (errors in two or more coefficients tending to cancel one another), one would wisely use the linear coefficients identified from mild maneuvers as known values in the identification

SYSTEMS CONTROL INC PALO ALTO CALIF F/G 15/7
PROCEEDINGS OF THE SYMPOSIUM ON CONTROL THEORY AND NAVY APPLICA--ETC(U)
AUG 77 M D CILETTI, J S TYLER N00014-72-C-0327

N00014-72-C-0327

NL

5 of 8
ADA045603

100%

of the nonlinear coefficients from the more violent maneuvers. One even has the flexibility of trying the model reference technique, if necessary and advantageous, for the identification of a few coefficients which may not be identified by the extended Kalman filter process. The ability to specify many meaningful maneuvers combined with the ability to make as many passes of the measurement data as desired (along with a variety of processing conditions) provides a powerful procedure with which one may reasonably expect to identify the hydrodynamic coefficients from full scale maneuvering trials.

The Design of Maneuvering Trials

Ship trials are actually experiments carried out at full scale, just as scaled model tests are laboratory experiments. A major part of the experiment is the planning of the experiment so that conclusive results are obtained from the data to be observed. This means that maneuvers should be selected and certain state measurements obtained which will produce, in combination and after a proper and available data reduction technique, the values of the coefficients for that ship. One should predict the possible success of the trials before proceeding because effort, time, and money will be wasted on trials which have little probability of success. The combined computer programs of generating simulated noisy data and parametric identifying by the extended Kalman filter technique provide just the proper tools for planning or designing maneuvering trials. Many types of maneuvers of different "violence" could be simulated and the measured state variables processed through the identification procedure using all the different processing tricks (such as different noise level, different first estimates, etc.). Those maneuvers which in combination indicate a good identifiability of the important linear and nonlinear coefficients should be scheduled for the trials. One has to be realistic at this

stage and simulate only those maneuvers which can be reasonably performed by the ship and use only those measured state variables which can readily be measured by available instrumentation. By this process of planning, one knows ahead of time with some confidence that with the particular maneuvers specified and with the measurement of certain state variables that the trials will furnish acceptable estimates of the coefficients. He knows exactly what instruments he needs, what maneuvers to specify, and how that data can be most effectively analyzed (including which maneuvers will most effectively identify which coefficients). This approach is quite different from the usual approach wherein data is taken during some standard trial and then great efforts are exerted to try to make sense of the data by methods which are not necessarily effective in handling that type of data.

Present Investigations and Future Research

Under a research program sponsored by the Maritime Administration, we are presently "designing" maneuvering trials for a typical large tanker (VLCC) to determine the feasibility of "measuring" through maneuvering trials the significant linear and nonlinear coefficients of a simulation mathematical model. Since these supertankers are dynamically unstable (i.e. unable to maintain straight line motion without rudder control), the nonlinear coefficients are very important in the ship dynamics even for very mild maneuvers of the rudder. In fact, because of the dynamic instability, the ship will go into a steady turn with no deflection of the rudder. As was the procedure in the case of the Mariner ship, a mathematical model including the significant coefficients will be formulated. A great many realistic maneuvers, both mild and violent, will be simulated with this model, producing noisy measurement data for those state variables which can be actually measured on the ship. Various levels of noise will be used and all the variety of

techniques of processing the data, as discussed previously, will be used. The case with the VLCC ship is more difficult than that of the Mariner in that it will be necessary to identify the linear coefficients from mild maneuvers wherein the nonlinear forces are significant in order to reserve the more violent maneuvers for identifying the nonlinear coefficients. It is hoped to conduct free-running physical model tests, the data from which will be used to see if the coefficients of the model can be determined by the identification technique.

Work will continue with the Mariner ship with attempts to identify the nonlinear coefficients in a manner similar to the identification of the linear coefficients discussed in this paper.

The computer program developed can be used to identify the coefficients associated with any system that can be described by a mathematical model form similar to the one used here, such as perhaps a turbine, reduction, shaft, and propeller system if appropriate measurements can be made on parts of the system.

It is planned to expand the math model to include coupled roll, i.e. include the state variables of roll angle ϕ , roll rate $\dot{\phi}$, and roll acceleration $\ddot{\phi}$, in their linear and nonlinear form. One can envision a full scale trial in which the rudder is oscillated in the natural frequency of roll and from this type of maneuver the linear and nonlinear roll damping coefficients determined.

The technique and programs can be used to make sense out of and reduce noisy data obtained from laboratory experiments, such as constrained and unconstrained model testing in a towing tank.

In conclusion, a "tool" has been developed and now exists with which the Navy can effectively design and carry out maneuvering trials and thereby provide valuable information to be used in the design of ships and their control systems.

APPENDIX I

EQUATIONS OF MOTION

When the equations of motion are restricted to motion in the horizontal plane without roll in unrestricted water, the hydrodynamic forces on the vehicle can be expressed as functions of the pertinent motion variables as

$$X = X(u, v, r, \dot{u}, \dot{v}, \dot{r}, \delta)$$

$$Y = Y(u, v, r, \dot{u}, \dot{v}, \dot{r}, \delta)$$

$$N = N(u, v, r, \dot{u}, \dot{v}, \dot{r}, \delta)$$

where

X is the longitudinal force

Y is the transverse (lateral) force

N is the yaw moment

and all are referred to an axis system fixed in the ship and an origin not necessarily located at the center of gravity (in order to take advantage of geometric symmetries).

u, v, and r are the longitudinal, transverse,
and yaw (angular) velocities referred
to the chosen origin

Δu is the increment in u from the steady state straight
ahead velocity u_0

\dot{u} , \dot{v} , and \dot{r} are the derivatives with respect to time of the
above quantities

δ is the rudder deflection

When X, Y, and N are expanded in a Taylor series in terms of the motion variables with terms beyond the third order being dropped as well as those terms which are zero by symmetry considerations, and only linear acceleration terms maintained

(u, v, r), the following equations result.

$$\begin{aligned}
 X = & X_o + X_u(\Delta u) + X_{\dot{u}}\dot{u} + \frac{1}{2} [X_{uu}(\Delta u)^2 + X_{vv}v^2 + X_{rr}r^2 \\
 & + X_{\delta\delta}\delta^2] + X_{vr}vr + X_{r\delta}r\delta + X_{v\delta}v\delta + \frac{1}{6} X_{uuu}(\Delta u)^3 \\
 & + \frac{1}{2} [X_{vvu}v^2(\Delta u) + X_{rru}r^2(\Delta u) + X_{\delta\delta u}\delta^2(\Delta u)] \\
 & + X_{vru}vr(\Delta u) + X_{v\delta u}v\delta(\Delta u) + Y_{r\delta u}r\delta(\Delta u)
 \end{aligned} \tag{1}$$

$$\begin{aligned}
 Y = & Y_o + Y_vv + Y_{\delta}\delta + Y_{vu}v(\Delta u) + Y_r r + Y_{ru}r(\Delta u) + Y_{\delta u}\delta(\Delta u) \\
 & + \frac{1}{6} [Y_{vvv}v^3 + Y_{rrr}r^3 + Y_{\delta\delta\delta}\delta^3] + \frac{1}{2} [Y_{vrr}vr^2 \\
 & + Y_{v\delta\delta}v\delta^2 + Y_{vuuv}v(\Delta u)^2 + Y_{rvv}rv^2 + Y_{r\delta\delta}r\delta^2 \\
 & + Y_{ruu}r(\Delta u)^2 + Y_{\delta vv}\delta v^2 + Y_{\delta rr}\delta r^2 + Y_{\delta uu}\delta(\Delta u)^2] \\
 & + Y_{vr\delta}vr\delta + Y_{\dot{v}}\dot{v} + Y_{\dot{r}}\dot{r}
 \end{aligned} \tag{2}$$

$$\begin{aligned}
N = & N_o + N_v v + N_r r + N_\delta \delta + N_{vu} v(\Delta u) + N_{ru}(\Delta u) \\
& + N_{\delta u} \delta(\Delta u) + \frac{1}{6} [N_{vvv} v^3 + N_{rrr} r^3 + N_{\delta\delta\delta} \delta^3] \\
& + \frac{1}{2} [N_{vrr} v r^2 + N_{v\delta\delta} v \delta^2 + N_{vu} v(\Delta u)^2 + N_{rvv} r v^2 \\
& + N_{r\delta\delta} r \delta^2 + N_{ruu} r(\Delta u)^2 + N_{\delta vv} \delta v^2 + N_{\delta rr} \delta r^2 \\
& + N_{\delta uu} \delta(\Delta u)^2] + N_{vr\delta} v r \delta + N_v \dot{v} + N_r \dot{r}
\end{aligned} \tag{3}$$

where

Y_o and N_o are the initial values of transverse force and yaw moment in straight ahead motion due to asymmetrical propeller effects (single screw with a preferred direction of rotation)

and

$Y_{\text{subscript}}$ and $N_{\text{subscript}}$ are the partial derivatives of the Y and N functions, respectively, with respect to the subscript, taken at the equilibrium condition of straight ahead motion, i.e.

$$N_v = \left(\frac{\partial N}{\partial v} \right)$$

$$N_{\delta vv} = \left(\frac{\partial^3 Y}{\partial \delta \partial^2 v} \right)$$

If the reasonable assumption, based on theoretical and experimental hydrodynamics, is made that the forces due to acceleration are essentially linear (negligible nonlinear effects in \dot{u} , \dot{v} , and \dot{r}) then the solutions for \dot{u} , \dot{v} , and \dot{r} are given as

$$\dot{u} = f_1 / (m - X_u \dot{u}) \quad (4)$$

$$\dot{v} = \frac{(I_z - N_r \dot{r}) f_2 - (m x_G - Y_r \dot{r}) f_3}{f_4} \quad (5)$$

$$\dot{r} = \frac{(m - Y_v \dot{v}) f_3 - (m x_G - N_v \dot{v}) f_2}{f_4} \quad (6)$$

where

$$f_1 = X \text{ in Eq. (1) } - X_u \dot{u}$$

$$f_2 = Y \text{ in Eq. (2) } - Y_v \dot{v} - Y_r \dot{r}$$

$$f_3 = N \text{ in Eq. (3) } - N_v \dot{v} - N_r \dot{r}$$

$$f_4 = (m - Y_v \dot{v})(I_z - N_r \dot{r}) - (m x_G - N_v \dot{v})(m x_G - Y_r \dot{r})$$

m = mass of vehicle

I_z = moment of inertia of vehicle in yaw about the origin

x_G = the distance of the center of gravity forward of the origin

REFERENCES

1. "Stability and Motion Control of Ocean Vehicles," Martin A. Abkowitz, The MIT Press, Second Printing, 1972.
2. "Parametric Identification of Nonlinear Stochastic Systems Applied to Ocean Vehicle Dynamics," Michael N. Hayes, Sc.D. Thesis, Dept. of Ocean Engineering, MIT, August 1971.
3. "System Identification Applied to Maneuvering Trials," Hernani L. Brinati, O.E. and S.M. Thesis, Dept. of Ocean Engineering, MIT, June 1973.
4. "Application of the Extended Kalman Filtering Technique to Ship Maneuvering Analysis," John G. Lundblad, O.E. and S.M. Thesis, Dept. of Ocean Engineering, MIT, December 1974.

IDENTIFICATION OF MULTIVARIABLE GAS TURBINE DYNAMICS FROM STOCHASTIC INPUT-OUTPUT DATA*

Gerald J. Michael and Florence A. Farrar
United Technologies Research Center
East Hartford, Connecticut 06108

SUMMARY

An algorithm has been developed for the identification of multivariable gas turbine dynamics from stochastic input-output data. The algorithm is based on modern state estimation theory and has been employed to identify the parameters of a linear time-invariant F100/F401 turbofan computer model. Unknown parameters of the F100/F401 model were introduced as auxiliary state variables, thereby transforming the parameter identification problem to a nonlinear state estimation problem. The engine model was forced by commanded changes in main burner fuel flow and jet exhaust. Gaussian noise was added to the commanded fuel flow to model metering valve uncertainties. Noise-corrupted measurements consisted of fan turbine inlet temperature, fan and compressor speeds, and main burner and afterburner pressures. The identification procedure was carried out at three steady-state design points between idle and military thrust conditions. The algorithm is generally applicable to identification of multivariable systems for which noise-corrupted input-output data are available.

The results indicate that the identified turbofan stability and control derivatives represent a satisfactory engine description for purposes of nonlinear multivariable feedback control design using the piecewise-linear/piecewise-optimal approach. This approach was previously developed by United Technologies Research Center under contract to the Office of Naval Research.

*This research was sponsored by the Office of Naval Research under Contract N00014-73-C-0281, Contract Authorization NR 215-219. This paper summarizes results presented in more detail in: Michael, G. J. and F. A. Farrar, "Identification of Multivariable Gas Turbine Dynamics from Stochastic Input-Output Data." United Technologies Research Center Report R941620-3, Annual Technical Report, March 1975 (DDC Accession No. AD A006277).

RESULTS AND CONCLUSIONS

1. An algorithm was defined to identify linearized F100/F401 turbofan engine model dynamics from simulated stochastic input-output data. The two-step algorithm consisted of a matrix least-squares-fit technique followed by a nonlinear dynamic filter. The matrix least-squares fit was used to generate appropriate initial conditions for the nonlinear filter which, in turn, provided simultaneous estimates of engine state variables as well as the constant parameters which describe linearized engine dynamics. This identification procedure was evaluated at three steady-state design points between idle and military conditions by comparing identified and actual engine model time responses to perturbations in jet exhaust area and main burner fuel flow. Results indicate that linearized engine dynamics identified with this two-step algorithm provide an engine description satisfactory for nonlinear multivariable control design using the piecewise-linear/piecewise-optimal approach.
2. The matrix least-squares-fit identification technique used alone was adequate for extracting engine dynamics from data with little or no noise. For realistic noise levels, however, the matrix least-squares approach generated an engine description whose time response differed significantly from that of the actual engine model. Nevertheless, even with large noise levels, the matrix least-squares-fit approach provided parameter estimates adequate for initializing the mathematically more sophisticated nonlinear dynamic filtering algorithm.
3. Adequacy of the identified engine model for accurately defining engine time response depends on the signal-to-noise ratios of the perturbed engine state variable measurements. As these signal-to-noise ratios are decreased the identified engine description is degraded. This degradation results from the increasingly inaccurate initial parameter estimates provided to the nonlinear dynamic filter by the matrix least-squares algorithm under high-noise conditions. In these situations, reprocessing of the input-output data -- i.e., processing it through the nonlinear filter more than once -- significantly enhances the adequacy of the identified engine model. Identified engine models generated by reprocessing high-noise input-output data possessed time response characteristics which compared very favorably with those of the actual engine model.

INTRODUCTION

This research was motivated by the need to define an analytical method for identifying linearized jet engine dynamics directly from noise-corrupted engine data. Engine dynamics must be known to apply both conventional control design techniques and the piecewise-linear/piecewise-optimal approach to control synthesis developed by UTRC under a previous ONR contract (Ref. 1). It has been shown that controllers designed using this optimal technique can produce significant improvements in controlled system dynamic response. For example, application of the piecewise-linear/piecewise-optimal control synthesis technique to an F100/F401 turbofan engine simulation resulted in F100/F401 thrust response which was significantly more rapid than that for a conventional "fast acceleration" mode of control (Ref. 2). Identification of linearized engine dynamics from stochastic input-output data is the key to applying the developed control optimization method to a real rather than a simulated engine. In addition, on-line computation of engine dynamics provides the data necessary to develop and implement a self-adaptive control algorithm which optimizes propulsion system performance in flight.

Modern estimation theory provides the mathematical means for extracting unknown system parameters from stochastic input-output data. The objective of this study was to evaluate the effectiveness of a two-step algorithm, developed within the framework of optimal estimation theory, in identifying linearized jet engine dynamics for multivariable feedback control design. The two-step algorithm was to consist of a matrix least-squares fit for providing initial conditions for a nonlinear dynamic filter which would then generate the identified engine model. The approach was to use noise-corrupted input-output data generated at three F100/F401 turbofan engine steady-state design points using known linearized engine stability and control derivatives. This identification procedure was to be implemented at each of these three design points. Time responses of identified and actual engine models would then be quantitatively compared, using previously developed UTRC error indices (Ref. 1), to evaluate the adequacy of the identified engine models.

METHOD FOR IDENTIFICATION OF ENGINE DYNAMICS

An identification algorithm based on modern state estimation theory is presented in this section. The objective was to identify multivariable gas turbine engine dynamics directly from stochastic input-output data. Engine input, state, and output variables are introduced initially and the linearized engine model representation is described. Introduction of unknown engine parameters as auxiliary state variables, thereby transforming the parameter identification problem to a nonlinear state estimation problem, is then discussed.

Multivariable Engine Dynamics

Linearized F100/F401 turbofan engine dynamics were used to generate stochastic input-output data for this study. A known engine model was employed so that comparisons between it and the identified model could be made on the basis of time response characteristics as well as parameter accuracy. The engine control variables chosen were:

- jet exhaust area
- main burner fuel flow.

The engine states considered were:

- fan turbine inlet temperature
- main burner pressure
- fan speed
- high compressor speed
- afterburner pressure.

Output variables were selected to be the five engine states.

Linearized engine dynamics at a given steady-state operating point can be represented by

$$\dot{x} = Ax + Bu$$

$$u = u_c + \xi \quad (1)$$

$$z = x + \eta$$

where the vector x represents perturbations in the five engine state variables, the vector z represents measurements of the perturbations in the five engine state variables, the vector u represents perturbations in the two control variables, and the vector u_c represents commanded perturbations in the two control variables. The vectors ξ and η model uncertainties in the two control variables and five state variable measurements, respectively. The dot notation denotes differentiation with respect to time. The constant A and B matrices define engine perturbational dynamics about the given steady-state operating point. These matrices consist of appropriate engine partial derivatives evaluated at the specified operating point. Reference 2 contains a listing of F100/F401 A and B matrices for five design points ranging from idle to military conditions. Note that for five state and two control variables, A and B become 5×5 and 5×2 matrices, respectively.

Algorithm for Estimation of F100/F401 Engine Dynamics

An algorithm was developed to identify elements of the A and B matrices of Eq. (1). These elements describe engine time response in a small region about the given steady-state operating point. No unique or universally accepted procedure for system identification exists today. A survey of many system identification methods is presented in Ref. 3. For this study a nonlinear dynamic filter, initialized by a matrix least-squares-fit procedure operating directly on the noisy data, was employed to simultaneously estimate engine state variables as well as parameters of the A and B matrices. This approach has the advantage of reducing to the previously developed (Ref. 1) least-squares method when noise levels are low and all engine state variables can be measured. Under these conditions, the least-squares method is known to have excellent identification capabilities.

Parameters of the A and B matrices, assumed unknown for the purpose of system identification, were first introduced as additional states to be estimated. This leads to a nonlinear multivariable system. Nonlinear filtering theory was then employed to simultaneously estimate both engine states and the parameters of the A and B matrices. In recent years a great deal of research has been performed in the area of nonlinear state estimation (Refs. 3, 4, 5 and 6). The identification algorithm for this study was based in part on the nonlinear filter described in Ref. 5. This nonlinear filter differs from the usual extended Kalman filter in the following two respects. In the derivation of the nonlinear filter equations, second-order Taylor series terms in the expansion of the nonlinear functions which describe the system are retained. In addition, bias correction terms in the filter state estimate equations are introduced and used to partially account for the effects of neglected third- and higher-order terms. The general nonlinear system description and summary of the nonlinear filter equations are presented in Ref. 5.

DISCUSSION OF RESULTS

Application of the identification algorithm to identify F100/F401 engine dynamics is presented in this section. Generation of noise-corrupted simulated engine input-output data, noise statistics associated with realistic engine data, and determination of the initial mean of the engine parameters are set forth. The criterion employed to evaluate adequacy of the identified engine model is then described. In the final part of this section, actual and identified F100/F401 model responses are compared and discussed.

Application of the Estimation Algorithm to F100/F401 Engine Model Data

Noise-corrupted input-output data for the linear F100/F401 engine model described by Eq. (1) were generated at three power-lever angle (PLA) settings: PLA = 20, 47, and 73 deg. The 20 and 73 deg settings represent idle and military conditions, respectively, for the F100/F401 turbofan. Previous UTRC identification studies indicate good identification is achieved when step inputs are used to excite the engine. Step inputs, however, cannot be used in practice since all engine controls are rate-limited.

Jet exhaust area and main burner fuel flow were therefore ramped at their maximum slew rates (128 and 176 percent of military rating/sec, respectively) until a change equal to 10 percent of their steady-state value, at the given steady-state operating point, was reached. Jet exhaust area was ramped up first, held for 1 sec and then ramped back down to its nominal value. One-half second after jet exhaust area had returned to its nominal value, commanded main burner fuel flow was ramped up, held for 1 sec, and then ramped back down to its steady-state value. Jet exhaust area uncertainty was assumed negligible. Gaussian noise was added to commanded fuel flow and the five engine state variables to model metering valve and sensor uncertainties, respectively. Commanded control perturbations and measurements of the five perturbed states, u_c and z , respectively, were sampled every 4 msec over a 3 sec interval.

The nonlinear filter requires initial parameter estimates. Two approaches were evaluated to determine initial parameter estimates. Both approaches are based on a matrix least-squares-fit identification technique developed at UTRC. This identification technique, which was developed for deterministic or very low-noise input-output data, is described in Ref. 1.

The first approach for determining initial parameter estimates used commanded engine inputs and noise-corrupted engine state measurements directly in the least-squares-fit algorithm of Ref. 1. In the second approach, raw measurement data was first smoothed using first-order digital filters (Ref. 7). The resulting smoothed

state estimates were then used in the least-squares-fit algorithm. A more accurate description of engine dynamics was obtained from the UTRC least-squares method using smoothed-state data rather than raw measurement data. However, after the original noise-corrupted engine data were processed by the nonlinear filter, there was no significant difference between identified engine dynamics using initial parameter estimates determined from the noise-corrupted raw data and initial parameter estimates obtained from smoothed data. The first method, requiring less computation, was therefore used to determine the initial parameter estimates.

Noise-corrupted input-output data were typically processed more than once by the nonlinear filter. Final parameter estimates from the first pass through the filter were employed as initial parameter estimates for the second pass. This reprocessing can be repeated as many times as is desired to obtain an improved description of engine dynamics. The amount of improvement, however, decreases as the number of passes increases. UTRC obtained significant improvement in the time response of the identified model by reprocessing the measurement data through the nonlinear filter up to four times. More processing, however, resulted in only slight further improvements.

Criteria for Assessing Adequacy of the Identified Engine Model

Criteria for evaluating the goodness of an identified system model depend on the purposes for which the system is being identified. Two primary goals of system identification are (1) system analysis and (2) control design. When the identification intent is analysis (e.g., to improve a simulation model), accuracy of identified parameters on a parameter-by-parameter basis can be of prime importance. The parameter-by-parameter criterion is the most stringent for evaluating an identified system model. On the other hand, when identification results are to be used primarily for control design, the ability of the identified model to accurately predict time response of the actual model is a more appropriate criterion for judging adequacy of the identification (Ref. 3).

In this study comparison of identified and actual system time responses was used to assess adequacy of the identified system model as well as to evaluate the identification procedure. UTRC had previously defined (Ref. 1) normalized measures (termed error indices) of the goodness-of-fit between identified and actual engine model state variable responses. These error indices are normalized root-mean-square differences between actual and calculated engine time responses. They provide a quantitative and reliable means of assessing the ability of the identified model to predict the time response of the actual model. The Ref. 2 studies demonstrated that performance of an actual nonlinear engine model -- under a multivariable feedback control mode designed using identified linear models with low error indices -- was predictable from the identified linear model time response. In this study, then, the identified system model was considered adequate for multivariable control design when the magnitude of the error indices was equal to or less than those achieved in the Ref. 2 studies.

Comparison of Identified and Actual F100/F401 Engine Models

Linear F100/F401 engine dynamics were identified from stochastic input-output data by the least-squares-fit technique and by the nonlinear filter. Engine state variable responses -- fan turbine inlet temperature, fan and compressor speeds, main burner and afterburner pressures -- of identified and actual engine models were evaluated. The evaluation was enhanced by comparing identified and actual engine model response without process or measurement noise and by computing state variable error indices. The error index α_j represents a normalized measure of goodness-of-fit for the variable x_j . The error indices were calculated using engine model input-output data without process or measurement noise. Previous UTRC studies indicate that identified engine dynamics for which the maximum error index is as high as 0.32 are satisfactory for designing a nonlinear multi-variable controller using the piecewise-linear/piecewise-optimal approach (Refs. 1 and 2).

Maximum sensor noise standard deviations considered in this study for temperature, pressure and speed sensors were 3.0, 2.5, and 1.0 percent, respectively, of the steady-state signal values at the given design point. These standard deviations model higher uncertainties than those currently associated with state-of-the-art sensors. Standard deviation of the fuel flow driving noise was 1.6 percent of the steady-state main burner fuel flow. This standard deviation represents the uncertainty between commanded fuel flow and fuel flow actually entering the main burner. The selected fuel flow noise intensity provides that noise is passed through to fan turbine inlet temperature but not to rotor speeds. Gaussian noise statistics were employed for both measurement and driving noise processes. The smallest signal-to-noise ratios occur at PLA = 20 deg, representing data records with the highest uncertainty level. Results at PLA = 20 deg are therefore discussed first.

Noise-corrupted measurements of perturbations in fan turbine inlet temperature, fan and compressor speeds, main burner and afterburner pressures for the linear engine model at PLA = 20 deg are shown in Fig. 1. Also illustrated are the deterministic (i.e., negligible noise) jet exhaust area and noisy fuel flow control inputs which caused perturbations in the engine state variables. Initial engine model parameter estimates were determined by applying the matrix least-squares-fit identification method using the noise-corrupted measurement data (Fig. 1) and commanded perturbations in jet exhaust area and main burner fuel flow. Comparison of actual and least-squares-fit identified engine model responses for two representative state variables are shown in Fig. 2. These results demonstrate inadequacy of the least-squares-fit identification technique for high-noise situations. Recall that this technique produced excellent identification in a noise-free environment (Ref. 1).

Raw measurement data of Fig. 1 were smoothed using first-order digital filters. Smoothed values of engine states are shown in Fig. 3. The least-squares-fit identification technique was then applied using these smoothed state values. Actual and identified engine dynamic response are compared in Fig. 4. Comparison of least-squares-fit identified engine response without and with measurement data

smoothing (Figs. 2 and 4, respectively) shows the improvement in the identified engine model when measurement data are first smoothed before applying the least-squares-fit identification technique. However, the error indices of Fig. 4 indicate that engine dynamics identified from smoothed data and the least-squares-fit identification method are not satisfactory for engine control design when measurement noise levels are high.

The noise-corrupted data were then processed four times by the nonlinear filter. A schematic diagram of the identification procedure is depicted in Fig. 5. Actual and identified engine responses are compared in Fig. 6. Computed error indices for identified engine dynamics from the nonlinear filter are also shown in Fig. 6. These indices represent a reliable and quantitative measure of the adequacy of the identified model in predicting the time response of the actual model. The time histories depicted in Fig. 6, in conjunction with the computed error indices, indicate that engine descriptions adequate for multivariable control design can be extracted from noise-corrupted engine data using modern estimation theory.

Having identified an engine model adequate for predicting actual time response and for designing multivariable control, it does not necessarily follow that accurate element-by-element identification has been achieved. In practice, however, comparison of identified and actual time histories represents the only feasible criterion for judging the goodness of the identified model since, by definition, actual engine parameters are unknown and unavailable.

Improved identification -- reflected by uniformly lower error indices and due to larger signal-to-noise ratios -- was obtained at the two remaining design points (PIA = 47 and 73 deg). The larger signal-to-noise ratios result from the fact that a given input perturbation -- expressed as a percent of point -- produces a larger output perturbation at the higher power conditions of the F100/F401 turbofan model. Noise levels, expressed as a percent of point, generally increase less than the output perturbation thereby resulting in larger signal-to-noise ratios. In this respect the 20 deg power setting, for which detailed results have been presented, represents the most difficult operating condition at which to identify linearized engine dynamics.

To further illustrate the effect of noise levels on identification accuracy, Fig. 7 presents computed error indices for two levels of measurement uncertainty at PIA = 73 deg. System identification, after which the error indices were computed, took place in exactly the same manner as previously described -- a matrix least-squares-fit followed by a nonlinear filtering algorithm. Figure 7 clearly illustrates the larger error indices associated with decreased signal-to-noise ratios. For the larger noise level, Fig. 7 depicts the time responses of those engine state variables having the largest (0.148) and smallest (0.048) error indices. Note that even for the higher noise levels, the computed error indices indicate an identified engine model adequate for multivariable feedback control design.

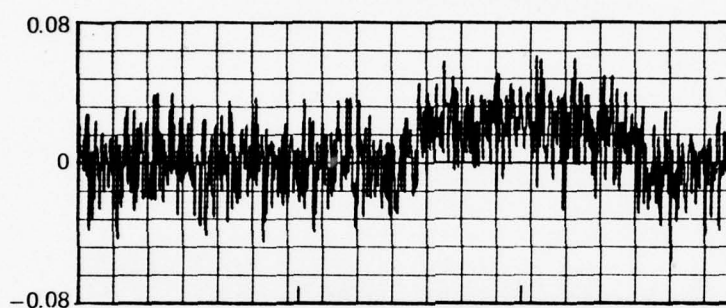
REFERENCES

1. Michael, G. J. and F. A. Farrar: An Analytical Method for the Synthesis of Nonlinear Multivariable Feedback Control. United Technologies Research Center Report M941338-2, prepared under Department of the Navy Contract N00014-72-C-0414, June 1973 (DDC Accession No. AD 762797).
2. Michael, G. J. and F. A. Farrar: Development of Optimal Control Modes for Advanced Technology Propulsion Systems. United Technologies Research Center Report N911620-2, prepared under Department of the Navy Contract N00014-73-C-0281, March 1974 (DDC Accession No. AD 775337).
3. Åström, K. J. and P. Eykhoff: System identification - A Survey. Automatica, Vol. 7, 1971, pp. 123-162.
4. Sage, A. P. and J. L. Melsa: System Identification. Academic Press, New York, 1971.
5. Athans, M., R. P. Wishner and A. Bertolini: Suboptimal State Estimation for Continuous-Time Nonlinear Systems from Discrete Noisy Measurements. IEEE Trans. Auto. Control, Vol. AC-13, Number 5, October 1968, pp. 504-514.
6. Wishner, R. P., J. A. Tabczynski and M. Athans: A Comparison of Three Non-Linear Filters. Automatica, Vol. 5, 1969, pp. 487-496.
7. Bryson, A. E., Jr., and Y. C. Ho: Applied Optimal Control. Ginn and Company, Waltham, Mass., 1969.

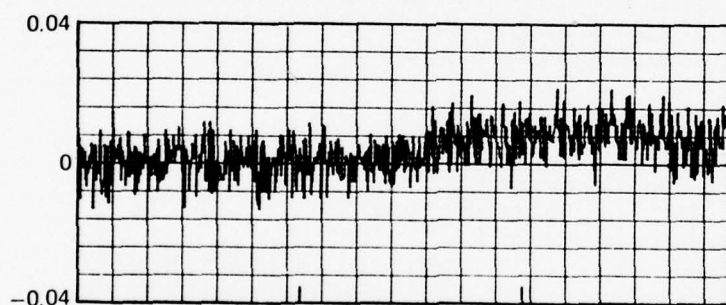
NORMALIZED F100/F401 ENGINE STATE AND CONTROL
PERTURBATIONS ABOUT PLA = 20 DEG DESIGN POINT

JET EXHAUST AREA AND FUEL FLOW PERTURBATIONS
CHOSEN AS 10 PERCENT OF OPERATING POINT — —
STATE VARIABLE PERTURBATIONS GENERATED
THROUGH LINEAR DYNAMICS

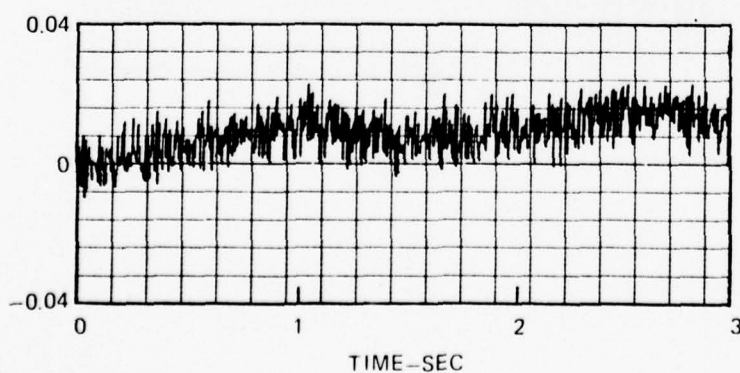
(a) MEASURED FAN TURBINE INLET TEMPERATURE



(b) MEASURED MAIN BURNER PRESSURE



(c) MEASURED FAN SPEED



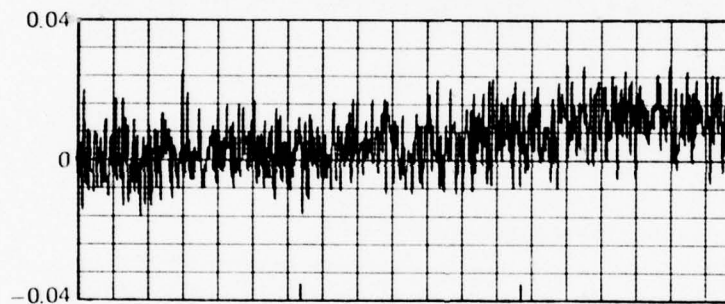
CONT'D

FIG. 1 (d)-(e)

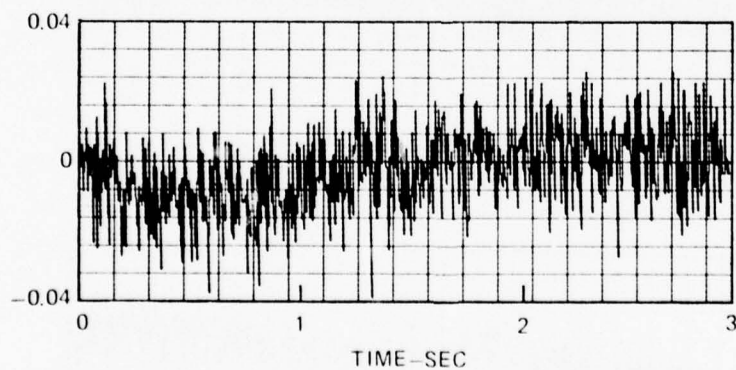
**NORMALIZED F100/F401 ENGINE STATE AND CONTROL
PERTURBATIONS ABOUT PLA = 20 DEG DESIGN POINT**

JET EXHAUST AREA AND FUEL FLOW PERTURBATIONS
CHOSEN AS 10 PERCENT OF OPERATING POINT — —
STATE VARIABLE PERTURBATIONS GENERATED
THROUGH LINEAR DYNAMICS

(d) MEASURED HIGH COMPRESSOR SPEED



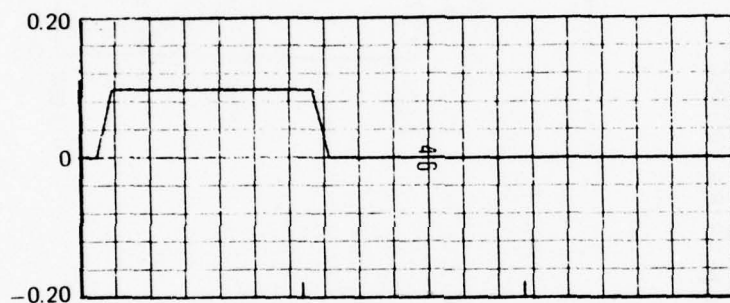
(e) MEASURED AFTERBURNER PRESSURE



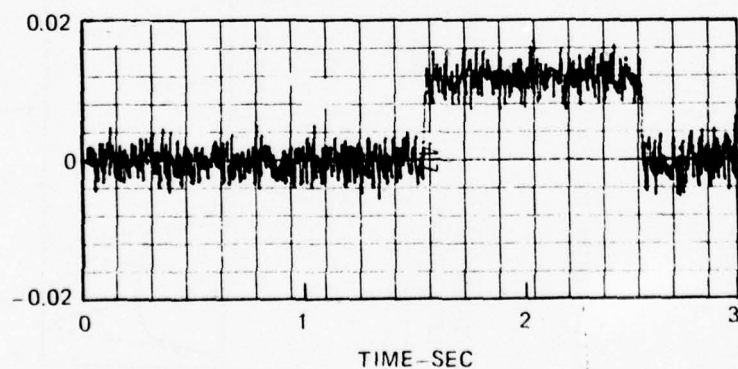
**NORMALIZED F100/F401 ENGINE STATE AND CONTROL
PERTURBATIONS ABOUT PLA = 20 DEG DESIGN POINT**

JET EXHAUST AREA AND FUEL FLOW PERTURBATIONS
CHOSEN AS 10 PERCENT OF OPERATING POINT—
STATE VARIABLE PERTURBATIONS GENERATED
THROUGH LINEAR DYNAMICS

(f) JET EXHAUST AREA



(g) MAIN BURNER FUEL FLOW

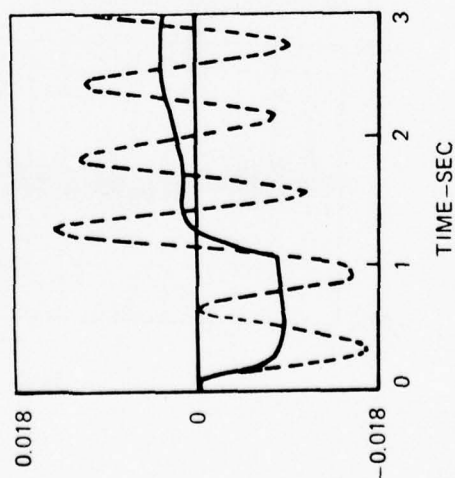


NORMALIZED RESPONSE OF ACTUAL AND IDENTIFIED F100/F401 ENGINE MODELS HAVING
LARGEST AND SMALLEST ERROR INDICES ABOUT PLA = 20 DEG DESIGN POINT

IDENTIFIED MODEL GENERATED THROUGH MATRIX LEAST-SQUARES-FIT PROCEDURE
WITHOUT NONLINEAR FILTERING

— ACTUAL RESPONSE
- - - IDENTIFIED RESPONSE

(a) PERTURBED AFTERBURNER PRESSURE
ERROR INDEX = 1.411



(b) PERTURBED FAN SPEED
ERROR INDEX = 0.829

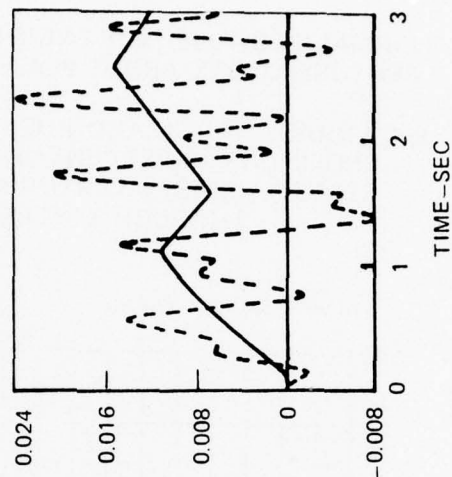
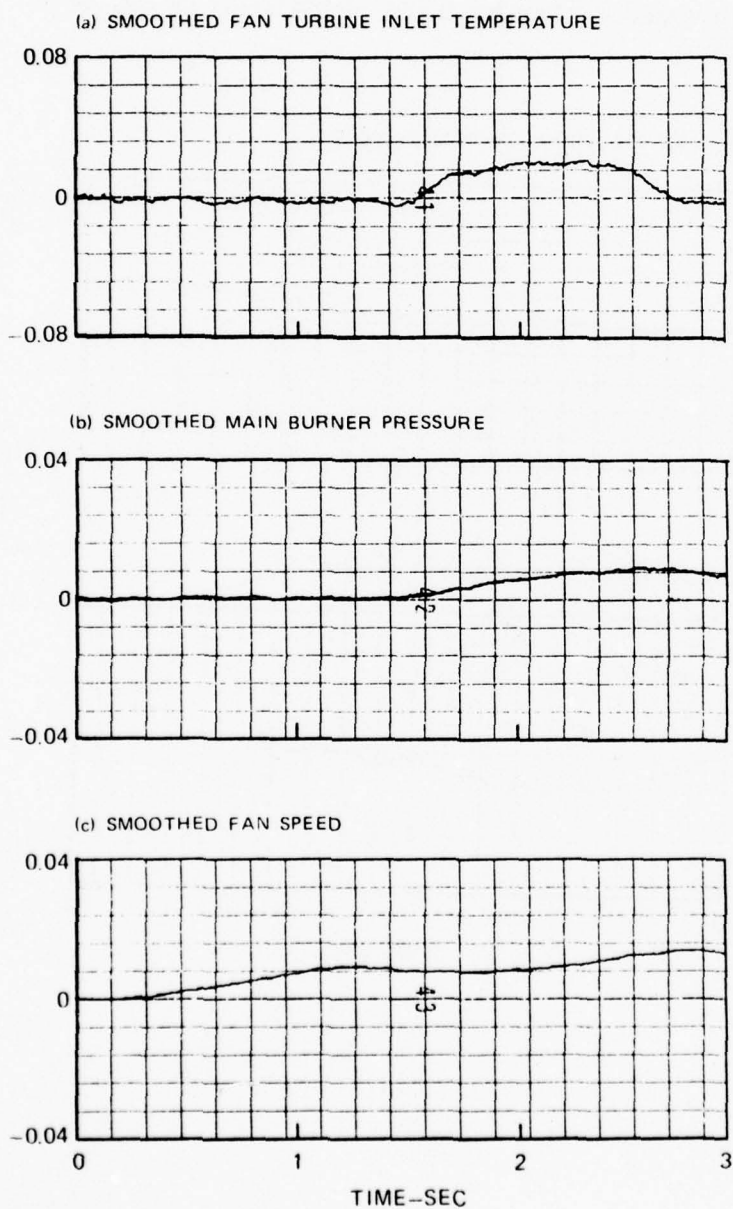


FIG. 2

FIG. 3 (a)-(c)

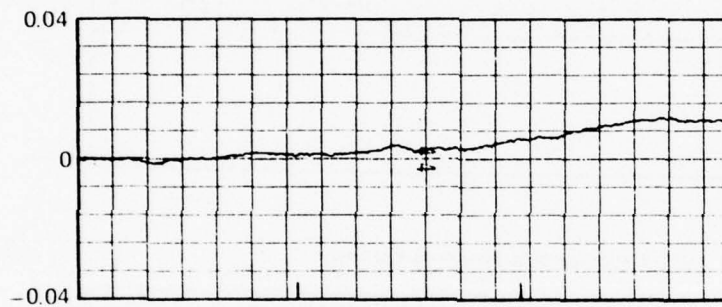
**NORMALIZED F100/F401 ENGINE MEASUREMENTS
SMOOTHED BY FIRST-ORDER DIGITAL FILTER**

RAW MEASUREMENT DATA PRESENTED IN FIG. 1

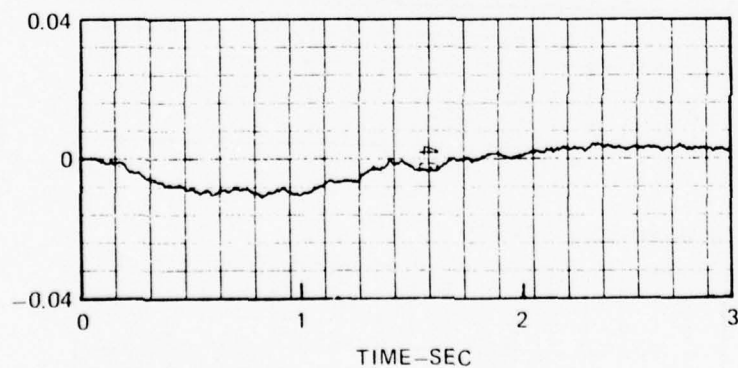


**NORMALIZED F100/F401 ENGINE MEASUREMENTS
SMOOTHED BY FIRST-ORDER DIGITAL FILTER
RAW MEASUREMENT DATA PRESENTED IN FIG. 1**

(d) SMOOTHED HIGH COMPRESSOR SPEED



(e) SMOOTHED AFTERBURNER PRESSURE



NORMALIZED RESPONSE OF ACTUAL AND IDENTIFIED ENGINE MODELS ABOUT PLA = 20 DEG DESIGN POINT

IDENTIFIED ENGINE MODEL GENERATED THROUGH MATRIX LEAST-SQUARES-FIT PROCEDURE
OPERATING ON THE SMOOTHED MEASUREMENT DATA PRESENTED IN FIG. 3

— ACTUAL RESPONSE - - - IDENTIFIED RESPONSE

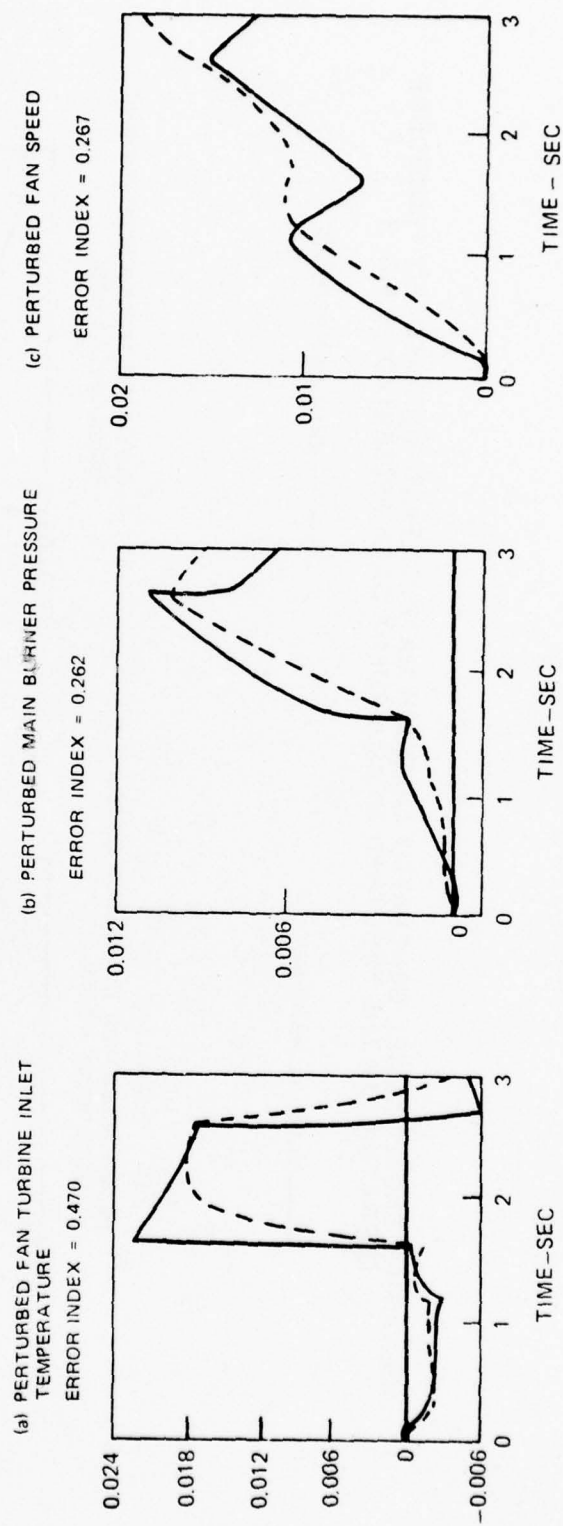


FIG. 4 (a)-(c)

NORMALIZED RESPONSE OF ACTUAL AND IDENTIFIED ENGINE MODELS ABOUT PLA = 20 DEG DESIGN POINT

IDENTIFIED ENGINE MODEL GENERATED THROUGH MATRIX LEAST-SQUARES-FIT PROCEDURE
OPERATING ON THE SMOOTHED MEASUREMENT DATA PRESENTED IN FIG. 3

— ACTUAL RESPONSE
--- IDENTIFIED RESPONSE

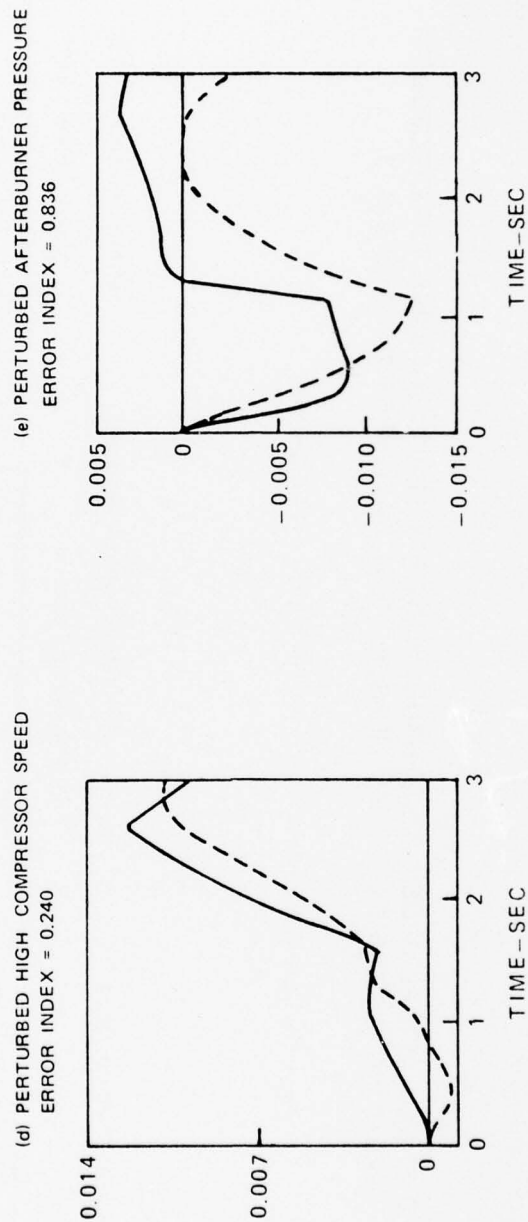


FIG. 4 (d)-(e)

SCHEMATIC DESCRIPTION OF F100/F401 ENGINE PARAMETER IDENTIFICATION PROCEDURE

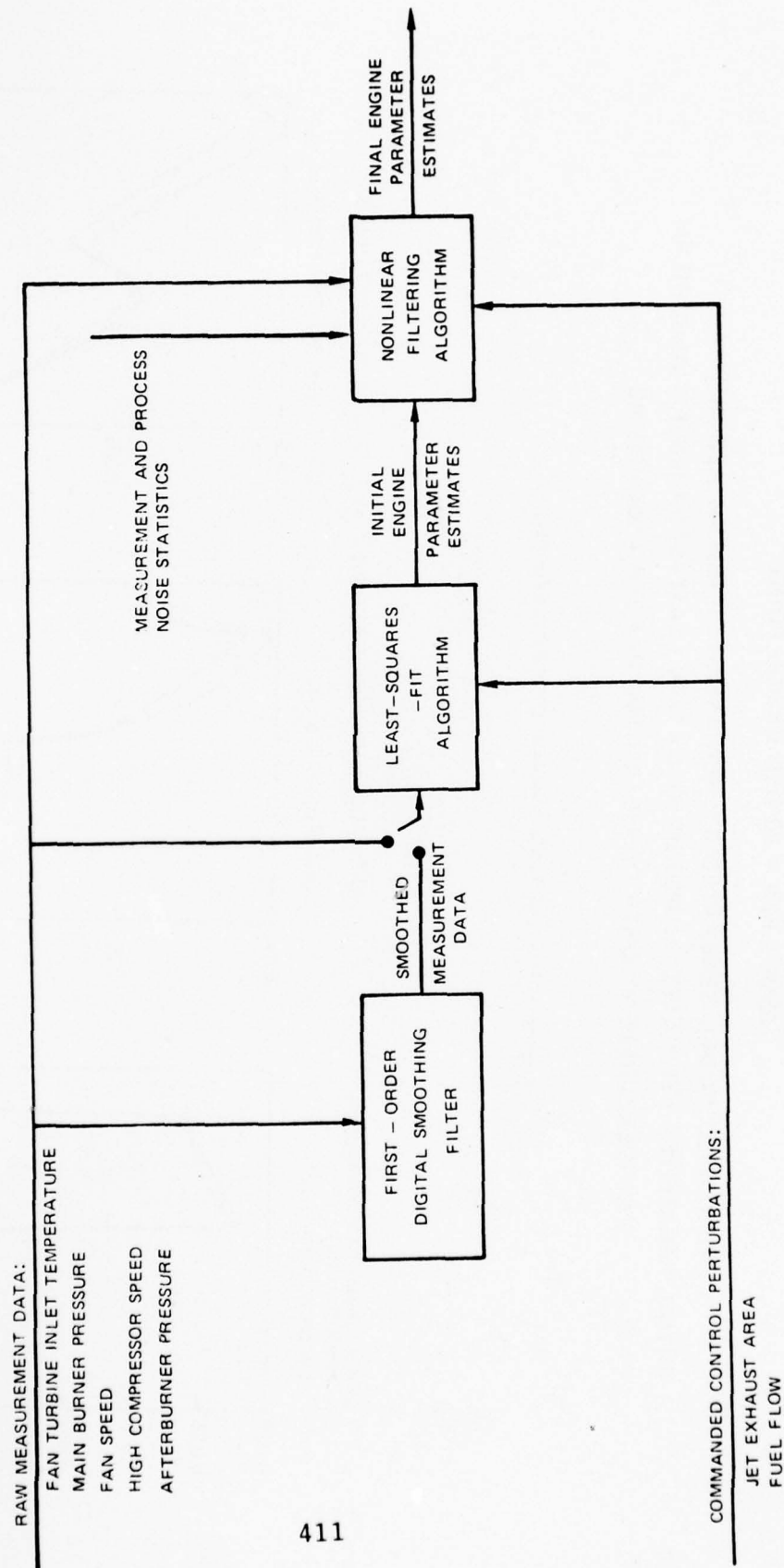


FIG. 5

NORMALIZED RESPONSE OF ACTUAL AND IDENTIFIED F100/F401 ENGINE MODELS ABOUT PLA = 20 DEG DESIGN POINT

IDENTIFIED MODEL GENERATED BY NONLINEAR FILTERING ALGORITHM
INITIAL PARAMETER ESTIMATES COMPUTED BY MATRIX LEAST-SQUARES-FIT ALGORITHM
RAW MEASUREMENT DATA OF FIG. 1 USED IN BOTH ALGORITHMS

— ACTUAL RESPONSE - - - IDENTIFIED RESPONSE

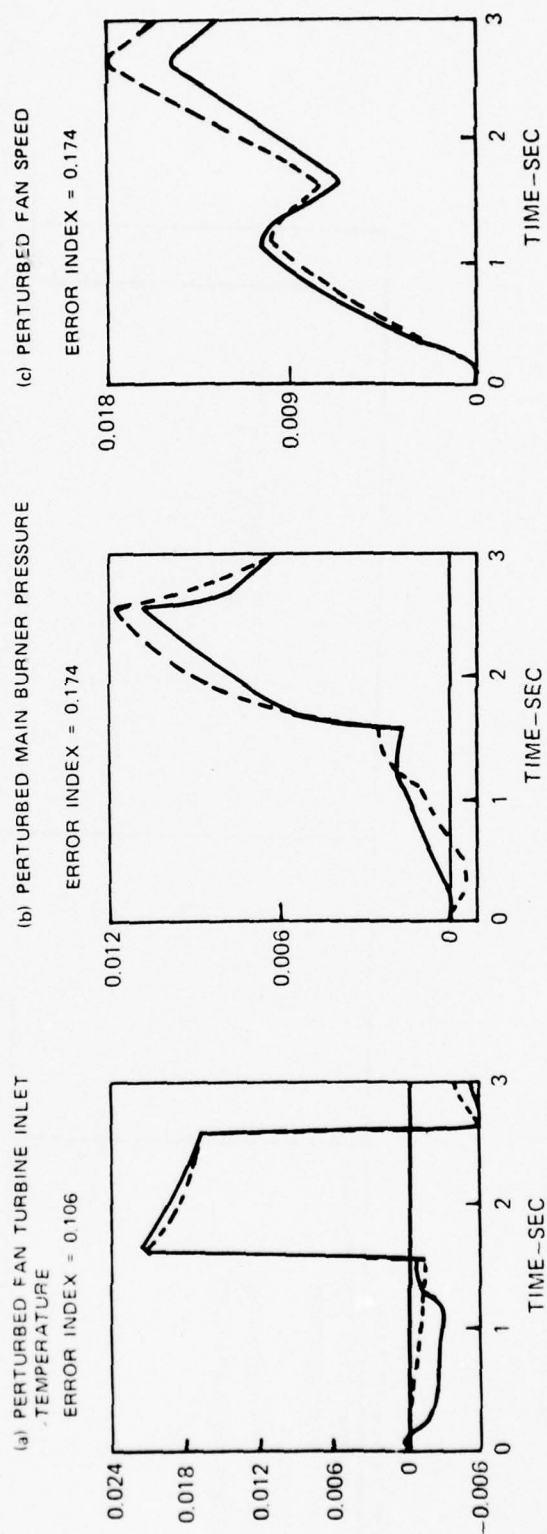


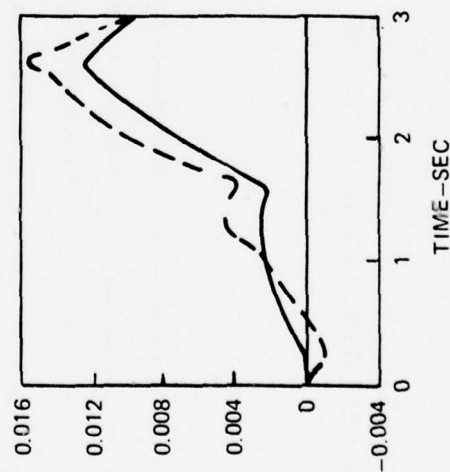
FIG. 6 (a)-(c)

NORMALIZED RESPONSE OF ACTUAL AND IDENTIFIED F100/F401 ENGINE MODELS ABOUT PLA = 20 DEG DESIGN POINT

IDENTIFIED MODEL GENERATED BY NONLINEAR FILTERING ALGORITHM
INITIAL PARAMETER ESTIMATES COMPUTED BY MATRIX LEAST-SQUARES-FIT ALGORITHM
RAW MEASUREMENT DATA OF FIG. 1 USED IN BOTH ALGORITHMS

— ACTUAL RESPONSE --- IDENTIFIED RESPONSE

(d) PERTURBED HIGH COMPRESSOR SPEED
ERROR INDEX = 0.283



(e) PERTURBED AFTERBURNER PRESSURE
ERROR INDEX = 0.147

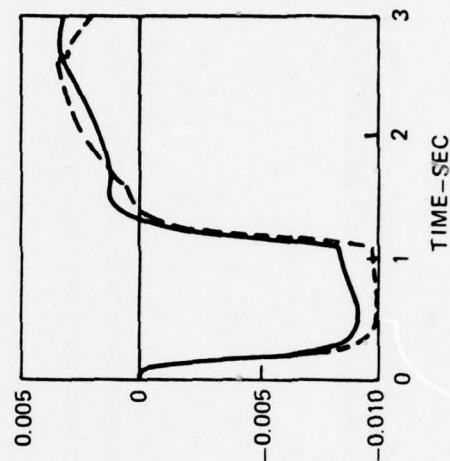


FIG. 6 (d)-(e)

NORMALIZED RESPONSE OF F100/F401 ENGINE MODELS IDENTIFIED FROM MEASUREMENT DATA WITH LOW AND HIGH LEVELS OF NOISE

COMPARISON OF ACTUAL AND IDENTIFIED MODEL RESPONSES HAVING LARGEST AND SMALLEST ERROR INDICES FOR THE HIGH NOISE LEVEL ABOUT PLA = 73 DEG DESIGN POINT

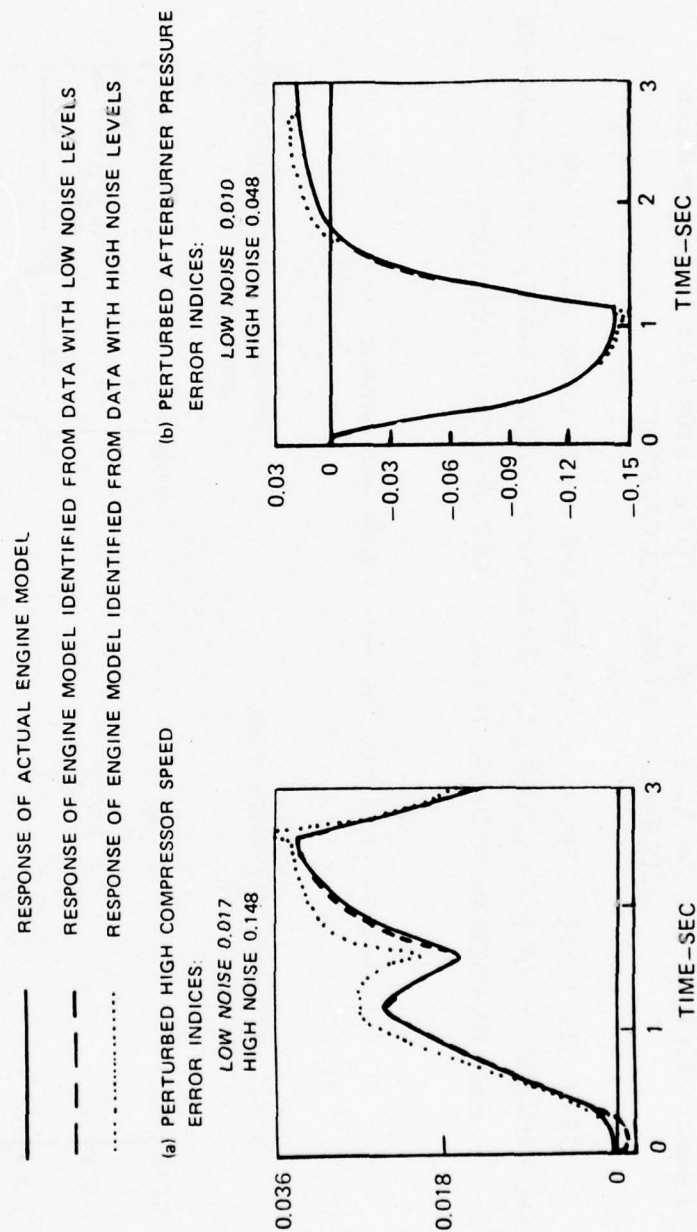


FIG. 7

CALIBRATION OF HIGH PRECISION NAVIGATORS
WITH MAXIMUM LIKELIHOOD ESTIMATION

by

Dr. Conrad E. Mueller
Dr. Gunter Stein

Honeywell Systems and Research Center (SRC)
2600 Ridgway Road N.E.
Minneapolis, Minnesota 55413

ABSTRACT

This paper summarizes recent advanced calibration analyses performed on an Inertial Measurement Unit (IMU) space-stabilized by two Electrically-Suspended-Gyros (ESG). The paper discusses the system model to be calibrated, the basics of the Maximum Likelihood Estimation (MLE) approach used for calibration, and the results.

I. INTRODUCTION

The basic calibration problem consists of separating out and then compensating for the effects of various IMU error sources such as accelerometer biases and scale factors, gyro drift rates, and platform misalignments, after observing only their accumulative effect.

Honeywell recently developed advanced ESG calibration techniques based on Maximum Likelihood Estimation (MLE) methods in order to (i) provide an off-line, analysis-oriented alternate calibration capability for the historical ESG system, (ii) determine basic ESG calibration limitations, and (iii) develop ways to overcome them.

II. SYSTEM MODEL

The ESGN IMU consists of an inertially stabilized gimballed platform carrying two electrically suspended gyros (ESG) for stabilization and a triad of integrating accelerometers for inertial velocity measurement. The two gyro spin vectors \hat{s}_1 and \hat{s}_2 are depicted in Figure 1. A spin axes frame is defined by the triad $\bar{e}_{g'} = (\hat{s}_1, \hat{s}_2, \hat{s}_1 \times \hat{s}_2)$. This frame drifts in time away from an initial alignment (C_0) with an inertial frame $\bar{e}_i(0)$,

$$(1) \quad \bar{e}_{g'}(0) = C_0 \bar{e}_i(0) = T_z(\phi_z^0) T_y(\phi_y^0) T_x(\phi_x^0) \bar{e}_i(0),$$

due to torques on the ESG's. Gyro torque theory stipulates that the spin axes triad at time t is

$$\bar{e}_{g'} = C(t) \bar{e}_i$$

where

$$\dot{C}(t) = \begin{bmatrix} 0 & \omega_z & -\omega_y \\ -\omega_z & 0 & \omega_x \\ \omega_y & -\omega_x & 0 \end{bmatrix} C(t) \quad C(0) = C_0$$

and

$$\begin{bmatrix} \omega_x \\ \omega_y \\ \omega_z \end{bmatrix} = \underbrace{\begin{bmatrix} \delta'_{10} \\ \delta'_{10} \\ -\delta'_{20} \end{bmatrix}}_{\substack{\text{constant} \\ \text{drift} \\ \text{coefficients}}} + \underbrace{\begin{bmatrix} \delta'_{12} & -\delta'_{13} & -\delta'_{11} \\ -\delta'_{13} & \delta'_{12} & \delta'_{11} \\ \delta'_{23} & -\delta'_{22} & -\delta'_{21} \end{bmatrix}}_{\substack{\text{g-sensitive} \\ \text{drift} \\ \text{coefficients}}} \bar{a}_{q'} + \underbrace{\begin{bmatrix} \delta'_{15} & \delta'_{16} \\ \delta'_{16} & \delta'_{15} \\ -\delta'_{26} & -\delta'_{25} \end{bmatrix}}_{\substack{\text{g}^2\text{-sensitive} \\ \text{drift} \\ \text{coefficients}}} \begin{bmatrix} a_{q'x}^2 \\ a_{q'y}^2 \end{bmatrix} + \underbrace{\begin{bmatrix} \delta'_{18} & \delta'_{19} \\ 0 & 0 \\ 0 & 0 \end{bmatrix}}_{\substack{\text{RAT-sensitive} \\ \text{drift} \\ \text{coefficients}}} \begin{bmatrix} \dot{r}^+ \\ \dot{r}^- \end{bmatrix} + \tilde{\omega}$$

or,

$$\begin{aligned} \bar{\omega} &= \Gamma_0 + \Gamma_1 \bar{a}_{q'} + \Gamma_2 D(\bar{a}_{q'}) \bar{a}_{q'} + \Gamma_3 \dot{r} + \tilde{\omega} \\ &= \Gamma_0 + \Gamma_1 \bar{a}_{q'} + \begin{bmatrix} \delta'_{15} & \delta'_{16} & 0 \\ \delta'_{16} & \delta'_{15} & 0 \\ -\delta'_{26} & -\delta'_{25} & 0 \end{bmatrix} \begin{bmatrix} a_{q'x} & 0 & 0 \\ 0 & a_{q'y} & 0 \\ 0 & 0 & a_{q'z} \end{bmatrix} \bar{a}_{q'} + \Gamma_3 \dot{r} + \tilde{\omega} . \end{aligned}$$

Here $\bar{a}_{q'}$ denotes acceleration expressed in the $\bar{e}_{q'}$ frame, and the equation

$$(2) \quad \dot{r}(t) = -\frac{1}{C} \left\{ \delta'_{20} + [\delta'_{22} \ \delta'_{23} \ -\delta'_{21}] \bar{a}_{q'} + [\delta'_{25} \ \delta'_{26}] \begin{bmatrix} a_{q'x}^2 \\ a_{q'y}^2 \end{bmatrix} - \omega_z \right\}$$

models the Redundant-Axis-Torquing (RAT) which maintains ESG spin axis orthogonality. The random drift variations, $\tilde{\omega}$, are modelled as Brownian motion,

$$\frac{d\tilde{\omega}}{dt} = \xi_3(t) \quad , \quad \tilde{\omega}(0) = 0$$

where $\xi_3(t)$ denotes standard Gaussian white noise.

To this point, twenty-three error parameters to be estimated have been introduced:

$$\{ \delta\phi_{ox}, \delta\phi_{oy}, \delta\phi_{oz}, \Gamma_0, \Gamma_1, \Gamma_2, \Gamma_3 \} \quad ,$$

assuming the initial nominal rotational angles $(\phi_z^0, \phi_y^0, \phi_x^0)$ which orient the spin axes relative to inertial axes in Equation (1) are

actually misaligned by an amount $\delta\phi_0 = (\delta\phi_{0x}, \delta\phi_{0y}, \delta\phi_{0z})$. The drift coefficients in Equation (2) need not be estimated since in an operating system the term $\dot{r}(t)$ is provided by the system itself and is not compensated for, but rather is delivered to the ESG's. The model for $\tilde{\omega}$ does not introduce new parameters to be calibrated, but allows one to analyze its effect on calibration and alignment of the other parameters.

The acceleration vector in the inertial frame involves two more error parameters, north and east deflections $d = (0, d_n, d_e)$ of the ideal local vertical frame. Thus

$$\bar{a}_i = T_z(-l) T_y(L) \begin{bmatrix} 1 & -d_e & -d_n \\ d_e & 1 & 0 \\ d_n & 0 & 1 \end{bmatrix} \begin{bmatrix} g_0 \\ 0 \\ 0 \end{bmatrix}$$

where l and L denote longitude and latitude angles and g_0 denotes the nominal value of gravitational acceleration.

The acceleration vector \bar{a}_g , expressed in the spin axes frame \bar{e}_g , is transformed thru 2 rotations β_2, β_3 to the platform proper. These 2 rotations represent random case alignment variations, pickoff

errors, and gimbal servo errors. Their sum β_s is modelled as a first-order vector Markov process with correlation time τ_s :

$$\frac{d}{dt} \beta_s = -\frac{1}{\tau_s} \beta_s + \xi_1(t), \quad \beta_s(0) \text{ unknown}$$

where $\xi_1(t)$ denotes standard Gaussian white noise. After two nominal rotations (45° , and β_1) which do not impact the set of error parameters to be calibrated, gravity is rotated through an incremental non-orthogonal rotation β , which was assumed to consist of unknown constants β_c as well as random variations $\tilde{\beta}$:

$$\beta = \beta_c + \tilde{\beta},$$

where the model for the random component is

$$\frac{d}{dt} \tilde{\beta} = -\frac{1}{\tau_p} \tilde{\beta} + \xi_2(t), \quad \tilde{\beta}(0) \text{ unknown.}$$

Gravity is now available in accelerometer axes \bar{e}_A . The instrument models are assumed to be (for $i = x, y, z$)

$$a_i = \frac{a_{Ai}}{K_i} + B_i + C_i(q_o^2 - a_{Ai}^2),$$

where only the accelerometer biases B_i and scale factors K_i were calibrated. (The accelerometer nonlinearities C_i were not calibrated at the system level; it was assumed they were adequately calibrated at the component level.)

Thus forty constant error parameters were modelled for C&A* in toto:

$$\mathcal{Z} = \{\delta\phi_o, \Gamma_o, \Gamma_1, \Gamma_2, \Gamma_3, d, \beta_s(0), \beta_c, \tilde{\beta}(0), K, B\}.$$

The complete IMU model is summarized in Figure 2.

III. CALIBRATION TECHNIQUES

To calibrate and align the ESG IMU we must estimate the various constant unknown parameters as they appear in the integrated system model shown in Figure 2. The initial misalignment angles $\delta\phi_o$ are actually 3 unknown initial values of 3 states, as are the orthogonal random case alignments $\beta_s(0)$ and the non-orthogonal random accelerometer alignments $\tilde{\beta}(0)$. Thus the unknown parameter vector can be re-ordered and then partitioned into nine unknown initial conditions for states evolving according to nine state-equations and a 31-vector of constants related to the inertial components themselves; i.e.,

$$\mathcal{Z} = \{\delta\phi_o, \beta_s(0), \tilde{\beta}(0)\} \cup \{\Gamma_o, \Gamma_1, \Gamma_2, \Gamma_3, d, \beta_c, K, B\},$$

$$\mathcal{Z} \triangleq \{x_o, \pi\} = \{x_o\} \cup \{\pi\}.$$

* C&A = Calibration and Alignment

Two C&A techniques were used to estimate the vector ξ -- "open-loop" and "closed-loop" C&A.

For "open-loop" C&A, a 15-state-vector was used, made up of the nine alignment states above plus three integrated specific accelerations \bar{V}_A ,

$$\frac{d}{dt} \bar{V}_A = \bar{a}_A, \quad \bar{V}_A(0) = 0$$

and three random drifts $\tilde{\omega}$, where

$$\frac{d}{dt} \tilde{\omega} = \xi_3(t), \quad \tilde{\omega}(0) = 0.$$

The nonlinear dynamics corresponding to the IMU math model are then symbolically written then as

$$\begin{aligned} \dot{x} &= f(x, t, \pi, \xi_1, \xi_2, \xi_3) \\ x(0) &= \{0, x_0, 0\} \end{aligned}$$

where $x \triangleq \{\bar{V}_A, \delta\phi, \beta_s, \tilde{\beta}, \tilde{\omega}\}$.

The only recorded measurements used in "open-loop" calibration were the velocities, \bar{V}_A , which are sampled at discrete times t_k , and hence the general nonlinear measurement equation

$$y_k = h(x_k, t_k, \pi) + \eta_k$$

becomes simply

$$y_k = \bar{V}_A(t_k) + \eta_k,$$

where η_k denotes a white observation noise process with statistics

$$E[\eta_k] = 0, \quad E[\eta_k \eta_j^T] = R \delta_{kj}.$$

The three white noise processes $\xi = (\xi_1, \xi_2, \xi_3)$ appearing in the dynamics for x itself are assumed to have statistics

$$E[\xi(t)] = 0, \quad E[\xi(t)\xi(\tau)^T] = Q\delta(t-\tau).$$

For "closed-loop" C&A, an 18-state-vector was formulated:

$$x = \{\bar{r}_i, \bar{V}_i, \delta\phi, \beta_s, \tilde{\beta}, \tilde{\omega}\},$$

where \bar{r}_i and \bar{V}_i denote inertial position and inertial velocity. The measurement used here was the inertial position, so

$$y_k = h(x_k, t_k, \pi) + \eta_k = \bar{r}_i(t_k) + \eta_k.$$

In either open-loop or closed-loop C&A, we have

$$\zeta = \{x_0, \pi\} = \{\delta\phi_0, \beta_s(0), \tilde{\beta}(0)\} \cup \{\Gamma_0, \Gamma_1, \Gamma_2, \Gamma_3, d, \rho_c, K, B\}$$

$$\dot{x} = f(x, t, \pi, \xi)$$

$$y_k = h(x_k, t_k, \pi) + \eta_k,$$

and the C&A problem for ESG was to estimate ζ in batch fashion after recording measurements $Y_N = \{y_1, y_2, y_3, \dots, y_N\}$.

IV. BASICS OF THE MAXIMUM LIKELIHOOD ESTIMATION APPROACH TO C&A

Maximum Likelihood Estimation (MLE) techniques produce an estimate $\hat{\zeta}$ of the vector ζ such that the probability of occurrence of the observed sequence of measurements is maximized. That is, the estimate $\hat{\zeta}$ is the parameter value most likely to have produced the observations. For convenience, the log of the likelihood function is maximized over ζ ,

$$L(\zeta) = \log \Pr\{\zeta_0, Y_N | \zeta\}$$

where the likelihood function

$$\Pr\{\zeta_0, Y_N | \zeta\} = \Pr\{\zeta_0, y_1, y_2, \dots, y_N | \zeta\}$$

is the joint probability of observing the samples $\{y_1, y_2, \dots, y_N\}$ and the initial guess ζ_0 , given the parameter value ζ .

For ESG C&A, the initial guess ζ_0 is assumed to be drawn from a multivariate Gaussian distribution with mean ζ and covariance P_0 ; i.e.,

$$\text{(distribution)} \quad \zeta_0 \stackrel{d}{=} N(\zeta, P_0)$$

$$\text{(mean)} \quad E[\zeta_0] = \zeta$$

$$\text{(error covariance)} \quad E[(\zeta_0 - \zeta)(\zeta_0 - \zeta)^T] = P_0$$

Thus, the likelihood function can be written as

$$\Pr\{\zeta_0, y_1, y_2, \dots, y_N | \zeta\} = N(\zeta, P_0) \prod_{k=1}^N \Pr\{y_k | Y_{k-1}, \zeta\}$$

and therefore

$$L(\zeta) = \log N(\zeta, P_0) + \sum_{k=1}^N \log \Pr\{y_k | Y_{k-1}, \zeta\}.$$

Reference [1] describes in detail how the sum of conditional probabilities above can be approximated by a sum of multivariate Gaussian densities

$$\sum_{k=1}^N \log N(\hat{y}_{k|k-1}, B_k)$$

provided an extended Kalman filter is used on the state vector x . The (log) likelihood function to be maximized is then

$$L(\zeta) = -\frac{1}{2} \|\zeta_0 - \zeta\|_{P_0^{-1}}^2 - \frac{1}{2} \sum_{k=1}^N \left(\log \det B_k + \|y_k - \hat{y}_{k|k-1}\|_{B_k^{-1}}^2 \right),$$

which is maximized by the value of ζ which solves

$$(3) \quad \frac{\partial}{\partial \zeta} L(\zeta) = 0.$$

Combinations of first-order gradient updates

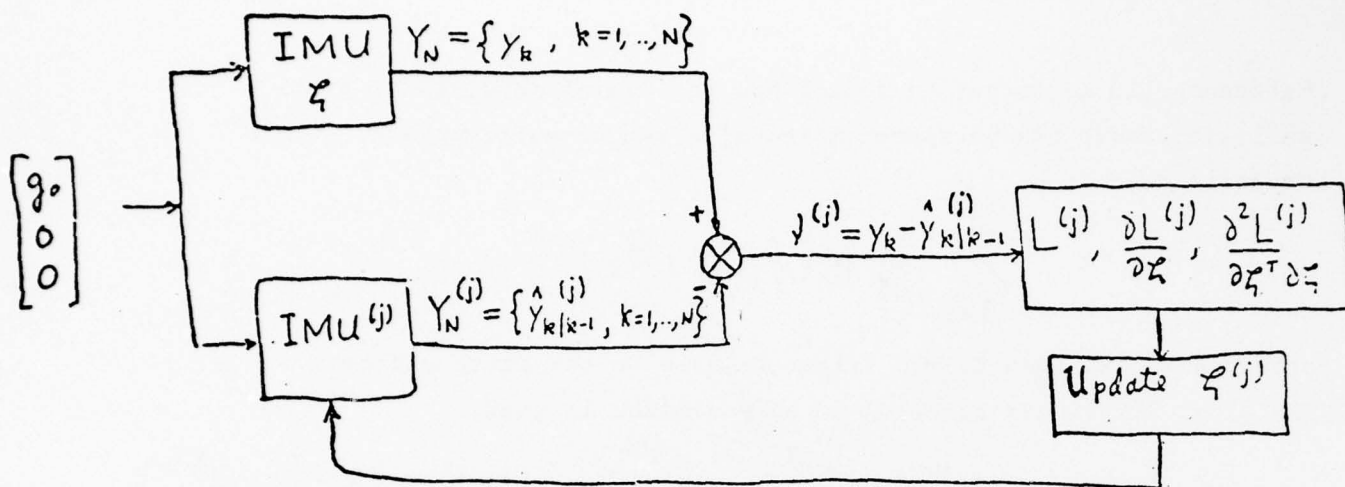
$$\zeta^{(j+1)} = \zeta^{(j)} + \epsilon \frac{\partial}{\partial \zeta} L^{(j)}$$

and second-order Newton-Raphson iterates

$$\zeta^{(j+1)} = \zeta^{(j)} - \left[\frac{\partial^2 L}{\partial \zeta^T \partial \zeta} \right]_{(j)}^{-1} \frac{\partial L}{\partial \zeta}^{(j)}$$

where used to solve Equation (3), thus achieving a compromise between convergence rate and computing effort.

The (one-step) predicted measurement appearing in $L(\zeta)$, $\hat{y}_{k|k-1}$, was computed by using an extended Kalman filter operating with parameters ζ . For a sequence of iterates $\zeta^{(j)}$, the MLE procedure becomes:



Thus, MLE requires repeated processing ($j = 0, 1, 2, \dots$) of the same observed history of IMU outputs, Y_N . This presents no difficulties for an off-line data processing application, but in an on-line system there could possibly be delays when switching from the C&A mode to the navigation mode.

The typical off-line ESG C&A procedure consists of nominally aligning the platform at some desired initial orientation with respect to inertial space,

$$C_0 = T_z(\phi_z^0) T_y(\phi_y^0) T_x(\phi_x^0) \quad ,$$

and then collecting measurements every 30 seconds for several days. The platform is then slewed to a second desired orientation and another data set is recorded. Repeated passes through the C&A data processing algorithms are then carried out. After the C&A data processing has converged to an acceptable (but still erroneous) ML estimate of the parameter ζ , the ESG platform is ready for cruise navigation, with the computer compensating the IMU outputs for the estimated ML values of ζ .

The various C&A errors are produced by process noises, observation noises, and by any parameters deliberately left uncalibrated. They contribute to subsequent navigation errors in the form of position errors due-to-C&A and heading errors due-to-C&A. Using MLE iterates which have converged to ζ^* ($\neq \zeta$) and assuming r_o denotes actual inertial position and \hat{r}_o denotes estimated, the first and second moments of navigation error $r_o - \hat{r}_o$ are

$$E[r_o - \hat{r}_o] = \frac{\partial [r_o - \hat{r}_o]}{\partial \zeta} E[\zeta - \zeta^*]$$

$$E\{[r_o - \hat{r}_o][r_o - \hat{r}_o]^T\} = \frac{\partial [r_o - \hat{r}_o]}{\partial \zeta} M \frac{\partial [r_o - \hat{r}_o]^T}{\partial \zeta},$$

where M denotes the C&A error covariance matrix,

$$M = E[(\zeta - \zeta^*)(\zeta - \zeta^*)^T].$$

Reference [1] contains definitions of the navigation error (due-to-C&A only) sensitivities

$$\frac{\partial [r_o - \hat{r}_o]}{\partial \zeta}, \quad \frac{\partial [v_o - \hat{v}_o]}{\partial \zeta}, \quad \text{and} \quad \frac{\partial [\delta\phi]}{\partial \zeta},$$

and shows that the square of a "Figure-of-Merit" (FOM),

$$FOM^2 = \frac{1}{T} \int_0^T [\delta v_e^2 + \delta v_n^2] dt$$

can be written as

$$E[FOM^2] = \text{Trace}[M S(T)]$$

where

$$S(\tau) = \frac{1}{T} \int_0^T \left\| \frac{\partial}{\partial \eta} [r_0 - \hat{r}_0] \right\|_W^2 dt .$$

These statistics which propagate C&A errors through navigation serve as a measure of goodness of the C&A process. For MLE, the theoretical Cramer-Rao lower bound on M is the inverse of the "Fisher Information Matrix", evaluated at ζ ,

$$-\frac{\partial^2 L}{\partial \eta^T \partial \eta}(\zeta) ,$$

and for full-parameter C&A, MLE theory assures that the ML estimate ζ^* is unbiased,

$$E[\zeta^* - \zeta] \longrightarrow 0 \quad \text{as } N \rightarrow \infty ,$$

and M asymptotically achieves the lower bound as $N \rightarrow \infty$,

$$M = E[(\zeta^* - \zeta)(\zeta^* - \zeta)^T] \longrightarrow \left[-\frac{\partial^2 L}{\partial \eta^T \partial \eta}(\zeta) \right]^{-1} .$$

Since the Fisher Information Matrix grows linearly with N, MLE with full-parameter C&A not only asymptotically achieves the theoretical lower bound, but ultimately achieves zero error. When some parameters are deliberately left uncalibrated, the estimates will be biased and there is no guarantee of achieving zero error. In linear estimation, standard Kalman filtering and MLE are equivalent.

The property of smallest C&A error under full-parameter, nonlinear estimation is the main advantage of the MLE algorithm, and renders it ideal for studies of fundamental C&A limitations of precision navigation systems. Furthermore, since it can also treat the case where the ζ parameter includes the noise statistics Q and R ,

$$\zeta = \{ \underline{x}_0, \pi, Q, R \} ,$$

estimation of internal platform noise magnitudes from actual system data is possible.

V. RESULTS

The mathematical model developed for the ESG platform featured adjustable complexity in terms of active error sources, platform orientations, and raw drift parameter values. Likewise, the MLE algorithm was made adjustable with respect to recognized error sources, noise assumptions, and initial uncertainties of error parameters. Figure 3 depicts the flexibility deliberately built in to permit tradeoff analyses on three important C&A issues:

- What platform orientations should be used for C&A?
- What error sources need to be calibrated?
- What initial error uncertainties and raw parameter values are required for successful C&A?

The remainder of Section IV presents some results for each of these three issues plus the results of a study to determine the minimum C&A time required to meet a spec on the FOM.

Platform Orientation Optimization

Two unique orientations which would improve the ESG system performance were determined, EPALD and CEM.

Past C&A studies have shown that the g^2 -sensitive drifts (Γ_2) are extremely difficult to separate in the presence of noise, and failure to separate them will cause significant errors as the latitude varies during subsequent navigation. Innovative consideration of existing ESG Torque Theory led to the discovery of the EPALD orientation which has some very desirable properties, especially for navigation over wide ranges of latitude. The EPALD orientation is illustrated in Figure 4. In this attitude, the Earth Polar Axis (EPA) falls along a long diagonal of a cube whose sides are defined by the two gyro spin axes and by their cross product. This motivates the name EPALD: Earth Polar Axis Long Diagonal. The significance of EPALD is that the effective constant drift of the platform (the combined effect of constant, g -dependent, and g^2 -dependent contributions from each gyro) reduces to the particularly simple form shown in Figure 4. To compensate for this effective drift at all latitudes, only 6 effective drift parameters (6 linear combinations of 18 separate gammas) need to be known accurately. This alleviates calibration problems significantly, and in EPALD navigation, renders the g^2 -dependent ramp drifts independent of latitude.

At least two orientations are required for C&A of the ESG platform. Thus an investigation was carried out to determine the optimal

C&A companion orientation to use with (positive) EPALD. A simple numerical search was developed, assuming a constant platform orientation matrix,

$$C(t) \equiv C_0 = T_z(0) T_y(\phi_y) T_x(\phi_x) .$$

The initial Euler angles ϕ_x and ϕ_y were sought which solved a reduced minimization problem: the original parameter vector

$$\mathcal{L} = \{ \delta\phi_0, \beta_s(0), \tilde{\beta}(0), \Gamma_0, \Gamma_1, \Gamma_2, \Gamma_3, d, \beta_c, K, B \}$$

was reduced to a 21-vector

$$\mathcal{L}_r = \{ \delta\phi_0, \Gamma_0, \Gamma_1, \Gamma_2 \}$$

and an approximate version of the expected value of the square of the Figure-of-Merit (FOM) was minimized over all Euler triples $(0, \phi_y, \phi_x)$.

The resulting optimal C&A orientation, CEM, is illustrated in Figure 5. It results in minimum FOM-due-to-C&A when used together with +EPALD for C&A and followed by +EPALD navigation along a "Standard cruise trajectory". Contours of constant (approximate) FOM^2 found in the search are shown in Figures 6 and 7. The hemispheres, drawn on a planar projection, are used because each candidate orientation can be described by two rotation angles. Notable points of the projection are designated in the figures. For example, the standard earth polar orientation (Gyro 2 north) is

the sphere's north pole, whereas the positive EPALD orientation lies in the southern hemisphere at 35 degrees latitude, -45 longitude.

The significance of the approximate $(FOM)^2$ contours is self evident. Contours with small values signify good companion orientations for EPALD. The best orientation is seen to fall very near earth polar at altitude 74 degrees, longitude 45 degrees, and corresponds to the gyro orientations with respect to inertial coordinates shown in Figure 5.

By using the MLE calibration algorithm on a platform in the CEM calibration orientation and navigating with the platform in the EPALD orientation, the mathematical FOM-due-to-calibration was improved four-fold, to almost one-half the error budget requirement. Because of the care in modeling measurement and process noise it is expected that these results will be achieved on actual system data.

C&A Error Model Study

Due to the performance margin referred to above, it was possible to perform tradeoff analyses to identify the minimum C&A error model that if calibrated would still meet the budget. The individual error sources were partitioned into major natural groups and these groups were deleted one at a time from the calibrated error model.

FOM-due-to-C&A was then evaluated without calibrating the deleted group but including the contribution of its uncalibrated values in the true FOM calculation. The group producing minimum performance deterioration when deleted was then permanently deleted, and then the remaining groups were deleted one at a time, etc. Results of these calibration model simplification studies are shown in Figure 8.

We see the expected half-budget FOM-due-to-calibration with full model calibration, and then that deletion of RAT gammas, east deflection, and initial conditions of platform alignment noises produces very little deterioration. Next, we can delete accelerometer scale factors (these are known well from VMU calibration), then accelerometer nonlinearities and biases (also known from VMU calibration), and finally, north deflection and g^2 -gammas. Only the last two steps put us beyond the budgeted requirement.

The Effect of Initial Error Uncertainties and Raw Parameter Values on the FOM-due-to-C&A

The dependence of the (best possible) FOM-due-to-C&A on initial error uncertainties and raw parameter values is summarized in Figure 9. Since the budget requirement is $FOM/GOAL \leq 1.0$, we can determine which orientations and/or what combinations of raw drift assumptions and initial uncertainties are required to meet spec.

We observe that there is little advantage of using CEM in place of -EPALD when all parameters are calibrated and raw drifts are (overly) optimistic. In this case, the gyros are initially placed in the EPALD cone and stay in the EPALD cone, actually yielding better results than +EPALD/CEM. However, under more realistic assumptions of raw drift, factors of improvement of 3 and 4 are possible using CEM for the first C&A orientation instead of -EPALD.

The Effect of C&A Time on the FOM-due-to-C&A

A brief preliminary study of FOM dependence on C&A time is summarized in Figure 10. It shows a minimum time required for C&A of about 36 hours.

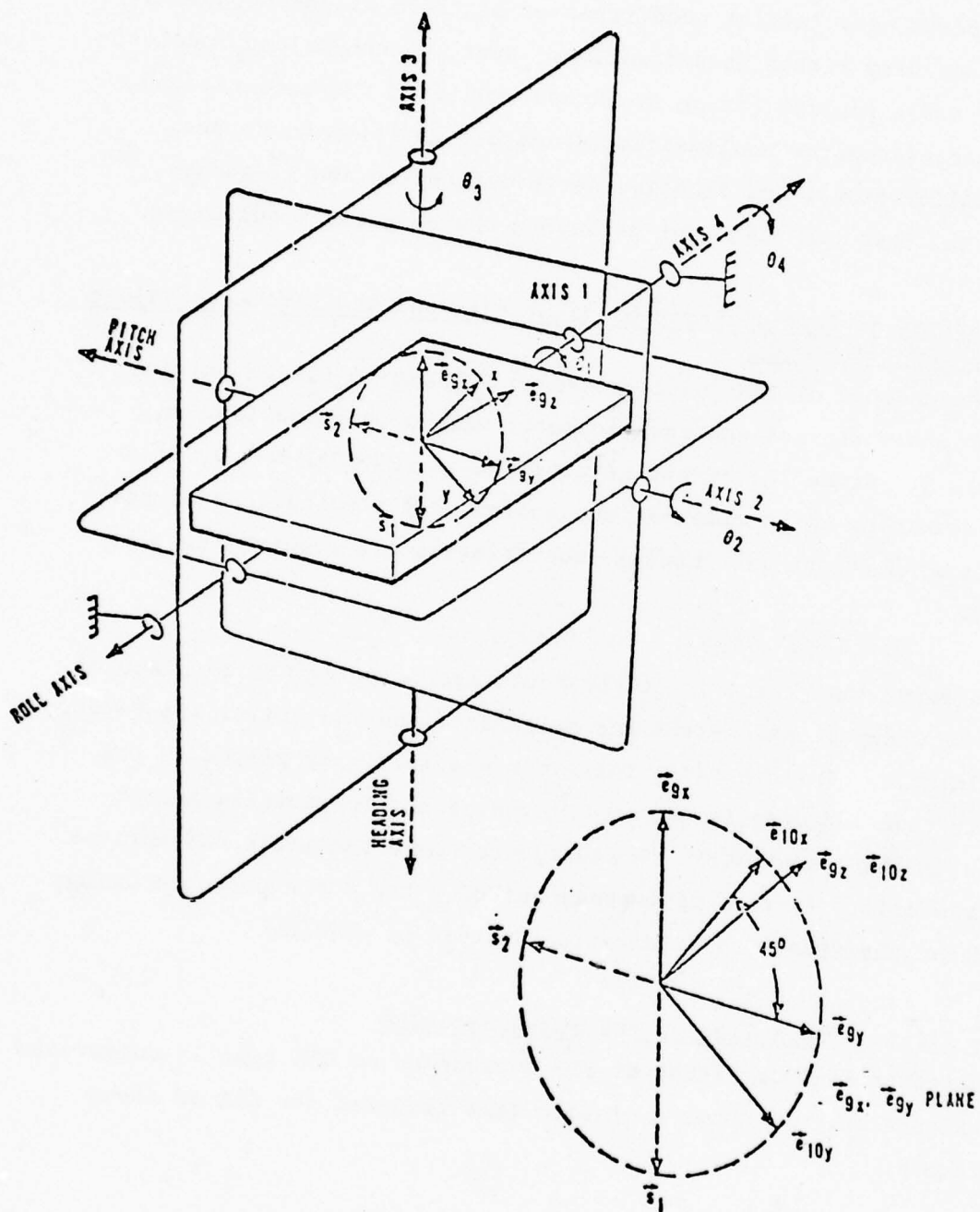


Figure 1. ESG Platform

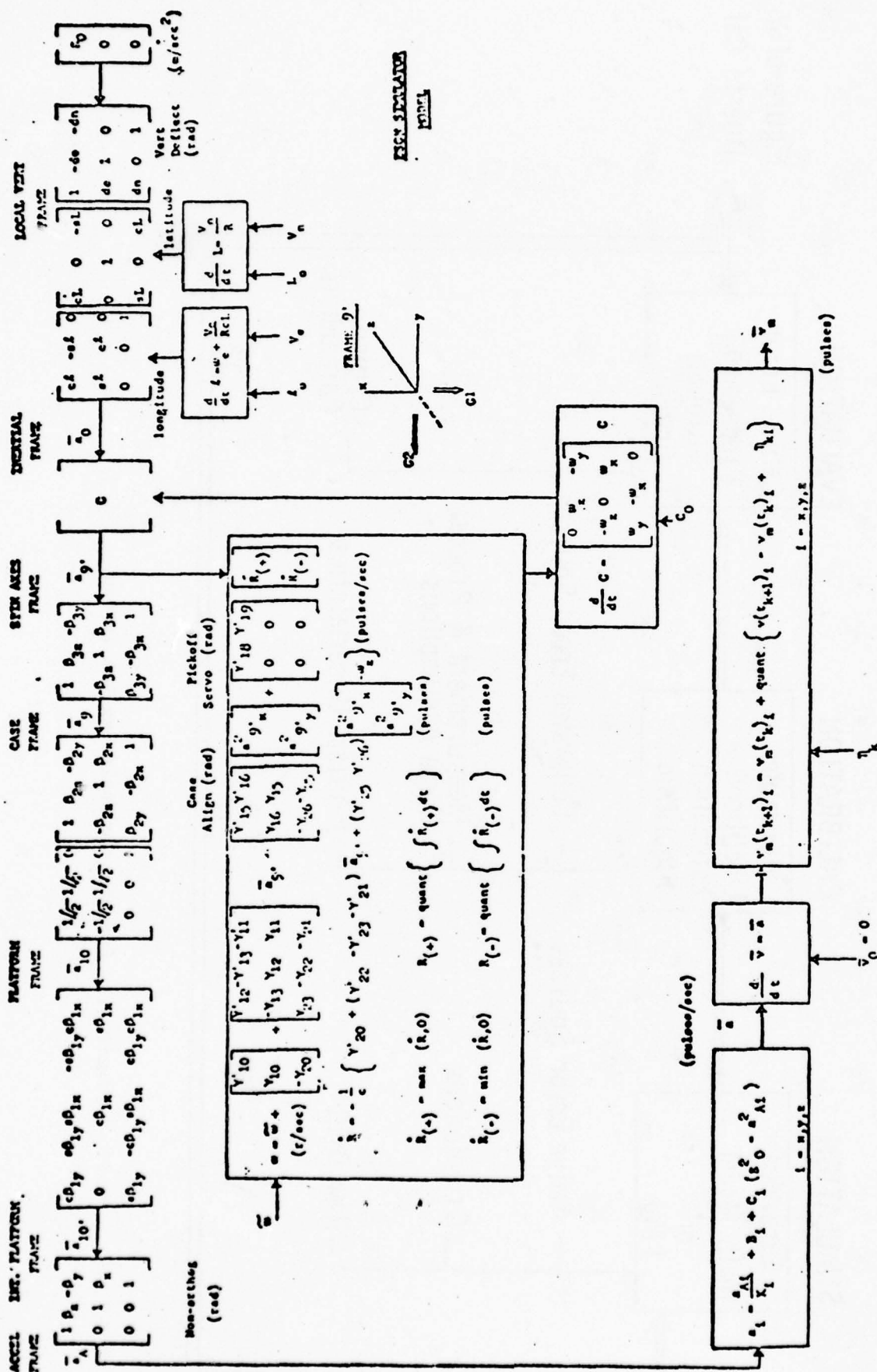


Figure 2. INU Math Model

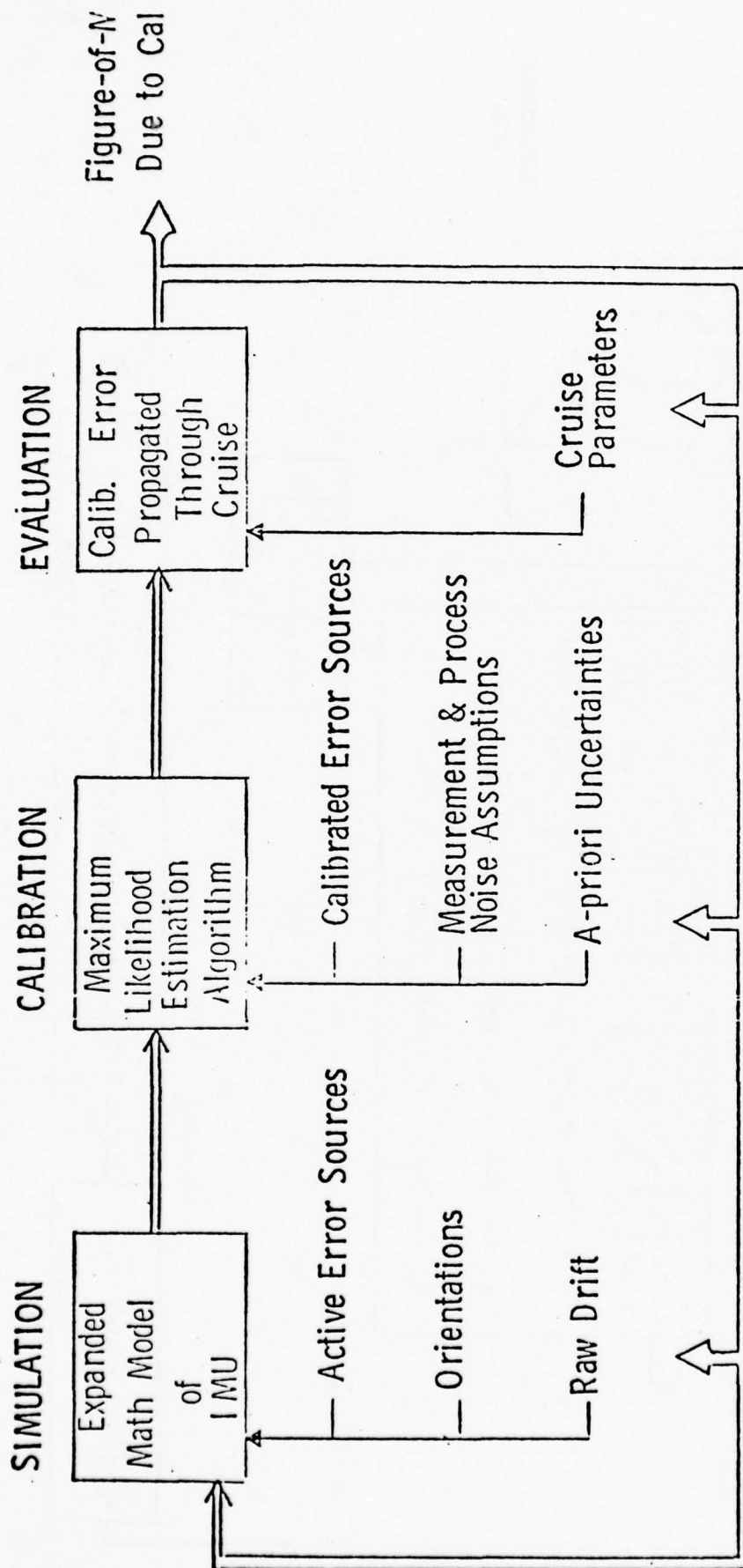
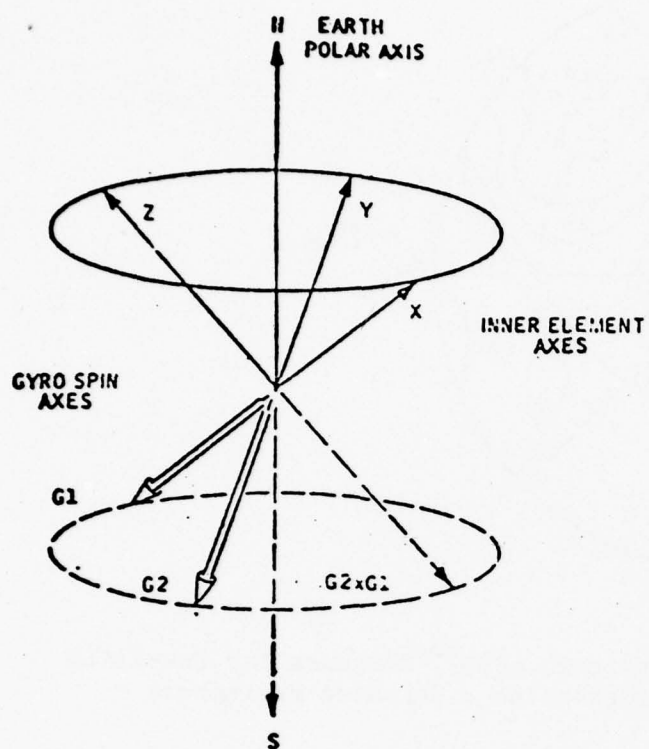


Figure 3. Approach to Analyzing C&A Issues



EFFECTIVE CONSTANT DRIFT
OF INNER ELEMENT

$$\omega = \omega_1 + \frac{\sin \text{LAT}}{\sqrt{3}} \omega_2$$

$$\omega_1 = \begin{bmatrix} \gamma'_{10} + (\gamma'_{15} + \gamma'_{16})/3 \\ \gamma_{10} + (\gamma_{15} + \gamma_{16})/3 \\ -\gamma_{20} - (\gamma_{25} + \gamma_{26})/3 \end{bmatrix}$$

$$\omega_2 = \begin{bmatrix} -\gamma'_{12} + \gamma'_{13} + \gamma'_{11} \\ \gamma_{13} - \gamma_{12} - \gamma_{21} \\ -\gamma_{23} + \gamma_{22} + \gamma_{21} \end{bmatrix}$$

Figure 4. EPALD Orientation

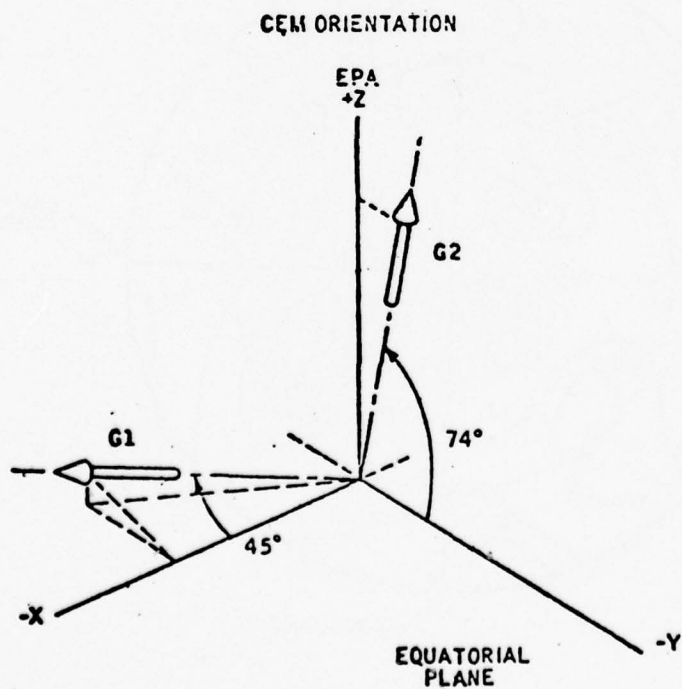


Figure 5. CEM Orientation

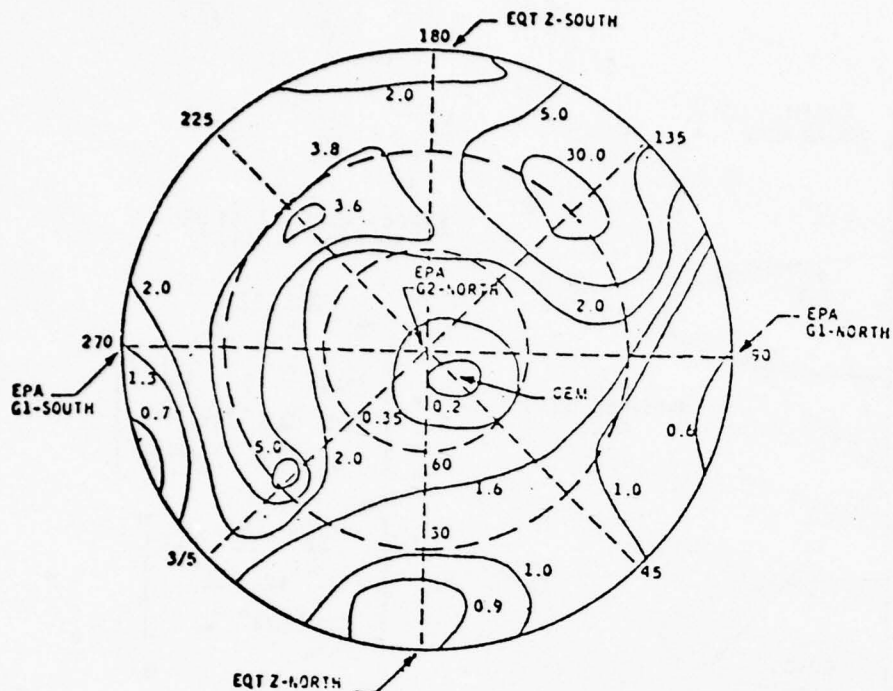


Figure 6. Approximate $(FOM)^2$ Contours for Pre-EPALD Orientation - Northern Hemisphere

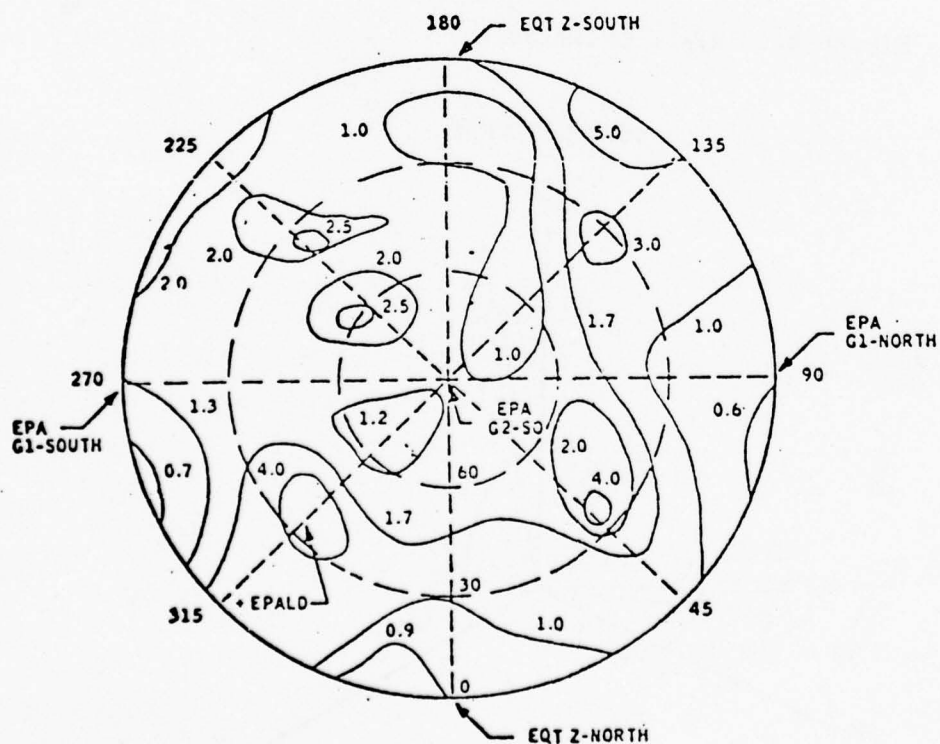
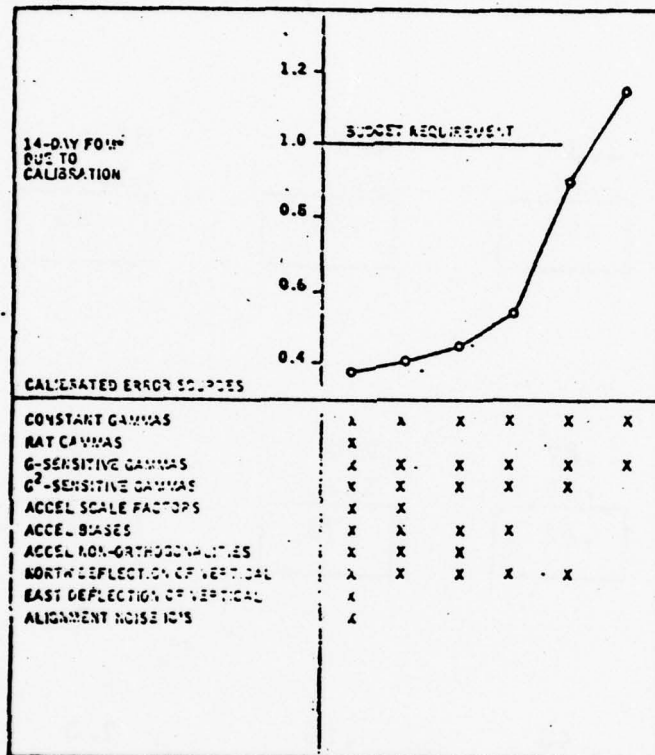


Figure 7. Approximate $(FOM)^2$ Contours for Pre-EPALD Orientation - Southern Hemisphere



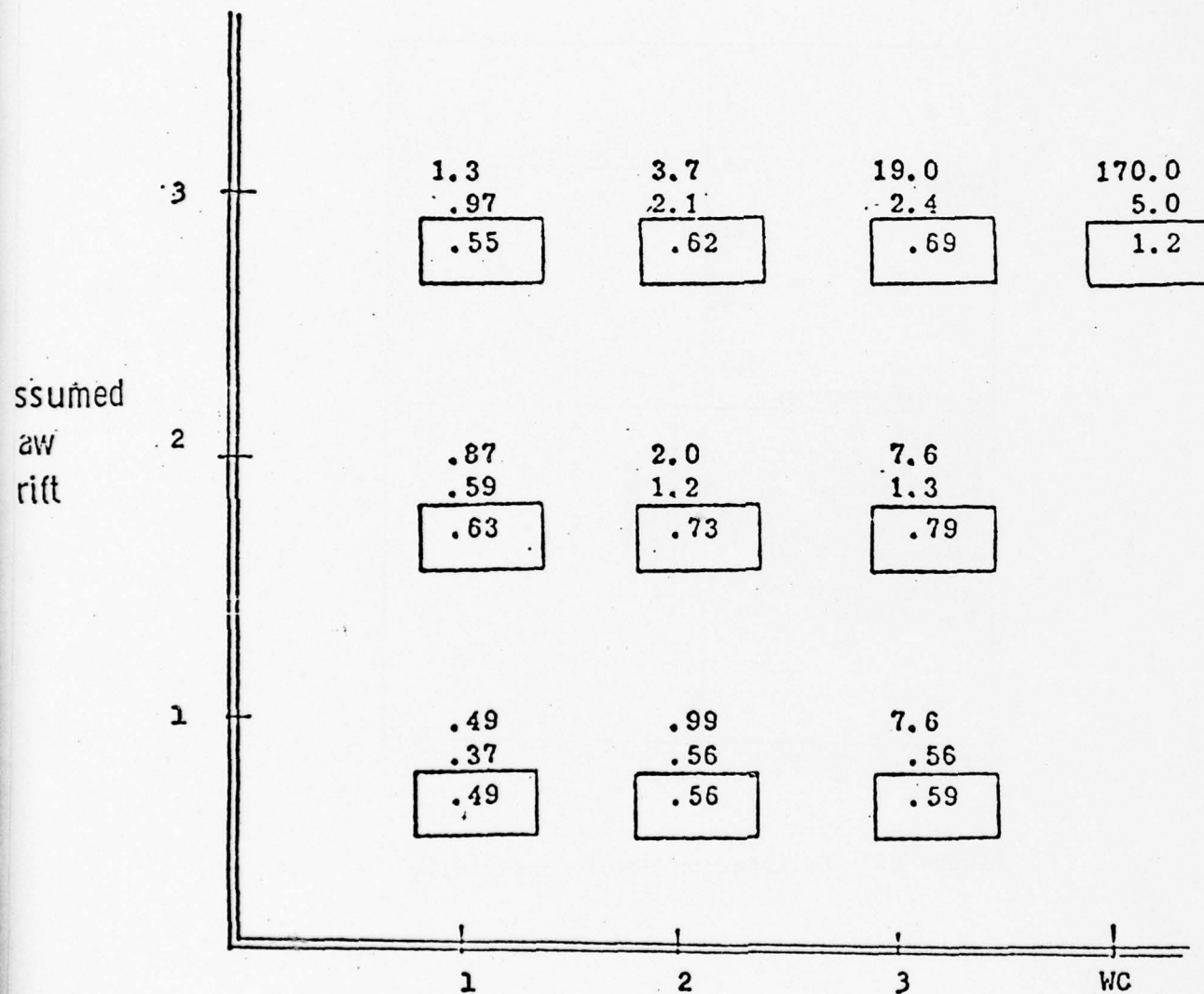
* SCALE FACTOR NOT SHOWN IN FORM CALCULATIONS.

Figure 8. Calibration Model Sensitivity

+ EPALD CAL; σ , γ_0 , γ_1 , γ_3 Calibrated

+ EPALD CAL; All Params Calibrated

+ EPALD/CEM CAL; All Params Calibrated



ASSUMED A-PRIORI UNCERTAINTIES

ALL CASES: +EPALD NAV. STD CRUISE

Figure 9

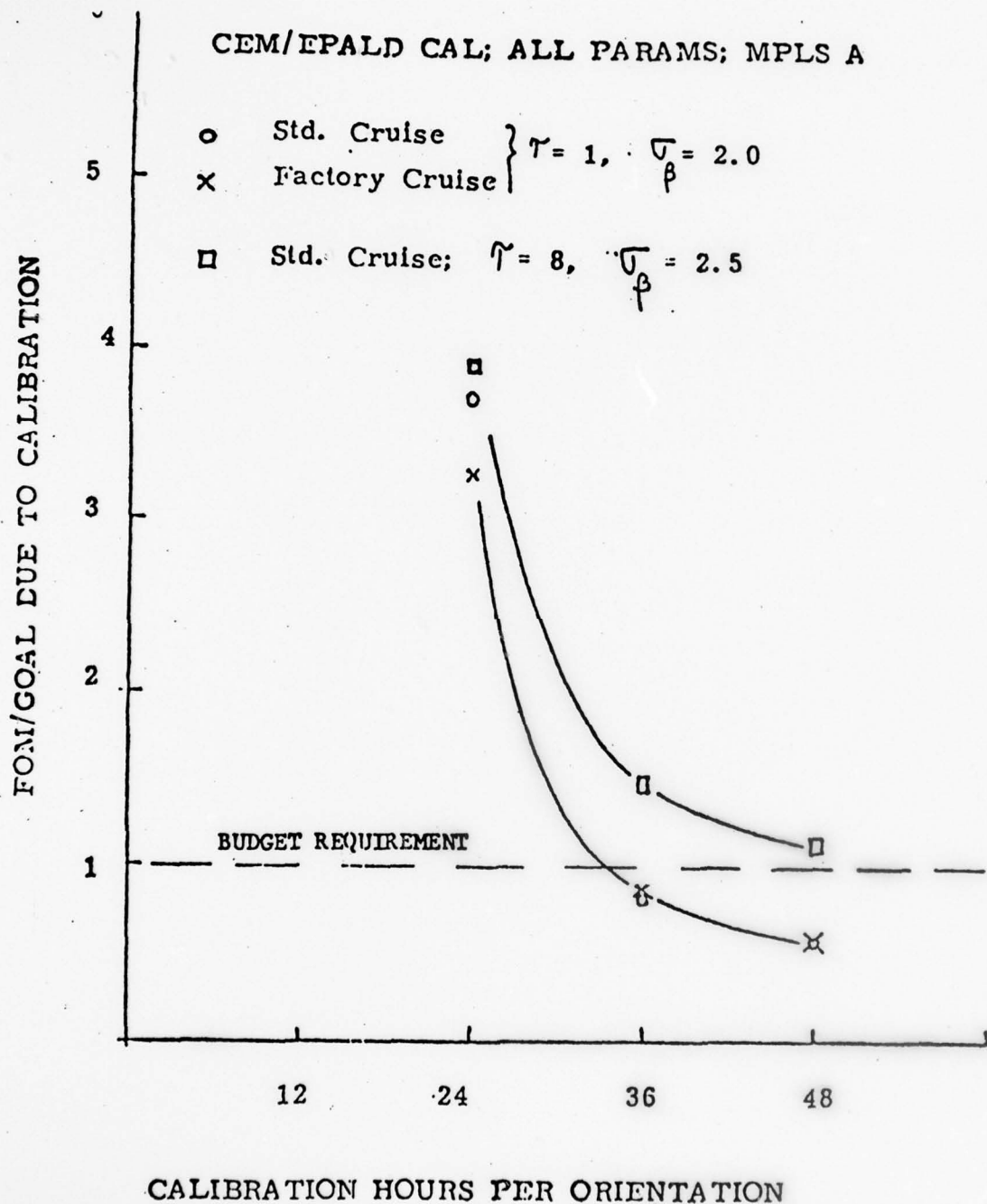


Figure 10. Results of Preliminary Study of Minimum Time Required for C&A

SESSION V
ESTIMATION

ESTIMATION OVERVIEW*

by

R.A. NASH

The Analytical Sciences Corporation
Reading, Massachusetts 01867

* The following figures include vuegraphs presented as an estimation overview.

OVERVIEW OF ESTIMATION THEORY RELATIVE TO NAVY APPLICATIONS

TASC

ESTIMATION OVERVIEW*

by

R.A. NASH

**The Analytical Sciences Corporation
Reading, Massachusetts 01867**

* The following figures include vuegraphs presented as an estimation overview.

OUTLINE

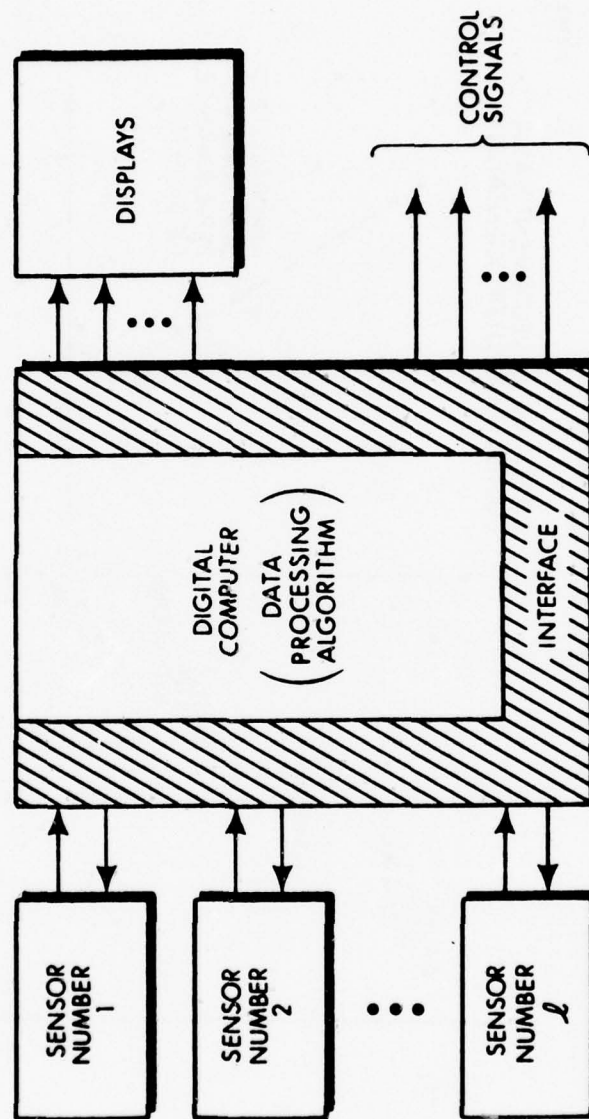
- KALMAN FILTERING / ESTIMATION THEORY – BASIC CONCEPTS
- GENERAL AREAS OF APPLICATION
- THREE “NON-TRADITIONAL” EXAMPLES
- PROBLEMS AND AREAS FOR FURTHER RESEARCH

KALMAN FILTERING/ ESTIMATION THEORY - BASIC CONCEPTS

TASC

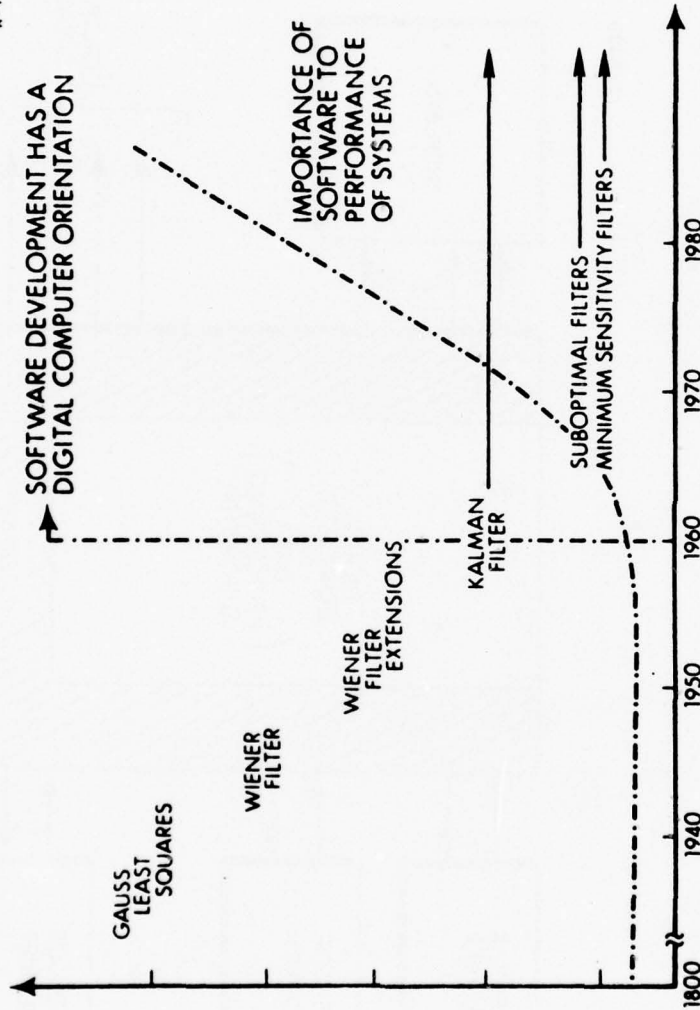
MODERN MULTISENSOR SYSTEM

R-6526



INCREASING ROLE OF SOPHISTICATED SOFTWARE IN MODERN SYSTEMS

R-1193



KALMAN FILTER OVERVIEW

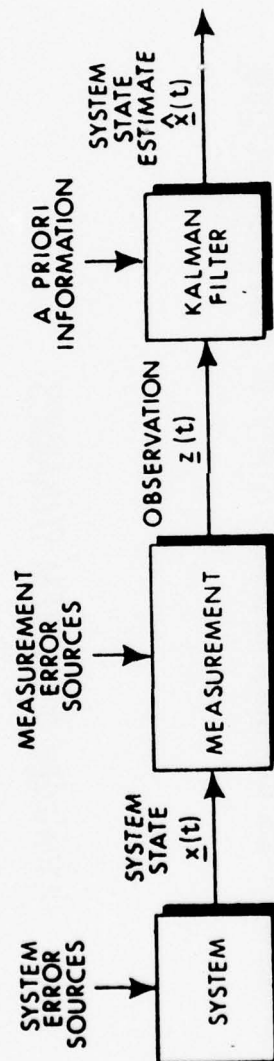
The KALMAN FILTER is a RECURSIVE DATA PROCESSOR which ESTIMATES the most probable STATE of a SYSTEM utilizing:

- knowledge of SYSTEM DYNAMICS
- MEASUREMENTS
- assumed STATISTICS of system and measurement errors
- INITIAL CONDITION information

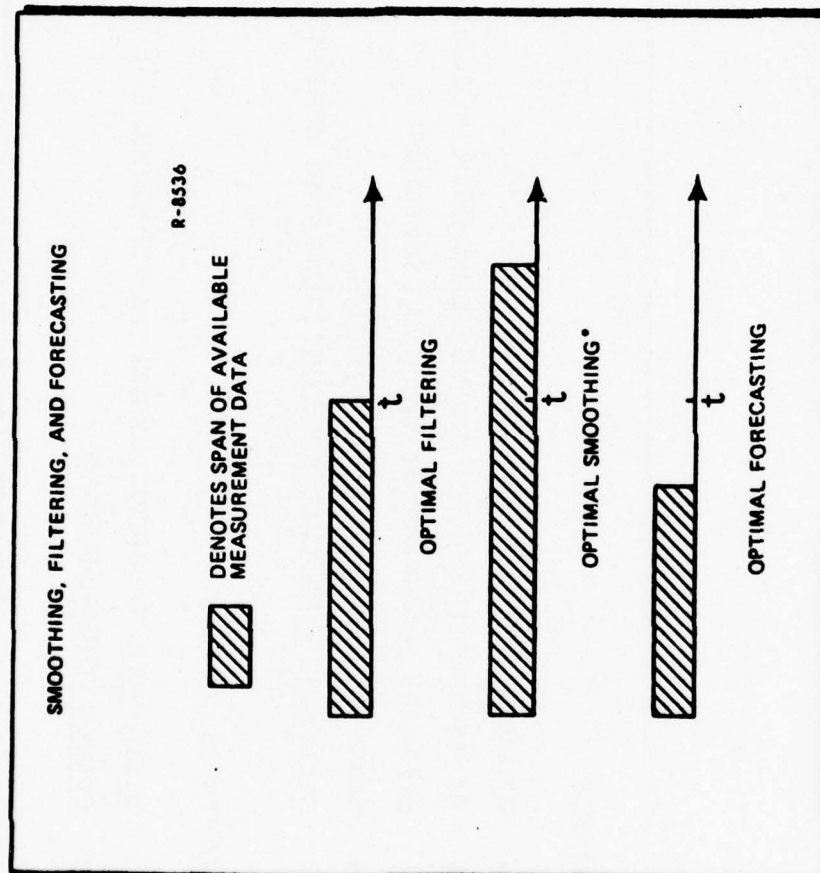
TASC

SYSTEM, MEASUREMENT AND ESTIMATOR

R-546-a



THREE TYPES OF ESTIMATION PROBLEMS



COMPETING FACTORS IN THE KALMAN FILTER FORMULATION

R-824

ADVANTAGES

- MINIMIZES SYSTEM ERROR (STATISTICAL)
- MAKES COMPLETE USE OF ALL MEASURED DATA (REDUNDANT)
- OPERATES UNDER ANY MEASUREMENT SCHEDULE
- GENERATES ITS OWN ERROR ANALYSIS
- RECURSIVE ESTIMATOR (DOES NOT STORE PAST MEASUREMENTS)

DISADVANTAGES

- SENSITIVITY TO ERRONEOUS MODELS, STATISTICS, ETC.
- COMPUTATIONAL BURDEN

TASC

COVARIANCE MATRIX

$$\tilde{\mathbf{x}} = \hat{\mathbf{x}} - \mathbf{x}$$

\mathbf{x} = SYSTEM STATE

$\hat{\mathbf{x}}$ = ESTIMATE OF THE SYSTEM STATE

$\tilde{\mathbf{x}}$ = ERROR IN THE ESTIMATE OF THE SYSTEM STATE

$$\mathbf{P} = E[\tilde{\mathbf{x}}\tilde{\mathbf{x}}^T]$$

GENERAL AREAS OF APPLICATION

TASC

KALMAN FILTERING AND RELATED IDEAS CAN BE APPLIED TO:

- **REAL-TIME SYSTEM INTEGRATION**
- **POST-TIME DATA PROCESSING**
- **COVARIANCE ANALYSIS (TRADE-OFF STUDIES
PRIOR TO BUYING HARDWARE)**

APPLICATIONS

NAVIGATION SYSTEM INTEGRATION

(ALIGNMENT, CALIBRATION, RESET,...; SSN'S, SSBN'S, SURFACE SHIPS, NAVAL AIRCRAFT,...)

TEST PROCEDURES AND POST-MISSION ANALYSIS

(INS AND COMPONENT PERFORMANCE EVALUATION, RANGE INSTRUMENTATION EVALUATION, TRANSPONDER SURVEYING, TRAJECTORY/TRACK RECONSTRUCTION,...; DASO/OT'S, SATRACK, SSN/SSBN PATROL EVALUATION, P-3C FLIGHT TESTS,...)

TRACKING AND SURVEILLANCE

(ORBIT RECONSTRUCTION; SIGNAL PROCESSING, TRAJECTORY ESTIMATION,...; NNSS, ASW, GUN FIRE CONTROL,...)

CORRELATION GUIDANCE

(PERFORMANCE PROJECTIONS, REAL-TIME "MAP MATCHING", QUANTIFICATION OF SIGNATURE STRENGTH,...; SLCM, SUBMARINE NAVIGATION AID,...)

OTHER - FAILURE DETECTION, MODEL IDENTIFICATION,
COMMUNICATION ANALOGS,...

TASC

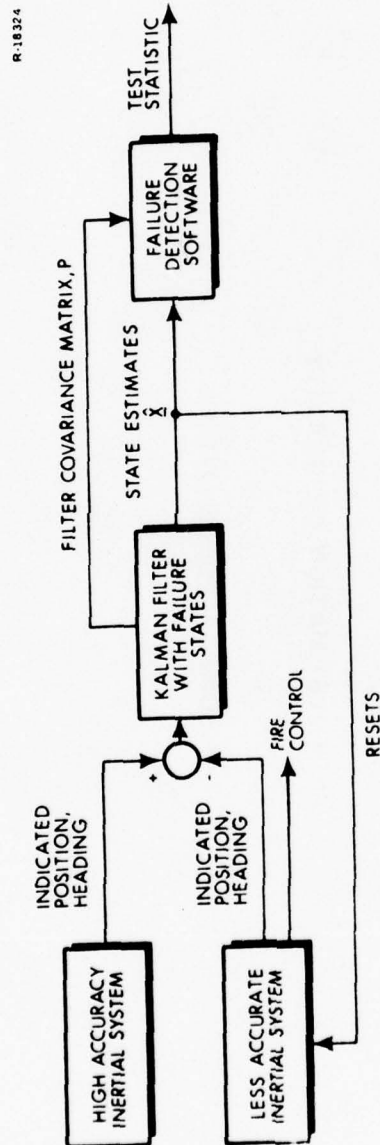
THREE

"NON-TRADITIONAL" EXAMPLES

- FAILURE DETECTION
- ESTIMATION OF GRAVITY
- OMEGA FORCE-FIT

FAILURE DETECTION FOR MULTIPLE NAVIGATION SYSTEMS

R-18324a



- PROVIDES FAULT MONITORING DURING INTERVALS BETWEEN EXTERNAL FIXES
- DESIGNED TO ISOLATE FAILURE MODES IN EITHER INERTIAL UNIT

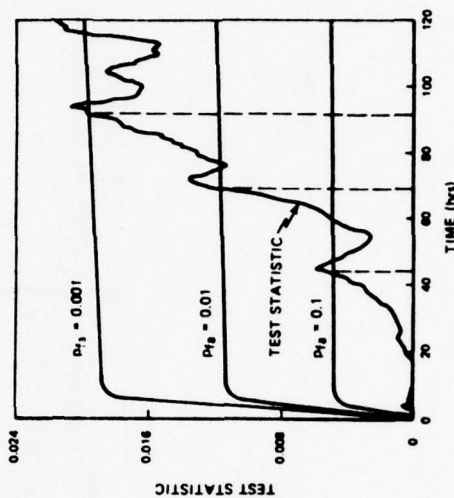
TASC

SIMULATION RESULTS FOR TASC FAILURE DETECTION ALGORITHM

CONDITIONS:

- DIRECT SIMULATION OF INERTIAL SYSTEM ERROR DYNAMICS
- GYRO RAMP FAILURE MODELED AT $t = 0$
- FAILURE DETECTION THRESHOLDS COMPUTED FOR 3 DIFFERENT PROBABILITIES OF FALSE ALARM (P_{fa})

459

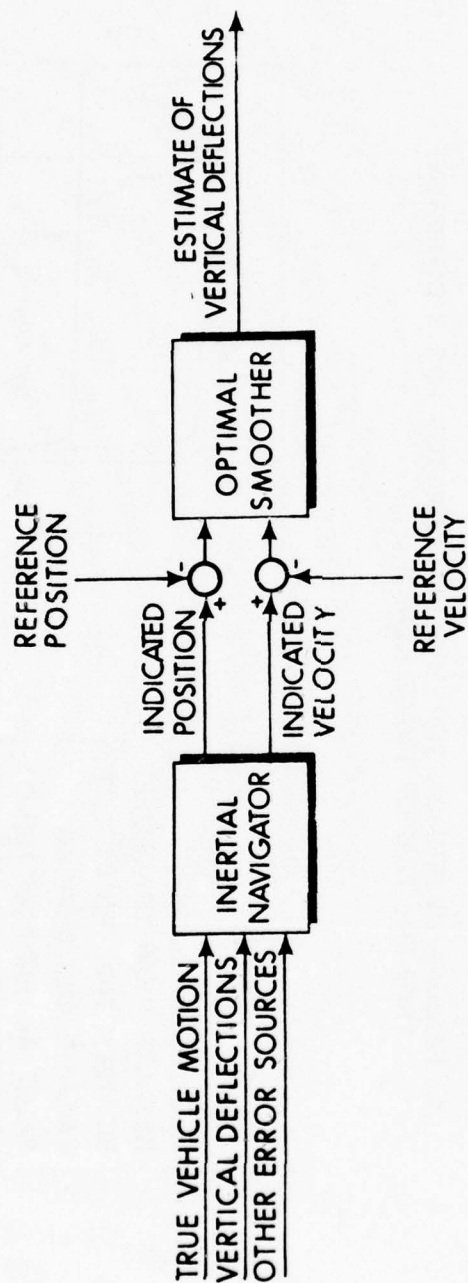


RESULTS SHOW TRADEOFF
BETWEEN TIME TO DETECT
FAILURE AND DESIRED
FALSE ALARM PROBABILITY

TASC

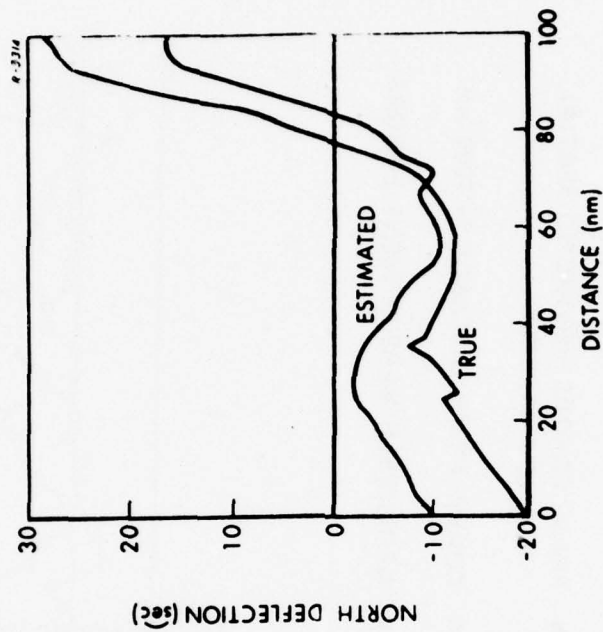
DIRECT RECOVERY OF GRAVITY

R-3308



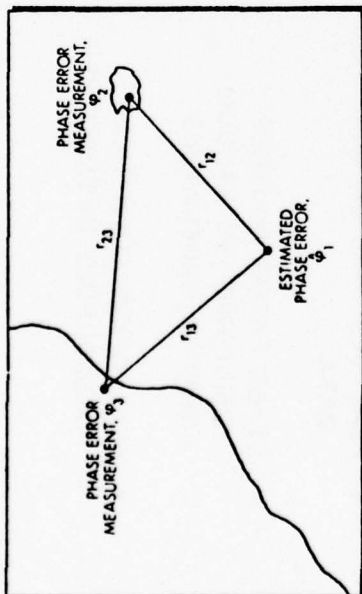
TYPICAL SIMULATION RESULTS

- HIGH QUALITY INS
- LORAN QUALITY POSITION REFERENCE
- EM LOG QUALITY VELOCITY REFERENCE
- REAL VERTICAL DEFLECTION DATA
- OTHER ERROR SOURCES SIMULATED BY RANDOM NUMBER GENERATORS
- DEFLECTION STATISTICS MISMODELED IN SMOOTHER



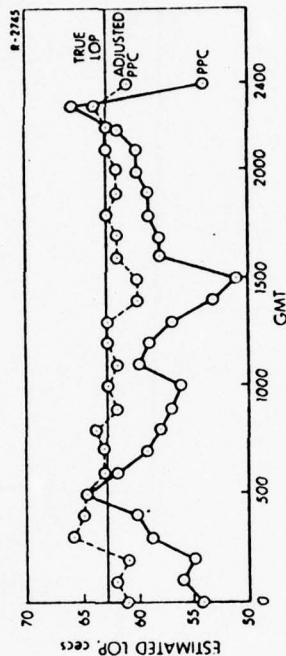
TASC

OMEGA FORCE-FIT PROPAGATION CORRECTIONS



- PHASE ERRORS—ISOTROPIC SPATIAL MARKOV PROCESS
- CORRELATION DISTANCE > 1000 nm
- NEGLIGIBLE MEASUREMENT ERRORS

- ESTIMATION RESULTS AT KINGS POINT, NY
- OVERALL REDUCTIONS IN RMS ERRORS OF 30–40%
- CURRENTLY IMPLEMENTED IN PUBLISHED CORRECTIONS



TASC

PROBLEMS AND AREAS FOR FURTHER RESEARCH

R-18326

- KALMAN FILTER REQUIREMENTS
AND IMPLEMENTATION DETAILS
- SUBOPTIMAL FILTER DESIGN
- MODULAR ESTIMATORS
- COMMUNICATION ANALOGS

KALMAN FILTER REQUIREMENTS

- EXACT KNOWLEDGE OF SYSTEM DYNAMICS
AND MEASUREMENT PROCESS (F, H)
- EXACT KNOWLEDGE OF ERROR SOURCE
STATISTICS (Q, R)
- EXACT KNOWLEDGE OF INITIAL COVARIANCES
- CONSIDERABLE COMPUTING CAPABILITY
(STORAGE, SPEED)

SOME NEW PROBLEMS POSED BY KALMAN FILTER SYSTEMS

R-18328

- IMPLEMENTATION DETAILS
- INPUT MODEL SELECTION
- SENSITIVITY
(A PRIORI VERSUS "REAL WORLD")

TASC

SUBOPTIMAL FILTER DESIGN APPROACHES

ORDER REDUCTION

HEURISTIC

OBSERVER THEORY

**MINIMUM VARIANCE REDUCED ORDER (MVRO)
OBSERVER/ESTIMATORS (ANALYSIS TOOL)**

STATISTICAL/DYNAMICAL UNCERTAINTY

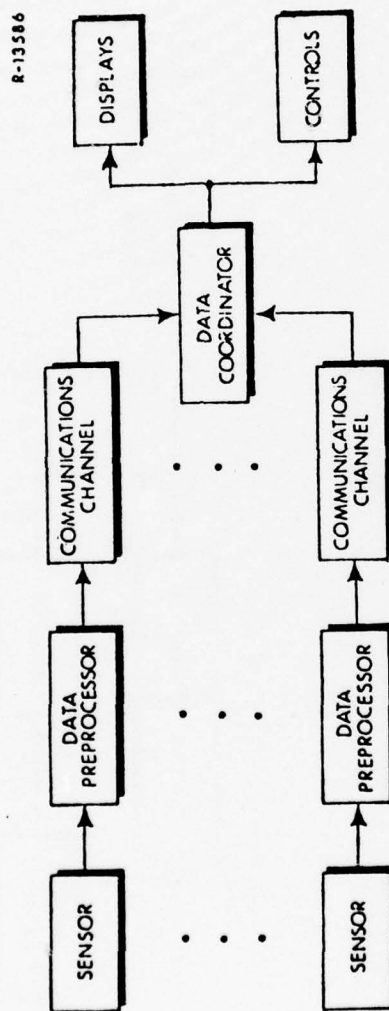
MINIMAX

BOUNDED NOISE

ADAPTIVE

TASC

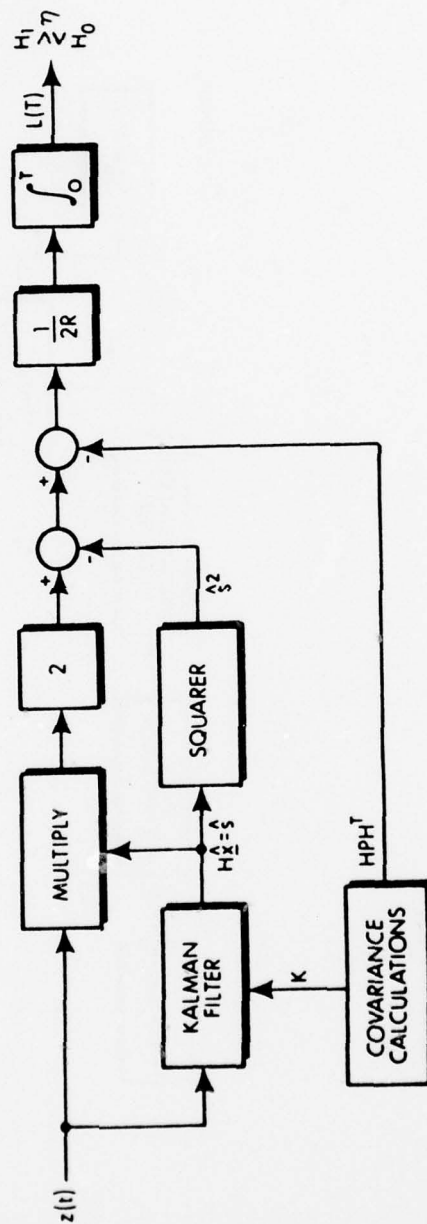
MODULAR ESTIMATION ARCHITECTURE



COMMUNICATION ANALOG EXAMPLE: BLOCK DIAGRAM OF OPTIMAL DETECTOR

(STATE-VARIABLE FORMULATION)

R-15609



CONTROL OF STABLE PROPORTIONAL NAVIGATION LAWS FOR MANEUVERING TASKS *

Roy B. Leipnik and Gary A. Hewer, Naval Weapons Center
and
Tyre Newton, Washington State University

The classic guidance law for missiles is proportional navigation (PN), which sets missile normal acceleration proportional to the line-of-sight rate (LOSR). If the missile sensor tends to be biased toward part of an extended target, the PN law is often counter-biased. When the target maneuvers, experience shows that PN and biased PN may become ineffective. The problem is to analyze and correct this.

Closer examination shows three obvious modifications of PN laws. First is to use higher derivatives of the LOSR. Second is to use other information, such as the lead angle and the angle of attack. Third is to compute the normal acceleration in a suitable reference frame. For a given guidance law, missile dynamics, and target behavior, two missile characteristics are desirable: controllability to a small miss-distance, and stability. These conflict to some extent. In this study, the three types of modifications of PN laws were considered as to miss-distance and stability, both by simulation and analytically for point targets. Exact solutions were derived (to obtain miss-distance) and Liapunov theory was applied (to obtain stability) for these nonlinear third-order differential equations. Analog and digital simulation were used to confirm and extend the theory.

The best results were obtained, for given PN constants, by using the normal acceleration in the line-of-sight frame rather than in the trajectory frame or the body-axis frame. Stability against arbitrary target maneuvers is maximized in this way. In fact, without saturation, stability then holds for arbitrary

* This paper was typed from a taped version of the oral presentation.

target maneuvers. Also, the missile velocity/target velocity ratio band for zero miss is larger in this frame.

Application of the derived results would be more confident if the actually sensed LOSR through the missile transfer function were used instead of the perfect or saturated-perfect LOSR. This depends strongly on missile design details and is difficult to handle in a general way, though of course computer simulation is available. An extension of Liapunov theory to handle sectoral stability in the parameter and initial-condition spaces would be quite helpful.

EXTENDING THE RANGE OF TACTICAL MISSILES
AGAINST JAMMING TARGETS

D.J. Yost and J.E. Kain
Applied Physics Laboratory
Johns Hopkins Road
Laurel, Maryland

ABSTRACT

The selection of missile guidance policies is in many cases governed by the types of electronic countermeasures (ECM) expected. One form of ECM is the standoff jammer whereby a specially equipped aircraft generates electromagnetic interference with sufficient power and appropriate frequency content so that missile fire control radar returns are unintelligible. This type of jamming as well as other forms of ECM has the effect of denying target range and range rate information to the intercept missile. Thus a missile designed to intercept a standoff or self-screening jammer must use a guidance policy which does not require missile-to-target range or range rate.

Though jamming may prevent target range and range rate measurement, target line-of-sight should be readily available as a missile guidance input. Thus an investigation has been undertaken to determine the feasibility of performing the midcourse guidance of the long range interceptor using only the passive angle data as observed from shipboard as well as from the interceptor. The problem of estimating range and range rate to the long range target was approached using the Extended Kalman Filter as well as the Second Order Gaussian Filter.

The mathematical model of this problem included a six state stochastic model for the target as well as noise states corresponding to the highly correlated interceptor inertial system errors. Monte Carlo results have indicated that the Extended Kalman Filter provides divergent estimates in some cases, yet the Second Order Gaussian Filter provides good results predictable through covariance analysis.

INTRODUCTION

The selection of missile guidance policies is in many cases governed by the types of electronic countermeasures (ECM) expected. One form of ECM is the standoff jammer whereby a specially equipped aircraft remains outside the effective missile intercept range and generates electromagnetic interference with sufficient power and appropriate frequency content so that missile fire control radar returns are unintelligible. Since the jammer power required is proportional to range squared while fire control radar power required is proportional to range to the fourth power, the jammer is at an advantage. Thus the intercept missile must be designed to deal with the problems posed by the standoff jammers as well as the higher performance self-screening jammer.

The jamming described above as well as other forms of ECM has the effect of denying target range and range rate information to the intercept missile. Thus, a missile designed to intercept a standoff or self-screening jammer must use a guidance policy that does not require missile to target range or range rate.

Though jamming may prevent target range and range rate measurement, target line of sight (LOS) should be readily available as a missile guidance input. Typically, a modified form of proportional navigation where missile normal accelerations are commanded proportional to missile velocity and missile to target LOS rate is used in an ECM environment. This type of guidance is effective at short ranges, but it does not provide the necessary trajectory shaping for long range intercepts.

In a clear environment where the target position and velocity are available on an uplink from the fire control radar, a midcourse guidance mode is available that shapes

the missile trajectory to place the missile close enough to the long range target so that proportional navigation or some other terminal guidance mode may be used. When the missile is restricted to fly proportional navigation over its entire trajectory, the maximum intercept range may be reduced by as much as a factor of two. If no alternate guidance is available, this allows the jammer to stand off at a range considerably less than the maximum clear environment missile intercept range and thus reduces the jamming power required by as much as a factor of four (Fig. 1).

One means of intercepting the long range standoff or self-screening jammer is to use existing midcourse guidance policies but generate estimates of target positions and velocities using only target LOS data. The target LOS should be available from the missile as well as the launch point (designated as a ship). This information, together with the missile position relative to the ship, might be used to solve a triangulation problem and thus to estimate the target location. Target velocity could be estimated by appropriately filtering the position estimate.

Another approach to target estimation is to utilize optimal filtering techniques. The approximate nonlinear optimal filters evaluated here make use of a stochastic model of the target and measurements and offers a considerable improvement in accuracy over the basic triangulation estimate.

In this paper the triangulation estimate, the extended Kalman filter and the Gaussian second-order filter are evaluated as target position and velocity estimators. An attempt was made to consider all potential measurement error sources including the easily modeled uncorrelated errors as well as the highly correlated errors due to the missile inertial system uncertainties. In all cases where specific values are required, data which reflects typical long range intercept missiles is used.

Additional studies including implementation considerations, effects on homing performance, and sensitivity studies are included in Ref. 1.

THE MISSILE DEFINITION

Before discussing the estimation problem, the nominal missile for which the majority of our studies were performed will be described. The missile will be assumed capable of long range intercepts on the order of 100 nmi. A typical long range trajectory which is the trajectory used for much of the analysis is presented in Fig. 2. The missile altitude is given by the following polynomial in time; i. e.,

$$y_m = -0.008t^2 + 1.7t \text{ (kft)} .$$

The missile was assumed to maintain a constant downrange velocity of 2.7 kft/s.

A seeker onboard the missile will be used to track the missile to target LOS in a missile-referenced coordinate system. The pointing errors caused by seeker measurements were assumed zero mean and uncorrelated in time with a data rate of 1 Hz and an rms error of 0.5° .

The missile contains an inertial reference unit (IRU) for determining missile position as well as for determining the inertial missile to target LOS. The error specifications associated with the IRU are given in Table 1.

Table 1
Nominal IRU Errors

IRU Errors	Symbol	rms Error
Gyro drift	\dot{A}	$10^\circ/\text{h}$
Initial attitude uncertainty	A_0	0.5°
Instrument dependent Position drift (per axis)	$\dot{\epsilon}_x$ $\dot{\epsilon}_y$	6 ft/s

The ship from which the missile was launched is assumed to track the target LOS to within a zero mean uncorrelated error with an rms of 4 mrad and a data rate of 1 Hz.

The nominal data processing rate was chosen as 1 Hz. The data may be processed either onboard the missile (requiring only an uplink) or onboard the ship (requiring both an uplink and downlink). From the standpoint of ECM, an uplink is far more reliable than a downlink and makes the missile processing more attractive.

THE MEASUREMENT MODELS

The studies performed here will be restricted to the vertical plane analysis; i.e., the ship, missile, and target will be constrained to remain in a vertical plane.

The vertical plane target LOS angles from the ship and target (σ_s and σ_m , respectively) are shown in Fig. 3 along with the missile and target cartesian position (x_m , y_m) and (x_T , y_T), respectively.

The ship to target and missile to target LOS angles σ_s and σ_m are given by

$$\sigma_s = \tan^{-1} \left(\frac{y_T}{x_T} \right) \quad (1)$$

and

$$\sigma_m = \tan^{-1} \left(\frac{y_T - y_m}{x_T - x_m} \right) . \quad (2)$$

The measured LOS angles σ'_s and σ'_m are modeled by

$$\sigma'_s = \tan^{-1} \left(\frac{y_T}{x_T} \right) + \eta_s \quad (3)$$

and

$$\sigma'_m = \tan^{-1} \left(\frac{y_T - y_m}{x_T - x_m} \right) + A_o + \dot{A} * t + \eta_m, \quad (4)$$

where t represents the time from missile launch, and η_s and η_m are the uncorrelated measurement errors with nominal statistics:

$$E(\eta_s) = E(\eta_m) = 0$$

$$E(\eta_s^2) = (0.004)^2 \text{ rad}^2$$

$$E(\eta_m^2) = (0.0057)^2 \text{ rad}^2.$$

The terms involving A_o and \dot{A} are the effects of inertial system errors on the measured missile to target LOS angle.

The measured values for missile position (x'_m , y'_m) are modeled as follows:

$$x'_m = x_m + \dot{\epsilon}_x * t - A_o * y_m \quad (5)$$

$$y'_m = y_m + \dot{\epsilon}_y * t + A_o * x_m. \quad (6)$$

There is assumed to be an independent linear time drift on each axis because of IRU instrument errors plus a term proportional to the initial attitude uncertainty. The initial attitude error tends to rotate the measured position from the actual position so that the position error owing to initial attitude error is orthogonal to the actual position vector (for small rotations). The initial attitude error magnitudes assumed here dominate the position error. For example at the nominal intercept, the one sigma missile altitude error owing to instrument uncertainty is 1.2 kft while the error associated with the initial attitude uncertainty is 4.7 kft.

It should be recognized that the inertial system errors represented in Eqs. (4), (5), and (6) are approximations of the actual errors. These expressions will nevertheless be used to generate what shall be considered "actual" measurements for the purpose of Monte Carlo studies.

In an attempt to develop an optimal filter for estimating the target states that accounts for the inertial system errors, one approach is to estimate the parameters A_0 , \dot{A} , $\dot{\epsilon}_x$, and $\dot{\epsilon}_y$ of Eqs. (4), (5), and (6). This would increase the number of states to be estimated by four and in practice might yield poor or even divergent estimates because of the modeling errors inherent in Eqs. (4), (5), and (6).

A more realistic measurement model might approximate A_0 , \dot{A} , $\dot{\epsilon}_x$, and $\dot{\epsilon}_y$ as first-order random processes with large time constants and empirically determined rms levels. This has the effect of "keeping the filter gains open" and masking the effects of system modeling errors. This approach would again increase the filter order by four states.

A model for the measured missile to target LOS which reflects the inertial system errors while adding only a single state is given by

$$\sigma_m'' = \tan^{-1} \left(\frac{y_T - y_m'}{x_T - x_m'} \right) + \frac{\beta}{R_{MT}} + \eta_m \quad (7)$$

and

$$\dot{\beta} = \eta_\beta - \beta/\tau_\beta \quad (8)$$

The term R_{MT} is the missile to target range, while the time constant τ_β and the strength of the white noise process η_β define the first order Markov process β . By equating σ_m' to σ_m'' , one finds that the stochastic process β/R_{MT} must represent the variable Z as defined by Eq. (9).

$$Z = \tan^{-1} \left(\frac{y_T - y_m}{x_T - x_m} \right) - \tan^{-1} \left(\frac{y'_T - y'_m}{x'_T - x'_m} \right) + A_0 + \dot{A} * t. \quad (9)$$

The random time function Z is defined by and summarizes the effect of the inertial system errors on the missile to target LOS. By selecting quantities with the appropriate statistics to represent A_0 , \dot{A} , $\dot{\epsilon}_x$, and $\dot{\epsilon}_y$, the random function Z can be computed over a given missile and target trajectory. Ten such samples of Z are shown in Fig. 4 using the statistics of Table 1 and the trajectory of Fig. 2. If the samples of Fig. 4 are multiplied by R_{MT} , Fig. 5 is the result. The random process $Z * R_{MT}$ was modeled by the first-order Markov process of Eq. (8). The time constant τ_β and the rms of β were selected as 400 seconds and 3 kft, respectively.

To develop the optimal filter, Eqs. (3) and (7) will be used to describe the measurements. The use of Eq. (7) to represent the missile to target LOS measurement lies primarily in its simplicity, but, also, the stochastic nature of the process β/R_{MT} should compensate for modeling errors inherent in Eqs. (4), (5), and (6).

THE TRIANGULATION ESTIMATE

One estimator for target position is the triangulation estimate. This simple estimator will be evaluated in order to show the improvement realized when optimal filtering theory is applied. In the vertical plane, the triangulation estimate is obtained by solving Eqs. (1) and (2) for x_T and y_T and approximating actual values of σ_m , σ_s , x_m , and y_m with measured values. The triangulation estimate (\hat{x}_T , \hat{y}_T) is given by

$$\hat{x}_T = \frac{x'_m \tan(\sigma'_m) - y'_m}{\tan(\sigma'_m) - \tan(\sigma'_s)} \quad (10)$$

and

$$\hat{y}_T = \hat{x}_T \tan(\sigma'_s) . \quad (11)$$

The evaluation of this nonlinear estimator in terms of the statistics of the required measurements can be done approximately using linearized covariance analysis. By defining

$$\hat{Y} = (\hat{x}_T, \hat{y}_T) \quad (12)$$

$$X = (x'_m, y'_m, \sigma'_m, \sigma'_s) , \quad (13)$$

Eqs. (10) and (11) can be written vectorially as

$$\hat{Y} = F(X) . \quad (14)$$

The covariance of \hat{Y} is approximated by

$$E[\hat{Y} - Y] (\hat{Y} - Y)^T = \frac{\partial F}{\partial X} E[X - \bar{X}] (X - \bar{X})^T \frac{\partial F^T}{\partial X} \quad (15)$$

$$P_{\hat{Y}} = \frac{\partial F}{\partial X} P_X \frac{\partial F^T}{\partial X} , \quad (16)$$

where $E[\]$ is the expected value of $[\]$, \bar{X} is the mean value of X , and $P_{\hat{Y}}$ and P_X are the covariance of \hat{Y} and X , respectively. The partial derivative $\partial F / \partial X$ has elements defined by

$$\left[\frac{\partial F}{\partial X} \right]_{ij} = \frac{\partial F_i}{\partial X_j} \quad (17)$$

The computations implied by Eqs. (16) were performed and the results verified by Monte Carlo simulation. The nominal missile and target were again used. Figures 6 and 7 show typical results.

Figure 6 shows that poor downrange estimation accuracy is to be expected during the early stages of flight prior to about 60 seconds. The triangle formed by the ship missile and target is very flat in this region making triangulation difficult. During the latter half of flight, downrange estimates are accurate to about 20 kft rms while altitude estimate errors (Fig. 7) are approximately 2 kft rms.

Note that, in order to use these estimates to generate acceleration commands, filtering would be required to generate a target velocity estimate as well as smoothed missile acceleration commands.

Note that optimal filtering could be applied at this point by assuming that Eqs. (10) and (11) defined "measurements" with statistics computed according to Eq. (15). This approach requires that all measurements in the vector X be available simultaneously so that the transformation $F(X)$ can be performed — a restriction removed using the more direct filter formulation to be discussed later.

AD-A045 603

SYSTEMS CONTROL INC PALO ALTO CALIF
PROCEEDINGS OF THE SYMPOSIUM ON CONTROL THEORY AND NAVY APPLICA--ETC(U)
AUG 77 M D CILETTI, J S TYLER

F/G 15/7

N00014-72-C-0327

NL

UNCLASSIFIED

6 of 8
ADA045603



THE STOCHASTIC TARGET MODEL

In order to develop a filter providing more accurate target position estimates as well as velocity estimates, a dynamic target model is required. The estimator should be capable of handling a variety of target trajectories, so a stochastic model is preferred.

The target acceleration along the vertical and horizontal directions are treated as independent first-order Markov processes. This yields the six-state target model of Eqs. (18) through (23):

$$\dot{A}_x = -A_x/\tau_x + \eta_{A_x} \quad (18)$$

$$\dot{A}_y = -A_y/\tau_y + \eta_{A_y} \quad (19)$$

$$\dot{V}_x = A_x \quad (20)$$

$$\dot{V}_y = A_y \quad (21)$$

$$\dot{x}_T = V_x \quad (22)$$

$$\dot{y}_T = V_y \quad (23)$$

The parameters required for defining this target are the statistics of the target states at time zero, the strengths of the white noise processes η_{A_x} and η_{A_y} , and the acceleration time constants τ_x and τ_y . The time constants τ_x and τ_y were selected as 20 seconds, and the initial target position and velocity standard deviations are given in Table 2.

Table 2
Initial Target State Standard Deviations

Target State	Standard Deviation at t = 0
Altitude	10 kft
Range	200 kft
Altitude rate	100 ft/s
Range rate	1000 ft/s

Since the target velocity and position states are non-stationary, some analysis is necessary to select appropriate white noise strengths so that target position and velocity states near intercept (taken here as 200 seconds) are reasonable.

The variances of the target states as a function of time can be computed by solving the differential equation for the propagation of the covariance matrix of the linear system given by Equations 18-23.

The approximate target altitude variance ($\sigma_{y_T}^2$) is given by

$$\sigma_{y_T}^2(t) = \sigma_{y_T}^2(0) + \sigma_{v_y}^2(0) t^2 + \sigma_{A_y}^2 * (2/3 \tau_y t^3 - \tau_y^2 \tau^2 + 2 \tau_y^4) \quad (24)$$

where the strength of the white noise process η_{Ay} is computed to force the y axis acceleration variance to be constant in time. A similar equation is valid for the downrange target state.

The target position and velocity standard deviations at $t = 200$ seconds for two values of rms target acceleration are shown in Table 3.

Table 3
Target State Standard Deviations Near Intercept

Target State	Target rms Acceleration	
	2.14 ft/s ²	21.4 ft/s ²
Altitude	23.5 kft	75.6 kft
Range	283 kft	292 kft
Altitude rate	224 ft/s	2000 ft/s
Range rate	1020 ft/s	2240 ft/s

Table 3 shows that for the initial state variances of Table 2 a target rms acceleration of 21.4 ft/s² (2/3 g) produces unrealistic target state standard deviations after 200 seconds. The value chosen for target rms acceleration for the purpose of filtering was 2.14 ft/s² or 0.0667 g.

THE NONLINEAR FILTERING PROBLEM

The target state estimation problem can now be placed in the format required by the modern optimal estimation techniques. Define the estimator state vector to be

$$X = \begin{bmatrix} A_x \\ A_y \\ V_x \\ V_y \\ x_T \\ y_T \\ \beta \end{bmatrix} \quad (25)$$

The state dynamics in continuous form are given by

$$\dot{X} = \begin{bmatrix} -1/\tau_x & 0 & 0 & 0 & 0 & 0 & 0 \\ 0 & -1/\tau_y & 0 & 0 & 0 & 0 & 0 \\ 1 & 0 & 0 & 0 & 0 & 0 & 0 \\ 0 & 1 & 0 & 0 & 0 & 0 & 0 \\ 0 & 0 & 1 & 0 & 0 & 0 & 0 \\ 0 & 0 & 0 & 1 & 0 & 0 & 0 \\ 0 & 0 & 0 & 0 & 0 & 0 & -1/\tau_\beta \end{bmatrix} X + \begin{bmatrix} \eta_{Ax} \\ \eta_{Ay} \\ 0 \\ 0 \\ 0 \\ 0 \\ \eta_\beta \end{bmatrix} \quad (26)$$

The measurement vector available at times t_i designated as Y is given by

$$Y_i = \begin{bmatrix} \tan^{-1} \frac{(X_6 - y'_m)}{(X_5 - x'_m)} + \frac{X_7}{R_{MT}} + \eta_{mi} \\ \tan^{-1} \left(\frac{X_6}{X_5} \right) + \eta_{si} \end{bmatrix} \quad (27)$$

where (x'_m, y'_m) is the measured missile position and η_{mi} , η_{si} are independent zero mean Gaussian sequences.

Though optimal filters for continuous systems with discrete measurements are available in the literature the approach used here will be to first discretize the continuous dynamics and use the fully discrete optimal filters.

The discretization of the system of Equation (26) is given by Equation 28.

$$X_{i+1} = \begin{bmatrix} e^{-T/\tau_x} & 0 & 0 & 0 & 0 & 0 & 0 \\ 0 & e^{-T/\tau_y} & 0 & 0 & 0 & 0 & 0 \\ T & 0 & 1 & 0 & 0 & 0 & 0 \\ 0 & T & 0 & 1 & 0 & 0 & 0 \\ T^2/2 & 0 & T & 0 & 1 & 0 & 0 \\ 0 & T^2/2 & 0 & T & 0 & 1 & 0 \\ 0 & 0 & 0 & 0 & 0 & 0 & e^{-T/\tau_\beta} \end{bmatrix} X_i + \begin{bmatrix} \omega_x \\ \omega_y \\ 0 \\ 0 \\ 0 \\ 0 \\ \omega_\beta \end{bmatrix}_i \quad (28)$$

where T is the sample period or the measurement data interval.

The statistics of the zero mean uncorrelated sequences ω_{xi} , ω_{yi} , $\omega_{\beta i}$ are given by

$$E(\omega_{xi}^2) = (1 - e^{-2T/\tau_x}) (0.00214 \text{ kft/s}^2)^2$$

$$E(\omega_{yi}^2) = (1 - e^{-2T/\tau_y}) (0.00214 \text{ kft/s}^2)^2$$

$$E(\omega_{\beta i}^2) = (1 - e^{-2T/\tau_\beta}) (3 \text{ kft})^2.$$

The estimation problem described by Equations 27 and 28 has discrete linear state dynamics and discrete nonlinear measurements. This problem falls into the class of nonlinear filtering problems frequently approached using the extended Kalman filter. When the extended Kalman filter fails to provide satisfactory results the second order Gaussian filter (Ref. 2) is available. Since the estimation problem described above has linear dynamics, only the "measurement processing" portion of the second order Gaussian filter is required.

The computations necessary for the extended Kalman filter and the second order filter are given below.

$$\tilde{X}_{i+1} = \Phi_i \hat{x}_i \quad (29)$$

$$P_{i+1}^- = \Phi_i P_i^+ \Phi_i^T + Q \quad (30)$$

$$K_{i+1} = P_{i+1}^- \frac{\partial H^T}{\partial X} \left[\frac{\partial H}{\partial X} P_{i+1}^- \frac{\partial H^T}{\partial X} + R + L \right]^{-1} \quad (31)$$

$$\hat{x}_{i+1} = \tilde{X}_{i+1} + K_{i+1} [Y - H(\tilde{X}_{i+1}) + \mu] \quad (32)$$

$$P_{i+1}^+ = \left[I - K_{i+1} \frac{\partial H}{\partial X} \right] P_{i+1}^- \quad (33)$$

The following linear dynamics are assumed:

$$X_{i+1} = \Phi_i X_i + \eta_i ; E[\eta_i \eta_j^T] = Q \delta_{ij}^* \quad (34)$$

and the discrete nonlinear measurement

$$Y_i = H(X_i) + \omega_i ; E[\omega_i] = 0 ; E[\omega_i \omega_i^T] = R ,$$

where ω_i is a vector of independent zero mean Gaussian sequences.

The computations for the extended Kalman filter consist of Eqs. (29) through (33) with

$$L_{ij} = 0 ; \mu_i = 0 ; \text{ for all } i \text{ and } j .$$

For the second-order Gaussian filter

$$\mu_i = \frac{1}{2} \sum_{j=1}^n \sum_{k=1}^n \frac{\partial^2 H_i}{\partial X_j \partial X_k} P_{jk}^- \quad (35)$$

$$L_{ij} = \frac{1}{2} \sum_p^n \sum_q^n \sum_r^n \sum_s^n \frac{\partial^2 H_i}{\partial X_p \partial X_q} \frac{\partial^2 H_j}{\partial X_r \partial X_s} P_{pr}^- P_{qs}^- . \quad (36)$$

At first glance Equations 35 and 36 appear quite formidable. In particular the computations required for L_{ij} increase as n^4 for an n th order state vector. This is significant when one considers that in general the computation of the extended Kalman filter is proportional to n^3 and lower powers of n . (Ref. 3) Thus for large n the L_{ij} computation may dominate the filter computational requirements.

* δ_{ij} is the Kronecker delta function.

When the measurement equation is a function of only two states (say r and s) the computation can be reduced significantly. Equations 35 and 36 can be reduced to

$$\mu_1 = \frac{1}{2} \left(\frac{\partial^2 H_1}{\partial X_r \partial X_s} P_{rr}^- + \frac{\partial^2 H_1}{\partial X_r \partial X_s} P_{rs}^- + \frac{\partial^2 H_1}{\partial X_s \partial X_s} P_{ss}^- \right) \quad (37)$$

$$L_{ij} = \frac{1}{2} \left(P_{rr}^- P_{ss}^- - P_{rs}^2 \right) \left(2 \frac{\partial^2 H_1}{\partial X_r \partial X_s} \frac{\partial^2 H_j}{\partial X_r \partial X_s} - \frac{\partial^2 H_i}{\partial X_r \partial X_s} \frac{\partial^2 H_j}{\partial X_r \partial X_s} - \frac{\partial^2 H_i}{\partial X_s \partial X_s} \frac{\partial^2 H_j}{\partial X_r \partial X_r} \right) + 2\mu_i \mu_j \quad (38)$$

These additional computations are insignificant when compared to the seven state extended Kalman filter computations.

An additional simplification as suggested by Choe (Ref. 4) which will be investigated is an approximation of Equation 36 by

$$L_{ij} = 2\mu_i \mu_j$$

In order to evaluate the performance of these filters the statistics of the estimate errors are required. If the measurement equation were linear, the covariance after measurement (P^+) from Equation 33 would be used. The square root of the diagonal elements of this matrix yields the standard deviation of the state estimate errors. The filters described above are derived from expansions of the nonlinear measurement equation about the estimate of the state prior to measurement (\hat{X}_{1+1}). Therefore the covariance matrix after measurement as computed by Equation 33 is only an approximation.

Thus in order to evaluate the nonlinear filters an additional computation must be made of the state estimation error statistics. This is accomplished via Monte Carlo methods whereby statistically accurate measurements are processed to generate realizations of the target state estimates and the associated errors over a typical missile and target trajectory. From a number of such error histories the ensemble statistics (mean and standard deviations) are computed. These statistics may be compared with those predicted by the nonlinear filter. Good correlation between the Monte Carlo and filter predicted standard derivations is an indication that the nonlinear functions involved are sufficiently smooth in the region about the actual states so that the nonlinear filter yields a "near" optimal estimate.

NONLINEAR FILTERING RESULTS

For the Monte Carlo studies discussed here the actual target and missile trajectories were fixed while generating each of the state error histories. The initial state estimates and the measurement error sequences are selected based on their prescribed statistics.

The Monte Carlo study with fixed target trajectory was performed using an intercept scenario similar to that shown by Figure 2, i.e., the target is incoming at 20 Kft altitude and 1000 ft/sec velocity and is intercepted at 200 seconds from missile launch. Simulated measurements based on statistical realizations of Equation 3-6 were computed over the missile flight at a 1 hz data rate. Twenty-five measurement histories were generated together with the corresponding target state estimates for the purpose of computing the Monte Carlo statistics.

For initialization of the filter, it was assumed that prior to missile launch an estimate of the target states was available with mean value equal to the actual value and standard deviations as given by Table 2.

Some results from the Monte Carlo analysis for the extended Kalman filter are seen in Figures 8-9. Note that the downrange target position (Figure 8) and velocity (Figure 9) Monte Carlo statistics differ markedly from the extended Kalman filter prediction.

From an inspection of the individual trajectories it was discovered that by "removing" several of the "poor" estimate histories from the Monte

Carlo computation, good agreement between the predicted and computed statistics could be obtained. Also in most cases the poor target estimate histories coincided with large initial target position errors. This is an indication that the region of measurement equation linearity is not sufficiently large to include the region of probable target state estimates early in missile flight. This problem can be overcome to some extent by providing more accurate initial target estimates.

In order to improve the region of acceptable filter performance the second order Gaussian filter was applied. Based on the experimental results with the particular nonlinear estimation problem investigated in Ref (2) it would appear that the major improvement from using the second order Gaussian filter would come from only the bias compensation term (μ).

In Ref (3) the opposite effect is noticed, i.e., the improvement is attributed solely to the gain compensation term (L). When the second order Gaussian filter is applied to the problem presented here, both nonlinear terms effect the estimation accuracy. When only the bias compensation term (μ) is added to the filter equations and the identical measurement sequences used in generating Figures 8 and 9 are processed, the divergent cases noted with the extended Kalman filter did not appear. The downrange filter performance with only the bias compensation term is shown in Figure 10. Note that the Monte Carlo standard deviation is higher than the predicted standard deviation. When the complete second order Gaussian filter was implemented the correlation of Figures 11-14 was observed. These four figures show the Monte Carlo standard deviations in good agreement with (or below) the filter predictions for both downrange and vertical positions and velocities.

It should be noted that the filter used by Choe in Ref (4) was somewhat different from the filter derived by Athens in Ref (2). Choe approximates the gain compensation term (L) by;

$$L_{ij} \approx 2\mu_i\mu_j \quad (39)$$

rather than using Equation 36. When the approximation of Equation 39 is used with the estimator discussed here the results are identical to Figures 11-14.

It should also be noted that the estimator performance as indicated by Figures 11-14 not only represents an evaluation of the particular filtering algorithms but also verifies the use of Equation 7 as an approximation to the measurement model.

As with the triangulation estimate the target estimation accuracy is poor early in flight but improves as intercept approaches to a more or less steady state value. Note that the optimal filtering technique has improved the position estimation by more than a factor of three as well as provided a filtered velocity estimate.

CONCLUSIONS

This paper has presented a possible solution to a problem of ever increasing importance in the light of advances in modern warfare - namely missile long range guidance without target range data. The target state estimation accuracy achieved using the Gaussian second-order filter to process the available target line-of-sight measurements should be sufficient to provide adequate intercept probabilities.

The advantages of modern filtering techniques are demonstrated by the significant improvement in estimation accuracy as compared with a more classical estimation approach. It is also shown that for the nonlinear multiple-measurement filtering problem, presented here, the complete Gaussian second order filter provides improved performance over the extended Kalman filter as well as the extended Kalman filter with a nonlinear bias correction term.

REFERENCES

1. J. E. Kain and D. J. Yost, "Extending the Intercept Range of Tactical Missiles Against Jamming Targets", TG-1264, February 1975.
2. M. Athans, R. P. Wishner and A. Bertolini, "Suboptimal State Estimation for Continuous Time Nonlinear Systems from Discrete Noisy Measurements"; 1968 Joint Automatic Control Conference, Ann Arbor, Michigan, June 1968, pp 364-382.
3. J. M. Mendel, "Computational Requirements for a Discrete Kalman Filter", IEEE Transactions on Automatic Control, Vol. AC-16, No. 6, December 1971, pp 748-758.
4. B. D. Tapley and C. Y. Choe, "Nonlinear Estimation Theory Applied to the Interplanetary Orbit Determination Problem", Third Symposium on Nonlinear Estimation Theory and its Applications, September 1972, pp 239-245.

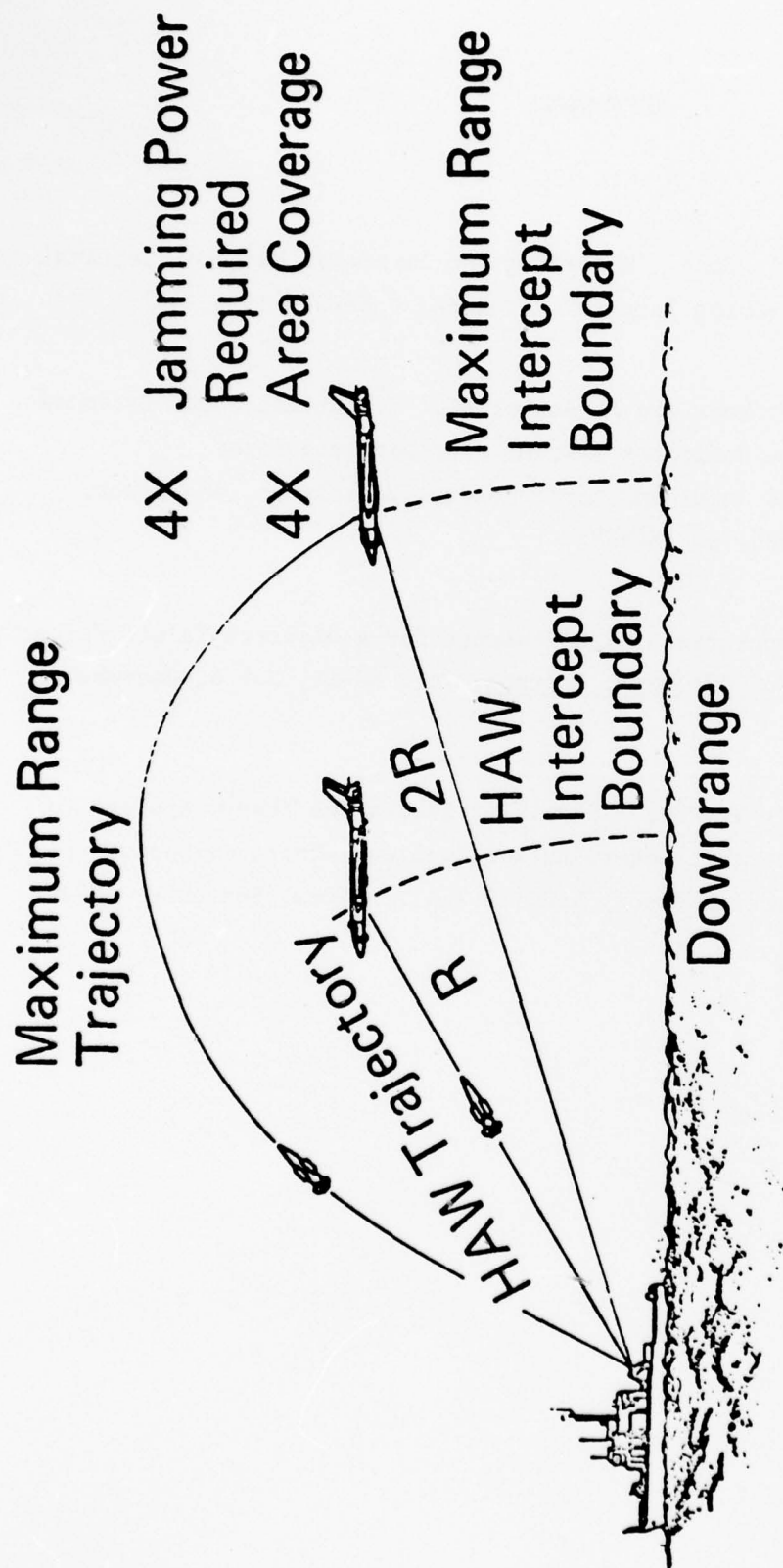


FIG. 1 Extended Intercept Range for Jamming Targets

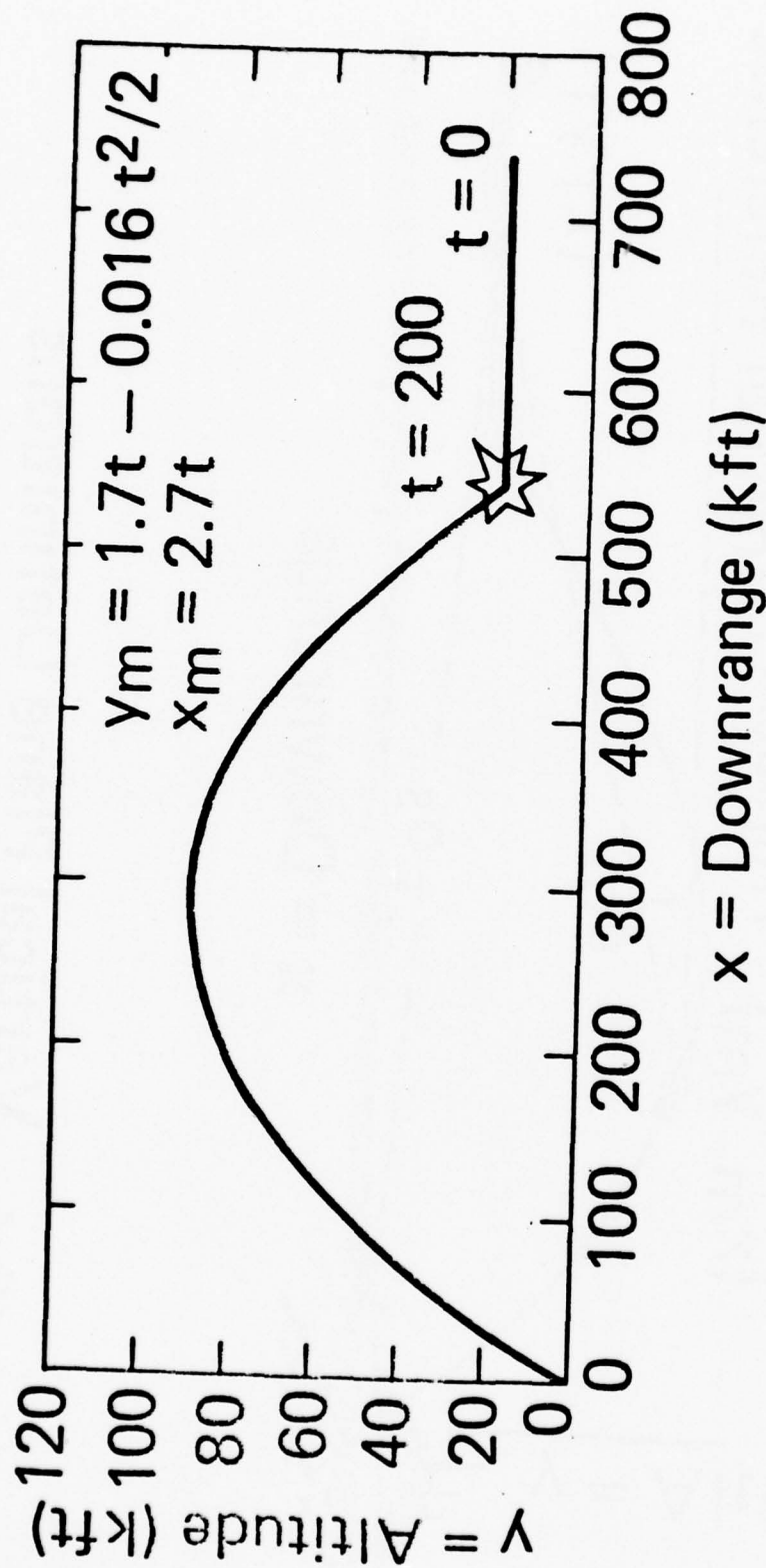


FIG. 2 Missile Intercept Trajectory for 1000 ft/s Incoming Target

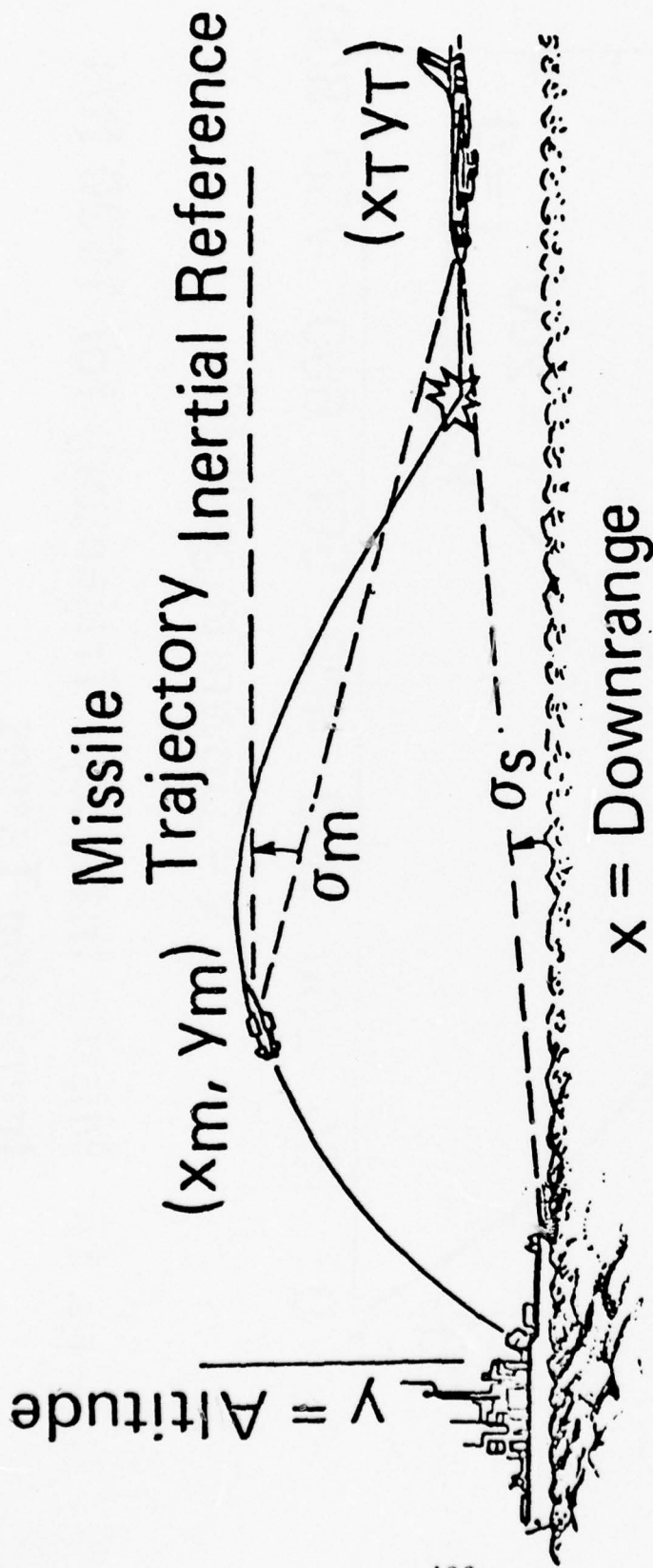


FIG. 3 Vertical Plane Definitions

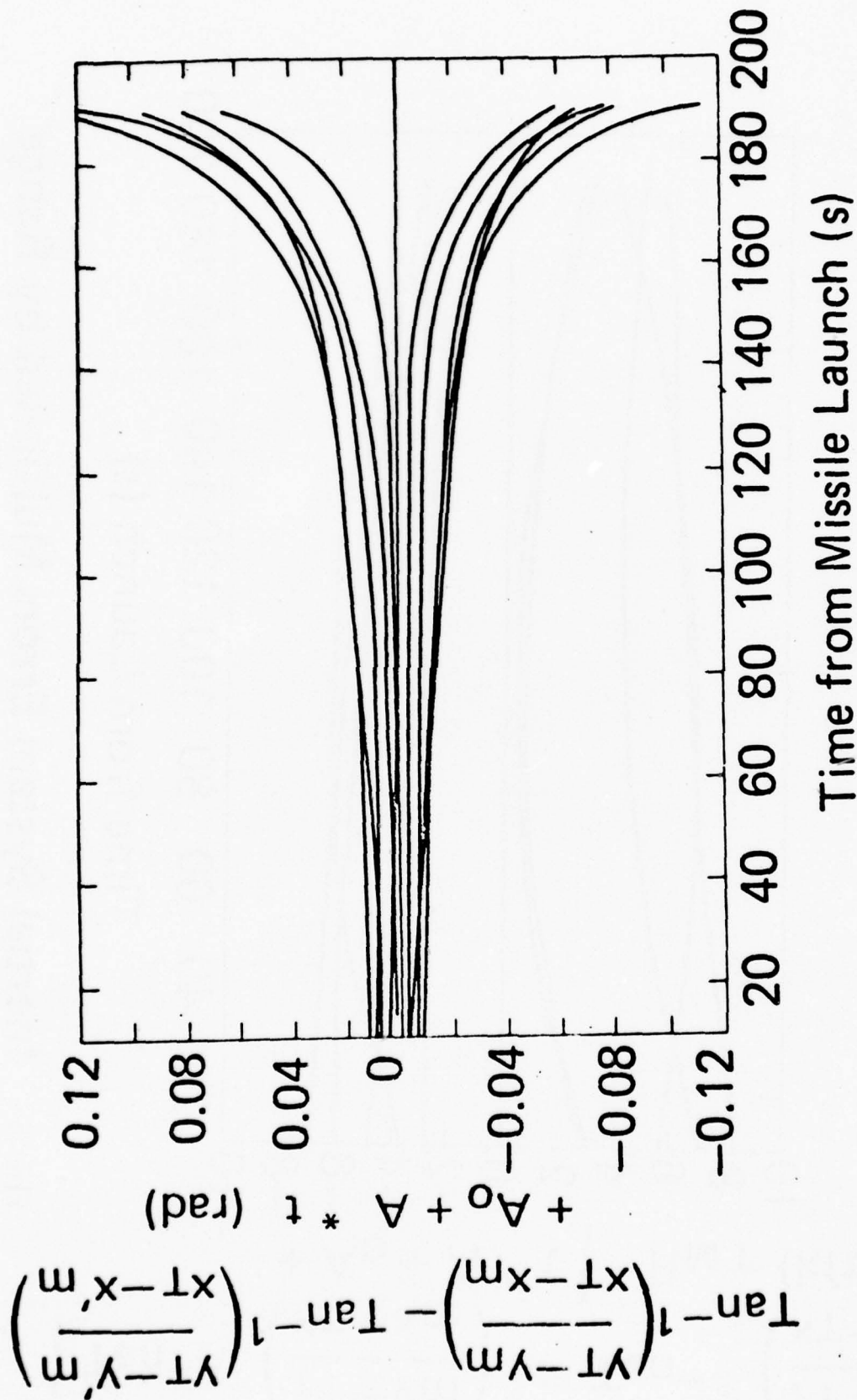


FIG. 4 Inertial System Errors

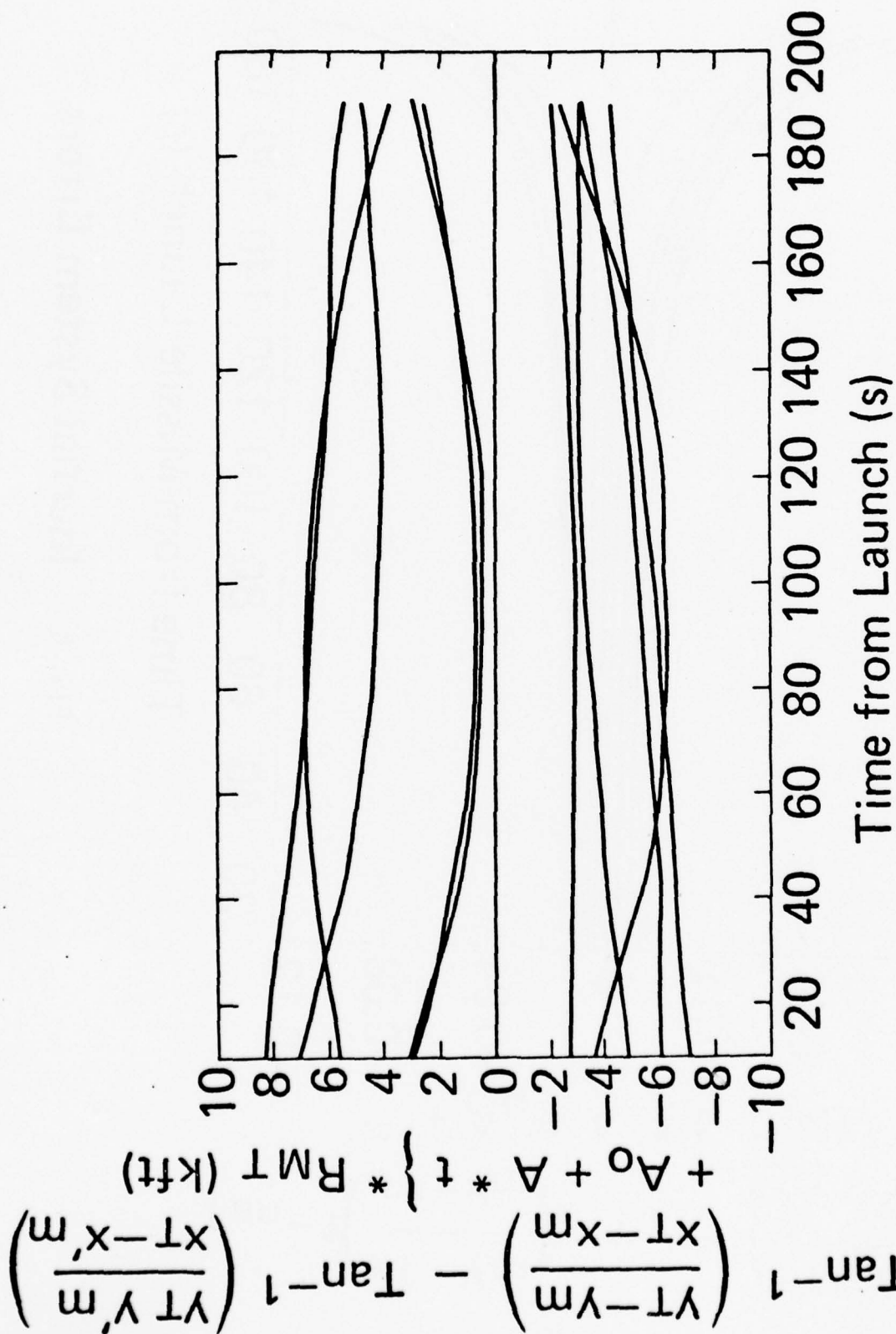


FIG. 5 Inertial System Errors Multiplied by Range

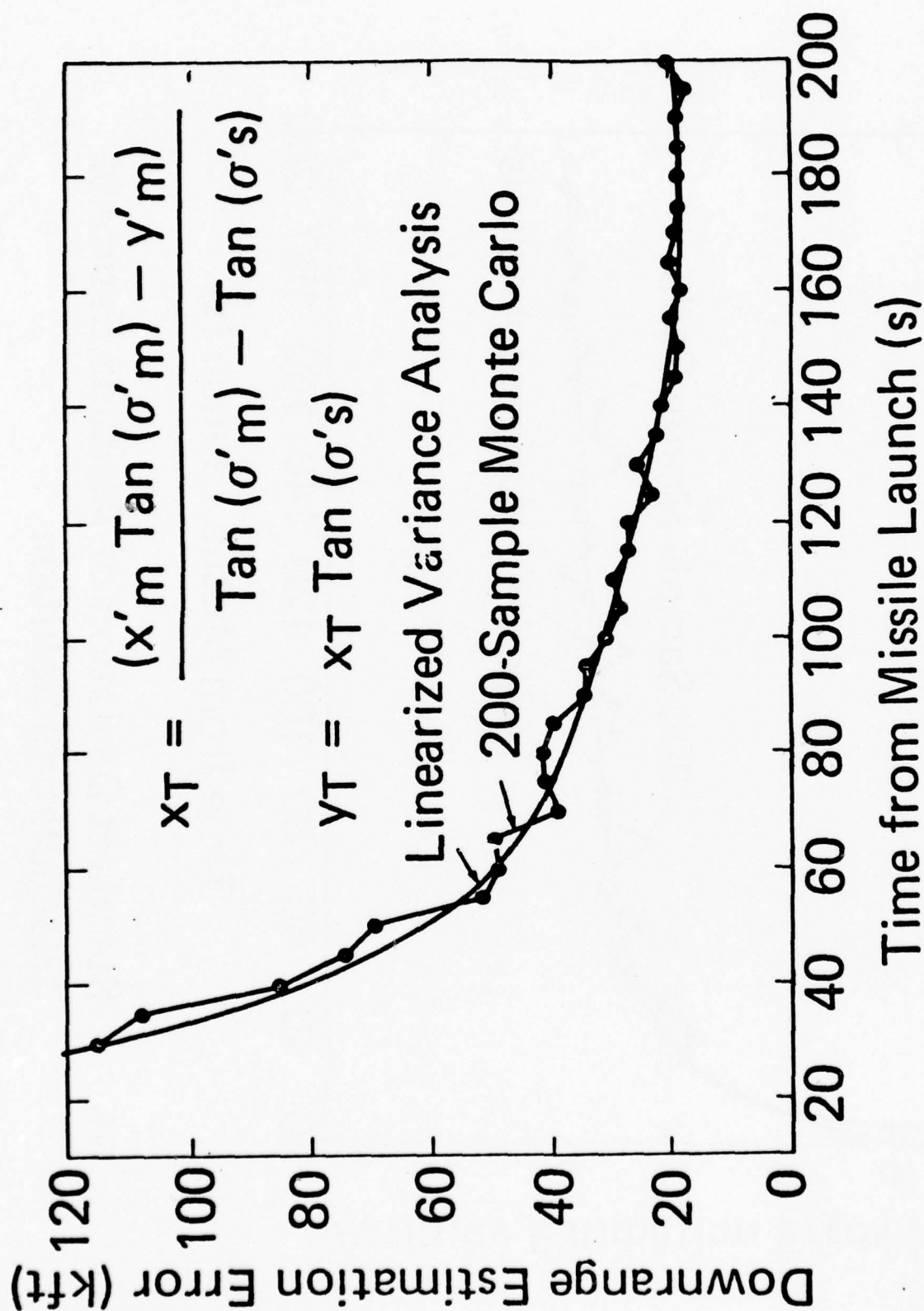


FIG. 6 Standard Deviation of Downrange Estimate
Triangulation Solution

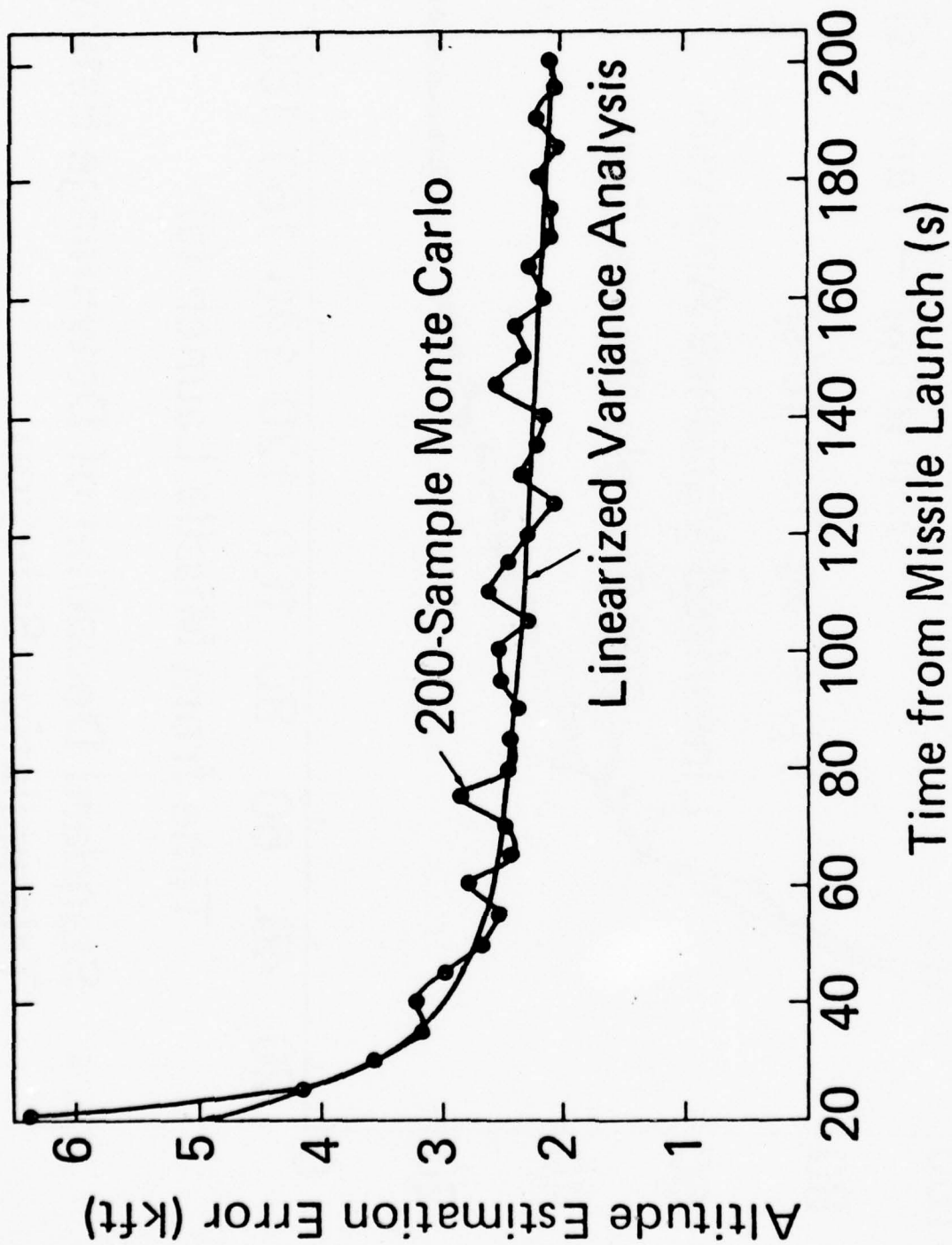


FIG. 7 Standard Deviation of Altitude Estimate
Triangulation Solution

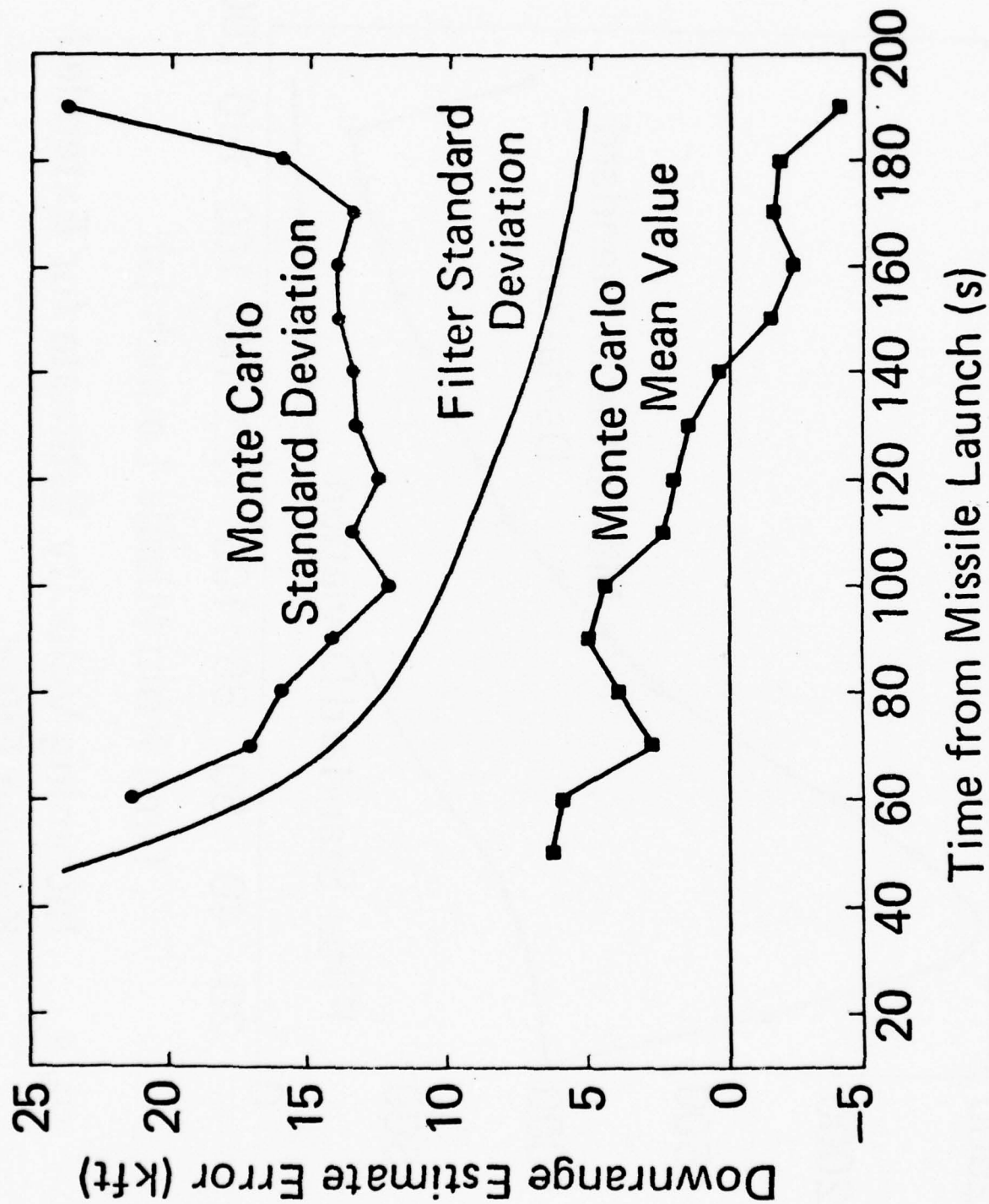


FIG. 8 Downrange Estimate for Extended Kalman Filter.

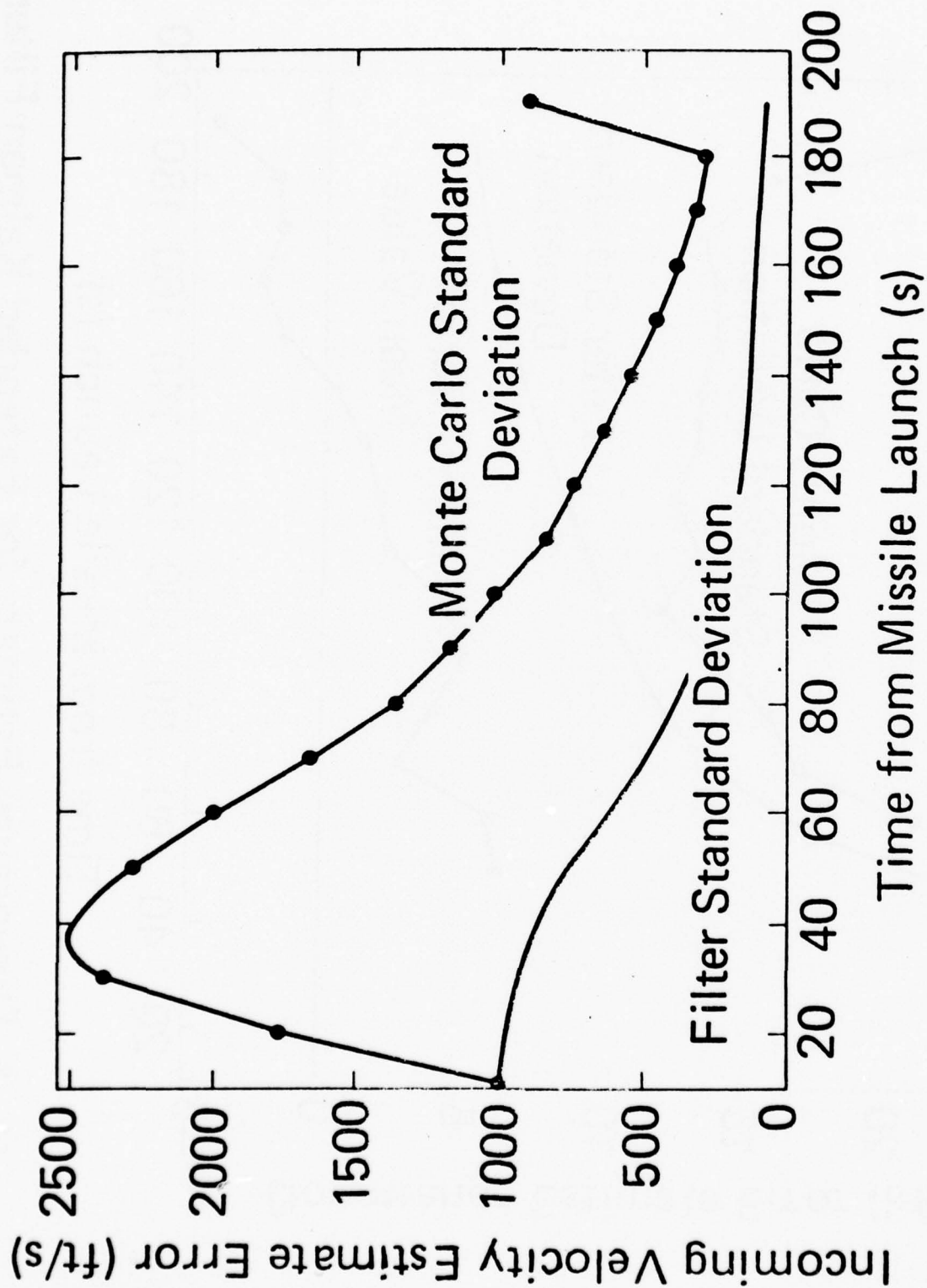


FIG. 9 Incoming Velocity Estimate for Extended Kalman Filter

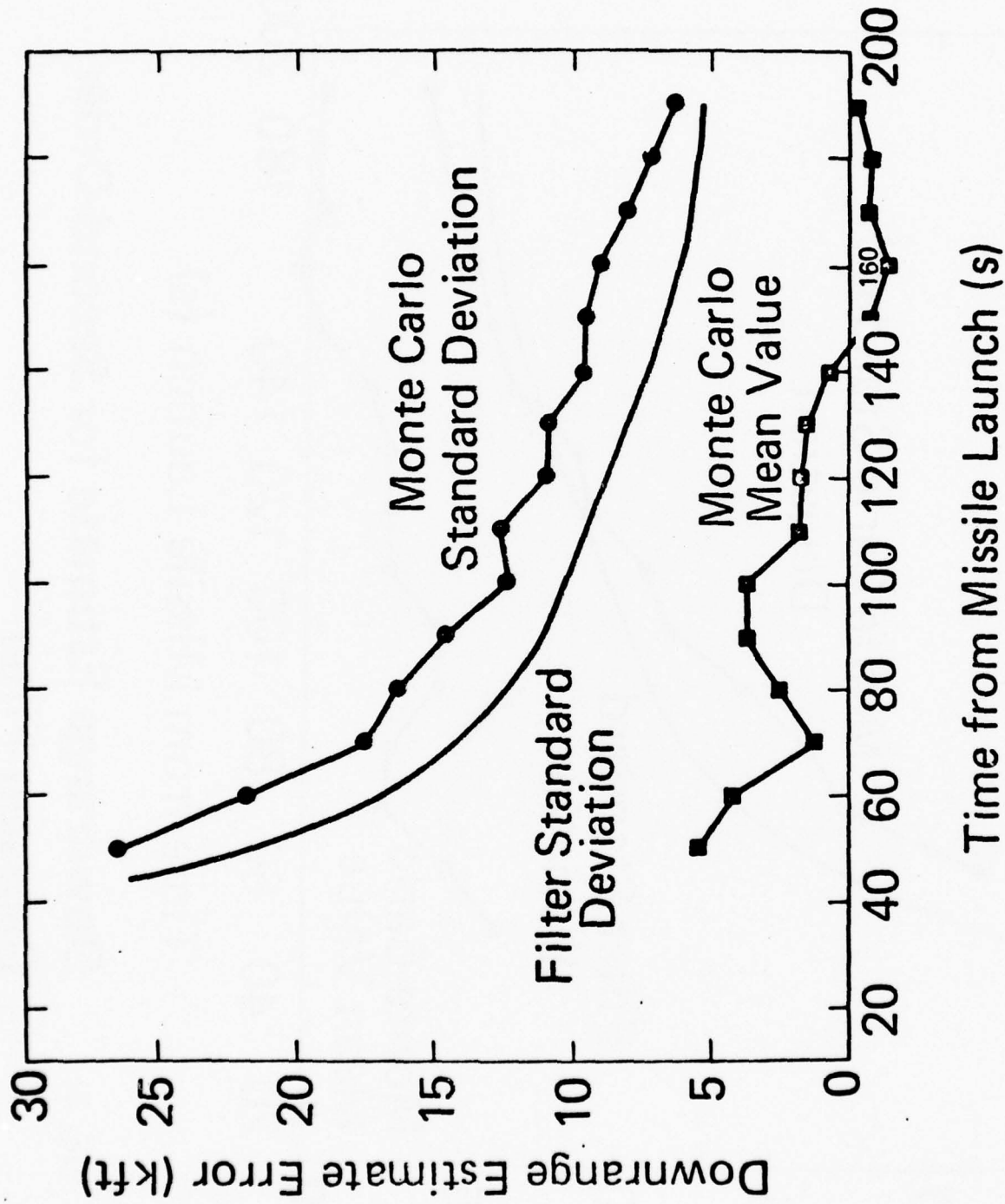


FIG. 10 Downrange Estimate for Extended Kalman Filter with Nonlinear Bias Compensation

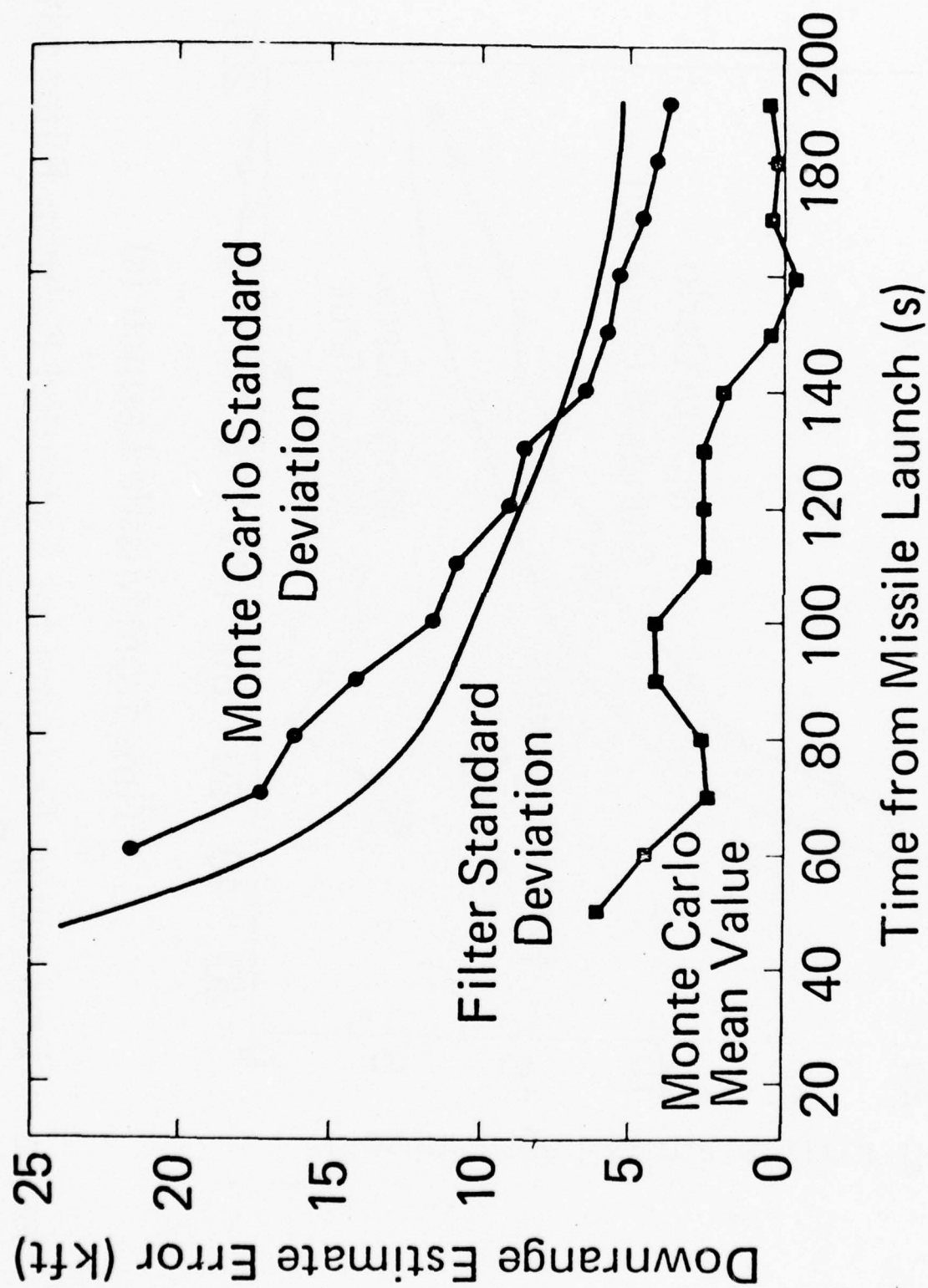


FIG. 11 Downrange Estimate for Second-Order Gaussian Filter

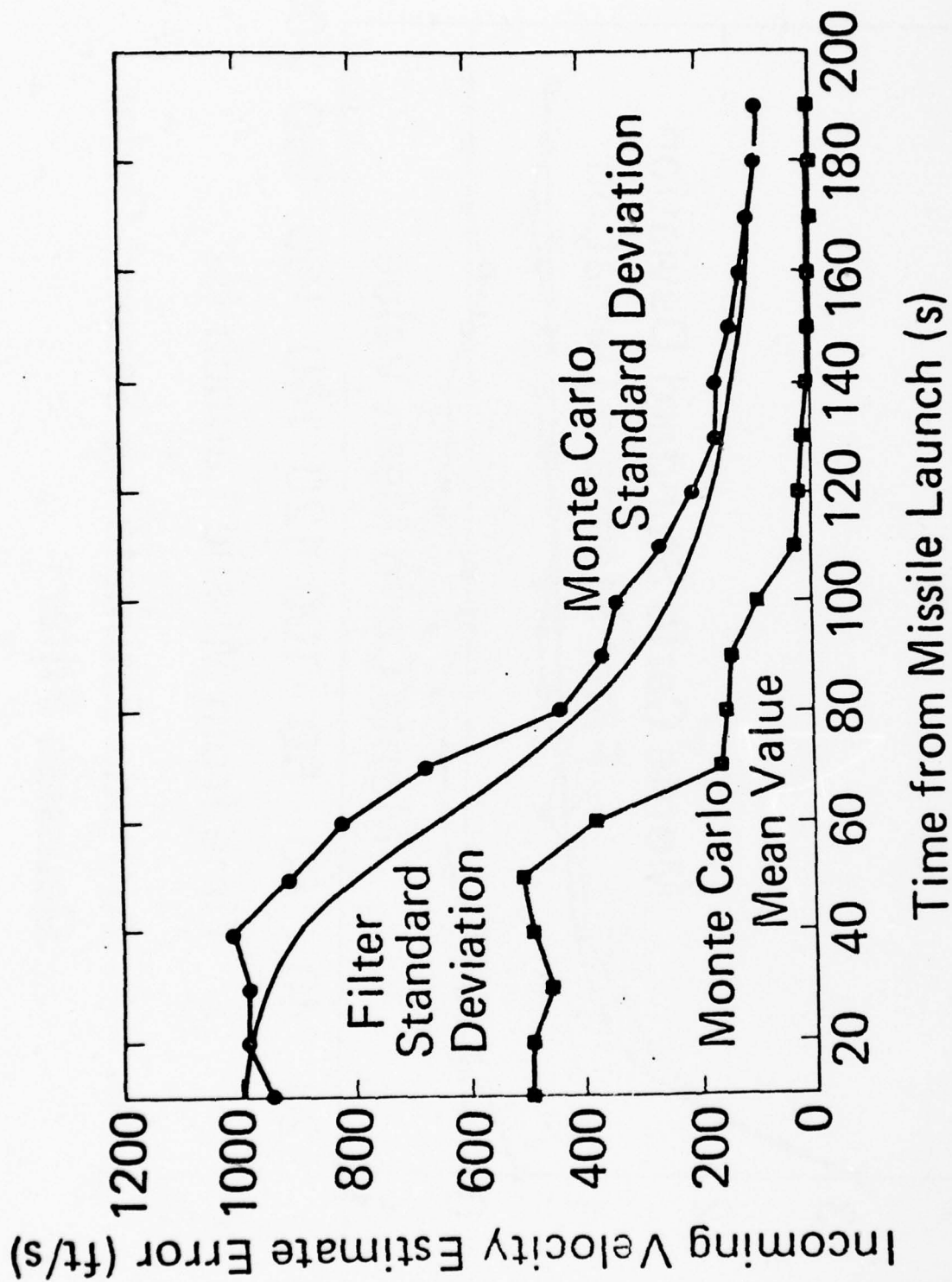


FIG. 12 Incoming Velocity Estimate for Second-Order Gaussian Filter

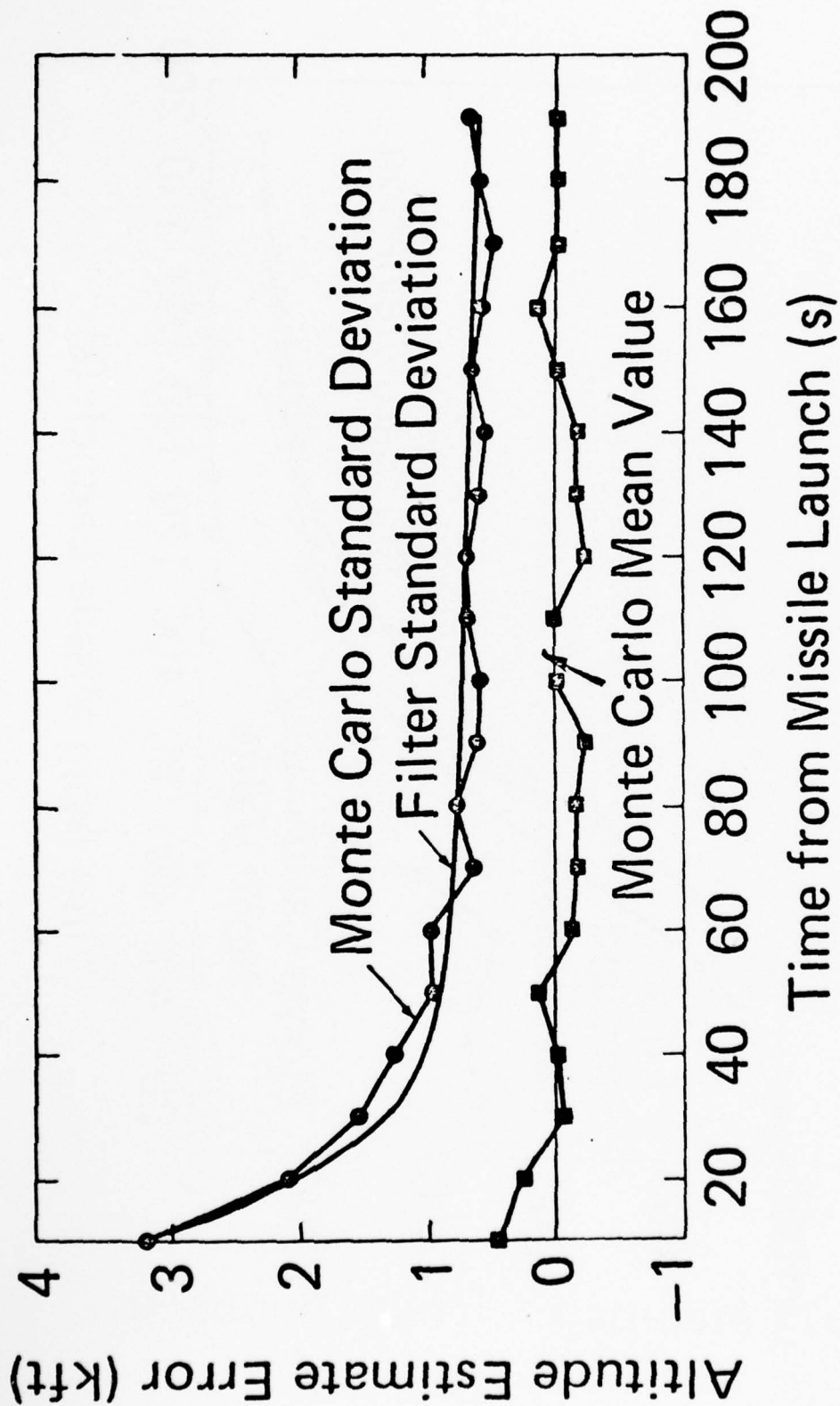


FIG. 13 Altitude Estimate for Second-Order Gaussian Filter

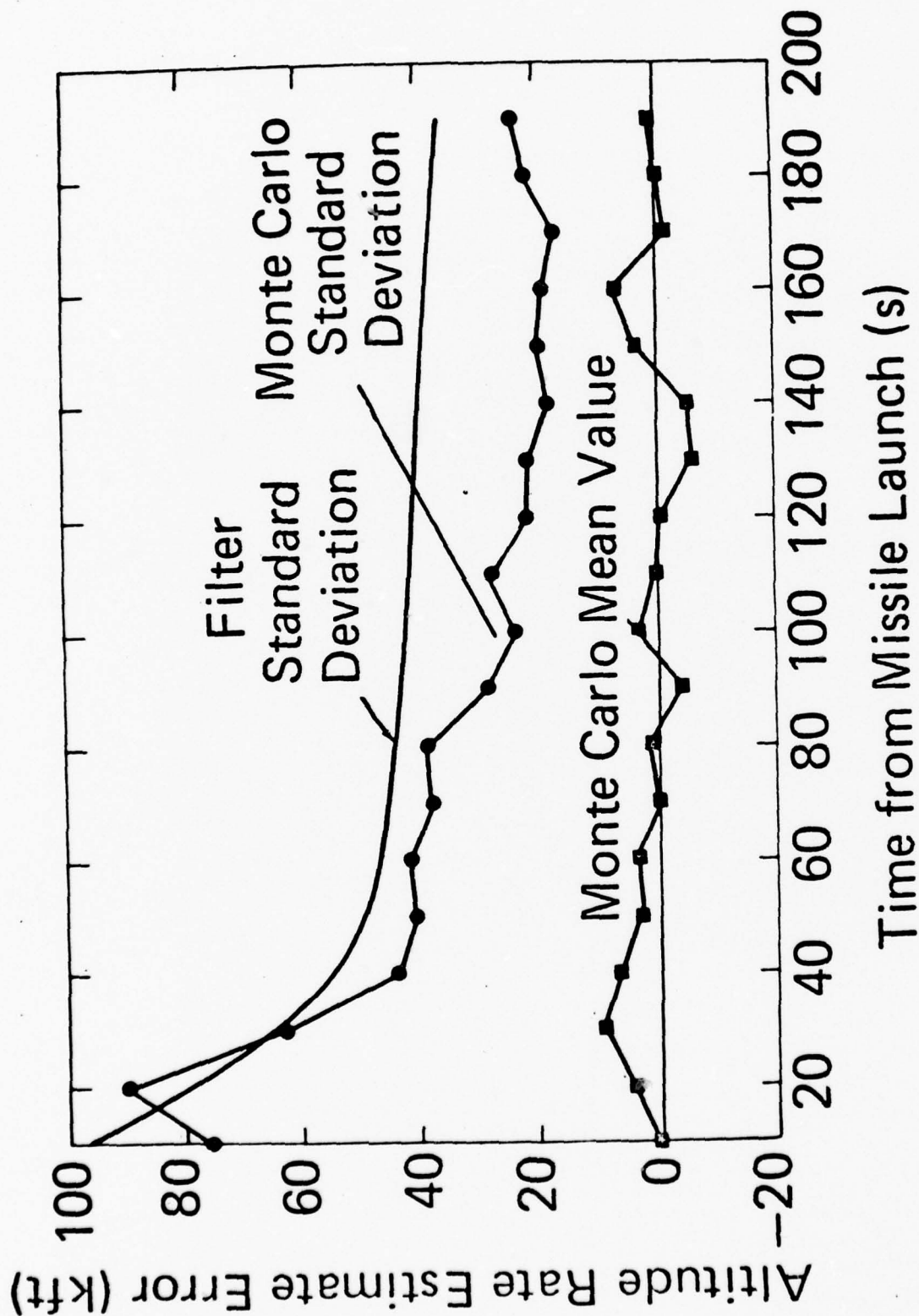


FIG. 14 Altitude Rate Estimate for Second-Order Gaussian Filter

SESSION VI

CONTROL

CONTROL OVERVIEW *

EUGENE YORE

Honeywell Systems and Research Center, Minneapolis

Some of the previous speakers alluded to the fact that some of the technical issues in getting control theory applied in operational systems are just a tip of the iceberg. There are significant management, marketing, and political issues that prevent or facilitate getting the theory into application, and the ultimate payoff (Figure 1). Before addressing technical detail, I would like to speak for a few minutes about these non-technical things, because I think they are crucial and they are probably more general than just control. Also, they apply to parameter identification and the estimation.

If you look at the problem of technology transfer, we run all the way from research to production, or operational systems going through the life of a program from advanced advanced to engineering development. In the early 1960's, pre-1965, the theory people were at the extreme end of one side of the spectrum and the hardware production operational systems were at the other end. Everybody agreed that that's where everybody else was. And, there was very little movement in between. Since then, there have been moves afoot to try to close that gap and, if you look at the production or hardware people, they see themselves as being all the way over to research.

On the other hand, if you look at the other end of the spectrum, the research people today see themselves getting into development and production, I think the truth is that the two ends of the spectrum are still far apart.

* This paper was typed from a taped version of the oral presentation.

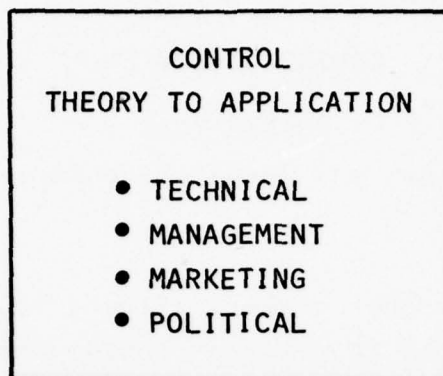


Figure 1

The research technology people have to understand the system's plan, and I would like to talk about just a couple of elements of what we have to understand.

We have to force ourselves to generate technology plans to address the system needs, and we must do it very early in programs if we are to have the impact on the program five years later. I think workshops like this are crucial to the exchange of future system needs, and technology capability to address those needs, and to helping these two ends of the spectrum at least talk the same language. There is another step that is necessary. There have to be workshops at higher levels of management, both in the Government and industry, to make commitments to these plans. And I know internally at Honeywell we are starting to do that up through group vice-president levels, and these plans get implemented in joint programs. You do not transfer technology with a report, you transfer it with people, and with capabilities in people. I think you do that with joint programs.

I would like to talk for just a minute about things I think facilitate or push these two ends of the spectrum together, and things that are inhibitors, that drive us apart (Figure 2). And these non-technical issues have to be addressed and overcome if we are to succeed.

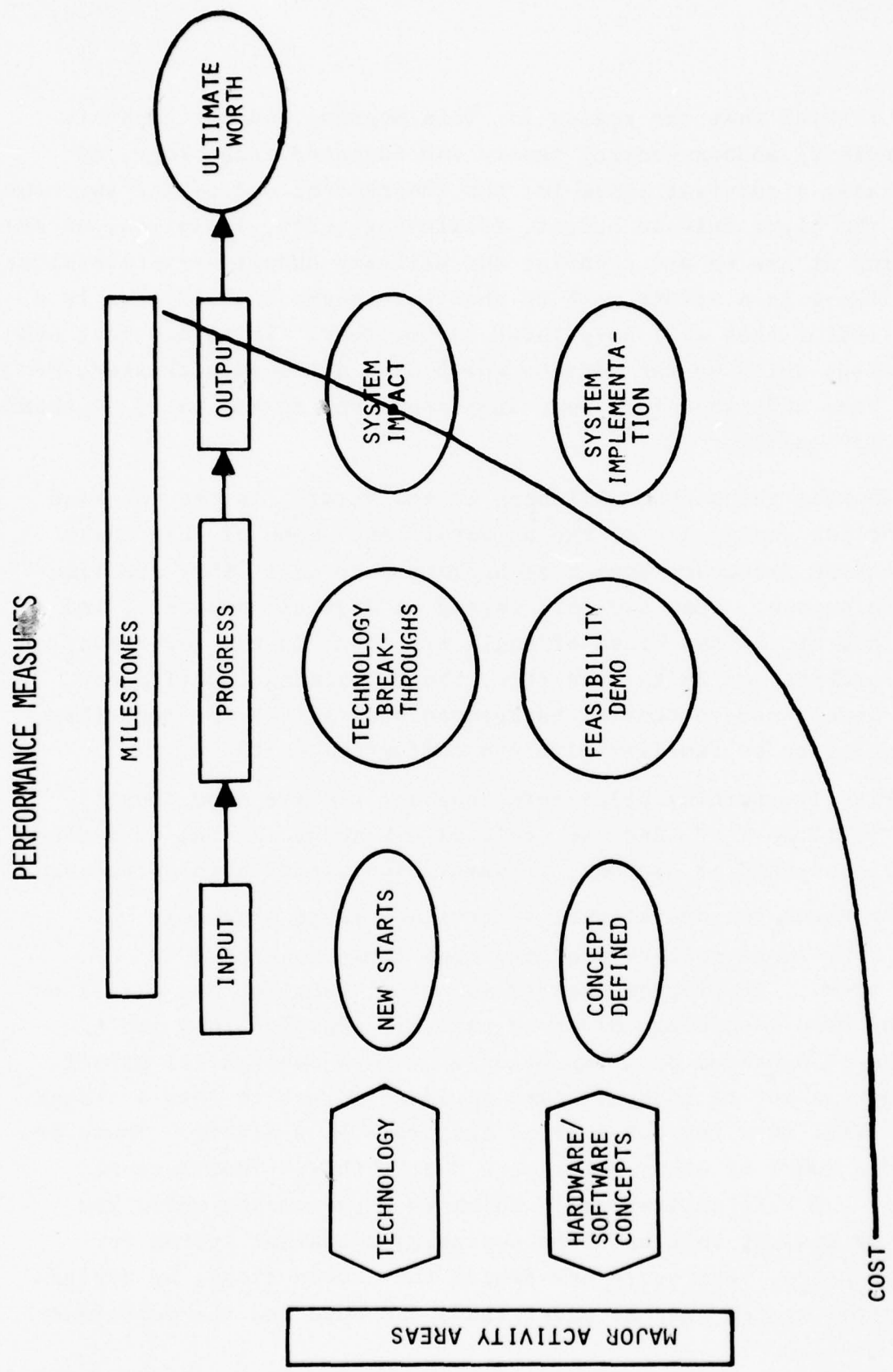


Figure 2

I think that the reason for this meeting and the emphasis on applying modern control theory and advanced technology, is partially a survival issue for the theoretical end of the spectrum. With the tight defense budget, escalating costs, inflation, we are looking at how we are spending our military budget very carefully; and, there is a strong push to show relevance; I think that is a facilitator that will help force us together. There are real system needs which we can address which have not been addressed, or have been addressed in a very cumbersome way in the past. I think that is healthy.

Another thing that will help in the future, is the new kind of analyst coming out of the universities. Some of them don't understand frequency domain techniques very well; they are time-domain people. They are well versed in digital computers, and if you look at the new breed of engineers, both in the government laboratories and in the industry, their training is different. They have a modern control background and that is the tool they are going to be familiar with and comfortable with.

Finally, nothing helps more than a directive from above - "You Shall Do It." And, we can't always count on that or depend on it, but when it happens, it sure helps expedite the process.

Programs for operational systems are large programs, with very large dollars and very high risks connected with them. The program manager is not willing to take a risk on an unproven technology or on an analysis approach that isn't proven on previous programs or doesn't show substantial payoff. It costs a lot of money to take an idea and get it into a system, and I will show you how I think that runs in a minute. There are a whole bunch of other problems - "we," "they," "not invented here," and "the analyst ego," which is a phenomenon where you have an analyst that has been designing a control system for twenty years. For every new system that comes along, he designs a control system, and he understands the spec and the performance.

He doesn't think he needs a new tool, which is probably true in a lot of cases. But, somehow, it is more than just a technical issue - his pride is at stake, and he has to obtain an ownership on these new tools.

Finally, there are organizational constraints (Figure 3) which I could talk a long time about. I won't, but the difference is that management on this side of the spectrum is primarily a top-down type of management, very high authority, a lot of power at the top; I think it is the other way on the other side of the spectrum.

There are many things that go into a good systems plan and a good technology plan (Figure 4). I just pulled out a few of them that I think are critical for transferring technology, and I have reversed the sides, here. I have research on the other side. I did that intentionally because I think that to get technology into a system, you have to look at the system first - what its objectives are, what the technical issues are. I think we have to look at all technical issues, not just the ones that are control issues. The paper yesterday on ultra-reliability was an example where the issue wasn't just an identification problem or a fault tolerance problem, it was a bigger problem the speaker was taking on, and it was a real technical issue in the system. I think out of those come technical needs which we can possibly address with theories like maximum likelihood, optimal control and Kalman filtering.

I think from these specific needs, we can build back up and get some more generic technology objectives, and so you are doing more than just a solution to one problem, a very specific application problem. I hope to show you some examples of this process later on when we start talking about technical needs.

It is also essential that we measure our performance process (Figure 5). How good are we at transferring technology? How good is the technology we transfer? And, if you look at this

ORGANIZATIONAL INHIBITORS		
TOPS DOWN	VS	BOTTOMS UP
RESEARCH	VS	ENGINEERING
TECHNOLOGY		HARDWARE
SMALL \$		BIG \$
UNEXPERIENCED		SENIOR
DEEP		BROAD

Figure 3

PLANS	
<u>SYSTEMS PLAN</u>	<u>TECHNOLOGY PLAN</u>
<ul style="list-style-type: none"> • SYSTEM OBJECTIVES • TECHNICAL ISSUES • TECHNICAL NEEDS 	<ul style="list-style-type: none"> • TECHNOLOGY OBJECTIVES • TECHNOLOGY STATUS • TECHNOLOGY NEED/ APPROACH

Figure 4

measuring of this performance, we have a whole bunch of theoretical work, new starts, and that's kind of the input to the system. The progress along the way is the feasibility demonstration at the laboratories, the flight tests.

Finally, the output is what the ultimate worth of that technology is, and that is in the system. We can do this at two different levels. One is just a technology level, and another level is the actual hardware/software. They look like this, and the ultimate payoff is a system impact where maybe you don't implement a full state optimal control system with the Kalman filter, but you have impacted the design - you have found a new

TRANSFER FACILITATORS AND INHIBITORS

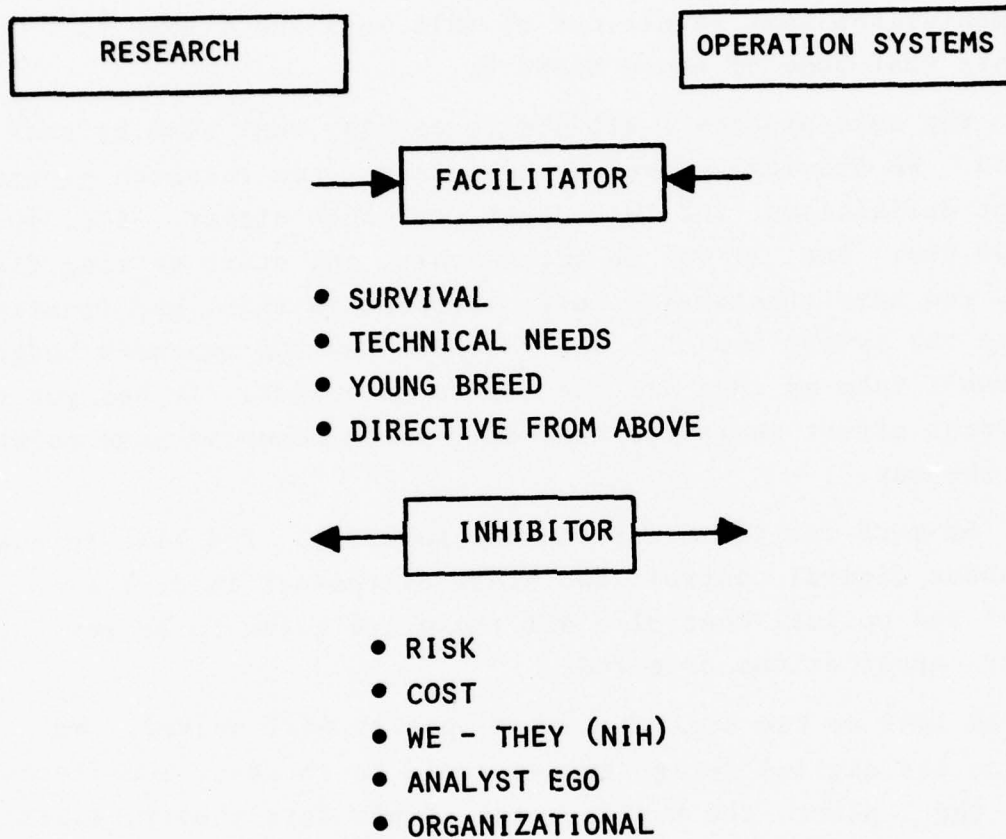


Figure 5

feedback law that people hadn't thought of before, or you have taught a new analyst some physical insight by giving him this rational procedure of modern control to go about his work. I think there are going to be examples where there are system implementations that result out of this work and I hope to indicate what some of those might be.

The cost problem I alluded to earlier must also be considered. We are really good at new starts, new research programs, concept definitions, and they don't cost much either - \$30, 40, 50, 100,000. But, if you go across this, and start getting flight tests, you have substantial costs invested in this, and finally over to the system impact. The research and the research budgets just can't take an idea all the way to an output. It has got to be a joint effort where you have the system money at some point along the way.

So much for the non-technical material. I'd like to now talk about digital control: the state-of-the-art in digital control and optimal control - all these are going to be very case history, applications oriented.

In 1965 we had digital control pretty well solved. We could do the digital design and we could do it several different ways - the Z-plane, the W-plane, the sample data theory, linear quadratic optimal control, and we could digitize analog systems (Figure 6). If you look at the point in time, the technology was way ahead of the state-of-the-art in hardware. The computers were big and they would not fit on airplanes. But that hardware has marched on; it's here; it's real today. I think if you look at the digital hardware implementation problem, from the control analyst's point of view, it presents to him a new problem in that the performance of his control laws is a function of hardware and software variables, such as sample rate, word length, and computational delay (Figures 7, 8). Computer programs have been developed to do that analysis satisfactorily. I

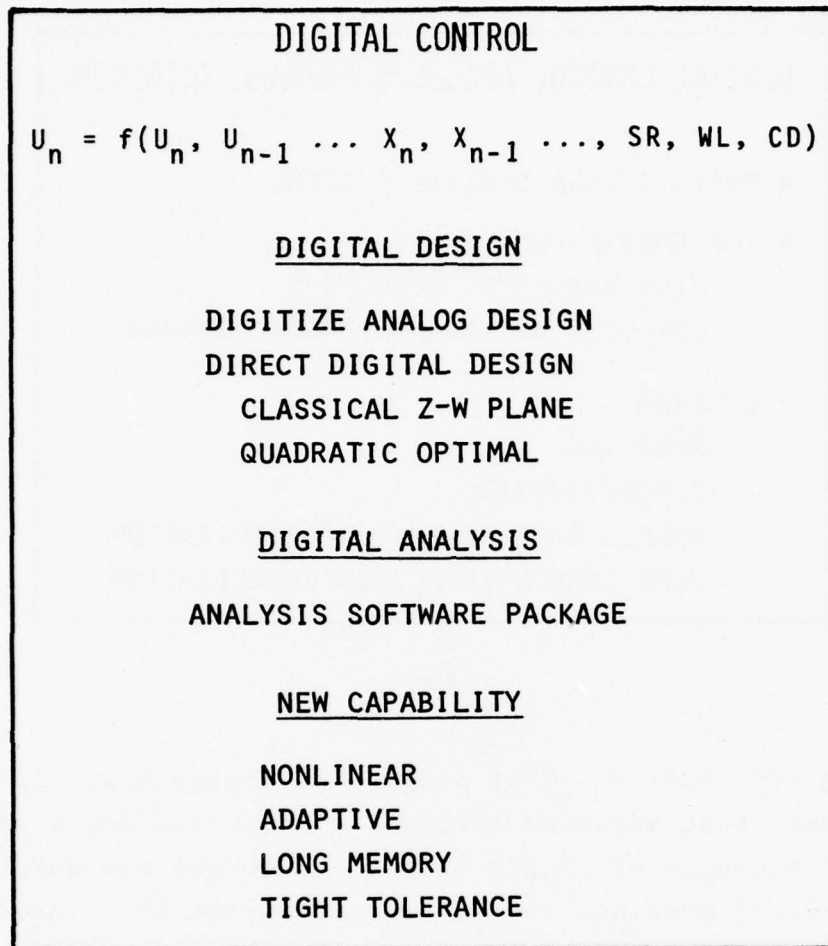


Figure 6

think digital control also gives us a new capability in adaptive control and I'll talk a little bit about one program I'm familiar with. Also, there's a lot of work being done in tighter tolerance and the built-in test and monitoring capability that you get with the digital system. We are also starting to do some work in non-linear filtering.

One program that Paul Blatt talked about was the A-7 digital multimode program. We were involved in that program very early before it went to a hardware stage, and developed a digital analysis software package to do some word-length sample

DIGITAL CONTROL ANALYSIS PACKAGE (DIGIKON)

- TREND TOWARD DIGITAL SYSTEMS
- IMPLEMENTATION ISSUES
 - HIGH BANDWIDTH SYSTEMS
 - LOW COST BUT SLOW MICROPROCESSORS
- DIGIKON
 - MODELING
 - DISCRETIZATION
 - SAMPLE RATE SELECTION/OPTIMIZATION
 - WORD LENGTH SELECTION/OPTIMIZATION

Figure 7

rate trade-off studies. That program is flying now. If you look at the impact that advanced technology had...you don't see it now. You've got a couple of sample rates; you've got one word-length; it's in a fixed machine, and it's hard to look at. There's the advanced technology. But, if you look at three to four years along the way, that software and analysis was done, and it said, "Yes, that computer's OK; yes, that sample rate's OK." So it impacted the system. Now if you look at where this fits on my original spectrum, this is a feasibility demonstration, flight test demonstration. It's not over on the far right hand side, yet; I think we are beginning to see an operational system on the J37, but we don't presently have a digital system production plan for the U.S. The last big airplane buy, the F-16, was a four-channel analog. So, the hardware wasn't quite far enough along for the digital to beat out the analog.

Now I'd like to talk about the history of optimal control as I know it from my perspective, and I want to go back a little bit in flight control (Figure 9). If you look at what happened in the beginning, we started out with an autopilot, heading-hold,

DIGITAL SYSTEM ANALYSIS SOFTWARE PACKAGE

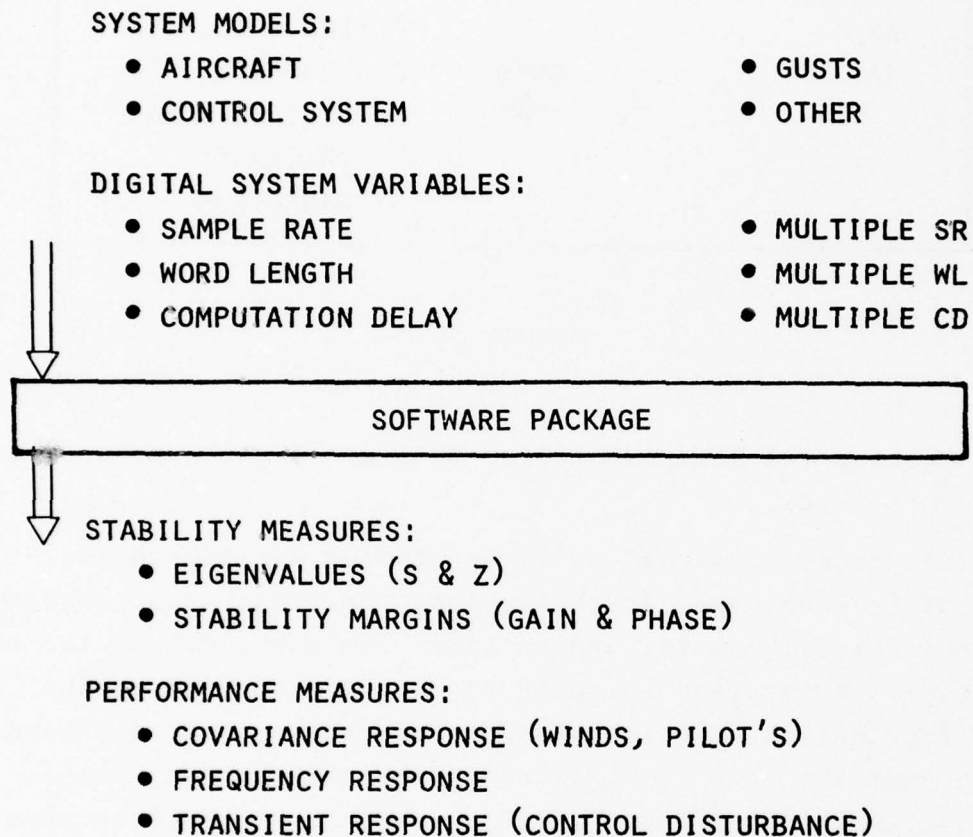


Figure 8

altitude-hold, and that was good; and we started building faster airplanes where we had trouble getting the natural stability, the aerodynamic stability throughout the flight envelope. The next step was to design a stability augmentation system. With the autopilot we just bought pilot relief, but when we started working with the SAS we started increasing the bandwidth of that control system and getting handling qualities, affecting flying qualities, and, as we demanded more and more out of the systems, we

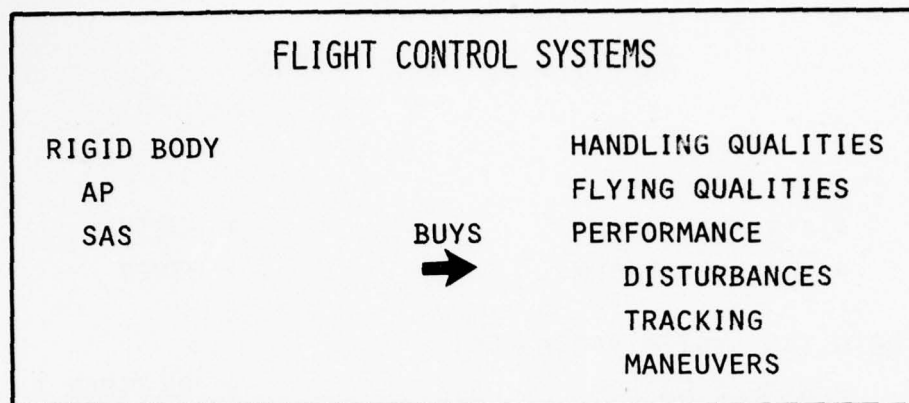


Figure 9

started pushing the bandwidth out. We started getting performance improvements, also.

This trend continued until we started exciting higher degrees of freedom, and, at that point, the first solution was to put bending filters in, and to limit the bandwidth of the control system. We started building bigger airplanes where the flexure frequencies were lower and it started pushing our bandwidth in, and the next step, after gain stabilization, phase stabilization, and bending filters, was to try to control some of the lower degrees of freedom in addition to the rigid body. And, in addition to increasing the bandwidth and doing all these good things, we started being able to think about controlling ride quality and accelerations at different stations along the fuselage. (Figure 10). We started being able to reduce peak stresses and think about increasing the tilt line of glide for the airplane. We were involved with Boeing, in the B-52 LAMS Program back in the early 1960's, with the flight test in 1967, and there was a big problem because it had 65 flexure modes below 10 hz (Figure 11). The objective was to use multiple control inputs to maintain existing handling qualities, improve the ride qualities at different locations on the fuselage, and to reduce the peak stresses at the wing root and on the stabilator (Figure 12).

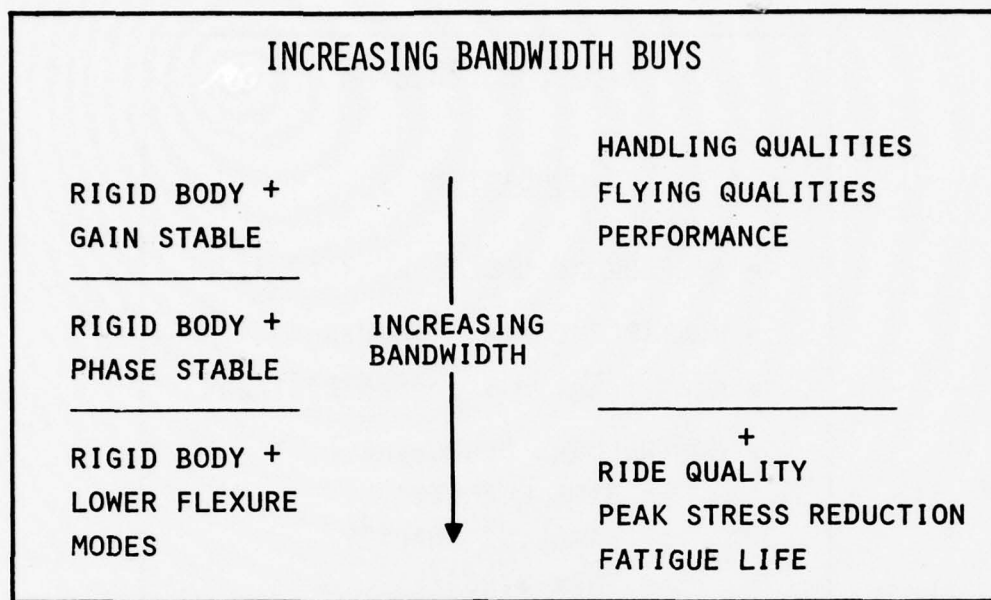


Figure 10

There's a lot of debate and hindsight surrounding this program, but in about 1965, we were having difficulty doing the analysis in designing this system using the classical approach. The reason was that the B-52 was a high-order system, with a lot of interaction and many degrees-of-freedom. An analyst just could not see through the whole problem. We got the opportunity to apply the optimal control to this problem, and we think it impacted the design. At that point in time, we could just design full-state variable feedback, and if you look at the control we came up with, we're really proud. It had required 27 sensors in pitch, and 30 in lateral. Then 81 man-months of engineering trial-and-error was used to simplify that design down to the 8 gain controller which was built, flown, and successfully flight tested.

Two things happened at that point in time. The B-52 program went on, and it became CCV. I want to talk about that in a minute; Paul Blatt talked about this a little bit in his overview. If you look at what happened, the responsibility for that design changed groups, and it reverted back to a conventional

B-52 LAMS PROGRAM

CONDITIONS

- 65 FLEXURE MODES $\omega_N < 10$ Hz
- MULTIPLE CONTROL INPUTS
- WING TORSION \rightarrow COCKED SPOILERS
- CONTROLLERD RESPONSES
 - RIDE QUALITY
 - HANDLING QUALITY
 - PEAK STRESSES
 - FATIGUE

RESULTS

- DESIGNED QUADRATIC OPTIMUM CONTROLLERS - 1 EACH FOR 3 EXTREME FLIGHT CONDITIONS
- SIMPLIFIED TO 1 CONTROLLER WITH 8 VARIABLE GAINS
- SENSOR CHOICE AND LOCATION BY TRIAL AND ERROR
- BUILT AND FLEW

Figure 11

FATIGUE DAMAGE RATES PER YEAR DUE TO TURBULENCE (THREE FLIGHT CONDITIONS)

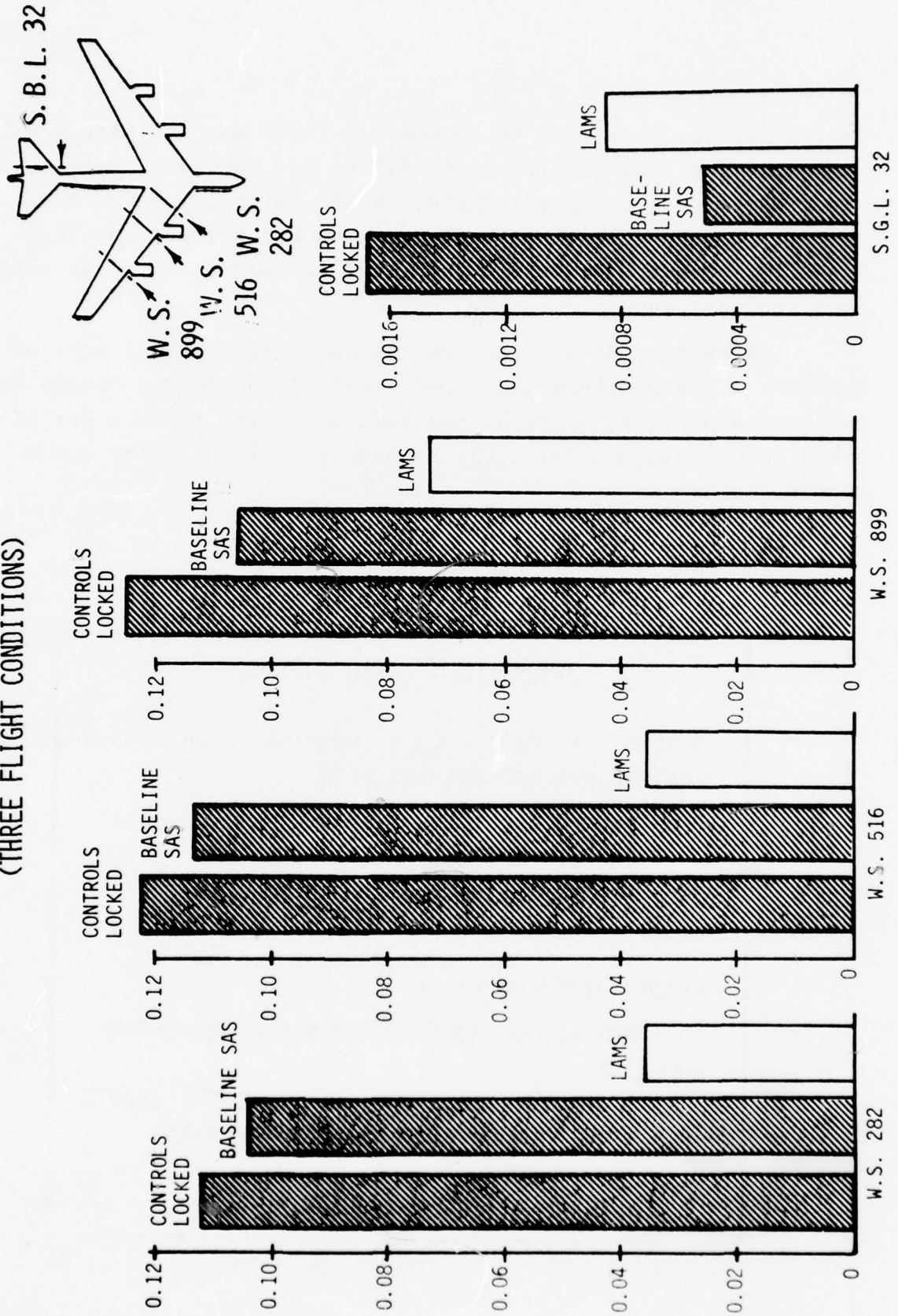


Figure 12

design for the next five to 10 years. There was a single mode design done for ride quality control, one for moderate control, and there was a step backwards there, as far as applying the technology. On the other hand, this program was a great forcing function, pushing the technology ahead and directing it at more practical problems.

At that point in time, we saw quadratic optimal control as handling large problems where conventional approaches become very cumbersome or fail; plus, having the capability to do a lot of other things (Figure 13). This opinion wasn't shared by other people, but we were not discouraged.

QUADRATIC OPTIMAL CONTROL

QUADRATICS ARE THE ONLY THEORIES WHICH DESIGN CONTROLLERS FOR SYSTEMS WITH

- MULTIPLE CONTROL INPUTS, MULTIPLE CONTROLLED OUTPUTS, MULTIPLE SENSED RESPONSES, MANY INTERCONNECTED DEGREES OF FREEDOM

QUADRATICS ALSO HANDLE

- BOTH AUTONOMOUS AND TIME-VARYING DYNAMICS
- BOTH STOCHASTIC AND DETERMINISTIC INPUTS
- BOTH FINITE-TIME AND INFINITE-TIME (STATIONARY) CONTROL CRITERIA
- DISCRETE OR CONTINUOUS

Figure 13

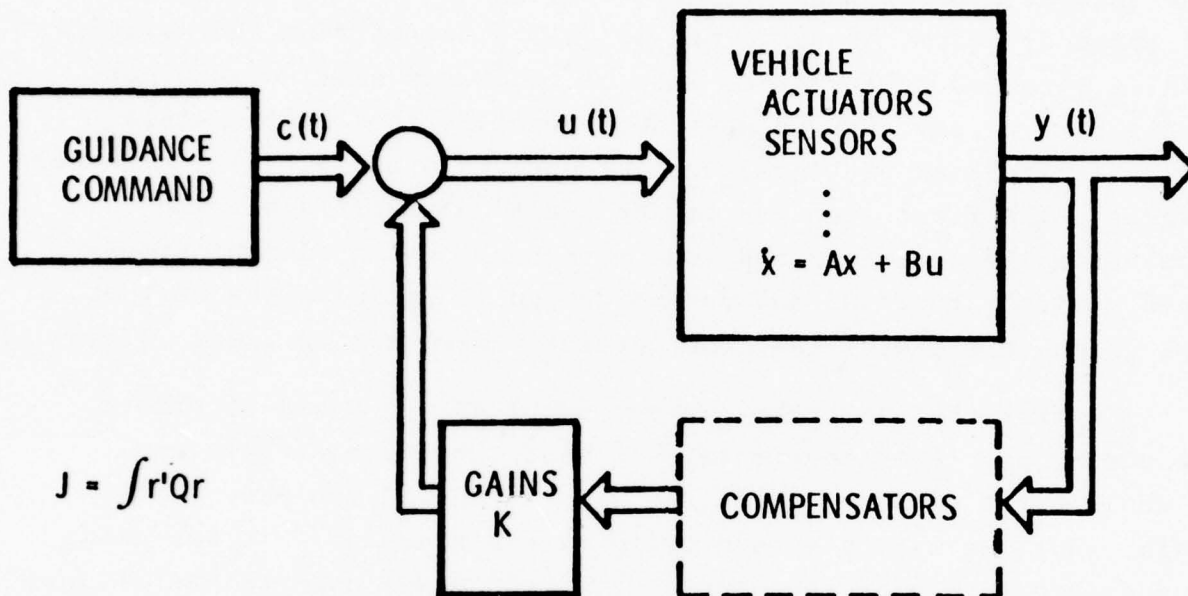
At that point optimal control could be used to design an ideal full-state feedback system, compute all the gains in a large system for every state, and choose the control system to minimize the quadratic performance index. But, in the B-52, when you look at those 81 gains, or 90 gains, or only a few of them that significantly affected performance, many of them were small or did not contribute a lot. So, we went about working the limited state variable feedback problems, both at Honeywell and at a lot of other places. The first step was to add practical constraints where you optimally constrain a Kalman filter or set an element cross-feed variable to zero, and do the design to optimize the rest of the gains to minimize the same quadratic performance index (Figure 14).

After the B-52 LAMS, we put about 40 man-years of effort to adding practical constraints to that theory, and there are a whole bunch of steps along the way. I showed you one, fixed gain. But, we have also addressed gain scheduling. In designing compensators, how do you handle data, and model uncertainty (Figure 15)? There's a very significant program now, funded by Langley, to examine insensitive designs - designs that are less sensitive to parameter or structure uncertainty in the model.

If we consider the present status of optimal control, it's clear that many people have algorithms in the computational capability to do the linear designs and evaluate those on full non-linear simulations (Figure 16). These algorithms are based upon the optimal control theory; they result in efficient algorithms; and they offer an engineer a rational procedure for going about the design (Figure 17).

There is still an awful lot of engineering art that goes into picking the performance criteria, the specifications, and designing to that. There is a very significant program being funded by ONR to put that connection between the time-domain optimal control design and the frequency domain conventional specifications on a more rigorous basis and reduce the trial-and-error associated with picking responses and quadratic weights to get an acceptable design to meet a performance criteria (Figure 18).

OPTIMAL CONTROL



$$\begin{bmatrix} u_1 \\ u_2 \\ u_3 \\ \vdots \\ u_m \end{bmatrix} = \begin{bmatrix} k_{11}(FC) & \cdot & k_{13} & \cdot & \cdot \\ k_{21} & \cdot & k_{23}(FC) & \cdot & \cdot \\ k_{31} & \cdot & k_{33} & \cdot & \cdot \\ k_{41}(FC) & \cdot & \cdot & \cdot & \cdot \\ \vdots & \cdot & \cdot & \cdot & \cdot \\ k_{m1} & \cdot & k_{m3} & \cdot & \cdot \end{bmatrix} \begin{bmatrix} x_1 \\ x_2 \\ x_3 \\ \vdots \\ x_n \end{bmatrix}$$

Figure 14

QUADRATIC OPTIMAL CONTROL RESEARCH MILESTONES

	1968	1969	1970	1971	1972	1973	1974
MODELING						NUMERICAL LINEARIZATION	
DATA MODEL UNCERTAIN				PARAMETER UNCERTAINTY	MULTILOOP STABILITY		
SIMPLE HARDWARE			FIXED GAIN	RATE MODEL FOLLOWING			SATURATING SYSTEMS
			PRACTICAL CONSTRAINTS	SENSOR CHOICE		DESIGN SPEC.	POLE PLACEMENT
PERFORMANCE	STEIN ALGORITHM	KONAR ALGORITHM		GAIN SCHEDULING	COMPENSATOR DESIGN		UPGRADE FIXED FORM
	CONTROL LOCATION	SENSOR LOCATION		INTEGRAL CONTROL			

Figure 15

QUADRATIC DESIGN PROCEDURES

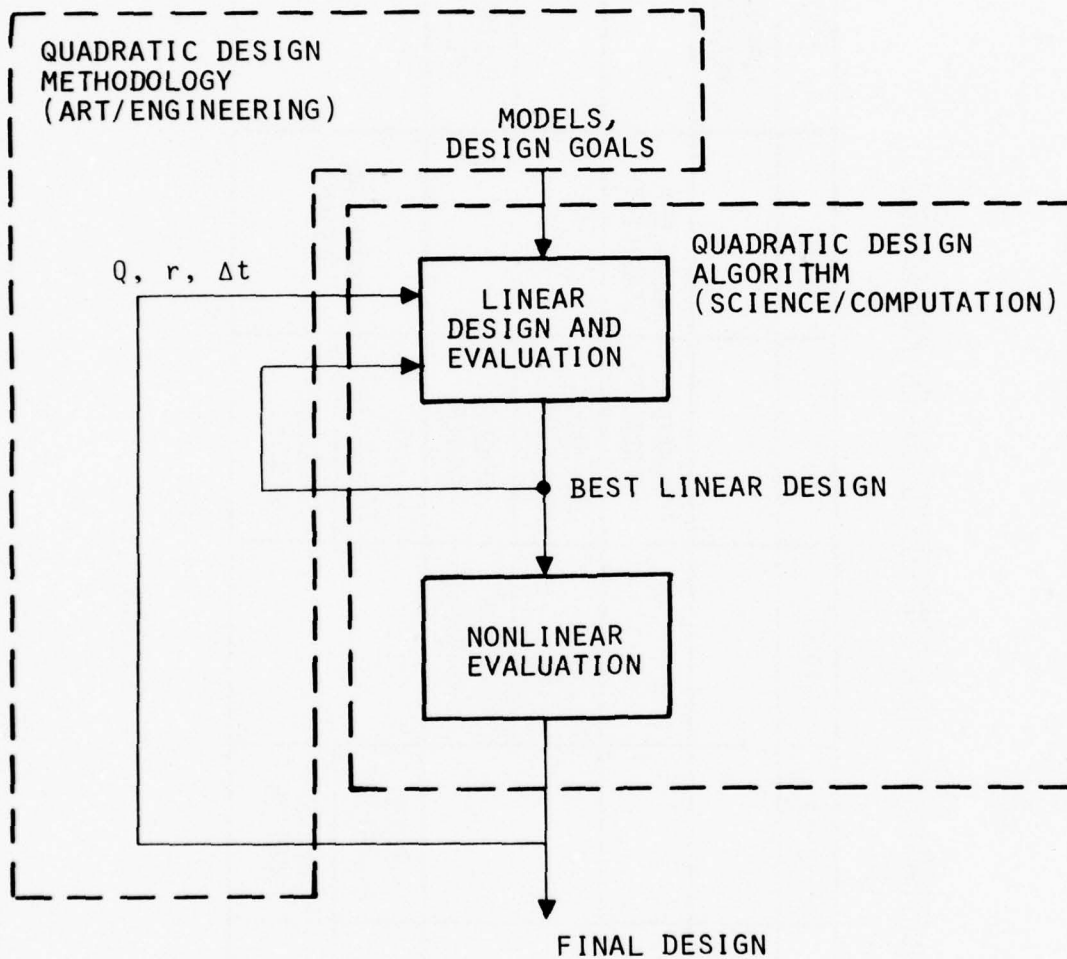


Figure 16

QUADRATIC DESIGN METHODOLOGY

DESIGN AND ANALYSIS SOFTWARE PACKAGE

- CONFIGURE CONTROL SYSTEMS
- COMPUTE CONTROL LAWS
- EVALUATE PERFORMANCE

OPTIMAL CONTROL THEORY

- MATHEMATICAL THEORY
- EFFICIENT ALGORITHMS

OPTIMAL CONTROL APPLICATION

- ENGINEERING
- RATIONAL PROCEDURE

Figure 17

OPTIMAL CONTROL BENEFITS

LOWER DESIGN COST

BETTER PERFORMANCE OR CHEAPER HARDWARE

COMPLEX CONTROL PROBLEMS

MULTIVARIABLE

MULTICRITERIA

INTERACTION

Figure 18

Performance criteria, when you go to design a control system, isn't just a cost functional. It includes short period damping frequencies, couplings, and Mill Spec 8785, plus several other constraints on actuators, bandwidths, etc. The objective of the ONR program is to put the relationship between that real specification and the quadratic weights and responses on a more mathematical basis. I have an example later on where it kind of shows the progress of that.

So much for the technology development. Figure 19 shows some applications which we have done and there are many more. We found out about some yesterday. We are going to hear about some more in this session today. In optimal control we continue to look for new applications and new applications in research, and on the other hand, we've seen almost an expeditious growth in its use in our product lines and on systems programs. There are several programs of interest.

The first one I'd like to consider is the CCV program. Paul Blatt indicated that the objective was to look at the control in the preliminary design cycle and determine how it can impact the vehicle mission performance (Figure 20). It looks at a multitude of different things, depending upon the airplane. There are two ways to look at CCV's. You can look at making a small perturbation in the existing airplane, and there have been several studies done trying to extrapolate existing data to assess the benefit of CCV's. Many people believe that the ultimate performance of CCV's is to go to a completely new design from scratch, with no stability constraints or aerodynamic constraints. It might end up with a vehicle which is much different, and there are some steps in this direction. The advanced technology fighter integration is an extreme, but it is an example of a step from a perturbation on the existing one to a whole new airplane.

Figure 21 shows some of the applications of optimal control to CCV problems that I am aware of. I'd like to talk about just one of these - the C-5A, because it is an example of how optimal

QUADRATIC OPTIMAL CONTROL APPLICATIONS PROGRAMS

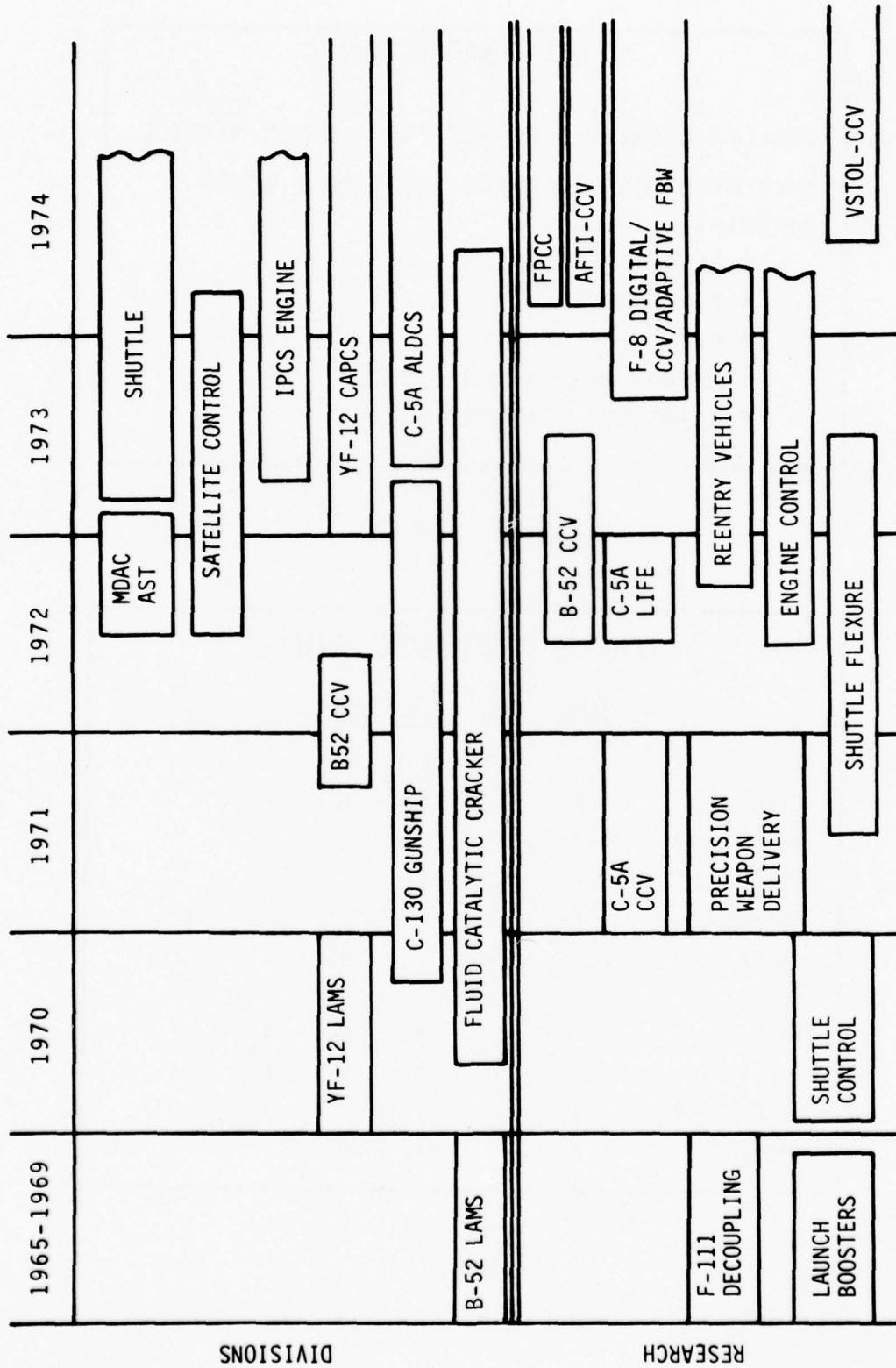


Figure 19

CCV CONCEPTS BUY

SMALLER LIGHTER AIRCRAFT FOR A GIVEN MISSION

INCREASED MISSION CAPABILITY FOR A GIVEN
AIRCRAFT

- FLIGHT ENVELOPE
- PAYLOAD
- RANGE
- ENERGY MANEUVERABILITY
- TRANSIENT MANEUVERABILITY

Figure 20

CONTROL CONFIGURED VEHICLES

	<u>LAMS</u>	<u>RQC</u>	<u>DLC</u>	<u>RSS</u>	<u>MLC</u>	<u>FMS</u>	<u>SP</u>
B-52	X	X	X				
C-5A	X	X	X	X	X		
YF-12	X	X					
F-104			X		X		
AST-MDAC	X	X				X	
JA-37		X		X			
F-101							X
AFTI			X	X	X		
F-8		X	X	X	X		X
TWIN OTTER	X	X			X		
SHUTTLE	X		X	X			

Figure 21

control impacted an operational system, or is in the process of doing that. Back in 1967/68, when we were working the B-52 LAMS program, there was a study passed to look at the C-5A. We looked at it and thought there was going to be a structural problem, a vibration or load keeping problem, but others were convinced there wasn't. The program went on, and in about 1962 they started getting a lot of flight test data which showed that the wings were wearing out at about a fifth to a fourth of their design life, and at that point, we got involved with Lockheed and Boeing on a program to design and implement an automatic load distribution control system on the C-5A. Because of their responsibilities, Lockheed made the decision to build the hardware in-house and just interface it with the Honeywell autopilot that was on that system. So optimal control was used in a parallel role to help do the requirement trade-offs, to define the requirements, and to check and simplify the control equations. They had an impact on the conventional configuration of that system, but it was not designed completely with the modern control theory.

A CCV program which is presently active is sponsored by NASA-Ames for the Twin Otter aircraft. It's in the first phase; handling qualities and ride quality are being investigated for low wing loading aircraft in the terminal phase of flight (Figures 22, 23). Figure 24 is an example of some of the trade-offs that have been done very rapidly using the optimal control theory to look at different sets of measurements, and different sets of force producers, and comparing them to the free aircraft in a conventionally designed control system.

Another effort that's being sponsored by the Air Force Flight Dynamics Laboratory takes flexstab and interfaces optimal control design algorithms with that program (Figure 25). Flexstab is a very large program to do preliminary design and analysis on aircraft, and it's the result of an awful lot of effort. I think everybody in the airplane business is probably familiar with the flexstab program. It is a real monster with the aerodynamics and

ACTIVE CONTROL TECHNOLOGY
FOR
LOW WING LOADING STOL

PHASE I - FLIGHT TEST

- HANDLING QUALITIES
- RIDE QUALITY

PHASE II - CONTROL CONFIGURATION

- MANEUVER LOAD CONTROL
- GUST LOAD CONTROL

Figure 22

structures. Adding the optimal control block provides the capability to define a configuration, come-down through a linear analysis and design, look at loads and do maybe a load relief control system and iterate back through the configuration without horrendous data transfer interface problems. The data is compatible. I don't think anybody's ever suggesting that you automate this whole thing, but the engineer will be in the loop here anyplace along the way, but at least it's made it easy for him.

Another application, which got just barely to the feasibility demonstration phase was the C-130 gunship. There was a technical reason for applying optimal control to that program, but that's not the reason it got used on that program (Figure 26). The technical reason was that the C-130 is an airplane that flies around in a 30-degree bank angle with the gun pointed out the side. You fly around in circles doing pylon turns and around trucks, or whatever, on trails, and you use roll to line up the elevation of

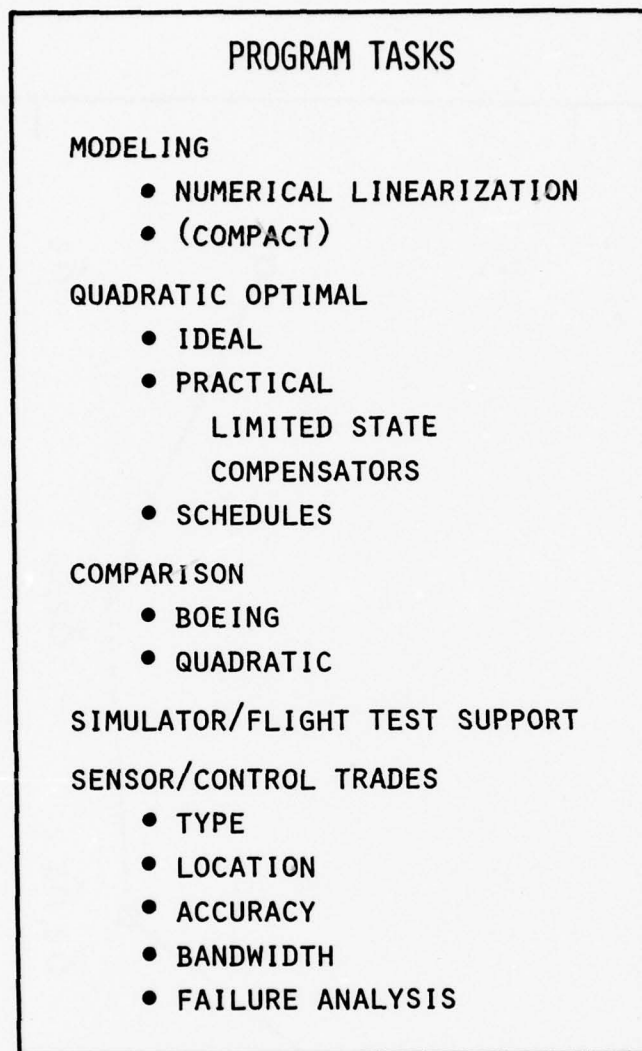


Figure 23

the gun and side-slip to line up azimuth and its over in a 30-degree bank. Pitch, roll and yaw are coupled. The objective was to improve the pilot response and to automate that. The way that optimal control got applied on the program was a kind of crusade by Colonel Parkenson at the Air Force Academy. He got involved in the program by riding around on gunships in Southeast Asia, studying the problem, learning the real-world system and constraints in the pilot's sphere,

MID PASSENGER STATION ACCELERATION VERSUS DESIGN COMPLEXITY

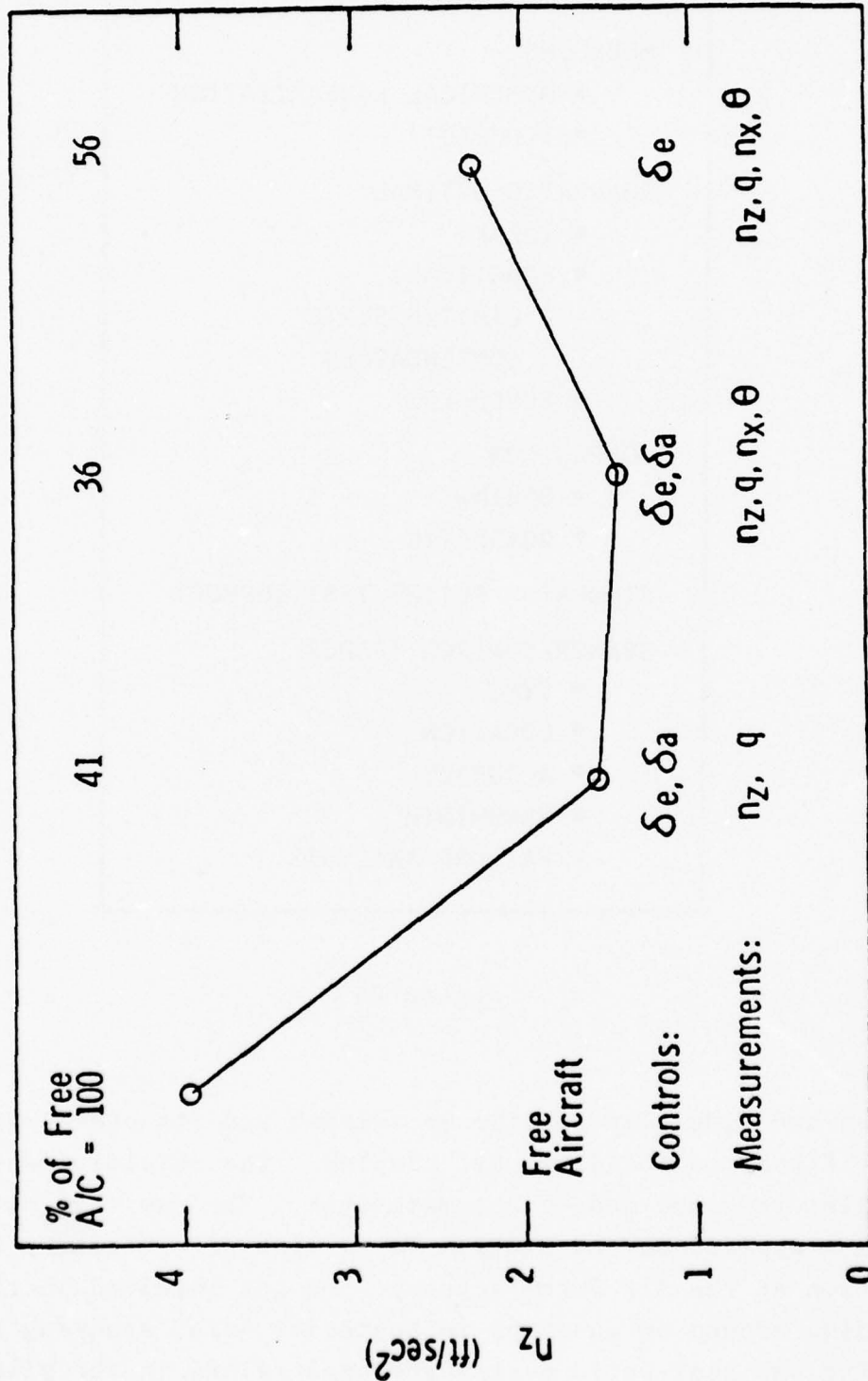


Figure 24

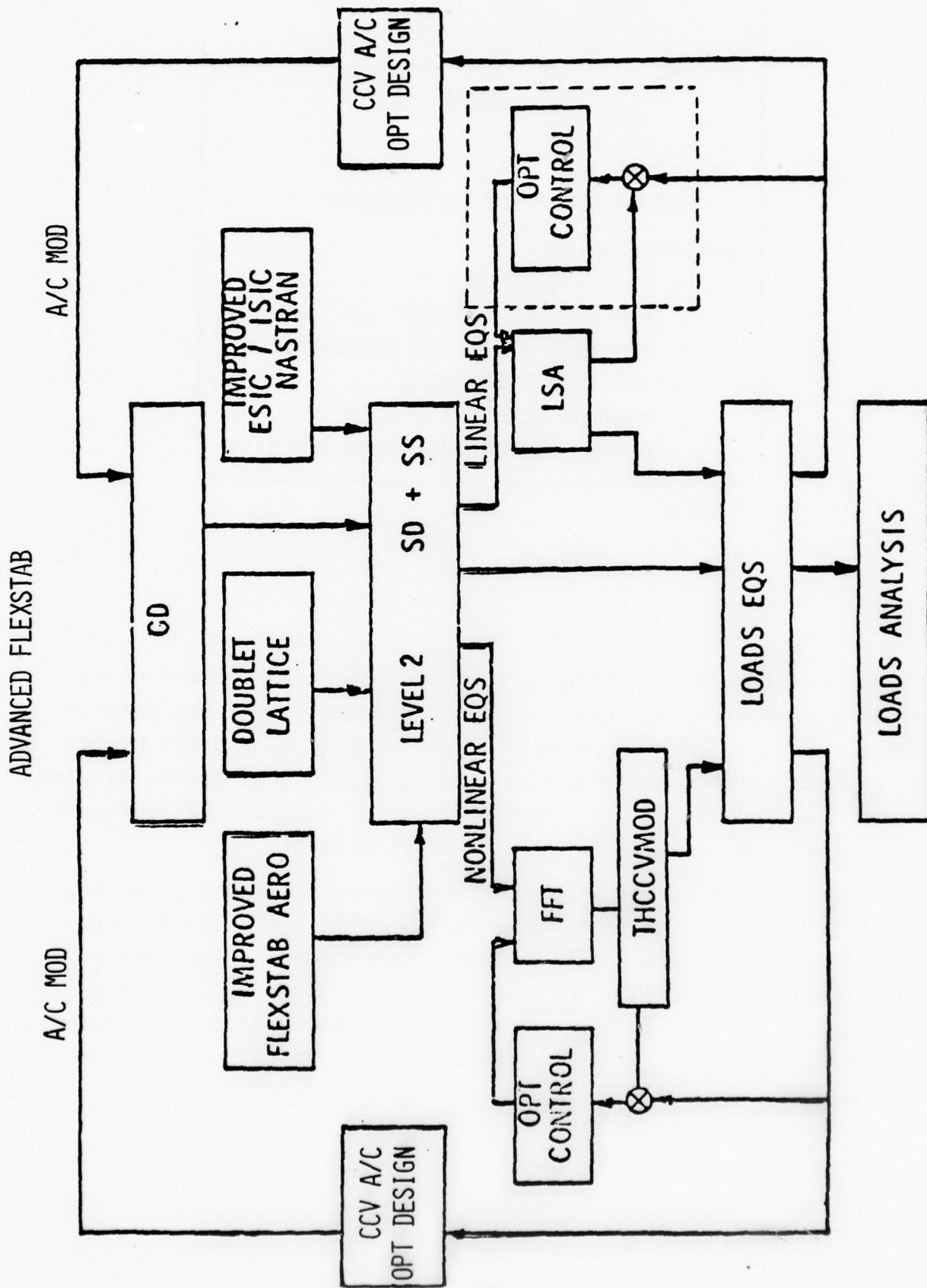
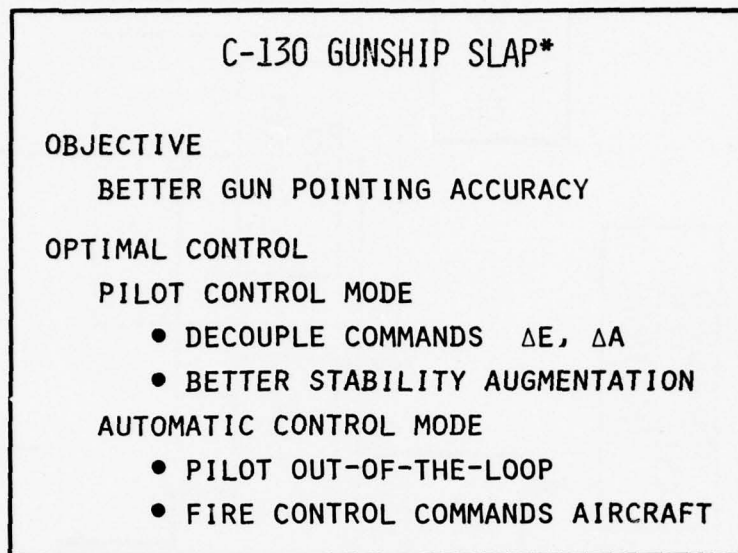


Figure 25



*USAFA

Figure 26

biases and really "sweating it out" with them. He gained their respect, and actually became a co-program manager of the program later. Because of his optimal control background and his belief in the modern technology he was able to impose them on the program. About the time the flight tests started the conflict in Southeast Asia came to an end and the program lost priority.

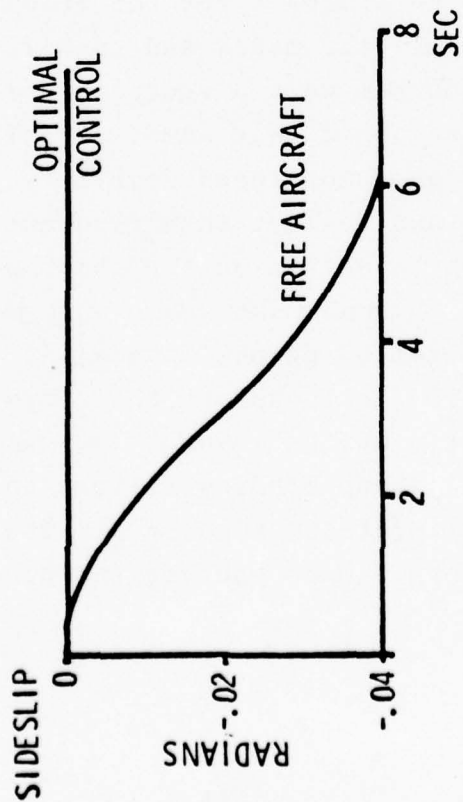
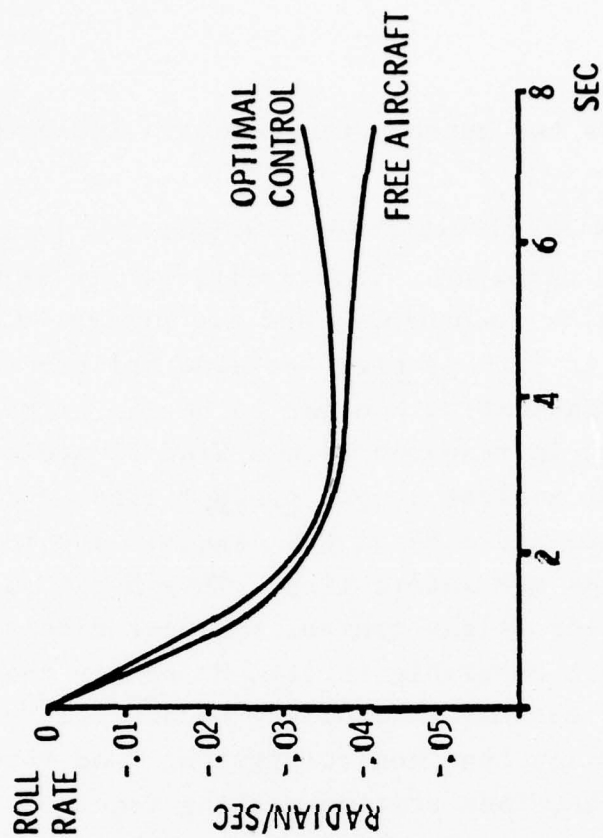
In the C-130 gunship there were other technical problems which involved software and integration of flight control with the fire control in a single computer and exceeding the limits of the computer. That kind of problem got in the way of carrying it all the way through to the operational system. But I think optimal control succeeded, and will probably be carried through on some similar program in the future.

Figure 27 shows two gunship responses to indicate how you are able to couple.

The next series of illustrations considers a program on the JA-37, a Swedish airplane. Internally, we are very concerned about transferring this technology, and are pretty well convinced that you have to do it with people. We also believed there were key people in the organization who had to be the prime movers. We teamed up a person in research with a kind of senior, grandfather flight control analyst in our product line, and we made them work together. And we had kind of CCV issues. The roles that they defined for themselves are interesting. They had to use the optimal control, and the senior flight control engineer didn't know or understand it, or have much ownership in it. He became the spec writer and the critic. The optimal control guy became the designer and the tool-user to develop that control system. And they butted heads for about three months, then started working together.

The engineer wanted to put an end to the optimal control once and for all, so he wouldn't let the researcher work the hard problem where he had all the modes and specifications for a large order system. He made him work a second-order system, short period. He gave him a frequency spec that comes out of the flutter group, where to get your DC gain for speed stability, to get your short period gain damping, and to meet this frequency constraint, he needed a very large attenuation on the short period. As you know, with just this second-order plant and just two feedbacks around it, you can't get 60 db per decade, it's only 20. So the researcher said, "Well (he looked at their system and it had bending filters in it), ah, ha, you've got bending filters in here, I'll just steal those bending filters and design the gain." Well, that got a foul protest, because all the work was in designing the bending filters. Once you got the bending filters anybody

OPTIMIZATION RESULTS C-130 PILOT CONTROL MODE



AILERON COMMAND

Figure 27

can pick the gains in five minutes. So, he was forced into using the optimal control to design the bending filters, and this was our start in the compensator design. Essentially what he did was augment the plant with some artificial or arbitrary filters with inputs, and used the quadratics to design the bending filters in addition to the gains. He ended up doing it in about three weeks, and that was pretty impressive to the classical guy, because he'd spent two years working on the problem, and, a novice in airplanes got as far in about a month. About that point in time, we sent them both to Sweden, and the engineer ended up in an argument with Professor Karl Astrom from Lund, who was the Swedish counterpart on this, on how to pick quadratic weights and responses. So, we started to win the battle.

In the time that remains I'd like to go through a list of different problems. Each one was motivated by a different real technical issue or system issue. We've designed CCV control laws for the NASA F-8 digital fly-by-wire program using the optimal control (Figure 28, 29). In that case, we were able to show performance improvements. Another program is an adaptive program at Langley. That program looks at three different adaptive concepts. We've looked at the old high-gain limit cycle concept like GE flys and F-111. We've flown in the F-15, and we wanted to look at that scheme to see how much better you could do implementing that digital computer. We picked a limit cycle, a model tracker scheme and a maximum likelihood scheme (Figure 30). We took all three of these through a competition through computer simulation. Figure 31 summarizes the concepts.

With these two schemes, you are just able to identify either implicitly or explicitly mg so they're about the same performance as the F-15 system. With this scheme we are able to identify more out of the data - pitching moment, velocity, angle-of-attack, and it

NASA F-8 PROGRAM

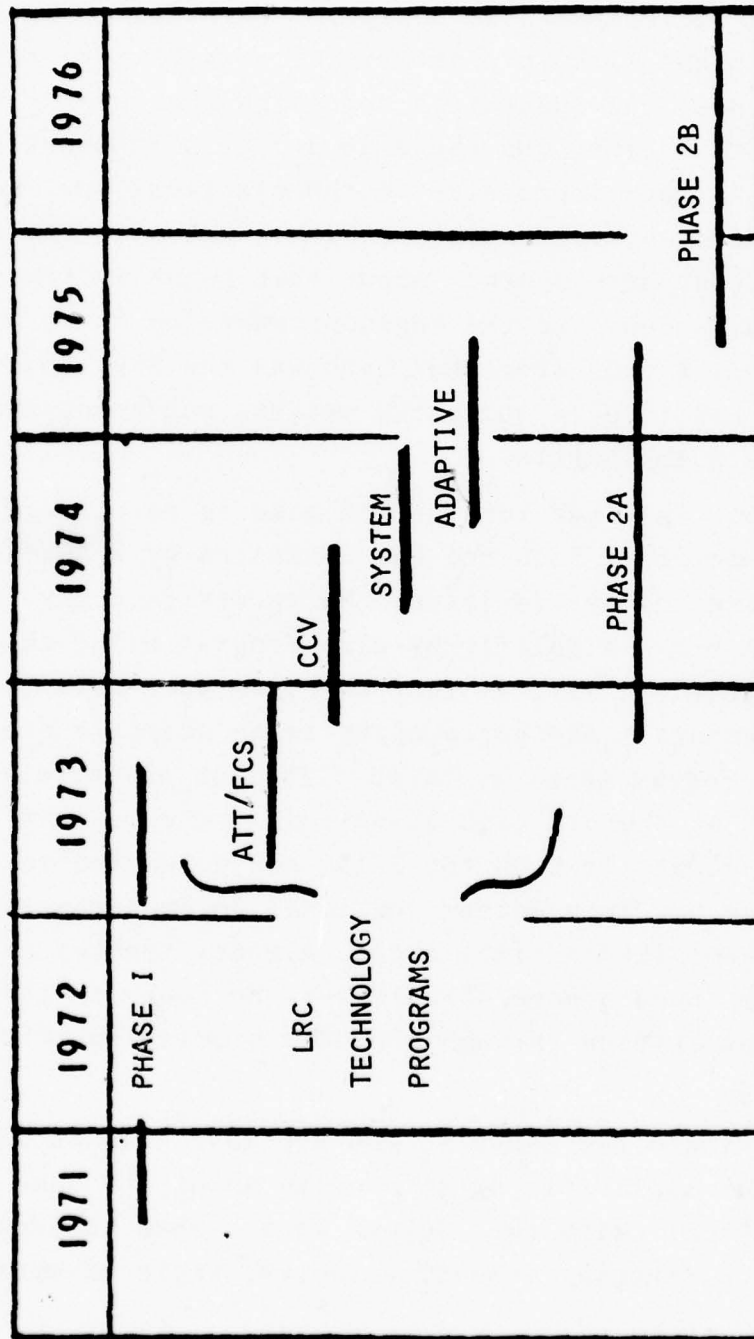


Figure 28

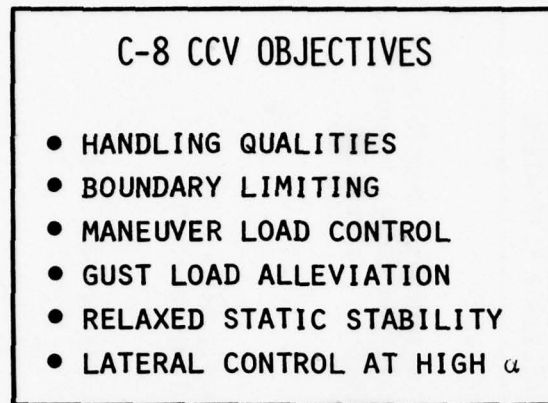


Figure 29

F-8 ADAPTIVE CONCEPTS

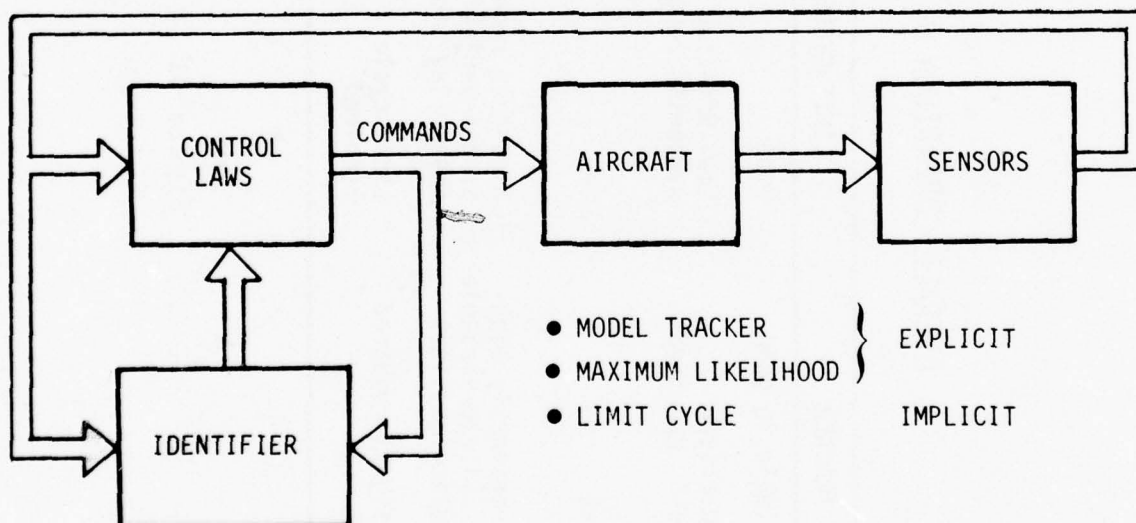


Figure 30

OVERALL COMPARISON OF CONCEPTS

	TRACKER	LIMIT CYCLE	MAX. LIKELIHOOD ESTIMATION
PERFORMANCE	Acceptable to good	Good	Good to excellent
GROWTH POTENTIAL	Low--Off-line synthesis required	Low--Off-line synthesis required	High--On-line synthesis possible --Air data functional redundancy Application possible
COMPUTER REQUIREMENTS	Minimal	Low	Medium
OPERATIONAL UTILITY	Not necessarily high-gain. Single-variable scheduling explicit	High-gain required Single-variable scheduling implicit	Not necessarily high-gain Multivariable scheduling Explicit
USER ACCEPTANCE	Test signal required	Limit cycle required	Test signal may be required

Figure 31

looks like there are substantial benefits to be gained from carrying this scheme on. One potential benefit is being able to eliminate air data in a triply-redundant task required data, which is always a problem.

Another area where optimal control has been applied is in re-entry vehicles (Figure 32). There are some very good technical reasons for addressing the problem with modern control theory, almost good enough that they outweigh the management, political and marketing type issues. If you look at the past, people have done frozen point designs, down nominal trajectories and spliced them together to design an optimal control system. With optimal control you can do the finite, time varying problem. This problem is characterized by very large parameter variations, very rapid parameter variations, and very large parameter uncertainties. In the past, people have done point mass trajectory determination, trajectory optimization, and then constrained the bandwidth of the control system to be wide enough that you could decouple it, and then control six-degrees-of-freedom. With the optimal control you can look at the coupled problem and compute steering gains also.

In the past, lateral, directional and longitudinal axis have been addressed separately, and then put together; sometimes you end up with constraints on pulling one maneuver, waiting for it to die out, and pulling the other maneuver. You couldn't pull both at once because you saturate and get limit cycles. With the optimal control's ability to handle the coupled maneuvers for a higher order system you are able to do this. The types of things you are looking for are lowering the design cost by the more rational procedure, trying to get a hardware cost. One potential benefit in looking at the coupled problem is that the bandwidth of the control system doesn't have to be artificially constrained to be high. You might also be able to reduce actuator bandwidth. Also, there are potential performance improvements to be gained by looking at the time-varying problem.

RE-ENTRY VEHICLE
QUADRATIC OPTIMAL CONTROL

ISSUES

TIME-VARYING	VS.	FROZEN POINT
COUPLED G&C	VS.	GUIDANCE THEN CONTROL
COUPLED 3 AXIS	VS.	LATERAL DIRECTIONAL AND LONGITUDINAL
DISCRETE	VS.	CONTINUOUS

PAYOFFS

DESIGN COST
HARDWARE COST
ACTUATOR BANDWIDTH
SENSORS
COMPUTER
PERFORMANCE

Figure 32

This same technique has been applied to tactical missiles and terminal control of tactical missiles (Figure 33), and the benefit I see there is in the conceptual stage -- you are able to look at the whole system (Figure 34) and do trade-offs and extensive looks at how a detector, a single detector bandwidth or specification, affects the whole system. Here is just an example of where we look at trade-offs on detector bandwidth versus miss distance (Figure 35). If you look at the component alone you get one answer; if you look at its effect on the total system, you get another answer.

CONTROL SCIENCES CAPABILITIES - TACTICAL MISSION

- INTEGRATED SYSTEM ANALYSIS
 - ANALYTICAL TRADE-OFFS FOR TOTAL SYSTEM
 - OPTIMUM TRADE-OFF BETWEEN SEEKER, VEHICLE, CONTROL PROVIDES PRACTICAL & OPTIMAL SYNTHESIS, ANALYSIS
 - TWO ANALYSIS TOOLS
 - MVOPT - MANEUVER VEHICLE OPTIMIZATION
 - DIGIKON - DIGITAL CONTROL

Figure 33

Jet engines are another area where optimal control has been applied by us and Gerry Michaels at UARL. About two years ago, we started looking at the J-85 engine. In engines there are really two control problems (Figure 36). If you look at fuel speed and fuel flow and possibly afterburner area, or afterburner fuel flow, you have an operating point, or an operating surface. Whereas, if you pick an exhaust area and a fuel flow, you get a given speed, and there is a whole plane associated with it. And, there are two control problems - one is to accelerate an engine from one point to another point on this plane without exceeding a surge constraint, where you blow fire out the front end (hence your constraint is where you melt the engine) or on the bottom side is another constraint called the blow-out, where you blow the fire out the back end of the engine.

The problem in which you blow the fire out the back end of the engine is a trajectory optimization problem - very non-linear, with non-linear constraints on state. There's also a regulator

INTEGRATED SYSTEM MODEL

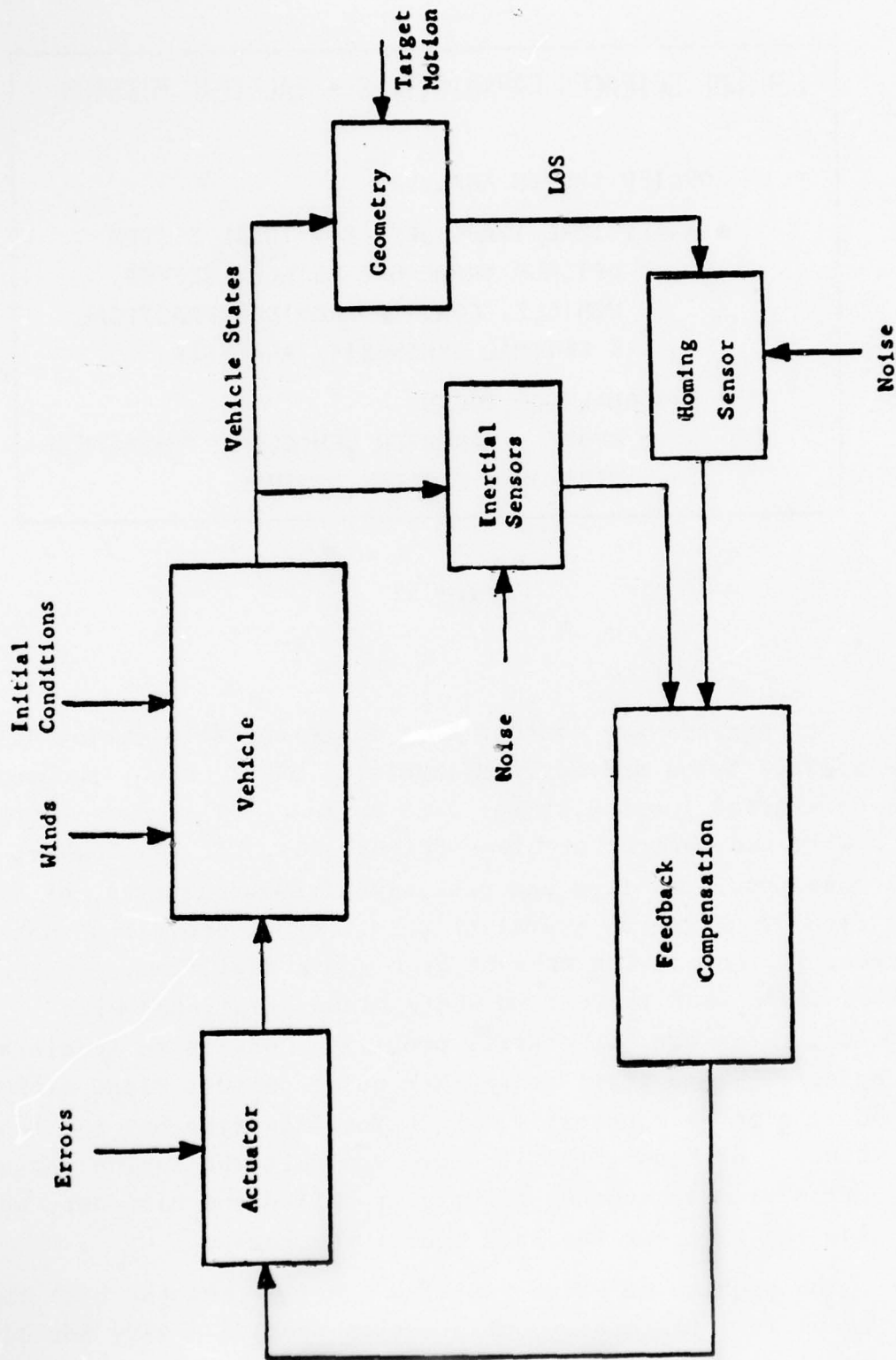


Figure 34

INTEGRATED SYSTEM PERFORMANCE EVALUATION

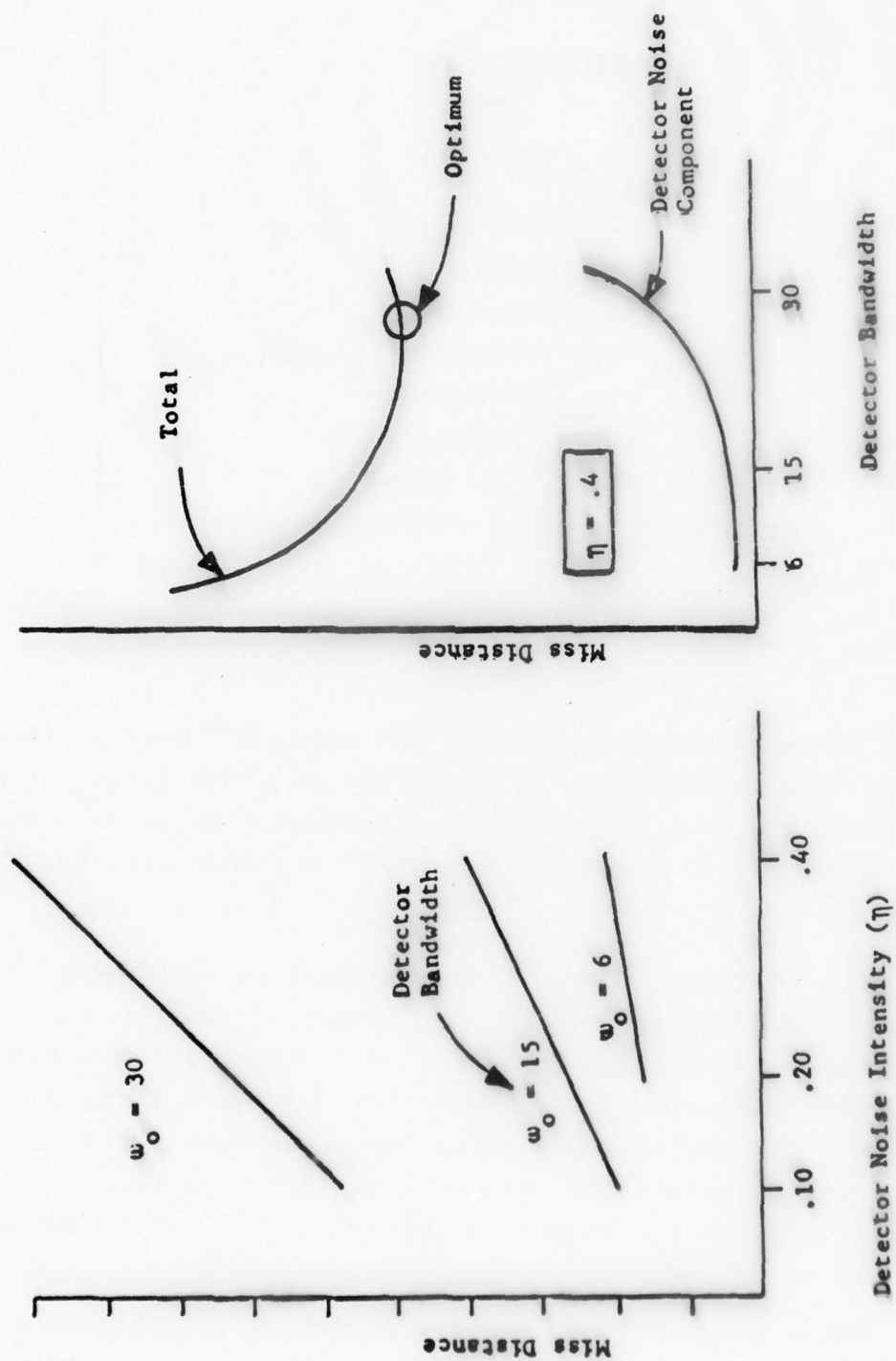


Figure 35

OPTIMAL CONTROL OF GAS TURBINE ENGINES

- ENGINE MODELING
PHYSICS
IDENTIFICATION
- STEADY STATE CONTROL
COMMAND OPTIMIZATION
QUADRATICS
- TRAJECTORY CONTROL
TRAJECTORY OPTIMIZATION
QUADRATICS
- SPECIAL MODES
- WIND TUNNEL TEST

Figure 36

problem of maintaining a point on the surface. Both of these problems have been addressed. Ed Beady at Pratt & Whitney has done extensive studies on the trajectory optimization problem using modern control. Gerry Michaels at UARL has done the regulator problem.

The J-85 engine went through a wind tunnel feasibility demonstration about a year ago, and Figure 37 shows a plot of Bode slams with an optimal controller. Essentially, a Bode slam is the old trick that is used to fool their engine controllers. It consists of pushing the power full forward, letting the engine accelerate and then pulling back. Do that very rapidly, and generally you can scoop the control system if you haven't paid attention to the detail.

Among other things that are happening in engines, people are starting to integrate the endflap with the engine and the exhaust (Figure 38). There is a hardware program in the Air Force

SPEED-PRESSURE BODE SLAMS

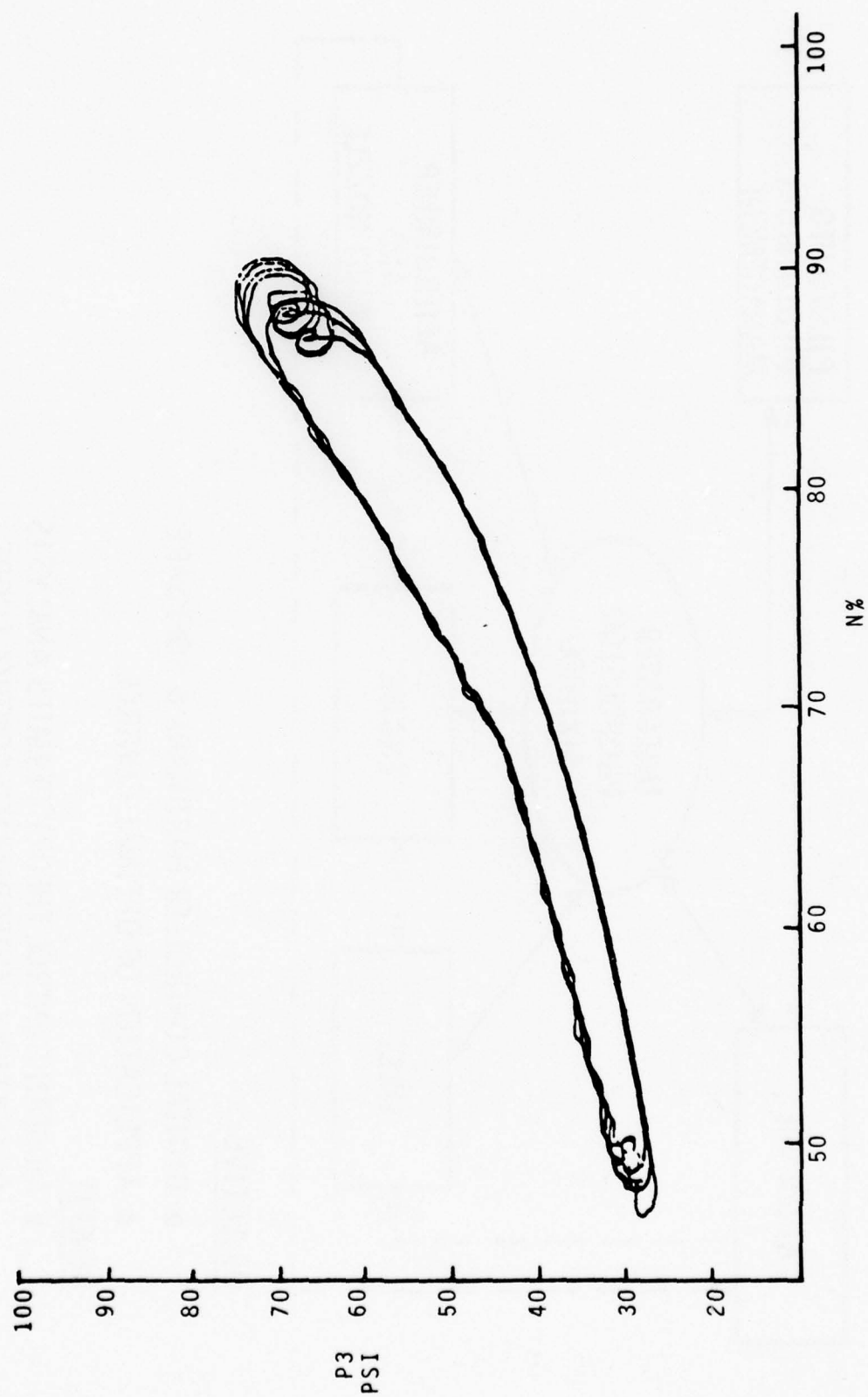
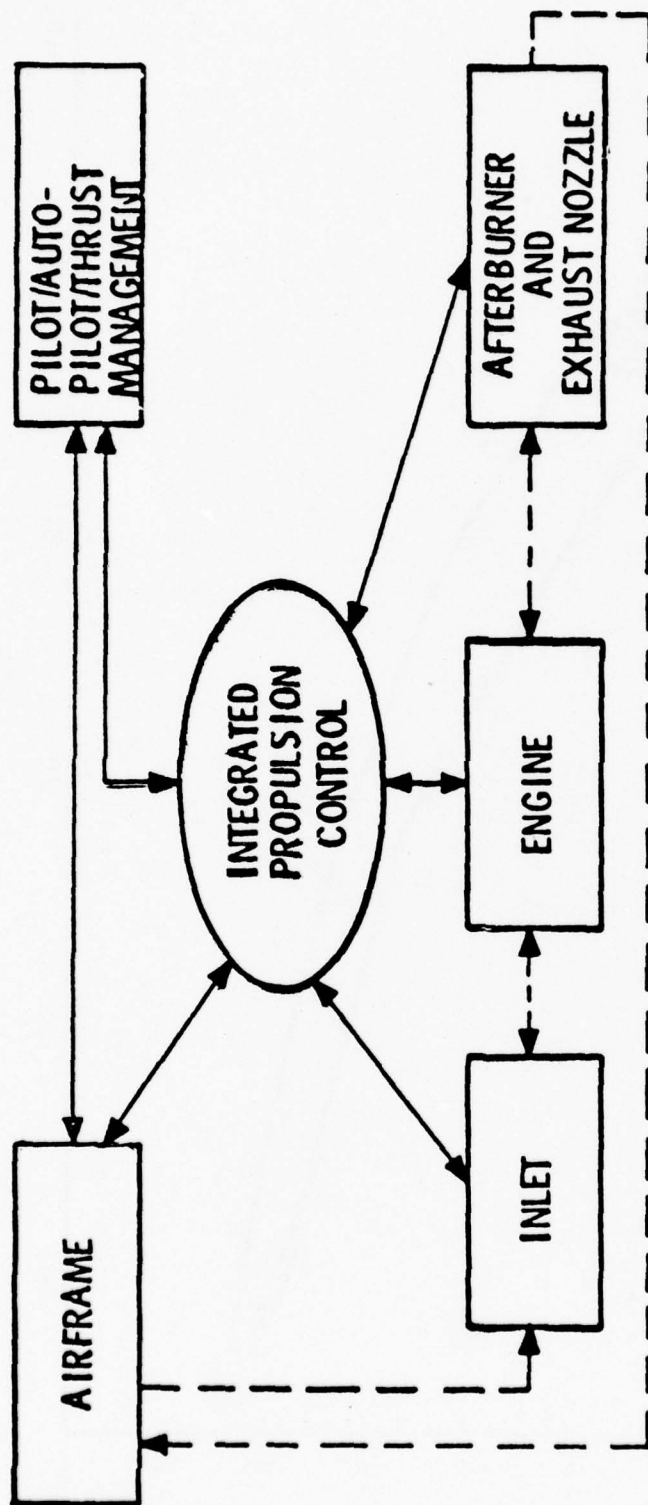


Figure 37

INTEGRATED PROPULSION CONTROL SYSTEM



OBJECTIVE

- DIGITAL CONTROLLER HARDWARE & SOFTWARE
- APPLICATION OF OPTIMAL CONTROL

BENEFIT

- MODERN CONTROL THEORY PERMITS ANALYSIS OF MULTIPLE, INTERRELATED CONTROL LOOPS

Figure 38

to do this integrated job implementing a digital computer and, at one point, we expect to do a parallel effort to apply optimal control to find better cross feeds which, because of program hardware problems and software problems, got eliminated from the program in the past. It's an example where there was a real technical need, but there was a program need that was overbearing and that was to hold the cost.

A joint technology demonstrator engine is being sponsored by the Air Force and the Navy. Future engines are getting more complicated with more control inputs. I think there's a real potential benefit to be gained by looking at the multi-variable problem in these complex engines, both the trajectory optimization and the regulator problem. I think there are some areas of research that need more work in engine control. One is modeling. The time delay problem before ignition is another and there are also some non-linear problems.

Another thing that's happening is that people are looking at the integration of the flight control with the propulsion control (Paul Blatt talked about this program). An example where this is needed is in high supersonic airplane at Mach 3+. A Concord has problems that are caused by coupling between the engine and flight control. The B-70 did, the YF-12 does. Essentially, I think, there are roles in this program; optimal control is being used to do the flight control, to do the propulsion control, and to do the integrated look at how you cross-feed these things.

In the engine business, there's been a lot of work, but there is a lot more work now on multi-variable control - more integration within the propulsion system, and coupling the two together (Figure 39). There have been both paper and pencil studies, and flight test studies out of NASA. The ultimate potential is flight path optimization, and fuel management. I think that's

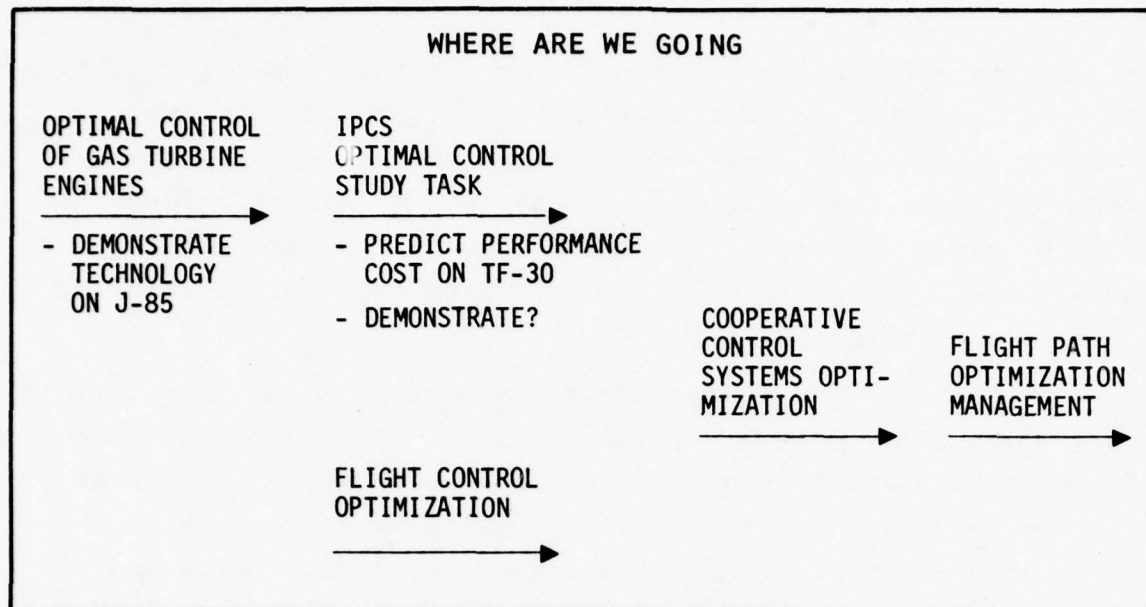


Figure 39

also been looked at by a lot of people, and I think in flight path optimization for the last couple of years, we have been waiting for the engine multivariable control and the integration to get caught up. The pressure of fuel costs will cause this to get a lot of attention in the future.

Problems with surface effect ships are another rich area for application of control theory. People at Aerojet are addressing those problems with optimal control; there are a lot of multi-variable problems there. The same applies to hydrofoils.

In summary, there are now an awful lot of problems where technology just needs to be applied. There are some technology problems which need research. I think we've got to become more concerned with the application, and we've got to become concerned with a lot of non-technical issues to succeed at the application.

THE APPLICATION OF STOCHASTIC CONTROL THEORY TO
NAVY FIRE CONTROL SYSTEMS

CHARLES F. PRICE
The Analytic Sciences Corporation (TASC)

In this paper "fire control" means tactical weapon systems that perform tracking, pointing, and homing guidance functions. This definition applies to systems involving missiles, guns, and in some cases, precision sensor control. Traditionally, the control and guidance techniques that have been applied to these systems can be rather simply described. Missile systems have for many years used proportional guidance, and tracking systems involving tracking and pointing functions have involved high-gain error type compensation techniques to close the tracking control loop. This paper indicates how some of the ideas of modern stochastic control theory have helped improve performance over that achieved with the classical techniques.

The systems of concern here are automatic, and they involve: (a) application of estimation theory to suppress tracking sensor errors, and (b) application of optimal control theory to achieve fire control objectives (Figure 1). In identifying these two functions, a separation principle is implied. That is, measurement data are first filtered to suppress the noise; then the filter outputs are employed to implement a control function to achieve the fire control objective.

The objective in fire control systems can be more simply stated than it can in some of the other applications discussed at this conference. Usually, the objective is to make a miss distance as small as possible, with a competing constraint on control level capability.

STOCHASTIC FIRE CONTROL SYSTEM CHARACTERISTICS

- RESTRICTED HERE TO AUTOMATIC SYSTEMS
- APPLY OPTIMAL ESTIMATION THEORY FOR TARGET TRACKING TO SUPPRESS SENSOR ERRORS
- APPLY OPTIMAL CONTROL THEORY TO ACHIEVE FIRE CONTROL OBJECTIVES

Figure 1

Figure 2 is a functional diagram for a fire control system which applies to missiles, guns, and sensors; some examples from all three of these applications are considered here. The system can contain a variety of instruments that sense the plant dynamic variables, as well as measure the weapon trajectory and its geometry relative to the target. All of the sen-

FIRE CONTROL SYSTEM STRUCTURE

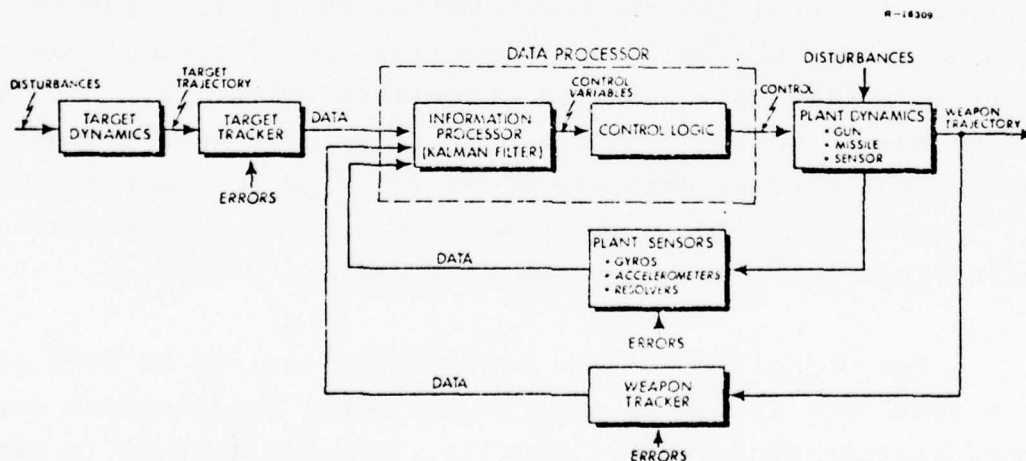


Figure 2

sor data is transmitted to an information processor, which is typically a state estimator such as a Kalman filter, or an extended Kalman filter, followed by control logic. Figure 3 gives a nonmathematical definition of a Kalman filter which highlights the fact that design of optimal data processors depends upon knowledge of the system dynamics, measurements, statistics, and in the case of target tracking systems, information about the target motion. Optimal control is summarized in Figure 4. A system model is needed to derive the control law, and the control is implemented using estimates of system state variables provided by the filter. In addition, the control law will depend upon the choice of the performance index. This very brief background highlights the fact that optimal filtering and control techniques are sensitive to knowledge of the plant, target dynamics, sensor statistics, disturbance statistics, and the choice of performance index (Figure 5).

KALMAN FILTER OVERVIEW

THE KALMAN FILTER IS A RECURSIVE* DATA PROCESSOR** WHICH ESTIMATES THE MOST PROBABLE STATE OF A SYSTEM UTILIZING:

- KNOWLEDGE OF SYSTEM DYNAMICS
- MEASUREMENTS
- ASSUMED STATISTICS OF SYSTEM AND MEASUREMENT ERRORS
- INITIAL CONDITION INFORMATION

* DOES NOT STORE PAST MEASUREMENTS

** COMPUTER PROGRAM OR DATA PROCESSING ALGORITHM

Figure 3

The first class of examples presented here concerns missile systems which have the objective of intercepting a target (Figure 6). Targets sometimes move and maneuver in unpredictable ways. Sensors measure this motion, incurring some measurement error; the missile has dynamics and nonlinear constraints. For instance, a missile has a limited acceleration capability. Thus, guidance laws are needed which inherently account for the stochastic and nonlinear dynamic properties of the missile system.

OPTIMAL CONTROL OVERVIEW

AN OPTIMAL CONTROL LAW SPECIFIES CONTROL LOGIC WHICH MINIMIZES (OR MAXIMIZES) A WELL DEFINED PERFORMANCE INDEX UTILIZING:

- KNOWLEDGE OF SYSTEM DYNAMICS
- ESTIMATES OF SYSTEM STATE VARIABLES

Figure 4

PERFORMANCE OF FIRE CONTROL SYSTEMS IS
SENSITIVE TO ERRORS IN DESIGN ASSUMPTIONS

- PLANT/TARGET DYNAMICS
- DISTURBANCE AND MEASUREMENT ERROR STATISTICS
- CHOICE OF PERFORMANCE INDEX

Figure 5

APPLICATION FOR MISSILE STOCHASTIC GUIDANCE LAWS

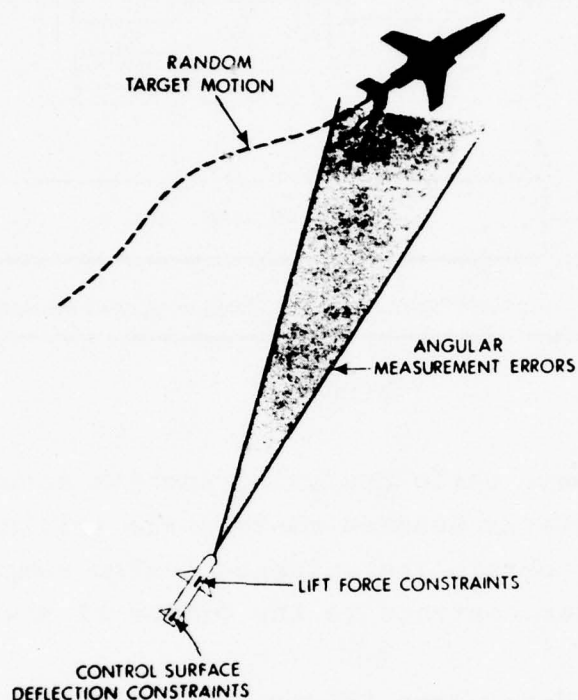


Figure 6

Figure 7 is a conceptual diagram for a CADETTM missile system model, that is useful for demonstrating the effect of different kinds of tracking algorithms (filtering techniques) and guidance algorithms (control logic for steering the missile) on missile performance, when various degrees of optimality are employed in the design. The term "CADET" refers to the Covariance Analysis Describing Function Technique, developed by TASC for analyzing nonlinear stochastic systems. (The method is much more

*CADET is a trademark of The Analytic Sciences Corporation.

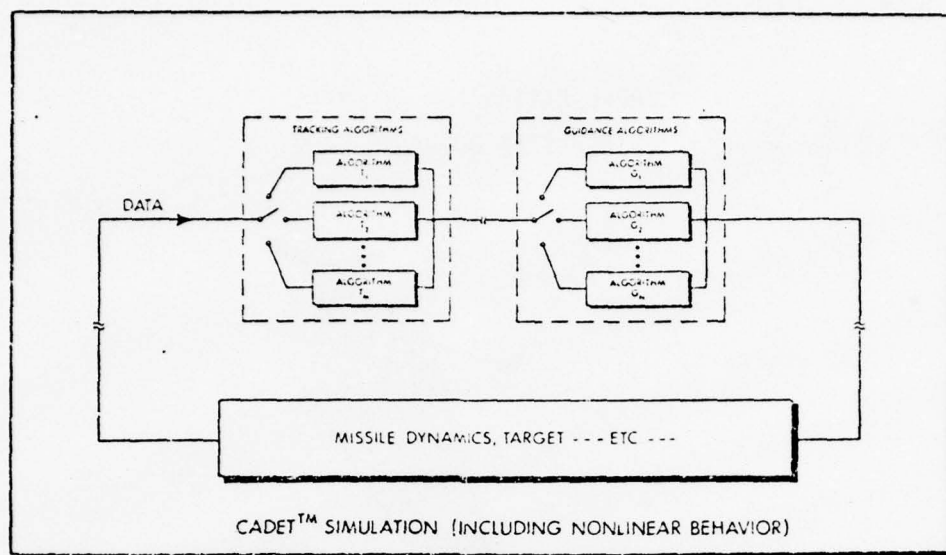


Figure 7

efficient than monte carlo analysis; and its accuracy compares favorably with several hundred monte carlo trials. The CADET model was used to obtain the guidance system comparisons presented below, under contract to the Office of Naval Research.

Five guidance laws (Figure 8) which involve various combinations of control logic and filtering techniques have been considered. The first, A, is a classical method -- proportional guidance with a first order filter whose parameters are optimized for the particular assumed noise statistics. In B, a Kalman filter is employed to optimally estimate the target line-of-sight rate needed to mechanize the proportional guidance law. In C and D, the control logic is derived by minimizing a performance index which is a weighted sum of the mean square miss distance and a quadratic integral penalty on the commanded acceleration. The difference between C and D is that C accounts for the target maneuver in mechanizing the control law, whereas D accounts for both the target maneuver and the missile autopilot. Law E is based upon minimizing the mean absolute miss distance, subject to the known missile acceleration limit.

GUIDANCE LAW DESIGNATIONS

A: PROPORTIONAL GUIDANCE; FIRST ORDER FILTER

B: PROPORTIONAL GUIDANCE; KALMAN FILTER

C: OPTIMAL LINEAR GUIDANCE, # 1; KALMAN FILTER

- Accounts for Target Maneuver Effects
- Minimize $\lim_{\lambda \rightarrow 0} E [(\text{miss})^2 + \lambda \int_0^{T_f} (\text{acceleration})^2 dt]$

D: OPTIMAL LINEAR GUIDANCE, # 2; KALMAN FILTER

- Accounts for Target Maneuver and Missile Autopilot Effects
- Minimize $\lim_{\lambda \rightarrow 0} E [(\text{miss})^2 + \lambda \int_0^{T_f} (\text{acceleration})^2 dt]$

E: OPTIMAL NONLINEAR GUIDANCE; KALMAN FILTER

- Accounts for Target Maneuver, Limited Missile Maneuver Capability, and Missile Autopilot Effects
- Minimize $E [|\text{miss}|]$ Subject to $|\text{acceleration}| \leq a_{\max}$

Figure 8

Figure 9 gives an indication of how these guidance laws perform if the design assumptions are matched to the CADET model. The miss distance is plotted versus the target acceleration bandwidth for each case. The greater the bandwidth, the more rapidly the target acceleration varies, causing progressively greater miss distance over the range of bandwidths considered. With the optimal techniques C, D, and E, the miss distance is about one-half that achieved with proportional guidance.

A proper evaluation of guidance laws requires analysis of their sensitivity to situations where the design assumptions are not matched to the CADET model, representing modeling uncertainty. Figure 10 displays the sensitivity of miss distance to

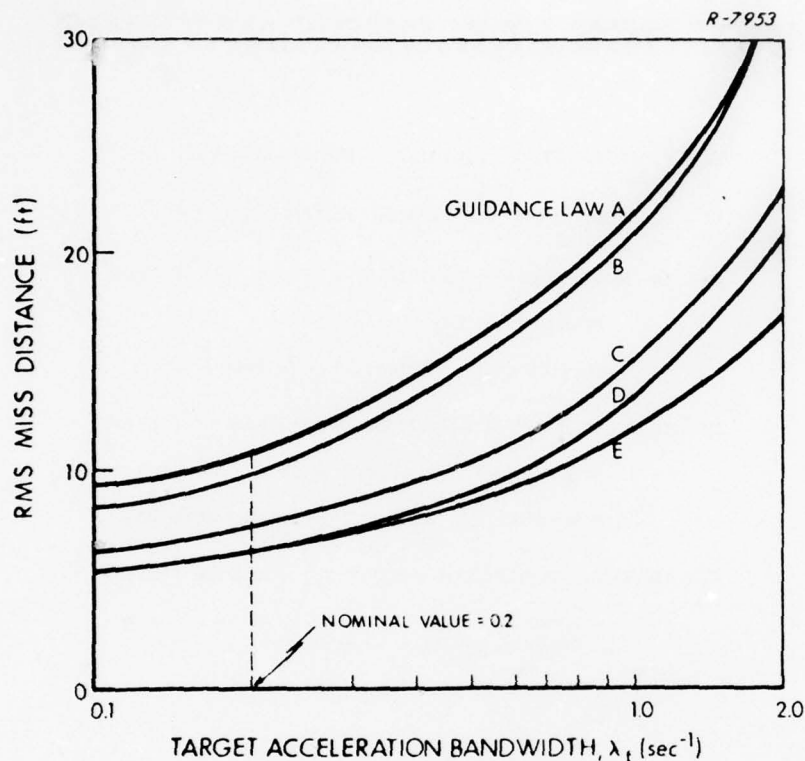
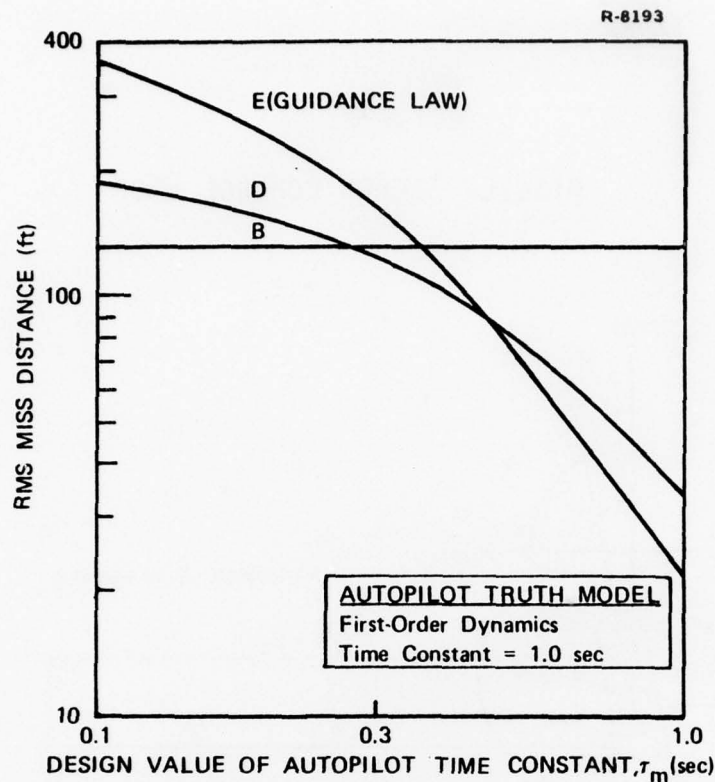


Figure 9

variations in the assumed value of the missile autopilot time constant for three of the laws defined in Figure 8. The case examined is one where the "true" (i.e., the value in the CADET model) autopilot time constant is one second. This could be typical of missile dynamics at high altitude. When the system design is matched to the truth model, proportional guidance (B) performs significantly worse than the optimal guidance techniques (D and E). However, if the design value of the time constant is much smaller than the true value, the optimal techniques perform worse than proportional guidance; the latter yields the same miss distance for all values of τ_m in Figure 10 because it does not depend upon an assumed value of the missile time constant. Consequently, it is important that accu-



rate values of design parameters be used in the optimal guidance laws.

The next application to be discussed is pointing and tracking systems. Figure 11 is an example of a seeker tracking system employing three different seeker control techniques. The seeker can measure the angular position of the target relative to its boresight and information about the seeker motion is provided by a rate gyro. Given these sensors, a model for the seeker dynamics, and a model for the target, a control law using a Kalman filter is designed with control gains which maintain a small seeker tracking error, ϵ . The conventional high gain compensation technique uses only the measurement of the tracking error, without the rate gyro information. The third design investigated was a suboptimal, compromise control technique that is simpler to implement than the optimal design, with some sacrifice in performance.

MISSILE SEEKER CONTROL LOOP

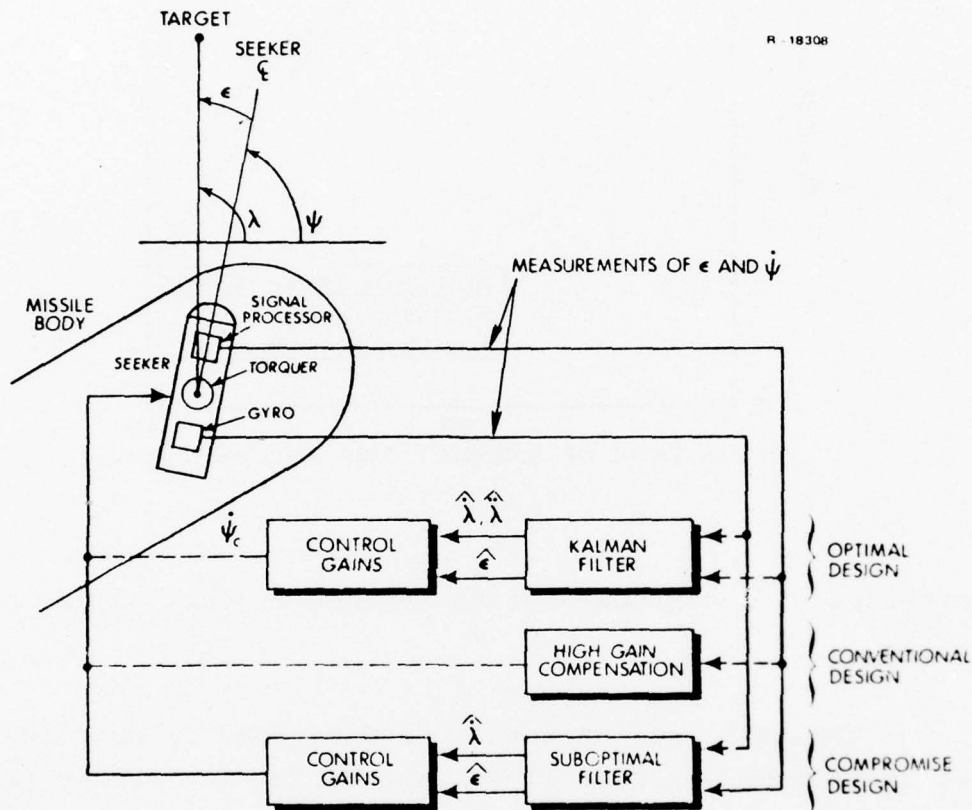


Figure 11

Performance comparisons for the above pointing and tracking techniques are shown in Figure 12 for a specific set of conditions that include a maneuvering target. Evidently the optimal and suboptimal designs offer significant improvement over the high gain design; the increment in improvement offered by the optimal method over the suboptimal method is a result of the fact that the former uses an estimate of target angular acceleration in the control law. The root-mean-square (RMS) con-

trol levels applied to the seeker for each case are shown in Figure 13.

Optimized pointing and tracking techniques are also useful against crossing targets -- i.e., targets that cross the sensor line-of-sight, as illustrated in Figure 13a. The pointing error achieved with the high gain compensation technique is shown in Figure 13b. Large errors occur in the crossover region because the target line-of-sight has large angular time-derivatives of all orders. For comparison, the pointing error achieved

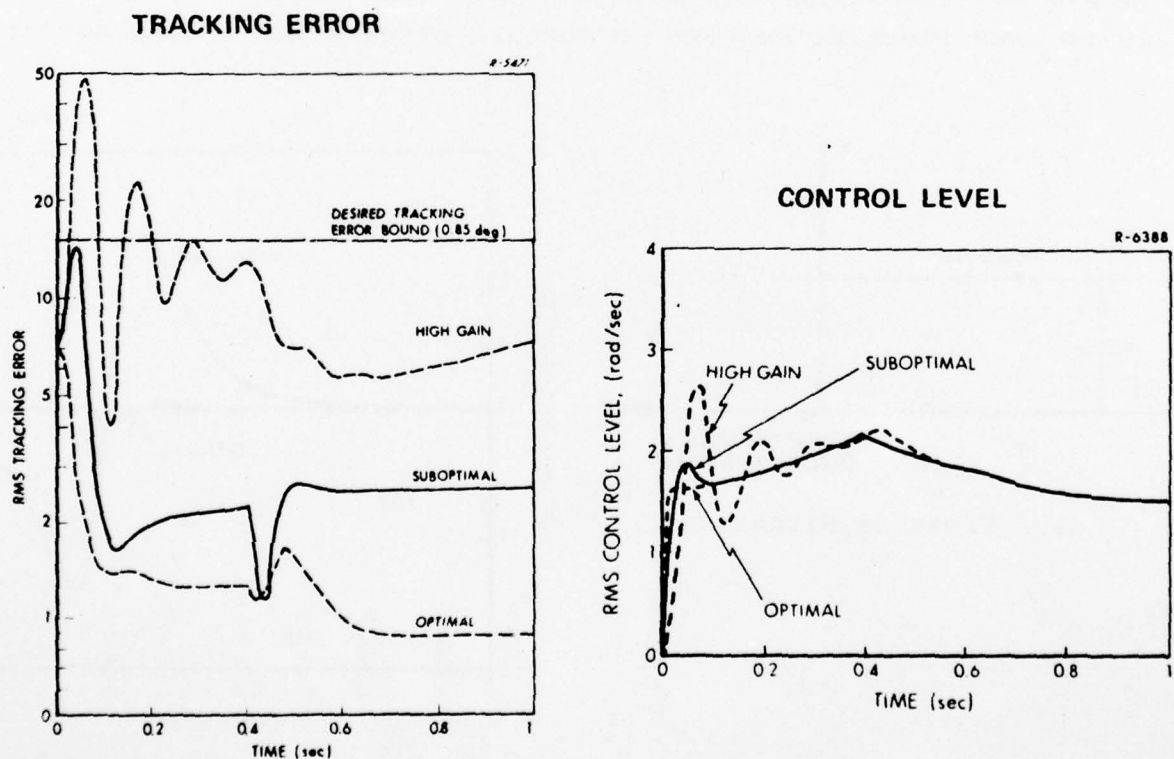
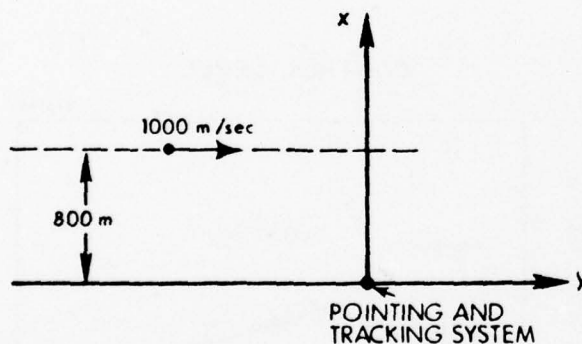


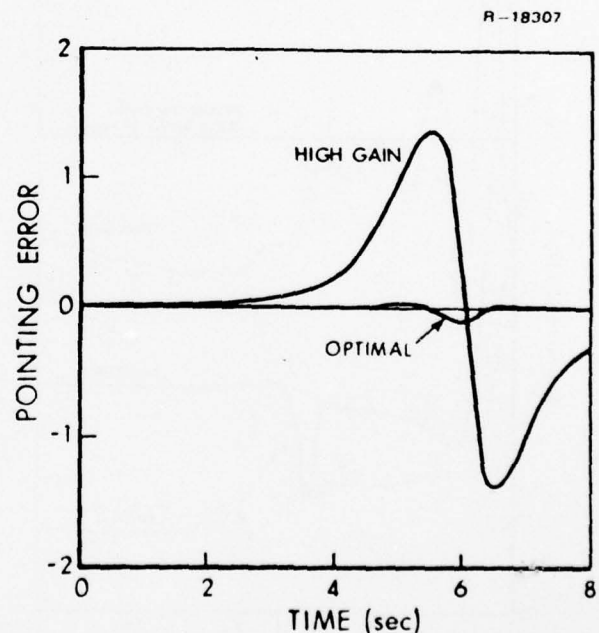
Figure 12

with an optimal design using a Kalman filter to estimate target angular rate and acceleration is also shown in Figure 13b. The observed improvement over high gain control can be critical for precision sensors that must maintain track of crossing targets.

From the above examples, it is clear that optimized pointing and tracking systems offer improved performance over conventional designs. However, just as in the case of missile guidance, the sensitivity of pointing accuracy to errors in the design assumptions upon which the pointing and tracking logic are based must be investigated. Consider the "on-axis" system shown in Figure 14 which has a sensor that measures the angular error between the pointing device and the target location. It also uses inertial sensors to measure orientation of the device



(a) Crossing Situation



(b) Comparison of High Gain and Optimized Pointing and Tracking Systems

Figure 13

POINTING SYSTEM STABILITY SENSITIVITY TO MODELING ERRORS

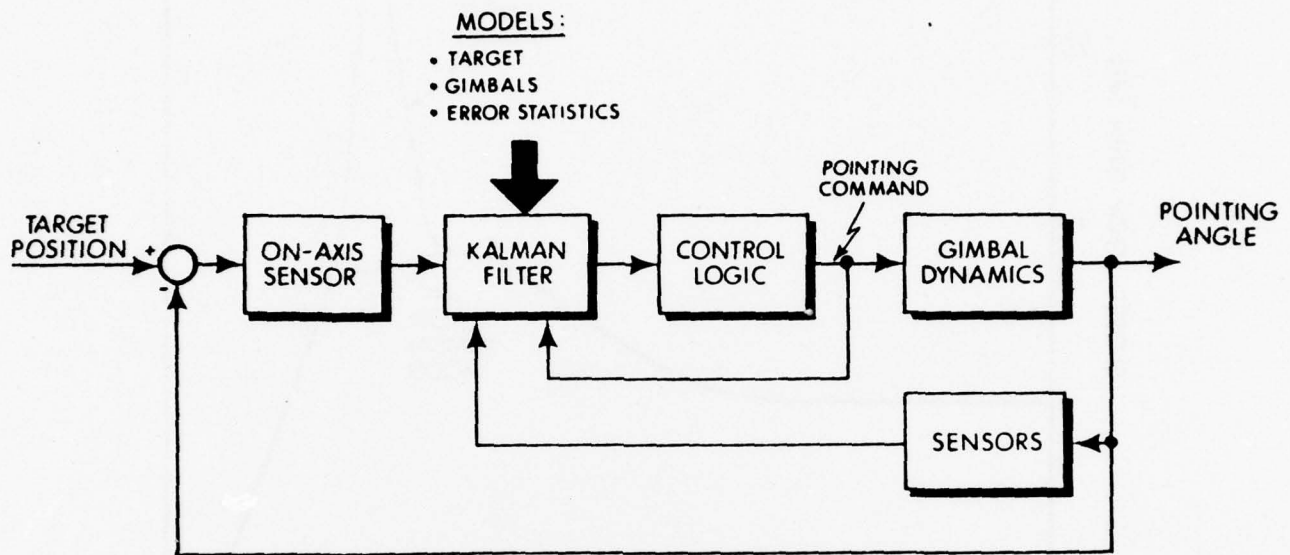


Figure 14

relative to an inertial reference frame. Observe that the seeker control loop in Figure 11 is an example of on-axis tracking.

The Kalman filter design in an on-axis system will be based upon dynamic models for both the target and the pointing device gimbal suspension system. If the pointing angle can be measured more accurately than the target position, the filter logic will attempt to eliminate the pointing angle from the on-axis sensor to obtain an equivalent measurement of target position relative to the inertial reference frame. In order to achieve an inertially referenced target position measurement, it is necessary to have a good model for the gimbal dynamics; if an inaccurate model is used, system stability may be adversely affected. This is illustrated in Figure 15 which compares the closed-loop frequency response of a system having

CLOSED LOOP FREQUENCY RESPONSE

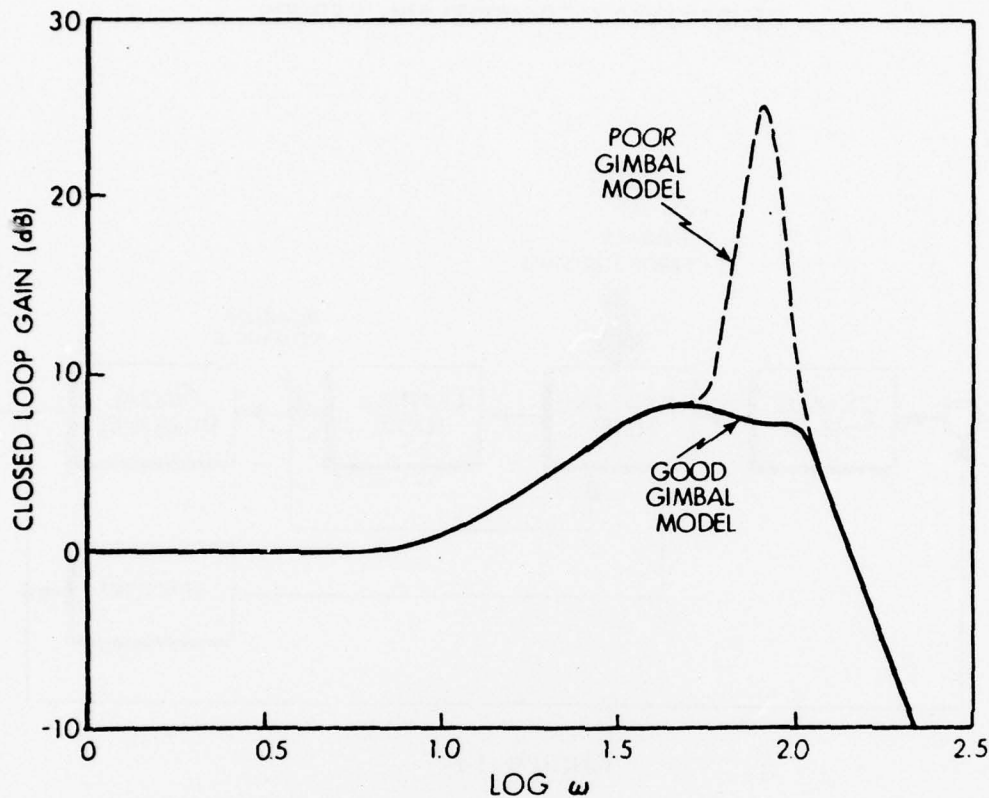


Figure 15

the structure of Figure 14, using both accurate and inaccurate gimbal models. Evidently the latter yields a nearly resonant closed loop system, which would have considerable response to noise and other disturbances.

Another sensitivity issue in tracking systems is the target behavior. Figure 16 demonstrates the performance that can be obtained with a Kalman filter which estimates target acceleration normal to the line-of-sight. Three target trajectories were examined having different acceleration spectra. The terms nonevasive, nominal, and highly evasive refer to increasing spectral bandwidths, respectively.

TRACKING SENSITIVITY TO TARGET MANEUVER CHARACTERISTICS

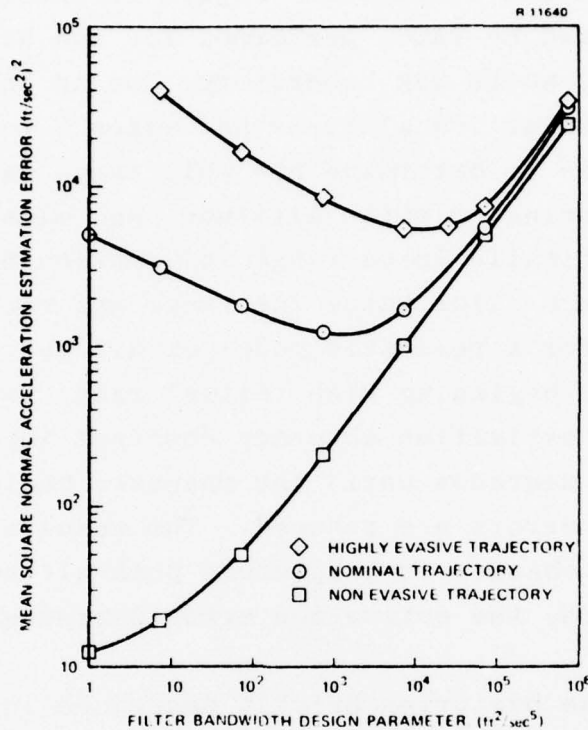


Figure 16

The mean square acceleration error is plotted in Figure 15 versus a filter bandwidth parameter. The latter is an element of the target "process noise" matrix (Q-matrix) used in calculating the filter gains. For each type of trajectory, there is an optimum bandwidth which minimizes the trade-off between the goals of noise suppression and following the target motion; this optimum is at the minimum of each curve in Figure 15. The curves also indicate that a filter optimized for one bandwidth may perform poorly if the actual target bandwidth is different from the assumed value. Thus, the sensitivity of tracking filter performance to target modeling errors is an important issue.

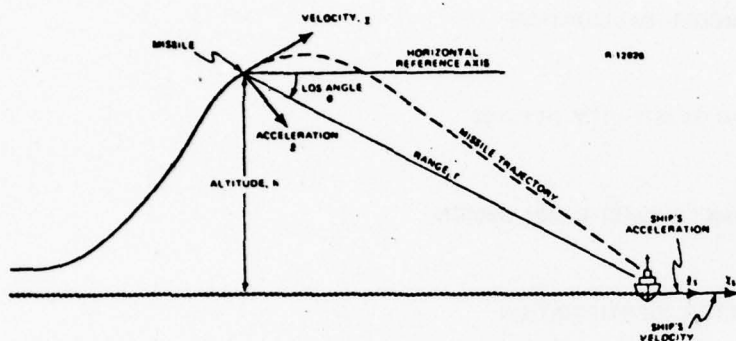
The utility of Kalman filtering for tracking targets is most dramatic when direct measurements of certain trajectory coordinates are not available. Figure 17 presents an application investigated by TASC, performed for the Naval Surface Weapons Center, White Oak Laboratory, for an anti-shipping missile which flies at low altitude and makes a terminal maneuver. The question was to determine how well range can be estimated from target bearing, missile altitude, and missile inertial data when the missile loses range information because of jamming. The figure illustrates the range and range rate estimation accuracy for a realistic model of all the error sources in the system. Beginning with initial range rate errors, the range rate estimation accuracy does not improve and the range accuracy degrades until the maneuver begins, after which the estimation errors are reduced. The results also show the sensitivity to changes in trajectory peak altitude; as the altitude increases, the estimation error decreases.

The case histories briefly described in this paper demonstrate that modern control and estimation theory has been useful in handling maneuvering targets, high velocity crossing targets, and range denied environments (Figure 18). Approaches that can reduce some of the effects of modeling errors are listed in Figure 19. Good model calibration is an obvious remedy; i.e., the control and estimation logic should be based upon an accurate system model. In many cases, some degree of modeling uncertainty must be tolerated; minimum sensitivity and minimax designs, can provide a degree of insensitivity to modeling errors.

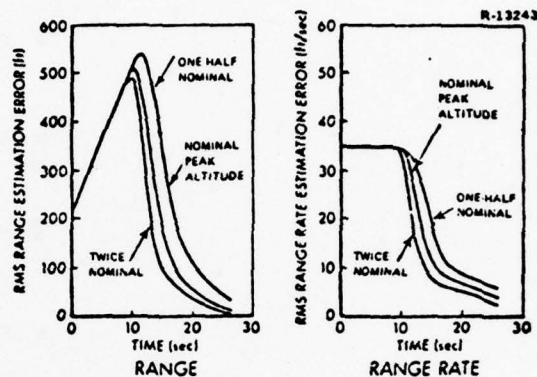
On-line parameter identification is closely related to the subject of off-line parameter identification discussed by others at this conference. Recursive data processing algorithms, such as the extended Kalman filter, are available for on-line

METHODOLOGY

- DEVELOP MODELS FOR MISSILE TRAJECTORY, SHIP, AND ERROR SOURCES
- DETERMINE THE RANGE AND RANGE RATE ESTIMATION ACCURACY ACHIEVABLE WITH AN OPTIMAL PROCESSOR



TRAJECTORY FOR AN ANTISHIPPING MISSILE



ESTIMATION ERROR SENSITIVITY
TO MISSILE TRAJECTORY HEIGHT

Figure 17

STOCHASTIC CONTROL THEORY CAN IMPROVE FIRE CONTROL SYSTEM PERFORMANCE AGAINST:

- MANEUVERING TARGETS
- HIGH-VELOCITY CROSSING TARGETS
- RANGE-DENIED ENVIRONMENTS

Figure 18

APPROACHES TO REDUCING EFFECTS OF MODELING ERRORS

- GOOD MODEL CALIBRATION
- MINIMUM SENSITIVITY DESIGNS
- "MINIMAX" (WORST CASE) DESIGN
- PARAMETER IDENTIFICATION
- ADAPTIVE TECHNIQUES

Figure 19

processing to estimate unknown or changing system parameters. These estimates can be used to implement adaptive techniques that make real-time adjustments to parameters in a Kalman filter or control law, thereby achieving estimation and control logic that is more closely matched to the true system dynamics.

The principle intent of this paper is to summarize some of the fire control applications where modern stochastic control theory is being used. Predictably, the most extensive applications of this technology are shipboard systems having relatively large digital computation capability. It is expected that the continuing advances in miniature computer hardware will make this technology accessible to the full range of Navy fire control systems.

THE CARRIER AIRCRAFT APPROACH PATH CONTROL SYSTEM
AS AN OPTIMAL CONTROL SYSTEM *

L.G. HOFMANN

SYSTEMS TECHNOLOGY, INC., PRINCETON, N.J.

ABSTRACT

Optimal control technology is applied to synthesize an approach path control system for a typical Navy carrier aircraft. A performance index is evolved which causes the optimal system to have feedback gains similar to those for a comparable system evolved using conventional analysis and simulation techniques. The optimal control problem formulation is the key to obtaining meaningful results. It includes stochastic models for the longitudinal and normal burble and gust environment, and sink rate commands, and a performance index consisting of the weighed sum of squares of airspeed error, integrated angle of attack error, sink rate error, elevator deflection, throttle deflection, elevator rate, and throttle rate. Numerical performance index weighting coefficients are evolved for the A-7E aircraft, and generalized weighting coefficients dependent upon key aircraft stability derivatives, are suggested for applications to other aircraft.

*This research was sponsored by the Naval Air Development Center, Warminster, Pennsylvania, as part of Contract No. N62269-73-C-0264. The author is indebted to colleague's Robert F. Ringland, John J. Shanahan, and Gary L. Teper for their valuable discussions and assistance with the computations.

†Principal Research Engineer

Introduction

This paper addresses representation of an A-7E Approach Path Control System (APCS) as synthesized using conventional frequency-domain and simulation techniques as the solution of a corresponding problem in optimal control. In principle at least, we endeavor to answer the question, "For what quadratic performance index is the conventionally-designed APCS optimal?" In other words, we wish to solve the so-called inverse optimal control problem. Rather than attempt a direct solution of the inverse optimal control problem, however, we have repetitively solved the (direct) optimal control problem while varying the weighting coefficients in the performance index in a systematic way to cause the optimal gain values to approach the conventional gain values. This approach was selected in preference to a formal solution of the inverse optimal control problem in the belief that we might more easily restrict the performance index to be a function of variables which are physically-meaningful in the context of this flight control problem. While the same restriction might have been imposed on a solution of the inverse optimal control problem, we were unable to appreciate how this could be done. The selected approach proved surprisingly adequate despite its lack of esoteric appeal.

The objectives were as follows:

- Specify a formulation for the APCS optimal control problem which can produce a solution which is similar to a conventionally-designed A-7E APCS.

- Identify the performance index form and values for the weighting coefficients that produce optimal control system gain values which are equal to their counterparts in the conventionally designed system.
- Generalize the performance index so that it might be used for the solution of other APCS synthesis problems.

The results are more than moderately successful in meeting all three objectives. In addition, some useful insights to further possible improvement of APCSs were obtained from the optimal control solutions, and one general insight pertinent to the effect of stochastic input bandwidth upon optimal system synthesis was also obtained.

The following sections will cover the aircraft-environment-control system model, the optimal control problem formulation and solution techniques, and results.

Aircraft, Environment, and Control System Models

The linearized Laplace-transformed perturbational equations of motion for the aircraft are given by the matrix equation, Eq. 1 (from Ref. 1).

AD-A045 603

SYSTEMS CONTROL INC PALO ALTO CALIF
PROCEEDINGS OF THE SYMPOSIUM ON CONTROL THEORY AND NAVY APPLICA--ETC(U)
AUG 77. M D CILETTI, J S TYLER

F/G 15/7

N00014-72-C-0327

NL

UNCLASSIFIED

7 OF 8
ADA045603



$$\begin{bmatrix}
 s - X_u^* & -X_w & g & 0 & 0 & 0 \\
 -Z_u^* & (1 - Z_w^*)s - Z_w & -U_0 s & 0 & 0 & 0 \\
 -M_u^* & -M_w^* s - M_w & s^2 - M_q s & 0 & 0 & 0 \\
 0 & 1 & -U_0 & 1 & 0 & 0 \\
 -s & 0 & -g & 0 & 1 & 0 \\
 0 & -s & l_x s^2 + U_0 s & 0 & 0 & 1
 \end{bmatrix}
 \begin{bmatrix}
 u \\
 w \\
 \theta \\
 \dot{h} \\
 a_x \\
 a_z'
 \end{bmatrix}
 =
 \begin{bmatrix}
 X_{\delta_e} & X_{\delta_T} & -X_u^* & -X_w \\
 Z_{\delta_e} & Z_{\delta_T} & -Z_u^* & -Z_w^* s - Z_w \\
 M_{\delta_e} & M_{\delta_T} & -M_u^* & -M_w^* s + \frac{M_q}{U_0} s - M_w \\
 0 & 0 & 0 & 0 \\
 0 & 0 & 0 & 0 \\
 0 & 0 & 0 & 0
 \end{bmatrix}
 \begin{bmatrix}
 \delta_e \\
 \delta_T \\
 u_g \\
 w_g
 \end{bmatrix}
 \quad (1)$$

Airspeed sensor responds to $u_a = u - u_g$

α sensor responds to $w_a = w - w_g$

Normal accelerometer located a distance l_x ahead of the c.g. responds to a_z'

Longitudinal accelerometer at c.g. responds to a_x

The basic numerical data for these equations is given in Table 1 for a typical power approach flight condition.

Figure 1 is a block diagram for a conventionally-designed APCS for the A-7E aircraft (Ref. 1). Provisions in the APCS for removal trim levels from sensor outputs and for lift compensation with bank angle, though of practical importance, have not been incorporated in Fig. 1. Certain other simplifications are made in order that the state vector in the optimal synthesis have as few elements as possible. Namely, a washout in the δ_e -to- δ_T crossfeed path has been neglected; the throttle and engine response lag and a filter in the feedback path to δ_T , $1/(s + 1)^2$, has been approximated by $0.5/(s + 0.5)$; and the forcing terms in the aircraft equations which depend upon \dot{w}_g have been neglected. An effective actuation lag of $10/(s + 10)$ in the δ_e path has been added, and a feedback of normal acceleration to elevator which has very low open-loop gain at this flight condition has also been neglected (Ref. 1). These simplifications are unlikely to affect the resulting design in an appreciable way.

Table 1

A-7E Geometry and Aerodynamic Derivatives for Power Approach

Note: Data for body-fixed stability axes

$$S = 375 \text{ ft}^2, \quad \bar{c} = 10.84 \text{ ft}, \quad z_j = 0.271 \text{ ft}, \quad \alpha_{TL} = 10.73 \text{ deg}$$

$$W = 24,000 \text{ lb}, \quad m = 746 \text{ slugs}, \quad \text{c.g. at } 28.6\% \text{ MAC}$$

$$I_{yy} = 68,000 \text{ slug-ft}^2, \quad l_x = 6.7 \text{ ft}$$

$$h = 0 \text{ ft}, \quad M = 0.1953, \quad U_0 = 218 \text{ ft/sec}, \quad \alpha_0 = 12 \text{ deg}$$

$$\rho = 0.002378 \text{ slugs/ft}^3, \quad a = 1,117 \text{ ft/sec}, \quad q = 56.51 \text{ lb/ft}^2$$

NONDIMENSIONAL DERIVATIVES	
C_L	1.105
$C_{L\alpha}$	3.870
$C_{L\dot{\alpha}}$	0
$C_{L\dot{M}}$	0
$C_{M\alpha}$	-0.514
$C_{M\dot{\alpha}}$	-0.750
C_{Mq}	-3.900
$C_{M\dot{M}}$	0
C_D	0.189
$C_{D\alpha}$	0.6113
$C_{D\dot{M}}$	0
T_M	-4480.
$C_{L\delta_e}$	0.518
$C_{M\delta_e}$	-0.648
$C_{D\delta_e}$	-0.0258

DIMENSIONAL DERIVATIVES	
X_u^*	-0.054534
X_w	0.064327
T_u	-0.005376
Z_u^*	-0.286953
$Z_{\dot{w}}$	0
Z_w	-0.528871
M_u^*	-0.000165
$M_{\dot{w}}$	-0.000289
M_w	-0.007964
$M_{\dot{\alpha}}$	-0.062987
M_{α}	-1.736239
M_q	-0.327532
X_{δ_e}	0.732836
Z_{δ_e}	-14.713536
M_{δ_e}	-2.188878
$X_{\Delta T}$	0.001317
$Z_{\Delta T}$	-0.000250
$M_{\Delta T}$	0.000004

*The starred derivatives are used to designate that thrust variations with speed (sometimes not available) have been included.

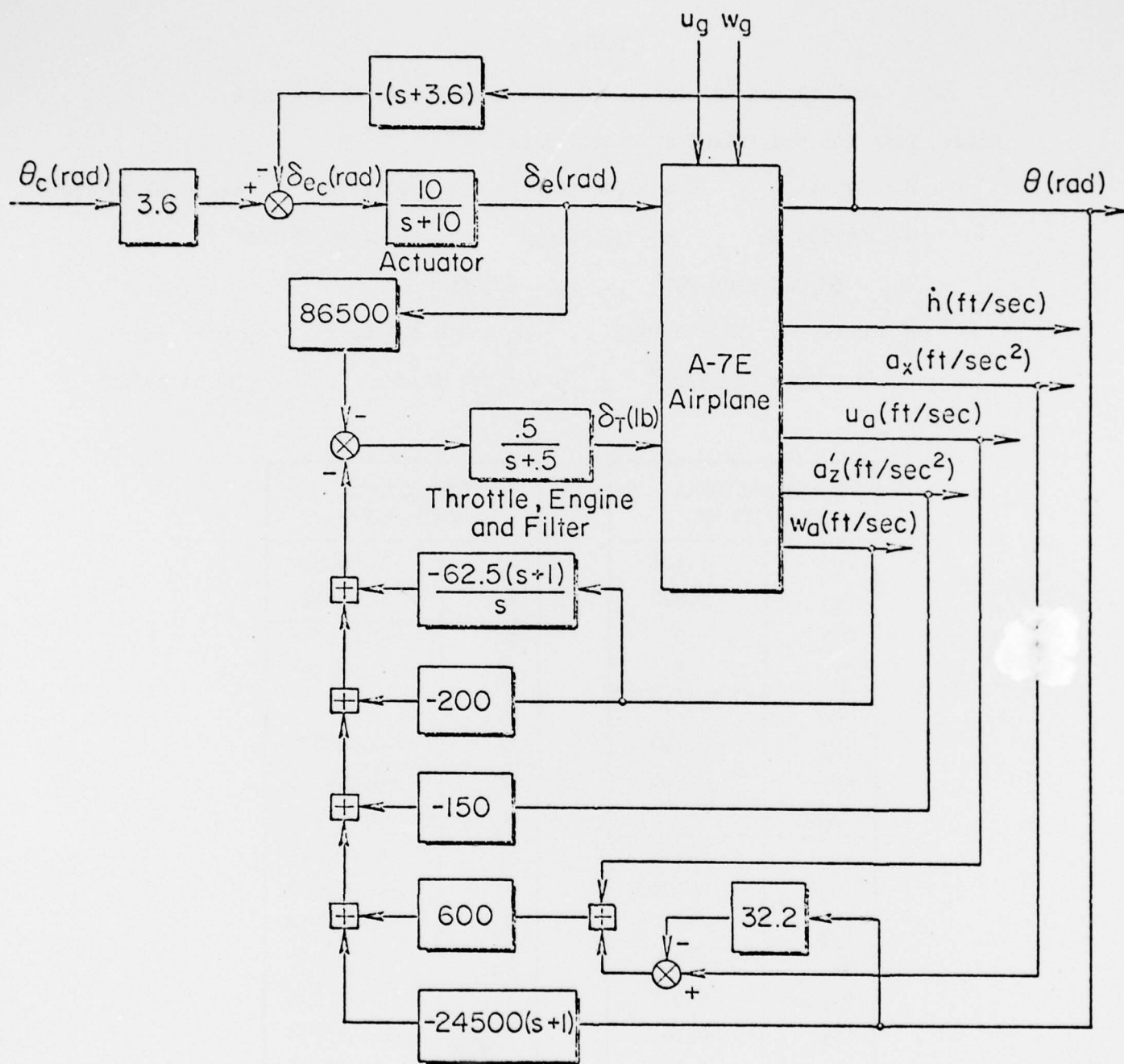


Figure 1. Approximation to the Conventionally Designed A-7E APCS.

The Laplace-transformed equations for the control system in Fig. 1 are

$$(s + 10.)\delta_e = 10. \{-(s + 3.6)\theta + 3.6\theta_c\} \quad (2)$$

$$\begin{aligned} s(s + .5)\delta_T = & .5 \{-86500. s\delta_e + 262.5(s + .238)w_a \\ & + 150. sa_z' - 600. su_a - 600. sa_x \\ & + 43820. s\theta + 24500. s^2\theta\} \end{aligned} \quad (3)$$

Figure 1 depicts the APCS as a pitch attitude control system (viz. θ_c) while in reality the objective is to control vertical speed. Therefore the appropriate commanded quantity is actually \dot{h}_c . The approximate scaling between \dot{h}_c and θ_c commands is the nominal airspeed, U_0 . The target closed-loop bandwidth for \dot{h}/\dot{h}_c (or \dot{h}/θ_c) is 1 rad/sec for this APCS.

The disturbance environment includes longitudinal and normal gust and burble components as well as a vertical speed (or pitch attitude) command. The gust and burble components will be modeled by low-pass filtered white noise.

$$\dot{u}_g = -\omega_{u_g} u_g + (2\omega_{u_g})^{1/2} \sigma_{u_g} n_1 \quad (4)$$

$$\dot{w}_g = -\omega_{w_g} w_g + (2\omega_{w_g})^{1/2} \sigma_{w_g} n_2 \quad (5)$$

The disturbance bandwidths are $\omega_{u_g} = \omega_{w_g} = 2.18$ rad/sec, the rms levels are $\sigma_{u_g} = 2.51$ ft/sec and $\sigma_{w_g} = 4.75$ ft/sec, and n_1 and n_2 are independent unit white noise sources. Vertical speed commands of interest are a step command to insure acceptable response dynamics and steady-state response characteristics, and a low-pass filtered white noise command to simulate ship motion effects during the deck-chasing mode of operation.

$$\ddot{h}_c = -\omega_{\dot{h}_c} \dot{h}_c + (2\omega_{\dot{h}_c})^{1/2} \sigma_{\dot{h}_c} n_3 \quad (6)$$

The command bandwidth is $\omega_{h_c} = 0.6$ rad/sec, the rms level of \dot{h}_c is $\sigma_{\dot{h}_c} = 1.54$ ft/sec*, and n_3 is an independent unit white noise source.

Models for the Optimally Designed APCS

It is necessary that conventional and optimal system designs be representable in common terms in order that the two APCS designs may be compared. Two steps taken to facilitate this comparison are

- Choose a state vector for optimal design that includes all linearly independent feedback variables used in the conventional design and an appropriate control vector. (That is, include the physically meaningful variables controlled by the feedback loops.)
- Express the conventional APCS design in terms of the state vector used in the optimal design.

The state vector, x , and control vector, u , are chosen as:

$$\underline{x}' = \{u_a, w_a, q, \theta, \delta_e, \delta_T, \int w_a dt, u, \dot{h}, -\dot{h}_e\} \quad (7)$$

$$\underline{u}' = \{\dot{\delta}_e, \dot{\delta}_T\} \quad (8)**$$

* This model is a cavalier approximation to a narrow-band random process having peak power at $\omega_p = 0.6$ rad/sec and a $2\sigma_{\dot{h}_c}$ value of 1.85 ft/sec² (Ref. 2, Table B-1). $\sigma_{\dot{h}_c}$ has been determined by $\sigma_{\dot{h}_c} = \sigma_{\ddot{h}_c} / \omega_p = 1.54$ ft/sec. A concern for simplicity is responsible for our use of this very simplified model for \dot{h}_c .

** The control vector in this formulation consists of the physical control rates. This formulation has been used by Kleinman, Baron, and Levison in Ref. 3 and by Rynaski and Whitbeck in Ref. 4 with considerable success. This formulation assures that the control rates demanded for optimal control will be amenable to moderation by appropriate adjustment of the control weighting coefficients in the performance index. This is an important feature which allows the designer of optimal systems to account for the rate limits which are characteristic of power actuation devices.

All quantities except a_z^1 and a_x in Eq. 3 are elements of the state vector. a_z^1 and a_x may be expressed in terms of state vector elements using Eq 1 and the result used to eliminate a_z^1 and a_x from Eq. 3. If the resulting expressions are evaluated using numerical values from Table 1, the following equations of the form $\underline{u} = -K\underline{x}$ are obtained for the conventionally designed APCS.

$$\begin{aligned} \dot{\delta}_e = & - \{ 0. u_a + 0. w_a - 10. q - 36. \theta + 10. \delta_e \\ & + 0. \delta_T + 0. \int w_a dt + 0. u + 0. \dot{h} + 0. (-\dot{h}_e) \} - 36. \theta_c \end{aligned} \quad (9)$$

$$\begin{aligned} \dot{\delta}_T = & - \{ 305. u_a - 76.2 w_a - 12700. q - 21910. \theta \\ & + 43480. \delta_e + .9159 \delta_T - 31.25 \int w_a dt \\ & + 0. u + 0. h + 0. (-\dot{h}_e) \} \end{aligned} \quad (10)$$

Equations 9 and 10 are in a suitable form for comparison with counterpart optimal APCS control laws.

Optimal system synthesis using time-domain techniques requires the "plant" equations in state vector form. That is in the form:

$$\dot{\underline{x}} = A\underline{x} + B\underline{u} + \underline{w}, \quad \underline{x}(0) = \underline{x}_0 \quad (11)$$

\underline{w} is the "process" noise vector, a vector with white noise elements. The steady-state covariance for the state vector, \underline{x} , in the presence of the control law, $\underline{u} = -K\underline{x}$, is the matrix $C = E[\underline{x}\underline{x}']$ given by the solution of

$$C(A - BK)' + (A - BK)C + W = 0 \quad (12)$$

where

$$W \delta(t - \tau) = E[\underline{w}(t)\underline{w}'(\tau)] \quad (13)$$

The performance index, J , is the expected value of a quadratic form of the states and controls.

$$J = E [\underline{x}' Q \underline{x} + \underline{u}' R \underline{u}] \quad (14)$$

Existence of an optimal solution requires that the R matrix be positive definite (Ref. 5).^{*} The Q and R matrices are here further restricted to be diagonal matrices in order that J be the weighted sum of mean square values for the states and controls. This restriction is sufficient (but not necessary) to assure that J is the weighted sum of mean square values for physically-meaningful variables within the context of this flight control problem.

Solution Technique

This section discusses the computational and procedural techniques used to solve for the optimal feedback gain matrix, to solve for the steady-state covariance of the state for closed-loop systems, and to accommodate the uncontrollable modes of the "plant" which are characteristic of this particular application.

Solution of the Steady-State Matrix Riccati Equation

It is well-known that the optimal feedback gains (in the sense of minimizing the performance index, J) are given by

$$K = R^{-1} B P \quad (15)$$

where P is the positive definite solution of the steady-state matrix Riccati equation

^{*} Q is often required to be positive semi-definite (e.g., Ref. 5). However, it has been demonstrated that optimal solutions may exist even when Q is a non-positive matrix (Ref. 6 and 7, pp. 35-37).

$$A'P + PA + Q - PBR^{-1}BP = 0 \quad (16)$$

when A, B, Q, and R are constant matrices (e.g., Refs. 5 and 8). The solution technique used is that described by Kleinman in Refs. 9 and 10. Kleinman's algorithm is an iterative approach which involves solving a sequence of steady-state covariance equations, the solution of which converges to the Riccati equation solution. It can be shown that the iterative scheme is analogous to Newton's method. The algorithm provides successive solutions which are characterized by monotone quadratic convergence.

Solution of the Steady-State Covariance Equation

Solutions of steady-state covariance equations are required in the course of solving the steady-state Riccati equation by the technique described above as well as in obtaining the covariance of the state vector for the closed-loop system.

The solution technique used transforms the covariance equation (Eq. 12) into an equation of the form:

$$C = F'CF + T \quad (17)$$

The transformed equation is then solved by a recursive technique which converges very rapidly. The algorithm is described in detail in Ref. 10.

Novel Features of the APCS Synthesis

Optimal synthesis problems are seldom formulated in a way which accounts for the finite bandwidth of the disturbance and command inputs. The finite bandwidth of these inputs has been accounted for in the formulation of the optimal APCS synthesis problem used herein. This feature also results in a

potential theoretical problem. Namely, only 7 of the 10 elements of the state vector for the APCS problem are controllable.* However, the statement on p. 679 of Ref. 5 implies that the "plant" need not be completely controllable if the uncontrollable modes are stable. Since the 3 uncontrollable modes correspond to the input shaping filter modes, and these modes are stable, existence of an optimal solution is still assured for the APCS problem.

The merits of including weightings on the control rates in the performance index for representing power actuation rate limitations has been discussed previously. It is an essential feature in our experience if one hopes to obtain optimal solutions which have some sense of practicality. A further benefit of this feature is that its inclusion effect induces lag filtering in the optimal controller which would otherwise be completely lacking. This lag filtering provides the potential for a "complementary filter" structure in the optimal controller. The effectiveness of complementary filtering as a practical technique in feedback control is well-known. It is comforting to know that it can be a part of the optimal controller structure because of the particular formulation of the problem used here.

Matching the Optimal Control Law to the Conventional Control Law

Matching of the optimal control law to the conventional control law is accomplished by trial-and-error adjustment of the diagonal elements of the

*It is obvious that the 3 modes corresponding to the shaping filters (see Eqs. 4-6) are not controllable by means of \underline{u} .

Q and R matrices. When a reasonable match is achieved, the resultant Q and R matrices may be regarded as specifying a performance index for which the conventional control law is approximately optimal.

This approach, while perhaps pedestrian, proved effective. The rather good match of control laws presented in the next section is the result of only 26 solutions of the optimal synthesis problem.

Results, Discussion, and Interpretation

The results of this control law matching process are presented below. The discussion points up certain implications of the optimal control law and addresses certain deficiencies. In addition, a generalized form of the performance index is given which should prove useful for synthesizing other APCs.

Effect of Stochastic Input Bandwidth

A finding of this research is that the sum of the optimal feedback gain for a controllable variable (such as u , w , or $\dot{h} = -w + U_0\theta$) with the gain for a corresponding variable containing an uncontrollable mode (such as $u_a = u - u_g$, $w_a = w - w_g$, or $(-\dot{h}_e) = \dot{h} - \dot{h}_c$, respectively) is invariant with any stochastic input bandwidth (such as ω_{u_g} , ω_{w_g} , ω_{h_c}) when only the latter variable is weighted in the performance index. This made it possible to pursue the initial matching of the optimal and conventional control laws using a state vector with seven in distinction to ten elements. This increased computational and engineering efficiency considerably in the matching task.

Best-Match Optimal Solution

The optimal control law which best matched the conventional law was obtained with $\omega_{hc}^* = 0$ in order to ensure unity-gain feedback of vertical speed. This optimal control law is:

$$\begin{aligned} \dot{\delta}_e = - \{ & \underline{.00876} u_a - \underline{.00549} w_a - \underline{10.1} q - \underline{12.2} \theta + \underline{9.54} \delta_e \\ & + .000101 \delta_T - .0139 \int w_a dt + .0805 u + 0. \dot{h} - \underline{.108} (-\dot{h}_e) \} \end{aligned} \quad (18)$$

$$\begin{aligned} \dot{\delta}_T = - \{ & 11.1 u_a + 10.2 w_a - 97.0 q - 3693. \theta + 105. \delta_e \\ & + .995 \delta_T - 18.1 \int w_a dt + 202. u + 0. \dot{h} + 58.2 (-\dot{h}_e) \} \end{aligned} \quad (19)$$

Equation 19 can be written in a slightly different and approximate form which compares more favorably with the conventional control law. Since the bandwidth of the elevator actuator lag is 9.54 rad/sec (refer to Eq. 18), it is evident that $\dot{\delta}_e$ will be very small in the frequency range within the bandwidth of the effective throttle, engine, and filter lag which is .995 rad/sec (refer to Eq. 19). Therefore $\dot{\delta}_e$ may be set to zero in Eq. 18, the resultant expression may be solved for $(-\dot{h}_e)$ and used to eliminate $(-\dot{h}_e)$ from Eq. 19 by substitution. The result of these operations is:

$$\begin{aligned} \dot{\delta}_T \doteq - \{ & \underline{6.42} u_a + \underline{7.36} w_a - \underline{5570.} q - \underline{10300.} \theta \\ & + 5270. \delta_e + \underline{1.05} \delta_T - \underline{25.7} \int w_a dt \\ & + \underline{247.} u + 0. \dot{h} + 0. (-\dot{h}_e) \} \end{aligned} \quad (20)$$

The significant terms on the right-hand sides of Eqs. 18 and 20 are underlined. The terms have been judged significant on the basis of the magnitude of the product of the gain and the root mean square value of the variable in the term.

The approximation to the optimal $\dot{\delta}_T$ control law, Eq. 20, now compares quite favorably with its conventional control law counterpart in Eq. 10. The main difference lies in the large gain (305.) on the u_g component of u_a in the conventional control law in comparison to 6.42 for the optimal control law. (The total inertial speed feedback gains; 305. and 247. + 6.42 = 253.42, respectively; are comparable however.) Another difference is the virtual absence of w_a feedback to the throttle in the control law of Eq. 20. This suggests that in conventionally designed APCs the gust-induced component of angle of attack feedback, while possibly beneficial at low frequencies, mainly increases throttle activity in a vain attempt to control gust-induced angle of attack changes by means of the throttle. The (inertial) plunge velocity component of the angle of attack feedback seems to serve a useful purpose only in the presence of high-gain, fairly broad-bandwidth feedback of airspeed (which includes the longitudinal gust component). The (inertial) plunge velocity feedback serves to moderate the futile application of thrust in response to longitudinal gust velocity in this case.

If the optimal $\dot{\delta}_e$ control law, Eq. 18, is expressed in a form appropriate to a pitch attitude command system, a favorable comparison with its counterpart conventional control law, Eq. 9, is obtained.

$$\begin{aligned} \dot{\delta}_e = - \{ & \underline{-.00876} u_a - .00549 w_a - \underline{10.1} q - \underline{35.7} \theta \\ & + \underline{9.54} \delta_e + .000101 \delta_T - .0139 \int w_a dt \\ & + .0805 u + 0. \dot{h} + \underline{.108} w + \underline{23.5} \theta_c \} \end{aligned} \quad (21)$$

The significant terms in the right-hand side of Eq. 21 are underlined as before. The other terms on the right-hand side are negligible.

The main difference between Eq. 21 and the counterpart conventional control law, Eq. 9, is the term $.108 w$ which is not present in Eq. 9. Use of a w feedback term in a conventionally designed APCS control law is discussed in Ref. 1. An apparent minor difference arises in connection with gains on θ and θ_c . These gains are not equal in magnitude in Eq. 21. However, the scaling of the variable which is labelled θ_c in the conventional APCS design is arbitrary in the context of the complete carrier-approach loop structure, with the result that this difference is more apparent than real.

The performance index which produced this optimal design is:

$$J = 6.19 \times 10^4 \sigma_{u_a}^2 + 6.21 \times 10^7 \sigma_{\delta_e}^2 + 0.5 \sigma_{\delta_T}^2 + 632. \sigma_{\int w_a dt}^2 \\ + 4.40 \times 10^4 \sigma_{(-\dot{h}_e)}^2 + 1.24 \times 10^6 \sigma_{\delta_e}^2 + 1.20 \sigma_{\delta_T}^2 \quad (22)$$

Root Mean Square Responses

Table 2 lists the root mean square responses to the vertical and horizontal turbulence components for the modified APCS system of Ref. 1, the approximation to it of Fig. 1, and the optimal control laws. The optimal and approximated optimal designs show essentially the same or better performance across the board with respect to the approximated Ref. 1 system. Increased weighting of mean square q in the performance index (Eq. 22) could have further reduced the root mean square value of q for the optimal system. This did not seem necessary, however, and the addition of this term would tend to erode the simplicity of the performance index. Similarly, increased weightings upon the mean square values of w_a , $\int w_a dt$, and $\dot{\delta}_T$ in the performance index could have decreased the root mean square values of w_a and $\int w_a dt$ while maintaining the effective

Table 2
Root Mean Square Response to Random Turbulence

RESPONSE VARIABLES	COMPLETE SYSTEM FROM REF. 1	APPROXIMATED REF. 1 SYSTEM	EXACT AND APPROXIMATED OPTIMAL CONTROL LAW
u_a (ft/sec)	2.98	2.79	2.52
α_a (deg)	1.40	1.08	1.17
θ (deg)	0.83	0.69	0.64 ^a
δ_T (lb)	1190	644	130
u (ft/sec)	1.81	1.59	0.62
$\int \alpha_a dt$ (deg-sec)	0.92	0.95	1.18
\dot{h} (ft/sec)	2.01	2.22	1.24
q (deg/sec)	0.82	0.56	0.89
δ_e (deg)	0.73	0.92	0.45

^aValue is 0.65 for the approximated optimal control law.

throttle, engine, and filter lag break frequency constant. However, the interaction between the weightings upon mean square w_a , $\int w_a dt$, and $\dot{\delta}_T$ was starting to become appreciable. This interaction is believed to be indicative of increasing system performance sensitivity to small changes in feedback gains, which is an undesirable characteristic for a practical system design. Therefore, further adjustment of these weightings was not pursued.

Table 3 lists the root mean square responses to the vertical and horizontal turbulence components and the vertical speed command inputs for the approximated

Table 3
Root Mean Square Response to Random Turbulence
and Vertical Speed Commands

RESPONSE VARIABLES	APPROXIMATED OPTIMAL CONTROL LAW
u_a (ft/sec)	2.52
α_a (deg)	1.21
θ (deg)	0.74
δ_T (lb)	155.
u (ft/sec)	0.62
$\int \alpha_a dt$ (deg-sec)	1.25
\dot{h} (ft/sec)	1.48
q (deg/sec)	1.02
δ_e (deg)	0.65
\dot{h}_e (ft/sec)	1.81

optimal control law, Eqs. 20 and 21. Comparison with the Table 2 values shows that the root mean square responses are only slightly increased by the addition of the vertical speed command inputs.

Time Responses and Possible Improvements

Figure 2 compares the time responses of the conventionally designed system and the system having the optimal control law in response to a step commanded path angle change. The figure shows the path angle (altitude rate) response for the optimal APCS to be much faster than that of the conventionally designed

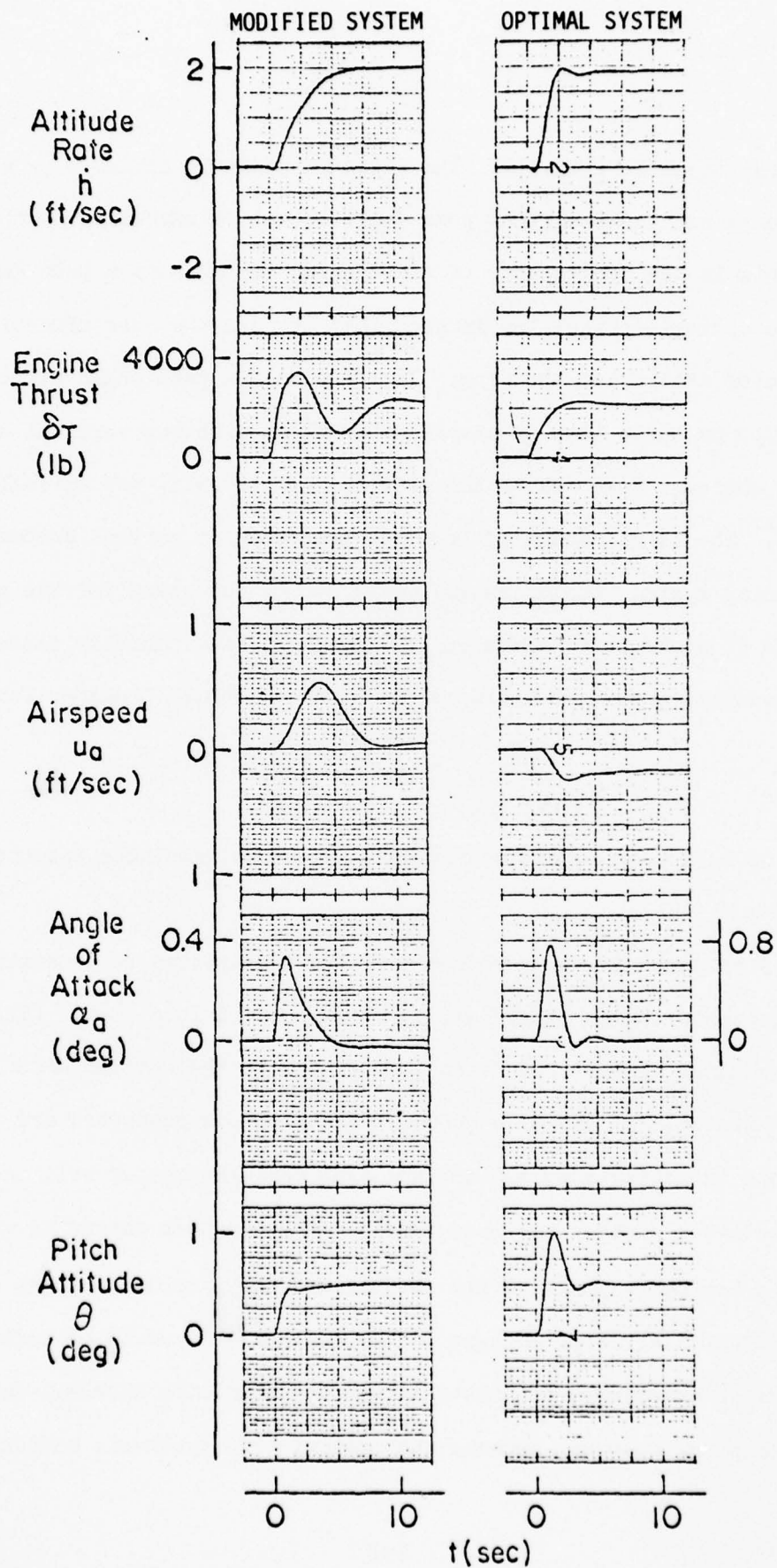


Figure 2. Time Response to $\gamma_c = +0.5$ deg. 595

APCS with less throttle activity. The rapid response is achieved by a rapid attitude change and the resultant peak angle-of-attack excursion is more than doubled. This is the consequence of configuring the APCS as a path angle command system. The optimal control law is such that it uses the most effective normal force generator available, the wing. In terms of its path angle responses, the airplane responds quite like an airplane having an airborne vertical speed sensor signal as a dominant feedback to the elevator as, in fact, the optimal control law demands. The large amount of lead now generated in current automatic carrier landing system (ACLS) designs would not be necessary for the optimal APCS because it would be provided in the airplane. For manually flown approaches, command augmentation such as would result in an effective transfer function of

$$\frac{\dot{h}_c}{\delta_{stick}} = K \frac{s + 0.5}{s + 0.125} \quad (23)$$

would have to be incorporated to provide conventional attitude responses to the stick.

Figure 3 compares the time responses of the two systems to deterministic burble disturbances (Fig. 16 of Ref. 1) with the ACLS loop open. (The current ACLS error channel transfer function is unsuited to the optimal APCS because of the lead it contains as noted above.) The altitude responses are comparable. However, this is achieved by the optimal APCS through greater reliance on angle-of-attack/attitude changes for maneuvering. The airspeed change is virtually ignored, the engine responds hardly at all, and the airplane reaches a higher peak angle-of-attack. Some changes in the optimal APCS would be necessary to make the system acceptable to pilots in the deterministic burble. This should not be surprising, however, because the optimal APCS synthesis accounted only

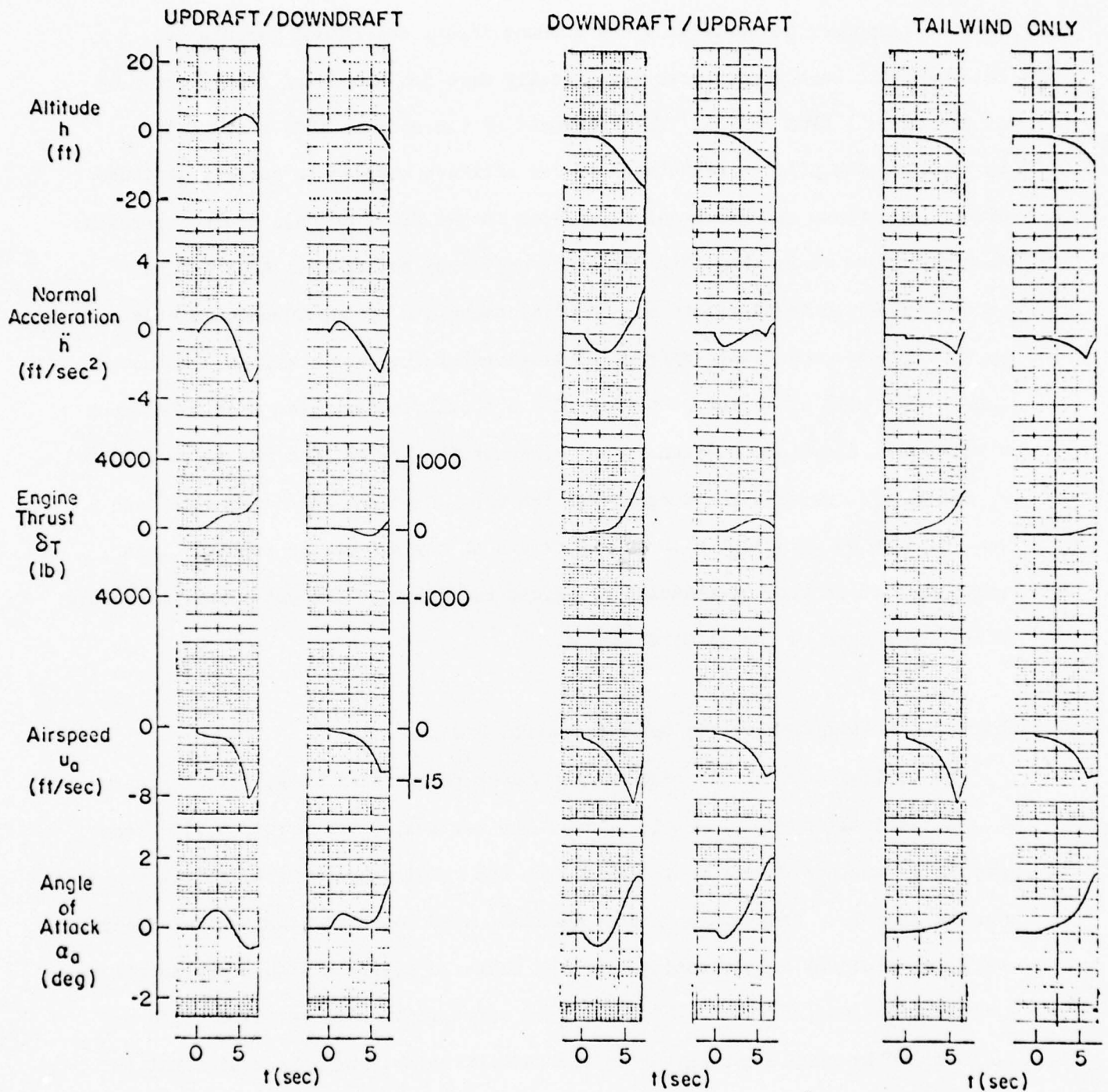


Figure 3. Time Response to Burble Model, ACLS Loop Open (Modified System responses are at the left and Optimal System responses are at the right of each pair.)

for the responses to vertical speed command inputs and random turbulence. Deterministic burble responses specifically were not accounted for in arriving at the optimal APCS design. This judgment of the optimal APCS deficiencies is based on the pilot's reluctance to use attitude changes to correct altitude errors when these changes require pull-ups in the final seconds of the approach. An approach to correcting this deficient aspect of the optimal APCS design procedures would be to reduce the spectral bandwidth of the turbulence model, so that it more accurately reflects the deterministic burble effect. As noted above, this will alter the partition of the total feedback gain upon u and upon w between u_a and u and between w_a and w , respectively, so that the gains upon u_a and w_a are increased. (Recall that the total feedback gain upon u , w , and \dot{h} was found to be invariant with the bandwidth of any stochastic input.) This would produce control laws having transient responses to the deterministic burble which are closer to the pilot's liking.

Practical Realization of the Optimal Control Law . .

The optimal control law requires feedbacks of inertial longitudinal speed, u , and vertical speed, \dot{h} . (\dot{h} is part of the vertical speed error, \dot{h}_e .) These quantities are not directly available from the usual complement of flight control sensors. However, a good approximation of inertial longitudinal speed may be obtained by complementing low-pass filtered airspeed with longitudinal acceleration-independent-of-pitch. A good approximation to vertical speed may be obtained by complementing barometric rate-of-climb (which is equivalent to low-pass filtered vertical speed) with normal acceleration. The steady 1 g present on the normal accelerometer output must be washed out, or more desirably,

biased out. The steady component of vertical speed must be contained in the ACLS (or pilot) generated \dot{h}_c .

Generalization of the Performance Index for APCS Design

At this point, it is worthwhile to render a speculation on how the performance index (Eq. 22) might be generalized for use in synthesizing similar APCSs for other aircraft. This speculative result is based upon the manner in which key stability derivatives affect the unit gain crossover frequencies for the important control loops.

$$\begin{aligned}
 J = & 6.21 \times 10^7 \sigma_{\delta_e}^2 + 4.40 \times 10^4 \left(\frac{-168.}{Z_{\delta_e} + Z_w M_{\delta_e} / M_w} \right)^2 \sigma_{\dot{h}_e}^2 \\
 & + 1.24 \times 10^6 \left(\frac{10.}{\omega_A} \right)^2 \sigma_{\delta_e}^2 \\
 & + k \left\{ 6.19 \times 10^4 \left(\frac{.001317}{X_{\delta_T}} \right)^2 \sigma_{\dot{u}_a}^2 + 0.5 \sigma_{\delta_T}^2 \right. \\
 & \left. + 632. \left(\frac{.000715}{X_{\delta_T} Z_{\dot{u}}^* / Z_w} \right)^2 \sigma_{\int w_a dt}^2 + 1.20 \left(\frac{0.5}{\omega_E} \right)^2 \sigma_{\delta_T}^2 \right\}
 \end{aligned} \tag{24}$$

ω_A is the actuator break frequency in the δ_e path, ω_E is the effective throttle, engine, and filter lag break frequency in the δ_T path, and k is a constant with a nominal value of unity. If one wishes to make relatively more use of thrust than of elevator control than results with $k = 1$, then k should be decreased. If relatively more use of elevator than thrust control than results with $k = 1$ is desired, then k should be increased. Given a sufficient increase in k , the resulting optimal designs will tend to resemble conventional autothrottle systems in distinction to conventional APCS systems.

Conclusion

This analysis represents a preliminary application of optimal control theory to the carrier approach problem. As such we find the results encouraging, and the above approach to this complex control problem worthy of further development.

References

- ¹Ringland, R. F., and L. G. Hofmann, "Approach Path Control System Design: Considerations, Requirements, and Examples," Rept. No. TR-1029-1, May 1974, Systems Technology, Inc., Hawthorne, Calif.
- ²Craig, S. J., R. F., Ringland, and I. L. Ashkenas, "An Analysis of Navy Approach Power Compensator Problems and Requirements, Rept. No. TR-197-1, Mar. 1970, Systems Technology, Inc., Hawthorne, Calif.
- ³Kleinman, D. L., S. Baron, and W. H. Levison, "A Control Theoretic Approach to Manned-Vehicle Systems Analysis," IEEE Trans., Vol. AC-16, No. 6, Dec. 1971, pp. 824-832.
- ⁴Rynaski, E. G., and R. F. Whitbeck, "The Theory and Application of Linear Optimal Control," Rept. No. AFFDL-65-28, Jan. 1966, Air Force Flight Dynamics Lab., Wright-Patterson AFB, Ohio.
- ⁵Athans, M., and P. L. Falb, Optimal Control: An Introduction to the Theory and Its Applications, McGraw-Hill Book Company, New York, 1966.
- ⁶McRuer, D., and D. Weir, "Relationships Between Optimal and Conventional 'Good' Systems — A Simple Case Study," SAE SP-358, May 1970, Society of Automotive Engineers.
- ⁷Hofmann, L. G., "Topics on Practical Application of Optimal Control to Single and Multiple Control-Point Flight Control Problems," Rept. No. AFFDL-TR-70-52, Feb. 1971, Air Force Flight Dynamics Lab., Wright-Patterson AFB, Ohio.
- ⁸Bryson, A. E., Jr., and Y. C. Ho, Applied Optimal Control, Ginn and Company, Waltham, Mass., 1969.
- ⁹Kleinman, D. L., "On An Iterative Technique for Riccati Equation Computations," IEEE Trans., Vol. AC-13, No. 1, Feb. 1968.

¹⁰Kleinman, D., "An Iterative Technique for Riccati Equation Computations,"
Tech. Memo. No. DLK-1, June 1970, Bolt, Beranek, and Newman, Inc.,
Cambridge, Mass.

F14A AIR COMBAT MANEUVERING CONTROL SYSTEM

W. BIHRLE, JR.
Grumman Aerospace Corporation

The F-14A supersonic air superiority fighter was designed to U.S. Navy specifications as a long-range, carrier suitable aircraft versatile enough to meet fighter escort, combat air patrol, and both subsonic and supersonic intercept mission requirements. A wide-spaced twin nacelle, variable sweep configuration was selected to fulfill the conflicting mission requirements in an optimum fashion. It was thought that unrestricted angle-of-attack flight in the subsonic-transonic speed regime also could be achieved with this configuration and thereby permit an expansion of the maneuvering envelope in the dog-fight arena beyond what had traditionally been considered possible. Consequently, the design objectives were that the aircraft possess good handling qualities up to and beyond maximum lift and be spin resistant or spin proof. These objectives were to be met without interfering with the longitudinal control authority so that the aircraft could be statically trimmed at an angle of attack of 38° and to overshoot to an angle of attack of approximately 65° during an accelerated maneuver. Navy concurrence with these objectives was obtained in 1970. This decision as well as the flight demonstrations in 1972 drew the attention of the aerospace community to high alpha flight and has prompted increased research in this area as typified by the NASA HIMAT program.

Today's paper reviews the ACM capability of the present production aircraft, and an ACM control system which is to be incorporated on future aircraft. The need for and the function of this control system as well as the studies that dictated the control laws are discussed.

DEFINITION OF TERMS AND ACRONYMS

ACM	Air Combat Maneuvering
AFCS	Automatic Flight Control System
ARI	Automatic Rudder Interconnect, positions the rudder and reduces differential stabilizer motion as a function of lateral stick movement at high alpha.
SAS	Stability Augmentation System
RSAS	Roll Stability Augmentation, as used for normal roll axis damping
CAS	Command Augmentation System, part of the RSAS, electrically positions the differential stabilizer as a supplement to pilot's mechanical positioning of the differential stabilizer.
YSAS	Yaw Stability Augmentation System, as used for normal directional axis damping
RARI	Rudder ARI, the rudder positioning function of the ARI
LARI	Lateral ARI, the differential stabilizer positioning function of the ARI
LRC	Langley Research Center
g	Acceleration due to gravity
C_L	Lift Coefficient
δ_a	Differential stabilizer deflection, half-angle
$C_{n\delta_a}$	Yawing moment coefficient due to differential stabilizer deflection
$C_{l\delta_a}$	Rolling moment coefficient due to differential stabilizer deflection

IMPORTANCE OF HIGH ALPHA CAPABILITY ON ACM TECHNIQUES

The absence of a lift curve break, wing rock, autorotative rolling moments, nose slice and pitch-up characteristics throughout the angle-of-attack range permits pilots to immediately discover the advantages of high angle-of-attack flight in the dogfight arena. Initially test pilots and then tactical group pilots developed ACM techniques that employed the high alpha capability by flying mock dogfights against souped-up A-4, slatted F-4, and F-106 aircraft. The fleet, employing these techniques, has found the F-14 to be in a class by itself.

Flight experience has shown that, due to the unique high alpha characteristics, pilots not only exceed the angle-of-attack for maximum tracking lift but also the angle for maximum steady state lift (see Figure 1) and in so doing generate values of instantaneous "g" based on dynamic lift. This dynamic lift is appreciably higher than the maximum tracking lift. Pilots have never been able to employ maximum dynamic lift in the past. An unrestricted angle-of-attack capability, however, does more than allow the pilot to generate superior levels of instantaneous "g." Pilots have found that by flying above 30 degrees angle-of-attack, they effectively convert the aircraft into a flying speed brake. In this alpha region, longitudinal stick inputs through a double bob weight feel system permit the pilot to precisely command pure speed changes of rather large magnitude. Also, when flying in this high alpha region, the pilot finds it extremely easy to command the attitude changes required to point the aircraft at the target as he falls in behind his adversary. Therefore, through superior levels of instantaneous "g" and longitudinal deceleration, the F-14 pilot always ends up behind his adversary. Significantly, this scenario is taking place even though the ACM control system, to be discussed today, has not yet been made available to the fleet.

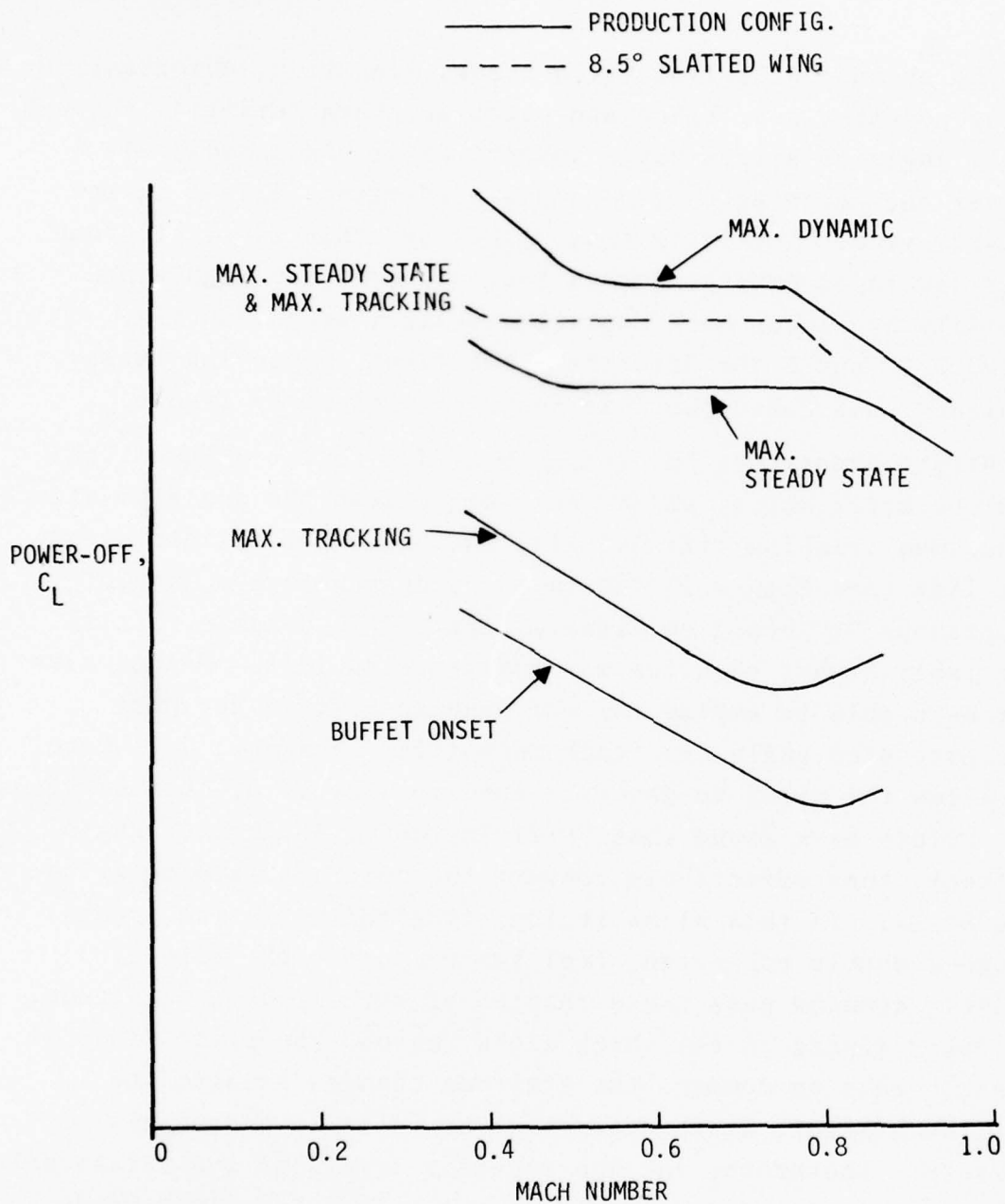


Figure 1. Aerodynamic Envelope for F-14A

NEED FOR ACM CONTROL SYSTEM

As shown in Figure 1, the maximum tracking C_L established in flight (using gun camera records) for the production configuration occurred well below the maximum steady-state C_L , as is always the case. Therefore, although the pilot could effectively employ the unrestricted alpha capability inherent in the F-14 configuration during a defensive maneuver, this was not the situation when tracking a target. It was desired, therefore, that objectionable levels of buffet intensity be eliminated throughout the alpha range.

A study¹, sponsored by the Naval Air Systems Command in 1966, identified the most important aerodynamic parameter responsible for producing departures and consequently spins was the yawing moment characteristic associated with the lateral control. A negative value (adverse yaw) for the $C_{n\delta_a}/C_{l\delta_a}$ ratio very effectively promoted spins. As shown in Figure 2, adverse yaw due to differential stabilizer deflection is realized above 20° angle-of-attack; reaching a maximum negative value at an angle of attack of 55°. It can be seen that at alpha 50°, the control produces yaw instead of roll at a level which simulates the rudder function at low alpha.

An analytical investigation demonstrated that, although the F-14 would not depart due to a stability problem, roll control induced departures indeed could be realized at high alphas. A LRC radio controlled drop model also verified that a departure at high alpha was possible which, unfortunately, could result in a fast flat spin. After full-scale flight tests verified the existence of this type of departure, pilots were instructed to

¹The Influence of the Static and Dynamic Aerodynamic Characteristics on the Spinning Motion of Aircraft. W. Bihle, Jr., Journal of Aircraft, Vol. 8, No. 10, October 1971.

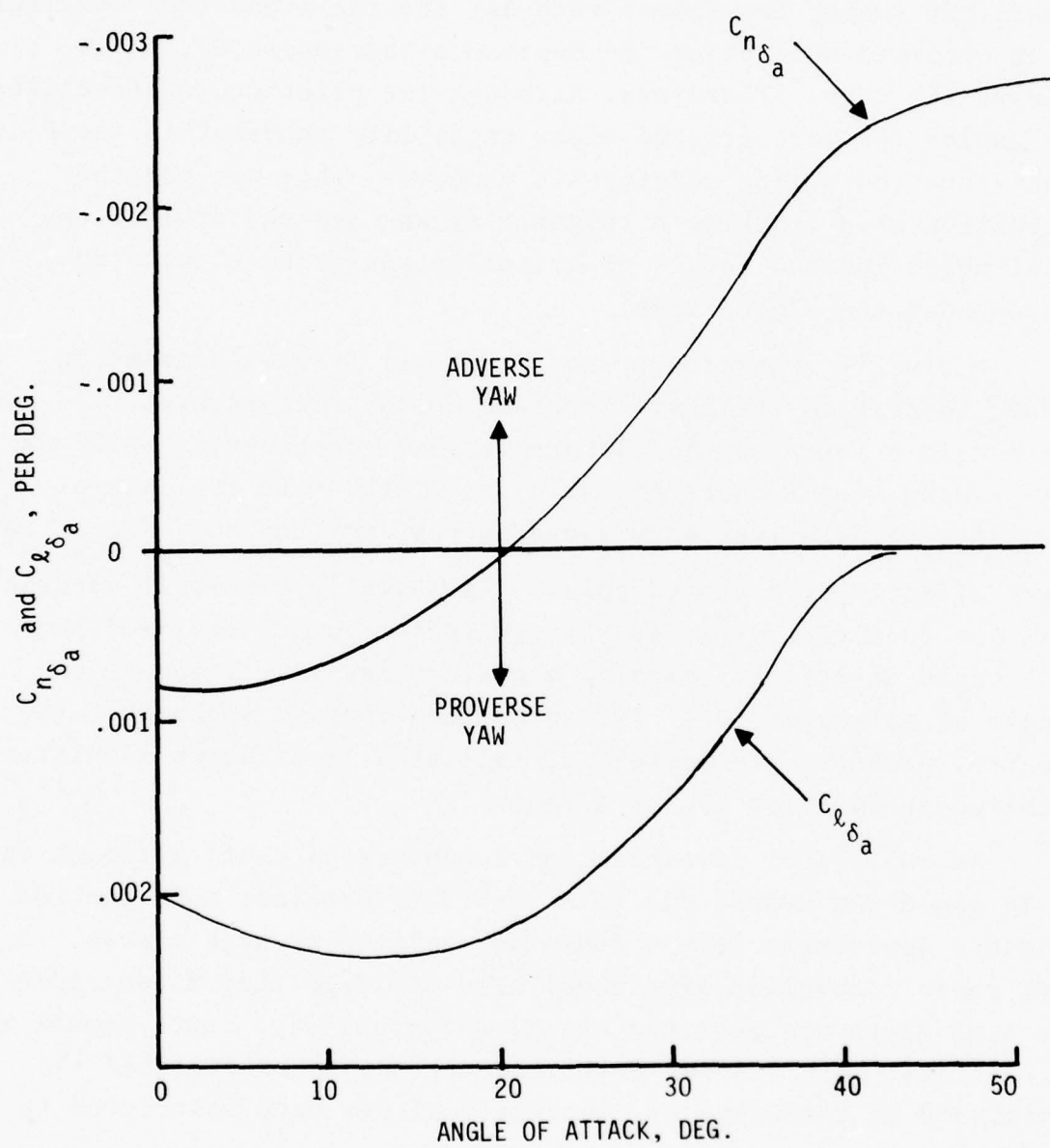


Figure 2. Control Characteristics of Differential Stabilizer
 $M = 0.2$

turn off the roll SAS before engaging in air combat maneuvers and to use restraint when employing the roll control above alpha 20°. This procedure, of course, put the burden on the pilot to avoid a control induced departure.

DEVELOPMENT OF REQUIREMENTS

In 1971, analytical and experimental (i.e., wind tunnel and radio controlled drop model) investigations were initiated to define the requirements for enhancing the high alpha maneuvering capability.

Maneuver Slats

Wind tunnel and flight test results demonstrated that deflecting the power approach configuration wing slats in the subsonic-transonic speed regime resulted in marked improvements in rate of climb, instantaneous and sustained maneuvering load factor, tracking capability and flying qualities. This being the case since the slat:

- Significantly increases lift and decreases drag at high values of C_L .
- Appreciably improves the level of lateral and directional stability at high alphas.
- Increases C_L for buffet onset.
- Appreciably reduces buffet intensity buildup.

The importance of the later two effects is indicated in Figure 1. As shown, the steady state lift which is high due to vortex lift and an automatic Mach-sweep programmer is further increased for the slatted configuration. However, even more important, the pilot could now track a target at this lift since tracking could be accomplished throughout the alpha range.

ARI

It was shown analytically that no combination of control inputs or maneuvers could induce departures leading to a spin if the differential stabilizer was neutralized above 20° angle

of attack. This conclusion was then verified using an instrumented LRC radio controlled model. Obviously, rolls would therefore have to be generated at very high alphas through application of the rudder (i.e., skidding the airplane) and thereby employing the effective dihedral ($-C_{l\beta}$) characteristic for producing rolling moments. It was decided to supply this rudder input automatically through a stick to rudder interconnect.

FUNCTIONAL DESCRIPTION OF CONTROL LAWS

The control laws developed to fulfill the requirements were constrained by the following guidelines:

- Existing hardware be employed whenever possible.
- Adverse effects on existing structure and systems be avoided,

The ACM control laws developed within these guidelines automatically activate the leading-edge wing slats, presently used in the power approach configuration, during subsonic maneuvers and introduces an equivalent Aileron-Rudder Interconnect (ARI) through use of the existing yaw and roll stability augmentation systems. The control laws did require the addition of a nose probe angle-of-attack sensor. Implementing the ACM requirements in this manner effectively maintained for the new systems the established safety (i.e., levels of redundancy and monitoring techniques) of the existing AFCS. It should be noted that, although the control laws fulfill the requirements admirably, they are nevertheless considered to be first generation high alpha control laws. This being the case since the high alpha performance theoretically achievable cannot be fully realized with these control laws.

The ARI is an auxiliary function of the YSAS and RSAS/CAS since it utilizes and combines with certain functions and components of those two SAS. At high alpha, the transition from normal SAS to ARI is smooth and not apparent to the pilot since the control operation is basically unchanged. The ARI reduces lateral stick motion to the differential tail from 12° to a maximum of 2° as a function of increasing alpha (LARI system) while crossfeeding lateral stick as a function of increasing alpha to rudder control (RARI system). An alpha probe mounted on the tip of the radome and an alpha computer provide accurate alpha information to operate the ARI system under all alpha and sideslip conditions.

The LARI function, i.e., the reduction of differential tail commanded per stick displacement, is more complex than the RARI function since it requires that the normal CAS commands be reduced proportional to increasing alpha while (negative) electrical stick commands are increased proportional to alpha and stick position which are of the opposite sign the pilot is commanding. Therefore, since the maximum authority of the RSAS is 5° and the pilot can command 7° , this technique results in a net of 2° of tail available to the pilot. This LARI system is turned on as a function of Mach number and angle of attack.

The rudder is crossfed by employing the lateral stick signal, derived from the RSAS, and is applied to the RARI where its gain is increased as alpha increases and in turn this signal is applied to the yaw series servo to operate the rudder. This system is also engaged as a function of alpha.

VERIFICATION AND DEFINITION OF CONTROL LAWS

Maneuver Slats

Flight tests were performed to measure the performance gains to be realized at different slat deflection angles and Mach numbers and to establish automatic extension and retraction slat schedules.

As would be expected, it was shown that slat effectiveness at high alpha increases with increasing deflection, especially at lower Mach numbers. For instance, the C_L for buffet onset is increased in going from an 8.5° to 11.5° slat deflection. Above this deflection, however, buffet intensity buildup increases. Although the 11.5° slat deflection was aerodynamically optimal, the 8.5° deflection was chosen since most of the slat effectiveness could be realized at this deflection with no associated mechanical or structural penalty. The schedule shown in Figure 3 was set as a function of Mach no. and angle of attack.

ARI

In July of 1973, the ARI control laws as well as other control departure and spin prevention techniques were evaluated performing several tracking and ACM tasks against an adversary on the LRC dynamic maneuvering simulator. It was concluded that the ARI system greatly improved the tactical effectiveness as well as the safety of the airplane at high angles of attack.

In October of 1973, a flight test program was initiated to select system gains and threshold values for the ARI system and to demonstrate that the system would prevent departures and spins for all wing sweeps, center-of-gravity locations, external store and speed brake configurations and asymmetric power conditions during subsonic normal, accelerated, and zero velocity

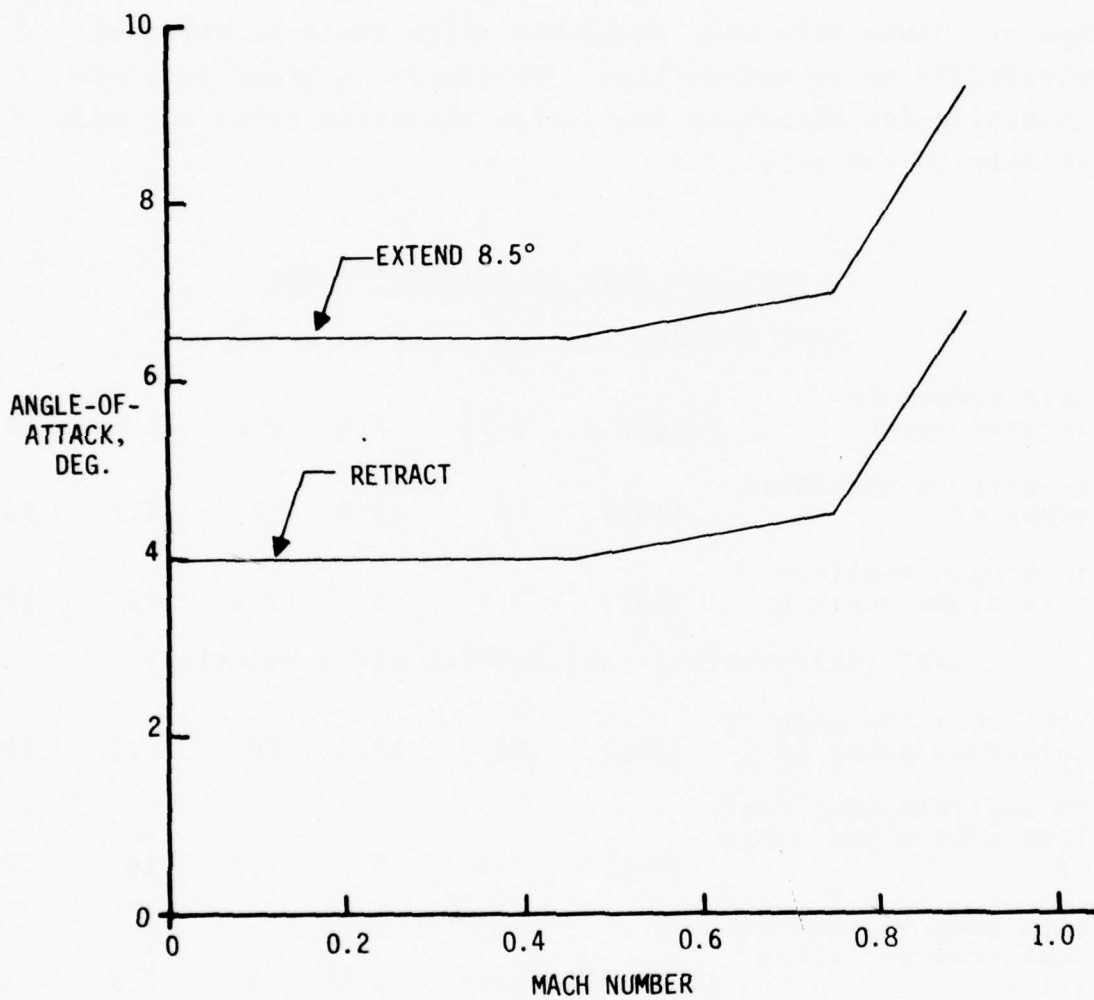


Figure 3. Automatic Slat Schedule.

vertical maneuvers when pro-spin controls (i.e., full application of the lateral and directional controls in opposite direction) were held for 15 seconds.

A variable gain calibrator (VGC) was incorporated in the flight test article. As shown in the following table, a large range of values were made available which could be selected individually or in combination. Obviously, a great deal of flexibility for adjusting the system characteristics was made available to the pilot.

VARIABLE GAIN CALIBRATOR VALUES

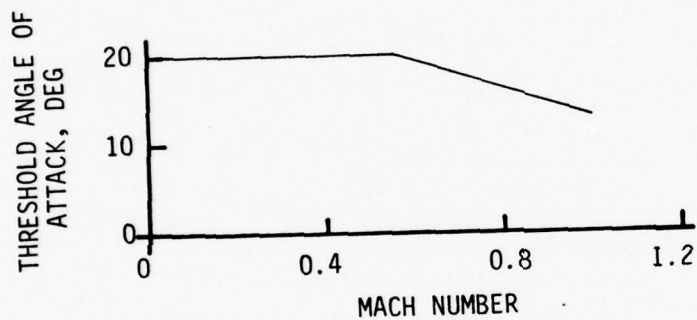
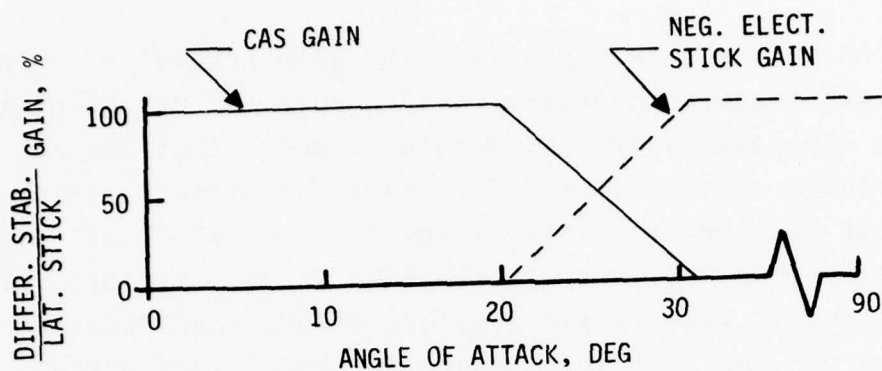
RARI (rudder-lateral stick relation)

Gain rudder to lateral stick	(deg/in)	6.33	7.6	9.6	12.66	19
0% Gain at threshold alpha of	(deg)	10	12.5	15	17.5	20
100% Gain realized over alpha range of	(deg)	2.5	5	7.5	10	12.5

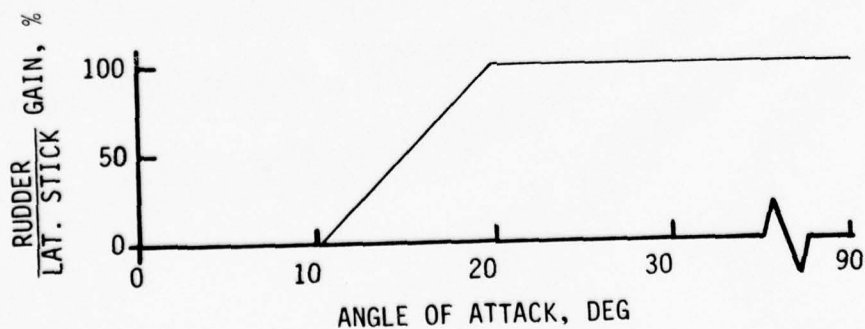
LARI (differential tail-lateral stick relation)

100% roll CAS gain at threshold alpha of	(deg)	15	17.5	20	22.5	25
0% roll CAS gain realized over alpha range of	(deg)	2.5	5	7.5	10	12.5
Gain (neg.) differential stab to lateral stick	(deg/in)	1.43	1.67	2	2.5	3.33
0% Gain at threshold alpha of	(deg)	15	17.5	20	22.5	25
100% Gain realized over alpha range of	(deg)	2.5	5	7.5	10	12.5

From this flight test program, the gain schedules shown in Figure 4 were found to meet the requirements for enhancing the high alpha ACM capability. It should be noted that the low alpha threshold value selected for the rudder-lateral stick gain was not required for rolling the aircraft above 30° alpha, as originally intended, but was found to further minimize kinematic coupling at low dynamic pressure flight conditions and thereby improve the roll performance in this flight regime.



(b) LARI SCHEDULES



(a) RARI SCHEDULE

Figure 4. ARI Schedules.

APPLICATION OF THE AUTOMATIC RUDDER
INTERCONNECT (ARI) FUNCTION IN
THE F-14 AIRCRAFT

By

J. H. Lindahl
Government and Aeronautical Products Division
Honeywell Inc.
Minneapolis, Minnesota

INTRODUCTION

Flight tests in the F-14 aircraft during 1972-1973 confirmed analytical data that the aircraft can be flown and adequately controlled through an extremely high angle-of-attack range. To achieve this expanded performance, the test pilot used flight techniques that were considered undesirable for use by operational pilots. Consequently, the Automatic Rudder Interconnect (ARI) function was defined so that operational pilots could utilize the aircraft's expanded flight envelope capability with normal control inputs.

This paper describes the major design considerations encountered during the integration of this new ARI function within the existing AFCS functions. The primary consideration during this effort was to maintain the flight safety aspects of the existing fail-op/fail-safe Yaw Stabilization Augmentation System (SAS) and fail-safe Roll Control Augmentation System (CAS) because the ARI function modifies control inputs to the Roll CAS and Yaw SAS functions.

The ARI function provides the capability to maintain subsonic roll maneuverability by means of lateral stick commands at high angles-of-attack. This is accomplished by commanding rudder deflections through the Yaw SAS series servos, while reducing the differential horizontal tail deflections through the Roll CAS series servos. Thus, roll maneuverability is provided by the rudder, while the differential tail deflections are cancelled to minimize

adverse Yaw effects. The fail-op/fail-safe SAS capabilities have been retained while mechanizing this self-monitored ARI capability. Built-in-test (BIT) of the ARI circuitry is also provided to detect ARI failures and to isolate these failures, where possible, from the SAS functions.

The resulting new AFCS configuration with the ARI function provides a practical solution to enhancing the air combat maneuverability of the F-14 in the high angle-of-attack flight regime.

BASIC ARI REQUIREMENTS

The ARI functional requirements provided for specific modification of the Rudder (RARI) control motions and Lateral (LARI) control motions (differential horizontal tail deflection). Lateral stick commands are switched into the rudder axis in place of the yaw SAS function when RARI is engaged. Negative lateral stick commands are blended into the Roll CAS function when LARI is engaged. Certain ARI control logic and ARI signal monitoring is also required along with reset capability to allow the pilot to clear momentary failures and re-engage the ARI/SAS functions. BIT requirements include fault detection and isolation of the added ARI circuitry within the AFCS.

RARI Control Functions

The rudder ARI provides for rudder deflections proportional to lateral control stick motions as a function of angle-of-attack (α) during subsonic, flaps-up flight. The RARI function is used in place of the Yaw SAS function whenever the angle-of-attack exceeds $+10^\circ$. RARI gain is scheduled linearly to provide zero gain at $10^\circ\alpha$ and maximum gain at $20^\circ\alpha$ and above, as shown in Figure 1.

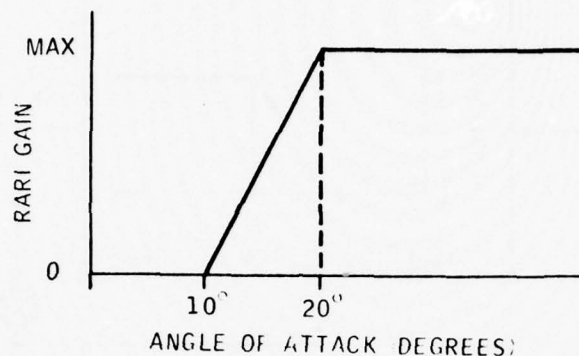


Figure 1. Lateral Stick to Rudder Gain Characteristic

During subsonic flight, the Yaw SAS signals are switched out at $\alpha = +10^\circ$. The RARI gain at $10^\circ\alpha$ is zero; thus there are no commands to the rudder through either the SAS or ARI under this specific flight condition. As the angle of attack increases above $+10^\circ$, the lateral stick commands provide the desired amount of rudder deflection to supplement the rolling commands to the aircraft.

LARI Control Functions

Lateral ARI control functions are somewhat more complex than RARI, as they are blended in and out with the Roll CAS function instead of simply switching from one function to the other, as shown in Figure 2.

The LARI/ROLL SAS gain blending is a function of angle of attack and Mach Number. An alpha start (α_s) signal is generated as a function of Mach Number as shown in Figure 3. A fixed alpha end (α_e) signal is established at $\alpha_s + 11^\circ$.

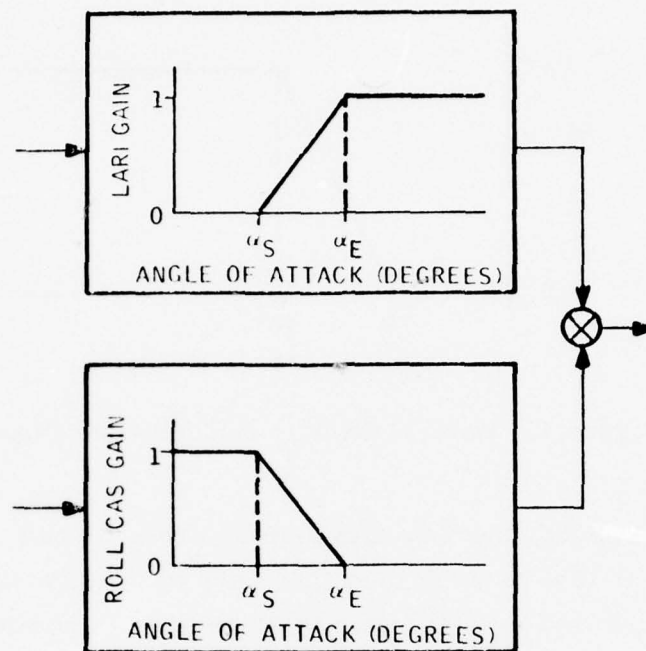


Figure 2. LARI/ROLL CAS Gain Blending

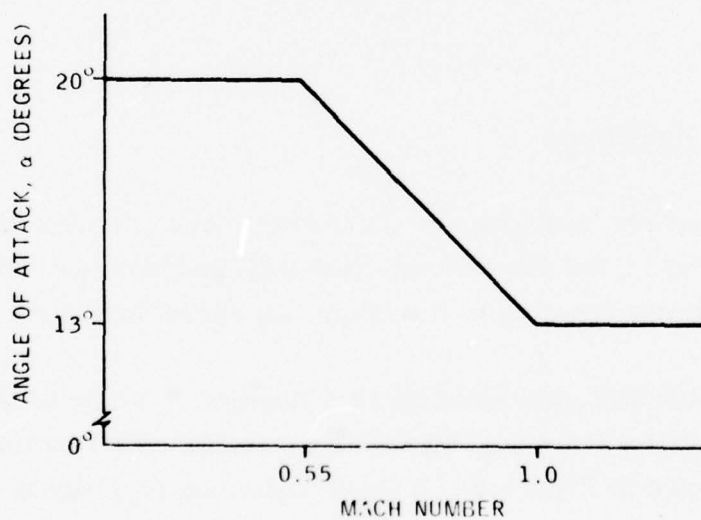


Figure 3. Alpha Start Characteristic

The lateral stick ARI command to the roll axis (differential tail deflection) is phased opposite to the mechanical input and CAS commands. Thus, during angle-of-attack operation ($\alpha > 24^\circ$ to 31°), with CAS gain at 0, the LARI signal is opposing the direct manual input of the pilot through the AFCS series type servos. This minimizes differential tail deflection and, consequently, adverse yaw effects due to differential tail motions at these high angle-of-attack flight conditions.

LOGIC REQUIREMENTS

The ARI function is intended to be operable at all times that the F-14 Aircraft is in the subsonic, flaps-up portion of its flight envelope. The pilot may momentarily turn off the ARI with the emergency disengage switch; or, at his option, he may disable ARI by disengaging the Roll CAS engage switch. Operation of Roll CAS increases the differential tail deflections at high angle-of-attack flight conditions when the LARI function is not operating. With Roll CAS engaged, however, ARI will be available and automatically operable in accordance with the logic interlocks listed below.

RARI Logic

The following logic statements must be satisfied in order to engage RARI.

- Angle of attack (α) greater than 10°
- Mach Number less than 1.0
- Roll CAS engaged
- Emergency disengage switch not activated
- Flaps up
- Mach signal comparator not tripped
- RARI signal comparator not tripped

Dual Mach Number signals are transmitted from the Central Air Data Computer (CADC) to the Automatic Flight Control System (AFCS), and a comparator is provided within the AFCS to ensure that Mach Number data agrees. Any significant disagreement will prevent RARI engagement. RARI command signals are also generated in two separate channels within the AFCS, and again these two signals are compared to ensure that RARI commands are valid when RARI is engaged. If either the Mach comparator or the RARI signal comparator is tripped, they can be reset with the pilot's master reset switch if the trouble has cleared.

LARI Logic

The logic statements below must be satisfied in order to engage LARI commands. LARI signal blending is also entirely automatic, normally controlled by angle-of-attack and Mach Number.

- Angle of attack (α) greater than 13° (Mach No. = 1.0) or α greater than 20° (Mach No. = 0.55) (see Figure 3)
- Mach number equal to or less than 1.0
- CADC validity signal present
- Emergency disengage switch not activated
- Flaps up
- Roll CAS engaged

Roll axis failures will still be detected, and the roll axis of the AFCS will automatically disengage when the normal failure lights indicate that a failure has occurred during LARI operation. The Roll CAS switch can be cycled off-on to reset the roll axis comparators, thus allowing Roll CAS/LARI operation if the failure has cleared.

BUILT-IN-TEST (BIT) REQUIREMENTS

Basic AFCS functions are tested by BIT as part of the ground On-Board Checkout (OBC) in order to isolate any failure to both the function affected and the device which has failed. RARI circuitry will similarly be tested by BIT; however, fault isolation is limited to the yaw computer device level, as ARI failure lights are not provided. The maintenance man or pilot can still isolate RARI faults to the RARI function, as he will have a yaw computer device failure light, but no functional failure light.

LARI fault detection is identified as a Roll CAS failure as well as a roll computer failure. This is necessary because the gain blending circuitry of Roll CAS and LARI commands utilize common parts for both functions.

The Pitch SAS and Roll CAS functions also include an automatic in-flight BIT for certain failure modes. This in-flight BIT of the roll axis will be inhibited when LARI is engaged.

EXISTING SAS CAPABILITIES

The basic fail-op/fail-safe capabilities of SAS must be retained while adding the ARI functions. The following description of the existing configuration illustrates the basic flight safety capabilities of the F-14 Yaw SAS and Roll CAS.

YAW SAS Configuration

A simplified block diagram of the Yaw SAS configuration is shown as Figure 4. Three channels of sensors and electronics are used with cross channel comparison to detect failures. The two servo channels are individually monitored.

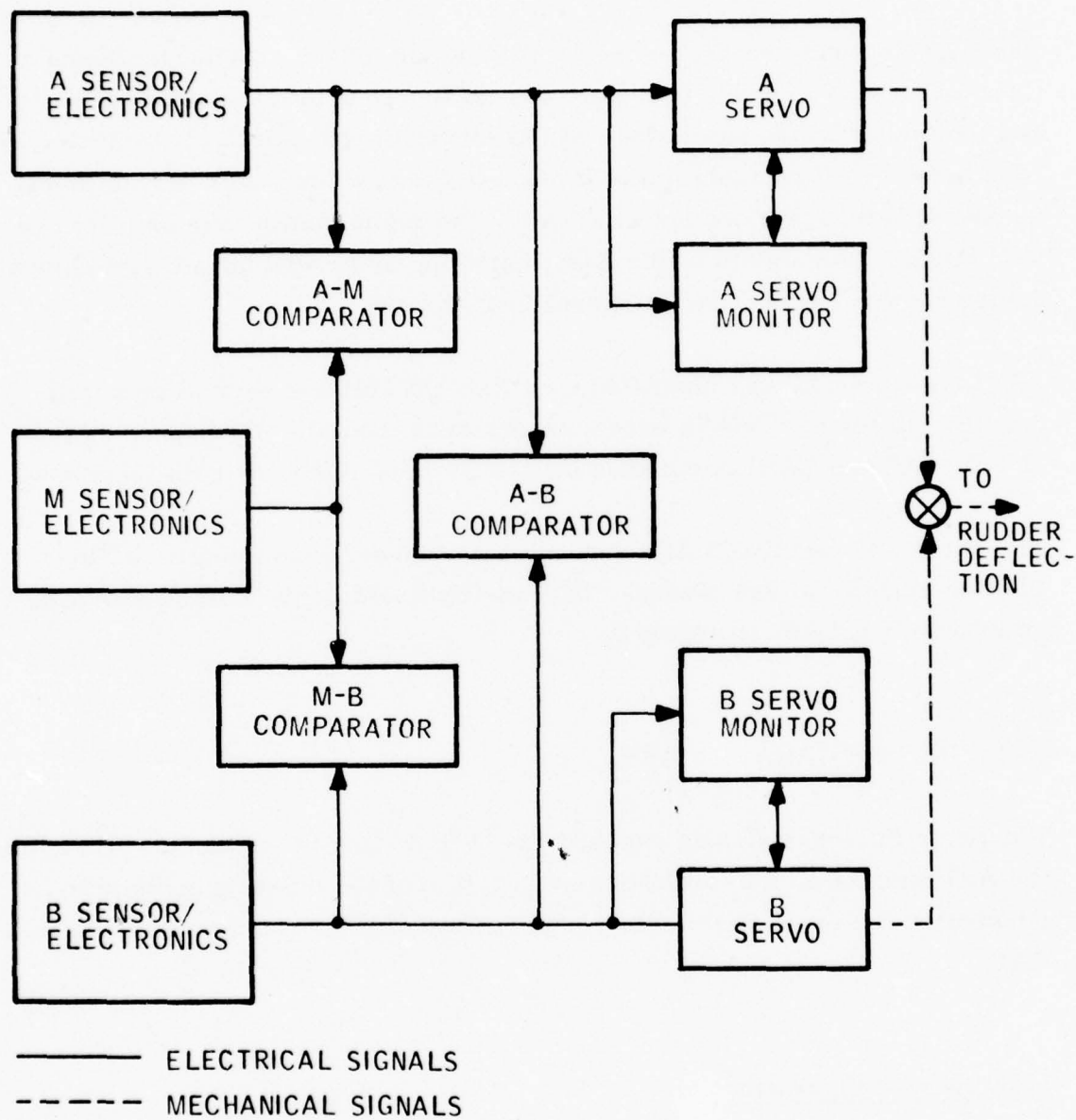


Figure 4. F-14 Yaw SAS Configuration

With appropriate gain changing and switching provisions, this configuration provides a fail-op capability for first failures and fail-safe disengage for second failures.

ROLL CAS Configuration

The Roll CAS configuration is illustrated in Figure 5. Dual sensors and electronic channels are used with a single comparator to detect sensor/electronic failures. The two servo channels are again individually monitored, the same as in the Yaw axis. A failure in the sensors or electronics disengages both servos and initiates in-flight BIT. Single channel operation may be utilized by the pilot following the 7-second in-flight BIT sequence by re-engaging the Roll CAS, with the failed channel remaining disengaged. A servo channel failure will result in immediate disengagement of only the failed channel, and the Roll CAS will operate at half gain and authority on the remaining channel.

ARI/SAS INTEGRATION

The ARI configuration which is being mechanized represents the results of various tradeoffs made relative to non-flight-safety redundancy requirements and hardware limitations. Initial definition called for a three-channel RARI mechanization and a dual-channel LARI mechanization. This initial configuration basically matched the redundancy levels of the Yaw SAS and Roll CAS to provide the equivalent fail-op/ fail-safe characteristics for RARI and LARI, respectively. This first approach had to be abandoned due to the large amount of circuitry which would have been required, making it necessary to provide an additional computer for the ARI functions.

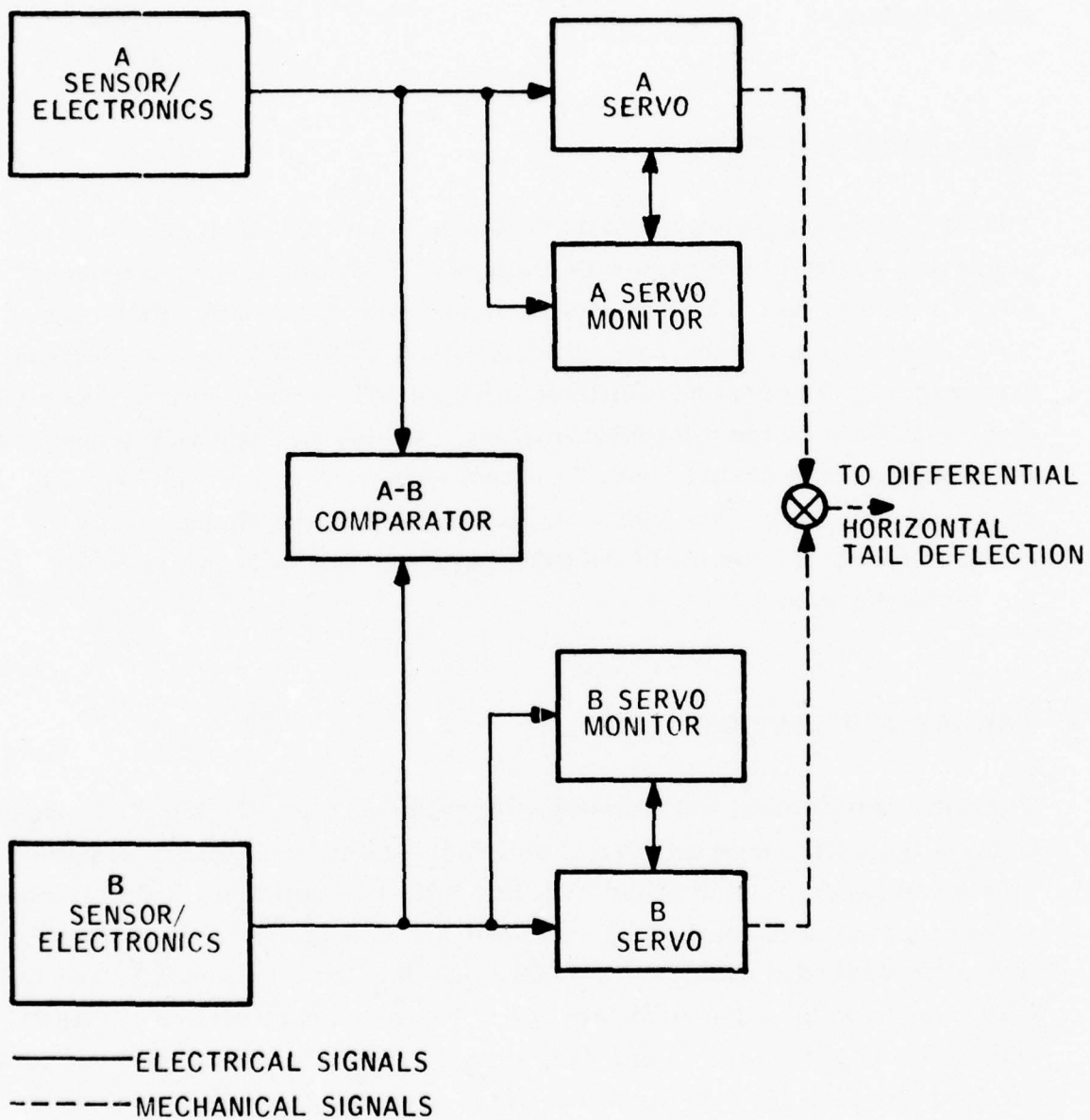


Figure 5. F-14 Roll CAS Configuration

Thus, a basic limitation was established to define an ARI configuration that could be mechanized within the existing AFCS computers. Primary flight safety requirements for SAS fail-op/fail-safe characteristics were retained; however, the RARI function need not be fail-operative. The resulting ARI mechanization meets the flight safety criteria and is physically contained within the AFCS computers.

YAW SAS/RARI Integration

A dual-channel RARI mechanization was defined for both the signal path and the Logic functions. The dual signal path ensures the integrity of the RARI signal which is fed into all three channels of the Yaw SAS electronics. A cross-channel comparator is utilized to sense any significant difference in the RARI command signals as shown in Figure 6. The output of the comparator is fed into the logic to prevent RARI engagement if the signal channels do not track. The dual RARI logic circuitry ensures that the Yaw SAS will not inadvertently be switched out due to single failures in the logic. Any dissimilarity in the two ARI logic channels will prevent RARI engagement. RARI failures (detected during on-board checkout) do not prevent the use of Yaw SAS, Roll CAS, or LARI, allowing the pilot to determine which flight restrictions, if any, should be observed.

The dual logic output is used to control three separate logic functions which in turn control the Yaw SAS/RARI switching in the yaw SAS electronics, as illustrated in Figures 7 and 8, respectively. The Roll CAS engage switch signal is also required for each of the three channel switch functions to give the pilot positive control of the RARI engage circuitry. The existing YAW SAS three-channel comparators protect the system from individual RARI switch function failures in the yaw axis electronics. Normal Yaw SAS failure indications will be generated for these switching element failures, as they are integral to the Yaw SAS mechanization.

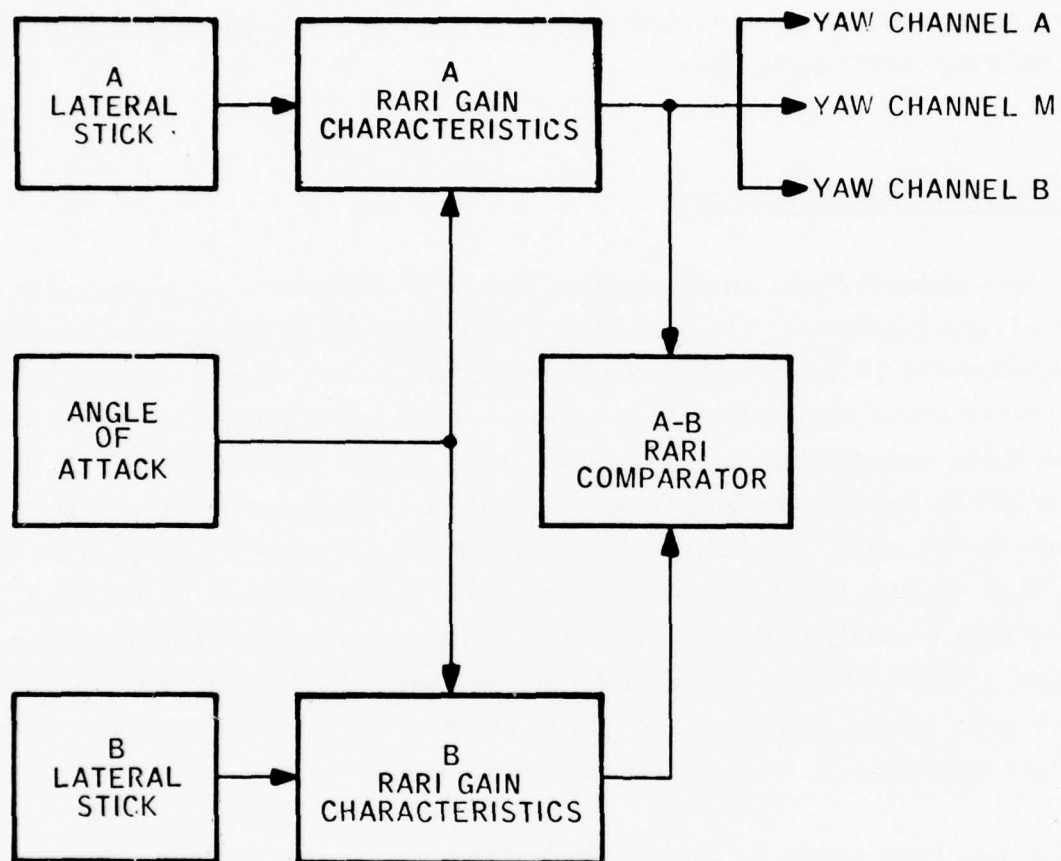


Figure 6. Dual RARI Signal Configuration

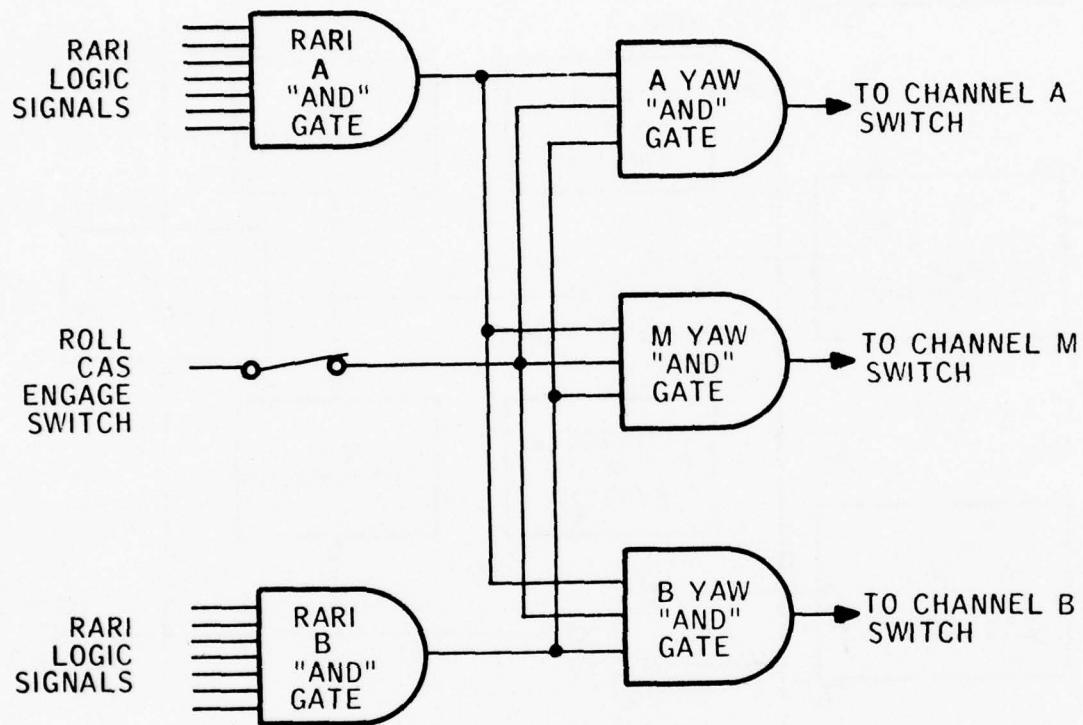


Figure 7. RARI Logic Configuration

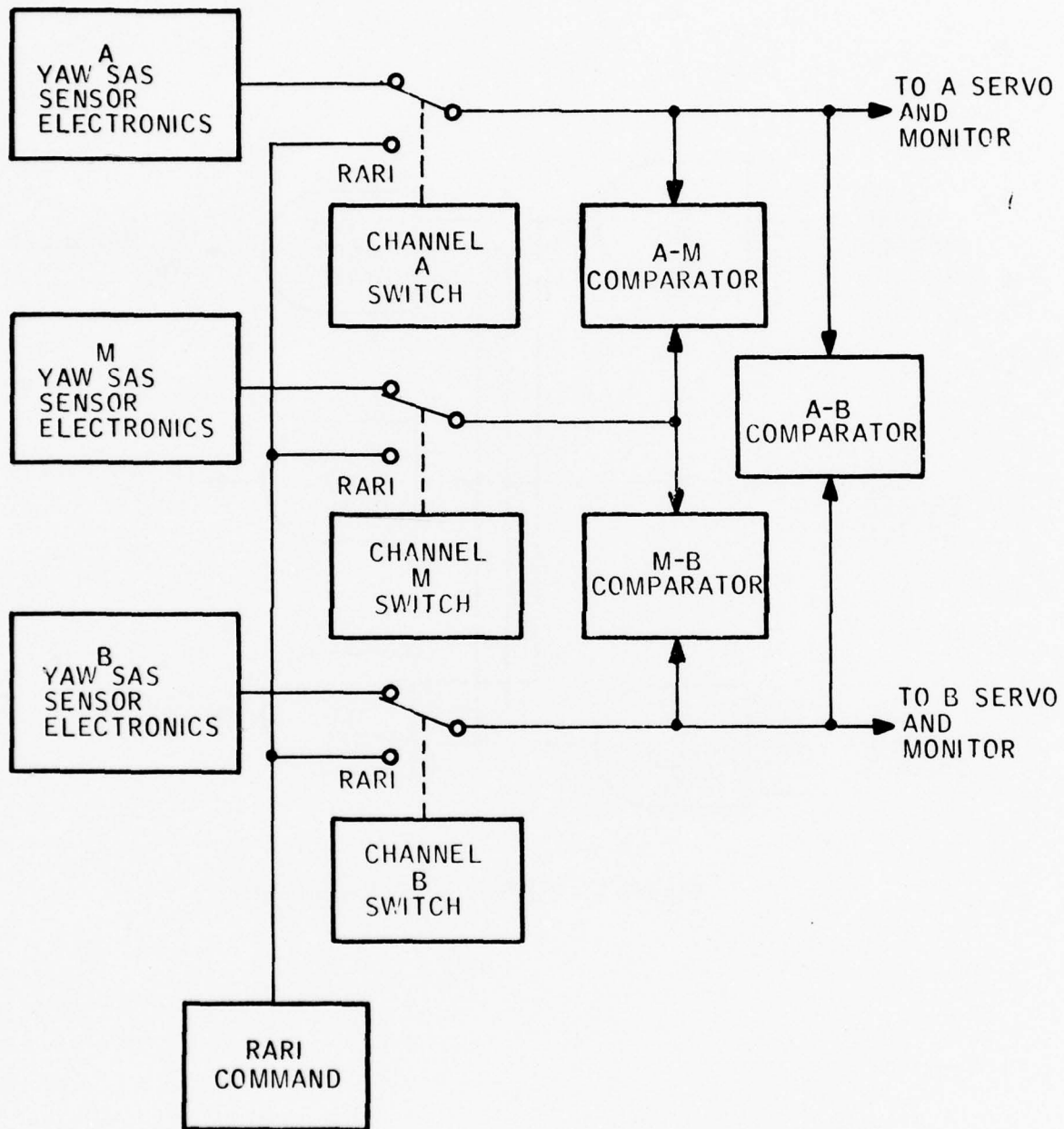


Figure 8. Yaw SAS/RARI Signal Interface

ROLL CAS/LARI Integration

Dual signal circuitry is also used to mechanize the LARI commands; however, the LARI logic is single channel. The dual LARI circuitry is basically required due to the blending of Roll CAS and LARI gains. One gain changer per channel can be utilized for this blending as shown in Figure 9, since the gain characteristics are the reciprocal of each other. The existing Roll CAS signal comparator is used to detect failures in the LARI circuitry; thus these failures cannot be isolated from the Roll CAS signal failures.

An in-flight failure that is detected by the Roll Bridge Comparator with LARI disengaged results in the normal in-flight BIT operation. The pilot may then re-engage the Roll CAS and operate on a single channel at half gain and half authority. Any subsequent flight condition change that results in LARI engagement will provide LARI operation also at half gain and half authority. If an in-flight failure is detected by the Roll Bridge Comparator with LARI engaged, the Roll CAS and LARI will automatically disengage and in-flight BIT will be inhibited. The pilot can re-engage dual channel Roll CAS/LARI if the failure clears itself. Single channel operation at half gain and authority is provided for LARI and/or Roll CAS operation following loss of one servo channel.

DESIGN ASSURANCE

The F-14 AFCS is in the fifth year of production, and incorporation of the ARI function at this stage of the program makes it necessary to ensure that the modified system retains its basic operation/environmental characteristics. The addition of the ARI capability to the AFCS is provided primarily by the addition of five circuit card assemblies within the existing computers. To verify the performance of these ARI circuits under simulated operational environments, the following analyses and special tests were initiated.

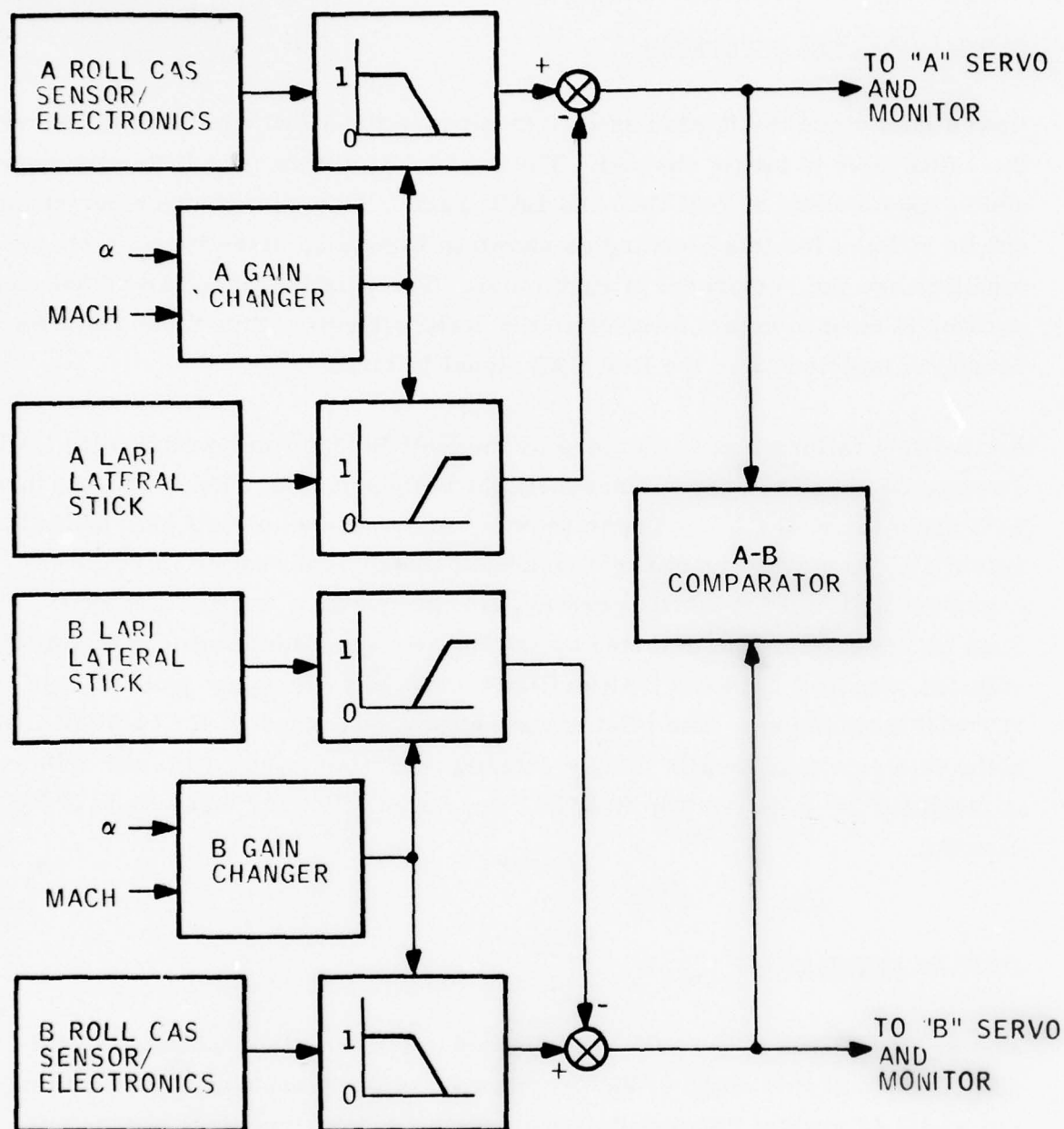


Figure 9. Roll CAS/LARI Signal Interface

SPECIAL ANALYSES

- Failure Mode and Effects Analysis
- BIT Ratio Analysis
- Reliability Prediction

SPECIAL DEVICE LEVEL TESTS

- Temperature
- Vibration

SPECIAL SYSTEM LEVEL TESTS

- System Compatibility
- Reliability Endurance
- Operational Level Maintainability (BIT)

The ARI addition has resulted in the following changes in the overall characteristics of the AFCS.

<u>ITEM</u>	<u>BEFORE ARI</u>	<u>WITH ARI</u>
Part Count	5500	6200
Predicted MTBF	1140 hr.	1040 hr.
Bit Effectiveness	95%	90%
Weight	54.5 lb.	57.0 lb.

SUMMARY

The successful mechanization and integration of the ARI function within the existing fail-op Yaw SAS and fail-safe Roll CAS of the F-14 is a current example of using automatic control techniques to improve an aircraft's operational capability. Flight safety is assured by testing the added ARI circuitry within the basic AFCS BIT capability, and by continuous monitoring during flight. Various analyses and special tests will ensure the integrity of the ARI circuitry under all flight environments. The program decisions made early in the program to mechanize the ARI function within the existing AFCS computers have provided the navy with a highly cost-effective approach for improving the air combat maneuverability of the F-14 aircraft.

LQG APPROACH TO SUBMARINE CONTROLLER DESIGN*
FOR NEAR SURFACE DEPTH KEEPING

JOHN WARE
Naval Ship Research and Development Center

This work that I am going to talk about was done at NSRDC and by Dave Kleinman, Bill Killingsworth, and Dick Smith at Systems Control, Inc., who were under contract to us during the initial period of development--which was about two years ago.

What I am going to talk about today is essentially the same thing that I talked about at a seminar here about a month ago. When I gave it at the seminar to a group of graduate students, it had an auxiliary title--"Is Optimal Control the Last Refuge of the Incompetent." Anyway, I've taken out all the equations and I'm going to hit on only a couple of minor, well, they look like minor topics now, but they were quite difficult problems for us at the time. I'd like to explain first of all what our goal was in this near surface depth keeping problem (Figure 1).

We've got the submarine near surface engaged in some type of activity which requires accurate control of depth. An easy way to envision this is the periscope problem. It is desirable to maintain depth within a foot or two feet, or ordered depth, and keep the pitch angle small. Although I don't like to mention specific submarines, this work was done for the Trident,

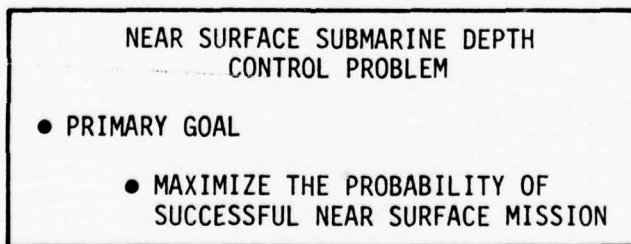


Figure 1

* This paper was typed from a taped version of the oral presentation.

and Trident is almost the length of two football fields. Imagine something that long keeping depth to within a foot, and maintaining pitch angles at considerably less than one degree. And that's our goal.

The primary goal is to maximize the probability of success of a near surface mission, which we translate into quadratic criteria of keeping the RMS depth and pitch angles small. We have a number of secondary goals which are shown in Figure 2, in order of importance. The first three relate to control power consumption, and related to those are goals of reducing system bandwidths; effectively we end up weighting control rates and control accelerations, which is a little bit unusual. We developed a realizable system (we had to), we minimized sensor impact, and this is a little bit different than most of the aircraft applications where we've seen additional sensors. We actually use less sensors in this control system than were used in conventional control systems. We didn't really have a very stringent requirement in minimizing computer load, but it's always a pretty wise thing to keep the number of computations small because they tend to grow larger and larger as time goes on. You better think way ahead of time about the amount of

- SECONDARY GOALS
 - MINIMIZE RADIATED NOISE
 - MINIMIZE HYDRAULIC POWER
 - MINIMIZE MECHANICAL WEAR
 - DEVELOP REALIZABLE SYSTEM
 - MINIMIZE SENSOR IMPACT
 - MINIMIZE COMPUTER LOAD

Figure 2

computation you can do--try to keep that small. I'll describe the problem a little bit more in detail.

We decided to use the optimal control approach for a number of reasons (Figure 3). One, we were more familiar with it than anything else, and it was also a secondary requirement of the task goal. Everything had been done previously by classical approaches and the question was, "Can we do any better by using optimal control approach?" The advantage of the modern approach is that it is highly structured. Everything you do fits into a very tight mathematical framework, and it reduces the amount of thinking that you have to do in many senses. You are guaranteed stability, and parameter insensitivity under certain conditions, and is quickly applicable to similar systems. Once you get your weighting matrices selected, and learn how they adjust, say, with submarine size, you can go to the next generation submarine supposedly very quickly.

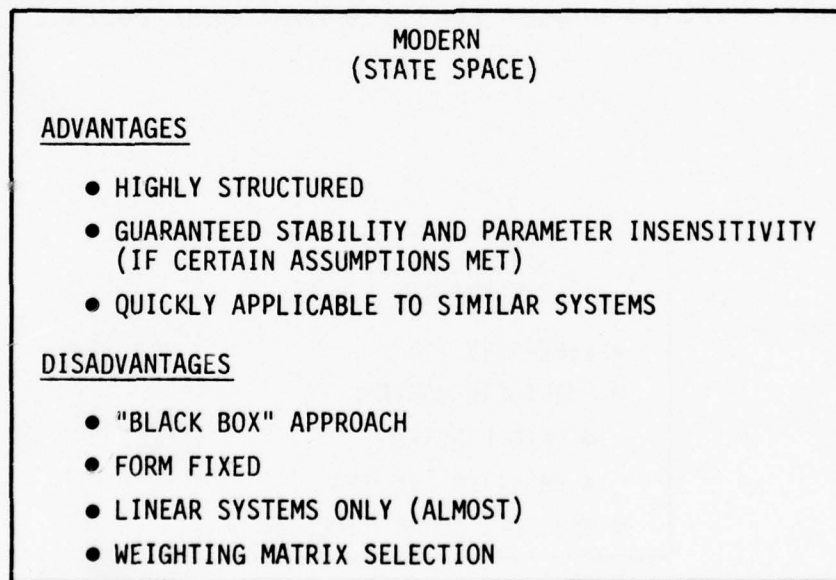


Figure 3

But the disadvantages are almost the same as the advantages. It's a disadvantage to take weightings and drop them into your computer program and grind the Riccati equation until you get a set of gains, because you don't get any insight into the problem.

It's also a disadvantage to have your form fixed by the control structure, the applicable control theory, which tells you "this matrix times this vector"--that's a real disadvantage. Also, it's applicable to linear systems only, almost, and you have the problem of using weighting matrices which is extremely difficult. I imagine we spent more of our time fooling around with weighting matrix selection than anything else.

So, a special problem we had for a submarine near surface was to determine if the submarine is linear. That turned out to be pretty easy (Figure 4). It turns out that in the near surface kind of environment, if we try to keep motion small, the submarine hull dynamics are basically very linear. In fact, we were even advised at one time by the hydrodynamicist that a linear model will be better than the nonlinear model.

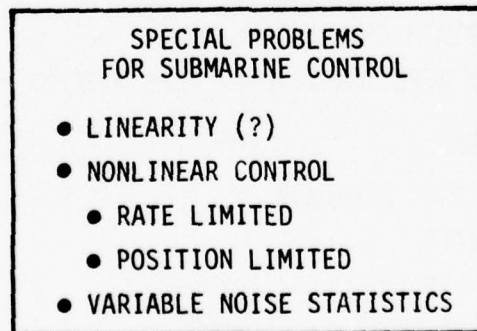


Figure 4

The nonlinearities are in the control system which is both rate and position limited. This turned out to be a quite significant problem.

Our next big problem was that we had variable noise statistics which come from the seaway. The submarine is so large that you can't move in response to the waves which are going overhead. The best you can do is try to keep the submarine fixed and ignore the waves. But depth is measured in a submarine with a pressure depth sensor located in the keel. Every time a wave goes over you measure effectively the height of the wave. But you don't want to respond to that, so we have a filtering problem and the noise statistics vary with a lot of parameters that we usually encounter at sea.

Near surface we also had the problems shown in Figure 5. The forces acting on the submarine are extremely high. They are orders and orders of magnitude greater than the forces and moments that can be applied by the effectors and it made a very difficult problem for us. If your noise forces are orders and orders of magnitude greater than what you can generate with the force effectors, what do you do? We found that mostly what you do is try to ignore them and hope they will go away because that's the only way you can maintain your depth at all. We also have a very low signal-to-noise ratio because the waves overhead in severe sea states might be 15 ft tall, and we are looking for variations in submarine depth in the order of 6-8 inches or a foot or two. We are really trying to pick out a very small signal in a very large amount of noise.

Most of the control problems (Figure 6) that have come up and been discussed over the past couple of days haven't really used estimation for control, and the problems that have had to go into estimation, haven't used the results of those estimations for control. It is the control estimation problems that are really sort of separate, and we didn't have that prerogative

NEAR SURFACE DEPTH CONTROL IS THE
MOST DIFFICULT PROBLEM

- HIGH FORCES
- SMALL FORCE EFFECTORS
- LOW SIGNAL TO "NOISE" RATIO

Figure 5

THE DEPTHKEEPING PROBLEM HAS
TWO MAJOR FACETS

- ESTIMATION
- CONTROL

Figure 6

of separating the two as nicely because of the really low signal to noise ratio.

The two sources of noise (Figure 7) are motions of the ship due to what are called first order wave forces, which are high frequency relative to the closed-loop frequencies. They are a frequency on the order of the wave height. The first order forces and moments typically have spectra that look like wave height spectra. Too fast to respond to, but they do move the boat. We also have the pressure depth variation, which I mentioned, which is due to waves.

The estimation problem (Figure 8) really turned out to be our greatest problem. The statistics of the sea are highly variable; they vary with the wind speed; frequency changes a lot with wind speed. They vary with wind direction and ship's heading with respect to the sea state heading, the sea can be

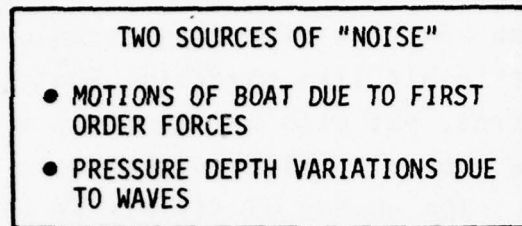


Figure 7

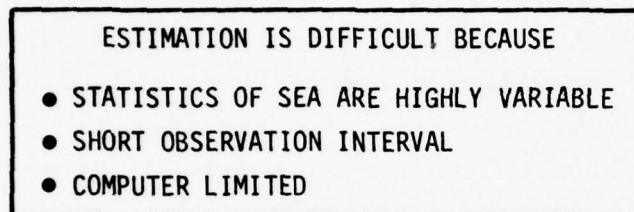


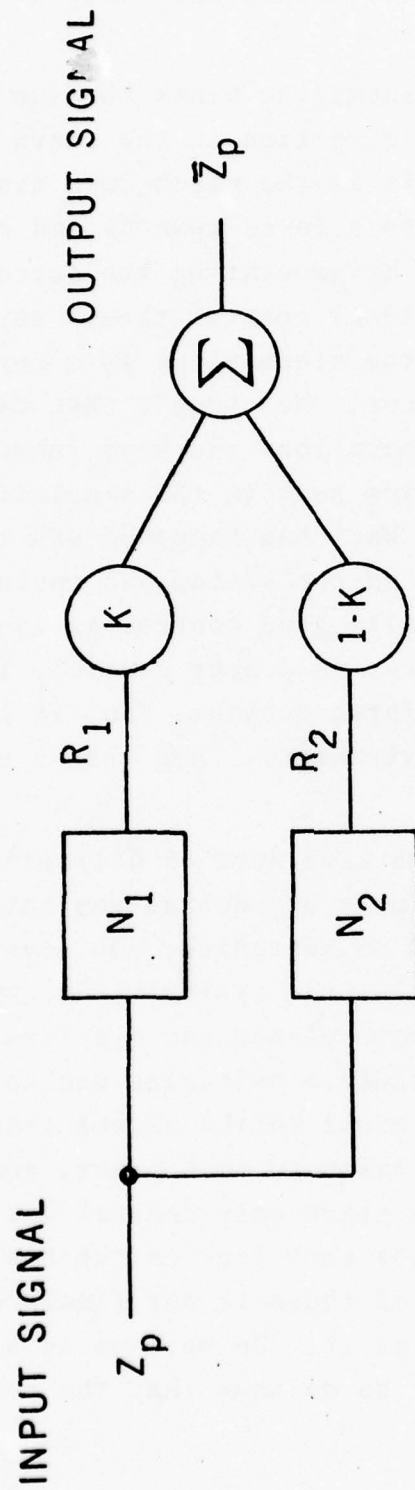
Figure 8

multidirectional rather than just all from one direction. So we have a problem of highly variable noise statistics and a relatively short observation interval in which to make some decision about what's going on, and what the statistics are, and to make some decision about adjusting filters to those variable statistics. If we are up near the surface for a 10-minute mission, we can't spend 5 minutes trying to determine what the statistics are--it's too late. We wanted to get estimations down in the orders of seconds--10's, 20's, 30's of seconds. And we couldn't also go to a full Kalman filter on-line estimation technique. We expected that we would be computer limited because of the requirement to be time-shared. As Mr. Stankey mentioned earlier, we're imbedded in a much larger environment--control is a very small frog in a very large pond.

So, we went to an adaptive filtering technique (Figure 9). What we did was a little bit like something that is frequently done in aircraft control, but also unlike it in a very significant way. We built a number of filters that were designed for different conditions. The number of filters we have is two. But rather than the aircraft concept of let's pick one or the other or the other, we built filters that, when linearly combined, gave responses that looked like a spectrum of the conditions between the two end points. The K-factor which selects one or the other of the filters; for example, if K turns out to be 0.5, we have generated a filter whose characteristics are midway between, roughly speaking, the two filters N1 and N2. And that's a lot different than what's done customarily in aircraft. We are able to take a filter here and a filter there and, by properly selecting K, sweep the whole range of characteristics between the two filters. The algorithm I have indicated for selecting K is one of quite a few that we looked at. It is not the algorithm we selected--as a matter of fact, I don't think we show anything today that we really did because of some restrictions. But, you can see the kind of thing that must be done. You sort of look at the residuals of the filters and try to push K in the direction of taking the filter with the lowest residual.

One of the great benefits of optimal control theory is that by not assuming a structure and not assuming what the gains are going to look like, you sometimes get some fairly unusual results that you would not have foreseen using a classical technique. One of the things that we found in the Trident when we first did this was that some of the gains we thought would turn out positive turned out negative. When we wanted the submarine to go up, the stern plane, which is at the back end of the boat, said dive. When we wanted the submarine to go down, the stern plane

ADAPTIVE FILTERING



$$K = \frac{\bar{R}_2^2}{\bar{R}_2^2 + \bar{R}_1^2}$$

Figure 9

went to rise. That counters intuition. But, it does indicate what is really happening.

What happens when a submarine wants to dive is that a force is generated in an upward direction at the stern and the submarine pitches down, and it is the pitch down that makes it go down. But you can generate a force upwards and counter that force and moment produced by generating the force upward on the forward plane, and the optimal control theory says that's the best thing to do--to use the stern plane as a force effector and not as a moment producer. We thought that was a really good idea and did some simulations and kept increasing the sea state and then the submarine sunk in the simulation. We couldn't figure out why. What had happened was that the forward actuator saturated, and the system was unstable. Now we had a problem. We had really good control as long as nothing saturated. And we had very, very poor control, instability, when we did saturate the forward plane. So, it looked like we had to go to multimode environment. And that's exactly what we did (Figure 10).

Well, you have to make some sort of decision. You can't switch your whole control mode as soon as you saturate, because that's a very violent kind of switching; you never want to put violent switching into real world systems. So, we designed a control system that used both planes and a system that used the stern plane only. We provided a switching mechanism that said: set a value, K , that is equal to the amount that the forward plane would be saturated, taken to some power, and use that as your indicator of how much stern-only control was required. As you probably noticed, we got very fond of the K 's and one minus K 's and you'll find a lot of those in our final control design theory if you take a look at it. We have no idea, theoretically, of the stability of this. We do know that the power that we

SUBMARINE CONTROL FORCES

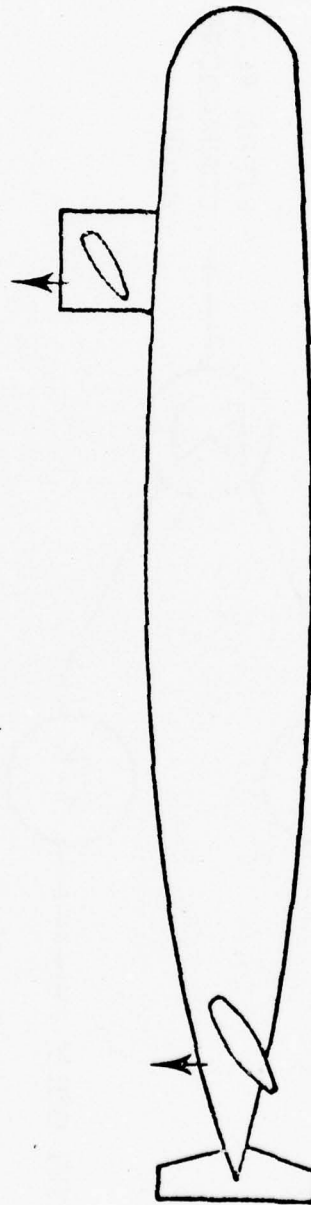
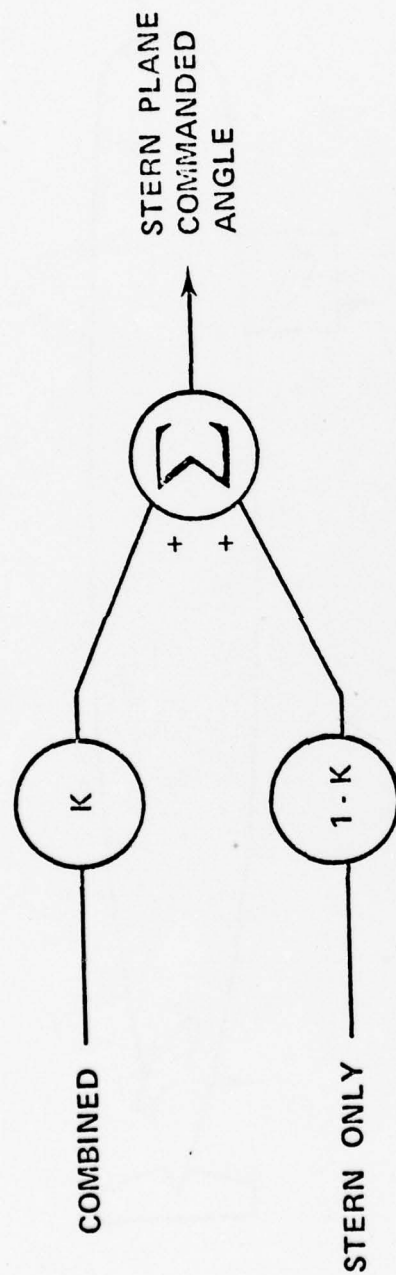


Figure 10

GAIN SWITCHING

STERN PLANE
COMMAND



$$K = \left(\frac{20}{\text{DBCOM}} \right)^{\gamma} \quad \text{/DBCOM/} > 20$$

OTHERWISE

$$K = 1$$

Figure 10 (Continued)

ke this ratio to, the Y , does affect stability. We have never
en able to make this system become unstable in simulation,
t we have never been able to prove that it's stable either.

I've been chided a little bit for not having the $U=LX$
aph. I think the $U=LX$ and the solution to the Riccati equa-
on itself are all pretty straightforward and our major problems
ose not from the optimal control, but the nonlinear kind of
blems we ran into.

SESSION VII
SUMMARY OF PANEL DISCUSSIONS

IDENTIFICATION PANEL SUMMARY

W. EARL HALL, JR.
Systems Control, Inc. (Vt)

The identification panel went through some of the various problems where parameter identification is important for aircraft. The problems that were concentrated upon the most were the aerodynamic coefficient problems, particularly with respect to post-test data processing.

The basic conclusions were (Figure 1) that the parameter identification algorithms are very well in hand, and this applied to the least squares, to the Kalman filter smoother, and to the maximum likelihood methods (this is based on comments by Bob Chen, Roger Burton, Martin Abkowitz, Richard Main and Narendra Gupta). However, the success of the parameter identification methods has placed increased emphasis on the modeling problem, and this modeling actually emerged throughout the entire discussion as that area where the basic research and the basic problems had to be resolved in order to have the most important effect on Navy systems.

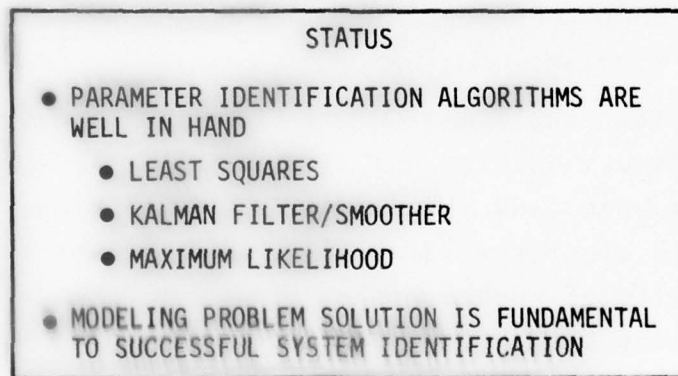


Figure 1

Figure 2 tries to summarize some of the methods. I think this sort of chart is really very hard to be general, because the success of any method depends on the person who is using it. It emerged, on the basis of comments from NSRDC and from NATC, as well as various others, that the least squares method with a filter is a good, fast, simple approach; it works best with simulations; seems to have fair accuracy for many flight test applications; and also for hydrodynamic applications.

The extended Kalman filter has now progressed to the point where it can be extremely fast with very good accuracy, but is limited to some extent by its inability to identify the process and measurement noise. However, as was pointed out by Bob Chen, many of these problems could be resolved by using smoothing, and, even though you couldn't identify Q and R directly, covariance matching techniques could be used to obtain answers that were certainly satisfactory for most flight test applications. Another advantage of the Kalman filter approach is that it's good for on-line applications and that seems to be one of the major places where it could be most widely used.

With regard to this problem of the ease of operation, Martin Abkowitz pointed out that, with experience, this can be made much simpler and I think that the experience of Calspan certainly indicates that good results can be obtained as experience is built up over a period of time.

The maximum likelihood method was generally characterized as being slow. It was pointed out that some of the recent advances which have been made in computational techniques have made this a very simple algorithm, as well as a very fast one. Again, however, the utility of such a method depends on the application and the person using them.

Figure 3 gives an example of some of the places where parameter identification has been applied in fixed-wing aircraft.

A COMPARISON BETWEEN LEAST SQUARES, EXTENDED KALMAN FILTERING
AND MAXIMUM LIKELIHOOD

ALGORITHM	COMPUTATION SPEED	ACCURACY	EASE OF OPERATION
1. LEAST SQUARES [LS] (WITH FILTER)	FAST	FAIR	SIMPLE
2. EXTENDED KALMAN FILTER [EKF]	SLOW → FAST	GOOD	DIFFICULT (A PRIORI COVARI- ANCE REQUIRED)
3. MAXIMUM LIKELIHOOD ⁽¹⁾ [ML] (WITH IMPROVED COMPUTATION TECHNIQUES)	SLOW → FAST ⁽²⁾	EXCELLENT	SIMPLE

NOTES: (1) MAXIMUM LIKELIHOOD METHOD MOST WIDELY USED FOR FIXED WING AIRCRAFT

(2) RECENT ADVANCES IN COMPUTATIONAL METHODS HAVE MADE THE MAXIMUM LIKELIHOOD METHOD APPLICABLE TO LARGE DIMENSIONAL PROBLEMS.

Figure 2

<u>APPLICATIONS</u>		
<u>FIXED WING</u>	<u>ROTARY WING</u>	<u>OTHER ATMOSPHERIC VEHICLES</u>
T-2	CH-53	HL-10
F-4	CH-47	M2/F3
F-14	UH-1	RV
F-15	ABC	
F-16		
F-17		
S-3		
F-111		
X-22		
<u>NON-AIRCRAFT APPLICATIONS</u>		
<ul style="list-style-type: none"> • BASIC OXYGEN FURNACE • BOILING WATER NUCLEAR REACTOR • HYDROCRACKER • ECONOMETRIC FORECASTING 		

Figure 3

Of course, it's been applied to many aircraft--these are ones I know about personally. T2, F4 - a high angle-of-attack for the F4; F14 through F17; the S3, Roger Burton talked about that; the F111; and, of course, the extensive programs at Calspan with the X22.

On the rotary wing aircraft, CH-53, CH-47, the UH-1 and the ABC helicopters have all been extensively analyzed with some success. We've also gotten into nonstandard vehicles--HL10, M2/F3, and reentry vehicles. I should also point out the significant applications have been achieved in non-aircraft examples, on the order of complexity which we can expect in even the worst operational situations with Navy requirements. Examples are basic oxygen furnace, boiling water nuclear reactors, the hydrocracker (and Larry Taylor made sure that I put the econometric forecasting on there).

The parameter identification algorithms seem to be pretty well in hand. Experience is the key factor in determining the success of the method, but there are other criteria and we didn't get into that. Given that these methods are successful, then emphasis shifted to the modeling problem which has emerged as a key problem.

Figure 4 shows some of the points that were made and the trade-off of computational modeling complexity. In using this as an example, the point that was made was that in attempting to analyze the nonlinear flight regime, what's the best way to go? Do you actually try a big nonlinear model, or do you try a bunch of sequential linear models and identify those? Well, it's desirable, of course, to, in total, for say a simulation application, be able to identify all coefficients necessary to be able to reproduce the response.

One subject of discussion for about 10 minutes was: do we use a "bunch" of linear programs or do we try to identify the entire polynomial of a nonlinear function, if polynomials were the functions we use? Of course, we could use others. But in this particular case, I am talking about polynomials.

The advantage of the piece-wise linear models is that they give the minimum number of parameters and correlate strongly with what we call the classical stability derivatives. However, in practical application, it means we must have many flight test points. We can use fewer test points, but now we need to have some a priori knowledge of how the polynomial segments will tie together. Of course, we could attempt to identify with large maneuvers, either in aircraft or in surface or subsurface ships, the complete nonlinear functions. However, this type of identification is very sensitive to instrumentation and numerical errors. No general conclusion was reached here. It was only that the trade-off criteria in one form or another were cited and this subject is a matter of future research.

AERODYNAMIC MODELING - I
TYPE OF REPRESENTATION

- COMPLETE AERODYNAMIC MODEL IS HIGHLY NONLINEAR AND CONTAINS A LARGE NUMBER OF UNKNOWN PARAMETERS

$$\dot{q} - \left(\frac{I_x - I_y}{I_y} \right) p r + \frac{I_e \Omega_e}{I_y} + \frac{M_T x}{I_x} = C_0 + C_\alpha \alpha + C_{\alpha^2} \alpha^2 + \dots + C_{\delta_s} \delta_s$$

$$+ C_\beta \beta + C_{\beta^2} \beta^2 + C_{\alpha\beta} \alpha \beta + \dots$$

- DESIRABLE OBJECTIVE: DETERMINE COEFFICIENTS OF ALL INDEPENDENT VARIABLES (I.E., THE COEFFICIENTS OF POLYNOMIAL EXPANSIONS OF THE AERODYNAMIC FORCES AND MOMENT)
- ALTERNATIVE REPRESENTATIONS:

	ADVANTAGES	DISADVANTAGES
PIECEWISE LINEAR	<ul style="list-style-type: none"> • MINIMUM PARAMETERS • CLASSICAL "STABILITY DERIVATIVE" 	<ul style="list-style-type: none"> • MANY FLIGHT TEST POINTS
PIECEWISE POLYNOMIAL	<ul style="list-style-type: none"> • FEWER TEST POINTS 	<ul style="list-style-type: none"> • A PRIORI KNOWLEDGE OF POLYNOMIAL SEGMENTS
ENTIRE POLYNOMIAL	<ul style="list-style-type: none"> • COMPLETE DESCRIPTION WITH FEWEST TEST POINTS 	<ul style="list-style-type: none"> • MOST SENSITIVE TO INSTRUMENTATION AND NUMERICAL ERRORS

Figure 4

In terms of what is necessary for determining the accuracy of the model required, there are several techniques. Richard Main pointed out that, in his experience at the Flight Research Center, it was necessary to use some identification program iteratively to correct errors by changing the model structure. This, of course, needs a technique which is very fast. Another technique which was mentioned is that of using hypothesis testing methods to come up with better models to correlate with a particular set of data. Such a hypothesis testing technique which has been successfully demonstrated under ONR research is to take flight test data and to pass it through some sort of program, using, for example, subset regression which is parameterized on an a priori structure through both wind tunnel data and physical knowledge. Using various hypothesis testing techniques and correlating the data, it is possible to come up with a most significant variables response for one particular flight condition. This doesn't replace the basic physical intuition and wind tunnel testing, but it is to verify intuition and, where necessary, indicate where we should upgrade the model.

The next topic which was discussed, brought with it general agreement that input design coupled with model structure determination is a critical point. Martin Abkowitz pointed out that it is his feeling (and I'll try and quote him as exactly as I can) that we should spend 95% of our time in planning trials and simulating those trials before we enter into an extensive model and parameter identification program. And the next figure shows how such a process would work, where we would actually use a six degree-of-freedom simulation; attempt to, on the basis of the simulation, come up with model structure, parameter identification, and model verification techniques; use these to upgrade our simulation and test various inputs, noise levels, both in process and measurement noise; to iterate through the entire scheme in order to plan such a flight test.

We spend quite a lot of time discussion hydro-vehicles (Figure 5). This was actually quite a long discussion and we were actually on the verge of getting very heated. I've attempted to summarize what the principal conclusions were in the figure, although I hope we may have a chance to discuss this further.

As far as the surface ship problem is concerned, there should be a large emphasis on the seaway modeling as opposed to, say, the actual modeling of the ship itself. Dr. Cummins of NSRDC pointed out the extensive work is going on in collecting models for seaways, that existing data indicated that the Pierson-Moskowitz and the Neumann spectra were not adequate for most control design purposes, and that further work did have to be done here. The question was raised as to whether or not parameter identification could help to do that--given that wave spectra tend to be nonrational functions. This question, I think, is going to be dependent to a large extent on programs and actually trying and testing the ability to identify process noise. Some research is indicated here.

On subsurface vehicles, Dr. Feldman indicated that (as he did in his paper on the first day), the basic modes and simulations appeared to be in good shape, but there are certain problems that appear to require nonlinear identification. This is

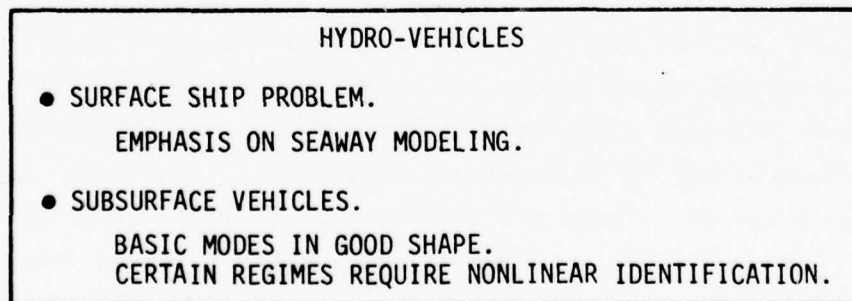


Figure 5

a basic problem where system identification may be applicable. Now, they have some identification programs, extended Kalman filter programs, that they have tried and they are attempting to use these now. These particular algorithms do not appear to have good properties in the presence of noise. On the other hand, this could be just a matter that extensive testing was not done.

Where are we now? Let me just point out that Kalman filtering, as I think Ray Nash summarized yesterday, has really come to a point of significant payoff for the Navy. This is, of course, based on extensive research. I would point out that the Office of Naval Research has, for the past three years, sponsored extensive research in parameter identification and linear identification programs based on maximum likelihood; it has lead to linear and nonlinear model structure determination algorithms; on-line and real time algorithms; and linear and nonlinear input design. Now, much of this basic research has been translated to highly visible and successful results to joint ONR and NATC programs.

On the basis of this work and the panel discussion, the conclusions that I gave yesterday, I think, are still basically valid. That a lot of the basic work has been done, that by integrating the algorithms with the various test programs and the test objectives that significant advances, at least in terms of upgrading some of the models necessary for control and estimation, appear feasible at this time.

ESTIMATION PANEL SUMMARY*

RAYMOND A. NASH, JR.
The Analytic Sciences Corporation

Figure 1 illustrates my view on the application of estimation theory. Considering the presentations yesterday and the panel discussion we had, I would perhaps add one additional application which isn't called out explicitly, the pointing of communication antennas. Also, I think if I had to make a general judgment, I would guess that the submarine navigation community has probably made the greatest use of estimation theory concepts.

I want to make the same point I made yesterday— that the covariance analysis mathematics associated with estimation theory is a very powerful "before-the-fact" tool to allow one to make configuration design trade-off studies which, hopefully, will save you money downstream. The problem often here is getting the funding, the front money, to get this done, because often people want to see hardware built right away.

Again, Fig. 1 is my attempt to summarize the kinds of things I said yesterday, along with the panel discussion that we had. I think we are all in agreement that estimation theory is a mature technology at this time, and that modeling is still the real problem. And, I'll make two comments here first. When people make components and subsystems of certain systems, the data they take is not for the purpose of structuring or constructing a model. Rather, this would be for the purpose of passing certain kinds of specifications, and that the data is typically not sufficient and typically not the right kind of data from which to obtain model structures. Now, there are

* This written record is an edited transcription of Dr. Nash's verbal remarks.

ESTIMATION THEORY SUMMARY

- ESTIMATION THEORY IS A MATURE TECHNOLOGY.
- MODELLING IS STILL THE REAL PROBLEM.
 - NOT MUCH TEST DATA.
 - NOT THE RIGHT KIND OF TEST DATA.
- THIS LEADS TO A NEED FOR "MINIMUM-SENSITIVITY" DESIGN PROCEDURES.
- OTHER FRUITFUL AREAS OF RESEARCH INCLUDE:
 - MODULAR ESTIMATION (MICRO-PROCESSORS AT THE SENSOR.)
 - FAILURE DETECTION ALGORITHMS.
 - COMMUNICATION ANALOGS (ASV-DETECTION OF CHARACTERISTIC SPECTRAL LINES).
 - EXTENSION OF ESTIMATION CONCEPTS TO TWO AND THREE DIMENSIONAL RANDOM PROCESSES ("MAP MAKING", MAP MATCHING, LARGE DATA BASE UPDATING, . . .).

Figure 1

two implications of that statement. One is the obvious application of identification theory, as Earl Hall has discussed. The second leads to a need for what I'll call minimum sensitivity design procedures—the design of estimators which are not sensitive to assumptions about the model. I guess a lot of people like to use the word robust estimators, in this particular case.

I indicated yesterday that some analytical tools do exist today for minimum sensitivity design. I would also point out that another very powerful (albeit, brute force) way to go about this kind of thing, is simply to solve the mathematics associated with the reduced-order filter in the real world, examining tabulations like error budgets and making engineering judgments as to what states are important, what states are not important, whether to guess high or low on Q-matrices, and this kind of thing.

The last bullet on Fig. 1 refers to other fruitful areas of reserach. Again, I mentioned most of these areas yesterday, but let me touch on them briefly again. The concept of modular estimation, i.e., putting some sort of micro-processor, "at the sensor" for purposes of data smoothing and data compression. John Deyst also alluded to this earlier today. I think this kind of thing is necessary and is coming.

I talked about one particular application of failure detection—utilizing Kalman filters—yesterday. John Deyst has mentioned some other related concepts this morning.

Regarding communication analogues, the last slide I showed yesterday had to do with showing how one could use the Kalman estimator to recursively calculate the likelihood ratio

ection theory problem. Also, in the course of the discussion yesterday, another area came out. In the anti-submarine business, what one likes to do is listen to what one is the target and attempt to identify characteristic lines, and I believe that this is done to a large extent by the operator using visual techniques. One only Kalman filtering kinds of techniques for automatic detection of these particular spectral lines.

And then finally, there is the extension of estimation concepts to two- and three-dimensional random processes, speaking specifically of things like spatial random processes here. I gave one example yesterday that had to do with the Omega radio navigation system, and I talked a little about correlation guidance. I really believe that this is a really exciting new area for application of estimation

You'd be surprised how little is known about the properties of two- and three-dimensional spatial random processes.

In the one-dimensional kind of domain, we always like linear systems which when excited by white noise, "produce" the right auto-correlation functions. However, in two dimensions, for example, you are dealing with partial differential equations. And it turns out that if you excite the partial differential equation, with white noise, you don't get an analytic auto-correlation, you get a Bessel function, the structure is considerably more complicated. I feel that these concepts can be used in the area of navigation, correlation guidance map-matching, and large data processing. The data base might be topography, it might be bathymetry data, or it might be magnetic field data. The problem that occurs here is that you collect data from one or more kinds of sensor, and obtained a data base that has a quality associated with it, and then later you

developed a new kind of sensor, a new kind of survey procedure and get another data base, and the idea is how can you merge this data base in an efficient way. One way to do it is recursive estimation theory kinds of concepts, and I think we've just scratched the surface in this particular area.

CONTROL PANEL SUMMARY *

DR. EUGENE YORE
Honeywell

I would like to go back to my theme from this morning, and I think what was happening the last three days was a workshop that moved from the theoretical R&D towards the practical operational problems. I think there was one significant presentation on the Trident that started to give us a little bit of appreciation for what is involved at the operational end of the spectrum; and I think there were two papers, one on "Ultra Reliability" and John Deyst's "Fault Tolerance" that, from a research point of view, showed a great deal of knowledge about the operational problem and the real system problems. I thought those were very good papers.

In the audience, during the course of the three days, I saw some research people writing equations during lab presentations on problems, and I saw some lab people not paying attention during equations. But, I think in general, we have moved toward the overlap that I think is necessary between research and production, at least in understanding and vocabulary. What I would like to do is talk about a few applications in the controls area, but before I do that, I would like to just go back to my performance measure, and say that in applying optimal control or control theory or modern control, the ultimate value is in the operational phase, and as we progress in this direction, our transfer, our applications become more and more valuable. We are starting to get a lot of flight test feasibility demonstrations here. Understanding the systems problems, getting our applications all the way over there. These were applications that I was aware of coming into this; I think we have added the Trident submarine up here; I think we have also added the helicopter take-off and the work that Dr. Fred Schmidt has done at Ames, and I think that is all we really added

* This paper was typed from a taped version of the oral presentation.

to this side of the column. There were several other things along the way.

There are two things that need to be done at this point. One thing is that we haven't transferred all the technology we have now. We haven't worked all the problems that we know how to work. We have got to continue to understand the operational systems better and their real problems in order to effect that transfer and there is a whole bunch of areas I want to talk about in a little detail.

The second thing I think is happening in the course of this application is that we are finding new research problems that we need to be really working on in parallel before we can ever succeed at the goal of getting into the operational areas.

There were some common needs, technology needs, and common system trends that ranged across a whole bunch of different areas. Digital control is coming, and its impact is being felt and seen. The issue of central digital computation versus distributed or dedicated is still very much an issue in a lot of these systems. The fact of life, a real trend toward microprocessors is beginning to be seen, and it was evident in several of the papers and applications in some of the papers.

From the system's point of view, it was interesting to see that there were some systems, some of the subsurface submarines where cost and the control hardware cost didn't seem to be as driving a factor as in the airplane. Reliability was a driver across almost all these systems, and it related very heavily, in addition to cost, to operator acceptance. Whether we are able in the future to get the operator confident in our automatic control system, to get them turned on and used, we have got to address the questions of fault tolerance and reliability.

We heard about new problems, or rather, problem areas where modern technology can be applied beneficially; in surface ships we heard about maneuvering problems, steering problems, replenishment at sea, where performance seemed to be an issue. An underriding

technical issue seemed to be modelling again - in surface ships and in the modelling of the seaway. Cost and reduced manning is another area that is receiving a lot of attention, and it seems that it is going to be a system driver in the future.

Surface effect ships look like a new program with a lot of decisions to be made yet. What are the best effectors? Configuration? Sensors? Modes? Ride quality seems to be one of the key technical drivers, but there are others: maneuvering and it seems to be a very crucial area where in that spectrum from research to advanced development, we are still pretty far over on the advanced development side and stand a chance of impacting a program before we get saddled with hardware constraints.

In the submarine, some of the things that we heard as driving the technical problems were fault detection, depth-keeping performance, high speed maneuvering (which is a problem that probably needs to be addressed in the future), and stability augmentation; there was some discussion about the potential of using control and control configured vehicle concepts in the design of a submarine to determine the position and sizing of the surfaces.

In aircraft, the driver appears to be cost and that is seen in a lot of different ways. Rising fuel costs indicate a need for another thrust in flight management and fuel optimization; fault tolerance was another way it was evident; and integration.

In the carrier auto-land problem, there seems to be a big modelling problem. It sounds like the systems that have been built aren't getting used because of the reaction the pilots have to using them.

This is an illustration I made of technology needs, or areas where I felt some research was required, before I came, and some of these things are supported with additional systems needs. If you look at non-linear control with CCV, where we are trying to drive control surfaces down, it becomes necessary to operate with control surfaces saturated part of the time. We heard about that problem again this morning in the submarine. I think this is a crucial area for more work.

In jet engines, there is a time-delay problem, and non-linear problems. A lot of modelling issues need to be addressed, and it looks like Jerry Michaels has a start on those with some of his systems modelling work. That is an area that also needs some fundamental research and more things than just control and application. It concerns 3-D flows and general dynamics and so forth.

We heard a little bit this morning about a multi-loop stability problem as related to saturation in submarines. We have the same problems in airplanes. When we start integrating more and more loops, like in the C130 gun ship where we are trying to control all three axes with all the cross-coupling, when we start combining engines with airplanes and looking at cross feeds, we end up with multi-loop problems and solutions. I think for some people who have been doing work in this area, it probably doesn't require a lot of work, but there is some need in that area. I think there are multi-rate stability problems in digital systems where you want to drive the fast loops at high rates, slower loops at lower rates, so you don't load your computer down. These need to be addressed. Those are being addressed somewhat in the space shuttle flight control problem.

There are many areas where modelling is an issue for partial differential equation systems. One that wasn't mentioned at all was towed-arrays, and the problem of controlling depths of towed-arrays-essentially long strings that you drag out in the water.

Micro-processors and their impact on future systems have already been talked about. I think this is a farther out need; it's awfully hard to get operational people or digital computer people supporting this right now, but when we start looking at putting micro-processors together and parallel configurations or parallel computing, if you look at the problem with micro-processors, they are actually pretty slow, and you need to put

a lot of them together, and first of all you have to install a simple data bus between them. But, if you go and do a detailed design of that data bus, it becomes very, very complex with interrupts and transfer of data between different micro-processors and so forth.

There is a need to study architecture, not from a computer point of view, but from a flight control law point of view, a hierarchical control, or a distributed control. I think there has been some work done in large processors at Ames and some other places. We need to get serious about it in the aerospace industry.

Finally, before I came, I saw costs as being an overriding driver on almost every system I looked at, and it seems like now maybe there are some systems where the cost of the control relative to the rest of the system is pretty small. It might not be that driving.

If you look at the technology status, I think I have changed my mind on where some of these things go. There is an awful lot of systems that need more modelling work, new start modelling work on them. Digital analysis and quadratic optimal control is ready to transfer and we should be pushing very hard to apply it to new programs where there are technical issues that warrant it, or some benefit.

I talked a little bit about a program that NASA Langley is sponsoring in insensitive control. Dave Kleinman talked about this a bit from the submarine point of view. I talked a little bit about a program that ONR is sponsoring and both of these are new starts, that will have a very rapid payoff in cost here, and will get input through optimal control as soon as the results are available. So, as far as status need, I think that pretty well summarizes it.

There is one other area that in a very general sense is indicative of the advance control system trends through which we can achieve payoffs using optimal control, and that is in mission performance integration, and I am not sure, but I think this is a trend which we certainly must address with the modern control, with our thinking anyway, and that is mechanization, primarily cost.

SESSION VIII
INFORMAL CONTRIBUTIONS

REMARKS ON LQG SUBMARINE CONTROL

DAVID L. KLEINMAN
University of Connecticut

I want to try to get a chance to mention very quickly some of the technical problems that arose over this two-year effort on near surface depth keeping. I am going to try to keep to the control theoretic problem phase rather than to some of the sometimes more important operational problems, such as failure detection or the like. And there are just four things I'd like to discuss just briefly. Some of them are appropriate to control systems in general, and some of them are geared more to the specifics of the submarine problem.

Figure 1 lists some of the problems that John Ware mentioned. One of the very difficult problems facing us was the problem of designing optimal linear control systems with saturating controls, which by itself is a misnomer--you just can't do it. Here the problem is that the forward plane effector very often saturates in near surface depth-keeping, especially in high sea states or at low speeds. This saturation factor is a position limiting effect and a rate limiting effect. On the other hand, the stern plane usually is not saturated. So the big question is, "What do you do with the stern plane when the forward plane is up against its limits?" If nothing is done the result is very often instability because of the fact that the stern plane tends to go the wrong way when you try to correct depth.

The approach taken to correct this problem was a construction of a nonlinear type of control, and it worked very well. But, we can't actually theoretically prove stability or, at best, a limit cycle, but this control has worked marvelously well in the application.

NEAR SURFACE DEPTH KEEPING PROBLEMS

- OPTIMIZATION WITH SATURATING CONTROLS
- PERFORMANCE EVALUATION METHODS
- SUCTION FORCE/MOMENT ESTIMATION
- DESENSITIZE DESIGN

Figure 1

OPTIMIZATION WITH SATURATING CONTROLS

- FORCE/MOMENT EFFECTORS; δb , δs
 - δb OFTEN SATURATES IN NSDK FOR HIGH SEA STATES
 - BOTH POSITION AND RATE SATURATION
 - δs ALMOST ALWAYS BELOW STOPS
 - WHAT TO DO WITH δs WHEN $\delta b = \delta b_{\max}$
 - $\delta s = L_s x$ MAY PRODUCE INSTABILITY DUE TO FULL STATE FEEDBACK TO δs
 - APPROACHES
 - USE SPLIT-PLANES CONTROL CONFIGURATION
 - USE δs -ONLY CONTROL DURING SATURATION PERIODS--
NONLINEAR CONTROL
- $$\delta s = (1-k) \delta s_1 + k \delta s_2 \quad k \sim \left| \frac{\delta b_{\max}}{\delta b_{\text{com}}} \right|^\beta$$
- TRANSLATE INTO COMMAND PITCH ANGLE

Figure 1 (Continued)

There are other possible approaches to the problem of saturating controls in a multiple control environment. The classical technique of split plane control, where the stern plane controls pitch, and the forward plane controls depth, does not get into these kinds of instability effects when one control saturates. The submarine may do something strange, but it won't do something very disastrous.

Another method of approach might be to translate depth error to command pitch angle, and instead of trying to keep the boat level, give up a little on that requirement to help you out on depth. But, this is one class of problems that we came up with, got a solution to, but just were not able to really spend the full time in looking at it over the contract period.

Figure 2 lists the issue involved in evaluating a control system. "How do you begin to evaluate it? Is it good? Is it bad? What can you really say?" There are a million and one measures that an analyst can apply toward the system. The common ones that control people are using are things like eigenvalues, or zeros, poles and zeros, closed loop stability margins, step response, things like this. And, usually these things are gotten around by adjusting the weighting matrices and the quadratic criteria.

But, on the other hand, the submarine itself has to operate in a random seaway. So the designer is really faced with running a simulation and taking a look at near surface depth keeping in random seaways, or with external types of input.

The questions here deal with choosing input forcing functions to use in evaluating the performance of a submarine. You'd really like to run the submarine in a random seaway. The problem, of course, is that the random seaway is not very easily expressible as white noise into a linear filter, which we all like, but rather some non-Gaussian density, a complex type of process that's been crying to be modeled since the early days of Von Neuman and beyond.

PERFORMANCE EVALUATION METHODS

- CONTROL THEORETIC MEASURES
 - EIGENVALUES
 - LOOP PHASE MARGINS
 - RELATION TO DYNAMIC RESPONSE
- SIMULATION METHODS
 - TYPE OF INPUT FORCING FUNCTION
 - PULSE RESPONSE VS. RANDOM SEAWAY
 - HOW LONG TO RUN SIMULATION
 - PROBABILISTIC MEASURES

Figure 2

AD-A045 603

SYSTEMS CONTROL INC PALO ALTO CALIF
PROCEEDINGS OF THE SYMPOSIUM ON CONTROL THEORY AND NAVY APPLICA--ETC(U)
AUG 77 M D CILETTI, J S TYLER

N00014-72-C-0327

F/G 15/7

NL

UNCLASSIFIED

8 of 8
ADA045603



END
DATE
FILMED
11-77
DDC

The length of the simulation must also be chosen. Should it be 10 minutes, 20 minutes, or 2 hours of actual physical time (not computer time)? You just really cannot solve this very easily because of the problems and nonlinear statistics in the input forcing functions. How do you begin to talk about the measures that come out of the simulation? What kind of statistical measures should one use? The probability of broach, percent time the planes are saturated, depth errors, just what? It is desirable to relate the simulation results to the control theoretic measures in some way, so that in the process of design you can get at the methods which will be used to eventually evaluate the system.

There is an overall need also, to evaluate performance in simulations, in a language that is familiar to operational personnel. This is the problem that control people always have. I can go to somebody in this room and say, we've got 30-40 degrees phase margin; they'll say, "hey, you've got a good system." I'll go to a submariner--they'll say "What?" So, it's this problem of language that must be overcome.

Figure 3 illustrates an area that we did not look at in the work, but it is nevertheless a very interesting problem. The forces that move the submarine near the surface, what are called the suction forces, are fairly low frequency pulse-like forces or moments. The planes counteract. Estimation of these pulse-like, or suction, forces before they really start moving the boat is of interest. Well, we did not really look into it, but some ideas along this line can be gotten from the use of observers, Kalman filters, or the possible use of vertical accelerometers. I might add that in our work we did not use any Kalman filters for the dynamic filtering of the vehicle equations. We used some Kalman filtering ideas in the adaptive filtering of the sensor signals, but not in the vehicle, which is the usual way one tends to think of Kalman filters.

SUCTION FORCE/MOMENT ESTIMATION

- SUCTION IS PRIMARY EXTERNAL INPUT
 - PULSE-LIKE OF DURATION ~ 20 SEC
 - LOW FREQUENCY
- ESTIMATION OF EXTERNAL FORCES CAN RESULT IN IMPROVED NSDK
 - OBSERVERS
 - KALMAN FILTERS
 - ACCELEROMETERS
- PROBLEM IS DIFFICULT SINCE SUCTION FORCES ARE INCLUDED IN HIGH FREQUENCY, MAGNITUDE SEAWAY FORCES

Figure 3

I think there are possibly some advantages here. We have shown the feasibility of trying to do some estimation of the forces in a submarine with long time lags--the name of the game is "build-in lead." If you can get lead on the forces acting on the boat, you can move your planes that much sooner and here another few seconds can translate to a foot or two in minimizing depth errors.

The problem, unfortunately, is very hard because the suction forces, although large in magnitude, are buried in a much higher frequency, much higher magnitude seaway type of motion. So, the thing is, how do you separate out a lower frequency force out of a much higher frequency force while not throwing tremendous amounts of phase-lag or time-delay? If a simple filter that just cuts off as a sharp low pass filter is used, the time lag in the problem is so high that the estimate of the suction forces don't do any good.

The final problem (Figure 4) is the whole problem of trying to design for inaccuracies, or low sensitivity. It's a universal problem. In submarine work, it tends to be just as bad, if not worse than anything else. The coefficients of the submarine's linear equations are often uncertain; there are dynamical approximations made to actuator dynamics and various other things. There are speed variations, and the submarine depends very critically on the parameters and the variations. Our approach was to design to the nominal parameters, of course, and to try as best we could to minimize the effect of the parameter variations in an ad hoc way: design the system, run a simulation, make some variations in the parameters, and adjust gains if necessary to keep things sort of on the low sensitivity side. There were various unmodeled time lags and time delays in the problem that sometimes came up just on your Friday afternoon. Some person would call up and say, "Hey, by the way, do you remember the half a second time lag in such and such loop?" So, there's a

DESENSITIVE DESIGN

- ACCURACY OF LINEAR MODEL FOR CONTROL DESIGN
 - COEFFICIENTS UNCERTAIN
 - DYNAMICAL APPROXIMATIONS
 - SPEED VARIATIONS
- DESIGN FOR NOMINAL PARAMETERS
 - MINIMIZE EFFECTS OF PARAMETER VARIATIONS
 - UNMODELED TIME LAGS
 - TRADE-OFF PERFORMANCE
- EFFECTS OF IMPLEMENTATION
 - QUANTIZATION ERRORS
 - DIGITAL CONTROL
 - NONLINEARITIES
- LOW SPEED PROBLEMS

Figure 4

problem of keeping your design robust enough to be able to handle some unmodeled time lags without destabilizing the entire system, which really means using some additional phase margins. And, then there's the whole issue of trading off performance, the little bit you are possibly willing to trade, forced by the desensitized design.

The other problems in desensitivity have to do with implementation, which is further downstream. The effects of quantization errors and the effects of digital control with a digitized analog design must be examined in conjunction with implementation on a computer. This creates inaccuracies that you'd like to have your control system insensitive to.

Finally, there are a myriad of nonlinearities--everything from hysteresis in the planes, back-lash, sensor characteristics and the like that we consider. Now it is very nice to be able to consider these nonlinearities before the fact in the design process rather than taking the design and ginning it around a little bit, and saying, "Well, it'll work under such and such conditions." These problems become very severe at the extremes of the speed range. At low speed in the submarine, there's what is called the plane reversal effect where, if you want to make the submarine go down, you have to put the planes on rise. It's very nice to have your modeling exact here, or have your control system insensitive, so you don't do the wrong thing. This is sometimes very difficult to do if you have a mis-matched modeled system. At the high speed end, you've got to be careful because a wrong move there can send you to the bottom very quickly.

These are just some of the problems that came up from a technical point of view. We think we've solved some of them, or at least got a head start. Others we haven't done very much on, and there are about a million more that I don't have the time to mention.

LIST OF ATTENDEES

JULY 15, 1975
CONTROL THEORY AND NAVAL APPLICATIONS
SYMPOSIUM
ATTENDEES

Martin A. Abkowitz
Massachusetts Institute of
Technology

Reidar Alvestad
Naval Ship R&D Center

Robert B. Asher
Air Force Academy

Irving Ashkenas
Systems Technology, Inc.

A. V. Balakrishnan
Optimization Software, Inc.

Mark J. Balas
U. S. Naval Surface
Weapons Center

William F. Ball
Naval Weapons Center

William Bihrlé
Grumman Aerospace Corp.

Paul E. Blatt
Air Force Flight
Dynamics Lab.

Walter J. Blumberg
Naval Ship R&D Center

Lawrence Bradley
The Analytic Sciences Corp.

R. K. Brands
Naval Postgraduate School

Stuart L. Brodsky
Office of Naval Research

A. E. Bryson
Stanford University

Margaret Bullock
Operations Research, Inc.

Robert A. Burton
Naval Air Test Center

Robert Chen
NASA, Ames Research Center

Michael D. Ciletti
University of Colorado

Craig Comstock
Naval Postgraduate School

John Connors
Naval Surface Weapons Center

William E. Cummins
Naval Ship R&D Center

John Deyst
C. S. Draper Laboratory

Warren R. Diamond
Naval Ship Engineering Center

Pierre Dogan
C. S. Draper Laboratory

Brian Doolin
NASA, Ames Research Center

Florence A. Farrar
United Aircraft Research Lab.

Jerome P. Feldman
Naval Ship R&D Center

Gary L. Gross
Naval Air Development Center

Narendra K. Gupta
Systems Control, Inc. (Vt)

Grant R. Hagen
Naval Ship R&D Center

Bert Hall
McDonnell Douglas

W. Earl Hall
Systems Control, Inc. (Vt)

Ralph A. Harrah
Naval Air Systems Command

Gary Hower
Naval Weapons Center

Marle D. Hewett
Naval Air Test Center

Irving Hirsch
Boeing Company

Lee Gregor Hoffman
Systems Technology, Inc.

James E. Kain
Johns Hopkins University

Jayant S. Karmarkar
Systems Control, Inc. (Vt)

David L. Key
Army Air Mobility

Donald E. Kirk
Naval Postgraduate School

David L. Kleinman
University of Connecticut

Robert C. Kolb
Naval Electronics Laboratory
Center

William S. Lapp
Naval Undersea R&D Center

L. J. Latham
Naval Air Test Center

Choung M. Lee
Naval Ship R&D Center

Roy B. Leipnik
Naval Weapons Center

Jack H. Lindahl
Honeywell

Isham Linder
Naval Postgraduate School

Samuel M. Lum
Naval Sea Systems Command

Paul Madden
Systems Control, Inc. (Vt)

Allen H. Magnuson
Naval Ship R&D Center

Richard Maine
University of California
at Los Angeles

James S. Meditch
University of California
at Irvine

Jerry Mersky
Optimization Software, Inc.

George Meyer
NASA, Ames Research Center

Gerald L. Michael
United Technologies Research
Center

Dave Moran
Naval Space R&D Center

Conrade E. Mueller
Honeywell

Walter McNeil
NASA, Ames Research Center

Duane [unclear]
Systems Technology, Inc.

Raymond A. Nash
The Analytic Sciences Corp.

Tyre Newton
Washington State University

David Pekelman
University of Pennsylvania

John Worth Pitsenberger
Department of the Navy

David Powell
Stanford University

Charles F. Price
The Analytic Sciences Corp.

Robert Ringland
Systems Technology, Inc.

William Ward Rosenberry
Naval Ship R&D Center

David Russell
University of Wisconsin

J. Ruzicka
Optimization Software, Inc.

E. G. Rynaski
CALSPAN Corporation

M. Sidar
NASA, Ames Research Center

David Siegel
Office of Naval Research

Allan Smith
NASA, Ames Research Center

Richard G. Smith
Systems Control, Inc. (Vt)

William E. Smith
Naval Ship R&D Center

John A. Sorensen
Systems Control, Inc. (Vt)

Harold W. Sorenson
Applied Systems Corp.

Harold Stalford
Naval Research Laboratory

Richard Stankey
Naval Ship Engineering Center

Gunter E. Stein
Honeywell

Lawrence W. Tavlör
NASA, Langley Research Center

George Thaler
Naval Postgraduate School

Hal Titus
Department of the Navy

James S. Tyler
Systems Control, Inc. (Vt)

Dennis Vensel
Johns Hopkins University

John Ware
Naval Ship R&D Center

Stein Weissenberger
NASA, Ames Research Center

Theodore J. Williams
Purdue Laboratory for Applied
Industrial Control

W. Wingate
Naval Surface Weapons Center

Eugene E. Yore
Honeywell

David Yost
Johns Hopkins University

John Zvara
Aerospace Systems, Inc.